JOURNAL OF BACTERIOLOGY, Mar. 2010, p. 1269–1278 Vol. 192, No. 5
0021-9193/10/$12.00 doi:10.1128/JB.01048-09

The Cyclic-di-GMP Phosphodiesterase BinA Negatively Regulates Cellulose-Containing Biofilms in *Vibrio fischeri*[▽]

Christine M. Bassis and Karen L. Visick*

Department of Microbiology and Immunology, Loyola University Medical Center, Maywood, Illinois

Received 7 August 2009/Accepted 22 December 2009

Bacteria produce different types of biofilms under distinct environmental conditions. *Vibrio fischeri* has the capacity to produce at least two distinct types of biofilms, one that relies on the symbiosis polysaccharide Syp and another that depends upon cellulose. A key regulator of biofilm formation in bacteria is the intracellular signaling molecule cyclic diguanylate (c-di-GMP). In this study, we focused on a predicted c-di-GMP phosphodiesterase encoded by the gene *binA*, located directly downstream of *syp*, a cluster of 18 genes critical for biofilm formation and the initiation of symbiotic colonization of the squid *Euprymna scolopes*. Disruption or deletion of *binA* increased biofilm formation in culture and led to increased binding of Congo red and calcofluor, which are indicators of cellulose production. Using random transposon mutagenesis, we determined that the phenotypes of the Δ*binA* mutant strain could be disrupted by insertions in genes in the bacterial cellulose biosynthesis cluster (*bcs*), suggesting that cellulose production is negatively regulated by BinA. Replacement of critical amino acids within the conserved EAL residues of the EAL domain disrupted BinA activity, and deletion of *binA* increased c-di-GMP levels in the cell. Together, these data support the hypotheses that BinA functions as a phosphodiesterase and that c-di-GMP activates cellulose biosynthesis. Finally, overexpression of the *syp* regulator *sypG* induced *binA* expression. Thus, this work reveals a mechanism by which *V. fischeri* inhibits cellulose-dependent biofilm formation and suggests that the production of two different polysaccharides may be coordinated through the action of the cellulose inhibitor BinA.

Bacterial biofilms play important roles in the environment and in interactions with eukaryotic hosts (for reviews, see references 17 and 32). Exopolysaccharides are a major component of biofilms (23), and many bacteria, including *Pseudomonas aeruginosa*, *Escherichia coli*, and *Salmonella* spp., have the ability to produce multiple different exopolysaccharides (23). For some of these bacteria, it has been demonstrated that the different polysaccharides contribute to biofilm formation in different settings. For example, several strains of *Salmonella* require an exopolysaccharide called O-antigen capsule to form biofilms on human gallstones but not to form biofilms on glass or plastic (11). Conversely, the exopolysaccharides cellulose and colanic acid are required for optimal biofilm formation by *Salmonella* spp. on glass and plastic but are not required for biofilm formation on human gallstones (11, 35). For some bacteria, a particular exopolysaccharide promotes attachment to one surface but seems to interfere with attachment to other surfaces. One example of this is *E. coli* O157:H7, which requires the exopolysaccharides poly-β-1,6-*N*-acetylglucosamine (PGA), colanic acid, and cellulose for optimal binding to alfalfa sprouts and plastic (27). In contrast, these polysaccharides are not required for binding by *E. coli* O157:H7 cells to human intestinal epithelial (Caco-2) cells and binding was actually enhanced in cellulose and PGA mutants, suggesting that while these polysaccharides are important for attachment to sprouts and plastic, they interfere with attachment to Caco-2 cells (27).

The marine bacterium *Vibrio fischeri* is known to produce at least two different exopolysaccharides that play roles in biofilm formation, the symbiosis polysaccharide (Syp) and cellulose (12, 59, 60). The Syp polysaccharide is critical for the formation of a biofilm-like aggregate at the initiation of symbiosis with the Hawaiian bobtail squid *Euprymna scolopes* (59). The natural condition(s) under which *V. fischeri* cells use cellulose in biofilm formation is not yet known. However, in other bacteria, cellulose contributes to the ability to attach to a variety of surfaces, including plant roots, other plant cells, mammalian epithelial cells, glass, and plastic (27, 28, 31, 35, 37, 45).

Although *V. fischeri* biofilm formation appears to be important for interaction with its symbiotic host and is likely also to be important in the marine environment outside the host, wild-type *V. fischeri* cells do not produce substantial biofilms under a variety of standard laboratory conditions. *V. fischeri*'s ability to form biofilms in culture, however, is greatly enhanced when the *syp* biosynthetic gene cluster (Fig. 1) is induced by overexpression of the response regulator SypG, the sensor kinase RscS, or the sensor kinase SypF (12, 59, 60).

In culture, *V. fischeri* also forms biofilms when cellulose production is induced. Cellulose contributes to the biofilms formed when either SypF or the putative response regulator VpsR is overexpressed (12). Additionally, overexpression of the diguanylate cyclase MifA induces biofilm formation and increases binding to two dyes that are cellulose indicators, Congo red and calcofluor (34, 37, 54).

The product of diguanylate cyclase activity, cyclic diguanylate (c-di-GMP), is an intracellular signaling molecule that plays an important role in regulating biofilm formation and motility (reviewed in references 10, 22, 38, 39, 48, and 56). C-di-GMP is produced from two GTP molecules by diguanylate cyclases with conserved GGDEF domains and is depleted

* Corresponding author. Mailing address: Department of Microbiology and Immunology, Loyola University Chicago, 2160 S. First Ave., Bldg. 105, Rm. 3860A, Maywood, IL 60153. Phone: (708) 216-0869. Fax: (708) 216-9574. E-mail: kvisick@lumc.edu.

▽ Published ahead of print on 8 January 2010.

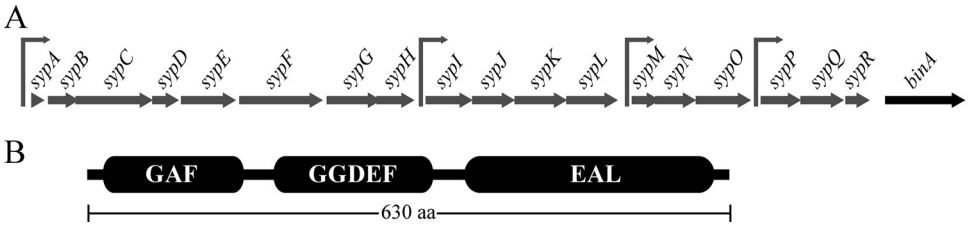

FIG. 1. The *binA* gene and its predicted protein. (A) The *binA* gene (VFA1038) is located downstream from and oriented in the same direction as the *syp* gene locus. Individual genes are indicated by block arrows, and the four known or putative promoters within the *syp* locus are indicated by line arrows. (B) The BinA protein (630 amino acids [aa]) is predicted to have three domains, GAF (~Q20 to L151), GGDEF (~H205 to A338), and EAL (~L374 to D611), as indicated. Only the EAL domain is well conserved.

by hydrolysis to linear pGpG by phosphodiesterases (PDEs) with EAL or HD-GYP domains. There is evidence of increased cellulose production in response to increased c-di-GMP levels in many bacteria (36, 41). In general, high levels of c-di-GMP enhance biofilm formation and low levels of c-di-GMP enhance motility (39).

Here we report that *V. fischeri* biofilm formation also increases in the absence of BinA, a GGDEF/EAL domain protein encoded by a gene that is adjacent to the *syp* cluster. We also report the discovery of genes involved in biofilm formation by *binA* mutants and the identification of amino acids that are critical to BinA activity. Finally, we suggest a mechanism by which the production of two different polysaccharides may be coordinated by BinA.

MATERIALS AND METHODS

Media. *E. coli* strains were grown in LB (13) or brain heart infusion broth (Difco, Detroit, MI). *V. fischeri* strains were grown in LBS (16, 46), SWT (60), or HMM (42) containing 0.3% Casamino Acids and 0.2% glucose (60). Congo red plates were made by the addition to LBS medium of 40 μg/ml Congo red and 15 μg/ml Coomassie blue before autoclaving. The following antibiotics were added to growth media where necessary, at the indicated final concentrations: chloramphenicol, 25 μg/ml in LB or 2.5 μg/ml in LBS; kanamycin, 50 μg/ml in LB or 100 μg/ml in LBS; tetracycline (Tc), 15 μg/ml in LB and either 5 μg/ml in LBS or 30 μg/ml in HMM; erythromycin, 150 μg/ml in brain heart infusion broth or 5 μg/ml in LBS; ampicillin, 100 μg/ml in LB. For solid media, agar was added to a final concentration of 1.5%. For motility experiments, TBS (1% tryptone, 342 mM NaCl, 0.225% agar) motility plates containing or lacking 35 mM $MgSO_4$ were used (33).

Strains and strain construction. The *V. fischeri* strains, plasmids, and primers utilized in this study are listed in Tables 1, 2, and 3, respectively. The parent *V. fischeri* strain used in this work was ES114, a strain isolated from *E. scolopes* (5). All derivatives were generated by conjugation. *E. coli* CC118 λ*pir* (19) containing pEVS104 was used to carry out triparental matings as previously described (52). *E. coli* strains Tam1 (Active Motif, Carlsbad, CA), GT115 (Invivogen, San Diego, CA), and Top10 (Invitrogen, Carlsbad, CA) were used for cloning and conjugations. Standard molecular biology techniques were used for all plasmid constructions. Restriction and modifying enzymes were purchased from New England Biolabs (Beverly, MA), Promega (Madison, WI), or Fermentas (Glen Burnie, MD). DNA oligonucleotides used for amplifying or modifying *binA* were obtained from MWG Biotech (High Point, NC). We constructed mutants by both vector integration (Campbell insertion mutagenesis [6]) and allelic replacement approaches as described previously (references 21 and 14, respectively). Mutants were verified by Southern analysis (14, 52). We complemented the *binA* mutant with *binA* located either in single copy in the chromosome at the Tn*7* site or by multicopy expression from a low-copy-number plasmid. For the former complementation, we utilized a tetraparental mating approach with strains carrying pEVS104 and pUX-BF13 as described previously (14).

To determine which genes contribute to biofilm formation by the Δ*binA* mutant strain, we performed a random transposon (Tn) mutagenesis of the Δ*binA* mutant strain using the mini-Tn*5* delivery vector pEVS170 (26). To determine the locations of specific Tn insertions, the Tn and flanking DNA were cloned using the origin of replication within the Tn as follows. Chromosomal DNA was isolated and digested with HhaI, which cuts outside of the Tn. Following ligation, *E. coli* cells were transformed and plasmid-containing cells were selected with erythromycin. The Tn insertion site was then determined by sequencing from the Tn end into the flanking chromosomal DNA.

We generated the *binA* EAL domain mutations (resulting in codon changes E402A and L404A) using the Change-IT kit (USB, Cleveland, OH) with template pCMA9, which contains the wild-type *binA* gene, and phosphorylated primers Phos-lacZ-up-rev and either 1038AAL or 1038EAA, respectively. The *binA* gene was sequenced from the resulting clones, pCMA25 and pCMA27, to verify the presence of only the desired mutation. To verify the stability of the mutant proteins, we generated FLAG epitope derivatives. To do so, we used primers 1038_SmaI_F and binA-FLAG-NcoI-R in PCRs with pCMA9, -25, and -27 as templates, followed by cloning to obtain pMSM17, -18, and -19.

Crystal violet-based biofilm assays. Crystal violet was used to assess biofilm formation as follows. Strains were grown statically in HMM (with Tc, as appropriate) at room temperature (22 to 23°C) overnight and then subcultured into 3 ml of fresh medium with a starting optical density (OD) of ~0.1 and grown statically for 72 h (in the absence of added antibiotics) or 96 h (when antibiotics were present). Biofilms at the air-liquid interface were visualized by the slow addition of 1 ml of 1% crystal violet and incubation for 30 min, followed by rinsing with deionized water. We quantified staining by adding 2 ml 100% ethanol, vortexing with glass beads, and then measuring the OD at 600 nm. Alternatively, strains were grown with shaking at 28°C (both overnight and following subculturing) for 48 h and then crystal violet was added as described above.

TABLE 1. *V. fischeri* strains used in this study

Strain	Genotype	Reference or source
ES114	Wild type	5
KV1817	*binA*::pESY10 (Cm^r)	60
KV2614	*att*Tn*7*::P_{binA}-*lacZ*	This study
KV3818	*binA*::pCMA8 (Erm^r)	This study
KV4131	Δ*binA*	This study
KV4196	Δ*binA* attTn*7*::*binA*	This study
KV4197	Δ*binA sypG*::pAIA4	This study
KV4203	Δ*binA sypC*::pBTG49	This study
KV4205	Δ*binA sypF*::pCLD28	This study
KV4206	Δ*binA sypH*::pESY38	This study
KV4207	Δ*binA sypJ*::pTMO90	This study
KV4209	Δ*binA sypL*::pTMB53	This study
KV4211	Δ*binA sypN*::pTMB54	This study
KV4212	Δ*binA sypO*::pTMB55	This study
KV4213	Δ*binA sypP*::pCMA11	This study
KV4601	Δ*binA sypR*::pTMB57	This study
KV4607	Δ*binA bcsA* (VFA0884)::Tn*5* (Erm^r)	This study
KV4608	Δ*binA bcsC* (VFA0881)::Tn*5* (Erm^r)	This study
KV4611	Δ*binA bcsZ* (VFA0882)::Tn*5* (Erm^r)	This study
KV4612	DUP [′*sypR-binA*′]::pEAH50 (*binA*$^+$) (duplication of the *sypR-binA* intergenic region and insertion of *lacZ*)	This study

TABLE 2. Plasmids used in this study

Plasmid	Characteristic(s)	Reference or source
pAIA4	pEVS122 containing ~500-bp *sypG* fragment	21
pBTG49	pESY20 containing ~400-bp *sypC* fragment	This study
pCLD28	pESY20 containing ~500-bp *sypF* fragment	This study
pCMA8	pESY20 containing ~300-bp *binA* fragment	This study
pCMA9	pKV69 containing ~1.8-kb *binA* sequences generated using PCR and primers 1038_SmaI_F and 1038_SmaI_R	This study
pCMA11	pESY20 containing ~400-bp *sypP* fragment	This study
pCMA13	pJET1.2 containing ~2-kb region downstream of *binA* generated by PCR with primers 1038_end_ApaIF and 1038_down_BamHIR	This study
pCMA14	pJET1.2 containing ~2-kb region upstream of *binA* generated by PCR with 1038_up_SpeIF and 1038_beg_ApaIR	This study
pCMA15	pJET1.2 containing ~2-kb sequences upstream and downstream of *binA*, generated from pCMA13 and pCMA14, for deletion of *binA*	This study
pCMA16	pEVS79 containing ~4-kb fragment from pCMA15	This study
pCMA17	pEVS107 containing ~2-kb fragment of *binA* plus upstream regulatory sequences, generated using PCR and primers VFA1037RTF and 1038_ApaI_R, for inserting *binA*$^+$ at the Tn*7* site	This study
pCMA25	pKV69 + *binA* (E402A mutation)	This study
pCMA27	pKV69 + *binA* (L404A mutation)	This study
pEAH73	pKV69 + *sypG*	20
pESY20	Mobilizable suicide vector R6Kγ oriV, oriTRP4, Erm^r	34
pESY38	pESY20 containing ~400-bp *sypH* fragment	This study
pEVS79	High-copy-number plasmid, Cm^r	47
pEVS104	Conjugal helper plasmid (*tra trb*), Kan^r	47
pEVS107	Mini-Tn*7*, R6Kγ oriV, oriTRP4, Kan^r	29
pEVS122	R6Kγ oriV, oriTRP4, *lacZ*α, Erm^r	15
pEVS170	Mini-Tn*5* delivery plasmid, Erm^r, Kan^r	26
pJet1.2	Ap^r Kan^r cloning vector	Fermentas
pKV69	Mobilizable low-copy-number vector, Tc^r, Cm^r	52
pKV276	pKV69 + *sypG*-D53E	20
pUX-BF13	Encodes Tn*7* transposase (*tnsABCDE*), Ap^r	3
pMSM17	pKV69 (ΔCm^r) + wild-type *binA* (+3′ FLAG epitope sequences)	This study
pMSM18	pKV69 (ΔCm^r) + *binA*-AAL (+3′ FLAG epitope sequences)	This study
pMSM19	pKV69 (ΔCm^r) + *binA*-EAA (+3′ FLAG epitope sequences)	This study
pTMB53	pEVS122 containing ~400-bp *sypL* fragment	60
pTMB54	pEVS122 containing ~400-bp *sypN* fragment	60
pTMB55	pEVS122 containing ~400-bp *sypO* fragment	60
pTMB57	pEVS122 containing ~400-bp *sypR* fragment	60
pTMO90	pEVS122 containing ~400-bp *sypJ* fragment	This study

Calcofluor staining. To further assess cellulose production, calcofluor was used. Strains were grown as described above for the crystal violet staining of static cultures. A concentrated stock of calcofluor (Sigma-Aldrich, St. Louis, MO) was made as a 0.2% solution in 1 M Tris, pH 9.0, which was autoclaved to dissolve the reagent. Biofilms were visualized by the addition of 1 ml of 0.2% calcofluor and incubation for 30 min, followed by rinsing with deionized water and exposure to UV light.

TABLE 3. Primers used in this study

Primer	Sequence
1038_end_ApaIF	GGGCCCGGTACCCCCTACTTTCACTT
1038_down_BamHIR	GGATCCTCAGCGCATCAGTAATACAT
1038_up_SpeIF	ACTAGTTACGCTGGTTTGCTTCTCGT
1038_beg_ApaIR	GGGCCCTTCAGGAATGTCGATGGCAG
1038_SmaI_F	CCCGGGAGAATAAACTGCTACTATCT
1038_SmaI_R	CCCGGGTAATGATATTTTAGAGTGCC
1038_ApaI_R	GGGCCCTAATGATATTTTAGAGTGCC
VFA1037RTF	CGTGAAATCCCTTATTTTAGTG
Phos_lacZ_up_rev	CCTGTGTGAAATTGTTATCCG
1038AAL	AAATGGATTGGTTGTGCCGCGCTATT ACGTTGG
1038EAA	GGATTGGTTGTGAAGCGGCATTACGT TGGAATCACCC
binA-FLAG-NcoI-R	AAAAAACCATGGTTATTTATCATCATC ATCTTTATAATCCACAAAGTGAAAG TAGGGGG

Migration assays. We monitored motility as described previously (33, 34). Briefly, we grew *V. fischeri* strains in TBS to an OD (600 nm) of ~0.3 and then spotted 10-μl aliquots onto TBS or TBS-Mg^{2+} motility plates. We measured the diameter of the outer migrating band hourly over the course of 4 to 5 h of incubation at 28°C (55).

Quantification of c-di-GMP levels. To measure intracellular c-di-GMP concentrations, *V. fischeri* strains were grown statically in HMM overnight at room temperature, subcultured (400 μl of overnight culture into 40 ml of HMM), and then grown statically at room temperature for 72 h. Each culture was mixed with 205 μl of cold 0.19% formamide and incubated on ice for 10 min. Samples were centrifuged at 6,000 rpm for 10 min at 4°C. The pellets were resuspended in 300 μl of cold 80% acetonitrile–0.1% formic acid, vortexed for 30 s, and incubated on ice for 10 min. The samples were then centrifuged at top speed in a microcentrifuge, and the supernatants were removed and stored at −80°C until liquid chromatography-tandem mass spectrometry was performed using a Waters Acquity Ultra Performance liquid chromatograph connected to a Quatro Premeir XE mass spectrometer (Micromass Technologies). A bridged ethyl hybrid C_{18} Ultra Performance liquid chromatography column (50 by 2.1 mm, 1.7 μm; Waters) was used for separation using solvents described previously (53). The amount of c-di-GMP in our samples was estimated using a standard curve generated from c-di-GMP standards with concentrations of 0.12 μM, 1.1 μM, and 3.3 μM. We then estimated the intracellular concentration of c-di-GMP using 3.93×10^{-16} liters as the volume of a single cell and the number of bacteria in each sample as determined by colony count from the original culture.

Western immunoblot analysis. The expression of mutant BinA proteins was verified using FLAG epitope-tagged versions of the proteins produced in the Δ*binA* mutant (KV4131) from plasmids pMSM17 (wild-type BinA), pMSM18

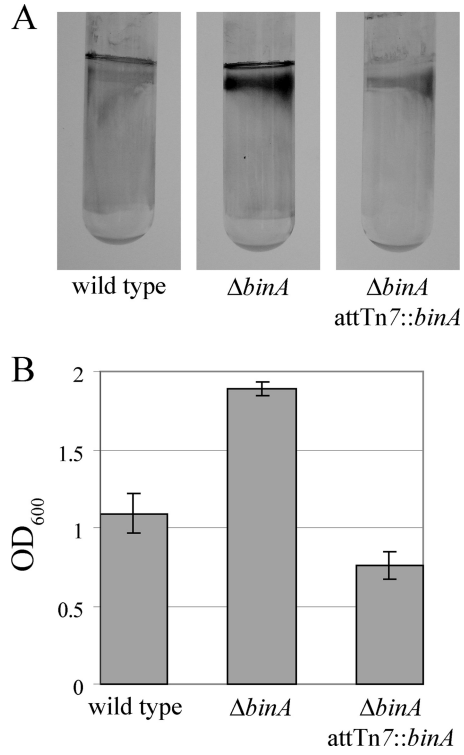

FIG. 2. Biofilm formation by the *binA* mutant. *V. fischeri* strains ES114 (wild type), KV4131 (Δ*binA*), and KV4196 (Δ*binA*/attTn*7*::*binA*$^+$) were grown statically for 72 h in HMM at room temperature and then analyzed for biofilm formation by crystal violet staining (A). Crystal violet staining was subsequently quantified from a triplicate set of tubes (B). Error bars represent ±1 standard deviation.

(BinA-AAL), and pMSM19 (BinA-EAA). Cells were grown with shaking in HMM containing Tc overnight. One-milliliter samples were pelleted, resuspended in loading buffer, and boiled, and a portion (15 μl) was loaded onto a 10% sodium dodecyl sulfate-polyacrylamide gel. After electrophoretic separation, proteins were transferred to a polyvinylidene fluoride membrane and probed with anti-FLAG antibodies (Sigma). Bands were visualized with a horseradish peroxidase-conjugated secondary antibody and ECL reagents.

β-Galactosidase assay. To assay transcription of the *binA* gene, we grew *V. fischeri* with shaking in HMM-Tc at 28°C overnight and then subcultured it into fresh HMM-Tc. The cultures were then grown with shaking at 28°C for 24 h. Samples were then assayed for β-galactosidase activity (30). The amount of protein in the extract was determined using the Lowry assay (25), and the β-galactosidase activity per milligram of protein in the sample was calculated.

RESULTS

BinA is a putative c-di-GMP phosphodiesterase that inhibits biofilm formation. Immediately adjacent to and downstream of the *syp* locus is a gene, VFA1038, that encodes a 630-amino-acid protein predicted to be involved in metabolism of the second messenger c-di-GMP (Fig. 1A). This putative protein contains both EAL and GGDEF domains (Fig. 1B), which are associated with c-di-GMP phosphodiesterase activity and diguanylate cyclase activity, respectively (reviewed in references 18 and 22). The EAL domain is highly conserved, with an EAL cd01948 E value of 4.00E-68. The GGDEF domain is much less conserved, with only 3 of 10 active-site residues conserved and a GGDEF cd01949 E value of 0.002. In addition, the I site, a sequence often located N terminal to the GGDEF motif that is involved in binding c-di-GMP (7, 8), was absent in VFA1038. Because the EAL domain is highly conserved and the GGDEF domain is poorly conserved, we hypothesized that the protein encoded by VFA1038 functions as a c-di-GMP phosphodiesterase.

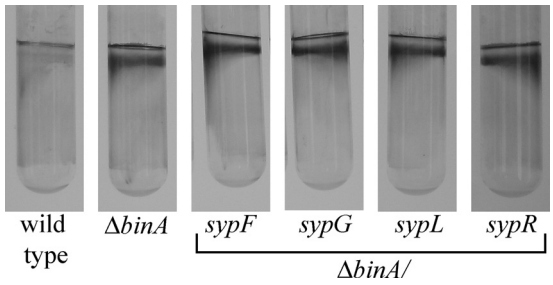

FIG. 3. Biofilm formation by *binA syp* double mutants. Mutants defective for both *binA* and various *syp* genes (KV4205, KV4197, KV4209, and KV4601) were analyzed for biofilm formation using the crystal violet assay following 72 h of static growth in HMM at room temperature. The assay was performed multiple times in triplicate using the double mutants indicated in the text; shown are a representative data set.

Since VFA1038 is predicted to encode a protein involved in the metabolism of c-di-GMP, an important regulator of biofilm formation, and VFA1038 is adjacent to the *syp* cluster, a locus known to be involved in biofilm formation, we asked whether VFA1038 plays a role in biofilm formation by *V. fischeri*. We found that two different VFA1038 insertional mutants exhibited increased biofilm formation, as observed through an increase in crystal violet staining of the test tube surface following growth of the mutants in static minimal medium (data not shown). Due to these results and others described below, we propose to name this gene *binA*, for biofilm inhibition.

To confirm that disruption of *binA* was responsible for the increased biofilm formation, rather than a polar effect or a secondary mutation, we constructed an in-frame *binA* deletion (Δ*binA*) mutant (KV4131). Like the insertional mutants, when grown statically, the Δ*binA* mutant exhibited enhanced biofilm formation, relative to that of wild-type *V. fischeri*, as measured by the crystal violet assay (Fig. 2). Complementation of the Δ*binA* mutant by the insertion of a single copy of *binA* at the Tn*7* site (KV4196) in the chromosome (Fig. 2) restored biofilm formation to low, wild-type levels. These results confirmed that loss of *binA* is responsible for enhanced biofilm formation in the mutants and indicated that BinA is indeed an inhibitor of biofilm formation.

The *syp* polysaccharide is not a major component of biofilms produced by the *binA* mutants. Because of the proximity of *binA* to the *syp* cluster, we hypothesized that biofilm formation by the *binA* mutants depends on the *syp* locus. To test this possibility, we constructed a series of double mutants and assayed static biofilm formation. The double mutants were obtained with the Δ*binA* mutant strain by insertional mutagenesis of the *sypC*, *sypF*, *sypG*, *sypH*, *sypJ*, *sypL*, *sypN*, *sypO*, *sypP*, and *sypR* genes (Table 1). All of the double mutants produced biofilms that were indistinguishable from that of the Δ*binA* mutant, as evaluated by crystal violet staining (Fig. 3 and data not shown). These data indicate that the *syp* polysaccharide is

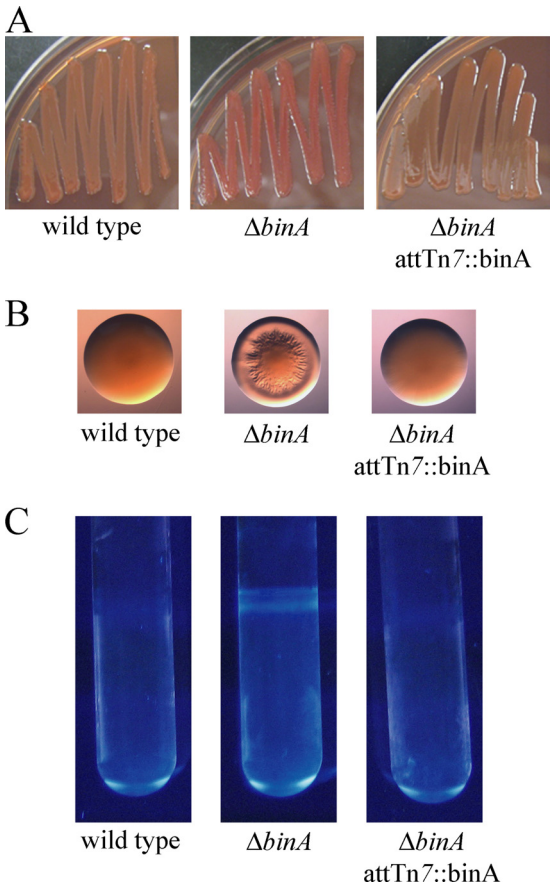

FIG. 4. BinA inhibits Congo red binding, wrinkled-colony formation, and Calcofluor binding. Congo red binding (A) and colony morphology (B) were assessed after 48 h of growth at room temperature on Congo red plates. (C) Calcofluor staining was assayed after 72 h of static growth in HMM at room temperature. The strains are the same as those indicated in Fig. 2.

not a major part of the biofilm formed by the Δ*binA* mutant. Thus, the activity of BinA must be directed at another target.

Both Congo red and calcofluor binding are enhanced in *binA* mutants. Because the activity of BinA in inhibiting biofilm formation was not directed at the *syp* locus, we sought to understand its role by using assays commonly found in the biofilm literature. In particular, increased biofilm formation is often associated with increased binding of the dyes Congo red and calcofluor. The binding of Congo red correlates, in many cases, with the production of cellulose and/or curli (e.g., see references 9 and 50). Calcofluor binds β-1,3 or β-1,4 linkages between D-glucopyranosyl units, such as those in cellulose (37, 54). When plated on Congo red plates, both insertion and deletion mutants of *binA* formed colonies that were darker red than those of wild-type *V. fischeri* (Fig. 4A and data not shown). In addition, the *binA* mutants formed wrinkled colonies, while those of the wild type were smooth (Fig. 4B and data not shown). Interestingly, this wrinkling phenotype did not occur when Congo red was absent from the base medium (LBS), indicating that Congo red actually stimulates wrinkled-colony formation by the *binA* mutant. Regardless of the cause, both the color and wrinkled-colony phenotypes were complemented by the addition of *binA*, either in single copy in the chromosome or on a plasmid (Fig. 4A and B and data not shown).

We also assayed calcofluor binding on plates and in liquid culture. With both approaches, the *binA* mutants exhibited increased calcofluor binding compared to wild-type *V. fischeri* (Fig. 4C and data not shown). The increased ability to bind calcofluor could be complemented by the introduction of a wild-type copy of *binA* (Fig. 4C). Together, these data indicate that BinA inhibits the production of a sugar with β-1,3 or β-1,4 D-glucose linkages, possibly cellulose.

Cellulose biosynthetic genes are required for biofilm formation by the Δ*binA* mutant strains. To identify the genes that contribute to biofilm formation by the *binA* mutants, we performed a random Tn mutagenesis of the Δ*binA* mutant. Because the Δ*binA* mutant produces colonies that are darker red than wild-type *V. fischeri* on Congo red plates (Fig. 4A), we screened for Tn mutants that had decreased colony color on Congo red plates. In a small screening of about 3,000 colonies, we identified eight mutants with either a white or a light red color (Fig. 5A and data not shown). Each of these colonies also failed to form wrinkled colonies (Fig. 5B and data not shown).

Southern analysis indicated that seven of the eight strains contained a clean single Tn insertion (data not shown). Among the seven strains with a single insertion, there were five different banding patterns, indicating five distinct Tn insertions (data not shown). We cloned and sequenced the Tn and flanking DNA from the five distinct insertion mutants. Each of the Tns in these strains had been inserted into the bacterial cellulose synthesis (*bcs*) locus (Fig. 5F and data not shown).

We chose to further characterize the *bcsA*, *bcsZ*, and *bcsC* mutants indicated in Fig. 5F by examining the ability of these mutants to form biofilms. Each of the Δ*binA bcs* mutants exhibited reduced crystal violet staining compared to that of the Δ*binA* mutant parent (Fig. 5C and D and data not shown); however, it was not reduced to the level of the wild type (Fig. 5C and D). These data suggested that BinA inhibits another component of biofilm formation in addition to cellulose or that some cellulose production was still possible in these double mutants. In support of the former hypothesis, disruption of the *bcs* operon eliminated all of the calcofluor staining observed with the *binA* mutant (Fig. 5E). Together, these data indicate that BinA is a negative regulator of cellulose production and that cellulose is a major contributor to biofilm formation by the Δ*binA* mutant.

Overexpression of BinA enhances motility. In general, c-di-GMP promotes biofilm formation and thus, loss of a c-di-GMP phosphodiesterase is often correlated with an increase in biofilm formation (18, 22, 39). Indeed, our data to date are consistent with the predicted role of BinA as a c-di-GMP phosphodiesterase. Alterations in c-di-GMP levels are also correlated with altered motility: increased c-di-GMP levels often correlate with decreased motility and decreased c-di-GMP levels with increased motility. Therefore, to determine if BinA plays a role in regulating motility in *V. fischeri*, we tested the ability of the *binA* deletion mutant (KV4131) to migrate on motility plates. Migration by the *binA* deletion mutant was indistinguishable from that of wild-type *V. fischeri* ES114 (Fig. 6A). That deletion of *binA* increases biofilm formation but has no effect on motility indicates some specificity in the role of

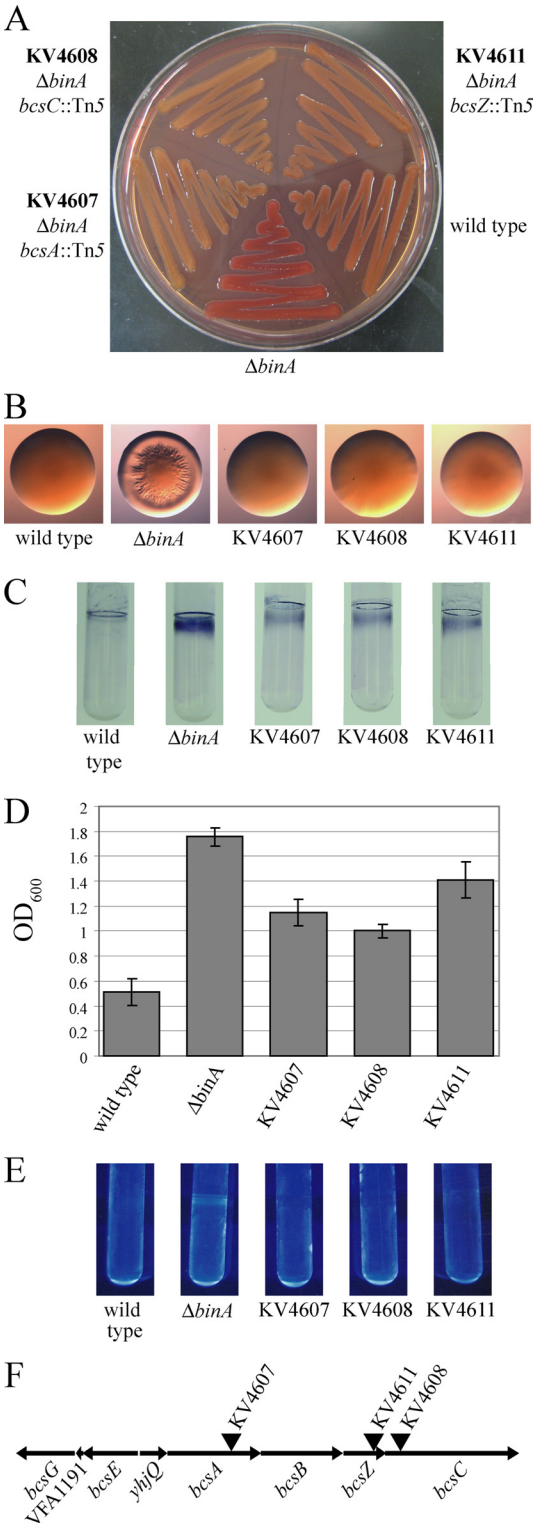

FIG. 5. Role of the cellulose operon in biofilm formation. Congo red binding (A) and colony morphology (B) were assessed after 48 h of growth at room temperature on Congo red plates. Crystal violet staining was visualized (C) and quantified (D) after 72 h of static growth in HMM at room temperature. Error bars represent ±1 standard deviation from a triplicate set of tubes. (E) Calcofluor staining was assessed after 72 h of static growth in HMM at room temperature. (F) The *bcs* locus (VFA0887 to VFA0881) with the locations of the Tn insertions indicated by inverted triangles.

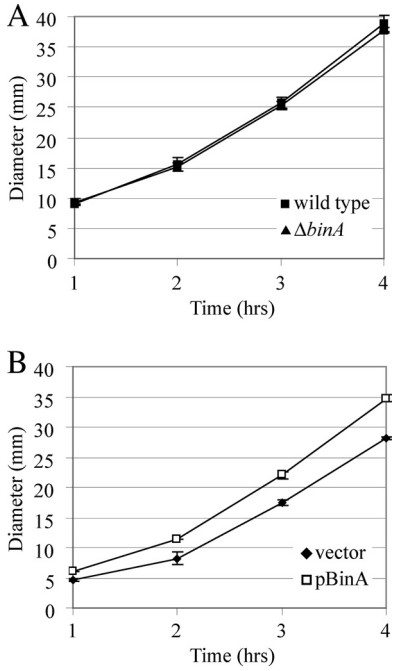

FIG. 6. Motility of *binA* mutant and overexpression strains. The motility of *V. fischeri* strains was monitored by measuring the diameter of the outer chemotaxis ring formed in TBS-Mg^{2+} soft agar over time. (A) Motility of the Δ*binA* mutant (KV4131) and its wild-type parent ES114. (B) Motility of wild-type strain ES114 carrying the control vector pKV69 or the *binA* overexpression plasmid pCMA9 (pBinA). Error bars represent ±1 standard deviation.

BinA. However, when BinA was overexpressed from a multicopy plasmid, *V. fischeri* exhibited increased migration compared to *V. fischeri* with a vector control (Fig. 6B). Thus, based on other examples in the literature (22), we propose that overexpression of BinA likely extends its predicted phosphodiesterase activity beyond its natural role, decreasing c-di-GMP levels in such a way that motility is enhanced.

BinA activity depends on the EAL domain. Thus, far, the data from bioinformatics, biofilm assays, and motility experiments are consistent with the hypothesis that BinA functions as a c-di-GMP phosphodiesterase. Typically, amino acid residues E and L of the EAL domain are required for c-di-GMP phosphodiesterase activity (4, 24, 49). Therefore, we asked if the activity of BinA indeed requires an intact EAL domain. To address this question, we constructed plasmids that overexpressed mutant alleles of *binA*. Specifically, we altered codons within the EAL domain to convert EAL to EAA (E402A) and AAL (L404A) to obtain BinA(EAA) and BinA(AAL), respectively.

To determine if these mutations altered BinA activity, we tested the ability of BinA(EAA) and BinA(AAL) to reduce Congo red binding by the Δ*binA* mutant. Overproduction of wild-type BinA in the Δ*binA* mutant reduced Congo red binding to levels similar to that of the wild-type control (Fig. 7A). In contrast, overproduction of BinA-EAA or BinA-AAL failed to reduce Congo red binding (Fig. 7A), suggesting that these proteins were inactive. We also assayed the activity of BinA(EAA) and BinA(AAL) during growth in culture. Specifically, we analyzed biofilms that formed during growth with shaking, as we found that these conditions resulted in impres-

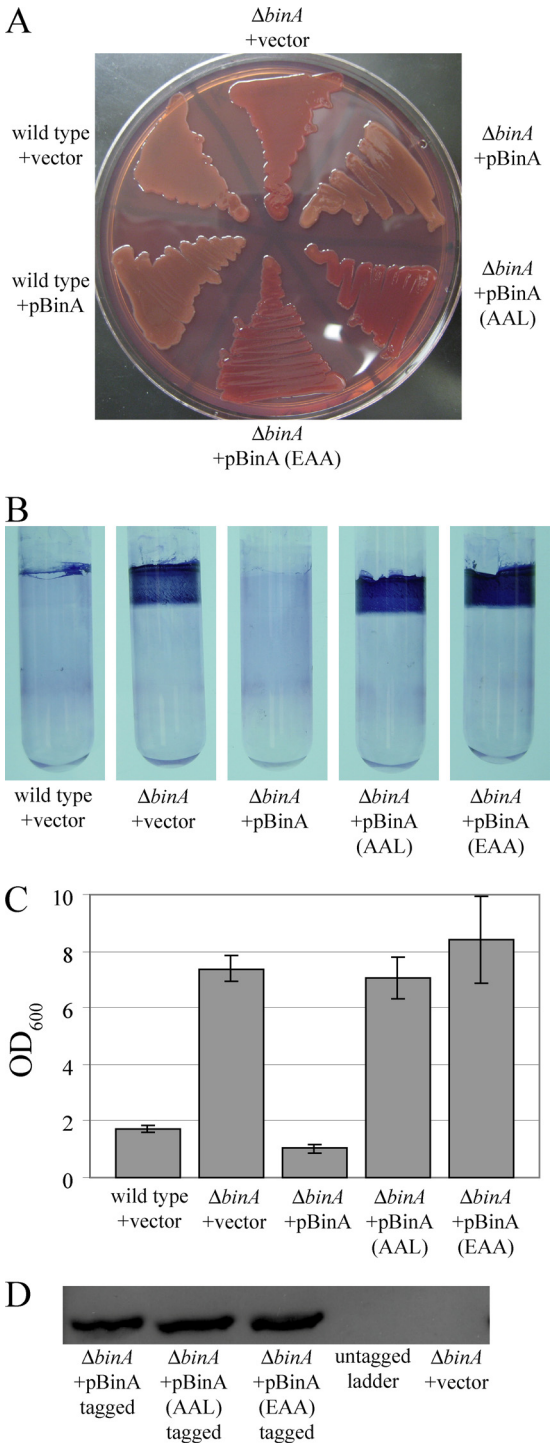

FIG. 7. Role of the EAL motif in BinA activity. The effect on BinA activity of mutating the EAL motif to AAL or EAA was monitored using Congo red binding (A) and crystal violet staining (B) of cultures grown in HMM-Tc under shaking conditions for 48 h at 28°C. Crystal violet staining was subsequently quantified from a triplicate set of tubes (C); error bars represent ±1 standard deviation. (D) Western immunoblot analysis of tagged versions of the BinA protein. BinA-expressing plasmids pMSM17, -18, and -19 were introduced into *binA* mutant KV4131. Whole-cell extracts were processed as described in Materials and Methods.

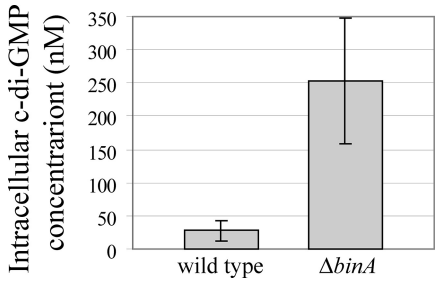

FIG. 8. Intracellular c-di-GMP concentrations. Each bar represents the average intracellular c-di-GMP concentration of three samples. The sample concentrations ranged from 0 nM to 53.4 nM for wild-type *V. fischeri* and from 86.7 nM to 413 nM for the Δ*binA* mutant (KV4131). The error bars represent ±1 standard error of the mean.

sive biofilm formation by the vector-containing Δ*binA* mutant that was fully complemented by overexpression of wild-type BinA (Fig. 7B and C). Under these conditions, the activity of BinA(EAA) and BinA(AAL) was undetectable (Fig. 7B and C). Independent experiments using tagged versions of the three proteins demonstrated that under these shaking growth conditions, the proteins were stably produced (Fig. 7D). Thus, in both Congo red and crystal violet assays, activity of BinA depends on the EAL residues, providing evidence that BinA functions as a c-di-GMP phosphodiesterase.

Loss of *binA* increases c-di-GMP levels. Because together our data suggested that BinA is a c-di-GMP phosphodiesterase, we hypothesized that the levels of c-di-GMP would increase in a *binA* mutant. To test this hypothesis, we measured c-di-GMP concentrations in wild-type and Δ*binA* mutant cells using high-pressure liquid chromatography–tandem mass spectrometry. We found the average c-di-GMP concentration to be significantly higher in Δ*binA* mutant cells (approximately 253 nM) than in wild-type cells (approximately 27.4 nM) (Fig. 8). These data verify the assignment of BinA as a c-di-GMP phosphodiesterase.

Connection to the *syp* locus. Given the location and orientation of the *binA* gene (Fig. 1A), we wondered whether expression of *binA* could be influenced by transcriptional activity at the nearby *syp* locus. In particular, overexpression of the response regulator SypG is known or predicted to induce transcription at four promoters (upstream of *sypA*, *sypI*, *sypM*, and *sypP*) (60). SypG is predicted to be a σ^{54}-dependent activator, and these four *syp* promoters are known or predicted to be σ^{54} dependent (60) (Fig. 1A). In contrast, there are no predicted σ^{54} promoter sequences in the 220-bp intergenic region between *sypR* and *binA*. To test whether *binA* transcription is influenced by SypG overexpression, we first assayed the reporter activity of a strain with the *sypR-binA* intergenic region fused to *lacZ* at a site distal to the *syp* locus (the Tn*7* site) and found no significant induction by SypG (data not shown). These data are consistent with the lack of predicted σ^{54}-dependent promoter sequences in that region. Next, we assayed reporter activity from a strain that contained the reporter at the *binA* locus; this strain contains a wild-type copy of *binA* at its native position (Fig. 9A). We found that overexpression of *sypG* and the increased-activity allele *sypG** induced *binA* expression three- and sevenfold, respectively (Fig. 9B). These data suggest that there may be some readthrough from tran-

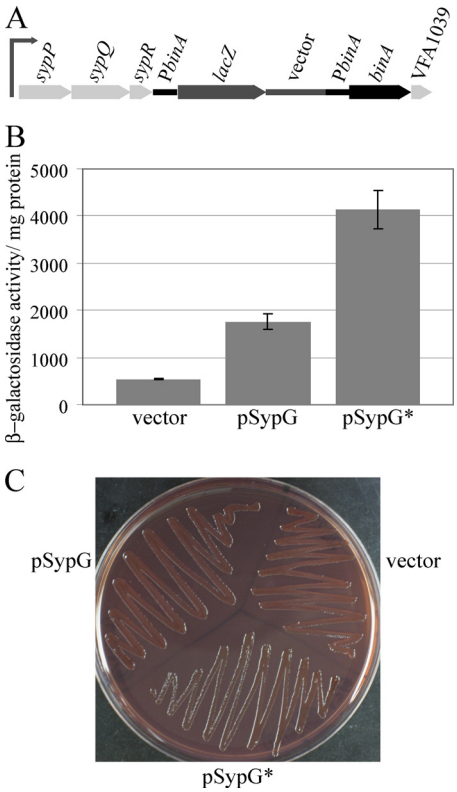

FIG. 9. Impact of the *syp* regulator SypG on *binA* expression and activity. (A) Diagram of the chromosomal region of the reporter strain KV4612, which contains pEAH50 inserted by homologous recombination with the *sypR-binA* intergenic region; this region is labeled P_{binA} for simplicity, although it is not known whether a promoter exists there. The 3′ end of *sypR*, the *sypR-binA* intergenic region, and the 5′ end of the *binA* gene are duplicated in the strain; one wild-type copy of *binA* is present. The drawing is not to scale. (B) β-Galactosidase activities of the *binA* mutant reporter strain KV4612 carrying the control plasmid pKV69 (vector), SypG overexpression plasmid pEAH73 (SypG), and SypG-D53E increased-activity allele plasmid pKV276 (SypG*). (C) Congo red binding by *sypN* mutant strain KV1838 carrying the indicated plasmids after 48 h of growth on a Congo red plate at room temperature.

scription of the *syp* locus, presumably the *sypPQR* operon (Fig. 1A and 9A). In support of a possible functional connection, we found that overproduction of SypG* caused a decrease in cellulose biosynthesis, as measured by dye binding on Congo red plates, independent of *syp* function (assayed in a *sypN* mutant) (Fig. 9C). However, overproduction of SypG* also caused a visible decrease in Congo red binding in a *binA sypN* mutant (data not shown), indicating that SypG may also have a BinA-independent effect on cellulose biosynthesis. These experiments further suggest coordination between *syp* and cellulose but indicate that additional factors are involved.

DISCUSSION

In this study, we investigated the function of the putative c-di-GMP phosphodiesterase BinA. One of the key roles for enzymes involved in c-di-GMP metabolism is to control biofilm formation. Indeed, we found that disruption of *binA* caused an increase in biofilm formation, as assayed by crystal violet staining. This increase in biofilm formation was due to increased cellulose production, as evident both from phenotypic assays of the *binA* mutant (Congo red and calcofluor assays) and from genetic studies in which disruption of the cellulose locus (*bcs*) restored wild-type phenotypes to the *binA* mutant. Thus, it appears that under standard laboratory conditions, *V. fischeri* turns off cellulose production using BinA.

Several lines of evidence support the assignment of BinA as a c-di-GMP phosphodiesterase. First, bioinformatics showed a strong conservation of the EAL domain, including key residues in the signature motif. Second, phosphodiesterase activity is often associated with decreased biofilm formation and increased motility, and this is true for BinA: disruption of *binA* increased biofilm formation, and its overexpression increased motility (Fig. 2 and 6). Third, replacement of critical amino acids within the EAL signature motif disrupted BinA function (Fig. 7). Fourth, our measurements using liquid chromatography-tandem mass spectrometry indicated that c-di-GMP concentrations are significantly higher in Δ*binA* mutant cells than in wild-type cells (Fig. 8).

There is precedence for "dual-domain" proteins (containing both GGDEF and EAL domains) to exhibit only diguanylate cyclase or only phosphodiesterase activity; generally, the activity corresponds to the well-conserved domain. For example, the *Pseudomonas aeruginosa* GGDEF/EAL domain protein BifA functions as a phosphodiesterase (24). Since our data are consistent with BinA functioning as a phosphodiesterase and because the putative GGDEF domain of BinA is poorly conserved, containing only 3 of 10 key active-site residues, BinA may be a dual-domain protein with only phosphodiesterase activity. Furthermore, the I site was absent, suggesting that the GGDEF domain likely does not even function in c-di-GMP binding. There are also examples in which the GGDEF or EAL domain has evolved away from enzymatic activity yet retains a function. One pertinent example is *E. coli* YcgF, an EAL domain protein that lacks phosphodiesterase activity yet appears to participate in protein-protein interactions (51). In our experiments, we observed that the BinA(AAL) and BinA(EAA) proteins retained residual activity during static growth in culture, as assayed by crystal violet staining (data not shown). Thus, it is possible that a non-enzymatically active BinA protein participates in protein-protein interactions. The influences of the GGDEF domain and also the putative GAF domain, which in other bacteria is involved in sensing environmental signals (2), on the activity of the BinA protein remain to be determined.

V. fischeri encodes 48 proteins with GGDEF and/or EAL domains. Only three other such *V. fischeri* proteins have been characterized: VFA1012, a GGDEF and REC domain protein for which no phenotype has yet been uncovered (21), and the diguanylate cyclases MifA and MifB, which are involved in the control of motility in the absence of magnesium (34). Loss of *binA* did not impact motility, regardless of whether magnesium was present or not (Fig. 6A and data not shown). These data suggest some level of specificity to the role of BinA. Although, in general, the regulation of c-di-GMP levels and localization in bacteria is poorly understood, it seems clear that there can be localized effects, based on the actions of diguanylate cyclases, phosphodiesterases, and proteins that bind c-di-GMP. The diguanylate cyclase(s) that promotes cellulose production in *V.*

fischeri is as yet unknown. However, the c-di-GMP binding protein is likely to be BcsA (Fig. 5F), by analogy with *Gluconoacetobacter xylinus*. It was in *G. xylinus* that c-di-GMP was initially uncovered and shown to be an allosteric effector of cellulose synthetic activity (40). BcsA is now known to contain a PilZ domain, one of several c-di-GMP binding domains (1, 44). *V. fischeri* has four genes predicted to encode PilZ domain proteins, *bcsA*, VF0527, VF0556, and VF1838 (1). Of these, disruption of only *bcsA* impacted biofilm formation by the *binA* mutant (Fig. 5 and data not shown). Because PilZ is not the only class of c-di-GMP binding proteins, it is possible that another, as yet unidentified, c-di-GMP binding protein could be impacted by BinA activity, such as a transcriptional regulator of *bcs* transcription.

While investigating the role of the cellulose locus, we found that mutations in *bcs* did not completely disrupt biofilm formation, as monitored by crystal violet staining (Fig. 5C). These data suggested that BinA negatively controls an additional biofilm component. One possibility could be expression of pili, which are a component of biofilm formation in many bacteria. *V. fischeri* encodes upwards of 10 pilus loci (43). However, our preliminary transmission electron microscopy experiments failed to uncover any evidence that pili were upregulated in the *binA* mutant (unpublished data). *V. fischeri* also has additional loci potentially involved in polysaccharide biosynthesis. One of these is a locus with some similarity to the *Vibrio* polysaccharide (*vps*-II) locus of *V. cholerae* (57, 58). Disruption of two genes within the *vps*-II-like locus of *V. fischeri* did not noticeably alter crystal violet staining of the *binA* mutant (unpublished data). However, it is likely that the construction of a triple mutant (*binA bcs vps*-II) would be necessary to eliminate a possible role for *vps*-II in the residual biofilm formation of the double mutant. It is worth noting here that in the course of experiments designed to understand the residual biofilm formation of this strain, we observed some influence of antibiotic addition on our biofilm phenotypes. Specifically, we found that Tc-based selection for the vector control in the *binA bcsA* double mutant eliminated the residual biofilm observed in static cultures (data not shown). In contrast, Tc-based selection for the vector control in the Δ*binA* mutant promoted the dramatic biofilm formation observed following growth of the culture with shaking (Fig. 7B); in the absence of Tc, the parent Δ*binA* mutant strain failed to form biofilms under the same conditions (unpublished data). Although these observations do not change any of our conclusions, they suggest a response to antibiotic treatment that needs to be characterized and point to the need for appropriate comparison sets.

We initiated our studies of *binA* because of the location and orientation of this gene with respect to the *syp* locus (Fig. 1A), hypothesizing that BinA would be involved in the control of Syp polysaccharide biosynthesis. Although this was not the case, other connections remained possible. Indeed, we found that the *syp* regulator and putative σ^{54}-dependent activator SypG could induce *binA* transcription. The induction likely occurred via readthrough from the adjacent *sypP* promoter (Fig. 1A and 9A), because the *binA* promoter region does not contain a putative σ^{54}-dependent promoter, and the *binA* promoter region fused to the *lacZ* reporter located at a site distal to the *binA* gene was not activated by SypG overexpression. These data suggest that *syp* cluster activation could indirectly increase the level of BinA protein, thus turning down cellulose production. Thus, potentially BinA coordinates an increase in *syp* polysaccharide production with a decrease in cellulose production. The timing and pattern of *syp* expression during colonization have not yet been determined. However, it is known that *syp* is required for symbiosis and at least one of the *syp* genes is required for the formation of a biofilm-like aggregate at the initiation of symbiosis (59, 60), suggesting that *syp* might be induced early in colonization. Further tests of this model will depend upon determining the conditions under which the two loci are naturally expressed, but BinA could potentially play a role in the transition from a cellulose-containing biofilm, possibly important in the marine environment, to a Syp-containing biofilm at the initiation of symbiosis. Disruption of the *binA* gene does not interfere with symbiosis (60); thus, either cellulose does not interfere with the function of the Syp polysaccharide or BinA is a redundant cellulose regulator under those environmental conditions.

In summary, in this work we have uncovered a mechanism by which *V. fischeri* prevents biofilm formation. This control mechanism is significant because it suggests that under certain environmental conditions it is disadvantageous to produce cellulose. It will be of interest to determine when cellulose production is induced and becomes important. Because of the medical importance of biofilm formation—and the accumulating evidence that environmental biofilms can provide a reservoir for infectious organisms—understanding how different organisms modulate different types of biofilms is key for the effective design of new antimicrobial treatments.

ACKNOWLEDGMENTS

We are grateful to Chris Waters for his assistance with high-pressure liquid chromatography–tandem mass spectrometry experiments designed to measure c-di-GMP levels in *V. fischeri*, Michael Misale for construction of tagged BinA mutants and Western blot analysis, and Satoshi Shibata for his assistance with electron microscopy. We also thank past and present members of the Wolfe and Visick labs for their input and critical reading of the manuscript and past and present members of the Visick lab for plasmid constructions.

This work was supported by NIH R01 grant GM59690 to K.L.V.

REFERENCES

1. **Amikam, D., and M. Y. Galperin.** 2006. PilZ domain is part of the bacterial c-di-GMP binding protein. Bioinformatics **22:**3–6.
2. **Aravind, L., and C. P. Ponting.** 1997. The GAF domain: an evolutionary link between diverse phototransducing proteins. Trends Biochem. Sci. **22:**458–459.
3. **Bao, Y., D. P. Lies, H. Fu, and G. P. Roberts.** 1991. An improved Tn*7*-based system for the single-copy insertion of cloned genes into chromosomes of Gram-negative bacteria. Gene **109:**167–168.
4. **Bobrov, A. G., O. Kirillina, and R. D. Perry.** 2005. The phosphodiesterase activity of the HmsP EAL domain is required for negative regulation of biofilm formation in *Yersinia pestis*. FEMS Microbiol. Lett. **247:**123–130.
5. **Boettcher, K. J., and E. G. Ruby.** 1990. Depressed light emission by symbiotic *Vibrio fischeri* of the sepiolid squid *Euprymna scolopes*. J. Bacteriol. **172:** 3701–3706.
6. **Campbell, A.** 1962. Episomes. Adv. Genet. **11:**101–145.
7. **Chan, C., R. Paul, D. Samoray, N. C. Amiot, B. Giese, U. Jenal, and T. Schirmer.** 2004. Structural basis of activity and allosteric control of diguanylate cyclase. Proc. Natl. Acad. Sci. U. S. A. **101:**17084–17089.
8. **Christen, B., M. Christen, R. Paul, F. Schmid, M. Folcher, P. Jenoe, M. Meuwly, and U. Jenal.** 2006. Allosteric control of cyclic di-GMP signaling. J. Biol. Chem. **281:**32015–32024.
9. **Collinson, S. K., P. C. Doig, J. L. Doran, S. Clouthier, T. J. Trust, and W. W. Kay.** 1993. Thin, aggregative fimbriae mediate binding of *Salmonella enteritidis* to fibronectin. J. Bacteriol. **175:**12–18.
10. **Cotter, P. A., and S. Stibitz.** 2007. c-di-GMP-mediated regulation of virulence and biofilm formation. Curr. Opin. Microbiol. **10:**17–23.

11. **Crawford, R. W., D. L. Gibson, W. W. Kay, and J. S. Gunn.** 2008. Identification of a bile-induced exopolysaccharide required for *Salmonella* biofilm formation on gallstone surfaces. Infect. Immun. **76:**5341–5349.
12. **Darnell, C. L., E. A. Hussa, and K. L. Visick.** 2008. The putative hybrid sensor kinase SypF coordinates biofilm formation in *Vibrio fischeri* by acting upstream of two response regulators, SypG and VpsR. J. Bacteriol. **190:** 4941–4950.
13. **Davis, R. W., D. Botstein, and J. R. Roth.** 1980. Advanced bacterial genetics. Cold Spring Harbor Laboratory, Cold Spring Harbor, NY.
14. **DeLoney, C. R., T. M. Bartley, and K. L. Visick.** 2002. Role for phosphoglucomutase in *Vibrio fischeri-Euprymna scolopes* symbiosis. J. Bacteriol. **184:**5121–5129.
15. **Dunn, A. K., M. O. Martin, and E. Stabb.** 2005. Characterization of pES213, a small mobilizable plasmid from *Vibrio fischeri*. Plasmid **54:**114–134.
16. **Graf, J., P. V. Dunlap, and E. G. Ruby.** 1994. Effect of transposon-induced motility mutations on colonization of the host light organ by *Vibrio fischeri*. J. Bacteriol. **176:**6986–6991.
17. **Hall-Stoodley, L., and P. Stoodley.** 2009. Evolving concepts in biofilm infections. Cell. Microbiol. **11:**1034–1043.
18. **Hengge, R.** 2009. Principles of c-di-GMP signalling in bacteria. Nat. Rev. Microbiol. **7:**263–273.
19. **Herrero, M., V. de Lorenzo, and K. N. Timmis.** 1990. Transposon vectors containing non-antibiotic resistance selection markers for cloning and stable chromosomal insertion of foreign genes in gram-negative bacteria. J. Bacteriol. **172:**6557–6567.
20. **Hussa, E. A., C. L. Darnell, and K. L. Visick.** 2008. RscS functions upstream of SypG to control the *syp* locus and biofilm formation in *Vibrio fischeri*. J. Bacteriol. **190:**4576–4583.
21. **Hussa, E. A., T. M. O'Shea, C. L. Darnell, E. G. Ruby, and K. L. Visick.** 2007. Two-component response regulators of *Vibrio fischeri*: identification, mutagenesis and characterization. J. Bacteriol. **189:**5825–5838.
22. **Jenal, U., and J. Malone.** 2006. Mechanisms of cyclic-di-GMP signaling in bacteria. Annu. Rev. Genet. **40:**385–407.
23. **Karatan, E., and P. Watnick.** 2009. Signals, regulatory networks, and materials that build and break bacterial biofilms. Microbiol. Mol. Biol. Rev. **73:**310–347.
24. **Kuchma, S. L., K. M. Brothers, J. H. Merritt, N. T. Liberati, F. M. Ausubel, and G. A. O'Toole.** 2007. BifA, a cyclic-di-GMP phosphodiesterase, inversely regulates biofilm formation and swarming motility by *Pseudomonas aeruginosa* PA14. J. Bacteriol. **189:**8165–8178.
25. **Lowry, O. H., N. J. Rosebrough, A. L. Farr, and R. J. Randall.** 1951. Protein measurement with the Folin phenol reagent. J. Biol. Chem. **193:**265–275.
26. **Lyell, N. L., A. K. Dunn, J. L. Bose, S. L. Vescovi, and E. V. Stabb.** 2008. Effective mutagenesis of *Vibrio fischeri* using hyperactive mini-Tn*5* derivatives. Appl. Environ. Microbiol. **74:**7059–7063.
27. **Matthysse, A. G., R. Deora, M. Mishra, and A. G. Torres.** 2008. Polysaccharides cellulose, poly-β-1,6-*N*-acetyl-D-glucosamine, and colanic acid are required for optimal binding of *Escherichia coli* O157:H7 strains to alfalfa sprouts and K-12 strains to plastic but not for binding to epithelial cells. Appl. Environ. Microbiol. **74:**2384–2390.
28. **Matthysse, A. G., and S. McMahan.** 1998. Root colonization by *Agrobacterium tumefaciens* is reduced in *cel*, *attB*, *attD*, and *attR* mutants. Appl. Environ. Microbiol. **64:**2341–2345.
29. **McCann, J., E. V. Stabb, D. S. Millikan, and E. G. Ruby.** 2003. Population dynamics of *Vibrio fischeri* during infection of *Euprymna scolopes*. Appl. Environ. Microbiol. **69:**5928–5934.
30. **Miller, J. H.** 1972. Experiments in molecular genetics. Cold Spring Harbor Laboratory, Cold Spring Harbor, NY.
31. **Monteiro, C., I. Saxena, X. Wang, A. Kader, W. Bokranz, R. Simm, D. Nobles, M. Chromek, A. Brauner, R. M. Brown, Jr., and U. Römling.** 2009. Characterization of cellulose production in *Escherichia coli* Nissle 1917 and its biological consequences. Environ. Microbiol. **11:**1105–1116.
32. **Moons, P., C. W. Michiels, and A. Aertsen.** 2009. Bacterial interactions in biofilms. Crit. Rev. Microbiol. **35:**157–168.
33. **O'Shea, T. M., C. R. DeLoney-Marino, S. Shibata, S.-I. Aizawa, A. J. Wolfe, and K. L. Visick.** 2005. Magnesium promotes flagellation of *Vibrio fischeri*. J. Bacteriol. **187:**2058–2065.
34. **O'Shea, T. M., A. H. Klein, K. Geszvain, A. J. Wolfe, and K. L. Visick.** 2006. Diguanylate cyclases control magnesium-dependent motility of *Vibrio fischeri*. J. Bacteriol. **188:**8196–8205.
35. **Prouty, A. M., and J. S. Gunn.** 2003. Comparative analysis of *Salmonella enterica* serovar Typhimurium biofilm formation on gallstones and on glass. Infect. Immun. **71:**7154–7158.
36. **Römling, U.** 2005. Characterization of the rdar morphotype, a multicellular behaviour in Enterobacteriaceae. Cell. Mol. Life Sci. **62:**1234–1246.
37. **Römling, U.** 2002. Molecular biology of cellulose production in bacteria. Res. Microbiol. **153:**205–212.
38. **Römling, U., and D. Amikam.** 2006. Cyclic di-GMP as a second messenger. Curr. Opin. Microbiol. **9:**218–228.
39. **Römling, U., M. Gomelsky, and M. Y. Galperin.** 2005. C-di-GMP: the dawning of a novel bacterial signaling system. Mol. Microbiol. **57:**629–639.
40. **Ross, P., Y. Aloni, H. Weinhouse, D. Michaeli, P. Ohana, R. Mayer, and M. Benziman.** 1986. Control of cellulose synthesis in *A. xylinum*. A unique guanyl oligonucleotide is the immediate activator of cellulose synthase. Carbohydr. Res. **149:**101–117.
41. **Ross, P., H. Weinhouse, Y. Aloni, D. Michaeli, P. Weinberger-Ohana, R. Mayer, S. Braun, E. de Vroom, G. A. van der Marel, J. H. van Boom, and M. Benziman.** 1987. Regulation of cellulose synthesis in *Acetobacter xylinum* by cyclic diguanylic acid. Nature **325:**279–281.
42. **Ruby, E. G., and K. H. Nealson.** 1977. Pyruvate production and excretion by the luminous marine bacteria. Appl. Environ. Microbiol. **34:**164–169.
43. **Ruby, E. G., M. Urbanowski, J. Campbell, A. Dunn, M. Faini, R. Gunsalus, P. Lostroh, C. Lupp, J. McCann, D. Millikan, A. Schaefer, E. Stabb, A. Stevens, K. Visick, C. Whistler, and E. P. Greenberg.** 2005. Complete genome sequence of *Vibrio fischeri*: a symbiotic bacterium with pathogenic congeners. Proc. Natl. Acad. Sci. U. S. A. **102:**3004–3009.
44. **Ryjenkov, D. A., R. Simm, U. Römling, and M. Gomelsky.** 2006. The PilZ domain is a receptor for the second messenger c-di-GMP. The PilZ domain protein YcgR controls motility in enterobacteria. J. Biol. Chem. **281:**30310–30314.
45. **Smit, G., S. Swart, B. J. Lugtenberg, and J. W. Kijne.** 1992. Molecular mechanisms of attachment of *Rhizobium* bacteria to plant roots. Mol. Microbiol. **6:**2897–2903.
46. **Stabb, E. V., K. A. Reich, and E. G. Ruby.** 2001. *Vibrio fischeri* genes *hvnA* and *hvnB* encode secreted NAD^+-glycohydrolases. J. Bacteriol. **183:**309–317.
47. **Stabb, E. V., and E. G. Ruby.** 2002. RP4-based plasmids for conjugation between *Escherichia coli* and members of the Vibrionaceae. Methods Enzymol. **358:**413–426.
48. **Tamayo, R., J. T. Pratt, and A. Camilli.** 2007. Roles of cyclic diguanylate in the regulation of bacterial pathogenesis. Annu. Rev. Microbiol. **61:**131–148.
49. **Tamayo, R., A. D. Tischler, and A. Camilli.** 2005. The EAL domain protein VieA is a cyclic diguanylate phosphodiesterase. J. Biol. Chem. **280:**33324–33330.
50. **Teather, R. M., and P. J. Wood.** 1982. Use of Congo red-polysaccharide interactions in enumeration and characterization of cellulolytic bacteria from the bovine rumen. Appl. Environ. Microbiol. **43:**777–780.
51. **Tschowri, N., S. Busse, and R. Hengge.** 2009. The BLUF-EAL protein YcgF acts as a direct anti-repressor in a blue-light response of *Escherichia coli*. Genes Dev. **23:**522–534.
52. **Visick, K. L., and L. M. Skoufos.** 2001. Two-component sensor required for normal symbiotic colonization of *Euprymna scolopes* by *Vibrio fischeri*. J. Bacteriol. **183:**835–842.
53. **Waters, C. M., W. Lu, J. D. Rabinowitz, and B. L. Bassler.** 2008. Quorum sensing controls biofilm formation in *Vibrio cholerae* through modulation of cyclic di-GMP levels and repression of *vpsT*. J. Bacteriol. **190:**2527–2536.
54. **Weiner, R., E. Seagren, C. Arnosti, and E. Quintero.** 1999. Bacterial survival in biofilms: probes for exopolysaccharide and its hydrolysis, and measurements of intra- and interphase mass fluxes. Methods Enzymol. **310:**403–426.
55. **Wolfe, A. J., and H. C. Berg.** 1989. Migration of bacteria in semisolid agar. Proc. Natl. Acad. Sci. U. S. A. **86:**6973–6977.
56. **Wolfe, A. J., and K. L. Visick.** 2008. Get the message out: cyclic-di-GMP regulates multiple levels of flagellum-based motility. J. Bacteriol. **190:**463–475.
57. **Yildiz, F. H., and G. K. Schoolnik.** 1999. *Vibrio cholerae* O1 El Tor: identification of a gene cluster required for the rugose colony type, exopolysaccharide production, chlorine resistance, and biofilm formation. Proc. Natl. Acad. Sci. U. S. A. **96:**4028–4033.
58. **Yildiz, F. H., and K. L. Visick.** 2009. *Vibrio* biofilms: so much the same yet so different. Trends Microbiol. **17:**109–118.
59. **Yip, E. S., K. Geszvain, C. R. DeLoney-Marino, and K. L. Visick.** 2006. The symbiosis regulator RscS controls the *syp* gene locus, biofilm formation and symbiotic aggregation by *Vibrio fischeri*. Mol. Microbiol. **62:**1586–1600.
60. **Yip, E. S., B. T. Grublesky, E. A. Hussa, and K. L. Visick.** 2005. A novel, conserved cluster of genes promotes symbiotic colonization and σ^{54}-dependent biofilm formation by *Vibrio fischeri*. Mol. Microbiol. **57:**1485–1498.

Review

Vibrio biofilms: so much the same yet so different

Fitnat H. Yildiz[1] and Karen L. Visick[2]

[1] Department of Microbiology and Environmental Toxicology, University of California, Santa Cruz, Santa Cruz, CA 95064, USA
[2] Department of Microbiology and Immunology, Loyola University Chicago, Maywood, IL 60153, USA

Vibrios are natural inhabitants of aquatic environments and form symbiotic or pathogenic relationships with eukaryotic hosts. Recent studies reveal that the ability of vibrios to form biofilms (i.e. matrix-enclosed, surface-associated communities) depends upon specific structural genes (flagella, pili and exopolysaccharide biosynthesis) and regulatory processes (two-component regulators, quorum sensing and c-di-GMP signaling). Here, we compare and contrast mechanisms and regulation of biofilm formation by *Vibrio* species, with a focus on *Vibrio cholerae*, *Vibrio parahaemolyticus*, *Vibrio vulnificus* and *Vibrio fischeri*. Although many aspects are the same, others differ dramatically. Crucial questions that remain to be answered regarding the molecular underpinnings of *Vibrio* biofilm formation are also discussed.

Vibrios and biofilms

Vibrio species are ubiquitous in aquatic ecosystems. Although many *Vibrio* species are free living, a small group can form pathogenic or symbiotic interactions with eukaryotic hosts. Indeed, these *Vibrio* species alternate between growth within their hosts and prolonged survival in aquatic habitats. *Vibrio cholerae*, for example, causes periodic occurrences of the severe diarrheal disease cholera. These epidemics typically result from consumption of drinking water contaminated with the pathogen. In between epidemics, *V. cholerae* survives within brackish water [1].

Like *V. cholerae*, the pathogens *Vibrio parahaemolyticus* and *Vibrio vulnificus* are most often delivered to human hosts through the consumption of contaminated water or food, particularly raw seafood. *V. parahaemolyticus* is responsible for the most common *Vibrio*-associated, seafood-borne gastroenteritis [2]. *V. vulnificus* causes gastroenteritis, severe wound infections and septicemia in susceptible hosts [3]. The symbiont *Vibrio fischeri* similarly alternates between free-living and host-associated lifestyles [4].

Adaptation of *Vibrio* species to changing parameters of the aquatic ecosystem, in addition to those of their respective hosts, is crucial to their survival and colonization success. One key factor for environmental survival and transmission is the ability to form biofilms (i.e. matrix-enclosed, surface-associated communities). The biofilm mode of growth is the preferred lifestyle in the microbial world as it enhances growth and survival by providing access to nutrients and protection from predators and antimicrobial compounds (reviewed in Ref. [5]).

The biofilm forming capacity of *V. cholerae* is well documented, both in natural habitats and under laboratory conditions (Figure 1a) [1,6,7]. Stool samples from cholera patients, for example, contain not only planktonic *V. cholerae* but also biofilm-like aggregates that are more infectious [8]. Furthermore, removal from water of particles >20 μm in diameter can reduce cholera incidence by 48% [9]. Taken together, these studies highlight the importance of the biofilm growth mode in both the intestinal and aquatic phases of *V. cholerae*'s life cycle. Biofilm formation also has a key role in host colonization by *V. fischeri* (Figure 1b) [10,11]. It is likely to also be important for the ecology, transmission and/or virulence of *V. vulnificus* and *V. parahaemolyticus*, which are found on surfaces of plankton and colonize shellfish [2,3], however, this area of research remains underdeveloped.

In recent years, numerous studies have investigated biofilm formation in *Vibrio* species. Many of these studies rely on colony morphology as an indicator of biofilm formation, including translucent (TR), opaque (OP) and rugose or wrinkled colonies; these and other methods for investigating *Vibrio* biofilms are described in Box 1. These studies have identified many key proteins, including those involved in the biosynthesis of flagella, pili and polysaccharides, and in the regulators that control their expression, predominantly two-component and quorum sensing regulators and the small signaling molecule c-di-GMP. Here, we compare and contrast mechanisms and regulation of biofilm formation in *Vibrio* species, focusing on *V. cholerae*, *V. parahaemolyticus, V. vulnificus* and *V. fischeri* as they are the species most intensively studied for biofilm formation.

Flagella are involved in initial stages of biofilm formation by *Vibrio* spp.

Biofilm formation begins when a bacterium reaches and attaches to a surface. After the initial attachment, subsequent formation of microcolonies and 3D structures is mediated by movement and growth of attached bacteria. In many bacteria, flagella-mediated motility promotes the initial stages of biofilm formation, usually by enhancing movement towards and along the surface [12]. In vibrios, the impact of motility seems to extend beyond attachment.

In *V. cholerae*, loss of flagellar genes usually results in decreased attachment, although the contribution of the flagellum varies between strains [6,13]. In *V. cholerae*

Corresponding author: Yildiz, F.H. (yildiz@metx.ucsc.edu).

0966-842X/$ – see front matter doi:10.1016/j.tim.2008.12.004 Available online 21 February 2009

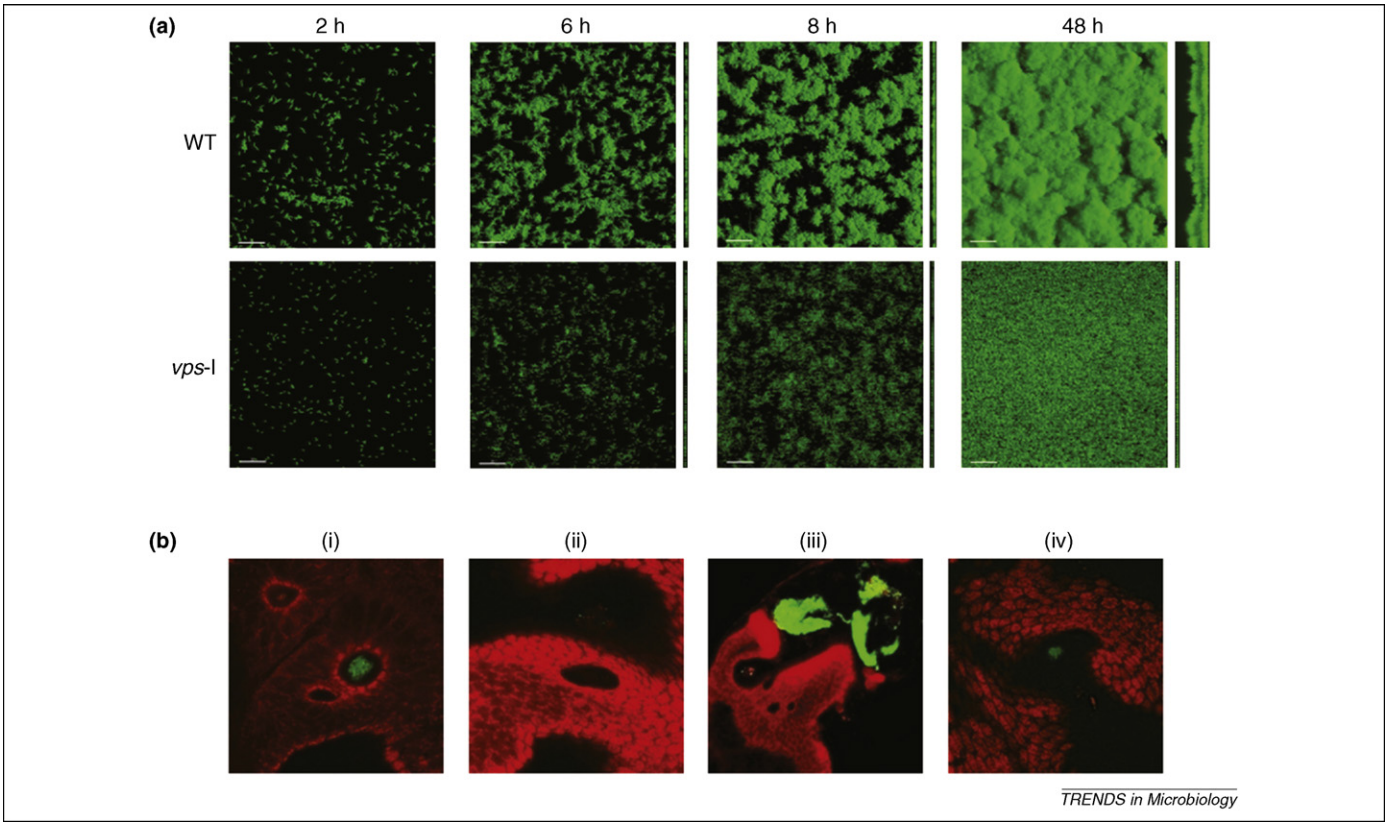

Figure 1. Biofilms of *V. cholerae* and *V. fisheri*. **(a)** 3D biofilm structures of green fluorescent protein (GFP) tagged wild-type *V. cholerae* and a *vps*-I cluster mutant (unable to produce VPS) formed after 2, 6, 8 and 48 h post-inoculation in once-through flow cell. Images were acquired with confocal laser scanning microscopy (CSLM) and top-down and side views of biofilms are shown. Scale bar indicates 30 μm. Data (but not images) are from Ref. [66]. **(b)** Biofilm-like aggregate formation on the light organ of squid. Newly hatched squid were inoculated with GFP tagged wild-type cells (i) or *sypN* polysaccharide mutant carrying vector control (ii), and wild-type cells (iii) or *sypN* mutant overexpressing the histidine kinase RscS (iv). Between 2–6 h post inoculation, squids were stained with Cell Tracker Orange (red color) and aggregate formation by *V. fisheri* strains was analyzed by CSLM. Data (but not images) are from Ref. [11].

O139, time lapse video microscopy [13] revealed that initial interactions between wild-type cells and a surface occurred rapidly: bacteria near the surface swam in circles, then exhibited more restricted movement. Some cells, tethered to the surface, alternated between short periods of jerky movement and no movement. The numbers of surface associated and immobilized bacteria increased over time, with subsequent formation of microcolonies and classical 3D structures. A *V. cholerae* O139 *flaA* mutant (lacking the major flagellin subunit), however, did not undergo this pattern of biofilm formation. Instead, the mutant aggregated in liquid culture, then subsequently settled onto the surface as immobilized clusters of cells [13]. After this settling, the biofilms developed relatively normally, indicting that the *flaA* mutant could form biofilms if it was allowed sufficient time.

Box 1. Experimental analysis of biofilm formation

There is a correlation between biofilm matrix production and colony morphology. Cells able to produce exopolymers have corrugated (also termed wrinkled or rugose), or in some cases mucoid, colony morphologies. Thus, changes in colony morphology have been extensively utilized to identify biofilm matrix components. For example, *V. parahaemolyticus* undergoes a reversible phase variation between opaque (OP) and translucent (TR) colony types (Figure I). OP colonies tend to result from increased polysaccharide production, and loss of the involved polysaccharide locus results in colonies that are TR [37,51]. Besides OP and TR morphotypes, *V. parahaemolyticus* forms rugose colonies that exhibit increased CPS production compared to parental TR or OP strains [69]. *V. vulnificus* produces OP, TR and rugose colony morphotypes [33,61,72], whereas *V. cholerae* undergoes phase variation to switch between the smooth and rugose colony morphotypes [7].

Biofilms formed at solid-liquid interfaces have been analyzed under static or flow conditions [66]. For static culture conditions, microorganisms are grown in microtiter dishes or test tubes and the extent of biofilm formation is followed by staining of the surface-associated biofilm with crystal violet. Pellicle formation has also been used to analyze biofilms formed at air-liquid interfaces under static conditions. To evaluate biofilm architecture, biofilms that form in static cultures or in the 'once-through' flow cell reactor can be analyzed using confocal laser scanning microscopy (CSLM), usually utilizing strains that express fluorescent proteins.

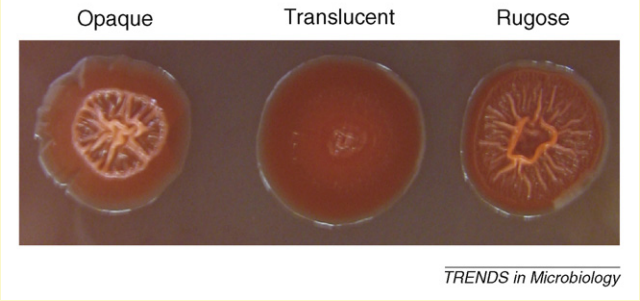

Figure I. Representative colony phenotypes of *V. parahaemolyticus*. Colony phenotypes of opaque, translucent and rugose strains of *V. parahaemolyticus* grown on Congo red plates are shown.

The planktonic aggregation of *flaA* mutants was subsequently attributed to increased production of an exopolysaccharide termed vibrio polysaccharide (VPS). Consistent with this result, these mutants formed rugose colonies. Surprisingly, any of several paralyzed (*mot*) mutants, which produce a flagellum but cannot rotate it, formed smooth colonies and poor biofilms [13,14]. A *flaA motX* double mutant also produced smooth colonies, indicating that disruption of *mot* can eliminate the VPS-inducing signal caused by loss of the flagellum [14]. Thus, *V. cholerae* could use the flagellar motor not only to promote motility but also to transmit a signal indicating interaction with a surface [14].

Such a possibility would not be unprecedented: *V. parahaemolyticus* uses its motor to decide when to switch from a swimming cell (polarly flagellated) to a swarmer cell (with lateral flagella) capable of moving on surfaces or in highly viscous media [15]. *V. parahaemolyticus* also uses its polar flagellum to promote biofilm formation [16]. *flgE* and *flgD* (hook) mutants are defective in attachment, pellicle formation (forming 'speckled' pellicles) and biofilm formation [16]. The severity of the defect depended on the strain background. For example, whereas TR *fla* mutants in submerged cultures could not adhere, OP *fla* mutants could adhere, but could not form complex 3D structures, even with prolonged incubation. These data indicate a role for the polar flagellum beyond biofilm initiation and/or in controlling other factors [16].

In *V. vulnificus* and *V. fischeri*, flagellum-mediated motility also promotes biofilm formation. For example, a *V. vulnificus flgE* (hook) mutant is defective for attachment both to polystyrene and to glass wool [17]. In *V. fischeri*, the *flrC* regulator is also required for biofilm formation [18]; prolonged incubation could overcome some, but not the entire defect.

Thus, motility has a key role in biofilm formation in the vibrios, as has been seen for other biofilm models. Interestingly, the role of motility seems to extend beyond simply allowing the cell to reach the right location. Understanding other role(s) for motility and/or the motility apparatus during biofilm development remains an important area of investigation.

Pili promote cell-surface and/or cell–cell interactions

In *V. cholerae*, at least three types of pili contribute to biofilm formation: mannose-sensitive haemagglutinin type IV pili (MSHA), toxin co-regulated pili (TCP) and chitin-regulated pili (ChiRP; formerly termed PilA) [19–22]. The relative importance of these pili varies under different conditions, and from strain to strain. MSHA, for example, is crucial for early attachment to abiotic surfaces in *V. cholerae* O1 El Tor strains, yet initial studies revealed no role in strain O139 [13]. Subsequent work revealed a role for the O139 MSHA pilus structural gene *mshA* in monolayer formation, and demonstrated that the *mshA* mutant could bypass this stage by aggregating as planktonic cells and subsequently settling and forming 3D biofilms [23]. Similarly, conflicting results for the importance of MSHA pili have been obtained for biofilm formation on various chitin substrates [19,20,22]. Thus, the contribution of MSHA to biofilm formation is impacted by both environmental and genetic factors.

The classic, virulence-associated pilus of *V. cholerae*, TCP, is involved in microcolony formation on an environmentally relevant substrate, chitin. A TCP pili mutant of El Tor N16961 formed monolayers, but not microcolonies, on a chitin substrate [21]. Recent work revealed that MSHA and TCP pili are inversely controlled at multiple levels [24], indicating the possibility that the two pilus types sequentially promote monolayer and 3D biofilm formation.

A role for ChiRP is less clear. ChiRP was required for competitive attachment to a chitin surface, crab shell, but largely unnecessary for individual attachment to chitin particles [20]. It is speculated that ChiRP might have a role other than adherence, such as orienting the cell optimally for chitin degradation [20].

V. parahaemolyticus also employs MSHA and ChiRP for biofilm formation. MSHA mutants form substantially reduced biofilms – a defect that could be overcome by prolonged incubation – and defective, speckled pellicles [16]. Like *V. cholerae*, strain background influenced the severity of the defect. ChiRP mutants fail to progress past monolayer formation [25]. In addition, both MSHA and ChiRP contribute to attachment to chitin particles [25].

In *V. vulnificus*, the type IV pilus structural protein PilA and, to a greater degree, the pre-pilin peptidase PilD, contribute to binding both to abiotic surfaces and to human epithelial cells [26,27]. The difference in relative importance of the two genes could be attributed to the retention by the *pilA* mutant of other types of pili, and/or to the role of PilD in processing other secreted proteins [26,27]. PilA and PilD are also necessary for prolonged attachment to oysters [28].

A role for pili in biofilm formation in *V. fischeri* has not been determined but is expected, given that the genome encodes eight putative pili loci, two of which contribute to efficient symbiotic colonization [29,30].

In general, although similar pili are used by vibrios for attachment, it seems that the genetic context of the cell and the type of surface it encounters (and/or other clues from the environment) can substantially influence the relative importance and thus usage of a particular type of pili for attachment.

Polysaccharides are the most prevalent component of *Vibrio* biofilms

Production of mature biofilms requires extracellular matrix components that hold the cells together and keep the biofilm attached to the surface. The capsular polysaccharide (CPS) or exopolysaccharide (EPS, or VPS in *V. cholerae*) loci involved in biofilm formation have been identified from numerous *Vibrio* spp. Expression of these loci is frequently correlated with biofilm-associated changes in colony morphology, in particular OP, rugose or wrinkled colonies (Box 1).

vps and vps-like loci

In *V. cholerae* O1 El Tor A1552, biofilm formation depends upon two linked loci, *vps*-I and *vps*-II (collectively termed *vps*), which encode structural proteins responsible for EPS production [7] (Figure 2a). *vps*-I and *vps*-II are separated by six genes (*rbmA-F*) that also are involved in biofilm

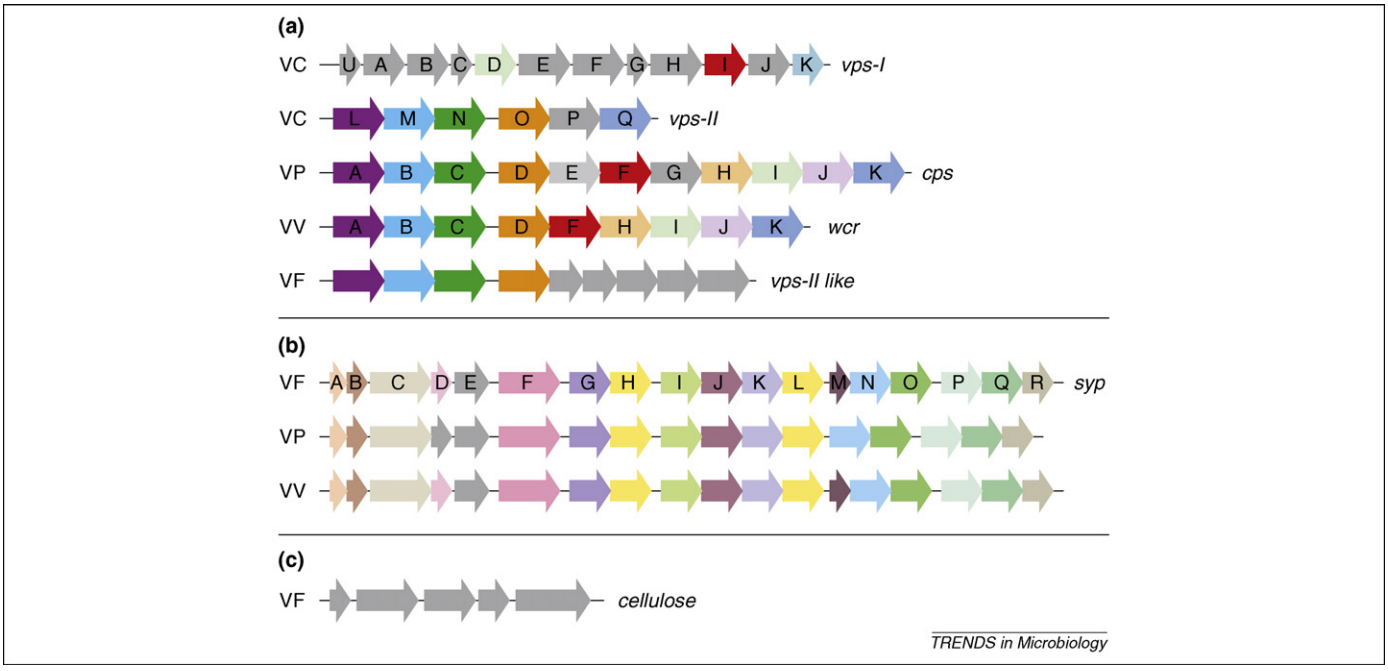

Figure 2. Polysaccharide loci in *Vibrio* spp. The three most prevalent loci with established roles in biofilm formation in *Vibrio* spp. are shown: **(a)** *vps* and *vps*-like, **(b)** *syp* and *syp*-like and **(c)** cellulose. In *V. cholerae*, the large *vps* locus encompasses 2 sub-loci, *vps*-I and *vps*-II; the polysaccharide loci of other vibrios is more similar to *vps*-II than to *vps*-I and thus for clarity these sub-loci are separated. (a) *V. cholerae* (VC) *vps* locus (*vps*-I (VC0916-VC0927) and *vps*-II (VC0934-VC0938*), V. parahaemolyticus* (VP) *cps* locus, *V. vulnificus* (VV) *wcr* locus (VVA0395-VVA0387; VV21582-VV21574) and a *vps*-II-like locus in *V. fischeri* (VF) (VF0352-VF0344). (b) *V. fischeri syp* locus (VFA1020-VFA1037) and similar loci in *V. parahaemolyticus* (VP1476–1458) and *V. vulnificus* (VV12658-VV12674). (c). *V. fischeri* cellulose locus (VFA0885-VFA0881). Genes (not drawn to scale) are represented by arrows. Gray arrows represent genes that are dissimilar to others in the same panel, whereas those with the same color exhibit sequence similarity. Genes are named as labeled.

formation but not polysaccharide production, with one exception: disruption of *rbmB* (a predicted VPS lyase) leads to an accumulation of polysaccharide [31]. VPS from *V. cholerae* O1 El Tor A1552 primarily contains glucose and galactose [7], with N-acetyl glucosamine, mannose and xylose representing minor constituents. This VPS is associated with rugose colony formation, matrix production, pellicles, 3D biofilms and resistance to chlorine [7,32]. Loss of *vps* eliminates these phenotypes.

The *vps* locus is conserved, in part, in other vibrios [29,33,34] (Figure 2a). No role in biofilm formation for the *vps*-like locus of *V. fischeri* has been observed to date [35]. Similarly, little is known about the *V. vulnificus* locus, *wcr*, other than that it is associated with the formation of both OP and rugose colonies [33,36]. *wcr* most resembles the *V. parahaemolyticus* locus, *cps*, which produces a CPS (CPSA), rather than an EPS like *V. cholerae* [37]. *cps* is required for OP colony morphology and pellicle formation, as its loss disrupts these phenotypes [34]. OP colonies have increased *cps* gene expression and produce more CPSA [34,37]. CPSA contains approximately equal amounts of fucose, galactose, glucose and *N*-acetylglucosamine, making it distinct from *V. cholerae* EPS [16,37]. Its production seems to require activated sulphur, as cysteine mutants fail to synthesize CPSA [16].

syp and syp-like loci

Biofilm formation in *V. fischeri* depends upon an 18 gene cluster of polysaccharide biosynthetic genes (*syp*) and associated regulators [11,38]. This locus is lacking in *V. cholerae*, but is conserved in *V. parahaemolyticus* and *V. vulnificus* (Figure 2b). Induction of *syp* expression results in wrinkled colonies, pellicle formation and matrix production; loss of specific *syp* genes largely restores the wild-type phenotype [11,18]. The Syp polysaccharide has not been purified, but seems to contain glucose or α-linked mannose [11]

Other polysaccharide loci

Biofilm formation by *V. fischeri* also depends upon a cellulose gene cluster similar to that found in *Salmonella* but absent in other vibrios [35] (Figure 2c). Numerous other polysaccharides and polysaccharide loci have been uncovered in *Vibrio* spp. (e.g. Refs [39,40]), although few have been investigated for roles in biofilm formation. Where investigated, a surprising number seem to have negative roles. For example, the group 1 CPS in *V. vulnificus* is associated with the production of OP colonies, but the loss of a representative gene increases attachment [41,42]. *V. cholerae* O139 contains a locus with genes for CPS and lipopolysaccharide (LPS) O antigen biosynthesis that also has a negative role in biofilm formation [43]. A third example is a putative O antigen CPS locus of *V. parahaemolyticus*, VP0214-VP0237, the loss of which increases attachment [16]. A deeper understanding of the roles of these possible polysaccharide loci awaits further investigation.

The *Vibrio* species studied to date produce distinct EPSs, and some if not all have the potential to produce multiple types of polysaccharides. Because biofilms gain their structural integrity largely from the EPS matrix component, these studies indicate a diversity of biofilms are produced. It is possible that these biofilms, thus, could have an important role in niche selection.

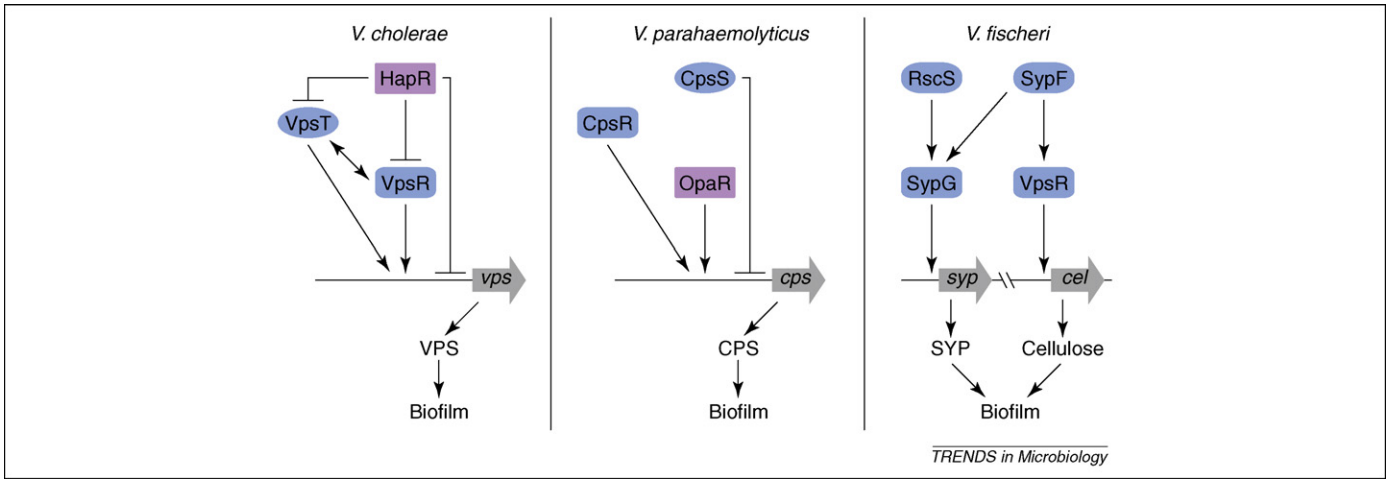

Figure 3. Regulation of biofilm formation in *Vibrio* spp. Biofilm formation in *V. cholerae* is positively regulated by the regulators VpsR and VpsT. The magnitude of transcriptional control of *vps* genes by VpsR is greater than that of VpsT. Expression of *vps* genes and the regulators VpsR and VpsT are negatively controlled by the HapR regulator. In *V. parahaemolyticus* expression of *cps* genes is negatively regulated by a homolog of VpsT, CpsS. In the absence of CpsS, OpaR and CpsR (HapR and VpsR homologs, respectively) positively control *cps* gene expression and biofilm formation. In *V. fischeri* transcription of *syp genes* and biofilm formation are positively controlled by the histidine kinases RscS and/or SypF, which act through response regulator SypG. SypF also positively regulates production of cellulose (*cel*), acting although the VpsR homolog of *V. fischeri*. The roles of VpsR and SypE as inhibitors in *V. fischeri* are poorly understood and thus these are omitted from this figure.

Transcriptional control of EPS production genes

In *Vibrio* species, regulation of exopolysaccharide production and biofilm formation is complex, and involves numerous transcriptional regulators, particularly two-component signal transduction and quorum sensing regulators (Figure 3). In a typical two-component system, a stimulus detected by a sensor histidine kinase (HK) is transformed into a cellular signal by a phosphorelay event that involves autophosphorylation of the HK at a conserved histidine residue. The phosphoryl group is then passed to a response regulator (RR) at a conserved aspartate residue, leading to activation and altered gene expression or protein function. Quorum sensing involves sensing and responding to population density (Box 2). Global regulators, such as CRP [44,45] and sigma factors RpoS and RpoN [32], have a role in biofilm formation in the vibrios, but they are not discussed here.

Two-component regulators

VpsR and VpsR-like regulators. In *V. cholerae*, the RR VpsR is a key regulator of biofilm formation. VpsR promotes transcription of the *vps* genes and formation of typical 3D biofilm structures [32,46]. Mutations that alter the residue predicted to be phosphorylated (D59) either inactivate this protein (D59A) or increase its activity (D59E) [14], thus supporting that phosphorylation on this residue is required for activation. However, the HK responsible for phosphorylation of VpsR has not been identified, as it is not physically linked to *vpsR*. Identifying the cognate HK will facilitate understanding the regulatory network controlling *vps* gene expression and how environmental signals regulate VPS production.

Under specific genetic conditions, *V. parahaemolyticus* also produces high levels of CPS and thus rugose colonies. Disruption of the *vpsR* homolog, *cpsR*, yields smooth colonies and decreases transcriptional activity of *cpsA* fused to a *lacZ* reporter in the rugose background [34]. However, CpsR is not required for basal levels of *cps* expression in TR or OP strains, as disruption of *cpsR* in these strains had no effect on *cps* transcription [34]. This contrasts with the role of VpsR, which is essential for transcription of *vps* genes in all forms of *V. cholerae*. It remains to be determined whether CpsR directly regulates transcription of *cps* genes.

V. fischeri also encodes a VpsR homolog. Disruption of *vpsR* leads to formation of mucoid colonies, which are indicative of enhanced polysaccharide production, indicating that VpsR might be a repressor [35]. When overexpressed, however, VpsR induces biofilm formation, indicating that it could also be an activator. Surprisingly, VpsR-induced biofilms depended not on a *vps*-like locus but on a putative cellulose biosynthesis cluster not found in other characterized vibrios (Figure 2c) [35]. Thus, VpsR seems to have a novel role in *V. fischeri*.

VpsT and VpsT-like. In *V. cholerae*, a second positive regulator is VpsT, a member of the UhpA (FixJ) family of transcriptional regulators [47]. VpsT shows homology to CsgD, which positively controls curli and cellulose production in *Salmonella enterica*. Disruption of *vpsT* yields smooth colonies and reduces *vps* expression, and biofilm formation [47]. Although the putative phosphorylation site in the receiver domain of VpsT is conserved, it is not necessary for the *in vivo* function of VpsT (J. Meir and F. Yildiz, unpublished). Thus, whether VpsT functions as a canonical RR remains unclear.

Characterization of *vpsT* and *vpsR* mutants in *V. cholerae* revealed different roles for these regulators in determining biofilm architecture. The *vpsT* mutant is still able to form biofilms (albeit distinct from its rugose parent), whereas *vpsR* and *vpsT vpsR* mutants produce only single cells or small microcolonies attached to the substratum [48]. The VpsR and VpsT regulons are largely identical, although VpsR exerts a larger impact on expression [48]. Thus, VpsR is essential for VPS production and biofilm formation, whereas VpsT seems to have an accessory role, possibly by increasing the level or activity of VpsR. Whether VpsT and VpsR serve as direct regulators of *vps* remains unknown.

Box 2. Quorum sensing

Quorum sensing is a mechanism that cells use to determine their population density. Signal synthases produce a diffusible molecule (autoinducer [AI]) that can accumulate in the extracellular environment. When the cell population is sufficiently high, and enough signal accumulates, this molecule binds to and activates cellular receptors. In *Vibrio* species, one consequence of this signaling is a phosphorelay that ultimately controls the synthesis of a global regulator and phenotypes that are more useful to a group of cells, such as luminescence, rather than to individuals [50]. Because biofilm formation is a behavior that depends upon a group of cells, it makes sense for bacteria to rely on quorum sensing regulators to control biofilm formation, and indeed they do. In *V. cholerae*, however, the sense of this control is not as might be expected: *V. cholerae* mutants, which are 'locked' into a regulatory state mimicking high cell density, are impaired in biofilm formation [54].

V. cholerae produces two AIs [50]. CAI-1 [(S)-3-hydroxytridecan-4-one] [73] is synthesized by CqsA and detected by CqsS. AI-2 [the furanosyl borate diester (2S,4S)-2-methyl-2,3,3,4-tetrahydroxytetrahydrofuran borate] is synthesized by LuxS and detected by the LuxQP receptor [50]. Information from the sensors is transduced through a phosphorelay, first to the LuxU phosphotransfer protein and then to LuxO, which is an RpoN dependent response regulator. At low cell density, when the concentrations of AIs are low, LuxO is phosphorylated and activates expression of a set of small regulatory RNAs (Figure Ia) [74]. The result is inhibition of expression of the major quorum sensing regulator, HapR. At high cell density, LuxO is dephosphorylated and expression of HapR is increased. Under these conditions, the *vps* genes and virulence-associated genes (*aphA*) are repressed (Figure Ib).

This regulation seems to be both direct and indirect as the empirically defined HapR binding motif was found in the promoter regions of both the *vps* locus and its regulator *vpsT* [32]. Mutants in *cqsA* that cannot produce the CAI-1 signal, a condition that should mimic low cell density, form thicker biofilms [55]. This indicates that CAI-1 signals are crucial for repression of biofilm formation via the quorum sensing regulatory circuitry. It is thought that quorum sensing ensures development of 'normal' biofilm structures that permit rapid dispersion of bacteria from the biofilm, thereby facilitating transmission.

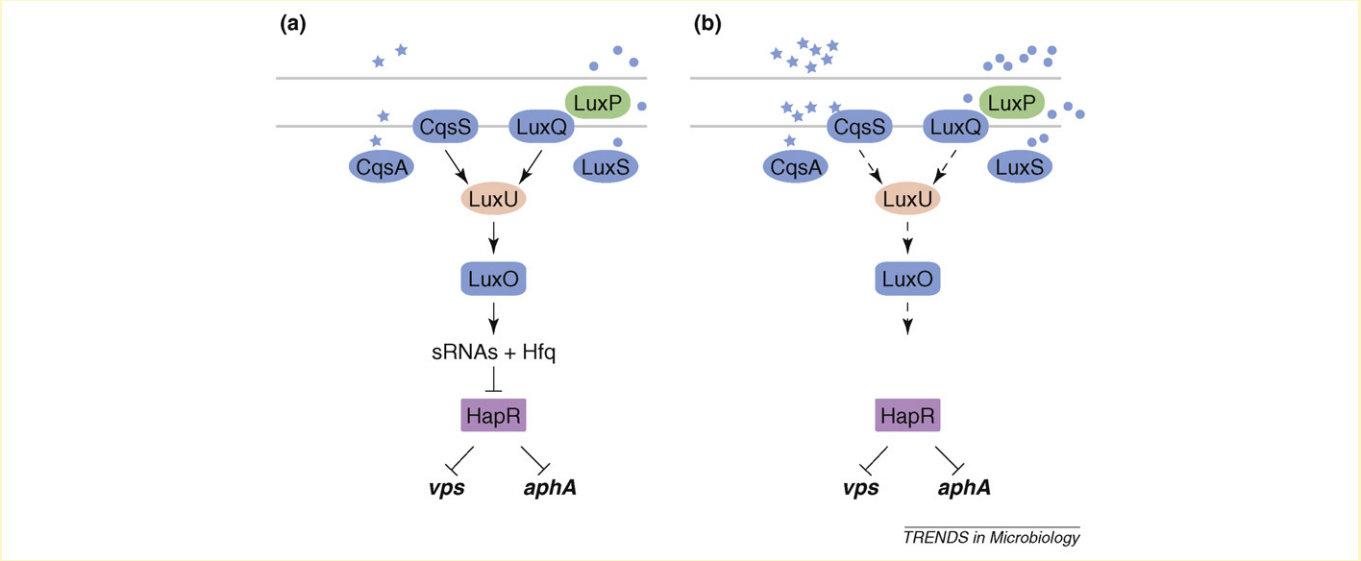

Figure I. *V. cholerae* quorum sensing. *V. cholerae* synthesizes two AIs, CAI-1 (stars) made by CqsA and AI-2 (circles) made by LuxS, that are detected by sensor kinases CqsS and LuxQ (working with periplasmic protein LuxP), respectively, which control a phosphorelay system. Low **(a)** and high **(b)** levels of autoinducers alter the signal transduction cascade, ultimately impacting biofilm formation and virulence gene expression. Abbreviations: Hfq, RNA binding protein; sRNAs, small regulatory RNAs.

A VpsT homolog, CpsS, also controls biofilm formation in *V. parahaemolyticus*, but as a negative regulator [34]. Introduction of a *cpsS* mutation into TR or OP strains derepresses *cpsA* transcription, resulting in rugose colonies. In TR strains, derepression is mediated through CpsR, whereas in OP strains, CpsR has an accessory role [34]. Thus, *V. cholerae* and *V. parahaemolyticus* use similar proteins, but they function in the opposite sense and to different degrees: CpsS is the dominant negative regulator in *V. parahaemolyticus*, whereas VpsT is a positive co-regulator in *V. cholerae*.

Other two-component regulators. In *V. vulnificus*, the RR NtrC contributes to biofilm formation through its transcriptional control of *gmhD* [49]. The GmhD protein, an ADP-l-glycero-D-manno-heptose-6-epimerase, is required for LPS and EPS production and biofilm formation [49]. The relative roles of LPS and EPS in biofilm formation, in addition to the identity of the EPS involved in this process, have yet to be determined.

In *V. fischeri*, two-component regulators have crucial roles in the control of biofilm formation, primarily through their activation of the *syp* polysaccharide locus. For example, the orphan HK RscS, when overexpressed, induces *syp* transcription, wrinkled colony and pellicle formation, and symbiotic biofilm formation [11]. RscS acts upstream of SypG, a *syp*-encoded RR that is proposed to be the direct activator of *syp* transcription [18].

Surprisingly, overexpression of SypG induced *syp* transcription but not the formation of wrinkled colonies or strong pellicles. However, overexpression of SypG in a *sypE* mutant, permitted wrinkled colony and pellicle formation [18]. Thus, SypE, a putative RR that is not predicted to bind DNA, seems to have an inhibitory role. RscS might therefore both activate SypG and inactivate SypE. Homologs of SypG are present in *V. vulnificus* and *V. parahaemolyticus*, but RscS and SypE are unique to *V. fischeri*.

Overexpression of a third *syp*-encoded regulator, SypF, also induces biofilm formation in *V. fischeri* [35]. This

regulator seems to function upstream of both SypG and VpsR: mutation of both regulators was necessary to eliminate all the biofilm phenotypes induced by SypF overexpression. The SypF-VpsR path seems to promote cell-surface attachment, whereas the SypF-SypG path seems to be responsible for cell–cell attachment [35].

Quorum sensing regulators

Vibrio species use quorum sensing (Box 2) to control numerous traits, including luminescence, virulence and biofilm formation. Best studied in *Vibrio harveyi*, in which the endpoint regulator is termed LuxR (reviewed in Ref. [50]), similar pathway components are found in all other vibrios studied to date.

The *V. parahaemolyticus* LuxR homolog, OpaR, positively regulates opacity, *cps* gene expression and biofilm formation [51]. Disruption of *opaR* in an OP strain yielded TR colonies, and overexpression of *opaR* in a TR strain increased *cps* expression and colony opacity [37]. A similar phenomenon is seen in both *V. vulnificus* and *V. fischeri*: mutants defective for the LuxR homologs, SmcR [52] and LitR [53], respectively, form TR colonies instead of the parental OP colonies; in the case of *V. vulnificus*, this disruption is associated with decreased biofilm formation. However, the molecular mechanisms causing decreases in colony opacity and biofilm formation and their connections to CPS or EPS production by *V. vulnificus* and *V. fischeri* are unknown.

In *V. cholerae*, the story is different (Figure 3). Mutants of the LuxR homolog, HapR, exhibit increased rugosity and increased *vps* expression [32,54,55]. These data indicate that HapR is a negative regulator of biofilm formation. HapR can directly bind DNA and repress expression of *vpsT* [56]. It can also control *vpsR* expression in some strains [32]. Thus, quorum sensing control of cell surface properties and biofilm formation is opposite in *V. cholerae* relative to the other vibrios. The ecological importance of this regulation is yet to be determined.

C-di-GMP signaling and biofilm formation

C-di-GMP is a ubiquitous second messenger that controls the transition from a free-living, motile lifestyle to a biofilm lifestyle in many bacteria (reviewed in Ref. [57]), including vibrios [58–62]. Increased c-di-GMP levels tend to promote biofilm formation and/or inhibit flagellar motility. C-di-GMP production and degradation is controlled by diguanylate cyclases (DGCs) and phosphodiesterases (PDEs), respectively [57] (Figure 4). Overexpression of these regulators tends to cause global effects. Intriguingly, vibrios contain much larger numbers of DGCs and PDEs than other bacteria [63]. The abundance of enzymes controlling synthesis and degradation of c-di-GMP in vibrios indicates the importance of c-di-GMP signaling to the biology of vibrios. Because different types of sensory domains are found in proteins predicted to function as DGCs or PDEs [63], one possibility is that cells adjust their c-di-GMP levels in response to environmental and intracellular signals and that c-di-GMP signaling has an important role in adaptation of vibrios to different environments.

In *V. cholerae*, c-di-GMP increases biofilm formation by stimulating transcription of *vps* genes and the positive transcriptional regulators *vpsR* and *vpsT* [60,64]. Mutants of the known or putative PDE genes, *mbaA*, *rocS*, *cdgC*, *cdpA* and *vieA*, exhibit enhanced biofilm formation, presumably because of increased c-di-GMP levels [65,66].

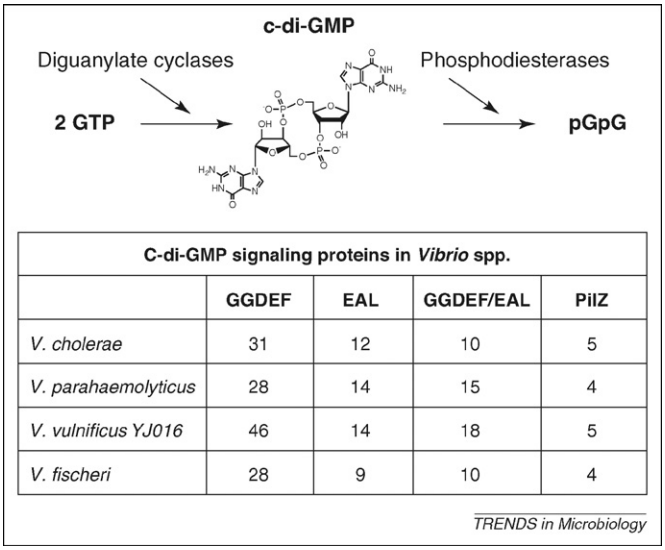

C-di-GMP signaling proteins in *Vibrio* spp.

	GGDEF	EAL	GGDEF/EAL	PilZ
V. cholerae	31	12	10	5
V. parahaemolyticus	28	14	15	4
V. vulnificus YJ016	46	14	18	5
V. fischeri	28	9	10	4

TRENDS in Microbiology

Figure 4. C-di-GMP signaling proteins in *Vibrio* spp. Cyclic di-guanosine-monophosphate (c-di-GMP) controls cell surface structures and biofilm formation in a diverse group of microorganisms. C-di-GMP is created from GTP (guanosine-5′-triphosphate) by diguanylate cyclase proteins that bear a GGDEF amino acid motif and degraded to the dinucleotide pGpG by phosphodiesterase proteins with EAL domains. C-di-GMP can be sensed by proteins with a PilZ domain. Numbers of genes encoding GGDEF, EAL, dual GGDEF and EAL or PilZ domain proteins in different *Vibrio* species are shown.

Recently, c-di-GMP also has been linked to the natural capacity of *V. cholerae* to generate rugose variants. For example, the prototype rugose strain A1552 expresses elevated c-di-GMP levels caused by a single amino acid change in a DGC protein, VpvC, relative to the smooth variant [67]. Disruption of *vpvC* in this rugose variant reduces overall c-di-GMP levels and causes cells to become similar to the smooth variant with respect to biofilm formation and *vps* transcription. Rugosity can also be generated by deletion of the master quorum sensing regulator *hapR*. This effect occurs through CdgA, a DGC whose mRNA abundance is increased in the *hapR* mutant; this increased CdgA presumably increases cellular c-di-GMP. Deletion of *cdgA* decreased *vps* transcription and restored smooth colony formation to the rugose *hapR* mutant [48]. Subsequent studies revealed that HapR serves as a direct regulator of *cdgA* [56].

Increased c-di-GMP level leads to a decrease in motility. In *V. cholerae*, as expected, mutations in DGC genes *cdgD* [60], *cdgH* [68] and *vpvC* [67] lead to an increase in motility, whereas mutations in PDE genes *vieA*, *rocS*, *cdgC* and *mbaA* lead to a decrease in motility relative to wild-type, when tested on Luria-Bertani medium (LB) soft agar motility plates [66].

In *V. parahaemolyticus*, increases in cellular c-di-GMP levels prevent swarming motility and promote biofilm formation. Two genes involved in c-di-GMP control, *scrG* and *scrC*, have been extensively characterized [58,59,69]. ScrG functions as a PDE: null mutants increase c-di-GMP and exhibit increased *cps* and decreased lateral flagellar

Box 3. Questions for future research

- What combination(s) of polysaccharides are being produced under various laboratory and environmental conditions?
- What are the constituents (protein or DNA) of biofilm matrices under laboratory, environmental and/or disease conditions?
- What other structural and regulatory factors are involved in biofilm formation?
- What are the environmental conditions that promote formation and dissolution of biofilms?
- What are the stimuli sensed by two-component systems regulating biofilms formation?
- What is the mechanism of c-di-GMP signaling and how is it connected to the regulatory network controlling biofilm formation?
- Do differences in regulation of biofilm formation reflect the importance of the biofilm lifestyle to each *Vibrio* spp. during their *in vivo* and *ex vivo* life cycles?

gene (*laf*) expression and, thus, enhanced biofilm formation and reduced swarming motility [59]. Null mutants defective for the *scrABC* operon behave similarly, whereas overexpression of *scrABC* yields the opposite results [58]. Interestingly, however, overexpression of *scrC* in the absence of *scrAB* (encoding putative pyridoxal-phosphate-dependent and extracellular solute-binding proteins, respectively) induces *cps*, not *laf*, expression [58]. Subsequent work revealed that ScrC is a bifunctional protein that functions as a DGC to synthesize c-di-GMP, but when co-produced with ScrAB, functions as a PDE and degrades c-di-GMP. Epistasis analysis indicates that ScrG and ScrABC act in the same regulatory circuitry and that *scrG* and *scrABC* double mutants show a cumulative effect at the level of *laf* and *cps* gene expression [58].

Relatively little is known about c-di-GMP and biofilm formation in *V. vulnificus* and *V. fischeri*. In *V. vulnificus*, expression of the DGC DcpA converted TR colonies of an acapsular mutant into OP colonies, but did not impact motility [61]. Overexpression of *dcpA* induced production of an EPS that was structurally distinct from the CPS, rugose colony formation and biofilm formation [61]. In *V. fischeri*, overexpression of the putative DGC MifA promotes cellulose biosynthesis and biofilm formation, indicating that c-di-GMP is a player in biofilm formation in this microbe as well [70].

How are c-di-GMP levels sensed by the cell? One protein domain that binds c-di-GMP is the PilZ domain. Of the five PilZ domain proteins in *V. cholerae*, two of these, PlzC and PlzD, have been recently shown to bind c-di-GMP and are known to regulate biofilm formation and/or motility [71]. Thus, PilZ domain proteins can function as c-diGMP receptors and regulate c-di-GMP-dependent processes in *V. cholerae* and likely in other vibrios.

It is becoming clear that, although *Vibrios* share common regulatory proteins and signaling systems, the biofilm regulatory circuitry is unique to each *Vibrio* spp. Differences in regulation might reflect the importance of the biofilm life style to each *Vibrio* spp. during their *in vivo* and *ex vivo* life cycles, differences in niche occupation, differences in environmental parameters that they respond to and/or parameters driving evolution of the pathogens and symbionts.

Concluding remarks

Biofilm formation, particularly on a biotic, possibly nutritional surface, seems likely to provide a substantial survival advantage to aquatic organisms such as *Vibrio* species. That these organisms use similar traits and regulators to solve the problem of biofilm formation is not unexpected. That they use such diversity in approaches – the relative importance of the traits and regulators, and even the sense (positive or negative) of control – is surprising and thus has the potential to provide great insights into the peculiar lifestyles of these microbes. Some outstanding research questions are listed in Box 3. Because biofilm formation is also part of the pathogenic lifestyles of *Vibrio* spp., elucidation of the molecular mechanisms and regulation of biofilm formation will provide the foundation for developing novel treatments and prevention strategies against *Vibrio*-associated illnesses.

Acknowledgements

We thank Emily Yip and Cindy DeLoney-Marino for photos of *V. fischeri* aggregates, Linda McCarter for *V. parahaemolyticus* pictures, and Kivanc Bilecen, Sinem Beyhan and Ates Gurcan for figure preparation. We also thank members of our laboratories, Karen Ottemann and Alan Wolfe for critical reading of the manuscript. Work in our laboratories investigating biofilm formation in *Vibrio* species was supported by NIH grants AI055987 to F.H.Y. and GM59690 to K.L.V.

References

1 Faruque, S.M. *et al.* (1998) Epidemiology, genetics, and ecology of toxigenic *Vibrio cholerae*. *Microbiol. Mol. Biol. Rev.* 62, 1301–1314
2 Nair, G.B. *et al.* (2007) Global dissemination of *Vibrio parahaemolyticus* serotype O3:K6 and its serovariants. *Clin. Microbiol. Rev.* 20, 39–48
3 Gulig, P.A. *et al.* (2005) Molecular Pathogenesis of *Vibrio vulnificus*. *J. Microbiol.* 43 (Spec No), 118–131
4 Visick, K.L. and Ruby, E.G. (2006) *Vibrio fischeri* and its host: it takes two to tango. *Curr. Opin. Microbiol.* 9, 632–638
5 Donlan, R.M. and Costerton, J.W. (2002) Biofilms: survival mechanisms of clinically relevant microorganisms. *Clin. Microbiol. Rev.* 15, 167–193
6 Watnick, P.I. and Kolter, R. (1999) Steps in the development of a *Vibrio cholerae* El Tor biofilm. *Mol. Microbiol.* 34, 586–595
7 Yildiz, F.H. and Schoolnik, G.K. (1999) *Vibrio cholerae* O1 El Tor: identification of a gene cluster required for the rugose colony type, exopolysaccharide production, chlorine resistance, and biofilm formation. *Proc. Natl. Acad. Sci. U. S. A.* 96, 4028–4033
8 Faruque, S.M. *et al.* (2006) Transmissibility of cholera: *in vivo*-formed biofilms and their relationship to infectivity and persistence in the environment. *Proc. Natl. Acad. Sci. U. S. A.* 103, 6350–6355
9 Colwell, R.R. *et al.* (2003) Reduction of cholera in Bangladeshi villages by simple filtration. *Proc. Natl. Acad. Sci. U. S. A.* 100, 1051–1055
10 Nyholm, S.V. *et al.* (2000) Establishment of an animal-bacterial association: recruiting symbiotic vibrios from the environment. *Proc. Natl. Acad. Sci. U. S. A.* 97, 10231–10235
11 Yip, E.S. *et al.* (2006) The symbiosis regulator *rscS* controls the *syp* gene locus, biofilm formation and symbiotic aggregation by *Vibrio fischeri*. *Mol. Microbiol.* 62, 1586–1600
12 O'Toole, G. *et al.* (2000) Biofilm formation as microbial development. *Annu. Rev. Microbiol.* 54, 49–79
13 Watnick, P.I. *et al.* (2001) The absence of a flagellum leads to altered colony morphology, biofilm development and virulence in *Vibrio cholerae* O139. *Mol. Microbiol.* 39, 223–235
14 Lauriano, C.M. *et al.* (2004) The sodium-driven flagellar motor controls exopolysaccharide expression in *Vibrio cholerae*. *J. Bacteriol.* 186, 4864–4874
15 Kawagishi, I. *et al.* (1996) The sodium-driven polar flagellar motor of marine *Vibrio* as the mechanosensor that regulates lateral flagellar expression. *Mol. Microbiol.* 20, 693–699

16 Enos-Berlage, J.L. *et al.* (2005) Genetic determinants of biofilm development of opaque and translucent *Vibrio parahaemolyticus*. *Mol. Microbiol.* 55, 1160–1182
17 Lee, J.H. *et al.* (2004) Role of flagellum and motility in pathogenesis of *Vibrio vulnificus*. *Infect. Immun.* 72, 4905–4910
18 Hussa, E.A. *et al.* (2008) RscS functions upstream of SypG to control the *syp* locus and biofilm formation in *Vibrio fischeri*. *J. Bacteriol.* 190, 4576–4583
19 Chiavelli, D.A. *et al.* (2001) The mannose-sensitive hemagglutinin of *Vibrio cholerae* promotes adherence to zooplankton. *Appl. Environ. Microbiol.* 67, 3220–3225
20 Meibom, K.L. *et al.* (2004) The *Vibrio cholerae* chitin utilization program. *Proc. Natl. Acad. Sci. U. S. A.* 101, 2524–2529
21 Reguera, G. and Kolter, R. (2005) Virulence and the environment: a novel role for *Vibrio cholerae* toxin-coregulated pili in biofilm formation on chitin. *J. Bacteriol.* 187, 3551–3555
22 Watnick, P.I. *et al.* (1999) A role for the mannose-sensitive hemagglutinin in biofilm formation by *Vibrio cholerae* El Tor. *J. Bacteriol.* 181, 3606–3609
23 Moorthy, S. and Watnick, P.I. (2004) Genetic evidence that the *Vibrio cholerae* monolayer is a distinct stage in biofilm development. *Mol. Microbiol.* 52, 573–587
24 Hsiao, A. *et al.* (2008) Post-transcriptional cross-talk between pro- and anti-colonization pili biosynthesis systems in *Vibrio cholerae*. *Mol. Microbiol.* 67, 849–860
25 Shime-Hattori, A. *et al.* (2006) Two type IV pili of *Vibrio parahaemolyticus* play different roles in biofilm formation. *FEMS Microbiol. Lett.* 264, 89–97
26 Paranjpye, R.N. *et al.* (1998) The type IV leader peptidase/N-methyltransferase of *Vibrio vulnificus* controls factors required for adherence to HEp-2 cells and virulence in iron-overloaded mice. *Infect. Immun.* 66, 5659–5668
27 Paranjpye, R.N. and Strom, M.S. (2005) A *Vibrio vulnificus* type IV pilin contributes to biofilm formation, adherence to epithelial cells, and virulence. *Infect. Immun.* 73, 1411–1422
28 Paranjpye, R.N. *et al.* (2007) Role of type IV pilins in persistence of *Vibrio vulnificus* in Crassostrea virginica oysters. *Appl. Environ. Microbiol.* 73, 5041–5044
29 Ruby, E.G. *et al.* (2005) Complete genome sequence of *Vibrio fischeri*: a symbiotic bacterium with pathogenic congeners. *Proc. Natl. Acad. Sci. U. S. A.* 102, 3004–3009
30 Stabb, E.V. and Ruby, E.G. (2003) Contribution of *pilA* to competitive colonization of the squid Euprymna scolopes by *Vibrio fischeri*. *Appl. Environ. Microbiol.* 69, 820–826
31 Fong, J.C. and Yildiz, F.H. (2007) The *rbmBCDEF* gene cluster modulates development of rugose colony morphology and biofilm formation in *Vibrio cholerae*. *J. Bacteriol.* 189, 2319–2330
32 Yildiz, F.H. *et al.* (2004) Molecular analysis of rugosity in a *Vibrio cholerae* O1 El Tor phase variant. *Mol. Microbiol.* 53, 497–515
33 Grau, B.L. *et al.* (2008) Further characterization of *Vibrio vulnificus* rugose variants and identification of a capsular and rugose exopolysaccharide gene cluster. *Infect. Immun.* 76, 1485–1497
34 Guvener, Z.T. and McCarter, L.L. (2003) Multiple regulators control capsular polysaccharide production in *Vibrio parahaemolyticus*. *J. Bacteriol.* 185, 5431–5441
35 Darnell, C.L. *et al.* (2008) The putative hybrid sensor kinase SypF coordinates biofilm formation in *Vibrio fischeri* by acting upstream of two response regulators. *SypG and VpsR. J. Bacteriol.* 190, 4941–4950
36 Smith, A.B. and Siebeling, R.J. (2003) Identification of genetic loci required for capsular expression in *Vibrio vulnificus*. *Infect. Immun.* 71, 1091–1097
37 Enos-Berlage, J.L. and McCarter, L.L. (2000) Relation of capsular polysaccharide production and colonial cell organization to colony morphology in *Vibrio parahaemolyticus*. *J. Bacteriol.* 182, 5513–5520
38 Yip, E.S. *et al.* (2005) A novel, conserved cluster of genes promotes symbiotic colonization and sigma-dependent biofilm formation by *Vibrio fischeri*. *Mol. Microbiol.* 57, 1485–1498
39 Bush, C.A. *et al.* (1997) Classification of *Vibrio vulnificus* strains by the carbohydrate composition of their capsular polysaccharides. *Anal. Biochem.* 250, 186–195
40 Nakhamchik, A. *et al.* (2007) Identification of a Wzy polymerase required for group IV capsular polysaccharide and lipopolysaccharide biosynthesis in *Vibrio vulnificus*. *Infect. Immun.* 75, 5550–5558
41 Chatzidaki-Livanis, M. *et al.* (2006) Genetic variation in the *Vibrio vulnificus* group 1 capsular polysaccharide operon. *J. Bacteriol.* 188, 1987–1998
42 Joseph, L.A. and Wright, A.C. (2004) Expression of *Vibrio vulnificus* capsular polysaccharide inhibits biofilm formation. *J. Bacteriol.* 186, 889–893
43 Kierek, K. and Watnick, P.I. (2003) The *Vibrio cholerae* O139 O-antigen polysaccharide is essential for Ca2+-dependent biofilm development in sea water. *Proc. Natl. Acad. Sci. U. S. A.* 100, 14357–14362
44 Fong, J.C. and Yildiz, F.H. (2008) Interplay between cyclic AMP-cyclic AMP receptor protein and cyclic di-GMP signaling in *Vibrio cholerae* biofilm formation. *J. Bacteriol.* 190, 6646–6659
45 Liang, W. *et al.* (2007) The cyclic AMP receptor protein modulates colonial morphology in *Vibrio cholerae*. *Appl. Environ. Microbiol.* 73, 7482–7487
46 Yildiz, F.H. *et al.* (2001) VpsR, a Member of the Response Regulators of the Two-Component Regulatory Systems, Is Required for Expression of *vps* Biosynthesis Genes and EPS(ETr)-Associated Phenotypes in *Vibrio cholerae* O1 El Tor. *J. Bacteriol.* 183, 1716–1726
47 Casper-Lindley, C. and Yildiz, F.H. (2004) VpsT is a transcriptional regulator required for expression of *vps* biosynthesis genes and the development of rugose colonial morphology in *Vibrio cholerae* O1 El Tor. *J. Bacteriol.* 186, 1574–1578
48 Beyhan, S. *et al.* (2007) Regulation of rugosity and biofilm formation in *Vibrio cholerae*: comparison of VpsT and VpsR regulons and epistasis analysis of *vpsT, vpsR*, and *hapR*. *J. Bacteriol.* 189, 388–402
49 Kim, H.S. *et al.* (2007) Role of NtrC in biofilm formation via controlling expression of the gene encoding an ADP-glycero-manno-heptose-6-epimerase in the pathogenic bacterium, *Vibrio vulnificus*. *Mol. Microbiol.* 63, 559–574
50 Waters, C.M. and Bassler, B.L. (2005) Quorum sensing: cell-to-cell communication in bacteria. *Annu. Rev. Cell Dev. Biol.* 21, 319–346
51 McCarter, L.L. (1998) OpaR, a homolog of *Vibrio harveyi* LuxR, controls opacity of *Vibrio parahaemolyticus*. *J. Bacteriol.* 180, 3166–3173
52 Lee, J.H. *et al.* (2007) Identification and functional analysis of *Vibrio vulnificus* SmcR, a novel global regulator. *J. Microbiol. Biotechnol.* 17, 325–334
53 Fidopiastis, P.M. *et al.* (2002) LitR, a new transcriptional activator in *Vibrio fischeri*, regulates luminescence and symbiotic light organ colonization. *Mol. Microbiol.* 45, 131–143
54 Hammer, B.K. and Bassler, B.L. (2003) Quorum sensing controls biofilm formation in *Vibrio cholerae*. *Mol. Microbiol.* 50, 101–104
55 Zhu, J. and Mekalanos, J.J. (2003) Quorum sensing-dependent biofilms enhance colonization in *Vibrio cholerae*. *Dev. Cell* 5, 647–656
56 Waters, C.M. *et al.* (2008) Quorum sensing controls biofilm formation in *Vibrio cholerae* through modulation of cyclic di-GMP levels and repression of *vpsT*. *J. Bacteriol.* 190, 2527–2536
57 Romling, U. and Amikam, D. (2006) Cyclic di-GMP as a second messenger. *Curr. Opin. Microbiol.* 9, 218–228
58 Ferreira, R.B. *et al.* (2008) *Vibrio parahaemolyticus* ScrC modulates cyclic dimeric GMP regulation of gene expression relevant to growth on surfaces. *J. Bacteriol.* 190, 851–860
59 Kim, Y.K. and McCarter, L.L. (2007) ScrG, a GGDEF-EAL protein, participates in regulating swarming and sticking in *Vibrio parahaemolyticus*. *J. Bacteriol.* 189, 4094–4107
60 Lim, B. *et al.* (2006) Cyclic-diGMP signal transduction systems in *Vibrio cholerae*: modulation of rugosity and biofilm formation. *Mol. Microbiol.* 60, 331–348
61 Nakhamchik, A. *et al.* (2008) Cyclic-di-GMP regulates extracellular polysaccharide production, biofilm formation, and rugose colony development by *Vibrio vulnificus*. *Appl. Environ. Microbiol.* 74, 4199–4209
62 Tischler, A.D. and Camilli, A. (2004) Cyclic diguanylate (c-di-GMP) regulates *Vibrio cholerae* biofilm formation. *Mol. Microbiol.* 53, 857–869
63 Galperin, M.Y. *et al.* (2001) Novel domains of the prokaryotic two-component signal transduction systems. *FEMS Microbiol. Lett.* 203, 11–21

64 Beyhan, S. *et al.* (2006) Transcriptome and phenotypic responses of *Vibrio cholerae* to increased cyclic di-GMP level. *J. Bacteriol.* 188, 3600–3613
65 Tamayo, R. *et al.* (2008) Role of cyclic Di-GMP during El tor biotype *Vibrio cholerae* infection: characterization of the *in vivo*-induced cyclic Di-GMP phosphodiesterase CdpA. *Infect. Immun.* 76, 1617–1627
66 Yildiz, F.H. and Kolter, R. (2008) Genetics and Microbiology of Biofilm Formation by Vibrio cholerae. In *Vibrio cholerae: Genomics and Molecular Biology* (Faruque, S.M. and Nair, G.B., eds), pp. 123–139, Caister Academic Press
67 Beyhan, S. and Yildiz, F.H. (2007) Smooth to rugose phase variation in *Vibrio cholerae* can be mediated by a single nucleotide change that targets c-di-GMP signalling pathway. *Mol. Microbiol.* 63, 995–1007
68 Beyhan, S. *et al.* (2008) Identification and characterization of cyclic diguanylate signaling systems controlling rugosity in *Vibrio cholerae*. *J. Bacteriol.* 190, 7392–7405
69 Boles, B.R. and McCarter, L.L. (2002) *Vibrio parahaemolyticus scrABC*, a novel operon affecting swarming and capsular polysaccharide regulation. *J. Bacteriol.* 184, 5946–5954
70 O'Shea, T.M. *et al.* (2006) Diguanylate cyclases control magnesium-dependent motility of *Vibrio fischeri*. *J. Bacteriol.* 188, 8196–8205
71 Pratt, J.T. *et al.* (2007) PilZ domain proteins bind cyclic diguanylate and regulate diverse processes in *Vibrio cholerae*. *J. Biol. Chem.* 282, 12860–12870
72 Grau, B.L. *et al.* (2005) High-frequency phase variation of *Vibrio vulnificus* 1003: isolation and characterization of a rugose phenotypic variant. *J. Bacteriol.* 187, 2519–2525
73 Higgins, D.A. *et al.* (2007) The major *Vibrio cholerae* autoinducer and its role in virulence factor production. *Nature* 450, 883–886
74 Lenz, D.H. *et al.* (2005) CsrA and three redundant small RNAs regulate quorum sensing in *Vibrio cholerae*. *Mol. Microbiol.* 58, 1186–1202

Molecular Microbiology (2009) 74(4), 782–789 ■
doi:10.1111/j.1365-2958.2009.06899.x
First published online 14 October 2009

MicroReview

An intricate network of regulators controls biofilm formation and colonization by *Vibrio fischeri*

Karen L. Visick*
Department of Microbiology and Immunology, Loyola University Medical Center, Maywood, IL 60153, USA.

Summary

The initial encounter between a microbe and its host can dictate the success of the interaction, be it symbiosis or pathogenesis. This is the case, for example, in the symbiosis between the bacterium *Vibrio fischeri* and the squid *Euprymna scolopes*, which proceeds via a biofilm-like bacterial aggregation, followed by entry and growth. A key regulator, the sensor kinase RscS, is critical for symbiotic biofilm formation and colonization. When introduced into a fish symbiont strain that naturally lacks the *rscS* gene and cannot colonize squid, RscS permits colonization, thereby extending the host range of these bacteria. RscS controls biofilm formation by inducing transcription of the symbiosis polysaccharide (*syp*) gene locus. Transcription of *syp* also requires the σ^{54}-dependent activator SypG, which functions downstream of RscS. In addition to these regulators, SypE, a response regulator that lacks an apparent DNA binding domain, exerts both positive and negative control over biofilm formation. The putative sensor kinase SypF and the putative response regulator VpsR, both of which contribute to control of cellulose production, also influence biofilm formation. The wealth of regulators and the correlation between biofilm formation and colonization adds to the already considerable utility of the *V. fischeri–E. scolopes* model system.

Introduction

Twenty years after the model system was established, the symbiosis between the bacterium *Vibrio fischeri* and its symbiotic host, the squid *Euprymna scolopes*, continues to provide rich and novel insights into a variety of problems in bacteria–host interactions (reviewed by Stabb, 2006; Visick and Ruby, 2006; McFall-Ngai, 2008; Ruby, 2008). Indeed, in the past year alone, researchers have uncovered numerous components of the bacteria–host interaction network, including the ability of the squid's symbiotic light organ to respond to light, colonization and bacterially released small molecules including autoinducers and a component of peptidoglycan, tracheal cytotoxin (Chun *et al.*, 2008; Tong *et al.*, 2009; Troll *et al.*, 2009). These studies suggest an interaction of a complexity that rivals that of traditional mammalian models. Furthermore, host defence cells called haemocytes contribute to specificity by binding to and engulfing non-native or mutant bacteria preferentially over native symbionts, thus demonstrating the utility of this system as a model for innate immunity (Nyholm *et al.*, 2009). Understanding of the evolution and ecology of the interaction has advanced through studies of natural populations combined with experimental manipulations, which suggested that a limited number of bacteria (1–2) likely enter and populate each of the six internal crypts that comprise the light organ of the newly hatched and initially uncolonized squid; as a result, polyclonal but segregated populations can exist within a single squid (Wollenberg and Ruby, 2009). Finally, genomic analysis of representative symbiotic and non-symbiotic *V. fischeri* strains led to the recognition that a single regulatory gene, *rscS*, could be sufficient to alter host specificity, as it enabled a fish symbiont to colonize squid (Mandel *et al.*, 2009). The molecular details underlying the influence of this regulator on colonization and specificity will be the main subjects of this review.

Symbiotic initiation and host specificity

The *V. fischeri–E. scolopes* symbiosis is highly specific. Juvenile squid hatch uncolonized but become colonized within hours following exposure to symbiosis-competent bacteria. Despite the presence of numerous other bacteria in the seawater, including closely related bacteria such as *Vibrio parahaemolyticus*, only *V. fischeri* successfully colonizes the squid's symbiotic light organ (McFall-Ngai

Accepted 22 September, 2009. *For correspondence. E-mail kvisick@lumc.edu; Tel. (+1) 708 216 0869; Fax (+1) 708 216 9574.

and Ruby, 1991). Furthermore, not all strains of *V. fischeri* are equally capable of colonizing, or are even symbiosis-competent (Nishiguchi *et al*., 1998; Ruby and Lee, 1998). For example, *V. fischeri* strains isolated from symbiosis with the fish *Monocentris japonica* generally fail to colonize *E. scolopes* (Mandel *et al*., 2009).

A number of factors contribute to this remarkable host specificity. Upon entering the light organ, *V. fischeri* must pass through mucus-filled ducts that contain outward-beating cilia (McFall-Ngai and Ruby, 1998; Visick and McFall-Ngai, 2000) and nitric oxide (Davidson *et al*., 2004), an antibacterial defence. In addition, the crypts contain halide peroxidase, a host defence protein that catalyses the production of hypochlorous acid, which is toxic to bacteria (Tomarev *et al*., 1993; Weis *et al*., 1996; Small and McFall-Ngai, 1999). Finally, macrophage-like haemocytes circulate within the crypts (Nyholm and McFall-Ngai, 1998). *V. fischeri* must survive each of these host-imposed stresses that presumably decrease the chances of colonization by other microbes.

Surprisingly, host specificity appears to begin even before the bacteria enter the ducts. Newly hatched juvenile squid exhibit a short permissive period in which non-symbionts (and even particles such as beads) can enter the light organ, followed by a non-permissive period during which nothing can enter (Nyholm *et al*., 2002). Subsequently, mucus is secreted to the surface of the light organ (Nyholm *et al*., 2000; 2002). *V. fischeri* aggregates within this mucus, an event that is critical to colonization (Nyholm *et al*., 2000; Yip *et al*., 2006). For example, a mutant lacking the sensor kinase RscS fails to aggregate, a phenotype that correlates well with its severe defect in symbiotic initiation (Visick and Skoufos, 2001; Yip *et al*., 2006). Studies of additional mutants have provided further support for the connections observed between aggregation and initiation of colonization (Millikan and Ruby, 2002; Whistler *et al*., 2006).

Some non-symbionts, such as the closely related *V. parahaemolyticus*, appear to be capable of adhering to the light organ, but others, such as the Gram-positive *Bacillus cereus*, are not, supporting the idea that specificity occurs at this stage of colonization (Nyholm *et al*., 2000). Furthermore, a 1:1 mixture of *V. fischeri* and the non-symbiont *V. parahaemolyticus* results in an aggregate consisting of more than 80% *V. fischeri* cells (Nyholm and McFall-Ngai, 2003). These latter data suggest that specificity results, in part, from a superior ability of *V. fischeri* to interact with the surface of the squid's light organ.

RscS and colonization

Initiation of symbiotic colonization requires a two-component sensor kinase gene that we designated *rscS*, for regulator of symbiotic colonization sensor (Visick and Skoufos, 2001). A subset of juvenile squid exposed to an *rscS* mutant remain uncolonized, while the rest become colonized only after a significant delay (Visick and Skoufos, 2001). Initial characterization failed to reveal defects in any known or suspected colonization traits, including motility and bioluminescence; however, subsequent studies (described below) uncovered an important role for RscS in inducing biofilm formation. The symbiotic defect of the *rscS* mutant is likely to be due to its failure to aggregate on the surface of the light organ, an event that we hypothesize to correspond to biofilm formation (Yip *et al*., 2006).

In the sequenced squid symbiont strain ES114, the *rscS* gene is located between *glpR* and *glpK*, genes involved in glycerol regulation and metabolism respectively (Visick and Skoufos, 2001; Ruby *et al*., 2005). When the genome of a second *V. fischeri* strain, the *M. japonica* isolate MJ11, became available, it was noted that *rscS* is absent from the *glp* locus (Mandel *et al*., 2009). Because the fish symbiont is not proficient at squid colonization, it was proposed that lack of *rscS* could account for the colonization deficiency of this strain. Indeed, introduction of *rscS* on a multicopy plasmid permits squid colonization by MJ11 (Mandel *et al*., 2009). These data demonstrated that RscS alone is sufficient to extend the host range of *V. fischeri* from fish to squid. In further support of this notion, disruption of *rscS* in a variety of *V. fischeri* isolates from different geographic locations impairs symbiotic initiation (Mandel *et al*., 2009). These results demonstrate that a single regulatory gene can alter the host range of an animal-associated microorganism and point to RscS and the genes it controls as key regulators of early steps in host colonization.

RscS and the syp *locus*

RscS is predicted to be a member of the histidine sensor kinase class of two-component regulators (Visick and Skoufos, 2001). Sensor kinases typically sense specific environmental signals and transduce that information by initiating a phosphorelay, resulting in the phosphorylation of their cognate response regulators and thus an output such as altered transcription of target genes (Gao and Stock, 2009). The gene for *rscS*, however, is not linked to a gene encoding a response regulator, and the 40 response regulators recognizably encoded in the *V. fischeri* genome made the hunt for a partner non-trivial (Hussa *et al*., 2007). Furthermore, neither a partner nor a target could be readily identified based on similarity in phenotype, as the *rscS* mutant does not exhibit any phenotype in culture (Visick and Skoufos, 2001).

A breakthrough in understanding the role of RscS came with the discovery of an 18-gene symbiosis

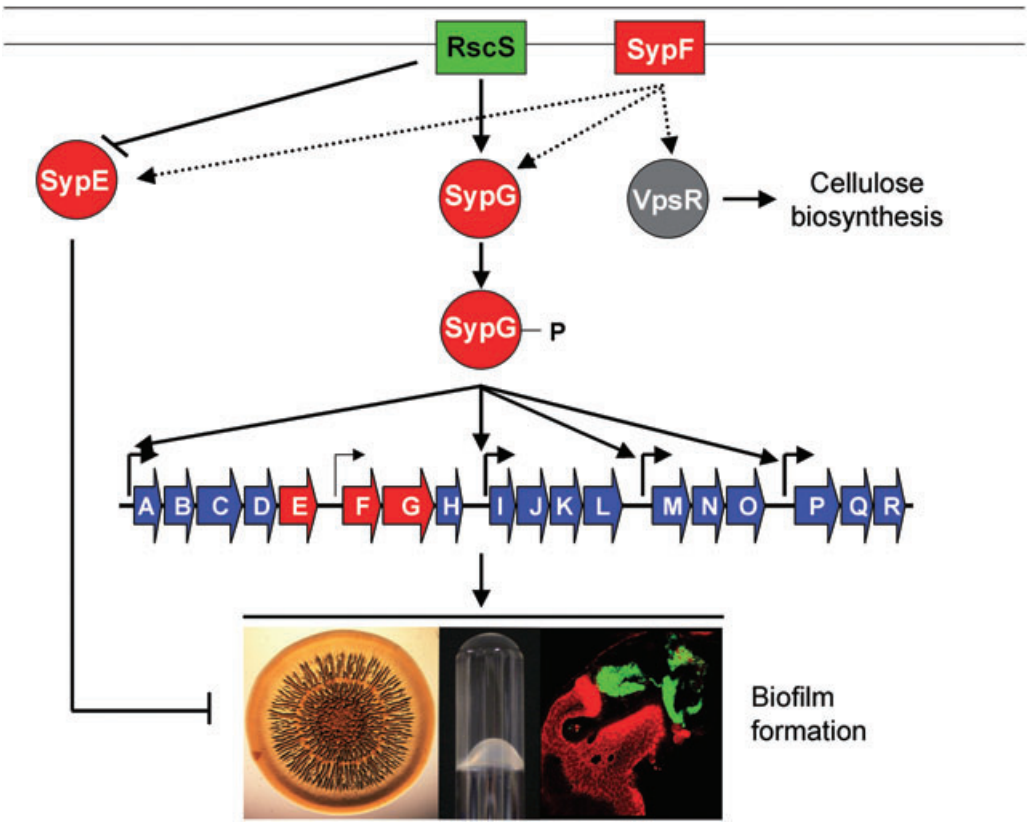

Fig. 1. Model for control of biofilm formation in *V. fischeri*. Depicted here is a model based on current data regarding the potential roles of the *syp* regulators. The sensor kinase RscS acts upstream of SypG, presumably serving as a phosphodonor in response to some as-yet-unidentified environmental signal, perhaps from the squid. Once phosphorylated, SypG is predicted to directly bind to sequences upstream of each of four *syp* operons to activate *syp* transcription by σ^{54}-containing RNA polymerase. The Syp proteins contribute to biofilm formation in culture, including the formation of wrinkled colonies and pellicles, as well as *in situ* biofilm formation and colonization. RscS overproduction also appears to inactivate SypE, which inhibits biofilm formation induced by overproduction of SypG at a level downstream from *syp* transcription; how RscS inactivates SypE is as yet unknown. Biofilm formation can be also induced by overexpression of a *sypF* allele with increased activity (SypF1) in a manner that depends in part on SypG and SypE, and in part on VpsR, which promotes cellulose biosynthesis.

polysaccharide gene locus, *syp* (Yip *et al*., 2005; 2006). Mutants defective for specific *syp* genes exhibit phenotypes similar to those of the *rscS* mutant: defective for symbiotic initiation, but not for a variety of traits tested in culture (Yip *et al*., 2005). The *syp* genes encode proteins with similarity to those involved in exopolysaccharide biosynthesis, including six putative glycosyltransferase genes. Of note, the *syp* locus also encodes two response regulators, potential partners for RscS. One of them, SypG, is a putative a σ^{54}-dependent enhancer binding protein, while the other, SypE, lacks any apparent DNA binding sequences.

A connection between RscS and *syp* was made when RscS was overproduced in a *syp* reporter strain. Because RscS is predicted to sense an environmental signal, potentially missing under standard laboratory conditions, a plasmid containing the *rscS* gene was mutagenized in an attempt to generate an allele with increased activity. This approach yielded a plasmid that substantially overproduces the RscS protein, resulting in increased transcription of the *syp* locus (Yip *et al*., 2006; Geszvain and Visick, 2008a). It also induces biofilm formation: whereas control cells produce smooth colonies, *rscS*-overexpressing cells produce wrinkled colonies (Fig. 1). This wrinkled colony phenotype is similar to other biofilm-forming *Vibrio* species such as *Vibrio cholerae*, which produces rugose colonies under certain conditions (Yildiz and Visick, 2009). Furthermore, *rscS*-overexpressing cells produce a thick pellicle at the air–liquid interface of statically grown cultures, a phenomenon not seen with wild-type *V. fischeri* (Yip *et al*., 2006); incredibly, these pellicles are so strong that the cultures can be inverted without loss of the liquid medium (Fig. 1). These biofilm phenotypes depend upon a functional *syp* locus as well as RscS overproduction.

The physiological importance of these biofilm phenotypes was underscored by the finding that RscS-overproducing cells form substantially enhanced aggregates on the surface of the light organ – upwards of 20× bigger than controls. As with the *in vivo* biofilms,

disruption of the *syp* locus eliminates or substantially reduces the size of the symbiotic aggregates induced by RscS. Importantly, this RscS-directed activity substantially promotes symbiotic colonization, as determined by competitive colonization experiments: squid inoculated with mixtures of vector-control and RscS-overexpressing wild-type cells become colonized exclusively by those that contain the RscS expression plasmid (Yip *et al*., 2006).

In summary, a major function of RscS appears to be in controlling the *syp* locus, resulting in biofilm formation and symbiotic colonization. The ability of RscS to induce squid colonization by normally non-symbiotic strain MJ11 can likely be attributed to its ability to promote symbiotic biofilm formation, although this idea has not yet been directly tested. In support of it, however, are the findings that the *syp* locus is conserved in MJ11 and that RscS overexpression promotes biofilm formation by MJ11 (Mandel *et al*., 2009).

RscS integrates positive and negative signals

RscS is predicted to be a hybrid sensor kinase. The C-terminus contains putative histidine kinase/ATPase (HisKA/HATPase), receiver (REC) and histidine phosphotransferase (Hpt) domains (Visick and Skoufos, 2001). This domain structure is similar to such well-characterized proteins as ArcB and BvgS that undergo two internal phosphorelay events prior to donation of the phosphoryl group to the cognate response regulator (Beier and Gross, 2008; Gao and Stock, 2009). Such additional domains involved in an intramolecular phosphorelay provide opportunities for multiple levels of control. The N-terminal region of RscS contains a large periplasmic domain flanked by two transmembrane helices, and a cytoplasmic PAS domain, all of which could contribute to sensory perception. The natural ligand(s) remains unknown, however.

Mutant alleles of *rscS* were constructed to study the roles of the various domains (Geszvain and Visick, 2008b). Perhaps not surprisingly, alterations of key residues in the HisKA and REC domains disrupt function, as measured by induction of *syp* transcription and biofilm formation. These data indicate that RscS functions as a kinase. In contrast, a substitution within the Hpt domain at a histidine predicted to be critical for phosphotransfer reduces but does not eliminate function. Perhaps the specific change facilitates phosphotransfer to the downstream response regulator from the conserved histidine within the HisKA domain, or perhaps the putative Hpt domain does not function as an Hpt. Additional work will be necessary to clarify the role of the predicted Hpt domain.

Substitutions of key residues in the PAS domain also abolish RscS activity. In RscS, the predicted location of the PAS domain is on the cytoplasmic face of the inner membrane, where it might be expected to respond to an internal cue. PAS domains in other proteins detect small molecules such as FAD or FMN, light or oxygen (Taylor and Zhulin, 1999). Alterations to residues predicted to be involved in binding FAD lead to a greater disruption in RscS activity than do substitutions in those predicted to be critical for FMN binding, suggesting that the PAS domain of RscS might bind to a FAD cofactor (Geszvain and Visick, 2008b).

Signalling by FAD, if it occurs, might be influenced by membrane localization and/or by signalling through the periplasmic loop or transmembrane regions. Indeed, membrane localization of RscS seems important, as a deletion derivative containing only the cytoplasmic portion of the protein (including PAS) exhibits reduced activity (Geszvain and Visick, 2008b). Surprisingly, however, deletions of the periplasmic loop result in increased activity, as do some substitutions within the first transmembrane helix, indicating that binding of an unidentified ligand to the periplasmic domain might inhibit, rather than activate, RscS activity. Together, these data reveal that RscS is a complex regulator, potentially integrating both inhibitory and stimulatory signals to initiate a phosphorelay that critically requires predicted phosphorylated residues in the HisKA and REC but not Hpt domains. An exciting future direction of this work will be to determine the nature of the signal(s) received by RscS.

RscS works upstream of SypG

The availability of RscS-induced phenotypes permitted a search for the response regulator(s) that functions downstream of RscS (Hussa *et al*., 2008). The *rscS* overexpression plasmid was introduced into each of 35 response regulator mutants (all but five of the 40 encoded by the *V. fischeri* genome), and the resulting phenotypes were evaluated. Most mutants exhibit biofilm phenotypes indistinguishable from those of the wild-type overexpression control. In several cases, some measures of biofilm formation (including glass attachment and pellicles) were impacted by disruption of specific response regulators, including *sypG*, *sypE*, *vpsR*, *flrC*, *arcA* and *VF1401*. However, wrinkled colony formation is affected only by the disruption of either *sypG* or *sypE*, and induction of *syp* transcription by RscS depends only on *sypG*. The strong requirement for SypG in all RscS-induced phenotypes suggests that RscS works upstream of SypG (Hussa *et al*., 2008).

Somewhat inconsistent with the above conclusion is the finding that overproduction of SypG alone does not induce the formation of wrinkled colonies or strong pellicles, although it does induce *syp* transcription. Furthermore, altering SypG by substituting glutamate for a conserved

aspartate, a change that in many other response regulators produces a constitutively active protein (e.g. Freeman and Bassler, 1999), increases *syp* induction but does not promote biofilm formation (Hussa *et al*., 2008). Although it is not always the case that the phenotypes of response regulators phenocopy those of their partner sensor kinases, these data raised the possibility that additional factors might be involved. Indeed, it was subsequently determined that deletion of the response regulator gene *sypE* permits the SypG overproduction strain to form wrinkled colonies and pellicles (Hussa *et al*., 2008). This latter work thus established conditions under which overproduced SypG and overproduced RscS could induce similar phenotypes, supporting the idea that these proteins could work together. Furthermore, it appears that overproduction of RscS must somehow lead to inactivation of SypE. The role of SypE will be discussed further below.

SypG and σ^{54} regulate syp *transcription*

SypG is a putative σ^{54}-dependent response regulator, and binding sites for σ^{54}-containing RNA polymerase exist within the *syp* locus (Fig. 1). Specifically, σ^{54} sites exist within each of the four largest gaps between genes of the 18-gene *syp* locus (Yip *et al*., 2005). Results from primer extension experiments designed to map the start sites of three of the genes (*sypA*, *sypI* and *sypM*) are consistent with the putative σ^{54}-dependent promoters, and mutagenesis studies verify that transcription of at least *sypD* and *sypN* depends upon the gene for σ^{54}, *rpoN* (Yip *et al*., 2005). Because σ^{54}-containing RNA polymerase requires a transcriptional activator to provide the energy for open complex formation (Buck *et al*., 2000), it seems reasonable that the *syp* locus would require an activator such as SypG to bind and activate transcription. Indeed, bioinformatic analysis revealed the presence of a conserved 22 bp sequence upstream of each of the putative σ^{54} binding sites that we hypothesize to be the SypG binding site (Yip *et al*., 2005). Our preliminary data support the importance of the conserved sequences in *syp* transcription (E.A. Hussa and K.L. Visick, unpublished), but the precise role remains to be determined.

SypE, a novel response regulator

Although RscS functions upstream of SypG, the regulatory network is far from straightforward. Biofilm formation, while readily induced by overexpression of RscS, requires inactivation of *sypE* when SypG is overproduced. However, loss of SypE impairs biofilm formation induced by RscS. Thus, SypE appears to play both positive and negative roles in biofilm formation. Loss of *sypE* exerts only small effects on *syp* transcription, regardless of whether RscS or SypG is overproduced, suggesting that its impact is not at the level of *syp* transcription (Hussa *et al*., 2008 and E.A. Hussa and K.L. Visick, unpublished). These data indicate that SypE controls biofilm formation at another level, such as post-transcriptional control of the synthesis of the Syp polysaccharide or via control of the synthesis of another component or regulator of the biofilm matrix.

SypE is an unusual two-component response regulator in that its REC domain is located in the centre of the protein (Yip *et al*., 2005). In addition, instead of the typical DNA binding domain, SypE contains a putative serine kinase domain in its N-terminus and a putative serine phosphatase domain in its C-terminus. The potential opposing activities of these domains suggest a possible molecular basis for the apparent dual role of this protein in controlling biofilm formation. The phosphorylation state of the REC domain might then determine which activity is favoured.

SypE thus is another complex regulator of biofilm formation in *V. fischeri*. Although the *syp* locus is conserved in many *Vibrio* species, *sypE* is generally lacking in these other *syp* loci (Yip *et al*., 2005). These data suggest that *V. fischeri* uses SypE to fine-tune its control of biofilm formation, perhaps to coordinate Syp production with other factors necessary for squid colonization. However, SypE itself is not a critical colonization factor, as disruption of *sypE* does not prevent symbiotic initiation (Hussa *et al*., 2007). Many intriguing questions remain to be answered about this unusual regulatory protein.

Roles for SypF and VpsR

In addition to the response regulators SypE and SypG, the *syp* cluster encodes a hybrid sensor kinase, SypF. Like RscS, SypF contains three domains predicted to be involved in a phosphorelay, HisKA/HATPase, REC and Htp, as well as a putative periplasmic loop (Yip *et al*., 2005). Overproduction of SypF exerts no discernible effect on biofilm formation. However, an increased activity allele, *sypF1*, was isolated that induces wrinkled colony formation, pellicle production, and increased adherence to a glass surface (Darnell *et al*., 2008). SypF1 contains a serine to phenylalanine change at amino acid 247. S247 is located within the HisKA domain, three residues N-terminal to the conserved histidine predicted to be the site of phosphorylation; a change at this position could impact kinase activity. However, the involvement of these conserved residues in a phosphorelay has not yet been assessed biochemically.

Given the location of *sypF* between the response regulator genes *sypE* and *sypG*, it seemed likely that one or

both would be necessary for SypF1-mediated induction of biofilm formation. However, the biofilm phenotypes are reduced, but not eliminated, in *sypE* and *sypG* mutants (Darnell *et al.*, 2008). Subsequent work revealed that the residual biofilm formation induced by SypF1 overexpression in *sypE* and *sypG* mutants depends on an unlinked gene encoding VpsR, a putative response regulator. Disruption of only *vpsR* also fails to eliminate biofilm formation, but a *vpsR sypG* double mutant mimics the uninduced wild type. These data indicate that, at least under these conditions, SypF contributes to biofilm control through two distinct pathways.

VpsR exhibits sequence similarity to a protein with the same name in *V. cholerae* (Yildiz *et al.*, 2001; Darnell *et al.*, 2008). The *V. cholerae* protein is a major regulator of biofilm formation, through its control of the *vps* polysaccharide locus (Yildiz *et al.*, 2001). Although *V. fischeri* contains genes similar to those within one segment of the *V. cholerae vps* locus (termed *vps-II*), this locus does not appear to be responsible for the biofilms induced by SypF1 overexpression. Instead, *V. fischeri* (but not *V. cholerae*) contains a cellulose biosynthesis locus that is necessary for biofilm formation induced by SypF1 overproduction (Darnell *et al.*, 2008). Similarly, overproduction of VpsR also induces the formation of a cellulose-dependent biofilm. The roles of SypF, VpsR, and cellulose in biofilm formation and symbiotic colonization need to be clarified although, intriguingly, a mutant defective for *vpsR* exhibits a small defect in symbiotic initiation (Hussa *et al.*, 2007).

Concluding remarks

Wild-type *V. fischeri* does not make impressive biofilms in culture. However, through genetic analysis and an appreciation of the natural symbiotic lifestyle of the organism, remarkable progress has been made to elucidate a complex regulatory network that controls biofilm formation (Fig. 1). The integrated signalling circuitry underlying biofilm development and symbiosis includes the hybrid sensor kinase RscS (a protein that is sufficient to broaden the host range of *V. fischeri* to include *E. scolopes*) and the downstream response regulator, SypG. Together, these proteins respond to as-yet-unknown squid or environmental signals and activate transcription of the symbiosis polysaccharide (*syp*) locus, which leads to biofilm-dependent initiation of colonization. An additional, novel response regulator, SypE, interacts with the RscS-SypG pathway and plays both positive and negative roles in control of biofilm formation. Adding to the complexity, production of the Syp polysaccharide might be coordinated with the biosynthesis of cellulose, through the putative sensor kinase SypF and the putative response regulator VpsR. A potential model that encompasses these findings is that multiple signals are received and integrated such that *V. fischeri* produces one type of biofilm (e.g. Syp-produced) at some stage(s) of its symbiotic or free-living life cycle and a distinct type (e.g. cellulose) at another stage(s).

While much remains to be understood, evidence to date suggests that some aspect of the *V. fischeri* interaction with its host activates biofilm formation – at least during the initial encounter, if not beyond. Negative control also appears to be important – perhaps to fine-tune synthesis of biofilm components, to produce a distinct type of biofilm under different conditions, or even to turn biofilm formation off when it is not needed. This system is one of the few in which factors involved in biofilm formation in culture have been clearly correlated with biofilm formation in a natural model of bacteria–animal associations. This ability to correlate biofilm formation in culture and during the association of *V. fischeri* with *E. scolopes* thus adds to the already considerable versatility and utility of this remarkable model system for the study of both benign and pathogenic interactions between bacteria and eukaryotes.

Acknowledgements

I thank Mark Mandel, Alan Wolfe, Jon Visick and past and present members of my lab for many wonderful discussions and for their suggestions on this manuscript, and Satoshi Shibata for donating an image for Fig. 1. I also gratefully acknowledge funding from the National Institutes of Health (GM59690 to KLV.), which supports our work investigating RscS, the *syp* locus and symbiotic colonization by *V. fischeri*.

References

Beier, D., and Gross, R. (2008) The BvgS/BvgA phosphorelay system of pathogenic *Bordetellae*: structure, function and evolution. *Adv Exp Med Biol* **631:** 149–160.

Buck, M., Gallegos, M.-T., Studholme, D.J., Guo, Y., and Gralla, J.D. (2000) The bacterial enhancer-dependent σ^{54} (σ^{N}) transcription factor. *J Bacteriol* **182:** 4129–4136.

Chun, C.K., Troll, J.V., Koroleva, I., Brown, B., Manzella, L., Snir, E., *et al.* (2008) Effects of colonization, luminescence, and autoinducer on host transcription during development of the squid–vibrio association. *Proc Natl Acad Sci USA* **105:** 11323–11328.

Darnell, C.L., Hussa, E.A., and Visick, K.L. (2008) The putative hybrid sensor kinase SypF coordinates biofilm formation in *Vibrio fischeri* by acting upstream of two response regulators, SypG and VpsR. *J Bacteriol* **190:** 4941–4950.

Davidson, S.K., Koropatnick, T.A., Kossmehl, R., Sycuro, L., and McFall-Ngai, M.J. (2004) NO means 'yes' in the squid-vibrio symbiosis: nitric oxide (NO) during the initial stages of a beneficial association. *Cell Microbiol* **6:** 1139–1151.

Freeman, J.A., and Bassler, B.L. (1999) A genetic analysis of the function of LuxO, a two-component response regulator involved in quorum sensing in *Vibrio harveyi*. *Mol Microbiol* **31:** 665–677.

Gao, R., and Stock, A.M. (2009) Biological insights from structures of two-component proteins. *Annu Rev Microbiol* **63:** 133–154.

Geszvain, K., and Visick, K.L. (2008a) Multiple factors contribute to keeping levels of the symbiosis regulator RscS low. *FEMS Microbiol Lett* **285:** 33–39.

Geszvain, K., and Visick, K.L. (2008b) The hybrid sensor kinase RscS integrates positive and negative signals to modulate biofilm formation in *Vibrio fischeri*. *J Bacteriol* **190:** 4437–4446.

Hussa, E.A., O'Shea, T.M., Darnell, C.L., Ruby, E.G., and Visick, K.L. (2007) Two-component response regulators of *Vibrio fischeri*: identification, mutagenesis and characterization. *J Bacteriol* **189:** 5825–5838.

Hussa, E.A., Darnell, C.L., and Visick, K.L. (2008) RscS functions upstream of SypG to control the *syp* locus and biofilm formation in *Vibrio fischeri*. *J Bacteriol* **190:** 4576–4583.

McFall-Ngai, M. (2008) Host-microbe symbiosis: the squid–Vibrio association – a naturally occurring, experimental model of animal/bacterial partnerships. *Adv Exp Med Biol* **635:** 102–112.

McFall-Ngai, M.J., and Ruby, E.G. (1991) Symbiont recognition and subsequent morphogenesis as early events in an animal-bacterial mutualism. *Science* **254:** 1491–1494.

McFall-Ngai, M.J., and Ruby, E.G. (1998) Sepiolids and vibrios: when first they meet. Reciprocal interactions between host and symbiont lead to the creation of a complex light-emitting organ. *Bioscience* **48:** 257–265.

Mandel, M.J., Wollenberg, M.S., Stabb, E.V., Visick, K.L., and Ruby, E.G. (2009) A single regulatory gene is sufficient to alter bacterial host range. *Nature* **458:** 215–218.

Millikan, D.S., and Ruby, E.G. (2002) Alterations in *Vibrio fischeri* motility correlate with a delay in symbiosis initiation and are associated with additional symbiotic colonization defects. *Appl Environ Microbiol* **68:** 2519–2528.

Nishiguchi, M.K., Ruby, E.G., and McFall-Ngai, M.J. (1998) Competitive dominance among strains of luminous bacteria provides an unusual form of evidence for parallel evolution in sepiolid squid-vibrio symbioses. *Appl Environ Microbiol* **64:** 3209–3213.

Nyholm, S.V., and McFall-Ngai, M.J. (1998) Sampling the light-organ microenvironment of *Euprymna scolopes*: description of a population of host cells in association with the bacterial symbiont *Vibrio fischeri*. *Biol Bull* **195:** 89–97.

Nyholm, S.V., and McFall-Ngai, M.J. (2003) Dominance of *Vibrio fischeri* in secreted mucus outside the light organ of *Euprymna scolopes*: the first site of symbiont specificity. *Appl Environ Microbiol* **69:** 3932–3937.

Nyholm, S.V., Stabb, E.V., Ruby, E.G., and McFall-Ngai, M.J. (2000) Establishment of an animal–bacterial association: recruiting symbiotic vibrios from the environment. *Proc Natl Acad Sci USA* **97:** 10231–10235.

Nyholm, S.V., Deplancke, B., Gaskins, H.R., Apicella, M.A., and McFall-Ngai, M.J. (2002) Roles of *Vibrio fischeri* and nonsymbiotic bacteria in the dynamics of mucus secretion during symbiont colonization of the *Euprymna scolopes* light organ. *Appl Environ Microbiol* **68:** 5113–5122.

Nyholm, S.V., Stewart, J.J., Ruby, E.G., and McFall-Ngai, M.J. (2009) Recognition between symbiotic *Vibrio fischeri* and the haemocytes of *Euprymna scolopes*. *Environ Microbiol* **11:** 483–493.

Ruby, E.G. (2008) Symbiotic conversations are revealed under genetic interrogation. *Nat Rev Microbiol* **6:** 752–762.

Ruby, E.G., and Lee, K.-H. (1998) The *Vibrio fischeri-Euprymna scolopes* light organ association: current ecological paradigms. *App Environ Microbiol* **64:** 805–812.

Ruby, E.G., Urbanowski, M., Campbell, J., Dunn, A., Faini, M., Gunsalus, R., *et al.* (2005) Complete genome sequence of *Vibrio fischeri*: a symbiotic bacterium with pathogenic congeners. *Proc Nat Acad Sci USA* **102:** 3004–3009.

Small, A., and McFall-Ngai, M. (1999) Halide peroxidase in tissues that interact with bacteria in the host squid *Euprymna scolopes*. *J Cell Biochem* **72:** 445–457.

Stabb, E.V. (2006) The *Vibrio fischeri-Euprymna scolopes* light organ symbiosis. In *The Biology of Vibrios*. Thompson, F.L., Austin, B., and Swings, J. (eds). Washington, DC: ASM Press, pp. 204–218.

Taylor, B.L., and Zhulin, I.B. (1999) PAS domains: internal sensors of oxygen, redox potential, and light. *Microbiol Mol Biol Rev* **63:** 479–506.

Tomarev, S.I., Zinovieva, R.D., Weis, V.M., Chepelinsky, A.B., Piatigorsky, J., and McFall-Ngai, M.J. (1993) Abundant mRNAs in the squid light organ encode proteins with a high similarity to mammalian peroxidases. *Gene* **132:** 219–226.

Tong, D., Rozas, N.S., Oakley, T.H., Mitchell, J., Colley, N.J., and McFall-Ngai, M.J. (2009) Evidence for light perception in a bioluminescent organ. *Proc Natl Acad Sci USA* **106:** 9836–9841.

Troll, J.V., Adin, D.M., Wier, A.M., Paquette, N., Silverman, N., Goldman, W.E., *et al.* (2009) Peptidoglycan induces loss of a nuclear peptidoglycan recognition protein during host tissue development in a beneficial animal-bacterial symbiosis. *Cell Microbiol* **11:** 1114–1127.

Visick, K.L., and McFall-Ngai, M.J. (2000) An exclusive contract: specificity in the *Vibrio fischeri-Euprymna scolopes* partnership. *J Bacteriol* **182:** 1779–1787.

Visick, K.L., and Ruby, E.G. (2006) *Vibrio fischeri* and its host: it takes two to tango. *Curr Op Microbiol* **9:** 632–638.

Visick, K.L., and Skoufos, L.M. (2001) Two-component sensor required for normal symbiotic colonization of *Euprymna scolopes* by *Vibrio fischeri*. *J Bacteriol* **183:** 835–842.

Weis, V.M., Small, A.L., and McFall-Ngai, M.J. (1996) A peroxidase related to the mammalian antimicrobial protein myeloperoxidase in the *Euprymna-Vibrio* mutualism. *Proc Natl Acad Sci USA* **93:** 13683–13688.

Whistler, C.A., Koropatnick, T.A., Pollack, A., McFall-Ngai, M.J., and Ruby, E.G. (2006) The GacA global regulator of *Vibrio fischeri* is required for normal host tissue responses that limit subsequent bacterial colonization. *Cell Microbiol* **9:** 766–778.

Wollenberg, M.S., and Ruby, E.G. (2009) Population structure of *Vibrio fischeri* within the light organs of *Euprymna scolopes* squid from Two Oahu (Hawaii) populations. *Appl Environ Microbiol* **75:** 193–202.

Yildiz, F.H., and Visick, K.L. (2009) *Vibrio* biofilms: so much the same yet so different. *Trends Microbiol* **17:** 109–118.

Yildiz, F.H., Dolganov, N.A., and Schoolnik, G.K. (2001) VpsR, a member of the response regulators of the two-component regulatory systems, is required for expression of *vps* biosynthesis genes and EPS (ETr) -associated phenotypes in *Vibrio cholerae* O1 El Tor. *J Bacteriol* **183:** 1716–1726.

Yip, E.S., Grublesky, B.T., Hussa, E.A., and Visick, K.L. (2005) A novel, conserved cluster of genes promotes symbiotic colonization and σ^{54}-dependent biofilm formation by *Vibrio fischeri*. *Mol Microbiol* **57:** 1485–1498.

Yip, E.S., Geszvain, K., DeLoney-Marino, C.R., and Visick, K.L. (2006) The symbiosis regulator RscS controls the *syp* gene locus, biofilm formation and symbiotic aggregation by *Vibrio fischeri*. *Mol Microbiol* **62:** 1586–1600.

JOURNAL OF BACTERIOLOGY, July 2008, p. 4576–4583 Vol. 190, No. 13
0021-9193/08/$08.00+0 doi:10.1128/JB.00130-08

RscS Functions Upstream of SypG To Control the *syp* Locus and Biofilm Formation in *Vibrio fischeri*▽

Elizabeth A. Hussa, Cynthia L. Darnell, and Karen L. Visick*

Department of Microbiology and Immunology, Loyola University Chicago, Maywood, Illinois 60153

Received 24 January 2008/Accepted 17 April 2008

Two-component signal transduction systems, composed of sensor kinase (SK) and response regulator (RR) proteins, allow bacterial cells to adapt to changes such as environmental flux or the presence of a host. RscS is an SK required for *Vibrio fischeri* to initiate a symbiotic partnership with the Hawaiian squid *Euprymna scolopes*, likely due to its role in controlling the symbiosis polysaccharide (*syp*) genes and thus biofilm formation. To determine which RR(s) functions downstream of RscS, we performed epistasis experiments with a library of 35 RR mutants. We found that several RRs contributed to RscS-mediated biofilm formation in *V. fischeri*. However, only the *syp*-encoded symbiosis regulator SypG was required for both biofilm phenotypes and *syp* transcription induced by RscS. These data support the hypothesis that RscS functions upstream of SypG to induce biofilm formation. In addition, this work also revealed a role for the *syp*-encoded RR SypE in biofilm formation. To our knowledge, no other study has used a large-scale epistasis approach to elucidate two-component signaling pathways. Therefore, this work both contributes to our understanding of regulatory pathways important for symbiotic colonization by *V. fischeri* and establishes a paradigm for evaluating two-component pathways in the genomics era.

Bacteria utilize two-component signal transduction pathways as "reflex" systems to sense and adapt to given environmental stimuli (9, 33, 38). Signaling via these systems is initiated by sensor kinase (SK) proteins, which autophosphorylate in response to a specific environmental cue. The phosphoryl group is subsequently transferred to a given response regulator (RR) or, in some cases, multiple RRs. The RR then promotes a given cellular output, often via the transcriptional activation of a subset of genes.

Two-component signaling systems are well suited to allow communication between symbiotic partners, mediating smooth transitions into, as well as maintenance within, such associations. Previous studies established that multiple two-component pathways are required for the initiation and maintenance of the symbiosis between the marine bioluminescent bacterium *Vibrio fischeri* and the Hawaiian squid *Euprymna scolopes* (19, 26, 36). At least 14 of the 40 putative RRs within the *V. fischeri* genome are required for efficient colonization. These include the luminescence regulator LuxO (15–17), the metabolic regulator ArcA (3), the global regulator GacA (39), the extracellular polysaccharide regulator SypG (10), and several less-characterized RRs (10).

Previous work also identified an SK protein, RscS (regulator of symbiotic colonization-sensor), that was required for symbiotic initiation (37). As an SK, RscS would be predicted to exert its influence through an RR protein. However, efforts to understand the RscS pathway were initially stymied by the lack of bioinformatic evidence. Frequently, sensor-regulator partners are encoded adjacently within the genome, often within or near the locus that they regulate. RscS is an orphan sensor, however, as it is not encoded adjacent to a predicted RR gene (37). In addition, while RscS is encoded within a locus of genes that function in glycerol metabolism, mutations in RscS do not alter the ability of *V. fischeri* wild-type strain ES114 to grow in media containing glycerol as the sole carbon source (37). Finally, general functional cues were also lacking; a disruption of *rscS* did not lead to defects in a number of phenotypes tested in culture.

Recently, however, we established that RscS activates the expression of the symbiosis polysaccharide (*syp*) cluster of genes (42). This cluster is composed of 18 genes organized into at least five putative operons (A to E, F to H, I to L, M to O, and P to R) (43; E. A. Hussa, K. Geszvain, and K. L. Visick, unpublished data). The *syp* gene products are predicted to function in polysaccharide synthesis and transport, and most are required for the initiation of symbiotic colonization (43). The overexpression of *rscS* results in the induction of *syp* transcription and *syp*-dependent biofilm formation (42).

With this discovery of culture phenotypes associated with RscS, it is now possible to use epistasis experiments to uncover the RR or RRs that function downstream of RscS. Recently, we identified and disrupted 35 of 40 putative RRs in the *V. fischeri* genome (10). Twelve of these genes were required for competitive colonization, a phenotype expected for the RR that functions downstream of RscS. However, many of these 12 RRs have established homologs and functions unrelated to those of RscS. For example, FlrC regulates flagellar synthesis (10, 12), whereas RscS does not appear to control motility (37). Furthermore, 9 of the 12 RRs are linked to a putative SK in the genome. These observations decreased, but did not eliminate, the potential of these RRs to relay the signal from RscS.

One candidate partner already known to affect *syp* transcription is SypG, a *syp*-encoded regulator that is also required for colonization (10, 43). SypG is predicted to be an RR in the

* Corresponding author. Mailing address: Department of Microbiology and Immunology, Loyola University Chicago, 2160 S. First Ave., Bldg. 105, Maywood, IL 60153. Phone: (708) 216-0869. Fax: (708) 216-9574. E-mail: kvisick@lumc.edu.

▽ Published ahead of print on 25 April 2008.

TABLE 1. Plasmids used in this study

Plasmid	Description	Source or reference
pCLD1	Cm^r derivative of pEVS107; Kan^r Cm^r	This study
pCLD6	pCLD1 + 3.2-kb ApaI/SpeI fragment from pEAH41 containing the *psypA-lacZ* fusion; Kan^r Cm^r	This study
pCLD19	Delivery vector carrying sequences flanking *sypE*	This study
pCLD46	pVSV105 carrying the *rscS1* allele; Cm^r	This study
pCLD48	pVSV105 carrying wild-type *sypE*; Cm^r	This study
pCR2.1-TOPO	Commercial cloning vector; Ap^r Kan^r	Invitrogen, Carlsbad, CA
pEAH41	pTMO82 carrying *psypA* upstream of *lacZ*; Ap^r Kan^r	This study
pEAH73	pKV69 carrying wild-type *sypG*; Cm^r Tc^r	This study
pES420	Mobilizable suicide vector, Em^r	21a
pEVS107	Mini-Tn*7* delivery plasmid; *mob*; Kan^r Em^r	18
pKG11	pKV69 carrying *rscS1* allele; Cm^r Tc^r	42
pKV69	Mobilizable vector; Cm^r Tc^r	37
pKV276	pEAH73 with D53E mutation in *sypG*; Cm^r Tc^r	This study
pTMO82	pCR2.1-TOPO carrying promoterless *lacZ*; Ap^r Kan^r	This study
pVSV105	Mobilizable vector; Cm^r	6

NtrC-like family of σ^{54}-dependent transcriptional activators. Like RscS, multicopy expression of *sypG* results in enhanced *syp* transcription and biofilm formation, as measured by glass attachment and pellicle formation (43); however, the pellicles are not as robust as those formed by RscS-overexpressing cells. In addition, the overexpression of SypG does not induce wrinkled-colony formation, another hallmark of RscS overexpression (42). Furthermore, the *sypG* gene is adjacent to two genes, *sypE* and *sypF*, that encode putative SK and RR proteins, respectively; thus, it is not clear whether SypG functions directly downstream of SypF or whether a more complicated regulatory scheme exists. Despite these complexities, the hypothesis that SypG functions downstream of RscS to control *syp* expression remained viable.

In this work, we surveyed putative *V. fischeri* RRs to identify those that function downstream of RscS. We report that several RRs contributed to RscS-mediated biofilm formation. However, the loss of *sypG* alone abrogated both RscS-mediated biofilm formation and *syp* transcription. These results thus identify SypG as being a critical link between the symbiosis regulator RscS and the processes that it controls and suggest that RscS and SypG function within the same signal transduction pathway.

MATERIALS AND METHODS

Strains and media. Plasmids and *V. fischeri* strains utilized in this study are listed in Tables 1 and 2, respectively. The parental *V. fischeri* strain used in this work was ES114, a strain isolated from *E. scolopes* (1). All derivatives were generated by conjugation, as previously described (4, 18, 37). *Escherichia coli* strains Tam1 λpir (Active Motif, Carlsbad, CA), DH5α, and Top10 (Invitrogen, Carlsbad, CA) were used for cloning and conjugative purposes. *V. fischeri* strains were grown in either the complex medium LBS (with 0.3% glycerol, where indicated) (8, 32) or HMM (27) containing either 0.3% tryptone (HMM-T) or 0.3% Casamino Acids and 0.2% glucose (43), where indicated. The following antibiotics were added to *V. fischeri* growth media, as necessary, at the indicated concentrations: chloramphenicol (Cm) at 2.5 μg/ml, erythromycin (Em) at 5 μg/ml, and tetracycline (Tc) at 5 μg/ml in LBS or 30 μg/ml in HMM (or HMM-T). The following antibiotics were added to *E. coli* growth media where necessary, at the indicated concentrations: Cm at 25 μg/ml, kanamycin (Kan) at 50 μg/ml, Tc at 15 μg/ml, or ampicillin (Ap) at 100 μg/ml.

Molecular techniques. The mini-Tn*7*-based reporters utilized within this study were generated by PCR amplification of the *sypA* promoter region using oligonucleotides VFA1019intR (TTTTTCGTACGTGATGGGAAATGACGTTGTG) and VFA1020per (CCGATGGCGTCCATATCAC) (MWG, High Point, NC). The product was then cloned into pTMO82, a derivative of pCR 2.1 TOPO (Invitrogen, Carlsbad, CA) carrying a promoterless copy of *lacZ*, via standard techniques. The resulting plasmid (pEAH41) expresses *lacZ* via the *sypA* promoter. The *sypA-lacZ* transcriptional fusion was then digested out of pEAH41 with ApaI and SpeI (New England Biolabs, Beverly, MA) and cloned into the mini-Tn*7* transposon within similarly digested plasmid pCLD1, a Cm^r derivative of pEVS107 (18). SypG overexpression vector pEAH73 is a derivative of pKV69 (Table 1) carrying *sypG* amplified from the *V. fischeri* genome using primers VFA1025RTF (GCTACACTTTCACTAGACGC) and SypG His R (GGTACCTCATTCCGATTCTTCATAG), obtained from MWG (High Point, NC).

Generation of a *sypE* deletion. We constructed the *sypE* deletion strain (Δ*sypE*) as follows: we amplified and cloned sequences 2 kb upstream and downstream of *sypE* into pCR2.1-TOPO and pESY20, respectively. The resulting plasmids were ligated together to produce a composite plasmid, pCLD19, that contained sequences flanking *sypE* but that lacked *sypE* itself. pCLD19 was introduced into ES114 by conjugation and selection for Em resistance (Em^r). Subsequent passage of the resulting colonies on Em allowed the identification of Em^r stable cells; in these cells, a single recombination event had occurred, promoting the integration of the entire plasmid into the chromosome. These cells were subsequently passaged nonselectively to identify Em-sensitive cells in which a second recombination event had occurred, leaving behind either Δ*sypE* or wild-type sequences. One Δ*sypE* strain, KV3299, was identified using a PCR approach and subsequently confirmed by Southern analysis using *sypE* and flanking DNA as a probe.

Generation of the D53E mutation in *sypG*. To obtain the D53E mutation in SypG, we performed site-directed mutagenesis using the Change-IT kit (USB, Cleveland, OH). Plasmid pEAH73 (Table 1) served as the template for primers SypG D53E-phosph (CCACATTTGGTGATTCTCGA**G**TTGAAACTGCCAGATATGTCAG) and Phos-lacZ-up-rev (CCTGTGTGAAATTGTTATCCG). Because the base change (in boldface type) introduces an XhoI site, we screened clones resulting from the mutagenesis with XhoI. A plasmid containing the XhoI site, pKV276, was subsequently identified, and the mutation was confirmed through sequence analysis of the *sypG* coding region using the Genomics Core Facility at the Center for Genetic Medicine at Northwestern University.

Glass attachment and pellicle assays. Strains were grown overnight in HMM containing 0.3% Casamino Acids and 0.2% glucose as well as 30 μg/ml Tc to select for plasmid pKV69 or pKG11. Cultures were then diluted to an optical density at 600 nm (OD_{600}) of 0.1 in the same medium and allowed to grow in static culture in either borosilicate glass culture tubes (for glass attachment assays) or 12-well culture plates (for pellicle assays) for 48 h at 22°C (or 28°C, in the case of experiments conducted with pEAH73). To assay attachment to glass, cultures were stained for 15 min with a 1% crystal violet (CV) solution and subsequently rinsed with deionized water, dried by aspiration, and photographed. Staining was then quantitated by adding 2 ml of 100% ethanol to stained tubes containing 1g of 1-mm glass beads. The tubes were then vortexed until stained material was completely removed from the tube surface. Stained material was quantitated by measuring the OD_{600} (22). The strength of pellicle formation was assessed by drawing a sterile toothpick through the culture surface; pellicles were scored using a scale of "−" to "+++," representing the amount of resistance encountered by the toothpick. A score of "−" was assigned

TABLE 2. *V. fischeri* strains used in this study

Strain[a]	Characteristic(s)	Reference or source
Without reporter		
ES114	Wild type	1
KV1548	VF2120 (*arcA*)::pEAH1	10
KV1585	VF1570::pKV174	10
KV1592	VFA1024 (*sypE*)::pEAH7	10
KV1593	VFA0179::pKV178	10
KV1594	VF1401::pKV177	10
KV1595	VF1396::pKV176	10
KV1596	VFA0561::pKV175	10
KV1612	VFA1017::pKV179	10
KV1640	VFA0041::pTMB26	10
KV1641	VF1054::pAIA1	10
KV1650	VFA0266::pTMB27	10
KV1651	VF1988::pTMB28	10
KV1654	VFA1012::pTMB31	10
KV1655	VF2343::pTMB32	10
KV1665	VF1909::pTMB33	10
KV1666	VFA1026 (*sypG*)::pAIA4	10
KV1668	VFA0211::pAIA6	10
KV1672	VFA0181::pTMB34	10
KV1714	VFA0795::pEAH10	10
KV1715	VF0454::pEAH11	10
KV1727	VF0526::pEAH4	10
KV1730	VF0095::pKV180	10
KV1787	Δ*sypG*	10
KV1809	VF1854::pEAH26	10
KV2164	VF2374::pEAH24	10
KV2165	VFA0216::pEAH25	10
KV2191	VF0937 (*luxO*)::pAIA3	10
KV2501	VF1689::pAIA2	10
KV2503	VFA0103::pAIA5	10
KV2505	VFA0802::pKV207	10
KV2507	VF0114::pKV209	10
KV2509	VFA0698::pKV214	10
KV2510	VF1833::pKV215	10
KV2636	VF1148::pTMB30	10
KV2637	VF1879::pKV216	10
KV2874	VFA0732::pKV208	10
KV3299	Δ*sypE*	This study
With reporter[a]		
KV3001	ES114 *att* Tn*7*::*psypA-lacZ*	This study
KV3395	KV1548 *att* Tn*7*::*psypA-lacZ*	This study
KV3396	KV1585 *att* Tn*7*::*psypA-lacZ*	This study
KV3398	KV1592 *att* Tn*7*::*psypA-lacZ*	This study
KV3399	KV1593 *att* Tn*7*::*psypA-lacZ*	This study
KV3397	KV1594 *att* Tn*7*::*psypA-lacZ*	This study
KV3400	KV1595 *att* Tn*7*::*psypA-lacZ*	This study
KV3419	KV1596 *att* Tn*7*::*psypA-lacZ*	This study
KV3420	KV1612 *att* Tn*7*::*psypA-lacZ*	This study
KV3421	KV1640 *att* Tn*7*::*psypA-lacZ*	This study
KV3422	KV1641 *att* Tn*7*::*psypA-lacZ*	This study
KV3429	KV1650 *att* Tn*7*::*psypA-lacZ*	This study
KV3430	KV1651 *att* Tn*7*::*psypA-lacZ*	This study
KV3423	KV1654 *att* Tn*7*::*psypA-lacZ*	This study
KV3424	KV1655 *att* Tn*7*::*psypA-lacZ*	This study
KV3425	KV1665 *att* Tn*7*::*psypA-lacZ*	This study
KV3426	KV1666 *att* Tn*7*::*psypA-lacZ*	This study
KV3427	KV1668 *att* Tn*7*::*psypA-lacZ*	This study
KV3428	KV1672 *att* Tn*7*::*psypA-lacZ*	This study
KV3431	KV1714 *att* Tn*7*::*psypA-lacZ*	This study
KV3432	KV1715 *att* Tn*7*::*psypA-lacZ*	This study
KV3532	KV1727 *att* Tn*7*::*psypA-lacZ*	This study
KV3433	KV1730 *att* Tn*7*::*psypA-lacZ*	This study
KV3232	KV1787 *att* Tn*7*::*psypA-lacZ*	This study
KV3508	KV1809 *att* Tn*7*::*psypA-lacZ*	This study
KV3521	KV2164 *att* Tn*7*::*psypA-lacZ*	This study
KV3509	KV2165 *att* Tn*7*::*psypA-lacZ*	This study
KV3510	KV2191 *att* Tn*7*::*psypA-lacZ*	This study
KV3518	KV2501 *att* Tn*7*::*psypA-lacZ*	This study
KV3519	KV2503 *att* Tn*7*::*psypA-lacZ*	This study
KV3520	KV2505 *att* Tn*7*::*psypA-lacZ*	This study
KV3533	KV2507 *att* Tn*7*::*psypA-lacZ*	This study
KV3534	KV2509 *att* Tn*7*::*psypA-lacZ*	This study
KV3535	KV2510 *att* Tn*7*::*psypA-lacZ*	This study
KV3547	KV2636 *att* Tn*7*::*psypA-lacZ*	This study
KV3548	KV2637 *att* Tn*7*::*psypA-lacZ*	This study
KV3522	KV2874 *att* Tn*7*::*psypA-lacZ*	This study
KV3620	KV3299 *att* Tn*7*::*psypA-lacZ*	This study

[a] Derivatives of these strains containing either pKG11 or pKV69 (or pEAH73, pKV276, pVSV105, pCLD48, or pCLD46, where indicated) were constructed and utilized as a part of this study.

where no pellicle was detected; "+" represents a very thin, easily disrupted pellicle; "++" represents a more cohesive (less easily disrupted) pellicle; and "+++" represents a thick pellicle that was difficult to disrupt.

β-Galactosidase assays. Samples were grown for 21 h in HMM-T. β-Galactosidase assays were conducted as described previously (21). The total amount of protein in each sample was assayed using Lowry assays (14), and β-galactosidase activity per mg protein in each sample was calculated.

RESULTS

Dependence of RscS on *V. fischeri* RRs for surface attachment. To identify RRs that function downstream of RscS, we introduced the RscS overexpression plasmid pKG11 or a vector control (pKV69) into each of 35 different RR mutants (10). Because RscS mediates biofilm formation in *V. fischeri*, we first assayed these strains for their abilities to attach to a glass surface using a CV stain to visualize biofilm-associated cells and cellular materials (see Materials and Methods). In control experiments, we found that the overexpression of RscS in wild-type cells enhanced the appearance of CV-stainable biofilm material (Fig. 1A) by 10-fold relative to the vector control (Fig. 1B). Upon a similar examination of the 35 RR mutant strains, we found that 29 of these mutants exhibited no significant differences in RscS-mediated glass attachment compared to vector controls (data not shown).

Of the remainder, only the RscS-overexpressing *sypG* mutant exhibited a biofilm phenotype indistinguishable from that of the vector control (Fig. 1). Because this phenotype is similar to the loss of RscS-induced biofilm formation that occurs upon the disruption of structural genes such as *sypN*, which encodes a putative glycosyltransferase (42, 43), we repeated our experiments using an in-frame deletion strain, Δ*sypG*. We found that the Δ*sypG* mutation also eliminated RscS-mediated attachment (Fig. 1). Additionally, the co-overexpression of both SypG and RscS in the Δ*sypG* mutant strain restored the glass attachment phenotype (data not shown). Thus, SypG functions downstream of RscS to facilitate attachment to a glass surface.

RscS-mediated attachment to glass was also altered by the loss of any of five other RRs (Fig. 1A). The loss of either VF0454, a putative homolog of the polysaccharide regulator VpsR (41), or the flagellar regulator FlrC resulted in decreased CV staining (2.5- and 2.3-fold, respectively) (Fig. 1). Mutations in *arcA*, VF1401, or *sypE* altered the pattern, but not the overall level, of staining (Fig. 1).

Because *sypE* is embedded in the *syp* cluster two genes upstream of *sypG*, we further assessed its specific role by constructing an in-frame deletion. The overexpression of RscS in the Δ*sypE* mutant resulted in a slightly diffuse pattern of CV-stained material, which did not differ quantitatively from *sypE*$^+$ cells (Fig. 1B). These results confirmed a minor role for SypE in RscS-mediated attachment to glass. Throughout the remainder of this work, we limited our studies to the Δ*sypE* strain.

Dependence of RscS on *V. fischeri* RRs for pellicle formation. Wild-type *V. fischeri* strains carrying pKG11 produced strong pellicles at the air-liquid interface of statically grown minimal medium cultures, while vector controls formed no detectable pellicle (Fig. 2A) (42). To identify the *V. fischeri* RRs that promote RscS-mediated pellicle formation, we grew the RR mutant strains carrying pKG11 or the vector control in minimal medium (HMM) for 48 h in static culture and assessed surface aggregation by dragging a sterile toothpick

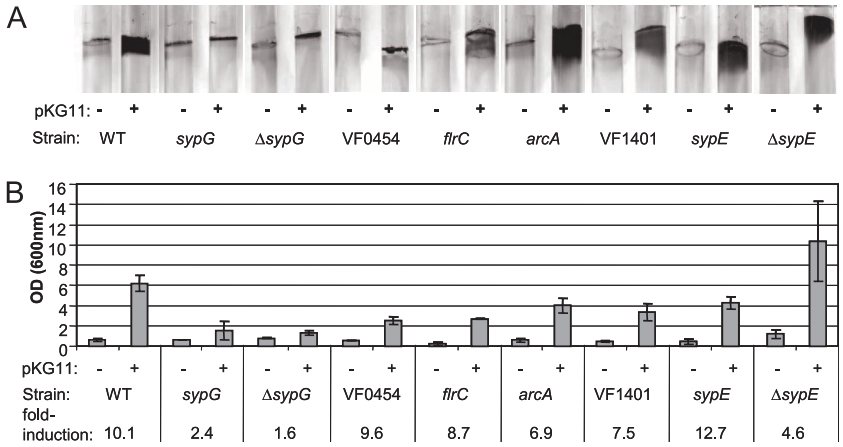

FIG. 1. RscS-mediated attachment to a glass surface in RR mutants. (A) Wild-type (WT) and RR mutant strains of *V. fischeri* carrying either RscS overexpression vector pKG11 (+) or the vector control, pKV69 (−), were grown statically in HMM containing glucose and Casamino Acids and stained with CV to visualize surface-attached material (representative photographs from an experiment conducted in triplicate). (B) Stain was removed by agitation with 1-mm glass beads and ethanol and quantitated by spectrophotometry. Induction represents the OD_{600} of a given strain carrying pKG11 divided by that of the same strain carrying the vector control.

through the culture surface (see Materials and Methods for a description of scoring). While 29 of the 35 RR mutant strains exhibited strong pellicle formation similar to that of the wild-type strain when multicopy RscS was present (data not shown), 6 displayed decreased pellicle formation or lacked pellicles entirely (Fig. 2). In particular, as observed with glass attachment assays, both *sypG* mutations (vector integration and in-frame deletion) abrogated RscS-mediated pellicle formation (Fig. 2A).

Disruption of five additional putative RRs resulted in decreased pellicle formation in RscS-overexpressing strains. Mutations in VF1401, *arcA*, VF0454, and *sypE* resulted in pellicles that were less dense and/or cohesive than those of RscS-overexpressing wild-type cells (Fig. 2A). The *flrC* mutant strain exhibited no detectable pellicle formation after 48 h (Fig. 2A). Previous reports suggested that biofilm formation is often delayed in nonmotile strains of bacteria (13). We therefore assayed pellicle formation after 72 h of incubation and found that pellicle formation by the *flrC* mutant increased; however, these pellicles remained less dense and less cohesive than those formed by the wild-type strain after either 48 or 72 h of incubation (Fig. 2B). These data indicate that *flrC* and/or motility influences RscS-mediated pellicle formation. Increased incubation time did not enhance pellicle formation by other RR mutant strains. Importantly, the *sypG* mutants did not form pellicles regardless of incubation time,

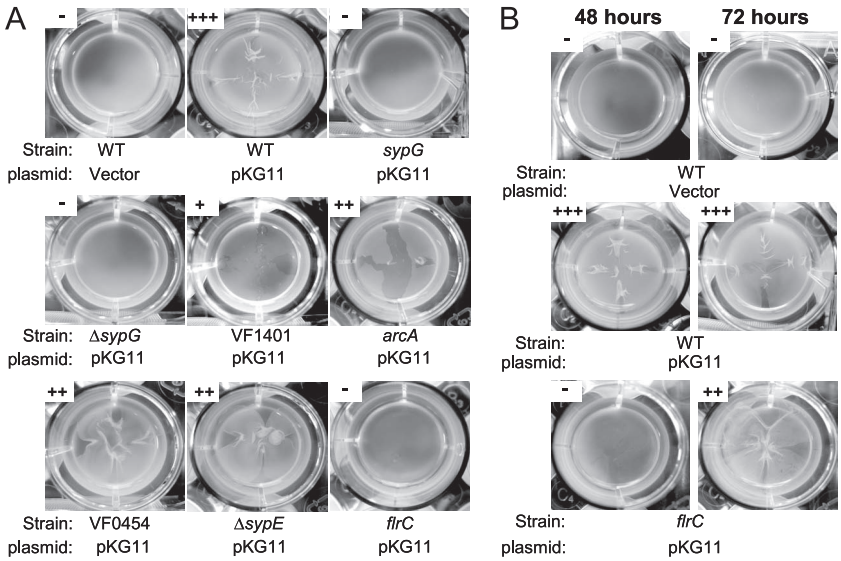

FIG. 2. RscS-mediated pellicle formation in RR mutants. Wild-type (WT) and RR mutant strains of *V. fischeri* carrying either pKG11 or a vector control (pKV69) were grown statically in HMM containing glucose and Casamino Acids for 48 h (A and B, as indicated) or 72 h (B). Pellicle formation was assessed by dragging a sterile toothpick through the culture surface and scored as described in Materials and Methods. Photographs are representative of samples from experiments conducted in triplicate.

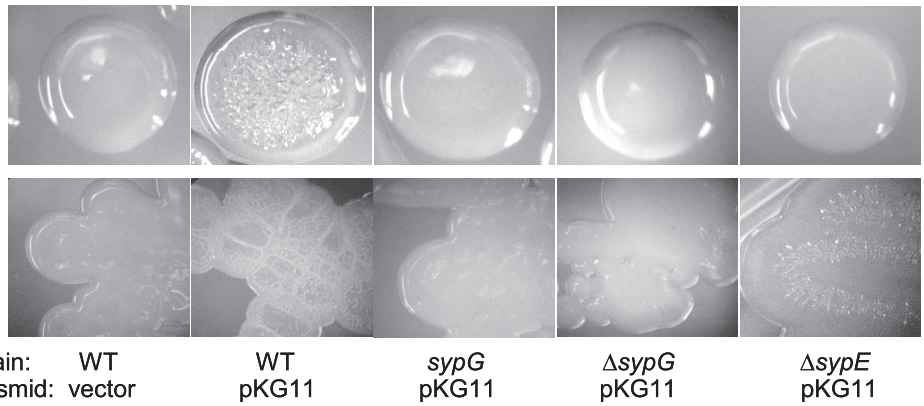

FIG. 3. RscS-mediated wrinkled-colony morphology in RR mutants. Wild-type (WT) and RR mutant strains of *V. fischeri* carrying either pKG11 or a vector control were streaked onto solid, complex medium (LBS with 0.3% glycerol and Tc) and allowed to grow for 3 days at room temperature. Photographs of individual colonies (top row) and also the heavy part of the streak (bottom row) were taken. Photographs are representative of at least three independent platings.

suggesting that *sypG* is absolutely required for this RscS-induced phenotype.

Dependence of RscS on *V. fischeri* RRs for wrinkled-colony morphology. Previous studies indicated that RscS-overexpressing *V. fischeri* cells formed colonies with a dry, wrinkled morphology (42). To identify the RR or RRs that control RscS-mediated wrinkled-colony formation, we examined the colonies formed on solid medium by each RR mutant carrying the vector control or pKG11. All mutants carrying the vector control formed smooth colonies that resembled those formed by the wild-type strain (Fig. 3 and data not shown). Wrinkled-colony formation induced by pKG11 occurred normally in 33 of the 35 RR mutants (data not shown). Only two mutations, in *sypG* and *sypE*, abrogated or reduced RscS-mediated wrinkled-colony formation.

Both *sypG* mutants exhibited completely smooth-colony morphology (Fig. 3). The wrinkling phenotype was restored when RscS and SypG were coexpressed in the Δ*sypG* mutant strain (data not shown), indicating that this RscS-mediated phenotype requires SypG. In contrast, the Δ*sypE* mutation resulted in a partial loss of RscS-mediated wrinkling. Individual *sypE* mutant colonies appeared smooth; however, the heavy part of the streak exhibited some dryness and wrinkling (Fig. 3). Thus, *sypE* plays an important role in, but is not completely required for, RscS-dependent wrinkling.

Dependence of RscS on *V. fischeri* RRs for *syp* transcription. All of the RscS-mediated biofilm phenotypes described above require the *syp* locus (42). Therefore, we assessed the effects of individual RR mutations on RscS-mediated *syp* transcription, measured via single-copy *sypA* promoter-*lacZ* fusions. Consistent with our previous studies (42), the multicopy expression of RscS from pKG11 caused a significant (75-fold) increase in *sypA* reporter activity in an otherwise wild-type background (Fig. 4).

Of the 35 RR mutants tested, 34 exhibited RscS-induced reporter activity at or above the level of the wild-type control (data not shown). The only exception was *sypG*: when RscS was overexpressed, the *sypG* vector integration and deletion mutants both exhibited significantly less reporter activity than did the wild-type strain (Fig. 4). Thus, not only is SypG the only RR required for all RscS-mediated biofilm phenotypes, it is also the only RR required for RscS to induce the expression of the *syp* cluster.

***sypG* overexpression in a *sypE* mutant mimics *rscS* overexpression.** Our results are consistent with the hypothesis that RscS functions upstream of SypG to induce *syp* transcription and biofilm formation. If the two regulators function together, then it might be expected that the two genes would induce similar phenotypes. Indeed, when overexpressed, SypG and RscS each induce *syp* transcription (43, 44). However, SypG overexpression, while promoting attachment to test tubes following growth under either static or shaking conditions (43), does not appear to cause wrinkled-colony formation or the production of strong pellicles (Fig. 5A and B, respectively). Based on these results, we formulated two hypotheses. First, SypG overexpressed in the absence of its SK might not be sufficiently activated (via phosphorylation) to induce the tran-

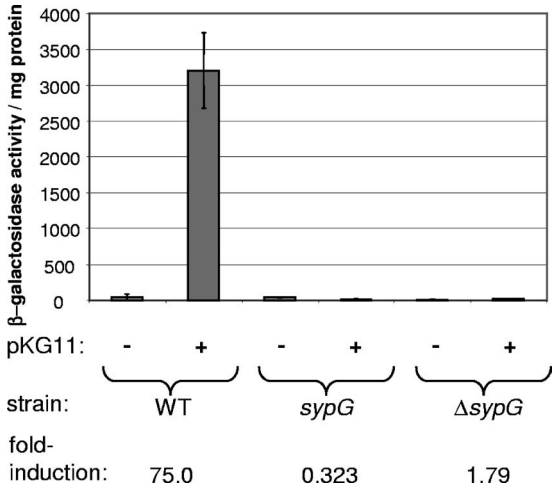

FIG. 4. RscS-mediated induction of *syp* transcription in RR mutants. Wild-type (WT) and RR mutant *sypA* reporter strains carrying either pKG11 or a vector control were grown with shaking in HMM-T at 22°C overnight. The level of transcription of the *sypA* reporter is reported as units of β-galactosidase activity per mg protein.

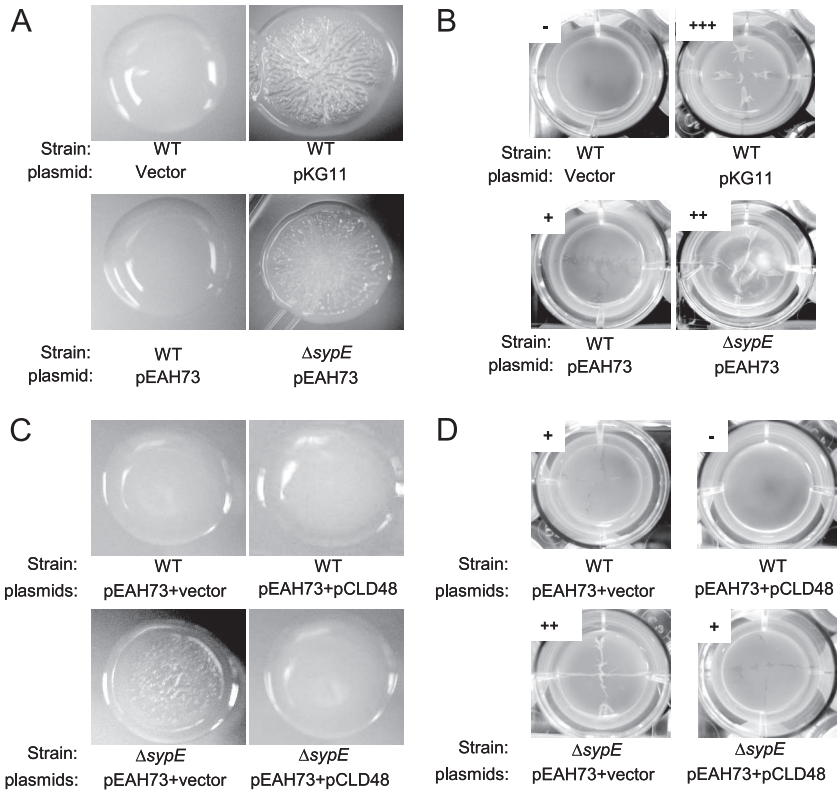

FIG. 5. SypG-mediated phenotypes in the absence of SypE. (A and C) Wild-type (WT) and Δ*sypE* mutant strains carrying the indicated plasmids were streaked onto solid, complex medium (LBS with 0.3% glycerol and Tc) and allowed to grow for 3 days at room temperature. Photographs are representative of samples from at least two independent platings. (B and D) Wild-type and Δ*sypE* mutant strains carrying the indicated plasmids were grown statically in HMM containing glucose and Casamino Acids at either 22°C (strains carrying the vector control and pKG11) or 28°C (strains carrying pEAH73). Pellicle formation was assessed by dragging a sterile toothpick through the culture surface and scored as described in Materials and Methods. Experiments were conducted in triplicate.

scription of the genes necessary for these phenotypes. Second, RscS could signal through more than one RR, either by activating an additional positive regulator or by inactivating a negative regulator, to induce the observed biofilm phenotypes. We favor the latter possibility, as our data thus far do not reveal another strong positive regulator of biofilm formation.

To distinguish these hypotheses, we sought a constitutively active allele of *sypG* through mutagenesis of the putative site of phosphorylation, aspartate 53. In other RRs such as CheY, NtrC, and LuxO, the substitution of Glu for Asp at that position has resulted in enhanced activity (7, 29, 30). The D53E substitution in SypG in fact resulted in a 3.5-fold increase in the SypG-mediated induction of the *sypA* promoter-*lacZ* reporter relative to that of wild-type SypG when expressed from a multicopy plasmid (data not shown). This allele did not, however, result in the appearance of wrinkled colonies or enhanced pellicles in wild-type *V. fischeri*.

Further attempts to clarify the roles of the various *syp* regulators, however, yielded an unexpected result: the overexpression of wild-type SypG (from pEAH73) in a Δ*sypE* mutant strain resulted in wrinkled colonies (Fig. 5A). These wrinkled colonies resembled those formed by RscS-overexpressing wild-type cells. Furthermore, we found that the Δ*sypE* strain carrying pEAH73 was capable of forming thick pellicles (Fig. 5B). To confirm that SypE inhibits SypG-mediated phenotypes, we complemented the Δ*sypE* mutation with *sypE* expressed from pCLD48, which is compatible with the SypG expression vector pEAH73. The co-overproduction of SypG and SypE in the Δ*sypE* strain restored smooth-colony morphology and weak pellicle formation (Fig. 5C and D, respectively), phenotypes similar to those of wild-type *V. fischeri* carrying pEAH73 and a vector control (pVSV105). Furthermore, the co-overproduction of SypE and SypG in the wild-type strain eliminated the formation of weak pellicles induced by the overexpression of SypG alone (Fig. 5D). These data reveal that phenotypes induced by SypG overexpression can mimic those induced by RscS, a result fully consistent with the hypothesis that the two regulators function together. They also support a model in which SypE is antagonistic to SypG, demonstrating the complexity of control over *syp*-dependent biofilm formation in *V. fischeri*.

DISCUSSION

The *V. fischeri* SK RscS was discovered as a determinant of colonization of the host squid, *Euprymna scolopes* (37). RscS regulates the expression of the *syp* cluster of genes and promotes cell-cell aggregation outside the squid light organ, an early event in colonization (42). Importantly, this biofilm-like behavior correlates with cell-cell aggregation phenotypes ob-

served in cells overexpressing RscS in culture (42). Until now, the identity of the downstream RR(s) in the two-component pathway represented by RscS has remained unclear.

To address this problem, we conducted epistasis experiments to identify the regulator(s) that functions downstream of RscS. Our data indicate that a mutation of six different RRs diminished RscS-mediated liquid biofilm phenotypes (i.e., pellicle formation and attachment to a glass surface): *arcA*, *sypE*, *sypG*, *flrC*, VF1401, and VF0454. Of these, only the loss of *sypG* completely eliminated the enhancement of liquid biofilms by RscS. The disruption of *sypG* also eliminated RscS-mediated wrinkled-colony formation. Only one other mutation, in the other *syp* cluster RR gene, *sypE*, diminished (but did not eliminate) the ability of RscS to promote wrinkling. Finally, the mutation of *sypG* alone eliminated the ability of RscS to induce the expression of a *syp* reporter.

Our data thus provide compelling genetic evidence that RscS and SypG function within the same two-component pathway. First, both RscS and SypG are required for the initiation of squid colonization (10, 37). Second, the overexpression of either RscS or SypG induces *syp* transcription and biofilm phenotypes (42, 43). Third, SypG is the only one of the 35 putative RRs tested that is required for all known functions of RscS.

Very few studies have established partnerships between orphan SKs and RRs. Some examples include UvrY and BarA in *E. coli* (23), ArcB and RssB in *E. coli* (20), DosT and DosR in *Mycobacterium tuberculosis* (25, 28), and CenK and CenR in *Caulobacter crescentus* (31). Often, in vitro phosphotransfer studies are utilized as evidence for such partnerships (31). Despite repeated attempts, both RscS and SypG proved difficult to purify, resulting in either low yields of protein (in the case of RscS) or aggregated, possibly unfolded protein (SypG) (E. A. Hussa and K. L. Visick, unpublished data). Thus, phosphotransfer experiments could not be performed. Due to the lack of biochemical data, it remains formally possible that RscS does not directly donate a phosphoryl group to SypG. There are at least four additional putative *V. fischeri* RRs that we were unable to disrupt in our previous mutagenesis study (10), one or more of which may function in the RscS pathway. Also, there is an additional *V. fischeri* RR, GacA, which was not considered in this study; mutation of GacA results in a growth yield defect that makes biofilm-related phenotypes difficult to study (39). However, the genetic evidence presented here demonstrates that RscS activity requires SypG; therefore, we assert that these additional RRs are likely not major components of the RscS pathway. There are also examples in which alternative paths of phosphotransfer are followed, such as the *E. coli* Rcs system, in which the RcsC kinase donates a phosphoryl group to an Hpt domain within an intermediate protein, RcsD (34). Intriguingly, encoded just upstream of *sypG* is a hybrid SK, SypF. However, unlike the loss of *sypG*, the disruption of *sypF* does not eliminate RscS-mediated wrinkled-colony formation (C. L. Darnell and K. L. Visick, unpublished data). Therefore, we think that it is unlikely that a substantial amount of RscS-initiated activation occurs via SypF.

It is abundantly clear, however, that the regulation of *syp*-dependent biofilms is complex. In support of this idea, in this study, we determined that the overexpression of SypG in a *sypE* deletion strain results in the formation of wrinkled colonies and pellicles mimicking those produced by wild-type strains overexpressing RscS. We interpret these data as further support of our model that RscS and SypG function in the same pathway. However, these results generate additional questions. For example, if SypE is required for the full expression of RscS-mediated biofilm phenotypes, then why does its loss allow biofilm formation to be induced by SypG overexpression?

SypE is not a typical RR: its phosphate-accepting receiver (REC) domain is centrally located and is not adjacent to a known DNA binding domain. Instead, C terminal to the REC domain is a putative protein phosphatase 2C domain (2) predicted to function as a serine phosphatase. N terminal to the REC domain is a region with weak similarity to the *Bacillus subtilis* RsbW protein, which acts as a serine kinase (5). If these domains function as predicted, it is possible that the phosphorylation of SypE could modulate its ability to serve as either a phosphatase or a kinase. Thus, we hypothesize that RscS may also function upstream of SypE in a manner that negates its antagonism of SypG-mediated phenotypes. In this model, the overexpression of RscS would both activate SypG and inactivate SypE, ultimately inducing wrinkled-colony formation. In contrast, the overexpression of SypG alone would not be sufficient to prevent SypE-mediated antagonism; thus, wrinkled-colony formation occurs only in the absence of SypE. A further understanding of how SypE functions awaits specific, mechanistic characterization of this protein and its unusual domains through mutagenesis studies.

This work also revealed roles for four additional RRs in *V. fischeri* biofilm formation (i.e., glass attachment and pellicle formation): FlrC, ArcA, VF0454, and VF1401. The first three of these RRs were previously shown to be involved in biofilm formation in other bacteria (10, 11, 13, 24, 35). In particular, VF0454 encodes a protein with high sequence identity to the *Vibrio cholerae* exopolysaccharide regulator VpsR; a distinct study from our laboratory has also uncovered an important role for VF0454 in biofilm formation (3a). Little is known about the final *V. fischeri* biofilm regulator, VF1401, except that it is required for competitive colonization and belongs to the family of σ^{54}-dependent transcriptional activators (10). At this time, we cannot determine whether these four RRs function specifically downstream of RscS or whether they have independent effects on biofilm formation, as wild-type strains of *V. fischeri* (i.e., strains not overexpressing *syp*) do not form robust biofilms in culture (40, 42, 43).

In summary, we have shown that the SK RscS functions primarily upstream of the RR SypG as a major two-component pathway involved in *V. fischeri* biofilm formation. This RscS/SypG-mediated signaling, however, is likely to be complex, involving at least one additional *syp* regulator, SypE, which appears to severely inhibit SypG-mediated biofilm formation. In addition, we have uncovered at least four other *V. fischeri* two-component regulators that feed into biofilm formation: FlrC, VF0454, ArcA, and VF1401. This work has thus provided a basis for understanding the complex control of biofilm formation in *V. fischeri*.

ACKNOWLEDGMENTS

We thank Therese O'Shea for construction of plasmid pTMO82 and Kati Geszvain and Jenny Wu for aid in phenotype screening in the early stages of this work. We also thank Steve Johnston for collabo-

ration in the yeast two-hybrid analysis. Additionally, we are grateful to Alan Wolfe and members of the Visick laboratory for providing useful insight into the manuscript.

This work was funded by the NIH grant GM59690, awarded to K.L.V.

REFERENCES

1. **Boettcher, K. J., and E. G. Ruby.** 1990. Depressed light emission by symbiotic *Vibrio fischeri* of the sepiolid squid *Euprymna scolopes*. J. Bacteriol. **172:** 3701–3706.
2. **Bork, P., N. P. Brown, H. Hegyi, and J. Schultz.** 1996. The protein phosphatase 2C (PP2C) superfamily: detection of bacterial homologues. Protein Sci. **5:**1421–1425.
3. **Bose, J. L., U. Kim, W. Bartkowski, R. P. Gunsalus, A. M. Overley, N. L. Lyell, K. L. Visick, and E. V. Stabb.** 2007. Bioluminescence in *Vibrio fischeri* is controlled by the redox-responsive regulator ArcA. Mol. Microbiol. **65:** 538–553.

3a. **Darnell, C. L., E. A. Hussa, and K. L. Visick.** 9 May 2008. The putative hybrid sensor kinase SypF coordinates biofilm formation in *Vibrio fischeri* by acting upstream of two response regulators, SypG and VpsR. J. Bacteriol. doi:10.1128/JB.00197-08.

4. **DeLoney, C. R., T. M. Bartley, and K. L. Visick.** 2002. Role for phosphoglucomutase in *Vibrio fischeri-Euprymna scolopes* symbiosis. J. Bacteriol. **184:**5121–5129.
5. **Dufour, A., and W. G. Haldenwang.** 1994. Interactions between a *Bacillus subtilis* anti-sigma factor (RsbW) and its antagonist (RsbV). J. Bacteriol. **176:**1813–1820.
6. **Dunn, A. K., D. S. Millikan, D. M. Adin, J. L. Bose, and E. V. Stabb.** 2006. New *rfp*- and pES213-derived tools for analyzing symbiotic *Vibrio fischeri* reveal patterns of infection and *lux* expression in situ. Appl. Environ. Microbiol. **72:**802–810.
7. **Freeman, J. A., and B. L. Bassler.** 1999. A genetic analysis of the function of LuxO, a two-component response regulator involved in quorum sensing in *Vibrio harveyi*. Mol. Microbiol. **31:**665–677.
8. **Graf, J., P. V. Dunlap, and E. G. Ruby.** 1994. Effect of transposon-induced motility mutations on colonization of the host light organ by *Vibrio fischeri*. J. Bacteriol. **176:**6986–6991.
9. **Hoch, J. A., and T. J. Silhavy (ed.).** 1995. Two-component signal transduction. ASM Press, Washington, DC.
10. **Hussa, E. A., T. M. O'Shea, C. L. Darnell, E. G. Ruby, and K. L. Visick.** 2007. Two-component response regulators of *Vibrio fischeri*: identification, mutagenesis, and characterization. J. Bacteriol. **189:**5825–5838.
11. **Junker, L. M., J. E. Peters, and A. G. Hay.** 2006. Global analysis of candidate genes important for fitness in a competitive biofilm using DNA-array-based transposon mapping. Microbiology **152:**2233–2245.
12. **Klose, K. E., and J. J. Mekalanos.** 1998. Distinct roles of an alternative sigma factor during both free-swimming and colonizing phases of the Vibrio cholerae pathogenic cycle. Mol. Microbiol. **28:**501–520.
13. **Kobayashi, K.** 2007. *Bacillus subtilis* pellicle formation proceeds through genetically defined morphological changes. J. Bacteriol. **189:**4920–4931.
14. **Lowry, O. H., N. J. Rosebrough, A. L. Farr, and R. J. Randall.** 1951. Protein measurement with the folin phenol reagent. J. Biol. Chem. **193:**265–275.
15. **Lupp, C., and E. G. Ruby.** 2004. *Vibrio fischeri* LuxS and AinS: comparative study of two signal synthases. J. Bacteriol. **186:**3873–3881.
16. **Lupp, C., and E. G. Ruby.** 2005. *Vibrio fischeri* utilizes two quorum-sensing systems for the regulation of early and late colonization factors. J. Bacteriol. **187:**3620–3629.
17. **Lupp, C., M. Urbanowski, E. P. Greenberg, and E. G. Ruby.** 2003. The *Vibrio fischeri* quorum-sensing systems ain and lux sequentially induce luminescence gene expression and are important for persistence in the squid host. Mol. Microbiol. **50:**319–331.
18. **McCann, J., E. V. Stabb, D. S. Millikan, and E. G. Ruby.** 2003. Population dynamics of *Vibrio fischeri* during infection of *Euprymna scolopes*. Appl. Environ. Microbiol. **69:**5928–5934.
19. **McFall-Ngai, M. J., and E. G. Ruby.** 2000. Developmental biology in marine invertebrate symbioses. Curr. Opin. Microbiol. **3:**603–607.
20. **Mika, F., and R. Hengge.** 2005. A two-component phosphotransfer network involving ArcB, ArcA, and RssB coordinates synthesis and proteolysis of sigmaS (RpoS) in *E. coli*. Genes Dev. **19:**2770–2781.
21. **Miller, J. H.** 1972. Experiments in molecular genetics. Cold Spring Harbor Laboratory, New York, NY.

21a. **O'Shea, T. M., A. H. Klein, K. Geszvain, A. J. Wolfe, and K. L. Visick.** 2006. Diguanylate cyclases control magnesium-dependent motility of *Vibrio fischeri*. J. Bacteriol. **188:**8196–8205.

22. **O'Toole, G. A., and R. Kolter.** 1998. Initiation of biofilm formation in *Pseudomonas fluorescens* WCS365 proceeds via multiple, convergent signalling pathways: a genetic analysis. Mol. Microbiol. **28:**449–461.
23. **Pernestig, A. K., O. Melefors, and D. Georgellis.** 2001. Identification of UvrY as the cognate response regulator for the BarA sensor kinase in *Escherichia coli*. J. Biol. Chem. **276:**225–231.
24. **Reid, D. W., and S. M. Kirov.** 2004. Iron, Pseudomonas aeruginosa and cystic fibrosis. Microbiology **150:**516; discussion, 516–518.
25. **Roberts, D. M., R. P. Liao, G. Wisedchaisri, W. G. Hol, and D. R. Sherman.** 2004. Two sensor kinases contribute to the hypoxic response of *Mycobacterium tuberculosis*. J. Biol. Chem. **279:**23082–23087.
26. **Ruby, E. G.** 1996. Lessons from a cooperative, bacterial-animal association: the *Vibrio fischeri-Euprymna scolopes* light organ symbiosis. Annu. Rev. Microbiol. **50:**591–624.
27. **Ruby, E. G., and K. H. Nealson.** 1977. Pyruvate production and excretion by the luminous marine bacteria. Appl. Environ. Microbiol. **34:**164–169.
28. **Saini, D. K., V. Malhotra, and J. S. Tyagi.** 2004. Cross talk between DevS sensor kinase homologue, Rv2027c, and DevR response regulator of *Mycobacterium tuberculosis*. FEBS Lett. **565:**75–80.
29. **Sanders, D. A., B. L. Gillece-Castro, A. L. Burlingame, and D. E. Koshland, Jr.** 1992. Phosphorylation site of NtrC, a protein phosphatase whose covalent intermediate activates transcription. J. Bacteriol. **174:**5117–5122.
30. **Sanders, D. A., B. L. Gillece-Castro, A. M. Stock, A. L. Burlingame, and D. E. Koshland, Jr.** 1989. Identification of the site of phosphorylation of the chemotaxis response regulator protein, CheY. J. Biol. Chem. **264:**21770–21778.
31. **Skerker, J. M., M. S. Prasol, B. S. Perchuk, E. G. Biondi, and M. T. Laub.** 2005. Two-component signal transduction pathways regulating growth and cell cycle progression in a bacterium: a system-level analysis. PLoS Biol. **3:**e334.
32. **Stabb, E. V., K. A. Reich, and E. G. Ruby.** 2001. *Vibrio fischeri* genes *hvnA* and *hvnB* encode secreted NAD^+-glycohydrolases. J. Bacteriol. **183:**309–317.
33. **Stock, A. M., V. L. Robinson, and P. N. Goudreau.** 2000. Two-component signal transduction. Annu. Rev. Biochem. **69:**183–215.
34. **Takeda, S., Y. Fujisawa, M. Matsubara, H. Aiba, and T. Mizuno.** 2001. A novel feature of the multistep phosphorelay in *Escherichia coli*: a revised model of the RcsC→YojN→RcsB signalling pathway implicated in capsular synthesis and swarming behaviour. Mol. Microbiol. **40:**440–450.
35. **Vilain, S., P. Cosette, G. A. Junter, and T. Jouenne.** 2002. Phosphate deprivation is associated with high resistance to latamoxef of gel-entrapped, sessile-like *Escherichia coli* cells. J. Antimicrob. Chemother. **49:**315–320.
36. **Visick, K. L., and E. G. Ruby.** 2006. *Vibrio fischeri* and its host: it takes two to tango. Curr. Opin. Microbiol. **9:**632–638.
37. **Visick, K. L., and L. M. Skoufos.** 2001. A two-component sensor required for normal symbiotic colonization of *Euprymna scolopes* by *Vibrio fischeri*. J. Bacteriol. **183:**835–842.
38. **West, A. H., and A. M. Stock.** 2001. Histidine kinases and response regulator proteins in two-component signaling systems. Trends Biochem. Sci. **26:**369–376.
39. **Whistler, C. A., and E. G. Ruby.** 2003. GacA regulates symbiotic colonization traits of *Vibrio fischeri* and facilitates a beneficial association with an animal host. J. Bacteriol. **185:**7202–7212.
40. **Wolfe, A. J., D. S. Millikan, J. M. Campbell, and K. L. Visick.** 2004. *Vibrio fischeri* σ^{54} controls motility, biofilm formation, luminescence, and colonization. Appl. Environ. Microbiol. **70:**2520–2524.
41. **Yildiz, F. H., N. A. Dolganov, and G. K. Schoolnik.** 2001. VpsR, a member of the response regulators of the two-component regulatory systems, is required for expression of *vps* biosynthesis genes and EPS^{ETr}-associated phenotypes in *Vibrio cholerae* O1 El Tor. J. Bacteriol. **183:**1716–1726.
42. **Yip, E. S., K. Geszvain, C. R. DeLoney-Marino, and K. L. Visick.** 2006. The symbiosis regulator RscS controls the *syp* gene locus, biofilm formation and symbiotic aggregation by *Vibrio fischeri*. Mol. Microbiol. **62:**1586–1600.
43. **Yip, E. S., B. T. Grublesky, E. A. Hussa, and K. L. Visick.** 2005. A novel, conserved cluster of genes promotes symbiotic colonization and sigma-dependent biofilm formation by *Vibrio fischeri*. Mol. Microbiol. **57:**1485–1498.

JOURNAL OF BACTERIOLOGY, July 2008, p. 4437–4446 Vol. 190, No. 13
0021-9193/08/$08.00+0 doi:10.1128/JB.00055-08

The Hybrid Sensor Kinase RscS Integrates Positive and Negative Signals To Modulate Biofilm Formation in *Vibrio fischeri*[▽]

Kati Geszvain† and Karen L. Visick*

Department of Microbiology and Immunology, Loyola University Chicago, Maywood, Illinois 60153

Received 11 January 2008/Accepted 16 April 2008

Overexpression of the *Vibrio fischeri* sensor kinase RscS induces expression of the *syp* (*s*ymbiosis *p*olysaccharide) gene cluster and promotes biofilm phenotypes such as wrinkled colony morphology, pellicle formation, and surface adherence. RscS is predicted to be a hybrid sensor kinase with a histidine kinase/ATPase (HATPase) domain, a receiver (Rec) domain, and a histidine phosphotransferase (Hpt) domain. Bioinformatic analysis also revealed the following three potential signal detection domains within RscS: two transmembrane helices forming a transmembrane region (TMR), a large periplasmic (PP) domain, and a cytoplasmic PAS domain. In this work, we genetically dissected the contributions of these domains to RscS function. Substitutions within the carboxy-terminal domain supported identification of RscS as a hybrid sensor kinase; disruption of both the HATPase and Rec domains eliminated induction of *syp* transcription, wrinkled colony morphology, pellicle formation, and surface adherence, while disruption of Hpt resulted in decreased activity. The PAS domain was also critical for RscS activity; substitutions in PAS resulted in a loss of activity. Generation of a cytoplasmic, N-terminal deletion derivative of RscS resulted in a partial loss of activity, suggesting a role for localization to the membrane and/or sequences within the TMR and PP domain. Finally, substitutions within the first transmembrane helix of the TMR and deletions within the PP domain both resulted in increased activity. Thus, RscS integrates both inhibitory and stimulatory signals from the environment to regulate biofilm formation by *V. fischeri*.

Bacteria commonly employ two-component regulatory systems to sense and respond to changes in their environment (42). These bacterial sensory systems are important during establishment of a symbiotic or pathogenic association; the bacteria detect the presence of a host organism and respond to the various environments encountered during migration through the host to the site of colonization (49). In the marine bioluminescent bacterium *Vibrio fischeri*, the sensor kinase component of a two-component regulatory pathway, RscS, is required for the bacterium to form a symbiotic association with its host organism, the Hawaiian bobtail squid (*Euprymna scolopes*) (47). In this symbiosis, colonization is initiated shortly after the juvenile squid hatch; *V. fischeri* cells form biofilmlike aggregates on the surface of the light organ in mucus secreted by the squid before migrating into the light organ crypts, multiplying to high cell density, and inducing bioluminescence (for reviews, see references 32, 40, 46). Strains in which *rscS* has been disrupted have a greatly decreased ability to colonize the squid (47) and do not aggregate in the mucus secreted by the squid (50).

RscS has been shown to regulate transcription of the *syp* (*s*ymbiosis *p*olysaccharide) gene cluster (50). The *syp* cluster is a group of 18 genes that encode proteins important for production of a surface polysaccharide. Most of the genes in this cluster are required for symbiosis, and disruption of these genes results in a severe colonization defect (51). Recently, an increased-activity allele of *rscS* (*rscS1*) was identified that greatly increased the transcription of the *syp* cluster in culture (50). This allele encodes a wild-type protein but has mutations in the transcript that increase protein levels (15a, 50). When present on a multicopy plasmid, *rscS1* induces various biofilm phenotypes in culture. These phenotypes include wrinkled colony morphology, adherence to glass surfaces, and pellicle formation. Furthermore, *rscS1* dramatically increases the size of the bacterial aggregates on the light organ and confers a dramatic advantage in competitive colonization assays (50).

rscS encodes a large (927-amino-acid) protein predicted to contain multiple domains involved in signal detection and relay. The most conserved domains are a histidine kinase/ATPase (HATPase) domain, a response regulator-like receiver (Rec) domain, and a histidine phosphotransferase (Hpt) domain (Fig. 1), suggesting that after autophosphorylation, the phosphoryl group is relayed within RscS before transfer to a cognate response regulator. One possible role of the phosphorelay of hybrid sensor kinases is to allow multiple regulatory inputs, similar to what occurs in the multiprotein phosphorylation cascade regulating sporulation in *Bacillus subtilis*. In this phosphorelay, multiple sensor kinases and phosphatases regulate the flow of phosphate and thus signal transduction (35). A second possible role for hybrid sensor kinases may be to act as "rheostats" that modulate the level of the response to the level of the input signal, as has been proposed for the *Bordetella* hybrid sensor kinase BvgS (8). It is not yet known whether these conserved sequences in RscS are necessary for its activity.

Commonly, the sensor region of a sensor kinase is located in

* Corresponding author. Mailing address: Department of Microbiology and Immunology, Loyola University Chicago, 2160 S. First Ave., Bldg. 105, Maywood, IL 60153. Phone: (708) 216-0869. Fax: (708) 216-9574. E-mail: kvisick@lumc.edu.

† Present address: Department of Environmental and Biomolecular Systems, Oregon Health and Sciences University, 20000 NW Walker Rd., Beaverton, OR 97006-8921.

▽ Published ahead of print on 25 April 2008.

its amino terminus. The sensor regions of sensor kinases are quite diverse, reflecting the wide array of signals detected by these proteins (30). The amino terminus of RscS has three structural features: a transmembrane region (TMR) with two predicted transmembrane (TM) helices (TM1 and TM2) which together define a large, 200-amino-acid periplasmic (PP) domain and a predicted PAS sensor domain located just carboxy terminal of TM2 (16) (Fig. 1). There are examples of sensor kinases that perceive their signal through each of these regions (PP domain, TMR, and PAS domain) (30). The most common class of membrane-bound sensor kinases is the class of sensor kinases thought to receive signals through their PP domains (30). For example, PhoQ in *Salmonella* detects Mg^{2+} and antimicrobial peptides through its ~150-amino-acid periplasmic domain (3, 7, 45). Other examples are the CitA/DcuS-like sensor kinases which detect concentrations of a signal molecule (citrate in the case of CitA) with a PAS-like fold in the PP domain (34, 37). While the large PP domain of RscS exhibits no similarity to PP domains involved in signal detection, this domain is conserved in putative proteins encoded by *rscS* alleles isolated from other *V. fischeri* strains (Mark Mandel, personal communication) and is present in a protein encoded by a putative *rscS* homolog from the coral pathogen *Vibrio shilonii* AK1 (accession number ZP_01865491). Thus, the PP domain of RscS may play a role in signal detection.

The TMR of membrane-bound sensor proteins has been implicated in sensing cell envelope stress, as well as in transduction of signal from the periplasm to the kinase domain. Many of the sensor kinases thought to perceive signals through their TMR have four or more TM helices (30). The sensor kinase LiaS from *B. subtilis* and its homologs, however, are predicted to have just two TM helices, like RscS. This sensor kinase responds to the presence of sublethal concentrations of antibiotics active against the cell wall, possibly through interaction of its TMR with the membrane protein LiaF (23). The role of the TMR in signal transduction has been studied most extensively with the bacterial chemoreceptors, in particular the aspartate receptor Tar (30). In these dimeric receptors, the two TM helices of each of the monomers form a four-helix bundle. The orientation of the helices relative to one another changes in response to ligand binding (13). In the case of Tar, ligand binding triggers a pistonlike movement of the signaling helix down toward the cytoplasm. This action regulates autophosphorylation of an associated histidine kinase (12, 33).

The third possible signal detection domain in RscS is its putative PAS domain. PAS domains are found in all kingdoms of life and have a conserved protein fold but limited sequence homology (19). They are important for detection of signals such as changes in light, redox potential, oxygen, and the presence of small ligands, such as ATP (44). Signal detection by PAS domains frequently requires the presence of a bound cofactor (44). Many sensor kinases have cytoplasmic PAS domains implicated in signal detection (30). For example, the O_2 sensor FixL from rhizobia possesses a heme-binding PAS domain; the interaction of O_2 with the heme cofactor results in inactivation of the kinase activity (17). *Escherichia coli* ArcB also has a cytoplasmic PAS domain; the interaction of oxidized quinones with this domain is thought to inhibit the kinase activity of this sensor kinase (29).

Despite the importance of the complex regulator RscS in inducing biofilm formation, little is known about the specific sequences essential for RscS activity. In this study, we examined the contribution of each RscS domain to protein activity by generating deletions and site-specific substitutions and evaluating their effects on *rscS1*-dependent biofilm phenotypes. Our results support the identification of RscS as a hybrid sensor kinase; replacement of predicted phosphorylated residues resulted in a decrease in or loss of biofilm formation. Moreover, our data demonstrate a critical role for PAS in RscS function. Finally, the other predicted sensor domains, TMR and the PP domain, contribute to RscS activity, and the PP domain has an apparently negative effect. These data allowed us to conclude that RscS integrates both positive and negative signals to regulate biofilm formation.

MATERIALS AND METHODS

Strains, plasmids, and media. Strains used in this study are listed in Table 1. *V. fischeri* strains constructed in this work were generated by conjugation as previously described (11, 47). A bacterial isolate from *E. scolopes*, ES114, was the symbiosis-competent parent strain used in this study (4). *E. coli* strains DH5α (48) and TOP10 (Invitrogen, Carlsbad, CA) were used as hosts for cloning and conjugation. *V. fischeri* strains were grown in complex medium (LBS [18, 41]) or in HMM (39) containing 0.3% Casamino Acids and 0.2% glucose (HMM-CAA-Glu) (51). Antibiotics were added, as needed, at the following final concentrations: chloramphenicol, 5 μg ml^{-1}; erythromycin, 5 μg ml^{-1}; and tetracycline (Tet), 5 μg ml^{-1} in LBS and 30 μg ml^{-1} in HMM. Agar was added to a final concentration of 1.5% for solid media.

Molecular techniques. Plasmids were constructed using standard molecular biology techniques with restriction and modifying enzymes obtained from New England Biolabs (Beverly, MA) or Promega (Madison, WI). Plasmids used or constructed in this study are listed in Table 1. All plasmids used in this study were derived from or are similar to pKG63, which lacks the *rscS* promoter but bears the *rscS1* (50) allele under control of the *lacZ* promoter (15a). Thus, all *rscS* alleles described in this work carry the ribosome binding site mutation and the silent mutation at the Leu-25 codon present in *rscS1* (50), as well as the described substitutions and deletions.

Site-directed mutagenesis. The large deletions in the periplasmic domain were generated by divergent PCR. Divergent primers specific for the end points of the desired deletions (Table 2) and Kod HiFi thermostable DNA polymerase (Novagen, Madison, WI) were used to PCR amplify around the appropriate *rscS1*-containing plasmid. The resulting PCR product was purified (GeneClean; Q-Biogene, Solon, OH), self-ligated, and transformed into TOP10 cells. The H323A, N345A, and F353A substitutions were generated by amplifying the 5′ end of *rscS* using primer *rscS1*-RBS-F and the appropriate mutagenic reverse primer and the 3′ end of *rscS* using the mutagenic forward primer and 9R2 (Table 2). The two fragments were then joined using splicing by overlap extension PCR (21) with *rscS1*-RBS-F and 9R2. The H867Q substitution was generated using a QuikChange kit (Stratagene, La Jolla, CA). The H412Q substitution was generated using the GeneEditor in vitro site-directed mutagenesis system (Promega, Madison, WI). The remaining substitutions were generated using a Change-It multiple-mutation site-directed mutagenesis kit (USB, Cleveland, OH).

Sequencing. The presence of mutations was confirmed by automated sequencing (Northwestern University Genomics Core Facility, Chicago, IL) of the *rscS1* gene on the various plasmids. One plasmid, pKG116 [*rscS1*(*L330R*)], contained a silent base change at codon 124. This alteration (GTA to GTG) had a negligible effect on Val codon usage (29% to 17%).

Western analysis. Cultures were grown in HMM-CAA-Glu with Tet overnight, and then 1-ml samples were removed and pelleted by centrifugation. Cells were resuspended in 50 μl of distilled H_2O with a protease inhibitor cocktail for use with bacterial cell extracts (Sigma Aldrich, St. Louis, MO), and a 5-μl aliquot was removed for quantitation by the assay of Lowry et al. (27). After quantitation, cells were diluted as necessary to bring all samples to the same protein concentration, and then 1 volume of 2× sodium dodecyl sulfate dye was added. Cells were lysed by boiling them for 5 min, and then extracts were loaded on an 8% sodium dodecyl sulfate-polyacrylamide gel electrophoresis gel. After electrophoretic separation, proteins were transferred to a polyvinylidene difluoride membrane and probed with anti-RscS antibodies as described elsewhere (15a).

TABLE 1. Plasmids and strains used in this study

Strain or plasmid	Genotype, characteristics, or construction	Source or reference
E. coli strains		
TAM1	*mcrA* Δ(*mrr-hsdRMS-mcrBC*) ϕ80*lacZ*ΔM15 Δ*lacX74 recA1 araD139* Δ(*ara-leu*)*7697 galU galK rpsL endA1 nupG*	Active Motif
DH5α	*endA1 hsdR17*(r_K^- m_K^+) *glnV44 thi-1 recA1 gyrA* (Nal^r) *relA* Δ(*lacIZYA-argF*)*U169 deoR* [ϕ80d*lac*Δ(*lacZ*)M15]	48
TOP10 F′	F′ [*lacI*^{q} Tn*10* (Tet^r)] *mcrA* Δ(*mrr-hsdRMS-mcrBC*) ϕ80*lacZ*ΔM15 Δ*lacX74 recA1 araD139* Δ(*ara-leu*)*7697 galU galK rpsL* (Str^r) *endA1 nupG*	Invitrogen
V. fischeri strains		
ES114	Wild type	4
KV2566	ES114 *att* Tn*7*::P*sypA*::*lacZ*	15a
Plasmids		
pJET1	Commercial cloning vector, Amp^r	Fermentas
pCR2.1-TOPO	Commercial cloning vector, Amp^r Kan^r	Invitrogen
pKV69	Mobilizable vector, Cm^r Tet^r	47
pKG63	pKV69 containing *rscS1* under control of P_{lacZ}, Cm^r Tet^r	15a
pKG92	pKV69 containing *rscS1*(ΔPP-large), Cm^r Tet^r	This study
pKG94	pKV69 containing *rscS1*(ΔPP-small), Cm^r Tet^r	This study
pKG99	pKV69 containing *rscS1*(*H323A*), Cm^r Tet^r	This study
pKG100	pKV69 containing *rscS1*(*F353A*), Cm^r Tet^r	This study
pKG102	pKV69 containing *rscS1*(*N345A*), Cm^r Tet^r	This study
pKG107	pKV69 containing *rscS1*(*H412Q*), Cm^r Tet^r	This study
pKG108	pKV69 containing *rscS1*(*H867Q*), Cm^r Tet^r	This study
pKG115	pKV69 containing *rscS1*(ΔN-term), Cm^r Tet^r	This study
pKG116	pKV69 containing *rscS1*(*L330R*), Cm^r Tet^r	This study
pKG123	pKV69 containing *rscS1*(*S9T*), Cm^r Tet^r	This study
pKG124	pKV69 containing *rscS1*(*S9A*), Cm^r Tet^r	This study
pKG125	pKV69 containing *rscS1*(*I13A*), Cm^r Tet^r	This study
pKG127	pKV69 containing *rscS1*(*D709A*), Cm^r Tet^r	This study

Wrinkled colony morphology. In most experiments, plasmid-bearing strains were streaked onto LBS-Tet plates and incubated at 28°C overnight. To obtain the photographs shown in Fig. 4, the bacteria were grown at 28°C in LBS-Tet for 6 h, and then a 10-μl aliquot was spotted on LBS-Tet plates and incubated at 28°C for 19 h. Spotting produced wrinkled morphology similar to that produced by streaking for single colonies, but it resulted in a uniform size, which allowed more direct comparisons among the different strains.

Surface adherence. Cultures were grown in HMM-CAA-Glu with Tet overnight and then diluted in 2 ml (final volume) to an optical density at 600 nm (OD_{600}) of 0.1. After 24 h of static incubation in glass tubes at 28°C, cells were stained with 1% (wt/vol) crystal violet for 15 min. Nonadherent cells and excess stain were washed away with several rinses of deionized H_2O, and the tubes were allowed to dry overnight. Quantitation was performed by adding 1 g of 1-mm glass beads and 2 ml of 95% ethanol to each tube, vortexing the tube for 10 s, and

TABLE 2. Primers used in this study

Primer	Sequence
ΔPPsmall-F	AAAGAATACACAATCCACACTATTTTT
ΔPPsmall-R	ACGACGATTATACAAAAATGAAGC
ΔPPlarge-R	ATATTGTTTTACAGGATGGTTCC
ΔPPlarge-F	ACCCAATCTGAAACGATAAAAAC
H323A-F	GTTAGATAAAATAAAAGCTGCCAATATTATTATCTTGC
H323A-R	GCAAGATAATAATATTGGCAGCTTTTATTTTATCTAAC
N345A-F	TATCTTTTGAATTAACAGCTCATCATAAAGATGGAAC
N345A-R	GTTCCATCTTTATGATGAGCTGTTAATTCAAAAGATA
F353A-F	CATAAAGATGGAACTTTAGCCTGGATAGATGTATC
F353A-R	GATACATCTATCCAGGCTAAAGTTCCATCTTTATG
NewΔNterm-F	GGATCCTTTATAGGAGTTAATGCAATGGAATTAATCC GCTCTGAAAAAGAA
D709A-F	TTAATTATCATGGCTAACCATATGCCTG
L330R-F	CAATATTATTATCTTGCGTCAATCCTTAGAAACAG
S9T-F	TTATTACGTTATACCCTGATCACAATCATT
S9A-F	CAATTATTACGTTATGCCCTGATCACAATCATT
I13A-F	TATAGCCTTATCACGGCCATTACTTGCACATTA
H412Q	GCAACTATGAGCCAGGAGCTGAGGACA
H867Q	GATTTAATGCTCAGTCGATAAAAGG
H867Q_pur	GATTTAATGCTCAGTCGATAAAAGG
Complement_H867Q-pur	CCTTTTATCGACTGAGCATTAAATC
rscS1-RBS-F	GGATCCTTTATAGGAGTTAATGCAATGAAA
9R2	GAGCCATTCCCAATATACC

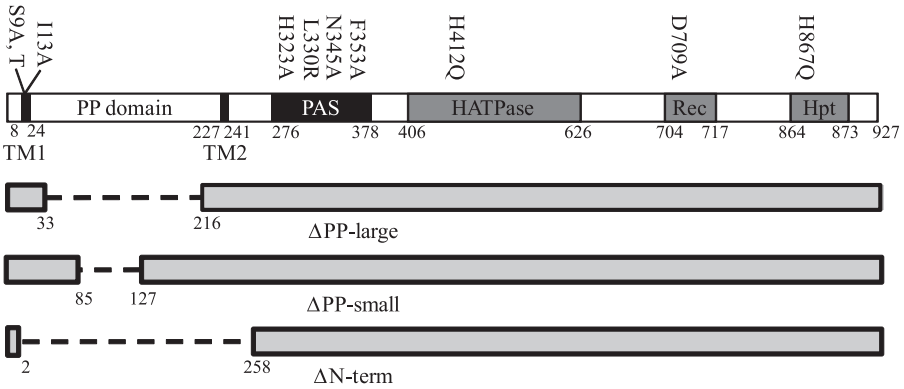

FIG. 1. Linear map of RscS domains. The locations of amino acid substitutions are indicated above the map, while deletions are shown below the map.

measuring the OD_{600} of the ethanol-crystal violet solution. The assay was performed in triplicate for each strain.

Pellicle formation. Cultures were grown in HMM-CAA-Glu with Tet overnight and then diluted in 3 ml (final volume) to an OD_{600} of 0.1. After 24 h of static incubation at 28°C, pellicle formation was assessed by drawing a pipette tip across the surface of the well. Formation of a visible film that was disrupted by the pipette tip was scored as positive for pellicle formation (+). Formation of a visible film only after 48 h of incubation was scored as ±. Strains which failed to form a film even after 48 h were scored as negative (−). The assay was performed in triplicate for each strain.

β-Galactosidase activity assays. Cultures were grown in rich medium (LBS) overnight, and β-galactosidase activity was measured as described previously (31). Total protein concentrations were determined by the method of Lowry et al. (27). The assay was performed in triplicate for each strain.

RESULTS

Putative phosphotransfer residues are important for RscS function. Sequence alignment predicted that RscS is a hybrid sensor kinase with HATPase, Rec, and Hpt domains (47), but to date, the importance of these regions for RscS activity has not been investigated. To determine if each of these putative domains contributes to RscS activity, we generated substitutions in residues predicted to be the targets of phosphorylation and assessed their effects on *rscS1*-dependent phenotypes. Specifically, we targeted the predicted autophosphorylated His in the HATPase domain (H412), the Asp site of phosphorylation in the Rec domain (D709), and the His in the Hpt domain (H867) (Fig. 1). Each of the His residues was replaced by Gln (H412Q and H867Q), while D709 was replaced by Ala (D709A).

Because the impact of RscS on biofilm formation has been observed only when an overexpression construct is used, we generated these and all other substitutions in the context of the increased activity allele *rscS1* carried on a multicopy plasmid. In each case, transcription of the *rscS* allele was driven exclusively from the vector-derived *lacZ* promoter. As controls, we used the unmutagenized *rscS1* plasmid pKG63 and vector pKV69. We then moved the resulting plasmids into *V. fischeri* and assessed RscS function. Specifically, we evaluated the abilities of the mutant alleles to produce protein and induce biofilm phenotypes, including *syp* transcription, wrinkled colony formation, pellicle formation, and surface attachment.

V. fischeri strains carrying plasmids with the H412Q and D709A substitution alleles produced full-length RscS protein, as evaluated by Western blot analysis (Fig. 2), but they exhibited severe defects in inducing biofilm phenotypes. First, these alleles failed to induce *syp* transcription, as monitored using a reporter strain bearing a chromosomal fusion of the *sypA* promoter to *lacZ* (P*sypA*::*lacZ*, KV2566 [Table 1]); the level of *syp* transcription induced by these alleles was 100-fold less than that induced by pKG63 (Fig. 3). Consistent with a loss of *syp* activation, these substitution alleles also failed to promote wrinkled colony formation under conditions in which pKG63 induces dramatic wrinkling (Fig. 4). Similarly, while pKG63 induced pellicle formation within 24 h, strains carrying the H412Q and D709A substitution alleles failed to form pellicles at the air-liquid interface even after 48 h (Table 3). Finally, these strains also failed to adhere to a glass surface, as visualized by crystal violet staining (Fig. 5A and B).

Like the H42Q and D709A substitution alleles, the H867Q allele produced wild-type levels of protein (Fig. 2). However, in contrast to the severe defects observed with the former alleles, H867Q induced moderate biofilm phenotypes. This substitution allele induced *syp* transcription to a level that was only fourfold less than the control level (Fig. 3). In agreement with this less severe effect on *syp* transcription, this strain also pro-

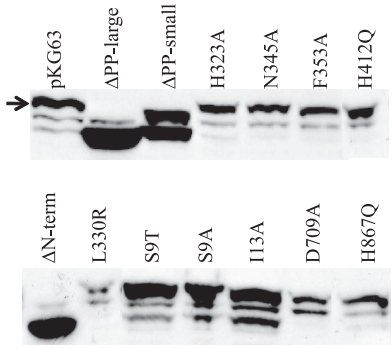

FIG. 2. Western blot analysis of RscS production by various mutant *rscS1* plasmids. The position of full-length RscS is indicated by an arrow. The lower two bands present in the pKG63 lane and the other full-length RscS derivatives represent a cross-reactive species and a putative proteolytic fragment of RscS, respectively (15a). ΔPP-large and ΔN-term roughly comigrate with the proteolytic fragment, while ΔPP-small is approximately the same size as the cross-reactive species.

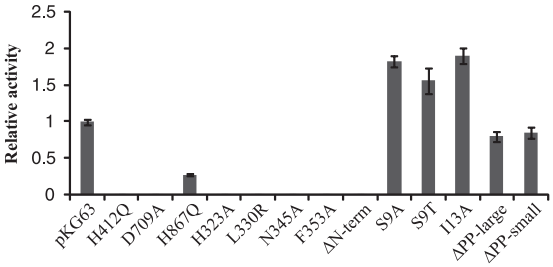

FIG. 3. Induction of *syp* transcription by RscS mutants. The β-galactosidase activity induced in the P*sypA*::*lacZ* reporter strain by a plasmid carrying a mutation was divided by the activity induced by pKG63 to derive the relative activity. The error bars represent propagation of the standard deviation.

duced moderate wrinkling (Fig. 4) and formed a pellicle at the air-liquid interface after 48 h (Table 3). Furthermore, the strain carrying the H867Q substitution allele retained some ability to adhere to a glass surface, forming a thin line of crystal violet-stained material at the air-liquid interface (Fig. 5A). These data suggest that the HATPase and Rec domains are required for RscS function, while the Hpt domain is partially dispensable.

RscS possesses a PAS signal detection domain critical for its activity. BLAST analysis (1) of the RscS amino acid sequence predicted that there is a PAS domain immediately carboxy terminal to TM2 (data not shown). Since PAS domains are commonly employed to detect environmental signals (44), we predicted that this domain is required to regulate RscS function. To further investigate the function of the putative PAS domain, we first generated a predicted structure. A first-approximation structural model (Fig. 6A) (SwissModel [2]) threaded the RscS PAS sequence onto the LOV1 domain of the Phot1 protein of *Chlamydomonas reinhardtii* (1N9L [14]), a flavin mononucleotide (FMN)-binding PAS domain. LOV (*l*ight, *o*xygen, or *v*oltage) domains comprise a subset of the PAS domain family and sense blue light through formation of a covalent cysteine-flavin adduct (9, 14). The ability to model the RscS sequence onto a PAS-like structure supported the hypothesis that RscS contains a PAS domain. However, the

TABLE 3. Pellicle formation by RscS mutants

Allele	Pellicle[a]
Empty vector	−
pKG63	+
H412Q	−
D709A	−
H867Q	±
H323A	−
L330R	−
N345A	−
F353A	−
ΔN-term	−
S9A	+
S9T	+
I13A	+
ΔPP-large	+
ΔPP-small	+

[a] +, formation of a visible pellicle within 24 h during incubation at 28°C; ±, formation of a visible pellicle within 48 h; −, failure to form a pellicle after 48 h.

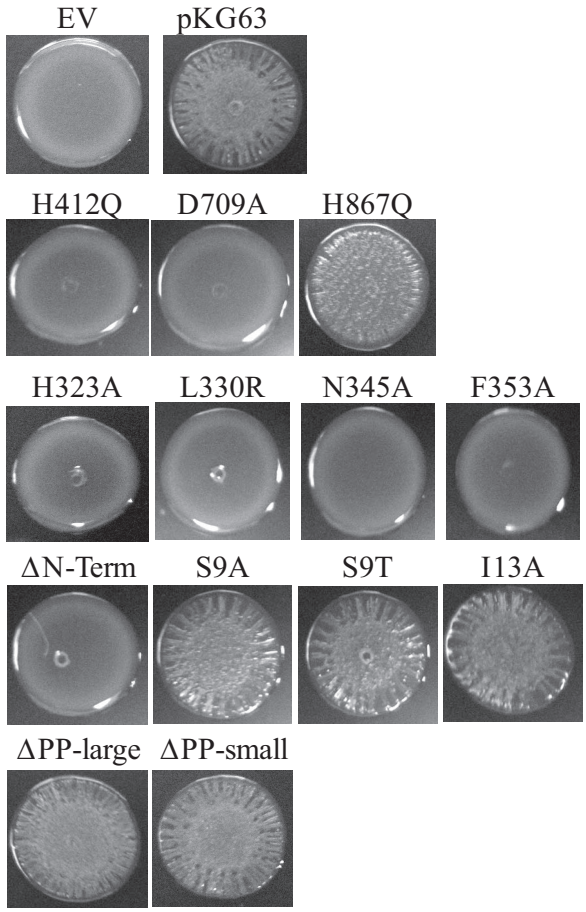

FIG. 4. Colony morphology of strains carrying RscS mutants. Bacteria were grown at 28°C in LBS-Tet for 6 h and then spotted on LBS-Tet plates and incubated at 28°C for 19 h. The experiment was performed at least in triplicate; representative results are shown. EV, empty vector.

RscS PAS domain lacks Cys residues, suggesting that it is not a canonical LOV domain. Furthermore, sequence alignment of RscS PAS, LOV1, and the related flavin adenine dinucleotide (FAD)-binding PAS domain of *Azotobacter vinelandii* NifL (Fig. 6D) revealed that the RscS PAS domain shares homology with NifL, especially in residues predicted to be important for FAD binding (24).

To determine if the putative PAS domain indeed regulates RscS function, we generated substitutions in PAS domain residues predicted to interact with a flavin cofactor based on the structure prediction and sequence alignment. In both FMN-binding LOV1 and FAD-binding NifL, a conserved Asn residue and an aromatic residue interact with the flavin ring of the respective cofactors (Fig. 6B and C). Replacement of the corresponding residues in RscS (Asn-345 and Phe-353) would thus be predicted to disrupt cofactor binding and RscS function. The NifL PAS domain further interacts with its FAD cofactor through a positive residue (corresponding to His-323 in RscS) and a hydrophobic residue (corresponding to Leu-330 in RscS) (24). Thus, disruption of these residues would be predicted to affect RscS function if the RscS PAS domain binds

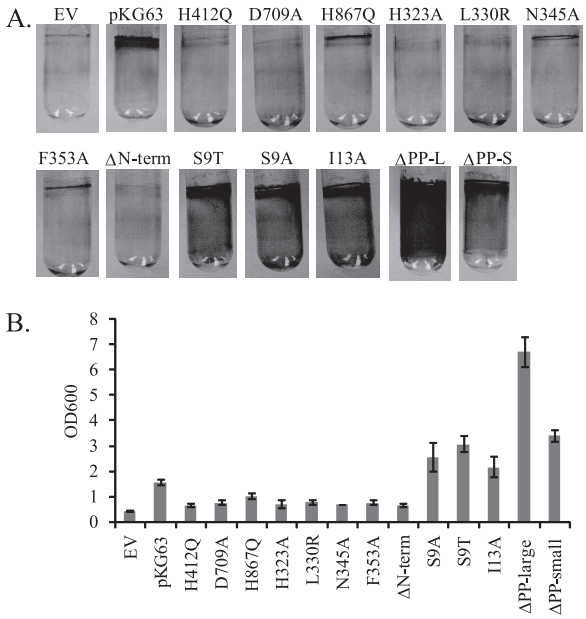

FIG. 5. Surface adherence of strains overexpressing the indicated *rscS* mutant constructs. (A) Photographs of crystal violet-stained glass tubes, showing variations in surface adherence. The experiment was performed in triplicate, and representative results are shown. (B) Quantitation of crystal violet staining. The error bars indicate the standard deviations. EV, empty vector.

a FAD cofactor. Therefore, we replaced H323, N345, and F353 with Ala and L330 with Arg.

V. fischeri strains carrying plasmids with the four PAS domain substitutions in *rscS* produced full-length RscS protein (Fig. 2) but exhibited severe defects in inducing biofilm formation. Each of the four PAS domain substitutions resulted in a profound loss of *syp* induction, and the transcription levels were approximately 100-fold lower than the level induced by pKG63 (Fig. 3). Consistent with this result, each substitution allele also failed to induce wrinkled colony formation on solid media (Fig. 4) and pellicle formation at the air-liquid interface (Table 3). Strains expressing the H323A and L330R substitution alleles also failed to adhere to a glass surface (Fig. 5A and B), while strains with the N345A and F353A substitution alleles exhibited a moderate ability to adhere to glass (Fig. 5A).

These experiments were performed at 28°C, the optimal growth temperature for *V. fischeri*. Historically, however, we have observed that incubation at room temperature increases RscS-mediated phenotypes (data not shown), and thus we asked if incubation at a lower temperature would restore activity to our PAS domain substitution alleles. Indeed, this was the case for the N345A and F353A substitutions. When incubated at room temperature, the strains carrying the N345A and F353A alleles both exhibited moderate wrinkling, surface adherence, and pellicle formation and induced *syp* transcription to levels near pKG63-induced levels (data not shown). However, strains carrying the H323A and L330R substitutions failed to exhibit *rscS1*-mediated phenotypes regardless of the temperature, and the results were indistinguishable from the results for the vector control (data not shown). Thus, the PAS domain is critical for RscS function, and the severe defect observed for substitutions (H323A and L330R) predicted to disrupt FAD binding but not FMN binding suggests that RscS may bind a FAD cofactor.

A cytoplasmic RscS derivative is partially active. Some membrane-bound sensor kinases become constitutively active when they are liberated from the membrane (6, 26), while others become nonfunctional (36). To determine what role membrane localization and/or sequences within the TMR and PP domain play in RscS function, we generated a cytoplasmic derivative of RscS lacking the putative TM helices and PP domain but retaining the PAS domain (ΔN-term; amino acids N3 through R257 removed [Fig. 1]) and tested its effect on RscS-dependent culture phenotypes. Western analysis showed that this deletion construct produced protein (Fig. 2). However, the deletion resulted in a loss of RscS function; the truncated protein failed to induce *syp* transcription (Fig. 3), wrinkled colony formation (Fig. 4), pellicles (Table 3), or surface adherence (Fig. 5A) when the assay was performed at 28°C. In contrast, incubation at a lower temperature restored partial activity, including moderate levels of *syp* transcription, wrinkled colony formation, thin pellicles, and moderate surface attachment (data not shown). Thus, full RscS activity may require localization to the membrane and/or essential sequences in the amino terminus.

The transmembrane domain is important for RscS function. The decrease in activity of the N-terminal deletion suggested a positive role for sequences in the PP domain and/or TMR. The TMR may directly detect environmental signals, or it may be important for transduction of the signal across the membrane from the PP domain. To determine the role of the TMR of RscS, we generated substitutions within the first putative TM helix (TM1) and determined their effects on RscS-dependent phenotypes. We focused on TM1 because modeling its sequence onto a helical wheel (data not shown) predicted the presence of a hydrophilic patch along one face of the helix. We predicted that this hydrophilic patch might serve as an interaction surface between the monomers within the RscS dimer or with another membrane protein. If it does, then disrupting this patch would alter these interactions and alter RscS function. To test this hypothesis, we replaced a hydrophilic Ser residue within the patch with a hydrophobic residue (S9A) or with another hydrophilic residue (S9T). Consistent with our hypothesis, strains carrying the S9A substitution allele exhibited an approximately twofold increase in *syp* transcription (Fig. 3). However, the S9T substitution also caused increased *syp* transcription, as did replacement of a residue outside the hydrophilic patch (I13A) (Fig. 3). The S9A, S9T, and I13A constructs each also slightly increased surface attachment (Fig. 5A) but induced the formation of wrinkled colonies (Fig. 4) and pellicles (Table 3) to an extent similar to that observed with strains carrying pKG63. Therefore, we propose that the identity of certain residues within TM1, but not their relative hydrophilicity, is important for RscS function.

The periplasmic domain negatively regulates RscS function. The loss of the N terminus led to a decrease in RscS function, while disruption of TM1 had the opposite effect. To determine what role the PP domain may play, we constructed mutations within this domain, leaving TM1 and TM2 intact. Because the PP domain has no significant homology to other proteins, we had no information to guide mutagenesis; therefore, we

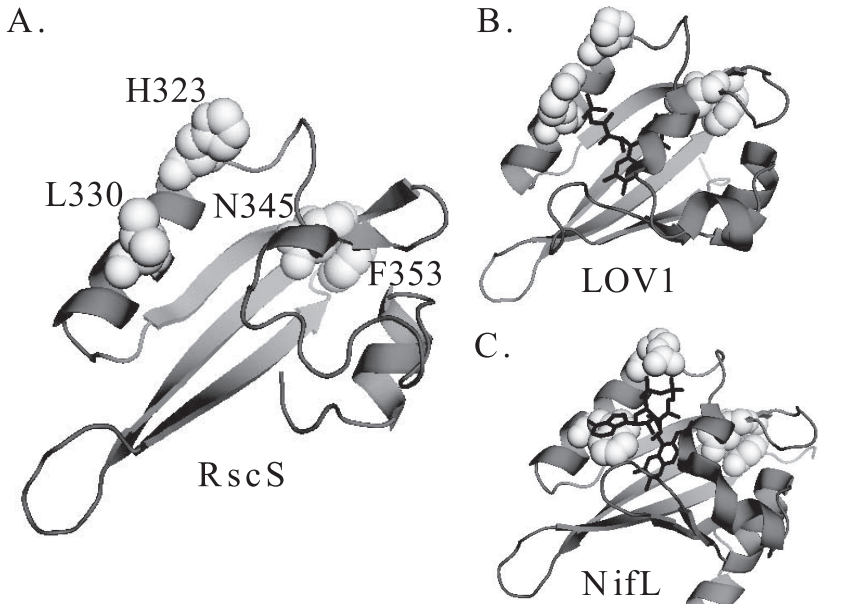

D.

```
RscS ------------AHDAIFILDKQGRLTWINQSYSALSGNTLEDI 307
NifL ELLPEIFRQTVEHAPIAISITDLKANILYANRAFRTITGYGSEEV 65
LOV1 ---------GLRHTFVVADATLPDCPLVYASEGFYAMTGYGPDEV 52

RscS EGKDLPSILQLDKIKHANIIILLQSLETGTSISFELTNHHKDGTL 354
NifL LGKNE-SILSNGTTPRLVYQALWGRLAQKKPWSGVLVNRRKDKTL 111
LOV1 LGHNC-RFLQGEGTDPKEVQKIRDAIKKGEACSVRLLNYRKDGTP 98

RscS FWIDVSITPILEPNGNIMHYIAVERDI--- 379
NifL YLAELTVAPVLNEAGETIYYLGMHRDTSEL 139
LOV1 FWNLLTVTPIKTPDGRVSKFVGVQVDVTS- 125
```

FIG. 6. RscS PAS domain. (A) RscS PAS domain sequence threaded onto the LOV1 domain of the Phot1 protein of *C. reinhardtii* (1N9L) (2, 14; http://swissmodel.expasy.org//). Residues subjected to mutagenesis in this study are shown in white spacefill and are labeled. (B) LOV1 domain of the Phot1 protein of *C. reinhardtii* (1N9L) (14). The FMN cofactor is indicated by black lines. Residues corresponding to the residues mutagenized in RscS are shown in white spacefill. (C) *A. vinelandii* NifL PAS domain structure (2GJ3) (24). The FAD cofactor is indicated by black lines. Residues corresponding to the residues mutagenized in RscS are shown in white spacefill. (D) Sequence alignment for the putative PAS domain of RscS, the *A. vinelandii* NifL PAS domain, and the LOV1 domain of the Phot1 protein of *C. reinhardtii*. Residues targeted for substitution in RscS and the corresponding residues in NifL and LOV1 are indicated by bold type. Crystal structures were visualized using the PyMOL molecular graphics system (http://www.pymol.org).

elected to examine the function of the PP domain by generating two deletions within it (Fig. 1). The deletion that we designated ΔPP-large removed 183 amino acids (Q33 through I216), leaving an 18-amino-acid linker between the two TM helices, while the deletion that we designated ΔPP-small removed 42 amino acids (amino acids 85 through 127) from the central portion of the domain.

V. fischeri strains carrying plasmids with these *rscS* deletions produced truncated RscS protein, as detected by Western analysis (Fig. 2). Both the large and small PP deletion constructs induced *syp* transcription to nearly wild-type levels (Fig. 3), suggesting that the PP domain is dispensable for this phenotype. Consistent with this result, strains carrying these two plasmids also produced wrinkled colonies on solid media (Fig. 4) and thick pellicles at the air-liquid interface (Table 3) to an extent similar to that observed with strains carrying pKG63. These results suggested that the PP domain is not required for RscS function other than as a membrane tether.

However, when we examined attachment, a different story began to emerge. The loss of the PP region of RscS (ΔPP-large) appeared to cause an increase in cell-cell aggregation. This effect was shown by formation of stringy cell aggregates during growth in shaking liquid cultures; these aggregates formed more quickly and to a greater extent in strains containing ΔPP-large than in strains carrying pKG63 (data not shown). Furthermore, strains carrying the ΔPP-large or ΔPP-small deletion alleles exhibited a dramatic increase in adherence to glass (Fig. 5A and B). Thus, these data suggested that removal of the PP domain resulted in increased RscS activity.

In the assay for surface attachment, the PP domain deletions not only increased the amount of crystal violet-stained material left on the glass surface but also changed the pattern of deposition. The wild-type protein induced surface attachment in a tight ring at the air-liquid interface, while both PP domain deletion alleles induced attachment throughout the culture (Fig. 5A). This effect could be seen quite clearly in surface attachment assays performed with various culture volumes. For pKG63-containing strains, the area of crystal violet stain-

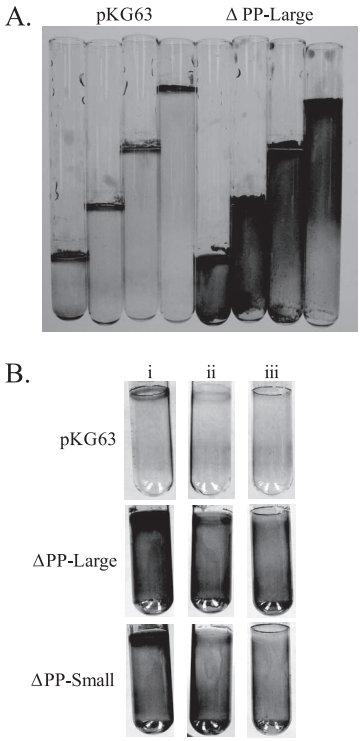

FIG. 7. Effect of air limitation on surface attachment. (A) Surface attachment assays performed with increasing volumes of culture. (B) Surface attachment assays performed with (i) normal airflow, (ii) airflow restricted with a cotton plug and Parafilm sealing the top, and (iii) airflow restricted by a mineral oil overlay.

ing was limited to the top of the tube, where the air-liquid interface was. In contrast, for strains carrying the ΔPP-large allele of *rscS*, staining occurred throughout the tube (Fig. 7A).

These results suggest that the wild-type protein fails to induce attachment below the air-liquid interface due to a negative signal relayed by the PP domain. For example, cells below the air-liquid interface may be exposed to lower levels of oxygen and thus be in a different redox state. In support of this idea, limiting airflow in the culture tubes using a mineral oil overlay or a cotton plug and Parafilm resulted in loss of the tight ring at the air-liquid interface for both pKG63 and PP domain deletion strains (Fig. 7B). In contrast, attachment below this ring was largely unaffected in cultures expressing the PP domain deletion constructs. The exact signal detected by the PP domain remains to be determined; nonetheless, these data support the conclusion that the PP domain modulates RscS activity under specific environmental conditions.

DISCUSSION

The work described here demonstrates that the *V. fischeri* symbiosis regulator RscS is a complex protein with multiple inputs for signal integration and relay. In its kinase domain, both the HATPase and Rec domains are required for RscS activity, while the Hpt domain is partially dispensable. In the amino-terminal sensor portion of the protein, disruption of the PP domain and TMR resulted in increased activity, while single amino acid substitutions in the PAS domain eliminated or severely impaired the function.

The identification of RscS as a hybrid sensor kinase suggested that after autophosphorylation the phosphoryl group progresses down the length of RscS through a phosphorelay before ultimately arriving at the target response regulator, as has been shown for the canonical hybrid sensor kinase ArcB (25). However, our results show that disruption of the Hpt domain results in only a partial loss of function. Intriguingly, the putative RscS homolog in *V. shilonii* has homology to *V. fischeri* RscS along the length of the protein but lacks a predicted Hpt domain (K. Geszvain, unpublished data). These data raise the possibility that at least some of the phosphoryl transfer along the length of RscS is independent of its Hpt domain. Thus, the phosphorelay may be branched, with some phosphoryl groups being transferred to the Hpt domain on RscS before being transferred to the response regulator and some phosphoryl groups being transferred from Rec to an unknown Hpt domain on a second protein. Such a phosphotransfer pathway is not unprecedented; in the Rcs capsular polysaccharide regulatory pathway of *E. coli*, the phosphoryl group is transferred from the Rec domain of the hybrid sensor kinase RcsC to the Hpt domain of another sensor kinase, RcsD (28). Alternatively, the phosphoryl group could be transferred directly to the downstream response regulator via H1 (H412), which has been shown to happen in vitro for ArcA/B (15). The *syp* cluster encodes three two-component regulators: two putative response regulators, SypG and SypE, and a predicted membrane-bound hybrid sensor kinase, SypF. SypG is required for all of the biofilm phenotypes induced by RscS in culture (15a, 22). Furthermore, we have found that SypG is required for biofilm formation induced by RscS(H867Q) and RscS(ΔPP-large) (unpublished data), suggesting that the activity of RscS is ultimately, if not directly, shuttled through SypG. SypE and SypF also play roles in RscS- and/or SypG-dependent phenotypes; however, their roles are complex and poorly understood (9a, 22). Thus, the regulatory consequences of RscS activation appear to be complex, involving interactions with multiple downstream targets.

While substitutions and deletions within the TMR and PP domain resulted in increased RscS activity, deletion of both domains together (ΔN-term allele) resulted in impaired function. Thus, while the TMR and the PP domain may detect or transmit a negative signal, there appears to be a positive role either for the TMR or the PP domain or for membrane localization itself. Possibly, membrane localization is required for activation of RscS through its PAS domain via a signal located predominately there, in much the same way that ArcB is proposed to be negatively regulated by quinones in the membrane (29). However, it is formally possible that the increased activity displayed by the TMR and PP domain mutant alleles is simply due to increased protein levels. This seems unlikely to be the case at least for the PP domain deletion alleles since they do not increase all RscS activities. For example, these alleles greatly increase surface attachment, yet they have little effect on *syp* transcription. Therefore, our data support a model in which the PP domain negatively regulates RscS function with residues in TM1 involved in transduction of this signal to the cytoplasmic domain, while the PAS domain located at the inner membrane positively regulates RscS activity.

Our results show that the PAS domain is critical for RscS function and support the hypothesis that there is a FAD cofactor bound to the domain. Replacement of H323 and replacement of L330 both resulted in a complete loss of RscS function, while the N345A and F353A substitutions both dramatically reduced activity at higher temperatures. A key difference between the FMN and FAD cofactors is the presence of the adenine base in the FAD cofactor. In NifL, a Trp residue (W87) base stacks with this adenine, stabilizing the interaction of the cofactor with the PAS domain (24). The corresponding residue in the FMN-binding LOV1 is a positively charged Arg (R74) (14), while in RscS it is a Leu residue (L330) (Fig. 6A). Replacement of L330 with Arg resulted in a complete loss of activity, consistent with the hypothesis that this positively charged residue repels binding of the hydrophobic adenine base of a FAD cofactor. The interaction between a positive residue and the phosphate group of FAD is thought to make a major contribution to the stability of FAD binding in flavoproteins (20). In NifL, this residue is R80 (24); the corresponding residue in RscS is H323, while in LOV1 it is P67 (14). Removing this positive residue from RscS (H323A) resulted in a complete loss of activity. Taken together, our data support the hypothesis that a FAD cofactor binds to the RscS PAS domain.

Can our data reveal anything about the nature of the signal(s) detected by RscS? FAD-binding PAS domains commonly act as redox sensors (43). For example, the oxidation state of the FAD cofactor bound in the *E. coli* aerotaxis sensor Aer is proposed to regulate the response of the protein to oxygen gradients and redox potential (38). Thus, RscS may sense the redox state of the cell through its PAS domain. At the same time, removal of the PP domain resulted in an apparent loss of sensitivity to low O_2 concentrations, as shown by increased surface attachment below the air-liquid interface of strains carrying the deletion alleles. This raises the intriguing possibility that a repressive O_2/redox state detected by the PP domain and an activating O_2/redox state detected by the PAS domain collaborate to limit RscS activity to a narrow window of optimal signal concentration. This is an attractive hypothesis because reactive oxygen species are present in the squid-secreted mucus that *V. fischeri* cells encounter early in the symbiosis (5, 10). Thus, RscS may detect a change in the redox state of the cell as the bacteria move from the relatively reducing environment of the seawater to the oxidizing environment of the squid.

ACKNOWLEDGMENTS

We thank Sean Crosson for his insights into PAS domain structure, Cindy Darnell for technical assistance, Alan Wolfe and members of our lab for critical reading of the manuscript and helpful suggestions, and Mark Mandel for sharing sequence data prior to publication.

This work was supported by NIH grant GM59690 awarded to K.L.V. and by the NIH through Ruth L. Kirschstein National Research Service Award 1 F32 G073523 from the NIGMS awarded to K.G.

REFERENCES

1. **Altschul, S. F., T. L. Madden, A. A. Schaffer, J. Zhang, Z. Zhang, W. Miller, and D. J. Lipman.** 1997. Gapped BLAST and PSI-BLAST: a new generation of protein database search programs. Nucleic Acids Res. **25:**3389–3402.
2. **Arnold, K., L. Bordoli, J. Kopp, and T. Schwede.** 2006. The SWISS-MODEL workspace: a web-based environment for protein structure homology modelling. Bioinformatics **22:**195–201.
3. **Bader, M. W., S. Sanowar, M. E. Daley, A. R. Schneider, U. Cho, W. Xu, R. E. Klevit, H. Le Moual, and S. I. Miller.** 2005. Recognition of antimicrobial peptides by a bacterial sensor kinase. Cell **122:**461–472.
4. **Boettcher, K. J., and E. G. Ruby.** 1990. Depressed light emission by symbiotic *Vibrio fischeri* of the sepiolid squid *Euprymna scolopes*. J. Bacteriol. **172:**3701–3706.
5. **Bose, J. L., U. Kim, W. Bartkowski, R. P. Gunsalus, A. M. Overley, N. L. Lyell, K. L. Visick, and E. V. Stabb.** 2007. Bioluminescence in *Vibrio fischeri* is controlled by the redox-responsive regulator ArcA. Mol. Microbiol. **65:**538–553.
6. **Cavicchioli, R., R. C. Chiang, L. V. Kalman, and R. P. Gunsalus.** 1996. Role of the periplasmic domain of the *Escherichia coli* NarX sensor-transmitter protein in nitrate-dependent signal transduction and gene regulation. Mol. Microbiol. **21:**901–911.
7. **Cho, U. S., M. W. Bader, M. F. Amaya, M. E. Daley, R. E. Klevit, S. I. Miller, and W. Xu.** 2006. Metal bridges between the PhoQ sensor domain and the membrane regulate transmembrane signaling. J. Mol. Biol. **356:**1193–1206.
8. **Cotter, P. A., and A. M. Jones.** 2003. Phosphorelay control of virulence gene expression in Bordetella. Trends Microbiol. **11:**367–373.
9. **Crosson, S., and K. Moffat.** 2001. Structure of a flavin-binding plant photoreceptor domain: insights into light-mediated signal transduction. Proc. Natl. Acad. Sci. USA **98:**2995–3000.

9a. **Darnell, C. L., E. A. Hussa, and K. L. Visick.** 9 May 2008. The putative hybrid sensor kinase SypF coordinates biofilm formation in *Vibrio fischeri* by acting upstream of two response regulators, SypG and VpsR. J. Bacteriol. doi:10.1128/JB.00197-08.

10. **Davidson, S. K., T. A. Koropatnick, R. Kossmehl, L. Sycuro, and M. J. McFall-Ngai.** 2004. NO means 'yes' in the squid-vibrio symbiosis: nitric oxide (NO) during the initial stages of a beneficial association. Cell. Microbiol. **6:**1139–1151.
11. **DeLoney, C. R., T. M. Bartley, and K. L. Visick.** 2002. Role for phosphoglucomutase in *Vibrio fischeri-Euprymna scolopes* symbiosis. J. Bacteriol. **184:**5121–5129.
12. **Draheim, R. R., A. F. Bormans, R. Z. Lai, and M. D. Manson.** 2006. Tuning a bacterial chemoreceptor with protein-membrane interactions. Biochemistry **45:**14655–14664.
13. **Falke, J. J., R. B. Bass, S. L. Butler, S. A. Chervitz, and M. A. Danielson.** 1997. The two-component signaling pathway of bacterial chemotaxis: a molecular view of signal transduction by receptors, kinases, and adaptation enzymes. Annu. Rev. Cell Dev. Biol. **13:**457–512.
14. **Fedorov, R., I. Schlichting, E. Hartmann, T. Domratcheva, M. Fuhrmann, and P. Hegemann.** 2003. Crystal structures and molecular mechanism of a light-induced signaling switch: the Phot-LOV1 domain from *Chlamydomonas reinhardtii*. Biophys. J. **84:**2474–2482.
15. **Georgellis, D., A. S. Lynch, and E. C. Lin.** 1997. In vitro phosphorylation study of the arc two-component signal transduction system of *Escherichia coli*. J. Bacteriol. **179:**5429–5435.

15a. **Geszvain, K., and K. L. Visick.** Multiple factors contribute to keep levels of the symbiosis regulator RscS low. FEMS Microbiol. Lett., in press.

16. **Geszvain, K., and K. L. Visick.** 2006. Roles of bacterial regulators in the symbiosis between *Vibrio fischeri* and *Euprymna scolopes*. Prog. Mol. Subcell. Biol. **41**:277–290.
17. **Gilles-Gonzalez, M. A., G. Gonzalez, and M. F. Perutz.** 1995. Kinase activity of oxygen sensor FixL depends on the spin state of its heme iron. Biochemistry **34:**232–236.
18. **Graf, J., P. V. Dunlap, and E. G. Ruby.** 1994. Effect of transposon-induced motility mutations on colonization of the host light organ by *Vibrio fischeri*. J. Bacteriol. **176:**6986–6991.
19. **Hefti, M. H., K. J. Francoijs, S. C. de Vries, R. Dixon, and J. Vervoort.** 2004. The PAS fold. A redefinition of the PAS domain based upon structural prediction. Eur. J. Biochem. **271:**1198–1208.
20. **Hefti, M. H., J. Vervoort, and W. J. van Berkel.** 2003. Deflavination and reconstitution of flavoproteins. Eur. J. Biochem. **270:**4227–4242.
21. **Horton, R. M.** 1997. *In vitro* recombination and mutagenesis of DNA. SOEing together tailor-made genes. Methods Mol. Biol. **67:**141–149.
22. **Hussa, E. A., C. L. Darnell, and K. L. Visick.** 25 April 2008. RscS functions upstream of SypG to control the *syp* locus and biofilm formation in *Vibrio fischeri*. J. Bacteriol. doi:10.1128/JB.00130-08.
23. **Jordan, S., A. Junker, J. D. Helmann, and T. Mascher.** 2006. Regulation of LiaRS-dependent gene expression in *Bacillus subtilis*: identification of inhibitor proteins, regulator binding sites, and target genes of a conserved cell envelope stress-sensing two-component system. J. Bacteriol. **188:**5153–5166.
24. **Key, J., M. Hefti, E. B. Purcell, and K. Moffat.** 2007. Structure of the redox sensor domain of *Azotobacter vinelandii* NifL at atomic resolution: signaling, dimerization, and mechanism. Biochemistry **46:**3614–3623.
25. **Kwon, O., D. Georgellis, and E. C. Lin.** 2000. Phosphorelay as the sole physiological route of signal transmission by the Arc two-component system of *Escherichia coli*. J. Bacteriol. **182:**3858–3862.
26. **Kwon, O., D. Georgellis, A. S. Lynch, D. Boyd, and E. C. Lin.** 2000. The ArcB sensor kinase of *Escherichia coli*: genetic exploration of the transmembrane region. J. Bacteriol. **182:**2960–2966.
27. **Lowry, O. H., N. J. Rosebrough, A. L. Farr, and R. J. Randall.** 1951. Protein measurement with the Folin phenol reagent. J. Biol. Chem. **193:**265–275.

28. **Majdalani, N., and S. Gottesman.** 2005. The Rcs phosphorelay: a complex signal transduction system. Annu. Rev. Microbiol. **59:**379–405.
29. **Malpica, R., G. R. Sandoval, C. Rodriguez, B. Franco, and D. Georgellis.** 2006. Signaling by the arc two-component system provides a link between the redox state of the quinone pool and gene expression. Antioxid. Redox Signal. **8:**781–795.
30. **Mascher, T., J. D. Helmann, and G. Unden.** 2006. Stimulus perception in bacterial signal-transducing histidine kinases. Microbiol. Mol. Biol. Rev. **70:**910–938.
31. **Miller, J. H.** 1972. Experiments in molecular genetics. Cold Spring Harbor Laboratory Press, Cold Spring Harbor, NY.
32. **Nyholm, S. V., and M. J. McFall-Ngai.** 2004. The winnowing: establishing the squid-vibrio symbiosis. Nat. Rev. Microbiol. **2:**632–642.
33. **Ottemann, K. M., W. Xiao, Y. K. Shin, and D. E. Koshland, Jr.** 1999. A piston model for transmembrane signaling of the aspartate receptor. Science **285:**1751–1754.
34. **Pappalardo, L., I. G. Janausch, V. Vijayan, E. Zientz, J. Junker, W. Peti, M. Zweckstetter, G. Unden, and C. Griesinger.** 2003. The NMR structure of the sensory domain of the membranous two-component fumarate sensor (histidine protein kinase) DcuS of *Escherichia coli*. J. Biol. Chem. **278:**39185–39188.
35. **Perego, M., C. Hanstein, K. M. Welsh, T. Djavakhishvili, P. Glaser, and J. A. Hoch.** 1994. Multiple protein-aspartate phosphatases provide a mechanism for the integration of diverse signals in the control of development in *B. subtilis*. Cell **79:**1047–1055.
36. **Piazza, F., P. Tortosa, and D. Dubnau.** 1999. Mutational analysis and membrane topology of ComP, a quorum-sensing histidine kinase of *Bacillus subtilis* controlling competence development. J. Bacteriol. **181:**4540–4548.
37. **Reinelt, S., E. Hofmann, T. Gerharz, M. Bott, and D. R. Madden.** 2003. The structure of the periplasmic ligand-binding domain of the sensor kinase CitA reveals the first extracellular PAS domain. J. Biol. Chem. **278:**39189–39196.
38. **Repik, A., A. Rebbapragada, M. S. Johnson, J. O. Haznedar, I. B. Zhulin, and B. L. Taylor.** 2000. PAS domain residues involved in signal transduction by the Aer redox sensor of *Escherichia coli*. Mol. Microbiol. **36:**806–816.
39. **Ruby, E. G., and K. H. Nealson.** 1977. Pyruvate production and excretion by the luminous marine bacteria. Appl. Environ. Microbiol. **34:**164–169.
40. **Stabb, E. V.** 2006. The *Vibrio fischeri-Euprymna scolopes* light organ symbiosis, p. ●●●–●●●. *In* F. L. Thompson, B. Austin, and J. Swings (ed.), The biology of vibrios. ASM Press, Washington, DC.
41. **Stabb, E. V., K. A. Reich, and E. G. Ruby.** 2001. *Vibrio fischeri* genes *hvnA* and *hvnB* encode secreted NAD^+-glycohydrolases. J. Bacteriol. **183:**309–317.
42. **Stock, A. M., V. L. Robinson, and P. N. Goudreau.** 2000. Two-component signal transduction. Annu. Rev. Biochem. **69:**183–215.
43. **Taylor, B. L., A. Rebbapragada, and M. S. Johnson.** 2001. The FAD-PAS domain as a sensor for behavioral responses in *Escherichia coli*. Antioxid. Redox Signal. **3:**867–879.
44. **Taylor, B. L., and I. B. Zhulin.** 1999. PAS domains: internal sensors of oxygen, redox potential, and light. Microbiol. Mol. Biol. Rev. **63:**479–506.
45. **Vescovi, E. G., Y. M. Ayala, E. Di Cera, and E. A. Groisman.** 1997. Characterization of the bacterial sensor protein PhoQ. Evidence for distinct binding sites for Mg^{2+} and Ca^{2+}. J. Biol. Chem. **272:**1440–1443.
46. **Visick, K. L., and E. G. Ruby.** 2006. *Vibrio fischeri* and its host: it takes two to tango. Curr. Opin. Microbiol. **9:**632–638.
47. **Visick, K. L., and L. M. Skoufos.** 2001. Two-component sensor required for normal symbiotic colonization of *Euprymna scolopes* by *Vibrio fischeri*. J. Bacteriol. **183:**835–842.
48. **Woodcock, D. M., P. J. Crowther, J. Doherty, S. Jefferson, E. DeCruz, M. Noyer-Weidner, S. S. Smith, M. Z. Michael, and M. W. Graham.** 1989. Quantitative evaluation of *Escherichia coli* host strains for tolerance to cytosine methylation in plasmid and phage recombinants. Nucleic Acids Res. **17:**3469–3478.
49. **Xu, J., H. C. Chiang, M. K. Bjursell, and J. I. Gordon.** 2004. Message from a human gut symbiont: sensitivity is a prerequisite for sharing. Trends Microbiol. **12:**21–28.
50. **Yip, E. S., K. Geszvain, C. R. DeLoney-Marino, and K. L. Visick.** 2006. The symbiosis regulator RscS controls the *syp* gene locus, biofilm formation and symbiotic aggregation by *Vibrio fischeri*. Mol. Microbiol. **62:**1586–1600.
51. **Yip, E. S., B. T. Grublesky, E. A. Hussa, and K. L. Visick.** 2005. A novel, conserved cluster of genes promotes symbiotic colonization and σ^{54}-dependent biofilm formation by *Vibrio fischeri*. Mol. Microbiol. **57:**1485–1498.

RESEARCH LETTER

Multiple factors contribute to keeping levels of the symbiosis regulator RscS low

Kati Geszvain & Karen L. Visick

Department of Microbiology and Immunology, Loyola University Chicago, Maywood, IL, USA

Correspondence: Karen L. Visick, Department of Microbiology and Immunology, Loyola University Medical Center, 2160 S. First Ave. Bldg. 105, Maywood, IL 60153, USA. Tel.: +1 708 216 0869; fax: +1 708 216 9574; e-mail: kvisick@lumc.edu

Present address: Kati Geszvain, Department of Environmental and Biomolecular Systems, Oregon Health and Sciences University, 20000 NW Walker Rd, Beaverton, OR 97006-8921, USA.

Received 10 December 2007; accepted 18 April 2008.
First published online 28 May 2008.

DOI:10.1111/j.1574-6968.2008.01209.x

Editor: Julian Ketley

Keywords
sensor kinase; histidine kinase; RscS; polysaccharide; symbiosis.

Abstract

Increased activity alleles (*rscS1* and *rscS2*) of the symbiosis regulator RscS induced both *syp* transcription and biofilm formation in *Vibrio fischeri*. Neither allele encodes a protein variant; instead they carry mutations near the putative ribosome-binding site and, in the case of *rscS1*, an additional silent mutation at codon Leu25. In this study, we found that endogenous levels of RscS are very low under the culture conditions examined and that the increased activity alleles dramatically increased the levels of protein. Of the two mutations present in *rscS1*, the Leu25 mutation, which replaces a rare with a more common Leu codon, appeared to make the greater contribution to increased activity. Our results suggest that RscS levels are maintained at low levels in the cell by the presence of a weak promoter, possible inefficient ribosome binding and the presence of rare codons in the 5′ end of the gene. Restriction of RscS levels may be important to prevent spurious signalling by this sensor kinase in the absence of a squid host.

Introduction

Two-component regulatory systems permit bacteria to rapidly sense and respond to changes in their environment (reviewed in Stock *et al.*, 2000). Thus, they are commonly used during bacterial colonization of a host, whether the ultimate outcome of colonization is symbiosis or pathogenesis. One example of a symbiotic association that utilizes two-component regulators during colonization is that between the marine bioluminescent bacterium *Vibrio fischeri* and the Hawaiian bobtail squid *Euprymna scolopes* (reviewed in Nyholm & McFall-Ngai, 2004; Stabb, 2006; Visick & Ruby, 2006). Newly hatched squid are aposymbiotic and must acquire their bacterial symbionts from their seawater environment. Symbiotic initiation by *V. fischeri* requires the orphan sensor kinase RscS: a strain in which *rscS* has been disrupted fails to colonize squid, or does so only after a severe delay (Visick & Skoufos, 2001). In contrast, colonization is substantially enhanced when RscS is overexpressed (Yip *et al.*, 2006). These data support the importance of this two-component regulator in symbiotic colonization.

Our recent efforts to understand the role of RscS in symbiotic colonization led to the discovery that RscS regulates transcription of the symbiosis polysaccharide (*syp*) cluster, a group of 18 genes also required for initiation of the symbiosis (Yip *et al.*, 2006). However, this regulation was not uncovered until we isolated two increased activity alleles of *rscS* (*rscS1* and *rscS2*, Yip *et al.*, 2006). Plasmids bearing either of these two alleles (pKG11 and pKG13, respectively) dramatically increased *syp* transcription and induced a number of biofilm-associated phenotypes. Specifically, pKG11 induced wrinkled colony morphology and pellicle formation, two phenotypes not observed for the wild-type and vector control strains. pKG13 also induced

wrinkled colony morphology, although to a lesser extent than pKG11 (K. Geszvain & K.L. Visick, unpublished data). Surprisingly, we found that both alleles encoded wild-type RscS protein, but contained a mutation within or adjacent to the putative ribosome-binding site (RBS, Fig. 1a). Additionally, pKG11 carried a silent mutation within the codon for Leu25 (Fig. 1a). The lack of a protein change suggested that these alleles increased activity by increasing levels of RscS protein, either through increasing the levels of transcript or increasing the efficiency of translation of the *rscS* transcript. However, semi-quantitative reverse transcriptase (RT)-PCR showed no detectable difference in *rscS* transcript steady-state levels in cells carrying pKG11 (Yip *et al.*, 2006). Here, we test the hypothesis that the mutations in pKG11 and/or pKG13 caused an increase in the levels of RscS protein and dissect the relative importance of the two mutations present in pKG11.

Materials and methods

Media

Escherichia coli strains were grown in Luria–Bertani (LB). *Vibrio fischeri* strains were grown in the rich medium LBS (Graf *et al.*, 1994; Stabb *et al.*, 2001), or Hepes minimal medium with casamino acids and glucose (HMM–CAA–Glu) (Yip *et al.*, 2005). The following antibiotics were added, as needed, to the final concentrations indicated: chloramphenicol (Cm), 5 μg mL^{-1}; and tetracycline (Tet), 5 μg mL^{-1} in LBS, 30 μg mL^{-1} in HMM.

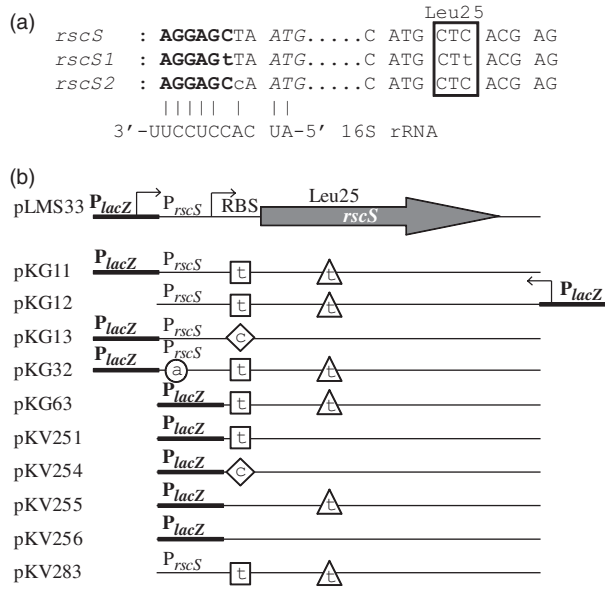

Fig. 1. Plasmids and mutations described in this study. (a) Mutations present in *rscS1* and *rscS2*. The putative RBS is shown in bold. The start codon is in italics while the 25th codon, encoding Leu, is boxed. Also shown is the 3′ end of the 16S rRNA of *Vibrio fischeri* (http://www.ergo-light.com/ERGO/) aligned to the putative RBS. (b) A linear representation of the plasmids used in this study. The location of mutations is indicated by a square for the RBS mutation present in *rscS1*, a triangle for the Leu25 mutation, a diamond for the RBS change present in *rscS2* and a circle for the promoter mutation present in pKG32.

Strains

Vibrio fischeri strain ES114 (Boettcher & Ruby, 1990) was the wild-type strain used in these experiments. Two derivatives of ES114 also were used. To identify the RscS protein, a strain which lacks the *rscS* gene was constructed: KV3378 (ES114Δ*rscS*). This strain was generated via recombination with pKG9 (Table 1) as follows. We used conjugation to deliver the unstable plasmid pKG9 into *V. fischeri* strain ES114, using standard techniques (Visick & Skoufos, 2001; DeLoney *et al.*, 2002). Following antibiotic selection for single recombinants in which pKG9 was integrated into the chromosome, we screened for cells that had undergone a second recombination event (identified by the loss of antibiotic resistance) to replace the wild-type copy of *rscS* with the deletion derivative (identified using PCR and confirmed by Southern analysis). To assess transcription of the *syp* locus, KV2566 (ES114 att Tn*7*::P*sypA-lacZ*) was constructed. To generate this strain, we introduced the suicide vector pEAH47 (Table 1) carrying a *lacZ* fusion to the *sypA* promoter into ES114 via a tetra-parental mating as described previously (O'Shea *et al.*, 2006). Following selection for the insertion of Tn*7* bearing the P*sypA-lacZ* reporter at the attTn*7* site, we screened for the loss of antibiotic resistance markers associated with the delivery and helper plasmids. In addition to the *V. fischeri* strains, the following strains of *E. coli* were used for the purposes of cloning and conjugation: DH5α (Woodcock *et al.*, 1989), TOP10 F′ (Invitrogen, Carlsbad, CA) and Tam 1 (Active Motif, Carlsbad, CA).

Plasmids

Plasmids used in this study are listed in Table 1. Plasmids were constructed using standard molecular biology techniques with restriction enzymes or PCR. To facilitate subcloning, a silent XhoI site was incorporated into *rscS* at L385 in both the pLMS33 and pKG11 plasmids via PCR amplification. To separate the two mutations present in *rscS1* as well as remove the P_{rscS} promoter, the *rscS* gene was amplified from either pLMS33-XhoI or pKG11-XhoI using primers specific for the RBS region (*rscS*-RBS-F, ggatccTTT AT**AGGAGC**TAATGCAATGAAA; *rscS1*-RBS-F, ggatccTTTA T**AGGAGt**TAATGCAATGAAA; or *rscS2*-RBS-F, ggatccTTT AT**AGGAGC**cAATGCAATGAAA) (where the letters in bold denote the putative RBS) and the M13-forward primer, which annealed to the opposite strand downstream of the gene. The resulting PCR product was cloned into

Table 1. Plasmids and strains used in this study

Plasmid	Description	References
pEAH47	pEVS107 with 1.6-kb VFA1019–*sypA* (VFA1020) intergenic region fused to *lacZ*	This work
pEVS107	Delivery vector for Tn*7*::*erm*	McCann *et al*. (2003)
pKG9	pEVS79 (Stabb & Ruby, 2002) with the *rscS* locus from *c*. 1 kb upstream to *c*. 1 kb downstream of the gene but with an internal EcoRI/ClaI fragment carrying *rscS* removed	This work
pKG11	pKV69 containing P_{rscS}-*rscS1*	Yip *et al*. (2006)
pKG12	pKV69 containing P_{rscS}-*rscS1*, opposite orientation relative to P_{lacZ}	This work
pKG13	pKV69 containing P_{rscS}-*rscS2*	Yip *et al*. (2006)
pKG32	pKG11 with P_{rscS} − 35 element mutation	This work
pKG63	pKV69 with *rscS1* under control of P_{lacZ}	This work
pKV69	Mobilizable vector, CmR, TetR	Visick & Skoufos (2001)
pKV251	pKV69 with RBS1 *rscS* under control of P_{lacZ}	This work
pKV254	pKV69 with *rscS2* under control of P_{lacZ}	This work
pKV255	pKV69 with Leu25 *rscS* under control of P_{lacZ}	This work
pKV256	pKV69 with wild type *rscS* under control of P_{lacZ}	This work
pKV283	pKG11 deleted for the *lac* promoter	This work
pLMS33	pKV69 containing *rscS* coding sequences plus 389 bp of sequence upstream of the ATG start codon, including P_{rscS}- *rscS* (located 44–70 bp upstream of the ATG start codon)	Visick & Skoufos (2001)
Strains	**Description**	**References**
ES114	*V. fischeri* wild type	Boettcher & Ruby (1990)
KV2566	ES114 att Tn*7*::P*sypA*::*lacZ*	This work
KV3378	ES114Δ*rscS*	This work

pCR2.1-TOPO (Invitrogen) and subsequently subcloned into pKV69.

Generation of anti-RscS antibody

To generate anti-RscS antibody, we first identified a 15 amino acid peptide near the carboxy-terminus of RscS (797-ELKRPSKYKLSDDA-810) that is predicted to be antigenic using the following Website: http://bio.dfci.harvard.edu/Tools/antigenic.pl. A search of the *V. fischeri* ES114 genome database at Integrated Genomics (http://www.ergo-light.com/ERGO/) revealed no significant matches, suggesting that this sequence is unique to RscS and thus would be specific for this protein. This peptide was generated and used to inject rabbits (Sigma Genosys, St Louis, MO); the resulting antiserum was subsequently purified with an affinity column (Alpha Diagnostic International, San Antonio, TX).

Western immunoblot analysis

Cells were grown in HMM–CAA–Glu with Tet at 22 °C overnight. Lysates were separated on 8% sodium dodecyl sulphate polyacyrlamide gel electrophoresis (SDS-PAGE), transferred to polyvinylidene difluoride membrane and probed with 1 : 500 dilution of affinity purified rabbit anti-RscS. Bands were visualized using a horseradish peroxidase-conjugated donkey anti-rabbit secondary antibody and ECL reagents. A Lowry assay was performed to ensure equal loading (Lowry *et al*., 1951).

β-Galactosidase assay

Cultures of the reporter strain KV2566 (P*sypA*::*lacZ*) carrying *rscS* or vector control plasmids were grown in LBS at 22 °C for 6–48 h. Samples were concentrated and cells were lysed using chloroform. *syp* transcription then was assessed by a β-galactosidase assay (Miller, 1972) and standardized to the amount of protein as determined by a Lowry assay (Lowry *et al*., 1951).

Results

The RscS protein naturally exists in limited quantities

The lack of protein substitutions present in the increased activity alleles *rscS1* and *rscS2* suggested that the mutations present in these alleles increased protein levels. However, strains bearing plasmids carrying these alleles (pKG11 and pKG13) did not produce sufficient amounts of RscS protein to detect by Coomassie staining (data not shown), and thus a more sensitive technique such as Western immunoblotting was required to analyze their levels. We, therefore, generated an anti-RscS antibody as described in Materials and methods. To evaluate the specificity of the purified antibodies, we performed a Western blot experiment using extracts from

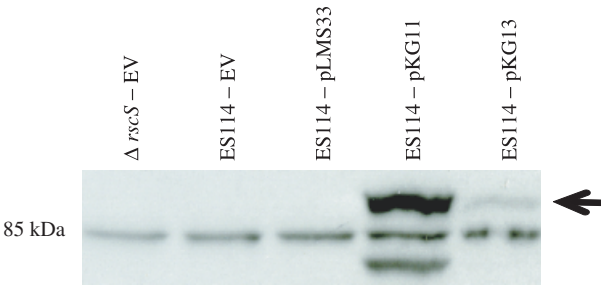

Fig. 2. Western immunoblot analysis of RscS expressed from different constructs. The putative full-length RscS is indicated by an arrow. The approximate location of the 85-kDa protein marker is indicated. EV = the empty vector, pKV69. Shown is a representative blot from three independent experiments.

V. fischeri carrying pKG11. The RscS antibody detected three species in this lysate, with the upper band (Fig. 2, arrow) roughly the correct size for RscS (predicted to be 106 kDa). To determine which of these bands represents RscS, we generated a *V. fischeri* strain in which *rscS* had been deleted (see Materials and methods) and introduced empty vector (pKV69) in order to treat the cells with the same antibiotics as those carrying *rscS* plasmids. We subsequently probed lysate derived from the Δ*rscS*–pKV69 strain with the RscS antibody. The middle of the three bands was still present in the *rscS* deletion, and thus we conclude that it represents a cross-reactive species (Fig. 2). However, both the top and the bottom bands were specific to RscS-containing strains. The faster migrating species may represent a proteolytic fragment of RscS.

Using this antibody, we then evaluated the relative levels of RscS produced by different *rscS* alleles. RscS was not detected in wild-type strains carrying the empty vector (pKV69, Fig. 2), suggesting that the endogenous *rscS* gene produces very little protein under the culture conditions we used [HMM–CAA–Glu with 30 μg mL^{-1} tetracycline (Ruby & Nealson, 1977; Yip *et al.*, 2005)]. RscS was also not detected in a strain carrying the wild-type *rscS* gene on a multicopy plasmid (pLMS33, Fig. 2). In fact, RscS was only detected in strains carrying the increased activity alleles (pKG11 and pKG13, Fig. 2). Consistent with their relative effects on *syp* cluster transcription (Yip *et al.*, 2006), pKG11 produced substantially more protein than pKG13 (Fig. 2). From this result, we conclude that the increased activity phenotypes associated with pKG11and pKG13 can be attributed to increased levels of RscS protein.

Transcription from the *rscS* promoter is weak

Each of the above plasmids, pLMS33 (wild-type *rscS*), pKG11 (*rscS1*), and pKG13 (*rscS2*), contain the *rscS* coding sequence and 389 bp of upstream sequence, including two predicted σ^{70}-binding *rscS* promoters [a major and a minor promoter (Visick & Skoufos, 2001), referred to collectively as P_{rscS}, Fig. 1b]. In each case, the *rscS* gene is also oriented correctly for transcription from the vector-derived *lacZ* promoter (P_{lacZ}). Therefore, transcription of *rscS* from these plasmids may be driven by either P_{rscS} or P_{lacZ}. Our data suggest that *rscS* transcription from these plasmids depends heavily on P_{lacZ}. First, pKG12, a subcloned plasmid variant in which *rscS1* was present in the opposite orientation relative to P_{lacZ} (and thus transcription would be dependent on the P_{rscS} promoters, Fig. 1b) exhibited substantially less RscS activity than pKG11 as measured by induction of *syp* transcription (Fig. 3) and failed to induce wrinkled colony morphology (data not shown). Second, in a screen for increased activity derivatives of pKG11 performed as described in Yip *et al.* (2006) but with pKG11 as the target for mutagenesis, we identified an allele with a mutation within the −35 hexamer of the major *rscS* promoter (TT**G**TAA to TT**A**TAA, pKG32) that decreased the similarity of the −35 element to the *E. coli* consensus (TTGACA) and thus may decrease binding of RNA polymerase (RNAP) to P_{rscS} (Busby & Ebright, 1994). Nonetheless, pKG32 results in approximately twofold increased RscS activity relative to pKG11 (Fig. 3). Third, deletion of P_{lacZ} from pKG11 to generate plasmid pKV283 resulted in a substantial decrease in *rscS* activity (data not shown). Together, these results indicate that P_{rscS} is a weak promoter; furthermore, they suggest that RNAP bound at this promoter may block

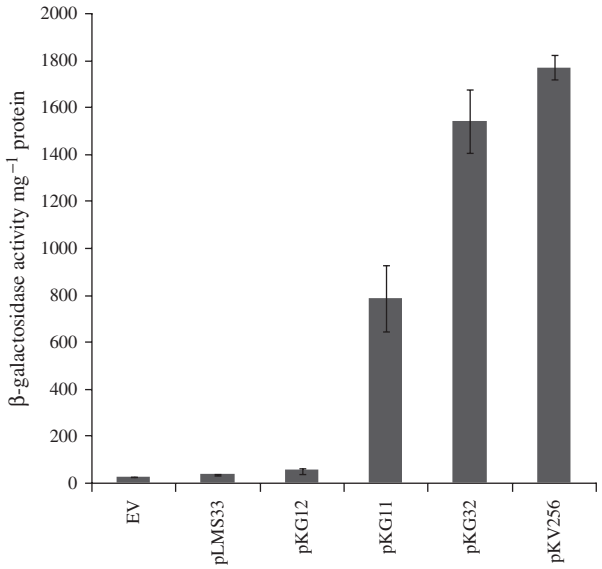

Fig. 3. The effect of different *rscS* alleles on *syp* transcription. Cultures of the reporter strain KV2566 (P*sypA*::*lacZ*) carrying the indicated plasmids were grown in LBS (Graf *et al.*, 1994; Stabb *et al.*, 2001) at 22 °C for 6 h, then *syp* transcription was assessed by a β-galactosidase assay (see Materials and methods). The assay was performed in triplicate, with error bars representing SD. EV = the empty vector, pKV69.

transcription from P_{lacZ}. Therefore, we predicted that removal of P_{rscS} would result in increased *rscS* transcription and increased RscS activity. This was in fact the case, cloning the wild-type *rscS* gene directly downstream of P_{lacZ} (pKV256, Fig. 1b) resulted in greatly increased RscS activity as shown by *syp* transcription (a 45-fold increase relative to pLMS33, Fig. 3). pKV256 also produced a substantial amount of RscS protein (data not shown) and, while pLMS33 has been shown to induce a slightly wrinkled colony morphology (Yip *et al.*, 2006), pKV256 induced dramatic wrinkling (data not shown).

The Leu25 mutation is primarily responsible for the *rscS1* phenotype

To determine which of the two mutations present on pKG11 (RBS1 and Leu25) were responsible for its phenotypes, we generated derivatives analogous to pKV256 but containing each individual mutation as well as the two together (Fig. 1b, Table 1) and screened their effect on RscS activity by assessing *syp* transcription. Plasmid pKG63, which carries the two mutations present in *rscS1*, increased *syp* transcription 1.2-fold relative to the wild type (Fig. 4). This moderate effect, compared with that seen for the double mutant plasmid pKG11, may be due to the high baseline activity of the wild-type allele in pKV256. pKV251 (RBS1) had a slight effect on activity (1.13-fold increased over wild-type, Fig. 4), while pKV255 (Leu25) increased activity 1.4-fold. In fact, the Leu25 mutation alone increased activity to a greater extent than the two mutations present together in pKG63 (Fig. 4). From these data we conclude that the Leu25 mutation was primarily responsible for the observed *rscS1* phenotypes.

We similarly asked whether the RBS2 mutation (Fig. 1b) would increase RscS activity in a construct lacking the *rscS* promoter (pKV254). Surprisingly, we found that it did not (Fig. 4). These data suggest that the context of this mutation is critical for its activity.

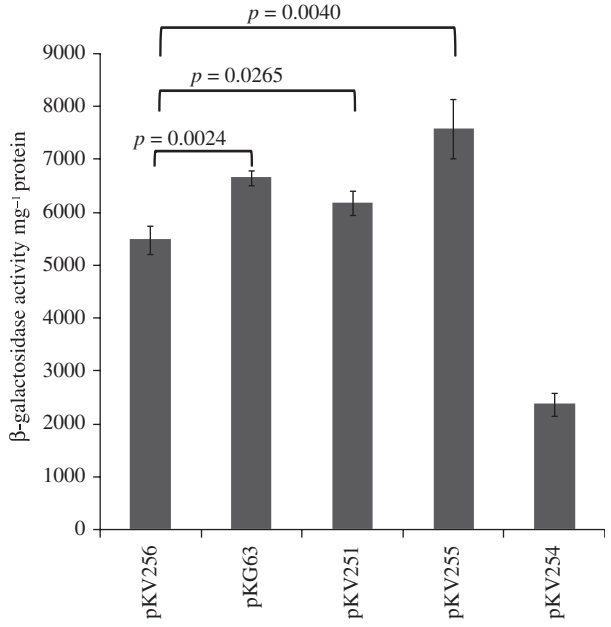

Fig. 4. Contribution of RBS1, RBS2 and Leu25 mutations to the *syp* transcription phenotype. Assays were performed as described in Fig. 3, except cultures were incubated at 22 °C for 48 h before removing samples. The *P* values refer to the variation between the two plasmids indicated by the brackets.

Discussion

In this study, we have generated antibodies specific for RscS and shown, using these antibodies, that pKG11 and pKG13 both increase protein levels above that of the wild type allele. Of the two mutations present on pKG11, the RBS mutation and the silent mutation at Leu25, Leu25 appears to make the greater contribution to the increased activity phenotype. Furthermore, our western analysis revealed that endogenous RscS levels are undetectable under the culture conditions we examined.

Together, our data suggest that RscS may be restricted to low levels in the cell by as many as three possible mechanisms. First, the natural promoter P_{rscS} appears to be weak. This is clear in the case of plasmids pKG12 and pKV283 (Fig. 1b), which contain the *rscS1* mutations but under control of P_{rscS}; unlike *rscS1* expressed from P_{lacZ}-P_{rscS} (pKG11) these constructs increase activity only slightly above that of empty vector (Fig. 3 and data not shown). Furthermore, the presence of P_{rscS} on the plasmid decreased RscS activity and a mutation within the major promoter predicted to weaken RNAP binding increased RscS activity (Fig. 3). Finally, semi-quantitative RT-PCR revealed very low levels of endogenous *rscS* transcript (data not shown). It remains to be seen if transcription of *rscS* is upregulated under a specific environmental condition, such as in response to the presence of a squid host. The promoter region of *rscS* appears to contain binding sites for the transcriptional regulators cAMP receptor protein (CRP) and GlpR (T.M. O'Shea and K.L. Visick, unpublished data), suggesting that RscS levels may be regulated in response to the nutritional state of the cell. Conversely, the low levels of *rscS* message detected may be due to transcript instability, as has been seen with other sensor kinase gene transcripts (Aiso & Ohki, 2003).

A second mechanism by which RscS levels are maintained at a low level may be through inefficient ribosome binding (Barrick *et al.*, 1994). This mechanism is suggested by the fact that both pKG11 and pKG13 contain changes within or adjacent to the RBS. However, these mutations do not increase complementarity between the RBS and the 16S rRNA; in fact the mutation present on pKG13 (RBS2)

decreases complementarity to the 16S rRNA (Fig. 1a). Therefore, these mutations may not directly alter ribosome binding but instead may alter formation of a secondary structure in the *rscS* message that occludes the RBS (de Smit & van Duin, 1990); the mutations in pKG11 and pKG13 may disrupt this structure and facilitate translation initiation. In support of an indirect effect on ribosome binding, we found that RBS2 increased RscS activity in the P_{lacZ}-P_{rscS} plasmid (Yip *et al.*, 2006) but decreased activity in the P_{lacZ} plasmid (Fig. 4; compare pKV254 to pKV256). The different 5′ UTRs of the two plasmids may form alternative secondary structures, resulting in differential effects of RBS2 on RscS activity.

A third mechanism keeping RscS levels low in the cell may be the use of rare codons. Our results show that the Leu25 mutation contributes significantly to the increased activity of *rscS1*. This mutation changes the 25th codon from CTC to CTT. The wild-type CTC codon is the rarest Leu codon, used in just 4% of *V. fischeri* Leu codons. The mutant CTT codon is found five times more frequently; in fact, it is the second most common Leu codon in *V. fischeri* (Nakamura *et al.*, 2000). It has been proposed that the presence of rare codons within the first 25 amino acids results in decreased translation efficiency as ribosomes stalled close to the initiation codon may block ribosome entry (Chen & Inouye, 1994). The Leu25 codon is located within a stretch of six amino acids ($L_{23}ML_{25}TRN_{28}$) of which all but the Met are encoded by rare codons, supporting the hypothesis that RscS is maintained at a low level through the use of rare codons in the message. Therefore, translation efficiency may be improved by the Leu25 mutation by increasing the efficiency of amino acid incorporation.

In summary, this work shows that increasing RscS protein levels is sufficient to increase RscS activity and that RscS protein levels are maintained at a low level in culture conditions. Because expression of RscS from pKG11 clearly enhances symbiosis (Yip *et al.*, 2006), it seems likely that high levels of RscS must be detrimental to some aspect of the *V. fischeri* life cycle, perhaps during long-term symbiotic maintenance or during survival in the seawater. Future studies will address these possibilities.

Acknowledgements

The authors thank Elizabeth A. Hussa for construction of the reporter strain KV2566, Cindy Darnell for technical assistance and members of the lab for critical reading of the manuscript and helpful suggestions. This work was supported by NIH grant GM59690 awarded to K.L.V. and by the NIH under the Ruth L. Kirschstein National Research Service Award 1 F32 G073523 from the NIGMS awarded to K.G.

References

Aiso T & Ohki R (2003) Instability of sensory histidine kinase mRNAs in *Escherichia coli*. *Genes Cells* **8**: 179–187.

Barrick D, Villanueba K, Childs J, Kalil R, Schneider TD, Lawrence CE, Gold L & Stormo GD (1994) Quantitative analysis of ribosome binding sites in *E. coli*. *Nucleic Acids Res* **22**: 1287–1295.

Boettcher KJ & Ruby EG (1990) Depressed light emission by symbiotic *Vibrio fischeri* of the sepiolid squid *Euprymna scolopes*. *J Bacteriol* **172**: 3701–3706.

Busby S & Ebright RH (1994) Promoter structure, promoter recognition, and transcription activation in prokaryotes. *Cell* **79**: 743–746.

Chen GT & Inouye M (1994) Role of the AGA/AGG codons, the rarest codons in global gene expression in *Escherichia coli*. *Genes Dev* **8**: 2641–2652.

DeLoney CR, Bartley TM & Visick KL (2002) Role for phosphoglucomutase in *Vibrio fischeri–Euprymna scolopes* symbiosis. *J Bacteriol* **184**: 5121–5129.

de Smit MH & van Duin J (1990) Secondary structure of the ribosome binding site determines translational efficiency: a quantitative analysis. *Proc Nat Acad Sci USA* **87**: 7668–7672.

Graf J, Dunlap PV & Ruby EG (1994) Effect of transposon-induced motility mutations on colonization of the host light organ by *Vibrio fischeri*. *J Bacteriol* **176**: 6986–6991.

Lowry OH, Rosebrough NJ, Farr AL & Randall RJ (1951) Protein measurement with the Folin phenol reagent. *J Biol Chem* **193**: 265–275.

McCann J, Stabb EV, Millikan DS & Ruby EG (2003) Population dynamics of *Vibrio fischeri* during infection of *Euprymna scolopes*. *Appl Environ Microbiol* **69**: 5928–5934.

Miller JH (1972) *Experiments in Molecular Genetics*, Cold Spring Harbor Laboratory Press, Cold Spring Harbor, NY.

Nakamura Y, Gojobori T & Ikemura T (2000) Codon usage tabulated from international DNA sequence databases: status for the year 2000. *Nucleic Acids Res* **28**: 292.

Nyholm SV & McFall-Ngai MJ (2004) The winnowing: establishing the squid-*Vibrio* symbiosis. *Nat Rev Microbiol* **2**: 632–642.

O'Shea TM, Klein AH, Geszvain K, Wolfe AJ & Visick KL (2006) Diguanylate cyclases control magnesium-dependent motility of *Vibrio fischeri*. *J Bacteriol* **188**: 8196–8205.

Ruby EG & Nealson KH (1977) Pyruvate production and excretion by the luminous marine bacteria. *Appl Environ Microbiol* **34**: 164–169.

Stabb EV (2006) The *Vibrio fischeri–Euprymna scolopes* light organ symbiosis. *The Biology of Vibrios* (Thompson FL, Austin B & Swings J, eds) ASM Press, Washington, DC.

Stabb EV & Ruby EG (2002) RP4-based plasmids for conjugation between *Escherichia coli* and members of the *Vibrionaceae*. *Methods Enzymol* **358**: 413–426.

Stabb EV, Reich KA & Ruby EG (2001) *Vibrio fischeri* genes *hvnA* and *hvnB* encode secreted NAD(+)-glycohydrolases. *J Bacteriol* **183**: 309–317.

Stock AM, Robinson VL & Goudreau PN (2000) Two-component signal transduction. *Annu Rev Biochem* **69**: 183–215.

Visick KL & Ruby EG (2006) *Vibrio fischeri* and its host: it takes two to tango. *Curr Opin Microbiol* **9**: 632–638.

Visick KL & Skoufos LM (2001) Two-component sensor required for normal symbiotic colonization of *Euprymna scolopes* by *Vibrio fischeri*. *J Bacteriol* **183**: 835–842.

Woodcock DM, Crowther PJ, Doherty J, Jefferson S, DeCruz E, Noyer-Weidner M, Smith SS, Michael MZ & Graham MW (1989) Quantitative evaluation of *Escherichia coli* host strains for tolerance to cytosine methylation in plasmid and phage recombinants. *Nucleic Acids Res* **17**: 3469–3478.

Yip ES, Geszvain K, DeLoney-Marino CR & Visick KL (2006) The symbiosis regulator RscS controls the *syp* gene locus, biofilm formation and symbiotic aggregation by *Vibrio fischeri*. *Mol Microbiol* **62**: 1586–1600.

Yip ES, Grublesky BT, Hussa EA & Visick KL (2005) A novel, conserved cluster of genes promotes symbiotic colonization and σ^{54}-dependent biofilm formation by *Vibrio fischeri*. *Mol Microbiol* **57**: 1485–1498.

JOURNAL OF BACTERIOLOGY, July 2008, p. 4941–4950 Vol. 190, No. 14
0021-9193/08/$08.00+0 doi:10.1128/JB.00197-08

The Putative Hybrid Sensor Kinase SypF Coordinates Biofilm Formation in *Vibrio fischeri* by Acting Upstream of Two Response Regulators, SypG and VpsR[▽]

Cynthia L. Darnell, Elizabeth A. Hussa, and Karen L. Visick*

Department of Microbiology and Immunology, Loyola University Medical Center, Maywood, Illinois

Received 7 February 2008/Accepted 5 May 2008

Colonization of the Hawaiian squid *Euprymna scolopes* by the marine bacterium *Vibrio fischeri* requires the symbiosis polysaccharide (*syp*) gene cluster, which contributes to symbiotic initiation by promoting biofilm formation on the surface of the symbiotic organ. We previously described roles for the *syp*-encoded response regulator SypG and an unlinked gene encoding the sensor kinase RscS in controlling *syp* transcription and inducing *syp*-dependent cell-cell aggregation phenotypes. Here, we report the involvement of an additional *syp*-encoded regulator, the putative sensor kinase SypF, in promoting biofilm formation. Through the isolation of an increased activity allele, *sypF1*, we determined that SypF can function to induce *syp* transcription as well as a variety of biofilm phenotypes, including wrinkled colony formation, adherence to glass, and pellicle formation. SypF1-mediated transcription of the *syp* cluster was entirely dependent on SypG. However, the biofilm phenotypes were reduced, not eliminated, in the *sypG* mutant. These phenotypes were also reduced in a mutant deleted for *sypE*, another *syp*-encoded response regulator. However, SypF1 still induced phenotypes in a *sypG sypE* double mutant, suggesting that SypF1 might activate another regulator(s). Our subsequent work revealed that the residual SypF1-induced biofilm formation depended on VpsR, a putative response regulator, and cellulose biosynthesis. These data support a model in which a network of regulators and at least two polysaccharide loci contribute to biofilm formation in *V. fischeri*.

In nature, the preferred lifestyle of many bacterial cells is growth within a biofilm, a community of microbes attached to a surface and/or to each other and embedded in a matrix consisting primarily of secreted polysaccharides. Biofilm cells exhibit different properties than individual, planktonic cells, such as increased resistance to antimicrobial agents, altered gene expression, and reduced metabolic rates (reviewed in references 11, 13, 14a, and 40). Because of these properties, and the fact that many human infections occur in the context of a biofilm, a critical area of research is in understanding how biofilms form, persist, and disperse.

To date, a number of organisms have been intensively studied for their biofilm-forming properties, including *Pseudomonas aeruginosa* (17, 25, 36, 46), *Staphylococcus* spp. (1, 3, 30, 48), and *Vibrio cholerae* (23, 42, 45, 50, 51). In these model systems, it has become apparent that numerous traits, such as motility and polysaccharide production, contribute to optimal biofilm formation. It is further evident that the regulatory control over these processes can be quite complex. For example, *V. cholerae*, which forms biofilms in the natural environment and during intestinal colonization of individuals with cholera (14, 41), uses multiple regulators to control biofilm formation. One of these is VpsR, a putative two-component response regulator protein that alters the transcriptome to produce a biofilm-competent state under specific environmental conditions (5, 22, 49). Two important targets of VpsR are the *vpsI* and *vpsII* (vibrio polysaccharide) loci, which produce VPS, the secreted polysaccharide that makes up the bulk of the *V. cholerae* biofilm matrix (49). Additional regulators, such as VpsT, a putative response regulator, HapR, a quorum-sensing regulator, and proteins that modulate the levels of the second messenger cyclic diguanylate (c-di-GMP), also control this locus (5, 9, 18, 54); thus, a complex network of regulation controlling biofilm formation exists.

While not traditionally considered an important model for biofilm formation, *Vibrio fischeri* contains a novel locus recently shown to be involved in polysaccharide production and biofilm formation. *V. fischeri* requires this 18-gene cluster, termed *syp* for *sy*mbiosis *p*olysaccharide, to colonize its symbiotic host, the squid *Euprymna scolopes* (Fig. 1A) (53). In this highly specific model of symbiosis, *E. scolopes* acquires its bacterial symbiont soon after hatching (reviewed in references 29, 37, and 43). *V. fischeri* cells from seawater form a biofilm-like aggregate on the surface of the symbiotic organ before entering pores and migrating to the sites of colonization. The *syp* cluster and an unlinked regulator, RscS, appear to be critical for the initial aggregation outside the pores; disruption of *rscS* or a representative *syp* gene resulted in a loss of aggregate formation and a defect in colonization (44, 52, 53). Furthermore, induction of the *syp* cluster by multicopy expression of RscS resulted in substantially increased aggregation on the surface of the symbiotic organ; it also caused, in laboratory culture, a variety of cell-cell aggregation phenotypes, including wrinkled colony and pellicle formation (52). These data revealed a link between symbiotic aggregation and biofilm formation in culture and suggested that symbiotic aggregation represents a type of natural biofilm formation that is crucial for *V. fischeri* to colonize *E. scolopes*.

* Corresponding author. Mailing address: Department of Microbiology and Immunology, Loyola University Chicago, 2160 S. First Ave., Bldg. 105, Rm. 3860A, Maywood, IL 60153. Phone: (708) 216-0869. Fax: (708) 216-9574. E-mail: kvisick@lumc.edu.

▽ Published ahead of print on 9 May 2008.

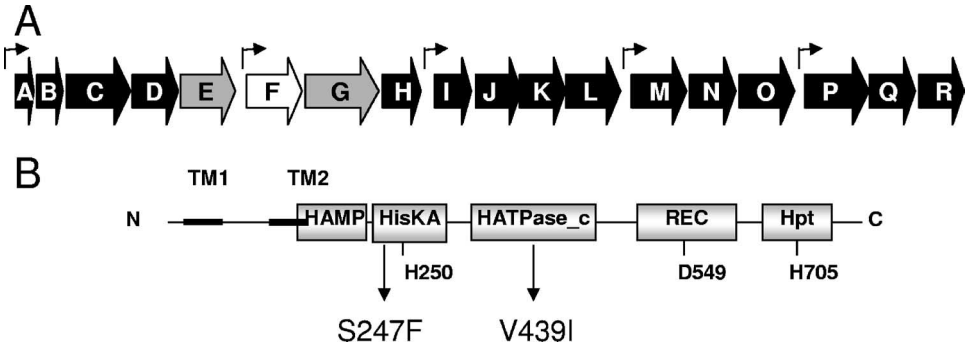

FIG. 1. The *syp* cluster and the SypF protein. (A) The *syp* cluster contains 18 genes (*sypA* to *-R*) that encode putative polysaccharide synthesis and transport proteins as well as four putative regulatory proteins, three of which are two-component regulators. The genes that are the subject of the manuscript are shown with gray (*sypE* and *sypG*) and white (*sypF*) arrows, while the remaining genes are shown with black arrows. The small bent arrows above the genes indicate known and putative promoters. (B) Domain structure of the hybrid sensor kinase SypF. SypF contains conserved histidine (H250, H705) and aspartate (D549) residues typical of hybrid sensor kinases. The putative SypF1 protein contains two substitutions, S247F in the HisKA domain and V439I in the H_ATPase domain, relative to that encoded within the annotated genome.

Control of *syp* expression appears complex. The unlinked regulator *rscS* encodes the sensor kinase portion of a two-component regulatory system. Two-component systems are widely used by bacteria to respond to their environment (reviewed in references 4, 7, and 20). A signal is sensed by the sensor kinase, resulting in autophosphorylation; the phosphoryl group is then passed to a response regulator. The activated response regulator then performs some function, such as inducing transcription, to elicit a cellular response. Indeed, we have found that RscS works upstream of SypG, a *syp*-encoded σ^{54}-dependent response regulator, to induce *syp* transcription and biofilm formation (21).

Located immediately upstream of *sypG* are genes for two other putative two-component regulators, *sypE* and *sypF* (Fig. 1A). The *sypE* gene encodes a putative response regulator that lacks a DNA-binding domain, while *sypF* encodes a putative sensor kinase. Our data to date suggest that SypE affects phenotypes induced by RscS and SypG; however, it appears to affect these phenotypes either positively or negatively, depending on which regulator is overexpressed, through an as-yet-unknown mechanism (21). A role for SypF has not yet been investigated. SypF appears to be a hybrid sensor kinase, with two putative transmembrane regions with a 120-amino-acid chain between them, a HAMP sensory domain, and putative domains typically involved in a phosphorelay (HisKA, HATPase_c, REC, and Hpt) (2, 35) (Fig. 1B).

Due to the complexity of the putative SypF protein and the intriguing location of its gene between two regulators required for biofilm formation, we sought a deeper understanding of its function. As part of this work we identified an increased activity allele, termed *sypF1*, that strongly induced biofilm-associated phenotypes. We found that these phenotypes depended in part on the *syp* locus and in part on another putative polysaccharide regulator, *vpsR*. These experiments thus reveal another layer in the complex control exerted by *V. fischeri* over polysaccharide production and biofilm formation.

MATERIALS AND METHODS

Media. *V. fischeri* strains were grown in SWT (53), LBS (15, 38), or HEPES minimal medium (HMM) (34) containing 0.3% Casamino Acids and 0.2% glucose (53). *Escherichia coli* strains were grown in LB (10) or brain heart infusion medium (Difco, Detroit, MI). The following antibiotics were added as needed, at the final concentrations indicated: ampicillin (Ap), 100 μg ml^{-1}; chloramphenicol (Cm), 25 μg ml^{-1} for *E. coli* and 2.5 μg ml^{-1} for *V. fischeri*; erythromycin (Em), 150 μg ml^{-1} for *E. coli* and 5 μg ml^{-1} for *V. fischeri*; kanamycin (Kn), 50 μg ml^{-1} for *E. coli* and 100 μg ml^{-1} for *V. fischeri*; tetracycline (Tc), 15 μg ml^{-1} for *E. coli* and 5 μg ml^{-1} [in LBS] or 30 μg ml^{-1} [in HMM] for *V. fischeri*. For solid media, agar was added to a final concentration of 1.5%.

Strain and plasmid construction. Wild-type *V. fischeri* ES114 (6) was used as the parent strain for these studies. Strains derived from ES114 and plasmids used in this study are described in Tables 1 and 2, respectively. *E. coli* strains TAM1 λ *pir* (Active Motif, Carlsbad, CA), TOP10 F′ (Invitrogen, Carlsbad, CA), and DH5α (47) were used for cloning, and *E. coli* CC118 (19) containing pEVS104 (39) was used to carry out triparental matings as described previously (44).

To overexpress *sypF*, we amplified the *sypF* gene using primers sypFexpF (AAGCGGGGACACCACCC) and 1026RTR (GAGGATAGCCAGAGAAGT GG), cloned the fragment into PCR cloning vector pCR2.1-TOPO (Invitrogen, Carlsbad, CA), and then subcloned it into the mobilizable pKV69 (44) to obtain

TABLE 1. *V. fischeri* strains used in this study

Strain	Genotype	Reference
ES114	Wild-type isolate from *E. scolopes*	6
KV1715	*vpsR*::pEAH11	22
KV1787	Δ*sypG*	22
KV1838	*sypN*::pTMB54	53
KV2283	*sypI*::pTMO89	This study
KV2481	*sypB*::pESY33	This study
KV3001	Wild-type attTn*7*::P$_{sypA}$ *lacZ*	21
KV3030	*sypB*::pESY33 attTn*7*::P$_{sypA}$ *lacZ*	This study
KV3031	*sypN*::pTMB54 attTn*7*::P$_{sypA}$ *lacZ*	This study
KV3232	Δ*sypG* attTn*7*::P$_{sypA}$ *lacZ*	21
KV3291	Δ*sypG vpsR*::pEAH11	This study
KV3299	Δ*sypE*	21
KV3378	Δ*rscS*	Gesvai and Visick[a]
KV3513	*vpsR*::pEAH11 attTn*7*::P$_{sypA}$ *lacZ*	This study
KV3514	*sypI*::pTMO89 attTn*7*::P$_{sypA}$ *lacZ*	This study
KV3586	Δ*sypE vpsR*::pEAH11	This study
KV3619	Δ*sypG vpsR*::pEAH11 attTn*7*::P$_{sypA}$ *lacZ*	This study
KV3620	Δ*sypE* attTn*7*::P$_{sypA}$ *lacZ*	21
KV3621	Δ*rscS* attTn*7*::P$_{sypA}$ *lacZ*	This study
KV3769	*VFA0884*::pCLD28	This study
KV3965	Δ*sypG* Δ*sypE*	This study
KV3968	Δ*sypG* Δ*sypE* attTn*7*::P$_{sypA}$ *lacZ*	This study
KV3970	*VF0352*::pCLD49	This study
KV4146	*VF0349*::pCLD57	This study

[a] K. Gesvain and K. L. Visick, submitted for publication.

TABLE 2. Plasmids used in this study

Plasmid	Relevant characteristics	Reference
pCLD6	Mini-Tn*7* delivery plasmid; mob; Kn^r Cm^r attTn*7*::P_{sypA}-*lacZ*	21
pCLD19	pESY20 + 2 kb upstream and downstream of *sypE*	21
pCLD28	pESY20 + 5′,3′-truncated *VFA0884*	This study
pCLD29	*sypF1* subcloned into pKV69; Cm^r Tc^r	This study
pCLD42	*vpsR* subcloned into pKV69; Cm^r Tc^r	This study
pCLD49	pESY20 + 5′,3′-truncated *VF0352*	This study
pCLD54	Wild-type *sypF* subcloned into pKV69; Cm^r Tc^r	This study
pCLD57	pESY20 + 5′,3′-truncated *VF0349*	This study
pCR2.1-TOPO	Commercial cloning vector; Ap^r Kn^r	Invitrogen
pEAH11	pEVS122 + 5′,3′-truncated *vpsR* (VF0454)	22
pESY20	pEVS122 cut with EcoRI (partial), filled in, and self-ligated	31
pEVS107	Mini-Tn*7* delivery plasmid; mob; Kn^r Em^r	27
pEVS122	R6Kγ *oriV oriT*RP4, Em^r, *lacZ*α	12
pJET1	Commerical cloning vector; Ap^r	Fermentas
pKV69	Mobilizable vector; Cm^r Tc^r	44
pMAC3	pKV69 expressing SypF-V439I; Cm^r Tc^r	This study
pMAC4	pKV69 expressing SypF1; Cm^r Tc^r	This study

pMAC3. A similar approach was used to generate a *vpsR* overexpression construct pCLD42, using primers VpsRF (AAGGATCCCATTTGTGAGACGAG ATAAGG) and VpsRR (AAGGATCCCATTTGTGAGACGAGATAAGG) and PCR cloning vector pJET1 (Fermentas, Glen Burnie, MD) as an intermediate cloning vector. The *sypF* overexpression plasmid pMAC3 was passaged through *E. coli* mutator strain CC130 (26) and introduced into ES114 by conjugation. The resulting colonies were examined for wrinkled colony formation. We isolated the plasmid (pMAC4) from one wrinkled colony and subcloned the *sypF* portion into pKV69 to obtain the *sypF1* overexpression plasmid pCLD29. The sequences of the *sypF* and *vpsR* genes in these constructs were obtained using forward, reverse, and/or gene-specific primers using the Genomics Core sequencing facility at Northwestern University. Sequence analysis revealed a single point mutation in pMAC3 (resulting in a V439I substitution), so a wild-type copy of *sypF* was cloned using sypFexpF and VFA10265R (CCTGCCCTGACATAT CTG), yielding pCLD54.

We constructed several *V. fischeri* mutants using a vector integration approach (8) as follows: we cloned an internal fragment of the target gene into the suicide vector pEVS122 (12) or its derivative pESY20 (31), generally by first cloning the appropriate PCR product into pCR2.1-TOPO. The resulting plasmid was introduced into *V. fischeri*. The resulting Em^r colonies were presumptive mutants, generated through homologous recombination to produce two truncated, nonfunctional copies of the gene. The mutants were subsequently verified by Southern analysis using the vector sequences as probe as described previously (53). The internal fragments for disrupting VFA0884, VF0349, and VF0352 were generated with primer sets VFA0884-c-F (CCGGTTGCAATTGAACTTTT AT)/VFA0884-c-R (GAGTTAAAGGAATGTCTTGCG), VF0349-c-F (CGTC TGCGCGTGCTACTC)/VF0349-c-R (AGCTGCTGCTTCAATAACGG), and VF0352-c-F (GTACCCTAACAAAGGCATTTG)/VF0352-c-R (CTGATACCG TAAGGAGTAAAG), respectively.

The Δ*sypG* Δ*sypE* double mutant was constructed by allelic replacement, using the Δ*sypG* parent strain and the Δ*sypE* deletion construct pCLD19, as previously described (21).

β-Galactosidase assay. Strains were grown (in triplicate) with shaking in HMM with Tc at 28°C overnight and then subcultured into fresh medium and grown for 20 h. Aliquots (1 ml) of cells were removed, concentrated, resuspended in Z-buffer, and lysed. The β-galactosidase activity (28) and the protein concentration (24) of each sample were assayed. β-Galactosidase units are reported as units of activity per mg of protein.

Crystal violet assay of biofilm formation. Strains were grown with shaking in HMM with Tc at 28°C overnight and then subcultured into fresh medium to an optical density at 600 nm (OD_{600}) of 0.1. Cultures were then grown for 48 h under static or shaking conditions and stained with 1% crystal violet. Tubes were rinsed with deionized H_2O and photographed. We quantified staining by adding 2 ml 100% ethanol and 1 g glass beads (1 mm), vortexing, and then measuring the OD_{600}.

Pellicle assay. Strains were grown with shaking in HMM with Tc at 28°C overnight and then subcultured to an OD_{600} of 0.1 in 3 ml of fresh medium in 12-well microtiter dishes. Cultures were then grown at room temperature for 48 h. The strength of the pellicle was evaluated by disrupting the air-liquid interface with a sterile pipette tip after 48 h of incubation. Cultures with no pellicle were scored as −; cultures with an easily broken pellicle were scored as +; cultures with an intermediate strength were scored as ++; cultures with a strong pellicle that was able to be lifted from the culture intact were scored as +++. To facilitate photography of the pellicles after they had formed, 25 μl of 100 mg/ml Coomassie blue was added to provide contrast, and the pellicles were disturbed so that they could be visualized.

RESULTS

An increased activity allele of *sypF* induces wrinkled colony formation. Biofilm formation by *V. fischeri* is controlled by at least three regulators, a sensor kinase (RscS) and two response regulators (SypG and SypE) encoded within the *syp* locus (Fig. 1A) (53). Between the two *syp* genes lies *sypF*, which encodes a putative sensor kinase. The juxtaposition of these latter genes suggested a common function. Thus, we hypothesized that SypF might act upstream of SypG and/or SypE to control biofilm formation. To probe the role of SypF, we assayed the biofilm phenotypes of a *sypF* mutant, as well as a wild-type strain of *V. fischeri* overexpressing *sypF* (from the multicopy plasmid pCLD54). Like the wild type and vector control, these strains did not induce wrinkled colony formation, pellicle production, adherence to glass, or *syp* transcription, although overexpression of *sypF* caused a slight aggregation of cells during growth with shaking in a minimal medium (HMM) (data not shown).

We thus hypothesized that our culture conditions might not include a strong activating signal recognized by this regulator. Therefore, we sought a constitutively active allele of *sypF* through random mutagenesis experiments (see Materials and Methods). Of over 10,000 colonies screened, we found a single colony that exhibited a wrinkled colony phenotype (Fig. 2A). We verified through subcloning experiments that the *sypF* portion of the plasmid was responsible for the wrinkled colony phenotype. The sequence of the *sypF1* allele carried by pCLD29 differed from that of *sypF* in the annotated genome at two positions, resulting in protein changes S247F and V439I. S247F is located within the HisKA domain and is three residues N-terminal to the conserved histidine predicted to be the site of phosphorylation; a change at this position could impact the predicted kinase activity of SypF (Fig. 1). The latter substitution, V439I, appears unimportant, as a strain carrying plasmid pMAC3, which carries *sypF* with only this change, behaved like a strain carrying wild-type *sypF* on pCLD54 (i.e., no impact on biofilm formation) (Fig. 2A and data not shown; see also Fig. 3A, 4A, and 5A, below). For the purposes of these studies, we used pMAC3 to control for the impact of SypF1 (expressed from pCLD29) on biofilm formation by *V. fischeri*.

Wrinkled colony formation by SypF1 depends on multiple regulators. Because the *sypF1* allele mediated wrinkled colony formation, a phenotype previously associated with *syp* function, we asked whether SypF1-induced wrinkled colony formation required an intact *syp* cluster. We introduced pCLD29 or the vector control into mutants defective for representative *syp*

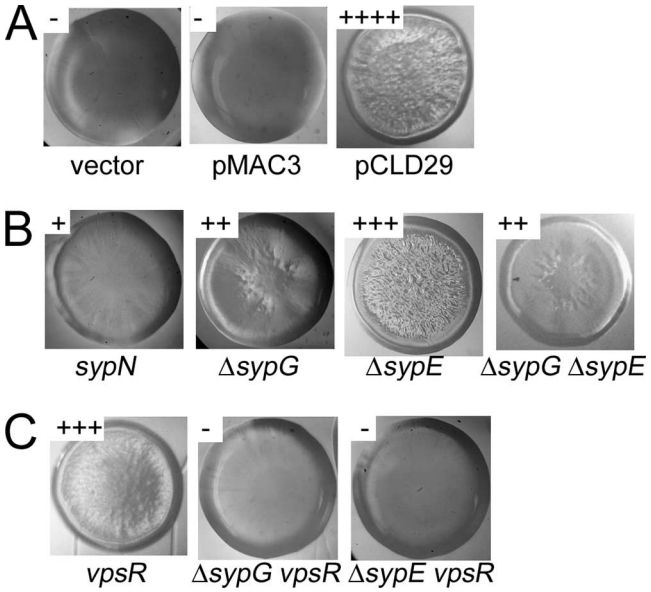

FIG. 2. Wrinkled colony morphology. Wrinkled colony formation was assessed by streaking strains on LBS with Tc and 0.3% glycerol. (A) Colonies formed by strains carrying the vector control, pMAC3 (*sypF* overexpression) or pCLD29 (*sypF1* overexpression). (B) Colonies formed by pCLD29-containing *syp* mutant strains, as indicated. (C) Colonies formed by pCLD29-containing *vpsR* mutant strains and *vpsR syp* double mutant strains.

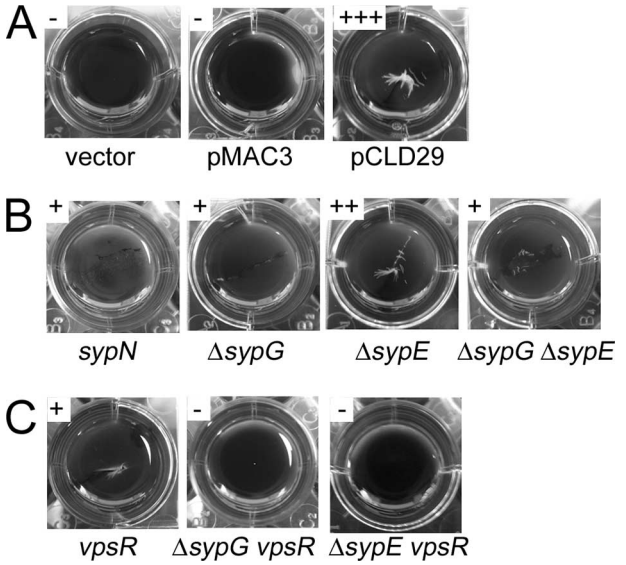

FIG. 3. Pellicle formation. Pellicles were assayed by culturing strains in HMM with Tc in 12-well microtiter dishes for 72 h. A pipette tip was dragged over the air-liquid interface to visualize the pellicle, and Coomassie blue was added to enhance the contrast. (A) Pellicle formation (or lack thereof) by strains carrying the vector, pMAC3, or pCLD29. (B) Pellicle formation by pCLD29-containing *syp* mutant strains. (C) Pellicle formation by pCLD29-containing *vpsR* mutant and *vpsR syp* double mutant strains. Scores were assigned as described in Materials and Methods.

structural genes: *sypB*, which encodes a putative OmpA-like outer membrane protein, and *sypI* and *sypN*, which encode putative glycosyltransferases. In these mutants, the ability of SypF1 to induce wrinkling was substantially reduced (Fig. 2B and data not shown). These data suggest that the *syp* cluster contributes to SypF1-induced wrinkling.

Our previous work revealed that wrinkled colonies induced by overexpressing the sensor kinase RscS were dependent upon the *syp*-encoded response regulator SypG, and to a lesser extent, SypE, a non-DNA-binding response regulator (21). To determine if these response regulators were required for SypF1-mediated wrinkled colony formation, we assayed the impact of SypF1 in mutants deleted for *sypG* or *sypE*. Deletion of either regulator caused a substantial reduction in, but not elimination of, wrinkling induced by SypF1 (Fig. 2B). To determine whether *sypE* and *sypG* together accounted for the ability of SypF1 to induce wrinkled colony formation, we constructed a strain in which both were deleted and then evaluated the resulting colony morphology induced by *sypF1*. Wrinkled colony formation in this strain was also substantially reduced, but again not eliminated (Fig. 2B). From these data, we conclude that SypE and SypG contribute to wrinkling induced by SypF1, but that another factor is also involved.

SypF1 induces pellicle formation. Another phenotype associated with the *syp* cluster is the formation of strong pellicles at the air-liquid interface of static cultures (52). We therefore assessed the ability of SypF1 to induce pellicle formation. We grew the *sypF1*-overexpressing strains statically in a minimal medium, HMM, for 48 h in a 12-well polystyrene microtiter dish. We found that overexpression of *sypF1* in the wild-type strain caused the formation of a strong pellicle that could be lifted from the culture as an intact aggregate. To aid comparisons between this pellicle and those formed in other mutant backgrounds, we applied a sterile pipette tip to the surface of the pellicle and assigned a score (see Materials and Methods) to the resistance encountered; we scored the pellicles produced by pCLD29-containing wild-type cultures as +++ (Fig. 3A).

To determine whether these pellicles depended upon *syp* structural genes, we assayed pellicle formation by the SypF1-overexpressing *syp* mutants (*sypB*, *sypI*, and *sypN*). The *syp* structural mutations substantially disrupted pellicle formation induced by SypF1: the pellicles that formed were very thin and easily broken (scored as +) (Fig. 3B and data not shown). These data support the conclusion that the product of the *syp* locus makes an important contribution to cell-cell interactions under these conditions.

We next assayed the dependence of SypF1-induced pellicle formation on *sypG* and *sypE*. Deletion of *sypG* substantially reduced, but did not eliminate, pellicle formation induced by SypF1 (scored as +) (Fig. 3B); this pellicle was easily broken into segments, supporting the hypothesis that Syp is important for cell-cell interactions. Deletion of *sypE* also reduced pellicle formation, though not as severely as the *sypG* mutant (scored as ++). Finally, a strain in which both *sypG* and *sypE* were deleted still retained some SypF1-induced pellicle formation. These data further support the hypothesis that SypF1 may function through an additional regulator.

SypF1 increases adherence to glass. A third phenotype associated with the *syp* locus is adherence to a glass surface (21, 52, 53), as assayed by crystal violet staining of cultures grown in HMM. Therefore, we asked whether SypF1 overexpression caused an increase in crystal violet-stainable material of statically

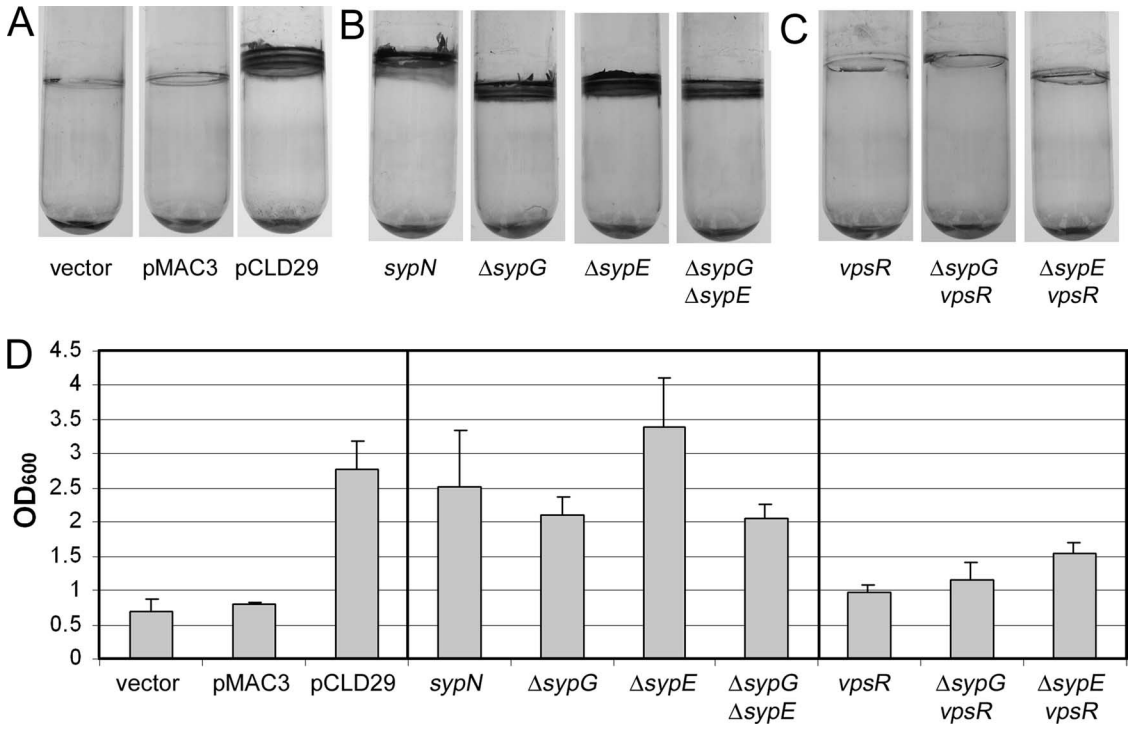

FIG. 4. Crystal violet staining of glass-attached material following static growth. Glass-attached materials following growth of cells under static conditions were assayed by subculturing into 2 ml HMM with Tc and incubating at room temperature for 48 h and then staining with 1% crystal violet. (A) Crystal violet staining of glass-attached material from cultures of vector-, pMAC3-, and pCLD29-containing cells. (B) Crystal violet staining of glass-attached material from cultures pCLD29-containing *syp* mutants. (C) Crystal violet staining of glass-attached material from cultures of pCLD29-containing *vpsR* mutant and *vpsR syp* double mutant strains. (D) Quantification of the crystal violet-stained material from tubes shown in panels A to C (and additional tubes not shown), solubilized as described in Materials and Methods. Error bars represent standard deviations.

grown *V. fischeri* cultures. We found that wild-type cultures carrying pCLD29 exhibited enhanced crystal violet staining at the air-liquid interface (Fig. 4A and D).

To determine if the SypF1-mediated enhancement of adherence to glass was dependent on *syp*, we evaluated attachment by pCLD29-containing *syp* mutants. We found that the *sypB*, *sypI*, and *sypN* genes were dispensable for this phenotype (Fig. 4B and data not shown). This result was somewhat surprising, since SypF1-mediated pellicle formation, a phenotype that occurs under similar static conditions, was disrupted by the loss of these genes. Like the structural genes, *sypG* and *sypE* did not appear to be important for the SypF1-induced adherence to glass under static conditions (Fig. 4B). Together with the pellicle data, our results suggested that the role of the *syp* cluster under these conditions involves promoting cell-cell, rather than cell-surface, interactions. They also supported the existence of a separate pathway, downstream from SypF, involved in mediating adherence to glass.

We also evaluated the ability of SypF1 to induce attachment to glass when cells were grown with shaking, a phenotype first observed in *V. fischeri* with the overexpression of the response regulator SypG (53). Under these conditions, SypF1 induced substantial cell clumping: the cells appeared aggregated, both at the air-liquid interface and the bottom of the tube, with the rest of the broth remaining relatively clear (Fig. 5A). Like SypG overexpression, SypF1 also induced a robust staining pattern with crystal violet (Fig. 5D and G).

Disruptions of *sypB*, *sypI*, and *sypN* each altered the appearance of the crystal violet-stained material and reduced aggregation (Fig. 5B and E and data not shown). Similarly, the loss of the regulators *sypG*, *sypE*, or both altered staining and decreased clumping (Fig. 5B, E, and G), though the *sypE* mutant had a less severe defect. Despite the different staining pattern, quantification revealed no significant differences in the amounts of crystal violet staining in these mutants relative to the control (Fig. 5G). We speculate that the qualitative difference in staining may result from apparent differences in the aggregation properties of the mutant cultures relative to the wild type (Fig. 5A). Taken together, these results further indicate that, under SypF1-overexpressing conditions, the *syp* regulators play more important roles in cell-cell adherence (as measured by aggregation) than in cell-surface attachment (as measured by crystal violet staining).

***sypF1* induces *syp* transcription.** To begin to understand the mechanism by which *sypF1* overexpression promotes the observed biofilm phenotypes, we asked whether pCLD29 induced transcription of the *syp* locus and, if so, whether induction depended upon SypG or SypE. We introduced pCLD29 and the vector control into strains that carried a P_{sypA}-*lacZ* transcriptional reporter (21) and measured the resulting β-galactosidase activity. Relative to the vector control, pCLD29 induced a 10-fold increase in β-galactosidase activity of the wild-type reporter strain (Fig. 6A). This induction was completely dependent on SypG, as its loss eliminated the observed induc-

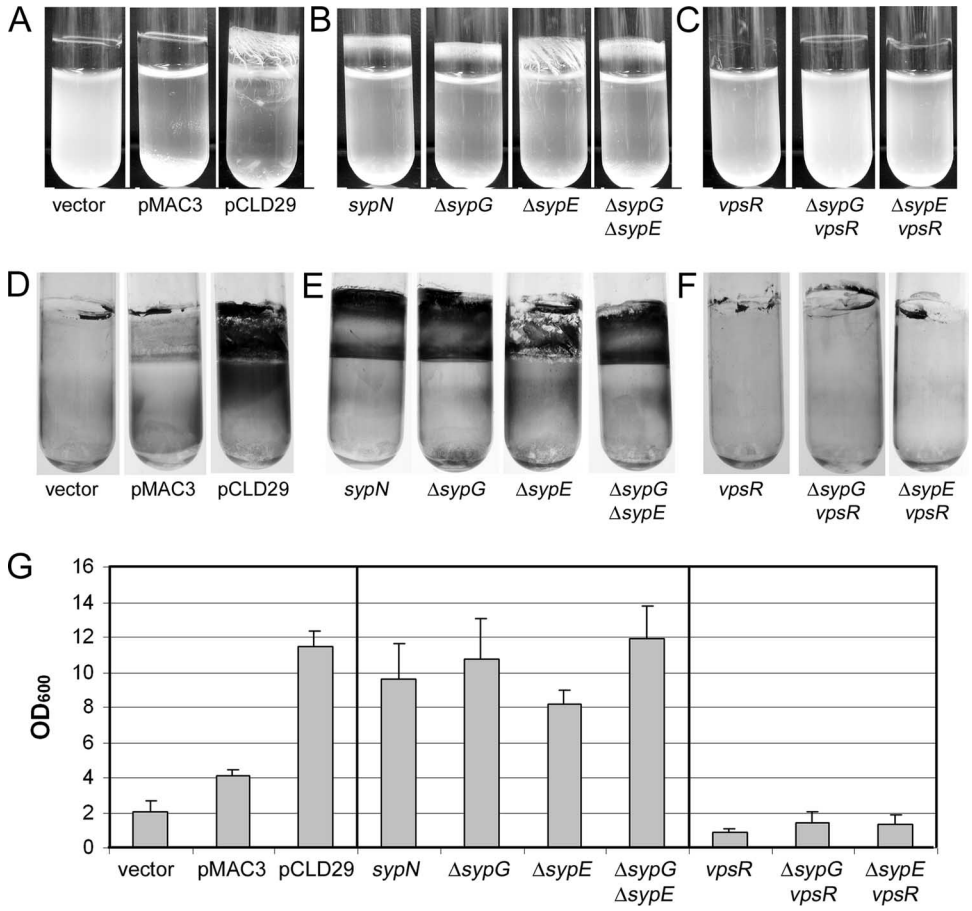

FIG. 5. Crystal violet staining of glass-attached material following growth with shaking. Glass-attached materials following growth of cells under shaking conditions were assayed by subculturing into 2 ml HMM with Tc and incubating at 28°C for 48 h (A to C) and then staining with 1% crystal violet (D to F). (A and D) Cultures of vector-, pMAC3-, and pCLD29-containing cells. (B and E) Cultures of pCLD29-containing *syp* mutants, as indicated. (C and F) Cultures of pCLD29-containing *vpsR* mutant and *vpsR syp* double mutant strains, as indicated. (G) Quantification of the crystal violet-stained materials from tubes shown in panels D to F (and additional tubes not shown), solubilized as described in Materials and Methods. Error bars represent standard deviations.

tion (Fig. 6B). The induction was also somewhat dependent on SypE, as a deletion of this gene reduced SypF1-mediated induction by sixfold (Fig. 6B). However, disruptions of other *syp* genes (*sypB*, *sypI*, and *sypN*) also caused reductions in *sypA* transcription (Fig. 6B and data not shown), making it somewhat difficult to interpret the *sypE* results. In any event, because SypE has no predicted DNA-binding domain, the effect of SypE is likely to be indirect. Not surprisingly, induction of

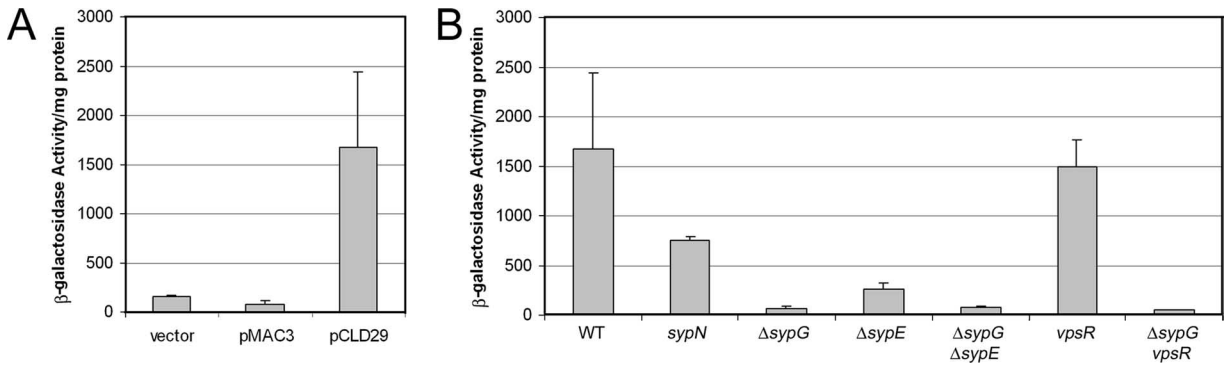

FIG. 6. β-Galactosidase activity. Transcription of the *syp* locus was monitored using a fusion of the *sypA* promoter region upstream of a promoterless *lacZ* gene, inserted in the chromosome at the Tn*7* site of wild-type and mutant cells. Cells were grown in HMM with Tc for 24 h. (A) Transcription from P_{sypA}-*lacZ* in cells carrying the vector control, pMAC3, or pCLD29. (B) Transcription from P_{sypA}-*lacZ* in pCLD29-containing wild-type (WT), *syp*, or *vpsR* mutant cells, as indicated. Error bars represent standard deviations.

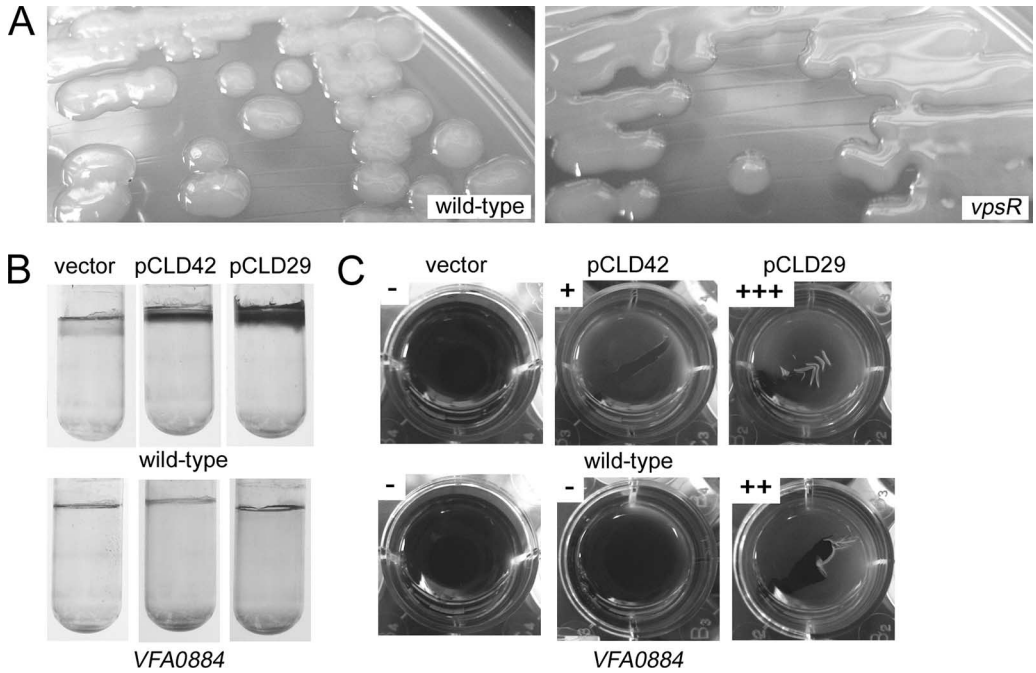

FIG. 7. Biofilm phenotypes of *vpsR* mutant and *vpsR* overexpression strains. Biofilms were produced upon disruption or overexpression of *vpsR*. (A) Colony morphology of vector (pKV69)-containing wild-type and *vpsR* mutant cells. (B) Crystal violet staining of glass-attached material from static cultures of wild-type or VFA0884 mutant cells carrying the vector control, pCLD42 (*vpsR* overexpressing), or pCLD29. (C) Pellicle formation by wild-type or VFA0884 mutant cells with vector, pCLD42, or pCLD29. Scores were assigned as described in Materials and Methods. Cells were grown as described in the legends for Fig. 2, 3, and 4.

the *syp* cluster was also eliminated in the *sypG sypE* double mutant (Fig. 6B). These data suggest that SypF1 primarily acts upstream of SypG in controlling *syp* transcription.

Some SypF1-induced phenotypes also depend upon *vpsR*. Together, our data support a role for *syp* and *syp* regulators in the phenotypes induced by SypF1, but it is clear that there are *syp*-independent effects. Because SypF is a sensor kinase, we hypothesized that it might signal through an additional response regulator(s) to promote the observed phenotypes. *V. fischeri* encodes 40 putative response regulators, including SypG and SypE. Of these, a prime candidate was VF0454. This gene encodes a protein with high sequence similarity to the *V. cholerae* gene *vpsR* (68% identity, 84% similarity over 441 amino acids [with one gap] of the *V. fischeri* ES114 protein with *V. cholerae* O1 biovar El tor [e-value, 6e-174]), which controls the *vps* polysaccharide locus (22, 35, 49).

Careful observation of a VF0454 vector integration mutant revealed that it formed colonies that were opaque and mucoid compared to the wild type (Fig. 7A and data not shown), suggesting that VF0454 may serve as a repressor of exopolysaccharide production. Therefore, we designated this gene *vpsR*, for vibrio polysaccharide regulator. Loss of *vpsR* also impacted the biofilm phenotypes induced by *sypF1* overexpression. Most significantly, the increase in crystal violet-stainable material produced under both static and shaking conditions appeared to be completely abrogated in the *vpsR* mutant (Fig. 4C and D and 5F and G). Loss of *vpsR* also altered wrinkled colony formation and reduced the strength of pellicle formed (Fig. 2C and 3C). The resulting pellicle was substantially defective in attaching to the surface of the well, suggesting a role for VpsR in cell-surface attachment. Finally, despite the loss of *vpsR*, the pCLD29-containing cultures, when grown in HMM with shaking, retained their characteristic clumping, although the amount appeared somewhat reduced (Fig. 5C). Together these data support an important role for VpsR in some SypF-induced phenotypes, particularly the cell-surface phenotypes revealed by crystal violet staining, and a lesser role in others. These effects appeared to be independent of SypF1-mediated *syp* transcription, as loss of *vpsR* did not alter this activity (Fig. 6C).

Because most SypF-induced phenotypes were not abolished by loss of *sypG* and *sypE*, or of *vpsR*, we asked whether SypF worked through both pathways. To determine if these regulators together could account for all of the SypF-induced phenotypes, we constructed *sypG vpsR* and *sypE vpsR* double mutants. Like the single *vpsR* mutant, these double mutants exhibited a mucoid phenotype, though this phenotype was lost when SypF1 was overexpressed (data not shown). The formation of wrinkled colonies and pellicles was completely abrogated in both pCLD29-containing double mutants (Fig. 2C and 3C). Crystal violet staining of double mutant cultures grown under either static or shaking conditions looked similar to that of the *vpsR* single mutant, indicating VpsR is responsible for these phenotype (Fig. 4C and 5C). Furthermore, the shaken cultures themselves were substantially less aggregated, appearing more similar to the vector control cultures (Fig. 5C). We obtained similar results when we evaluated SypF1-induced biofilm formation in a mutant defective for both *vpsR* and a *syp* structural gene, *sypP* (data not shown). These data support the

hypothesis that *syp* and a *vpsR*-dependent pathway together account for the SypF1 overexpression phenotypes.

VpsR overexpression impacts biofilm formation. To further evaluate the role of VpsR in biofilm formation, we constructed a plasmid that overexpresses the *vpsR* gene. After introducing this plasmid, pCLD42, into wild-type cells, we evaluated biofilm-associated phenotypes. Overexpression of VpsR was not sufficient to induce wrinkled colony morphology or alter crystal violet staining resulting from cultures grown under shaking conditions (data not shown). However, VpsR-overexpressing cultures were able to form weak pellicles (Fig. 7). Additionally, pCLD42 caused an increase in crystal violet staining from cultures grown under static conditions (Fig. 7). Together, these data support VpsR as an activator of biofilm formation.

Cellulose plays a role in *V. fischeri* biofilm formation. In *V. cholerae*, VpsR controls a large polysaccharide gene locus, *vps* (49, 51). Only a portion of this locus is conserved in *V. fischeri* (16). To determine whether this *vps*-like locus was responsible for the phenotypes induced by either SypF1 or VpsR overexpression, we disrupted two representative genes, VF0349 and VF0352. However, neither of these mutations disrupted the observed biofilm phenotypes (data not shown).

Subsequent exploration of the biofilms induced by these regulators revealed an increase in Congo red binding, a phenotype indicative of, among other things, cellulose biosynthesis. *V. fischeri* contains a cellulose biosynthetic gene cluster (*VFA0881-885*) similar to that found in *Salmonella* (32, 33, 35). To evaluate the role of this locus in the observed phenotypes, we constructed a mutant defective for *VFA0884*, which encodes the catalytic subunit of a putative cellulose synthase, and introduced either pCLD29 (*sypF1*) or pCLD42 (*vpsR*). Loss of VFA0884 disrupted the Congo red binding induced by these regulators (data not shown). Furthermore, this mutation eliminated glass attachment induced by SypF1 or VpsR (Fig. 7B). Finally, the pellicles formed by SypF1 in the *VFA0884* mutant were reduced to levels similar to the *vpsR* mutant; VpsR-induced pellicles were completely dependent on *VFA0884* (Fig. 7C). Together, these data support a role for cellulose in biofilm formation by *V. fischeri* under these conditions.

DISCUSSION

The significance of microbial biofilms as major survival strategies under both environmental and host conditions is well-accepted. Control of biofilm formation in numerous systems is complex (e.g., *V. cholerae* [5, 9, 50, 51, 54]). Here, we have shown that biofilm formation in *V. fischeri* also depends on multiple regulators. Our discovery of an increased activity allele, *sypF1*, revealed a role for this putative hybrid sensor kinase in the transcriptional control of *syp*, a polysaccharide locus necessary for symbiotic colonization. In addition, multicopy expression of *sypF1* induced biofilm phenotypes, including the formation of wrinkled colonies on solid medium and cell-cell aggregating, surface attachment, and pellicle formation in liquid medium. Surprisingly, we found that SypF1 appears to work through at least two response regulators, SypG and VpsR: disruption of both regulators was required for the complete loss of both wrinkled colony and pellicle formation induced by SypF1 overexpression. Multicopy expression of VpsR could also induce biofilm phenotypes (Fig. 7B and C), and these were found to be dependent on cellulose biosynthesis. Together, these data extend our knowledge of the complex control of biofilm formation by *V. fischeri* and suggest that SypF may coordinate *syp* activity through SypG with cellulose through VpsR.

Perhaps the simplest phenotype induced by overexpression of *sypF1* was transcription of the *syp* locus, as monitored with a *lacZ* reporter fused downstream from the *sypA* promoter. Reporter activity was increased 10-fold by SypF1, and this induction depended completely on SypG, a putative DNA-binding response regulator thought to directly activate *syp* transcription (53) (E. A. Hussa and K. Visick, unpublished data). Transcription did not depend fully upon any other regulator, although loss of SypE impacted the overall levels of induction, as did, to a lesser extent, loss of representative Syp structural proteins (encoded by *sypB*, *sypI*, and *sypN*). Perhaps these results indicate a form of feedback control on *syp* transcription. Importantly, *syp* transcription did not depend on VpsR, a response regulator predicted to control polysaccharide production: loss of the *vpsR* gene did not impact *sypA* transcription induced by SypF1 overexpression. Finally, SypF1-mediated *sypA* transcription also did not depend upon RscS, a sensor kinase known to act upstream of SypG (21) (C. Darnell and K. Visick, unpublished data). Together, these data support the hypothesis that SypF1 activates *syp* transcription by working upstream of SypG.

Despite this apparent connection between SypF and SypG with respect to *syp* transcription, a number of biofilm phenotypes induced by overexpression of *sypF1* did not depend exclusively on SypG, or in the case of attachment to glass, on SypG at all. Biofilm phenotypes are complex, requiring many factors to produce a complete structure (including, for example, motility, pili, exopolysaccharide, secreted proteins, and in some cases DNA) (reviewed in references 11 and 13). Furthermore, different phenotypes require different subsets of these factors. Therefore, to evaluate the role of SypF in biofilm formation, we assessed three major phenotypes (wrinkled colony morphology, surface attachment, and pellicle formation). Through this comprehensive approach, combined with mutant analyses, we were able to uncover a role for VpsR. Whereas loss of either SypG or VpsR severely impacted only a subset of the SypF1-induced phenotypes, loss of both regulators abolished all of them. Surprisingly, although VpsR (but not SypG) was required for attachment to glass induced by SypF1 under shaking conditions (Fig. 5), VpsR overexpression did not induce a similar phenotype (data not shown). These results suggest the involvement of other factors controlled by SypF1.

SypF also appeared to work upstream of SypE, though the impact of *sypE* disruption was less severe than that of *sypG* disruption and similar to disruption of *syp* structural genes, suggesting a less important regulatory role for SypE. At this time, our data support the hypothesis that SypE contributes to SypF-mediated biofilm formation, but whether SypE can be considered a direct downstream regulator remains uncertain, as its loss eliminates none of the observed phenotypes. Indeed, our preliminary data suggest that an additional RR may also be involved in the complex phenotypes induced by SypF; this possibility is currently under investigation (Darnell and Visick, unpublished). However, from the data presented here, we con-

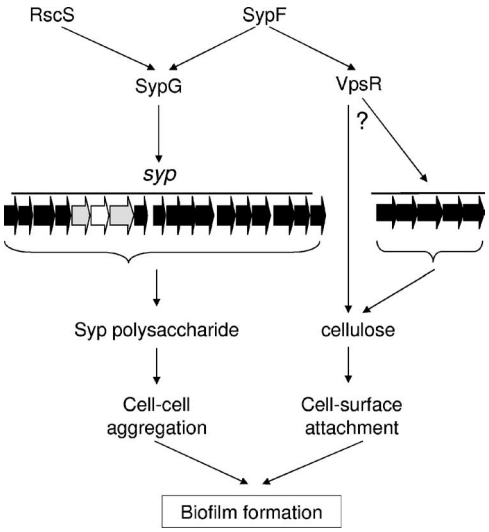

FIG. 8. Model for the roles of *syp* regulators in biofilm formation in *V. fischeri*. Transcription of the *syp* locus can be induced by overexpression of RscS or SypF (SypF1), acting through SypG. The Syp structural proteins contribute to the production of a Syp polysaccharide, involved in cell-cell aggregation phenotypes, such as wrinkled colonies and pellicles. SypE contributes by an unknown mechanism to these phenotypes; it also appears to inhibit SypG activity (not depicted). SypF overexpression may activate VpsR, ultimately promoting cellulose operon (VFA0881-885) expression or cellulose synthesis. The result of these interactions is enhanced cell-surface interactions. Block arrows indicate genes (depicted in gray for *sypE* and *sypG* and in white for *sypF*), and line arrows indicate activation. The question mark indicates that the level at which VpsR exerts its effect is not yet known.

clude that SypG and VpsR appear to represent major regulators involved in relaying the SypF-initiated signal.

Using these data and previous work (21, 52, 53) as a guide, we have developed a working model for the roles of the various *syp* regulators described to date (Fig. 8). SypF and RscS each have the potential to serve as phospho-donors to SypG, which we propose directly activates *syp* transcription. We previously reported that SypE may serve, under some circumstances, as an inhibitor of SypG activity, although SypE is required for full RscS and SypF activity (reference 21 and this work). As a result of these activities, a *syp*-dependent polysaccharide is produced, contributing to the formation of wrinkled colonies and pellicles and other phenotypes. In addition, SypF may directly or indirectly activate VpsR. Although the role of this protein as a response regulator is unclear, given the relative lack of conservation of key residues involved in phosphorylation (22, 49), genetic evidence supports the role of the *V. cholerae* homolog as a response regulator (23). Regardless of its specific activity, the *V. fischeri* protein apparently functions upstream of cellulose biosynthesis and thus biofilm formation. In other bacteria such as *Salmonella*, cellulose biosynthesis is controlled through posttranscriptional mechanisms, including through the availability of c-di-GMP (32, 33). Therefore, our simple model (Fig. 8) shows VpsR as a transcriptional regulator of the cellulose biosynthetic locus or as an indirect regulator of cellulose biosynthesis.

We propose that cellulose is responsible for initial attachment during static growth and that subsequent cell-cell interactions depend upon the Syp polysaccharide (Fig. 8). This hypothesis is supported by the following data: loss of VpsR or VFA0884 (but not SypG) disrupted surface attachment induced by SypF1 during static growth. The subsequent development of pellicles depended heavily on SypG. Disruption of *vpsR* did not prevent pellicle formation, but the pellicles that formed failed to attach properly to the well. These data suggest different roles for the two polysaccharides.

Similar to VpsR in *V. cholerae* ($VpsR_{VC}$), in which this protein has been most thoroughly investigated (5, 49), VpsR in *V. fischeri* ($VpsR_{VF}$) appears to be an orphan response regulator encoded within an analogous region of the large chromosome. The two proteins exhibit high sequence similarity yet appear to play distinct roles. $VpsR_{VF}$ controls cellulose biosynthesis; in contrast, *V. cholerae* doesn't contain a cellulose locus. While $VpsR_{VC}$ activates transcription of the *vps* polysaccharide locus, $VpsR_{VF}$, appears to serve both as a positive regulator of cellulose biosynthesis and as a negative regulator of an unknown polysaccharide, as evidenced by the increased mucoidy of a *vpsR* mutant. A further understanding of $VpsR_{VF}$ function awaits a more thorough investigation of its regulon through array studies.

It is possible that by overexpressing an increased activity allele of *sypF*, we are creating artifactual phenotypes: an overabundance of active SypF may phosphorylate response regulators that are not biologically relevant. However, SypG is encoded directly downstream of *sypF*, suggesting a likely connection between these regulators. VpsR also seems to be a relevant target, given that it is unlinked to a known sensor kinase and it clearly plays a role in polysaccharide production in its own right. Finally, the *vpsR* mutant exhibited a small defect in colonization of the squid when competed with the wild-type strain, suggesting a biologically relevant role (22). Thus, while SypF1 may improperly donate phosphoryl groups to other response regulators that contribute to phenotypes not identified here, this work nonetheless reveals regulators and phenotypes involved in biofilm formation by *V. fischeri*.

Taken together, this work elucidates a role for SypF in controlling the *syp* locus and thus contributing to the production of a *syp*-generated polysaccharide. It also provides evidence for a second distinct arm for polysaccharide production coordinated by SypF through VpsR, resulting in cellulose production. These two polysaccharides make differential contributions to the observed SypF-induced biofilms. Thus, this work further demonstrates the complexity of biofilm formation and regulation in *V. fischeri*, a nontraditional model of biofilm formation.

ACKNOWLEDGMENTS

We thank Mark Clementz, Deborah Muganda, and Emily Yip for their experimental contributions to this work and Alan Wolfe and Christine Anderson for their review of the manuscript.

This work was supported by NIH grant GM59690 awarded to K.L.V.

REFERENCES

1. **Al Laham, N., H. Rohde, G. Sander, A. Fischer, M. Hussain, C. Heilmann, D. Mack, R. Proctor, G. Peters, K. Becker, and C. von Eiff.** 2007. Augmented expression of polysaccharide intercellular adhesin in a defined *Staphylococcus epidermidis* mutant with the small-colony-variant phenotype. J. Bacteriol. **189:**4494–4501.
2. **Altschul, S. F., T. L. Madden, A. A. Schäffer, J. Zhang, Z. Zhang, W. Miller, and D. J. Lipman.** 1997. Gapped BLAST and PSI-BLAST: a new generation of protein database search programs. Nucleic Acids Res. **25:**3389–3402.
3. **Begun, J., J. M. Gaiani, H. Rohde, D. Mack, S. B. Calderwood, F. M.**

Ausubel, and C. D. Sifri. 2007. Staphylococcal biofilm exopolysaccharide protects against *Caenorhabditis elegans* immune defenses. PLoS Pathog. **3:**e57.
4. **Beier, D., and R. Gross.** 2006. Regulation of bacterial virulence by two-component systems. Curr. Opin. Microbiol. **9:**143–152.
5. **Beyhan, S., K. Bilecen, S. R. Salama, C. Casper-Lindley, and F. H. Yildiz.** 2007. Regulation of rugosity and biofilm formation in *Vibrio cholerae*: comparison of VpsT and VpsR regulons and epistasis analysis of *vpsT*, *vpsR*, and *hapR*. J. Bacteriol. **189:**388–402.
6. **Boettcher, K. J., and E. G. Ruby.** 1990. Depressed light emission by symbiotic *Vibrio fischeri* of the sepiolid squid *Euprymna scolopes*. J. Bacteriol. **172:**3701–3706.
7. **Calva, E., and R. Oropeza.** 2006. Two-component signal transduction systems, environmental signals, and virulence. Microb. Ecol. **51:**166–176.
8. **Campbell, A.** 1962. Episomes. Adv. Genet. **11:**101–145.
9. **Casper-Lindley, C., and F. H. Yildiz.** 2004. VpsT is a transcriptional regulator required for expression of *vps* biosynthesis genes and the development of rugose colonial morphology in *Vibrio cholerae* O1 El Tor. J. Bacteriol. **186:**1574–1578.
10. **Davis, R. W., D. Botstein, and J. R. Roth.** 1980. Advanced bacterial genetics. Cold Spring Harbor Laboratory, Cold Spring Harbor, NY.
11. **Donlan, R. M., and J. W. Costerton.** 2002. Biofilms: survival mechanisms of clinically relevant microorganisms. Clin. Microbiol. Rev. **15:**167–193.
12. **Dunn, A. K., M. O. Martin, and E. Stabb.** 2005. Characterization of pES213, a small mobilizable plasmid from *Vibrio fischeri*. Plasmid **54:**114–134.
13. **Dunne, W. M., Jr.** 2002. Bacterial adhesion: seen any good biofilms lately? Clin. Microbiol. Rev. **15:**155–166.
14. **Faruque, S. M., K. Biswas, S. M. Udden, Q. S. Ahmad, D. A. Sack, G. B. Nair, and J. J. Mekalanos.** 2006. Transmissibility of cholera: in vivo-formed biofilms and their relationship to infectivity and persistence in the environment. Proc. Natl. Acad. Sci. USA **103:**6350–6355.

14a. **Geszain, K., and K. L. Visick.** 28 May 2008. Multiple factors contribute to keeping levels of the symbiosis regulator RscS low. FEMS Microbiol. Lett. doi:10.1111/j.1574-6968.2008.01209.

15. **Graf, J., P. V. Dunlap, and E. G. Ruby.** 1994. Effect of transposon-induced motility mutations on colonization of the host light organ by *Vibrio fischeri*. J. Bacteriol. **176:**6986–6991.
16. **Grau, B. L., M. C. Henk, K. L. Garrison, B. J. Olivier, R. M. Schulz, K. L. O'Reilly, and G. S. Pettis.** 2008. Further characterization of *Vibrio vulnificus* rugose variants and identification of a capsular and rugose exopolysaccharide gene cluster. Infect. Immun. **76:**1485–1497.
17. **Guvener, Z. T., and C. S. Harwood.** 2007. Subcellular location characteristics of the *Pseudomonas aeruginosa* GGDEF protein, WspR, indicate that it produces cyclic-di-GMP in response to growth on surfaces. Mol. Microbiol. **66:**1459–1473.
18. **Hammer, B. K., and B. L. Bassler.** 2003. Quorum sensing controls biofilm formation in *Vibrio cholerae*. Mol. Microbiol. **50:**101–104.
19. **Herrero, M., V. de Lorenzo, and K. N. Timmis.** 1990. Transposon vectors containing non-antibiotic resistance selection markers for cloning and stable chromosomal insertion of foreign genes in gram-negative bacteria. J. Bacteriol. **172:**6557–6567.
20. **Hoch, J. A., and K. I. Varughese.** 2001. Keeping signals straight in phosphorelay signal transduction. J. Bacteriol. **183:**4941–4949.
21. **Hussa, E. A., C. Darnell, and K. L. Visick.** 25 April 2008. RscS functions upstream of SypG to control the *syp* locus and biofilm formation in *Vibrio fischeri*. J. Bacteriol. **190:**4576–4583.
22. **Hussa, E. A., T. M. O'Shea, C. L. Darnell, E. G. Ruby, and K. L. Visick.** 2007. Two-component response regulators of *Vibrio fischeri*: their identification, mutagenesis and characterization. J. Bacteriol. **189:**5825–5838.
23. **Lauriano, C. M., C. Ghosh, N. E. Correa, and K. E. Klose.** 2004. The sodium-driven flagellar motor controls exopolysaccharide expression in *Vibrio cholerae*. J. Bacteriol. **186:**4864–4874.
24. **Lowry, O. H., N. J. Rosebrough, A. L. Farr, and R. J. Randall.** 1951. Protein measurement with the folin phenol reagent. J. Biol. Chem. **193:**265–275.
25. **Ma, L., H. Lu, A. Sprinkle, M. R. Parsek, and D. J. Wozniak.** 2007. *Pseudomonas aeruginosa* Psl is a galactose- and mannose-rich exopolysaccharide. J. Bacteriol. **189:**8353–8356.
26. **Manoil, C., and J. Beckwith.** 1985. Tn*phoA*: a transposon probe for protein export signals. Proc. Natl. Acad. Sci. USA **82:**8129–8133.
27. **McCann, J., E. V. Stabb, D. S. Millikan, and E. G. Ruby.** 2003. Population dynamics of *Vibrio fischeri* during infection of *Euprymna scolopes*. Appl. Environ. Microbiol. **69:**5928–5934.
28. **Miller, J. H.** 1972. Experiments in molecular genetics. Cold Spring Harbor Laboratory, New York, NY.
29. **Nyholm, S. V., and M. J. McFall-Ngai.** 2004. The winnowing: establishing the squid-*Vibrio* symbiosis. Nat. Rev. Microbiol. **2:**632–642.
30. **O'Gara, J. P., and H. Humphreys.** 2001. *Staphylococcus epidermidis* biofilms: importance and implications. J. Med. Microbiol. **50:**582–587.
31. **O'Shea, T. M., A. H. Klein, K. Geszvain, A. J. Wolfe, and K. L. Visick.** 2006. Diguanylate cyclases control magnesium-dependent motility of *Vibrio fischeri*. J. Bacteriol. **188:**8196–8205.
32. **Romling, U.** 2002. Molecular biology of cellulose production in bacteria. Res. Microbiol. **153:**205–212.
33. **Ross, P., R. Mayer, and M. Benziman.** 1991. Cellulose biosynthesis and function in bacteria. Microbiol. Rev. **55:**35–58.
34. **Ruby, E. G., and K. H. Nealson.** 1977. Pyruvate production and excretion by the luminous marine bacteria. Appl. Environ. Microbiol. **34:**164–169.
35. **Ruby, E. G., M. Urbanowski, J. Campbell, A. Dunn, M. Faini, R. Gunsalus, P. Lostroh, C. Lupp, J. McCann, D. Millikan, A. Schaefer, E. Stabb, A. Stevens, K. Visick, C. Whistler, and E. P. Greenberg.** 2005. Complete genome sequence of *Vibrio fischeri*: a symbiotic bacterium with pathogenic congeners. Proc. Natl. Acad. Sci. USA **102:**3004–3009.
36. **Sakuragi, Y., and R. Kolter.** 2007. Quorum-sensing regulation of the biofilm matrix genes (*pel*) of *Pseudomonas aeruginosa*. J. Bacteriol. **189:**5383–5386.
37. **Stabb, E. V.** 2006. The *Vibrio fischeri-Euprymna scolopes* light organ symbiosis, p. 204–218. *In* F. L. Thompson, B. Austin, and J. Swings (ed.), The biology of vibrios. ASM Press, Washington, DC.
38. **Stabb, E. V., K. A. Reich, and E. G. Ruby.** 2001. *Vibrio fischeri* genes *hvnA* and *hvnB* encode secreted NAD^+-glycohydrolases. J. Bacteriol. **183:**309–317.
39. **Stabb, E. V., and E. G. Ruby.** 2002. RP4-based plasmids for conjugation between *Escherichia coli* and members of the Vibrionaceae. Methods Enzymol. **358:**413–426.
40. **Stoodley, P., K. Sauer, D. G. Davies, and J. W. Costerton.** 2002. Biofilms as complex differentiated communities. Annu. Rev. Microbiol. **56:**187–209.
41. **Tamplin, M. L., A. L. Gauzens, A. Huq, D. A. Sack, and R. R. Colwell.** 1990. Attachment of *Vibrio cholerae* serogroup O1 to zooplankton and phytoplankton of Bangladesh waters. Appl. Environ. Microbiol. **56:**1977–1980.
42. **Tischler, A. D., and A. Camilli.** 2004. Cyclic diguanylate (c-di-GMP) regulates *Vibrio cholerae* biofilm formation. Mol. Microbiol. **53:**857–869.
43. **Visick, K. L., and E. G. Ruby.** 2006. *Vibrio fischeri* and its host: it takes two to tango. Curr. Opin. Microbiol. **9:**632–638.
44. **Visick, K. L., and L. M. Skoufos.** 2001. A two-component sensor required for normal symbiotic colonization of *Euprymna scolopes* by *Vibrio fischeri*. J. Bacteriol. **183:**835–842.
45. **Wai, S. N., Y. Mizunoe, A. Takade, S. I. Kawabata, and S. I. Yoshida.** 1998. *Vibrio cholerae* O1 strain TSI-4 produces the exopolysaccharide materials that determine colony morphology, stress resistance, and biofilm formation. Appl. Environ. Microbiol. **64:**3648–3655.
46. **Waite, R. D., A. Papakonstantinopoulou, E. Littler, and M. A. Curtis.** 2005. Transcriptome analysis of *Pseudomonas aeruginosa* growth: comparison of gene expression in planktonic cultures and developing and mature biofilms. J. Bacteriol. **187:**6571–6576.
47. **Woodcock, D. M., P. J. Crowther, J. Doherty, S. Jefferson, E. DeCruz, M. Noyer-Weidner, S. S. Smither, M. Z. Michael, and M. W. Graham.** 1989. Quantitative evaluation of *Escherichia coli* host strains for tolerance to cystosine methylation in plasmid and phage recombinants. Nucleic Acids Res. **17:**3469–3478.
48. **Yarwood, J. M., D. J. Bartels, E. M. Volper, and E. P. Greenberg.** 2004. Quorum sensing in *Staphylococcus aureus* biofilms. J. Bacteriol. **186:**1838–1850.
49. **Yildiz, F. H., N. A. Dolganov, and G. K. Schoolnik.** 2001. VpsR, a member of the response regulators of the two-component regulatory systems, is required for expression of *vps* biosynthesis genes and EPS(ETr)-associated phenotypes in *Vibrio cholerae* O1 El Tor. J. Bacteriol. **183:**1716–1726.
50. **Yildiz, F. H., X. S. Liu, A. Heydorn, and G. K. Schoolnik.** 2004. Molecular analysis of rugosity in a *Vibrio cholerae* O1 El Tor phase variant. Mol. Microbiol. **53:**497–515.
51. **Yildiz, F. H., and G. K. Schoolnik.** 1999. *Vibrio cholerae* O1 El Tor: identification of a gene cluster required for the rugose colony type, exopolysaccharide production, chlorine resistance, and biofilm formation. Proc. Natl. Acad. Sci. USA **96:**4028–4033.
52. **Yip, E. S., K. Geszvain, C. R. DeLoney-Marino, and K. L. Visick.** 2006. The symbiosis regulator RscS controls the *syp* gene locus, biofilm formation and symbiotic aggregation by *Vibrio fischeri*. Mol. Microbiol. **62:**1586–1600.
53. **Yip, E. S., B. T. Grublesky, E. A. Hussa, and K. L. Visick.** 2005. A novel, conserved cluster of genes promotes symbiotic colonization and σ^{54}-dependent biofilm formation by *Vibrio fischeri*. Mol. Microbiol. **57:**1485–1498.
54. **Zhu, J., and J. J. Mekalanos.** 2003. Quorum sensing-dependent biofilms enhance colonization in *Vibrio cholerae*. Dev. Cell **5:**647–656.

JOURNAL OF BACTERIOLOGY, Mar. 2007, p. 2571–2574 Vol. 189, No. 6
0021-9193/07/$08.00+0 doi:10.1128/JB.01761-06

The Sugar Phosphotransferase System of *Vibrio fischeri* Inhibits both Motility and Bioluminescence▽

Karen L. Visick, Therese M. O'Shea, Adam H. Klein, Kati Geszvain, and Alan J. Wolfe*

Department of Microbiology and Immunology, Loyola University Chicago, 2160 South First Ave., Bldg. 105, Maywood, Illinois 60153

Received 17 November 2006/Accepted 2 January 2007

Magnesium-dependent induction of *Vibrio fischeri* flagellar (Mif) biogenesis depends upon two diguanylate cyclases, suggesting an inhibitory role for cyclic di-GMP. Here, we report that cells defective for the sugar phosphotransferase system (PTS) exhibited a magnesium-independent phenotype similar to that of mutants of the Mif pathway. Unlike Mif mutants, PTS mutants also were hyperbioluminescent.

The second messenger, cyclic AMP (cAMP), is synthesized by adenylate cyclase (AC). In bacteria of the family *Enterobacteriaceae* (e.g., *Escherichia coli*), the activity of AC becomes enhanced by its interaction with the phosphorylated version of $EIIA^{Glc}$ (phospho-$EIIA^{Glc}$), the glucose-specific IIA component of the phosphoenolpyruvate (PEP):carbohydrate phosphotransferase system (PTS) (6, 17, 18, 20). The glucose-specific PTS is composed of three soluble, cytoplasmic proteins (EI, HPr, and $EIIA^{Glc}$) and one integral cytoplasmic membrane protein ($EIICB^{Glc}$). These proteins sequentially transfer a phosphoryl group from PEP to glucose, with the concomitant transport of the sugar across the membrane (Fig. 1). The presence of glucose in the environment pulls phosphoryl groups through the PTS, ensuring that the system's components remain essentially unphosphorylated; depletion of that glucose results in the accumulation of phospho-$EIIA^{Glc}$, which activates AC to synthesize cAMP. This cAMP binds cAMP receptor protein (CRP, also known as CAP), which then regulates the transcription of hundreds of genes, including *flhDC*, the master regulator of the *Enterobacteriaceae* flagellar regulon (for reviews, see references 6a, 10, 11, 17, and 30).

Cyclic di-GMP (c-di-GMP) is a newly appreciated second messenger, apparently unique to bacteria, that modulates diverse cellular processes (for a recent review, see reference 21). First identified as a positive effector of cellulose synthase in *Gluconoacetobacter xylinus* (reviewed in reference 22), c-di-GMP regulates transition from the motile, planktonic state to sessile, community-based behaviors, such as biofilm development. It tends to inhibit motility, both flagellar and twitching, while enhancing the biosynthesis of capsular components required by developing biofilms. c-di-GMP is synthesized by diguanylate cyclases (DGC) and degraded by phosphodiesterases (PDE) (21). Together these activities maintain the steady-state concentration of c-di-GMP (22). DGC activity has been associated with the highly conserved GGDEF domain. One PDE activity (to linear di-GMP) has been associated with the highly conserved EAL domain, while a second PDE activity (to two GMPs) has been associated with the HD-GYP domain (21). Finally, a c-di-GMP-binding domain (termed PilZ) was recently reported (2) and shown to inhibit flagellar assembly in *E. coli* (25).

Insights into the control of c-di-GMP production and its targets have come from our investigations of motility in the marine bacterium *Vibrio fischeri*. This bacterium, found as free-living, motile individuals or as a sessile community in association with the Hawaiian squid *Euprymna scolopes*, regulates the biogenesis of its flagella in response to the concentration of environmental magnesium (Mg^{2+}). In the presence of abundant Mg^{2+}, such as that found in seawater, *V. fischeri* cells possess flagella; when Mg^{2+} becomes limiting, they do not (14). This *M*g^{2+}-dependent *i*nduction of *f*lagellar (Mif) biogenesis depends upon at least two DGCs, one confirmed (MifA) and one putative (MifB) (Fig. 1). Unlike wild-type (WT) cells, mutants that lack MifA or MifB or both synthesize flagellin proteins and become motile even when Mg^{2+} is limiting (15). Since MifA (and likely also MifB) catalyzes the production of c-di-GMP, these observations are consistent with a model in which c-di-GMP inhibits flagellar biogenesis, while Mg^{2+} interferes with or overcomes that inhibition. Since overexpression of *mifA* did not exert a significant effect upon the transcription of flagellin genes, we have proposed that c-di-GMP acts posttranscriptionally (15).

Disruption of both *mifA* and *mifB* under Mg^{2+}-limiting conditions failed to promote the same level of migration that WT cells achieve in the presence of Mg^{2+}; this result suggests the existence of additional Mif pathway components. Therefore, during a recent study (15), we searched for those additional components using a screen for transposon (Tn) mutants that migrated in the absence of Mg^{2+}. The majority of the putative mutations mapped to *mifA*; however, several did not. Here, we report the characterization of one of the non-*mifA* mutants.

This non-*mifA* mutant (strain KV2657) exhibited a phenotype similar to those of *mifA* and *mifB* mutants: in the absence of Mg^{2+}, like the *mifA* vector integration (Campbell) mutant (*mifA*::pKV217; strain KV2672) or the *mifB* Campbell mutant (*mifB*::pTMO125; strain KV2532), it migrated sooner and more rapidly than the positive control, KV1421 (Fig. 2A and B). In the presence of Mg^{2+}, the migration rate of KV2657, like that of mutant *mifA* or *mifB*, was similar to that of the KV1421 control (Fig. 2A and C). Furthermore, even with Mg^{2+}, the control strain left a dense mass of poorly motile and nonmotile cells at the site of inoculation. The Tn mutant, in contrast, did not,

* Corresponding author. Mailing address: Department of Microbiology and Immunology, Loyola University Medical School, 2160 S. First Ave., Bldg. 105, Rm. 3846, Maywood, IL 60153. Phone: (708) 216-5814. Fax: (708) 216-9574. E-mail: awolfe@lumc.edu.

▽ Published ahead of print on 12 January 2007.

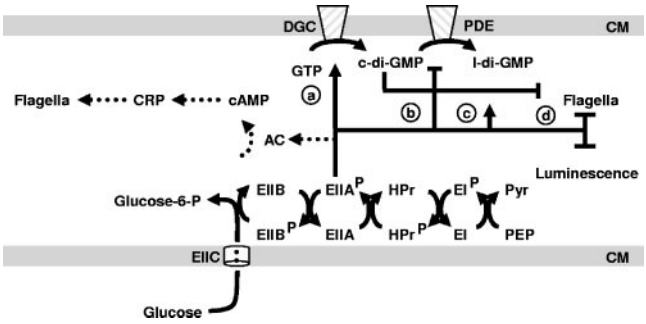

FIG. 1. The PTS and the proposed Mif pathways. CM, cytoplasmic membrane; l-di-GMP, linear di-GMP; EIIC and EIIB, subunits of the glucose-specific PTS transporter; EIIA, HPr, and EI, signaling components of the PTS pathway; Pyr, pyruvate. Dotted lines represent a pathway known to function in *E. coli*. See the text for the proposed interaction between the PTS and Mif pathways (a through d) and their effects upon flagellar biogenesis and on bioluminescence.

consistent with the hypothesis that a larger proportion of its cells became motile sooner than those of the control (Fig. 2A and data not shown), a behavior reminiscent of *mif* mutants (15).

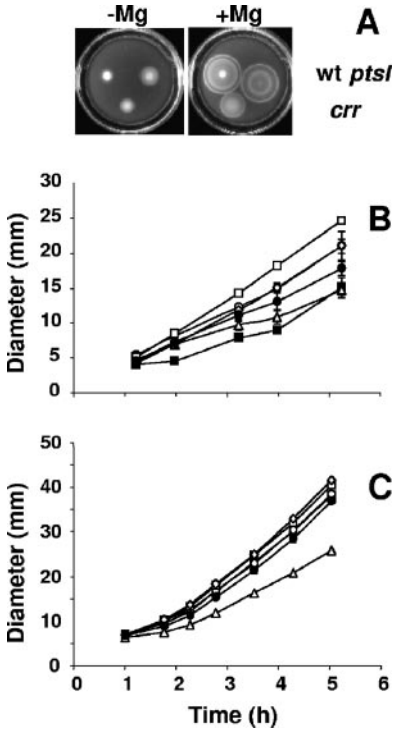

FIG. 2. Disruption of the *ptsHI-crr* operon permits migration in the absence of added Mg^{2+}. (A) Cells were grown overnight at 28°C in tryptone broth-saline (TBS) (5), inoculated onto the surface of TBS motility plates containing either no added Mg^{2+} (−Mg) or containing 35 mM $MgSO_4$ (TBS-Mg^{2+}) (+Mg) (14), incubated at 28°C for 5 hours, and photographed. wt refers to strain KV1421 and *ptsI* refers to strain KV2801 (*ptsI*::pTMO151), while *crr* refers to strain KV2850 (*crr*::pTMO152). (B and C) Displacement of the outer band of strains: KV1421 (WT; solid squares), KV2672 (*mifA*::pKV217; open squares), KV2532 (*mifB*::pTMO125; open diamonds), KV2657 (*ptsI*::Tn5; closed circles), KV2801 (*ptsI*::pTMO151; open circles), and KV2850 (*crr*::pTMO152; open triangles) in TBS (B) or in TBS-Mg^{2+} (C).

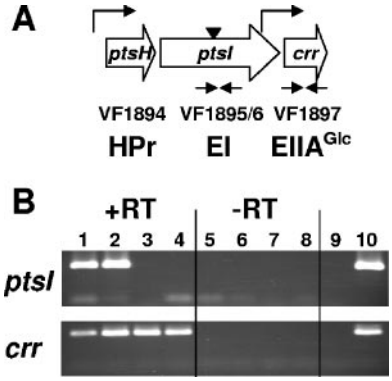

FIG. 3. Arrangement of PTS genes. (A) Schematic shows the putative operon structure, the gene products, and the approximate locations of the Tn*5* (inverted triangle) and the primers (inverted arrows) used for both the Campbell insertions and the RT-PCR shown in panel B. Bent arrows indicate putative promoters. (B) RT-PCR, performed as described previously (15), shows that the Campbell insertion allele *ptsI*::pTMO151 (strain KV2801) is not polar on the downstream *crr* gene. The parent strain KV1421 is shown as a control. *ptsI*, primers specific for *ptsI*; *crr*, primers specific for *crr*. Lanes 1, 2, 5, 6, strain KV1421; lanes 3, 4, 7, 8, strain KV2801; lane 9, negative control (distilled water); lane 10, positive control (ESR1 genomic DNA).

Sequence analysis revealed that the Tn in strain KV2657 inserted (along with its delivery vector) into VF1896 (Fig. 3A), an open reading frame (ORF) annotated to encode the C-terminal two-thirds of the PTS component EI; the N terminus of EI was annotated as VF1895 (23). We hypothesized that the annotation of separate ORFs resulted from a sequencing error. We thus amplified, cloned, and sequenced the annotated junction of VF1895 and VF1896 and determined that VF1895/VF1896 represents a single ORF (data not shown).

VF1895/VF1896 resides on chromosome 1 of *V. fischeri*, within a locus (VF1894 to -1897) (23) that bears a strong resemblance to the *ptsHI-crr* locus of *E. coli* K-12 (10, 24). The proteins encoded by VF1894, VF1895/VF1896, and VF1897 share extensive identity, respectively, to those encoded by *ptsH* (HPr, 79%), *ptsI* (EI, 73%), and *crr* ($EIIA^{Glc}$, 83%) (1, 27). On the basis of this identity and the data presented below, we designated the VF1894 to -1897 locus as the *V. fischeri* ortholog of the *E. coli ptsHI-crr* operon. To test this designation, we constructed Campbell mutations in both the VF1895/VF1896 (*ptsI*::pTMO151) and the downstream VF1897 (*crr*::pTMO152) genes, verifying their construction by Southern blotting analysis. Although the resulting strains (KV2801 and KV2850, respectively) grew as well as their WT parent in rich medium, they grew poorly or not at all in minimal medium supplemented with several sugars, including glucose, glucosamine, and *N*-acetylglucosamine (data not shown).

To confirm the role of *ptsI* in Mg^{2+}-dependent motility, we compared the migration behavior of strain KV2801 (the Campbell mutant) to that of strain KV2657, the original *ptsI* Tn insertion mutant (Fig. 2B). The Campbell mutant exhibited a similar behavior: in the absence of Mg^{2+}, it migrated sooner and faster than the control strain KV1421 (Fig. 2A and B); in the presence of Mg^{2+}, it behaved much like KV1421. Disruption of *ptsI* should preclude the phosphorylation of downstream components of the PTS pathways, including those specific for glucose, e.g., $EIIA^{Glc}$ (Fig. 1). To determine whether

EIIA^{Glc} also plays a role in controlling motility, we tested the *crr* Campbell mutant (strain KV2850): in the absence of Mg^{2+}, it began migrating considerably sooner than its WT parent (Fig. 2A and B). In the presence of Mg^{2+}, however, the *crr* mutant migrated quite a bit more slowly than either the WT or the *mifA* mutant (Fig. 2A and C). The reason for this behavior remains unknown but is unlikely to be due to differences in growth rate (data not shown).

The behavior of the *ptsI* mutant could be due either to an inability to phosphorylate downstream components or to a polar effect on the transcription of the downstream *crr* gene. In *E. coli*, the *ptsHI-crr* locus contains two minor promoters positioned upstream of *crr* within *ptsI* (10, 17, 26). Thus, a polar mutation in the *E. coli ptsI* gene does not eliminate transcription from *crr* (17). To determine whether this is also true of the *V. fischeri ptsHI-crr* locus, we performed reverse transcription (RT)-PCR (15) using primer pairs specific for *ptsI* and *crr* (Fig. 3A). In contrast to the control cells (strain KV1421), which possessed transcripts for both *ptsI* and *crr*, the Tn insertion mutant (strain KV2657) showed a transcript for only *crr* (Fig. 3B). These data demonstrate that the Tn insertion into *ptsI* does not exert polarity on the downstream *crr*. Thus, like its *E. coli* ortholog, the *V. fischeri crr* gene likely possesses its own promoter, and the effect of a *ptsI* deficiency likely results from an inability to phosphorylate EIIA^{Glc} and/or other downstream components.

In *E. coli*, phospho-EIIA^{Glc} activates flagellar biogenesis by enhancing AC activity. The resultant cAMP binds CRP, which activates transcription of *flhDC*, the operon that encodes the master activator of the *E. coli* flagellar regulon (11, 28). In contrast, the data for *V. fischeri* (which uses a regulatory system that does not include *flhDC*) are consistent with a negative role for phospho-EIIA^{Glc}, much like that for MifA, which appears to act subsequent to transcription (15). To determine whether EI and/or EIIA^{Glc} also act posttranscriptionally, we performed a semiquantitative RT-PCR analysis with *flaA*, *flaC*, and *flaE*, which encode major *V. fischeri* flagellins (12), and with *fliF*, predicted to encode the M ring, whose insertion into the cytoplasmic membrane constitutes the first step in building flagella (19). The cDNA levels were not substantially affected by the status of *mifB* (strain KV2825), *ptsI* (KV2801), or *crr* (KV2850) (data not shown). In contrast, the cDNA levels were substantially diminished but not eliminated by the disruption of *rpoN* (data not shown), which encodes σ^{54}, proposed to sit near or at the top of the hierarchical *V. fischeri* flagellar regulon (strain KV1513) (19, 29). We conclude that both the PTS and the Mif pathway impact flagellar biogenesis at similar levels.

Thus, we propose that phospho-EIIA^{Glc} interacts with the Mif system to regulate flagellar biogenesis, most likely at a posttranscriptional level (Fig. 1). This model is supported by the following observations: (i) *ptsI* and *crr* mutants of *V. fischeri* exhibited similar behavior, i.e., increased migration in the absence of Mg^{2+} (Fig. 2), suggesting that phospho-EIIA^{Glc} is a prerequisite for the inhibition of flagellar biogenesis; (ii) disruption of either *ptsI* or *crr* exerted no significant effect upon the transcription of flagellin genes; and (iii) these behaviors resemble those of *mif* mutants (15). We do not yet know how the Mif and PTS pathways interact, although we can imagine an interaction between phospho-EIIA^{Glc} and the Mif pathway

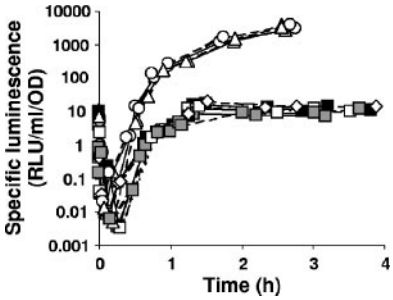

FIG. 4. The *ptsHI-crr* operon regulates bioluminescence. Cells were grown at 28°C in SWT (3) supplemented with extra NaCl (for a final concentration of 552 mM), and bioluminescence was measured over time. To account for any small differences in growth, specific luminescence (relative light units/ml/optical density unit [OD]) was plotted versus optical density. The experiment was performed with two independent isolates (denoted as solid and dotted lines) of the following strains: ES114 (WT, closed squares), KV2532 (*mifB*::pTMO125, open diamonds), KV2672 (*mifA*::pKV217, open squares), KV2801 (*ptsI*::pTMO151, open circles), KV2850 (*crr*::pTMO152, open triangles), and KV2826 (*mifA*::pKV217 Δ*mifB*, gray squares).

at any one of a number of levels (Fig. 1): phospho-EIIA^{Glc} could (i) activate a DGC; (ii) inhibit a PDE composed of an EAL domain and a nonconsensus "regulatory" GGDEF domain (21); (iii) interfere with the ability of c-di-GMP to interact with its target; or (iv) act independently. EIIA^{Glc}, either in its phosphorylated or nonphosphorylated form, tends to interact with a variety of proteins, including not only EIICB^{Glc} and AC (5a, 17) but also FrsA, which controls the fermentation-respiration switch (9). Alternatively, the effect could be mediated by another PTS component, e.g., EI or HPr.

To further our understanding of the relationship between the PTS and the Mif pathway, we also considered the following published observations: (i) in *E. coli*, phospho-EIIA^{Glc} activates AC to produce cAMP (6, 17, 20); (ii) cAMP binds and activates the transcriptional regulator CRP (30); and (iii) CRP of *V. fischeri* has been linked to the control of bioluminescence (J. L. Bose, U. Kim, W. Bartkowski, R. P. Gunsalus, A. M. Overley, K. L. Visick, and E. V. Stabb, submitted for publication; 7, 8, 13). We therefore asked whether a mutation in *mifA*, *mifB*, *ptsI*, or *crr* impacted bioluminescence. We grew WT and mutant cells in a tryptone-based seawater medium (which contains Mg^{2+}) and measured bioluminescence over time. To account for any small differences in growth, we plotted the specific luminescence (relative light units/ml/optical density unit) versus optical density (Fig. 4). Cells defective for *mifA* (KV2672) or *mifB* (KV2532) or both (KV2826) displayed bioluminescence patterns comparable to that of the WT strain (ES114). Surprisingly, however, mutants defective for either *ptsI* (KV2801) or *crr* (KV2850) exhibited substantially elevated levels of bioluminescence. Specifically, these mutations promoted an increase of over 300-fold in bioluminescence, allowing this naturally nonvisibly bioluminescent strain of *V. fischeri* to produce visibly detectable light. Given the clear differences in the bioluminescence patterns of these strains, these data support the conclusion that Mif and the PTS function in distinct pathways, at least with respect to bioluminescence.

At first glance, the observation that the PTS controls bioluminescence is not surprising: both cAMP and CRP have been

reported to activate bioluminescence in *V. fischeri* (J. L. Bose et al., submitted; 7, 8, 13), and it is well known that phospho-EIIA^{Glc} activates AC in *E. coli* (17). However, if phospho-EIIA^{Glc} activated AC in *V. fischeri* as it does in *E. coli*, then one would predict that the PTS would activate bioluminescence. Instead, the PTS appears to inhibit bioluminescence (Fig. 4). Similarly, phospho-EIIA^{Glc}, cAMP, and CRP activate transcription of the flagellar regulon in *E. coli* (11, 28); yet, phospho-EIIA^{Glc} appears to inhibit flagellar biogenesis in *V. fischeri* (Fig. 2). These parallel observations concerning the effect of the PTS on distinct cellular processes suggest that the influence of the *V. fischeri* PTS might exhibit some novel properties relative to those of its better-studied distant relative *E. coli*.

This work was supported by the estate of William G. Potts in support of medical research at the Stritch School of Medicine at Loyola Univeristy Chicago and by NIH grant GM59690, awarded to K.L.V., and NIH grant GM066130, awarded to A.J.W.

REFERENCES

1. **Altschul, S. F., T. L. Madden, A. A. Schäffer, J. Zhang, Z. Zhang, W. Miller, and D. J. Lipman.** 1997. Gapped BLAST and PSI-BLAST: a new generation of protein database search programs. Nucleic Acids Res. **25:**3389–3402.
2. **Amikam, D., and M. Y. Galperin.** 2006. PilZ domain is part of the bacterial c-di-GMP binding protein. Bioinformatics **22:**3–6.
3. **Boettcher, K. J., and E. G. Ruby.** 1990. Depressed light emission by symbiotic *Vibrio fischeri* of the sepiolid squid *Euprymna scolopes*. J. Bacteriol. **172:** 3701–3706.
4. Reference deleted.
5. **DeLoney-Marino, C. R., A. J. Wolfe, and K. L. Visick.** 2003. Chemoattraction of *Vibrio fischeri* to serine, nucleosides, and *N*-acetylneuraminic acid, a component of squid light-organ mucus. Appl. Environ. Microbiol. **69:**7527–7530.
6. **den Blaauwen, J. L., and P. W. Postma.** 1985. Regulation of cyclic AMP synthesis by enzyme III^{Glc} of the phosphoenolpyruvate:sugar phosphotransferase system in *crp* strains of *Salmonella typhimurium*. J. Bacteriol. **164:**477–478.

6a. **Deutscher, J., C. Francke, and P. W. Postma.** 2006. How phosphotransferase system-related protein phosphorylation regulates carbohydrate metabolism in bacteria. Microbiol. Mol. Biol. Rev. **70:**939–1031.

7. **Dunlap, P. V., and E. P. Greenberg.** 1985. Control of *Vibrio fischeri* luminescence gene expression in *Escherichia coli* by cyclic AMP and cyclic AMP receptor protein. J. Bacteriol. **164:**45–50.
8. **Dunlap, P. V., and E. P. Greenberg.** 1988. Control of *Vibrio fischeri lux* gene transcription by a cyclic AMP receptor protein-LuxR protein regulatory circuit. J. Bacteriol. **170:**4040–4046.
9. **Koo, B. M., M. J. Yoon, C. R. Lee, T. W. Nam, Y. J. Choe, H. Jaffe, A. Peterkofsky, and Y. J. Seok.** 2004. A novel fermentation/respiration switch protein regulated by enzyme IIAGlc in *Escherichia coli*. J. Biol. Chem. **279:**31613–31621.
10. **Kotrba, P., M. Inui, and H. Yukawa.** 2001. Bacterial phosphotransferase system (PTS) in carbohydrate uptake and control of carbon metabolism. J. Biosci. Bioeng. **92:**502–517.
11. **Macnab, R. M.** 1996. Flagella and motility, p. 123–145. *In* F. C. Neidhardt et al. (ed.), *Escherichia coli* and *Salmonella*: cellular and molecular biology, 2nd ed. ASM Press, Washington, DC.
12. **Millikan, D. S., and E. G. Ruby.** 2004. *Vibrio fischeri* flagellin A is essential for normal motility and for symbiotic competence during initial squid light organ colonization. J. Bacteriol. **186:**4315–4325.
13. **Nealson, K. H., A. Eberhard, and J. W. Hastings.** 1972. Catabolite repression of bacterial bioluminescence: functional implications. Proc. Natl. Acad. Sci. USA **69:**1073–1076.
14. **O'Shea, T. M., C. R. DeLoney-Marino, S. Shibata, S.-I. Aizawa, A. J. Wolfe, and K. L. Visick.** 2005. Magnesium promotes flagellation of *Vibrio fischeri*. J. Bacteriol. **187:**2058–2065.
15. **O'Shea, T. M., A. H. Klein, K. Geszvain, A. J. Wolfe, and K. L. Visick.** 2006. Diguanylate cyclases control magnesium-dependent motility of *Vibrio fischeri*. J. Bacteriol. **188:**8196–8205.
16. Reference deleted.
17. **Postma, P. W., J. W. Lengeler, and G. R. Jacobson.** 1996. Phosphoenolpyruvate:carbohydrate phosphotransferase systems, p. 1149–1174. *In* F. C. Neidhardt, R. Curtiss III, J. L. Ingraham, E. C. C. Lin, K. B. Low, B. Magasanik, W. S. Reznikoff, M. Riley, M. Schaechter, and H. E. Umbarger (ed.), *Escherichia coli* and *Salmonella*: cellular and molecular biology, 2nd ed. ASM Press, Washington, DC.
18. **Postma, P. W., J. W. Lengeler, and G. R. Jacobson.** 1993. Phosphoenolpyruvate:carbohydrate phosphotransferase systems of bacteria. Microbiol. Rev. **57:**543–594.
19. **Prüss, B. M., D.-J. Kim, S. Forst, R. T. Fleming, K. L. Visick, and A. J. Wolfe.** 2005. Genomics of flagella, p. 1–12. *In* B. M. Prüss (ed.), Global regulatory networks in enteric bacteria. Research Signpost, Kerala, India.
20. **Reddy, P., and M. Kamireddi.** 1998. Modulation of *Escherichia coli* adenylyl cyclase activity by catalytic-site mutants of protein IIA^{Glc} of the phosphoenolpyruvate:sugar phosphotransferase system. J. Bacteriol. **180:**732–736.
21. **Romling, U., M. Gomelsky, and M. Y. Galperin.** 2005. C-di-GMP: the dawning of a novel bacterial signaling system. Mol. Microbiol. **57:**629–639.
22. **Ross, P., R. Mayer, and M. Benziman.** 1991. Cellulose biosynthesis and function in bacteria. Microbiol. Rev. **55:**35–58.
23. **Ruby, E. G., M. Urbanowski, J. Campbell, A. Dunn, M. Faini, R. Gunsalus, P. Lostroh, C. Lupp, J. McCann, D. Millikan, A. Schaefer, E. Stabb, A. Stevens, K. Visick, C. Whistler, and E. P. Greenberg.** 2005. Complete genome sequence of *Vibrio fischeri*: a symbiotic bacterium with pathogenic congeners. Proc. Natl. Acad. Sci. USA **102:**3004–3009.
24. **Rudd, K. E.** 2000. EcoGene: a genome sequence database for *Escherichia coli* K-12. Nucleic Acids Res. **28:**60–64.
25. **Ryjenkov, D. A., R. Simm, U. Romling, and M. Gomelsky.** 2006. The PilZ domain is a receptor for the second messenger c-di-GMP. The PilZ domain protein YcgR controls motility in enterobacteria. J. Biol. Chem. **281:**30310–30314.
26. **Salgado, H., S. Gama-Castro, M. Peralta-Gil, E. Díaz-Peredo, F. Sánchez-Solano, A. Santos-Zavaleta, I. Martínez-Flores, V. Jiménez-Jacinto, C. Bonavides-Martínez, J. Segura-Salazar, A. Martínez-Antonio, and J. Collado-Vides.** 2006. RegulonDB (version 5.0): *Escherichia coli* K-12 transcriptional regulatory network, operon organization, and growth conditions. Nucleic Acids Res. **34:**D394–D397.
27. **Schäffer, A. A., L. Aravind, T. L. Madden, S. Shavirin, J. L. Spouge, Y. I. Wolf, E. V. Koonin, and S. F. Altschul.** 2001. Improving the accuracy of PSI-BLAST protein database searches with composition-based statistics and other refinements. Nucleic Acids Res. **29:**2994–3005.
28. **Soutourina, O., A. Kolb, E. Krin, C. Laurent-Winter, S. Rimsky, A. Danchin, and P. Bertin.** 1999. Multiple control of flagellum biosynthesis in *Escherichia coli*: role of H-NS protein and the cyclic AMP-catabolite activator protein complex in transcription of the *flhDC* master operon. J. Bacteriol. **181:**7500–7508.
29. **Wolfe, A. J., D. S. Millikan, J. M. Campbell, and K. L. Visick.** 2004. *Vibrio fischeri* σ^{54} controls motility, biofilm formation, luminescence, and colonization. Appl. Environ. Microbiol. **70:**2520–2524.
30. **Zheng, D., C. Constantinidou, J. L. Hobman, and S. D. Minchin.** 2004. Identification of the CRP regulon using in vitro and in vivo transcriptional profiling. Nucleic Acids Res. **32:**5874–5893.

JOURNAL OF BACTERIOLOGY, Aug. 2007, p. 5825–5838 Vol. 189, No. 16
0021-9193/07/$08.00+0 doi:10.1128/JB.00242-07

Two-Component Response Regulators of *Vibrio fischeri*: Identification, Mutagenesis, and Characterization▽

Elizabeth A. Hussa,[1] Therese M. O'Shea,[1] Cynthia L. Darnell,[1]
Edward G. Ruby,[2] and Karen L. Visick[1]*

Department of Microbiology and Immunology, Loyola University Chicago, Maywood, Illinois 60153,[1] and Department of Medical Microbiology and Immunology, University of Wisconsin—Madison, Madison, Wisconsin 53706[2]

Received 13 February 2007/Accepted 8 June 2007

Two-component signal transduction systems are utilized by prokaryotic and eukaryotic cells to sense and respond to environmental stimuli, both to maintain homeostasis and to rapidly adapt to changing conditions. Studies have begun to emerge that utilize a large-scale mutagenesis approach to analyzing these systems in prokaryotic organisms. Due to the recent availability of its genome sequence, such a global approach is now possible for the marine bioluminescent bacterium *Vibrio fischeri*, which exists either in a free-living state or as a mutualistic symbiont within a host organism such as the Hawaiian squid species *Euprymna scolopes*. In this work, we identified 40 putative two-component response regulators encoded within the *V. fischeri* genome. Based on the type of effector domain present, we classified six as NarL type, 13 as OmpR type, and six as NtrC type; the remaining 15 lacked a predicted DNA-binding domain. We subsequently mutated 35 of these genes via a vector integration approach and analyzed the resulting mutants for roles in bioluminescence, motility, and competitive colonization of squid. Through these assays, we identified three novel regulators of *V. fischeri* luminescence and seven regulators that altered motility. Furthermore, we found 11 regulators with a previously undescribed effect on competitive colonization of the host squid. Interestingly, five of the newly characterized regulators each affected two or more of the phenotypes examined, strongly suggesting interconnectivity among systems. This work represents the first large-scale mutagenesis of a class of genes in *V. fischeri* using a genomic approach and emphasizes the importance of two-component signal transduction in bacterium-host interactions.

The symbiosis between the Hawaiian squid *Euprymna scolopes* and the bacterium *Vibrio fischeri* serves as a model for symbiotic bacterium-host interactions. Previous studies have revealed a number of bacterial factors required for host colonization (24, 56), including motility (25, 49, 57) and luminescence (78). Many of these factors were identified by generating and testing specific hypotheses developed from an understanding of the general colonization process. To date, however, large-scale studies of colonization factors have been hampered by a deficit of genetic tools needed for bacterial mutant construction. Recently, however, the genome sequence of *V. fischeri* has been published (65). In addition, the availability of a useful suicide vector (17) has greatly facilitated mutant construction (73, 90). Thus, it is now possible to approach the investigation of *V. fischeri* biology from a genomic perspective.

One large-scale approach to understanding the biology of an organism is to mutagenize regulatory genes (such as two-component response regulators [RRs]), as each mutation potentially impacts the expression and/or function of a number of proteins. Both gram-negative and gram-positive bacteria utilize two-component signal transduction systems to sense and respond to different environmental stimuli, such as nutrient availability, pH, osmolarity, and host factors (5, 10). These signaling pathways are known to influence numerous processes in bacteria, including motility, bioluminescence, biofilm formation, and pathogenesis (31). Simple two-component signal transduction systems utilize two main protein components: (i) the sensor histidine kinase protein (SK), which functions as a dimer to autophosphorylate at a conserved histidine residue (using ATP as a phosphodonor) in response to a specific signaling event, and (ii) the RR, which catalyzes transfer of phosphate from the cognate SK to a conserved aspartate residue on its receiver or REC domain. More-complex "hybrid" systems consist of multiple phosphoryl-accepting histidine and aspartate residues within the same pathway. Regardless of the complexity of the upstream signal transduction pathway, the RR ultimately changes its activity upon phosphorylation to elicit a cellular response to the initial signal.

Typically, RRs contain two functional domains, a REC domain that participates in signal transduction and an effector domain necessary for the cellular response. Residues in the activation domain that are highly conserved among RRs provide a basis for identifying putative RRs. Studies of a number of such regulators, such as the well-characterized CheY, provide a basis for understanding the function of conserved residues in the activation domain. In *Escherichia coli* CheY, six amino acid residues play key roles in activation. Phosphorylation occurs on Asp57 (9), while two additional Asp residues, at positions 12 and 13, chelate a Mg^{2+} ion necessary for transfer of the activating phosphoryl group from the donor His (81). Three other amino acids, Thr87, Tyr106, and Lys109, convey the phosphorylation-associated conformational change that facilitates effector function (6, 12, 37, 38, 70).

In addition to their conserved activation domains, RRs contain effector domains responsible for eliciting a cellular re-

* Corresponding author. Mailing address: Department of Microbiology and Immunology, Loyola University Chicago, 2160 S. First Ave., Bldg. 105, Maywood, IL 60153. Phone: (708) 216-0869. Fax: (708) 216-9574. E-mail: kvisick@lumc.edu.
▽ Published ahead of print on 22 June 2007.

sponse to stimulation. Non-DNA-binding RRs (such as CheY) may directly impact protein function by affecting, for example, folding or stability; as a result they may also indirectly impact transcription of downstream target genes. DNA-binding RRs typically fall into three distinct subclasses, exemplified by NarL, OmpR, and NtrC (74). Members of each subclass maintain unique DNA sequence specificities and mechanisms of action. Members of the NarL subclass contain a classical helix-turn-helix (HTH) DNA-binding motif (4). Those of the OmpR subclass share a winged helix-turn-helix (wHTH) motif. In this latter motif, the traditional recognition helix used in major groove interactions with DNA is flanked by extended looped regions, which may interact with the minor groove of the target DNA sequence (46). The third, NtrC-like subclass consists of a structurally distinct group of RR proteins that serve as coactivators for RNA polymerase holoenzymes associated with the alternative sigma factor σ^{54}, and members of this subclass are known as σ^{54}-dependent RRs. These proteins contain two distinct effector domains. One domain binds DNA, while the other, approximately 240 amino acid residues in length, is responsible for oligomerization and ATP hydrolysis. Together with RNA polymerase containing σ^{54}, the two RR domains promote open complex formation during transcriptional initiation (54, 55, 59, 68, 80).

The importance of two-component regulators is underscored by their abundance in many sequenced bacterial genomes. For example, *E. coli* contains 32 two-component regulators (53). In *V. fischeri*, only five RRs have been described thus far: GacA, LuxO, ArcA, SypG, and SypE (8, 52, 83, 84, 90); of these, only the first three have been characterized by genetic disruption. Mutants that lack GacA exhibit pleiotropic effects in culture, fail to initiate symbiotic colonization (84), and fail to induce host development (83). LuxO and ArcA both serve as negative regulators of luminescence genes (8, 40–42, 52); however, of these two, only LuxO appears necessary during symbiotic initiation, suggesting that it controls symbiosis genes in addition to those governing luminescence (40–42, 52). Given that so few of these regulators have been characterized, we chose to identify, mutagenize, and characterize specific phenotypes mediated by *V. fischeri* RRs. This work demonstrates the feasibility of performing global screens for gene function in *V. fischeri* and represents an initial characterization of many two-component signal transduction pathways in this organism.

MATERIALS AND METHODS

Bioinformatics and statistics. Amino acid sequences of the *E. coli* K12 RRs CheY (47), OmpR (86), NarL (26), and NtrC (51) were obtained from the NCBI database and utilized as query sequences to search the genome of *V. fischeri* strain ES114 in the ERGO light database from Integrated Genomics (http://www.ergo-light.com/ERGO/). *V. fischeri* open reading frames (ORFs) that exhibited an expected threshold, or "E," value of <1 were further subjected to rpsBLAST analysis (44) to identify conserved domains. ORFs containing REC signal receiver domains were compared to CheY and other *E. coli* RR sequences by ClustalW amino acid alignment (76) to screen for conserved residues within this domain (D12, D13, D57, T87, Y106, and K109) (81). Putative RRs were then classified by using rpsBLAST (44) and ClustalW (76) analysis of each RR effector domain. Where indicated, Student's *t* tests (unpaired) were performed to generate a probability, or *P*, value to determine significance.

Strains and media. *V. fischeri* strain ES114 was the parent strain used in this study (7). *V. fischeri* strain KV1421 (58), which contains a chromosomal erythromycin resistance cassette (Tn*7*::*erm*) (48), was used as a control for motility and bioluminescence experiments. *E. coli* strains DH5α*λpir* (17), CC118*λpir* (29), and TAM1*λpir* (Active Motif, Carlsbad, CA) were used for cloning. Triparental matings to introduce plasmid DNA into *V. fischeri* utilized *E. coli* strain CC118*λpir* carrying the conjugation helper plasmid pEVS104 (73).

V. fischeri strains were grown in the following media. To test growth in a minimal medium, HEPES-MM was used (64). For routine culturing, either LBS (72) or SWT medium was used; the latter contains 0.5% tryptone, 0.3% yeast extract, and seawater salts (90). For motility experiments, cells were grown in TB-SW, a tryptone-based medium containing seawater salts, to maintain consistency with previously reported assays of *V. fischeri* motility (15). Previous work within the field indicates that increased medium osmolarity correlates with increased luminescence in culture (71). Thus, additional NaCl was added to SWT to a final concentration of 510 mM to assay for bioluminescence; we designated this medium as SWTS. *E. coli* strains were grown in LB (14), brain heart infusion (Difco), or SOC (66) medium. Where appropriate, antibiotics were added to the following final concentrations: chloramphenicol at 25 μg ml^{-1} for *E. coli* and 2.5 μg ml^{-1} for *V. fischeri*, kanamycin at 50 μg ml^{-1}, and erythromycin (ERY) at 5 μg ml^{-1} for *V. fischeri* and 150 μg ml^{-1} for *E. coli*. Agar was added to a final concentration of 1.5% for solid media.

Molecular and genetic techniques. Standard molecular biology techniques were used for all plasmid constructions. Restriction and modifying enzymes were purchased from New England Biolabs (Beverly, MA) or Promega (Madison, WI). To generate vector integration mutations (11) in each RR, DNA oligonucleotides used for amplifying internal fragments of RR genes (Table 1) were obtained from MWG Biotech (High Point, NC). Amplified PCR fragments were cloned into the *oriR6K*-based suicide vector pEVS122 (17), which was digested with the restriction enzyme SmaI. In some cases, internal fragments of RRs first were cloned using the TOPO TA cloning kit per the manufacturer's instructions (Invitrogen, Carlsbad, CA) and then subsequently subcloned into either pEVS122 or its derivative, pESY20 (58). Strains of *E. coli* carrying internal fragments of each RR in pEVS122 or pESY20 were used in triparental conjugations to introduce the DNA into wild-type *V. fischeri* strain ES114. ERY-resistant colonies that arose were presumptive RR mutants. To confirm each mutant, Southern blot analysis was performed as previously described (79) using digoxigenin-labeled pEVS122 as a probe to detect complementary sequences (Roche Molecular Biochemicals, Indianapolis, IN). Hybridization and detection were carried out as described previously (79). RR mutants resulting from these manipulations are shown in Table 2.

Stability of the duplication. Vector integration mutagenesis results in a partial duplication of the interrupted gene, and thus, recombination to yield a wild-type strain can occur. To determine whether such an event is frequent, we grew three *V. fischeri* RR mutants (KV1548, KV1703, and KV1704) for at least 10 generations in SWT in the absence of ERY selection. Cells were diluted and inoculated onto SWT plates (also nonselective). More than 200 colonies from each of the strains in triplicate were then patched onto LBS containing ERY and SWT plates to determine the percentage that retained ERY resistance.

Luminescence assays. To assay for potential bioluminescence defects, the RR mutants and ES114 were grown overnight in SWT- and subcultured into SWTS to a starting optical density at 600 nm (OD_{600}) of approximately of 0.03. At various times after inoculation, 1-ml samples were taken for luminescence and OD measurements. A TD-20/20 luminometer (Turner Biosystems, Sunnyvale, CA) set at factory settings was used to determine the relative light units integrated over a 6-second count.

Motility assays. To assay motility, KV1421 (58) and individual RR mutants were grown to the mid-exponential phase of growth (OD, ~0.3) in TB-SW, and 10-μl aliquots were inoculated onto TB-SW plates containing 0.225% agar (15, 85). Each mutant was spotted onto an individual plate along with a wild-type control. Over the course of 4 to 5 hours of incubation at 28°C, the diameter of migrating rings was measured.

Competitive symbiosis and growth assays. To assess the colonization capability of mutant *V. fischeri* strains, juvenile squid were inoculated into artificial seawater (Instant Ocean; Aquarium Systems, Mentor, OH) containing between 1,000 and 6,000 cells per ml of seawater. For competitive colonization assays, animals were inoculated with an approximately 1:1 ratio of mutant and wild-type cells. In the individual inoculation experiment, animals were inoculated with ES114 or KV1787 (Δ*sypG*) alone. The presence of bacterial strains within the light organs of juvenile squid was assessed through luminescence and homogenization/plating assays as described previously (63). The limit of detection based on these methods is 14 *V. fischeri* cells per squid. In competitive assays, colonization is reported as the log-transformed relative competitive index (log RCI). This number is generated by dividing the ratio of mutant to wild-type cells within the homogenate by the ratio present in the inoculum and subsequently determining the $\log_{10}$ value of that number.

TABLE 1. Primers used in this study

ORF name	Primer sequence	Primer name
VF0095	GACCTTAACTAGCACCAATATG	3153-c-F
	GATGAGCGAGATAAGCGTCC	3153-c-R
VF0114	CGTTACTTGTCAGAACAAGGC	155-F
	GAACATTTCACGTGTGCCTAG	155-R
VF0454	AAAAAGGTACCCATTGCAACGTTAGTTAATAAC	2061intF[a]
	TTTTTGGATCCTCTAAATCGATGTGGCTTGC	2061intR[a]
VF0526	AGGGACACGTTGTTTATTCTG	2425-c-F
	GTGTAAATCCGGCTGCTCG	2425-c-R
VF0923	CTACTGGGATGATTGCCGC	4095 F
	GCGAATGTATGAATAAGGGGAG	4095 R
VF0937	AAAAAGGTACCCGGCTCATGGCTCAATTG	LuxOintF[a]
	TTTTTGGATCCTCTAGCCAAGGGTCTCGG	LuxOintR[a]
VF1054	TCTGATTTGTGTGGACGACC	1666-c-F
	GATAGTCATGAGATACATCCG	1666-c-R
VF1148	ATGAACTCTTTGCTAGAGAAG	2414-c-F
	TATCTGGTTGGCTAAGCGG	2414-c-R
VF1396	CGCACAAATTGTAGAAACCC	459-c-F
	GGAACTGCGGGTATCTAAG	459-c-R
VF1401	GAAATTGTATGCAAACCATAC	1925-c-F
	ATTAGATGGAGCAAGTTGAGC	1925-c-R
VF1570	ACGAAGTGGTAACTCGCTC	1334-c-F
	CGAACAACGTTAGACTCATC	1334-c-R
VF1689	AAAAAGGTACCGTAGAGGAAGCGGTATTGG	2073intF[a]
	TTTTTGGATCCTATGGATGCCACCATTGCC	2073intR[a]
VF1783	AAAAAGGTACCCCTCGTTTAGAGGCGATTG	796intF[a]
	TTTTTGGATCCTGGTTGTCATCACCAATACG	796intR[a]
VF1854	CGTGATGGTGCTTGGTCC	5201F
	TCATCCGCAGTGATCGTATG	5201R
VF1909	CATCCGTTAATGCGTCGTGG	3374-c-F
	TTGCCGCCTTTCATCGCTTC	3374-c-R
VF1988	GAAGCACCAATTCGTGAAATG	846-c-F
	GTCACACGATGAGATACAGG	846-c-R
VF2120	GAACACGTAACTCGTAATACG	998-c-F
	AACCGTTGAACACATAGCGC	998-c-R
	GTTACGTGCACGAATAGTCAG	998-c-R2
VF2343	GATATTGAACTGACAGCTCTG	4741-c-F
	TGATACTACTGCTATTACTCTC	4741-c-R
VF2374	CTGCTCTTAGACTTAAAAATGCC	65F
	CTTTATATTGCTGAGGCGTTAG	65R
VFA0041	ACCACATCATTGTCCGCTC	1605-c-F
	CGCAATATCTGGCGTAAGG	1605-c-R
VFA0103	GGTTGATGATGAGCTCTCAG	3280-c-F
	CTCTTCACCATCCACTGGC	3280-c-R
VFA0179	AAAGGGATTAACAGAGTCAGG	3211-c-F
	GGTTTCTTGTGGCGGTTCG	3211-c-R
VFA0181	GAAGTATTACAAGATGAAGGC	3208-c-F
	CCTACATAGCTTTGACGCTG	3208-c-R
VFA0211	AAAAAGGTACCGGATCTAAAGGATTATCAATGGCG	3110intF[a]
	TTTTTGGATCCAAGACAAATGCGATTCAATGG	3110intR[a]
VFA0216	AAAGTAATGGACCTTGCTGAAGTC	3116F
	GATATGCGAACTCCATCTGAGAG	3116R
VFA0266	ACCATGTAGCAGAAACCATTG	629-c-F
	GGCGATATAACGTGCCTGC	629-c-R
VFA0436	CATGCTACCTAATCTTGATGGG	1948F
	ACCACTTCATCAGCATTTTCC	1948R
VFA0561	CGGACGGACTGATTGTCAG	140-c-F
	ACGTTCTCACCTGAATTAACC	140-c-R
VFA0608	TCCGCTCTGGCTCGTAAAC	737-c-F
	GCTACGTTAGCTACCTCAAG	737-c-R
VFA0732	ATGAGCCATTATTACGCTTTC	3084-c-F
	GCTGTGCAGACAGTTGCTG	3084-c-R
VFA0795	CGCTCGGAAATCATTAGCTC	2872-c-F
	GAACGATGCAATGTAGCGAC	2872-c-R
VFA0862	AAAAAGGTACCGGACGTTGTTTTCCACCAC	3758intF[a]
	TTTTTGGATCCACGGACATTCACCATCACG	3758intR[a]
VFA1012	AAAAAGGTACCCCTATCATGGGAGGGTTTG	3034intF[a]
	TTTTTGGATCCGCTGTTTGCCTTAATTGCTC	3034intR[a]
VFA1017	CTCAGATAGATAAAGCGTATTC	3040-c-F
	AATGCTTGAACGAATAGTGGG	3040-c-R
VFA1024	CAATGGCAGAGAAGCGCTG	3630-c-F
	TGTGTGAGGTCTGCATGTTG	3630-c-R
VFA1026	CCACTTCTCTGGCTATCCTC	3633-c-F
	CTCGGCGCATACTTCTTTAC	3633-c-R

[a] These primers contain additional sequences with engineered restriction sites.

TABLE 2. *V. fischeri* strains used in this study

Strain	Genotype	Reference
ES114	Wild type	7
KV1421	*att*Tn*7*::Ery^r	58
KV1548	VF2120 (*arcA*)::pEAH1	This study
KV1585	VF1570 (*torR*^{a})::pKV174	This study
KV1592	VFA1024 (*sypE*)::pEAH7	This study
KV1593	VFA0179::pKV178	This study
KV1594	VF1401::pKV177	This study
KV1595	VF1396 (*phoP*^{a})::pKV176	This study
KV1596	VFA0561::pKV175	This study
KV1612	VFA1017::pKV179	This study
KV1640	VFA0041 (*uhpA*^{a})::pTMB26	This study
KV1641	VF1054::pAIA1	This study
KV1650	VFA0266::pTMB27	This study
KV1651	VF1988 (*phoB*^{a})::pTMB28	This study
KV1654	VFA1012::pTMB31	This study
KV1655	VF2343 (*cpxR*^{a})::pTMB32	This study
KV1665	VF1909 (*narP*^{a})::pTMB33	This study
KV1666	VFA1026 (*sypG*)::pAIA4	This study
KV1668	VFA0211::pAIA6	This study
KV1672	VFA0181::pTMB34	This study
KV1703	VF2120 (*arcA*)::pTMB35	This study
KV1704	VF2120 (*arcA*)::pTMB36	This study
KV1714	VFA0795::pEAH10	This study
KV1715	VF0454 (*vpsR*^{a})::pEAH11	This study
KV1727	VF0526 (*phoP*^{a})::pEAH4	This study
KV1730	VF0095 (*ntrC*^{a})::pKV180	This study
KV1787	Δ*sypG*	This study
KV1809	VF1854 (*flrC*^{a})::pEAH26	This study
KV2164	VF2374::pEAH24	This study
KV2165	VFA0216::pEAH25	This study
KV2191	VF0937 (*luxO*^{a})::pAIA3	This study
KV2501	VF1689 (*expM*^{a})::pAIA2	This study
KV2503	VFA0103::pAIA5	This study
KV2505	VFA0802 (*cheV*^{a})::pKV207	This study
KV2507	VF0114 (*ompR*^{a})::pKV209	This study
KV2509	VFA0698 (*cheV*^{a})::pKV214	This study
KV2510	VF1833 (*cheY*^{a})::pKV215	This study
KV2636	VF1148 (*yehT*^{a})::pTMB30	This study
KV2637	VF1879 (*cheV*^{a})::pKV216	This study
KV2874	VFA0732::pKV208	This study

[a] Putative identity based on an e-value less than e^{-20}, per BLAST analysis, compared with regulators previously characterized in *E. coli*, *B. subtilis*, or *V. cholerae*.

To assess competitive growth in culture, *V. fischeri* RR mutant and marked wild-type strains were coinoculated into SWT medium at an approximately 1:1 ratio and the inoculum was plated. After at least 20 generations of growth in SWT, cells were diluted and plated again. The log RCI was calculated as described above.

RESULTS

Identification of putative RR proteins in the *V. fischeri* genome. To identify *V. fischeri* ORFs encoding putative RRs, we searched the genome for characteristic signal receiver (REC) domains and conserved residues therein (further detailed in Materials and Methods). In CheY, these conserved residues have been characterized as follows: the site of phosphorylation (Asp57), two additional aspartate residues (Asp12 and Asp13) necessary for maintaining a Mg^{2+} ion within the active site (81), and three residues (Thr87, Tyr106, and Lys109) that facilitate effector function (3, 12, 39). By these analyses, we identified 40 putative RR genes. For simplicity, we will refer to these proteins as RRs rather than putative RRs, although final confirmation that these identified proteins in fact function as RRs will require biochemical characterization not part of the current study. We further categorized the RR proteins into four main groups based on the nature of their predicted effector domains, represented by the following proteins: (i) CheY, which lacks a DNA-binding domain; (ii) NarL, which includes an HTH DNA-binding domain; (iii) OmpR, which contains a wHTH DNA-binding domain; and (iv) NtrC, with both a nucleotide binding domain and an HTH DNA-binding domain (Tables 3 to 6).

The first group of RRs, shown in Table 3, includes 15 ORFs that encode typical REC domains and, like CheY, lack distinct DNA-binding motifs. The *V. fischeri* homolog of CheY is likely encoded by VF1833. This gene is linked to other putative chemotaxis genes, including the RR genes *cheB* (VF1830) and *cheV* (VF1879). There exist two other CheV-like proteins (encoded by VFA0698 and VFA0802), which display 33.9% and 48.4% identity, respectively, to the VF1879-encoded CheV. These genes are present at distinct locations on chromosome 2, unlinked to any other genes involved in flagellar biosynthesis or chemotaxis (most of which are encoded on chromosome 1). Another RR in this group is *sypE* (VFA1024), a member of the recently identified *syp* cluster of genes involved in cell surface phenotypes and colonization (89, 90). SypE itself has yet to be characterized. The additional proteins in this group do not exhibit significant sequence similarity to known regulators.

The RRs in the second group contain, in addition to REC domains, HTH DNA-binding motifs found in RRs such as NarL (26) (Table 4). This class of six proteins includes GacA, as well as proteins with sequence similarity to known *E. coli* RRs. These include potential homologs of NarP, a regulator of genes involved in anaerobic respiration during nitrate limitation (61); UhpA, which regulates hexose phosphate transport (23, 32, 82); and YehT, an RR involved in multidrug resistance (30).

The third group contains 13 RR proteins that have a predicted wHTH DNA-binding domain, a motif found in RRs such as the outer membrane porin regulator OmpR (45, 80) (Table 5). Based on sequence similarity, VF0114 is likely an OmpR homolog. The only member of this class that has been characterized in *V. fischeri* is ArcA (8). Other RRs in this group exhibit similarity to characterized proteins, such as TorR, a regulator of the TMAO anaerobic respiratory system (69); PhoB, a phosphate regulator (43); and CpxR, an envelope stress regulator (16). The additional eight RRs within this family have no predicted homologs that have been characterized.

The fourth group consists of six putative σ^{54}-dependent RRs with sequence similarity to the nitrogen regulator NtrC (Table 6). In addition to REC and DNA-binding domains, proteins in this class contain a nucleotide binding domain required for σ^{54}-dependent transcriptional activation (59, 80). In addition to an NtrC homolog, likely encoded by VF0095, this group includes the luminescence regulator LuxO and VF1854, a putative homolog of the flagellar synthesis regulator FlrC, based on similarity to the *Vibrio cholerae* protein (34). SypG is another σ^{54}-dependent activator, which regulates expression of the *syp* cluster of genes (90). VF0454 exhibits similarity to the *V. cholerae* regulator of polysaccharide synthesis, VpsR. VF1401 has no previously characterized putative homolog.

TABLE 3. Putative RRs with no clear DNA-binding motif

ORF[a]	Length (amino acids)	Identity to CheY (%)[b]	Conserved residue[c]						Known or possible identity[d]	% Identity/ similarity[e]	Possible SK partner[f]
			D12	D13	D57	T87	Y106	K109			
VF0923	439	20.9	X	X	X			X			Unpaired
VF1054	157	26.4	X	X	X		X	X			VF1053
VF1689	368	23.3	X	X	X			X	ExpM[g]	32/53	Unpaired
VF1830	376	23.3	X	X	X				CheB	35/54	VF1831 (CheA)
VF1833	122	65.1	X	X	X	X	X	X	CheY	68/86	VF1831 (CheA)
VF1879	306	32.6	X	X	X	X		X	CheV[h]	30/55	VF1831 (CheA)
VFA0216	382	24.8	X	X	X						Unpaired
VFA0608	334	24.0	X	X	X			X			Unpaired
VFA0698	298	25.6	X	X	X	X		X	CheV[h]	28/53	Unpaired
VFA0732	267	22.5	X	X	X		X	X			VFA0733
VFA0795	331	23.3	X	X	X			X			Unpaired
VFA0802	313	27.1	X	X	X	X		X	CheV[h]	31/53	Unpaired
VFA1012	299	24.8		X	X	X		X			Unpaired
VFA1017	572	23.3	X	X	X		X	X			VFA1016
VFA1024	505	21.7	X	X	X			X	SypE[i]		VFA1025 (SypF)

[a] ORFs are designated VF if located on chromosome 1 and VFA if found on chromosome 2.
[b] Percent identity to *E. coli* CheY protein calculated by determining the number of identical residues per ClustalW alignment (76) and dividing by the number of amino acids in the shorter sequence.
[c] Presence (X) of amino acid residues conserved within REC domains of RR proteins (numbers shown represent placement within *E. coli* CheY).
[d] Possible identities were assigned to proteins whose e-values to the indicated *E. coli* (or alternative species, where indicated) gene were more significant than e^{-20}, per BLAST analysis (1, 67).
[e] Per BLAST alignment (bl2seq) using the Blosum 62 matrix across the length of the *V. fischeri* protein (28, 75).
[f] Identified as SK based on the presence of conserved histidine (H box) motifs by rpsBLAST analysis (44); putative homology, based on parameters outlined in footnote *d*, is indicated in parentheses.
[g] Compared to *Erwinia carotovora* sequence (2).
[h] Compared to *Bacillus subtilis* sequence (22).
[i] SypE has been previously named (90).

The genes of cognate RR and SK pairs are often physically linked on the chromosome. Therefore, we extended our analysis of RR genes to examine the functions of nearby genes. Using BLAST analysis, genes encoding the conserved SK domain involved in dimerization and phosphorylation, termed HisKA, were considered putative SKs. Interestingly, each of the RRs within the OmpR-like family is linked to a putative SK (Table 5). The RRs of the HTH and σ^{54}-dependent families each contain five (of six) seemingly paired members (Tables 4 and 6). In contrast, only 7 of the 15 RRs listed in Table 3 (lacking a DNA-binding motif) appear linked to SK genes.

Finally, we analyzed the distribution of RRs across each of *V. fischeri*'s two chromosomes. The larger chromosome, chromosome 1 (2.9 Mb, designated VF), encodes 22, or about half, of the RRs, 16 of which have known or tentatively assigned identities. The remaining 18 RRs are encoded on the smaller chromosome, chromosome 2 (1.3 Mb, designated VFA), and only five of them have assigned identities. Thus, in addition to the imbalance in the number of RRs with tentative assignments, the proportion of RRs on each chromosome is not representative of the size of the respective chromosomes. With two exceptions, we have not confirmed the putative identities of these genes; however, to aid the reader, we will include the putative assignments of the RR genes in parentheses following their gene numbers throughout this work.

Construction of RR mutants. To begin to characterize the two-component signal transduction systems of *V. fischeri*, we constructed mutant strains defective for individual *V. fischeri* RR genes. We chose to eliminate from our study the RR *gacA* gene (VF1627), as it has been characterized extensively, but included *luxO* (VF0937) and *arcA* (VF2120) as controls.

To mutate the RR genes with relative ease, we cloned an internal portion of each RR gene into a suicide vector (pEVS122 [17] or pESY20 [58]), marked with ERY resistance (Ery^r). Recombination of these constructs into the *V. fischeri* genome generates two truncated copies of the gene, which generally results in a null mutation (11). Although such mutations have the potential for polar effects on downstream genes

TABLE 4. Putative HTH RRs[a]

ORF	Length (amino acids)	Identity to CheY (%)	Conserved residue						Known or possible identity	% Identity/ similarity	Possible SK partner
			D12	D13	D57	T87	Y106	K109			
VF1148	238	28.7	X	X	X			X	YehT	51/73	VF1149 (YehU)
VF1627	214	28.7	X	X	X		X	X	GacA[b]		VF2082 (GacS)
VF1909	203	29.5	X	X	X	X	X	X	NarP	54/72	VF1908 (NarQ)
VF2374	209	23.3	X	X	X			X			Unpaired
VFA0041	202	24.8	X	X	X			X	UhpA	64/75	VF0040 (UhpB)
VFA0103	205	24.8	X	X	X	X		X			VFA0102

[a] See Table 3 footnotes for explanations of column heads.
[b] GacA has been previously identified and characterized (84).

TABLE 5. Putative wHTH RRs[a]

ORF	Length (amino acids)	Identity to CheY (%)	Conserved residue						Known or possible identity	% Identity/ similarity	Possible SK partner(s)
			D12	D13	D57	T87	Y106	K109			
VF0114	239	26.4	X	X	X	X	X	X	OmpR	83/94	VF0115 (EnvZ)
VF0526	226	21.7		X	X	X	X	X			VF0524, VF0525
VF1396	218	24.8	X	X	X		X	X			VF1397
VF1570	232	24.8		X	X	X	X	X	TorR	56/72	VF1619 (TorS)
VF1988	230	27.1		X	X	X	X	X	PhoB	80/91	VF1987 (PhoR)
VF2120	239	25.6		X	X		X	X	ArcA[b]		VF2122 (ArcB)
VF2343	227	26.4	X	X	X	X	X	X	CpxR	60/78	VF2344 (CpxA)
VFA0179	226	24.0		X	X	X	X	X			VFA0178
VFA0181	221	26.4	X	X	X	X		X			VFA0182
VFA0211	228	30.2		X	X		X	X			VFA0212
VFA0266	221	26.4		X	X	X	X	X			VFA0265
VFA0436	225	31.0		X	X		X	X			VFA0435
VFA0561	218	22.5	X	X	X	X	X	X			VFA0560

[a] See Table 3 footnotes for explanations of column heads.
[b] ArcA has been previously characterized (8).

(a possibility for numerous RR genes disrupted in this study), we will refer to our mutants simply as RR mutants; future work such as complementation and genetic analyses of the operon structure will be necessary to confirm the specific roles of RRs identified in this survey. Potential mutants were isolated by selection for Ery^r and subsequently confirmed using Southern blot analysis (see Materials and Methods). Resistant colonies arose at a frequency generally proportional to internal fragment length (i.e., larger fragments typically resulted in more-numerous resistant exconjugants). Although rarely, Southern analysis indicated that some isolates appeared to contain two copies of the suicide vector integrated in the RR gene. These strains were not used for further study. We constructed mutations in 35 of the 39 targeted RR genes in this manner. The remaining four RR genes (VF0923, VF1830 [*cheB*], VFA0436, and VFA0608) were recalcitrant to disruption despite multiple attempts; further experiments are required to determine whether these represent essential genes.

Since this method of making mutations has been used to a limited extent in *V. fischeri* and certainly has not been utilized on such a large scale, some additional characterization of this technique was warranted. First, we probed the lower size limit of homologous DNA that could be recombined successfully into the *V. fischeri* chromosome. We generated derivatives of our *arcA* mutant construct that truncated the original 314-bp gene fragment to 101 bp and 85 bp and introduced them into *V. fischeri*. ERY-resistant colonies were rare but arose with greater frequency with prolonged periods of conjugation. Southern analysis verified appropriate chromosomal insertion of the smaller *arcA* constructs in KV1703 and KV1704. In addition, we found that these strains (as well as our original *arcA* mutant, KV1548) exhibited increased luminescence (Fig. 2A), consistent with the function of ArcA as a negative regulator of bioluminescence (8). These results demonstrated that an 85-bp fragment is sufficient for homologous recombination in *V. fischeri*; thus, this method can be readily utilized for constructing mutations in small genes.

Second, we evaluated the stability of the *V. fischeri* vector integration mutants, as homologous recombination can occur to remove the partial duplication in these strains. We tested stability by growing three representative mutants for at least 10 generations in the absence of selective pressure. The three mutants contained duplications arising from recombination of 85-, 306-, and 651-bp regions of DNA (in *arcA*, VF0526 [*phoP*] and VF1854 [*flrC*], respectively). In two experiments, 100% of >200 colonies of each mutant strain remained resistant to ERY, suggesting that this type of mutation in *V. fischeri* is relatively stable and that constant selective pressure is unnecessary. Thus, the majority of subsequent experiments were carried out in the absence of selective pressure.

TABLE 6. Putative σ^{54}-dependent RRs[a]

ORF	Length (amino acids)	Identity to CheY (%)	Conserved residue						Known or possible identity	% Identity/ similarity	Possible SK partner(s)
			D12	D13	D57	T87	Y106	K109			
VF0095	467	28.7	X	X	X	X	X	X	NtrC	69/80	VF0096 (NtrB)
VF0454	445	17.1			X				VpsR[b]	67/84	Unpaired
VF0937	476	26.4		X	X	X		X	LuxO		VF0708, VF1036[c]
VF1401	475	25.6	X	X	X	X		X			VF1400
VF1854	477	31.8		X	X	X	X	X	FlrC[b]	78/85	VF1855 (FlrB)
VFA1026	500	21.7		X	X	X		X	SypG[d]		VFA1025 (SypF)

[a] See Table 3 footnotes for explanations of column heads.
[b] Compared to *Vibrio cholerae* proteins VpsR (88) and FlrC (34).
[c] LuxO likely functions in a phosphorelay, receiving its phosphate from phosphotransferase protein LuxU (VF0938), which likely responds to two sensor kinases, LuxQ (VF0708) and AinR (VF1036), a LuxN homolog (42).
[d] SypG has been previously named (90).

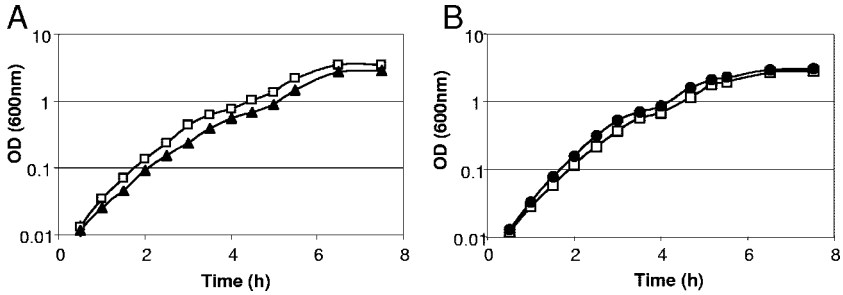

FIG. 1. Growth of RR mutants in culture. Growth of the control strain KV1421 (open squares) was measured in SWT medium over time and compared to growth of the *arcA* (A) (closed triangles) and VF1854 (*flrC*) (B) (closed circles) RR mutants. Experiments were performed in triplicate, and error bars are present but obscured by the icons representing each data point.

Impact of RR mutations on growth and luminescence. One of the hallmarks of *V. fischeri* biology is the ability to grow to high cell density and produce light. To address the involvement of two-component pathways in this process, we analyzed the ability of the 35 RR mutants to grow and luminesce. Because we have previously shown that the presence of the Ery^r marker decreases the luminescence and motility of *V. fischeri*, even in the absence of selection (58), we compared the growth and luminescence of the Ery^r RR mutants to those of KV1421, a derivative of the wild-type strain also marked with Ery^r. Upon plating of each mutant on solid medium composed of either the complex medium SWT or MM supplemented with a variety of carbon sources, we observed that only the *arcA* mutant generated consistently smaller colonies than did the control strain, KV1421. We further examined each of these strains in liquid SWT medium and found that most grew at a rate indistinguishable from that of the control. However, consistent with the observations of growth on solid medium, the *arcA* strain exhibited a significant, yet minor, deficit in growth, as measured by OD in SWT broth compared to that of the control (Fig. 1A). This result is consistent with previous observations (8). Conversely, a strain carrying a mutation in the putative homolog of the flagellar regulator *flrC* exhibited consistently higher OD measurements than did the control, indicating a possible growth advantage (Fig. 1B).

Bioluminescence of *V. fischeri* occurs at high cell density in response to the synthesis, release, and uptake of autoinducers (19–21). To date, the only RRs associated with luminescence are the negative regulators LuxO and ArcA (8, 52). To investigate whether other two-component regulators affect this pathway, we measured the bioluminescence of each mutant strain in SWTS medium relative to the control, KV1421. The growth characteristics of each RR mutant in SWTS generally paralleled those observed in SWT (data not shown). To account for any minor differences in growth or starting inoculum, we analyzed the specific luminescence of each strain relative to the OD. Representative experiments are depicted in Fig. 2.

Consistent with previous observations, mutations in *arcA* and *luxO* resulted in increased bioluminescence at high cell density (Fig. 2A) (42). Three different mutants defective for the RR ArcA displayed high levels of luminescence; all reached a level above the limit of detection at cell densities near or above an OD_{600} of 2. Additionally, the *luxO* mutant consistently achieved specific luminescence levels about fourfold above that of KV1421 (Fig. 2B). With few exceptions, most other RR mutant strains induced light production at rates similar to those of the wild type and achieved the same maximal levels (data not shown). For example, a mutant defective for the RR SypG, which exhibits substantial sequence similarity to the luminescence regulator LuxO, was indistinguishable from KV1421 (Fig. 2C). However, we did identify three RRs that appeared to enhance bioluminescence, as mutations that disrupted VFA0698 (*cheV*), VF1854 (*flrC*), or VF1148 (*yehT*) caused a small but reproducible decrease in bioluminescence levels compared to the control (Fig. 2D, E, and F, respectively). These data thus reveal additional minor players (either direct or indirect) in bioluminescence control.

Role of RRs in motility. In many bacteria, numerous environmental factors influence bacterial motility, making it another phenotype likely controlled by two-component regulation in *V. fischeri*. Therefore, we examined the motility of the 35 RR mutants by inoculating TB-SW soft agar plates each with an RR mutant and a control and measuring the diameter of the outer chemotaxis ring over time. Again, many RR mutants, such as the *sypG* mutant (Fig. 3A), exhibited no significant defect in motility compared to the control. However, we identified three classes of motility phenotype mutants: (i) those that appeared nonmotile, (ii) those with decreased migration, and (iii) those with increased migration relative to the control.

The first class of mutants, those that appeared nonmotile, included two strains (Fig. 3B). One was disrupted for VF1854, which encodes a putative homolog of *V. cholerae* FlrC, a protein necessary for flagellar gene expression (13, 60). The other contained a mutation in VF1833, the putative *cheY* gene. Because mutations in *cheY* are expected to disrupt chemotaxis rather than motility, we used a light microscope to examine the motility of these two strains and the control following growth in a liquid medium. We found that, whereas cells defective for the *flrC* homolog were nonmotile, those of the putative *cheY* mutant and the control were motile. Furthermore, our observations suggested that the *cheY* mutant cells exhibited far less frequent reversals than did the control (KV1421) cells, consistent with the smooth-swimming phenotype of typical *cheY* mutants. These data thus support the identification of VF1833 as *cheY* and of VF1854 as *flrC*.

The second class of mutants included five strains with decreases in migration (Fig. 3C). Two of these were strains defective for *arcA* and *luxO*. The *arcA* mutant (Fig. 3C, closed diamonds) exhibited a slight yet significant defect in migration rate. This is a phenotype not previously reported for this reg-

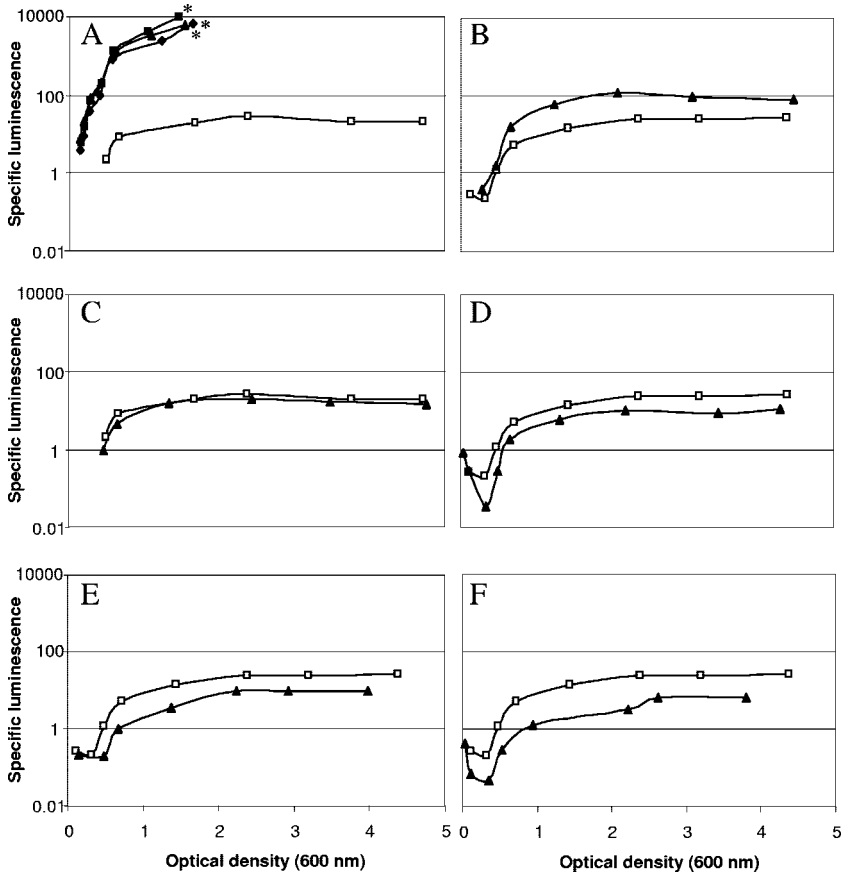

FIG. 2. Luminescence of RR mutants in culture. Specific luminescence (relative luminescence/OD_{600}) versus OD_{600} for KV1421 (open squares) was compared to *arcA* mutants (KV1548, KV1703, and KV1704; closed triangles, closed squares, and closed diamonds, respectively) (A), each of which reached levels of luminescence above the limit of detection (*), as well as to strains lacking the following RRs: *luxO* (B), *sypG* (C), VFA0698 (*cheV*) (D), VF1854 (*flrC*) (E), and VF1148 (*yehT*) (F). Shown are representative data from one of four independent experiments.

ulator; however, given the growth defect of this strain, verification of this result will require a growth-independent means of validation not part of this study. The *luxO* mutant (Fig. 3C, open triangles) exhibited the most severe motility defect of this class, with a greater-than-twofold decrease in the rate of motility on TB-SW soft agar plates relative to the control. This phenotype is consistent with that previously reported for a *luxO* mutant (41).

The second class of mutants also included those defective for VF0454 (*vpsR*) (Fig. 3C, closed squares), VF1909 (*narP*) (Fig. 3C, closed circles), and VF2343 (*cpxR*) (Fig. 3C, closed triangles). Disruption of VF2343 resulted in a slightly decreased rate of motility compared to the control. The two remaining strains were delayed in migration; each exhibited a strongly decreased rate of migration compared to that of the control until about 3 h postinoculation.

The third class of mutants contained a single strain, defective for VFA0698, which exhibited a small but reproducible increase in motility relative to the control (Fig. 3D). Intriguingly, VFA0698 is one of three RRs that exhibit sequence similarity to *cheV* (Table 3). In summary, these experiments supported the identification of LuxO as a motility regulator and revealed up to seven additional regulators that impact motility; additional experiments will be required to determine the mechanisms by which these RRs affect motility.

Multiple RRs play a role in colonization. Two-component regulators often mediate a bacterium's ability to sense and respond to host-specific signals during colonization. In fact, at least three such regulators, the RRs GacA and LuxO and the SK RscS, are known to affect the ability of *V. fischeri* to initiate colonization of the squid host (41, 79, 83, 84). To characterize our RR mutants with respect to symbiosis, we assayed the ability of the mutants to compete with the wild-type strain for colonization. In these experiments, we inoculated squid with approximately 1:1 mixtures of each RR mutant and a wild-type control. We evaluated successful colonization by measuring bioluminescence, which occurs when the bacteria have achieved a high cell density within the symbiotic light organ. We then isolated bacterial symbionts from colonized squid and determined the relative amounts of each of the two strains. To facilitate differentiation of the two strains, we marked one of the two strains using a stable plasmid that constitutively expresses *lacZ*, which does not affect competitive colonization (18), and plated the strains on medium containing X-Gal (5-bromo-4-chloro-3-indolyl-β-D-galactopyranoside). Finally, we calculated the RCI by normalizing the

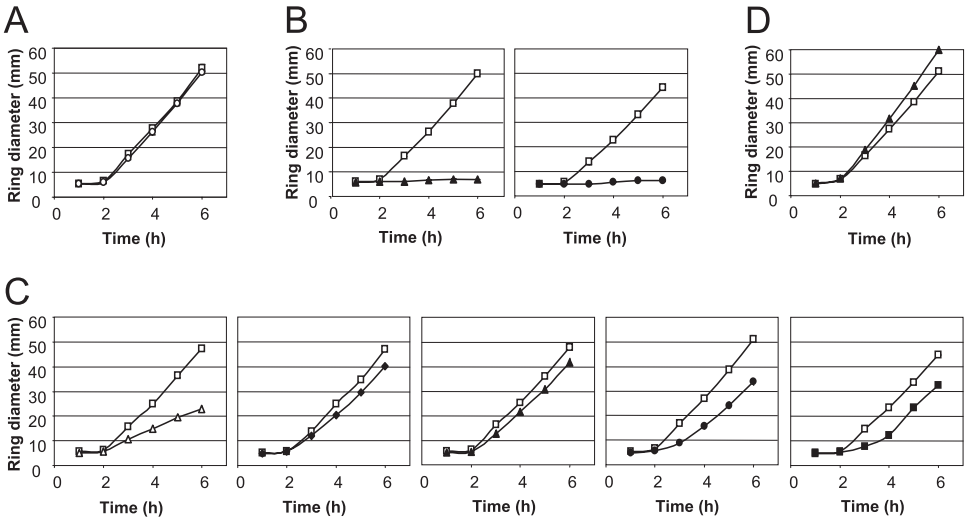

FIG. 3. Motility of RR mutants. Migration of KV1421 (open squares) was assayed over time in TB-SW soft agar plates by measuring the diameter of the outer motility ring and compared to that of strains lacking *sypG* (open circles) (A); *flrC* (closed triangles) and *cheY* (closed circles) (B); *luxO* (open triangles), *arcA* (closed diamonds), VF2343 (*cpxR*) (closed triangles), VF1909 (*narP*) (closed circles), and VF0454 (*vpsR*) (closed squares) (C); and VFA0698 (*cheV*) (closed triangles) (D). Experiments were conducted in triplicate, and error bars are present but obscured by the icons representing each data point.

ratio of output bacteria to the ratio of the input bacteria, which we report as a $\log_{10}$-transformed value (log RCI) for purposes of comparison (see Materials and Methods). A log RCI value below zero indicates a competitive disadvantage for an RR mutant; we report here only those mutants with a mean log RCI significantly less than zero as evaluated by Student's *t* test.

Of the 35 mutants that we tested, 23 exhibited no competitive defect in colonization. For example, squid inoculated with a strain defective for VF1396 consistently exhibited a log RCI of zero or greater (Fig. 4A). In contrast, 12 of the mutants tested exhibited a significant defect in competitive colonization in at least two independent experiments (Fig. 4B to D and data not shown). Subsequently, these 12 strains were also tested for competitive growth in culture. Most of the RR mutants that were competitively defective for colonization did not exhibit growth disadvantages in coculture (data not shown). Those that did exhibit statistically significant coculture differences are reported below.

Several mutants with defects in motility exhibited competitive defects (Fig. 4B). A mutation in *luxO*, a gene previously shown to be necessary for symbiotic initiation (41), resulted in a substantial competitive disadvantage (Fig. 4B, average log RCI of <-1.48). In addition, the *flrC* mutant was among the most severely compromised strains, as the inoculated squid yielded levels of mutant bacteria below our limit of detection (14 CFU/squid). It is likely that the lack of motility in this strain accounts for its colonization defect, as has been shown for other flagellar mutants (25, 49, 50). In coculture, the *flrC* mutant exhibited a competitive growth advantage in rich medium (data not shown), a phenotype that is unlikely to account for its colonization defect. A mutant defective for *cheY* was also severely defective in competition during colonization; a potential role for chemotaxis in symbiotic association will be discussed below. Although the *cheY* mutant exhibited a slight competitive growth disadvantage (average log RCI of -0.2286, $P = 0.0357$), this phenotype is unlikely to account for the severe colonization defect that we observed. Finally, three other RR mutants that displayed less-severe changes in motility also exhibited competitive defects: VF0454 (*vpsR*), VF1909 (*narP*), and VFA0698 (*cheV*). Notably, the *cheV*-like VFA0698 mutant (average log RCI of -0.8) exhibited increased motility, as well as decreased luminescence.

We also found five mutants that exhibited no defects in growth, luminescence, or motility and yet failed to compete effectively for symbiotic colonization (Fig. 4C). They were disrupted for the following RR genes: VF0095 (*ntrC*), VF1689 (*expM*), VF1988 (*phoB*), VFA0179, and VFA0181. Of these, only the *ntrC* mutant exhibited a slight competitive growth disadvantage in coculture experiments (average log RCI of -0.553, $P = 0.0018$). Further studies will be required to identify the pathways governed by each of these RRs and to determine whether they represent previously uncharacterized colonization determinants.

Finally, we also found that a strain that lacked the RR SypG was severely defective in competition. SypG has been shown to regulate transcription of a cluster of genes, *syp*, which are required for colonization (90); however, no mutations in *sypG* have previously been characterized. As shown in Fig. 4D, of nine animals inoculated with labeled ES114 and the *sypG* mutant, all were exclusively colonized with ES114.

Because SypG was the only RR that was completely excluded from the light organ and exhibited no motility or luminescence defect, we characterized *sypG* further by constructing an in-frame mutation to eliminate potential polar effects on the downstream gene *sypH*. We tested the Δ*sypG* mutant in single animal inoculations and found that under these conditions, the Δ*sypG* strain was severely defective in initiating symbiosis compared to the wild-type strain (a representative experiment is depicted in Fig. 5; $P = 0.01$). In fact, 5 of the 10 animals inoculated with the Δ*sypG* strain yielded no bacteria upon

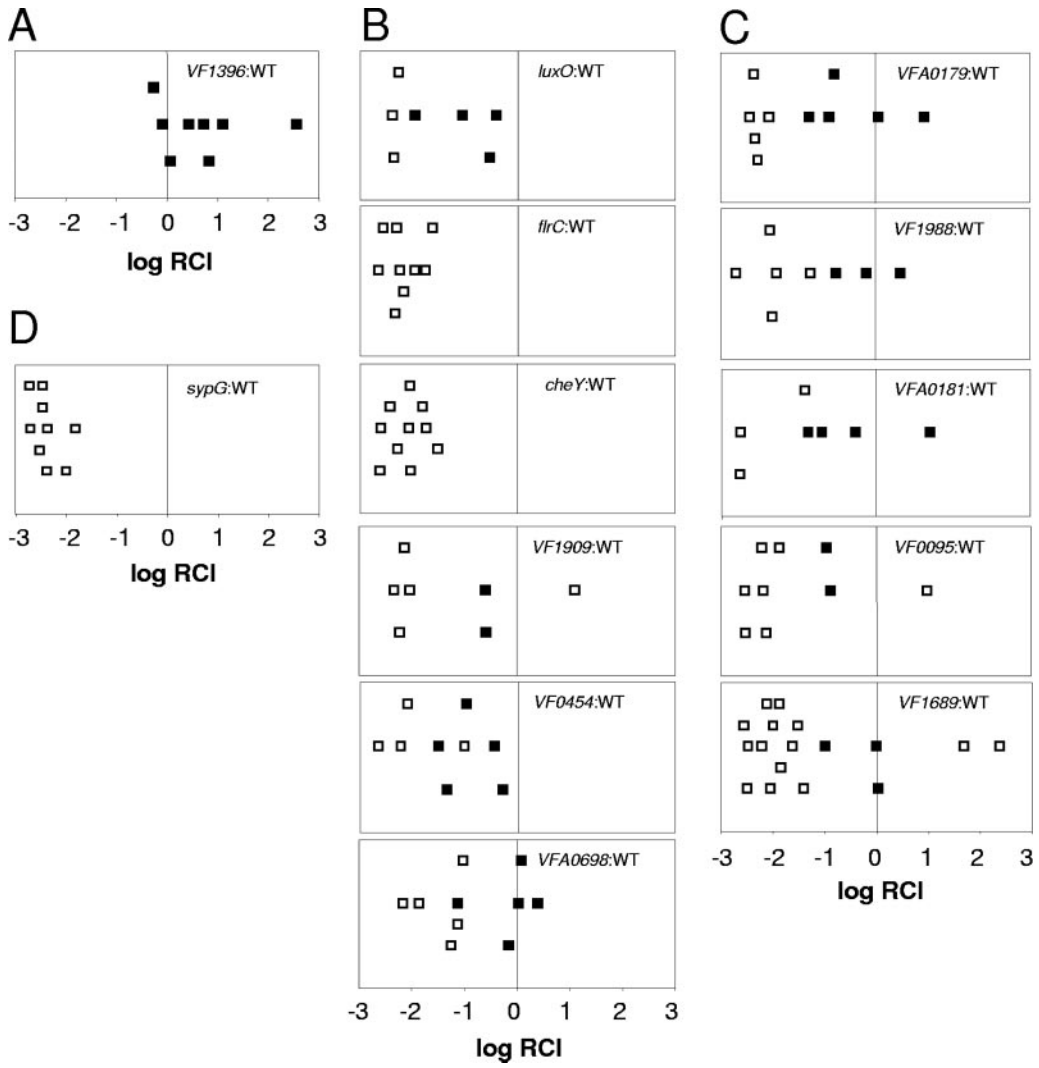

FIG. 4. Competitive colonization of RR mutants. Juvenile squid were coinoculated with RR mutant and marked wild-type (ES114) *V. fischeri* strains for approximately 18 h. The animals were then homogenized, and colonization was measured by the subsequent determination of the mutant-to-wild-type (WT) ratio of bacterial cells present within each squid (reported as log RCI; see Materials and Methods). A log RCI of <0 indicates that wild-type bacteria outnumber the mutant bacteria, indicating a competitive defect, whereas a log RCI of >0 indicates that mutant bacteria outnumber wild-type cells. Open squares represent animals in which either the mutant (log RCI, <0) or wild-type (log RCI, >0) cells were below the limit of detection (14 CFU/squid, in these experiments). Positioning along the *y* axis is arbitrary. (A) VF1396 mutant; (B) mutants which affect known symbiosis determinants (motility and/or luminescence); (C) strains which do not affect motility or luminescence; (D) a strain lacking *sypG*, which regulates the known symbiosis determinants within the *syp* cluster of genes.

homogenization (below the limit of detection, 14 CFU/squid). These data thus supported the prediction that SypG would be an important symbiotic regulator (90) and also revealed the utility of performing competition experiments to identify genes that might be necessary for symbiotic colonization even in the absence of competition.

DISCUSSION

To date, global genetic analyses and characterization of two-component signal transduction systems have been conducted in relatively few bacteria, largely in model organisms such as *Escherichia coli*, *Bacillus subtilis*, *Streptococcus pneumoniae*, and *Enterococcus faecalis* (27, 35, 36, 53, 77, 87). This work, conducted in the marine bacterium *V. fischeri*, adds to this relatively small data set. Through a bioinformatics approach, we identified 40 putative two-component RRs encoded by *V. fischeri* based, in part, on the presence of a canonical REC domain. Using a recently developed suicide plasmid and a vector integration approach, we subsequently mutated 35 of these regulators. We then examined several phenotypes in culture as well as the impact of these mutations on symbiotic colonization through competition analyses. This work demonstrated the feasibility of such a large-scale mutagenesis in *V. fischeri* and resulted in the identification of novel regulators of motility, bioluminescence, and colonization.

To identify RRs, we relied on bioinformatics approaches, searching the ERGO Light database (http://www.ergo-light.com/ERGO/) and then analyzing the candidates using rps-

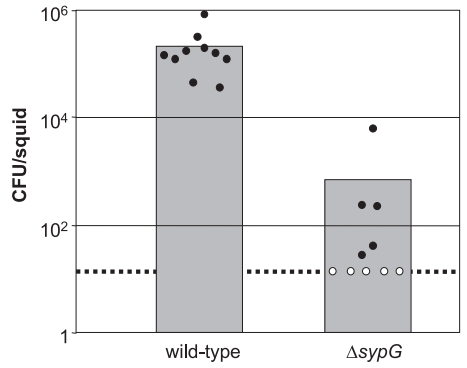

FIG. 5. Individual colonization of wild-type and Δ*sypG* strains. Individual animals (open or closed circles) were inoculated with wild-type (ES114; 1,390 cells/ml) or Δ*sypG* mutant (2,610 cells/ml) strains of *V. fischeri* for approximately 18 h and subsequently homogenized. Bacterial numbers were assessed by plating and are reported as CFU per squid. Open circles represent homogenates containing fewer than 14 CFU per squid (our limit of detection; dashed line). Gray boxes represent the average CFU for each strain of bacteria.

BLAST (44). We subsequently compared our results with data recently made available through the Center for Biological Sequence Analysis (CBS; http://www.cbs.dtu.dk/), which lists 47 putative RRs. The RRs that we identified through our analysis matched those listed by CBS, with the following exceptions. First, CBS listed 13 ORFs that we eliminated from our study, because further analysis indicated that those 13 ORFs contain both REC domains and sensory domains (i.e., the H box), and thus, they likely function as hybrid sensor kinase proteins rather than RRs. In addition, we identified five genes not listed by CBS. Four of these are CheY-like regulators that lack a DNA-binding domain: VF0923, VF1054, VFA0216, and VFA1017. Each of these contains a REC domain and most of the highly conserved residues therein (Table 3). We also included in our analysis VF0454 (*vpsR*), although it is unclear whether this regulator will indeed function as a RR. Alignments of this protein with LuxO (VF0937) revealed an overall conservation within the REC domain of the latter protein, supporting this assignment. However, like its *V. cholerae* homolog (88), VF0454 (*vpsR*) lacks several of the highly conserved residues in the REC domain (Table 6). Because our identifications were based on bioinformatics rather than biochemical analyses, further studies will be necessary to verify the function of these putative RRs as phosphate-accepting two-component proteins.

Our vector integration approach to interrupt the RR genes successfully yielded disruptions in 35 of the 39 RRs that we targeted for mutation with relative ease. As controls, we disrupted two previously characterized RRs, *luxO* and *arcA*. These mutations each resulted in phenotypes consistent with previous reports (8, 40–42). We can conclude, therefore, that our mutagenesis approach is capable of generating null mutations. Because many of the predicted RRs disrupted in this work appear to be encoded within operons (data not shown), the specific roles of these regulators must be addressed by complementation experiments in future work. Regardless of this caveat, this study reveals novel loci affecting downstream phenotypes such as colonization. It remains unclear why we were unable to obtain mutations in the remaining four genes. These may represent essential genes; however, this seems unlikely to be the case for VF1830 (*cheB*), which is predicted to play a role in chemotaxis.

Finally, we assessed the roles of the 35 RRs in two primary physiological traits in culture, bioluminescence and motility, as well as in the ability to compete with a wild-type strain for symbiotic colonization. We identified eight RR mutants with motility phenotypes, five with bioluminescence phenotypes, and 12 with symbiosis phenotypes. Of the symbiosis-defective strains, six exhibited alterations in either motility or bioluminescence or both, while six were wild type for these phenotypes. RRs required for symbiosis were found on each of the two chromosomes, with proportionally more of them mapping to the larger chromosome. They were also found in each of the four RR classes (regulators with no predicted DNA-binding sequences, with HTH or wHTH, or with σ^{54} activation domains). Intriguingly, of the six RRs that comprise the subgroup of σ^{54}-dependent RRs, five played roles in symbiosis, indicating the importance of this regulatory subclass in symbiotic colonization.

Of the six mutants defective for both symbiosis and other traits, the nonmotile *flrC* (VF1854) mutant is perhaps easiest to interpret: motility is essential for the initiation of symbiotic colonization (25, 49, 50), as demonstrated by the lack of *flrC* mutants found in the light organ in our experiments (Fig. 4B). A *cheY* mutant was similarly excluded from the light organ. This mutant also failed to migrate in soft agar plates; however, consistent with the predicted role of CheY as a chemotaxis regulator, the *cheY* mutant was actually motile but exhibited predominantly smooth swimming in liquid medium. These experiments indicate that chemotaxis may be important for symbiotic colonization. In support of this, we have similarly found that a mutant defective for *cheR*, another chemotaxis regulator whose loss results in smooth swimming, was also defective for colonization (14a). However, since both *cheY* and *cheR* mutants fail to migrate through soft agar, it remains formally possible that these strains fail to colonize not due to a lack of chemotaxis but due to an inability to penetrate the squid-secreted mucus layer. It will be necessary to construct specific chemoreceptor mutants or identify a squid-secreted chemoattractant to fully address this question.

Of the five additional mutants that exhibited decreases in motility, three also displayed symbiosis phenotypes (VF0454 [*vpsR*], VF1909 [*narP*], and *luxO*). Thus, it is tempting to speculate that reduced motility reduces colonization proficiency. This appears not to be true, however, in the case of the VF2343 and *arcA* mutants, which exhibited decreased motility but remained proficient for colonization. In addition, an interpretation for the *luxO* mutant, which was among the most severely compromised for motility, is complicated by the role which this regulator plays in the control of bioluminescence and other genes (40–42, 52).

Motility and colonization are also linked in the case of the mutant disrupted for VFA0698 (*cheV*). In this case, however, the mutant displayed an increase in motility. It also exhibited a decrease in bioluminescence. VFA0698 is one of three RRs predicted to encode a CheV-like protein, with both REC and CheW domains. In *Bacillus subtilis*, CheV functions to couple methyl-accepting chemotaxis proteins to the SK CheA, allow-

ing chemotactic signaling to occur (33, 62). Further experiments are required to determine whether any of the three *V. fischeri* CheV-like proteins performs such a function. The relative contribution to the symbiotic defect, if any, of the bioluminescence and motility phenotypes of the VFA0698 mutant remains unclear.

Perhaps most exciting are the six RRs whose loss caused a symbiosis defect but no alterations in bioluminescence or motility: VF0095 (*ntrC*), VF1689 (*expM*), VF1988 (*phoB*), VFA0179, VFA1081, and *sypG*. Of these, the most severe was the *sypG* mutant, which was excluded from the light organ. Because the insertional mutation in this strain could cause polar defects on a downstream gene, we further investigated the role of *sypG* by constructing an in-frame deletion and evaluating its ability to colonize juvenile squid in single-inoculation experiments. The results confirmed that this regulator plays an important role in symbiotic initiation (Fig. 5). The *sypG* gene resides within a large cluster of genes that are necessary for symbiotic colonization and function in polysaccharide biosynthesis (90). Our recent work demonstrates that *sypG* overexpression induces transcription of the *syp* genes, making it likely that this regulatory role accounts for the symbiotic requirement for SypG (90). Whether SypG controls additional colonization factors remains to be determined.

Of the remaining five RRs important for colonization, roles for VF0095 (*ntrC*), VF1689 (*expM*), and VF1988 (*phoB*) can be hypothesized based on bioinformatics. For example, VF1988, a putative PhoB homolog, could play a role in controlling genes based on phosphate availability. Similarly, the possible NtrC homolog VF0095 may respond to changing nitrogen levels. VF1689 may be a homolog of ExpM in *Erwinia carotovora*, which does not bind DNA but rather impacts the stability of the stationary-phase sigma factor σ^S (2). The remaining regulators (VFA0179 and VFA0181) contain predicted DNA-binding domains, which will likely facilitate investigations into their functions. Intriguingly, these two regulators are encoded near one another on the chromosome. These genes might thus represent a novel symbiosis locus.

Many of the RR mutants exhibited no defects or relatively minor defects in our competitive colonization experiments; however, this does not rule out the possibility that other RRs function in symbiosis. Whereas the competitive colonization experiments described herein were terminated 24 h after inoculation, other similar assays described in the literature are often extended to 48 h to account for the ability of a given bacterial strain to persist within the light organ after initial colonization. Thus, those RRs that are essential for persistence may not be defective (or may be only slightly defective) during the initial 24 h of symbiosis. Indeed, although we found no significant competitive defect for an *arcA* mutant at 24 h, recent work indicates that an *arcA* mutant exhibits a defect within 48 h (8). Additionally, it is possible that mixed inoculation with wild-type strains may complement some RR mutant phenotypes required for colonization. For example, an RR mutant unable to produce an unknown extracellular symbiosis determinant may be able to obtain that determinant from its wild-type neighbors during inoculation, thus masking a colonization phenotype. Thus, future experiments may identify additional RRs that function in symbiosis.

In summary, our results highlight the utility of a global approach for investigating gene function in *V. fischeri*. Together these experiments have provided a wealth of information regarding the roles of *V. fischeri* RRs in a variety of phenotypes, including symbiotic colonization. These results will serve as a starting point for understanding the connections between these global regulators and the physiological traits which they impact, particularly as microarray technology is applied to the mutant strains generated here.

ACKNOWLEDGMENTS

We thank Alan Wolfe, Jonathan Visick, and members of the Visick lab for critical reading of the manuscript.

This work was supported by NIH grants RR12294, awarded to E.G.R., and GM59690, awarded to K.L.V.

REFERENCES

1. **Altschul, S. F., T. L. Madden, A. A. Schäffer, J. Zhang, Z. Zhang, W. Miller, and D. J. Lipman.** 1997. Gapped BLAST and PSI-BLAST: a new generation of protein database search programs. Nucleic Acids Res. **25:**3389–3402.
2. **Andersson, R. A., E. T. Palva, and M. Pirhonen.** 1999. The response regulator *expM* is essential for the virulence of *Erwinia carotovora subsp. carotovora* and acts negatively on the sigma factor RpoS (sigma s). Mol. Plant-Microbe Interact. **12:**575–584.
3. **Appleby, J. L., and R. B. Bourret.** 1998. Proposed signal transduction role for conserved CheY residue Thr87, a member of the response regulator active-site quintet. J. Bacteriol. **180:**3563–3569.
4. **Baikalov, I., I. Schroder, M. Kaczor-Grzeskowiak, D. Cascio, R. P. Gunsalus, and R. E. Dickerson.** 1998. NarL dimerization? Suggestive evidence from a new crystal form. Biochemistry **37:**3665–3676.
5. **Beier, D., and R. Gross.** 2006. Regulation of bacterial virulence by two-component systems. Curr. Opin. Microbiol. **9:**143–152.
6. **Birck, C., L. Mourey, P. Gouet, B. Fabry, J. Schumacher, P. Rousseau, D. Kahn, and J. P. Samama.** 1999. Conformational changes induced by phosphorylation of the FixJ receiver domain. Structure **7:**1505–1515.
7. **Boettcher, K. J., and E. G. Ruby.** 1990. Depressed light emission by symbiotic *Vibrio fischeri* of the sepiolid squid *Euprymna scolopes*. J. Bacteriol. **172:** 3701–3706.
8. **Bose, J. L., U. Kim, W. Bartkowski, R. P. Gunsalus, A. M. Overley, N. L. Lyell, K. L. Visick, and E. V. Stabb.** 2007. Bioluminescence in *Vibrio fischeri* is controlled by the redox-responsive regulator ArcA. Mol. Microbiol. **65:**538–553.
9. **Bourret, R. B., J. F. Hess, and M. I. Simon.** 1990. Conserved aspartate residues and phosphorylation in signal transduction by the chemotaxis protein CheY. Proc. Natl. Acad. Sci. USA **87:**41–45.
10. **Calva, E., and R. Oropeza.** 2006. Two-component signal transduction systems, environmental signals, and virulence. Microb. Ecol. **51:**166–176.
11. **Campbell, A.** 1962. Episomes. Adv. Genet. **11:**101–145.
12. **Cho, H. S., S. Y. Lee, D. Yan, X. Pan, J. S. Parkinson, S. Kustu, D. E. Wemmer, and J. G. Pelton.** 2000. NMR structure of activated CheY. J. Mol. Biol. **297:**543–551.
13. **Correa, N. E., C. M. Lauriano, R. McGee, and K. E. Klose.** 2000. Phosphorylation of the flagellar regulatory protein FlrC is necessary for *Vibrio cholerae* motility and enhanced colonization. Mol. Microbiol. **35:**743–755.
14. **Davis, R. W., D. Botstein, and J. R. Roth.** 1980. Advanced bacterial genetics. Cold Spring Harbor Laboratory, Cold Spring Harbor, NY.

14a. **DeLoney, C., A. Wolfe, and K. L. Visick.** 2003. Abstr. 103rd Gen. Meet. Am. Soc. Microbiol., abstr. N-244. American Society for Microbiology, Washington, DC.

15. **DeLoney-Marino, C. R., A. J. Wolfe, and K. L. Visick.** 2003. Chemoattraction of *Vibrio fischeri* to serine, nucleosides, and *N*-acetylneuraminic acid, a component of squid light organ mucus. Appl. Environ. Microbiol. **69:**7527–7530.
16. **Dong, J., S. Iuchi, H. S. Kwan, Z. Lu, and E. C. Lin.** 1993. The deduced amino-acid sequence of the cloned cpxR gene suggests the protein is the cognate regulator for the membrane sensor, CpxA, in a two-component signal transduction system of *Escherichia coli*. Gene **136:**227–230.
17. **Dunn, A. K., M. O. Martin, and E. Stabb.** 2005. Characterization of pES213, a small mobilizable plasmid from *Vibrio fischeri*. Plasmid **54:**114–134.
18. **Dunn, A. K., D. S. Millikan, D. M. Adin, J. L. Bose, and E. V. Stabb.** 2006. New *rfp*- and pES213-derived tools for analyzing symbiotic *Vibrio fischeri* reveal patterns of infection and *lux* expression in situ. Appl. Environ. Microbiol. **72:**802–810.
19. **Eberhard, A., A. L. Burlingame, C. Eberhard, G. L. Kenyon, K. H. Nealson, and N. J. Oppenheimer.** 1981. Structural identification of autoinducer of *Photobacterium fischeri* luciferase. Biochemistry **28:**2444–2449.
20. **Engebrecht, J., K. Nealson, and M. Silverman.** 1983. Bacterial bioluminescence: isolation and genetic analysis of functions from *Vibrio fischeri*. Cell **32:**773–781.
21. **Engebrecht, J., and M. Silverman.** 1984. Identification of genes and gene

products necessary for bacterial bioluminescence. Proc. Natl. Acad. Sci. USA **81:**4154–4158.
22. **Fredrick, K. L., and J. D. Helmann.** 1994. Dual chemotaxis signaling pathways in *Bacillus subtilis*: a σ^D-dependent gene encodes a novel protein with both CheW and CheY homologous domains. J. Bacteriol. **176:**2727–2735.
23. **Friedrich, M. J., and R. J. Kadner.** 1987. Nucleotide sequence of the *uhp* region of *Escherichia coli*. J. Bacteriol. **169:**3556–3563.
24. **Geszvain, K., and K. L. Visick.** 2005. Roles of bacterial regulators in the symbiosis between *Vibrio fischeri* and *Euprymna scolopes*, p. 277–290. *In* J. Overmann (ed.), Molecular basis of symbiosis. Springer-Verlag, Berlin, Germany.
25. **Graf, J., P. V. Dunlap, and E. G. Ruby.** 1994. Effect of transposon-induced motility mutations on colonization of the host light organ by *Vibrio fischeri*. J. Bacteriol. **176:**6986–6991.
26. **Gunsalus, R. P., L. V. Kalman, and R. R. Stewart.** 1989. Nucleotide sequence of the narL gene that is involved in global regulation of nitrate controlled respiratory genes of Escherichia coli. Nucleic Acids Res. **17:**1965–1975.
27. **Hancock, L. E., and M. Perego.** 2004. Systematic inactivation and phenotypic characterization of two-component signal transduction systems of *Enterococcus faecalis* V583. J. Bacteriol. **186:**7951–7958.
28. **Henikoff, S., and J. G. Henikoff.** 1992. Amino acid substitution matrices from protein blocks. Proc. Natl. Acad. Sci. USA **89:**10915–10919.
29. **Herrero, M., V. de Lorenzo, and K. N. Timmis.** 1990. Transposon vectors containing non-antibiotic resistance selection markers for cloning and stable chromosomal insertion of foreign genes in gram-negative bacteria. J. Bacteriol. **172:**6557–6567.
30. **Hirakawa, H., K. Nishino, J. Yamada, T. Hirata, and A. Yamaguchi.** 2003. Beta-lactam resistance modulated by the overexpression of response regulators of two-component signal transduction systems in *Escherichia coli*. J. Antimicrob. Chemother. **52:**576–582.
31. **Hoch, J. A., and T. J. Silhavy (ed.).** 1995. Two-component signal transduction. ASM Press, Washington, DC.
32. **Island, M. D., B. Y. Wei, and R. J. Kadner.** 1992. Structure and function of the *uhp* genes for the sugar phosphate transport system in *Escherichia coli* and *Salmonella typhimurium*. J. Bacteriol. **174:**2754–2762.
33. **Karatan, E., M. M. Saulmon, M. W. Bunn, and G. W. Ordal.** 2001. Phosphorylation of the response regulator CheV is required for adaptation to attractants during *Bacillus subtilis* chemotaxis. J. Biol. Chem. **276:**43618–43626.
34. **Klose, K. E., and J. J. Mekalanos.** 1998. Distinct roles of an alternative sigma factor during both free-swimming and colonizing phases of the *Vibrio cholerae* pathogenic cycle. Mol. Microbiol. **28:**501–520.
35. **Kobayashi, K., M. Ogura, H. Yamaguchi, K. Yoshida, N. Ogasawara, T. Tanaka, and Y. Fujita.** 2001. Comprehensive DNA microarray analysis of *Bacillus subtilis* two-component regulatory systems. J. Bacteriol. **183:**7365–7370.
36. **Lange, R., C. Wagner, A. de Saizieu, N. Flint, J. Molnos, M. Stieger, P. Caspers, M. Kamber, W. Keck, and K. E. Amrein.** 1999. Domain organization and molecular characterization of 13 two-component systems identified by genome sequencing of Streptococcus pneumoniae. Gene **237:**223–234.
37. **Lee, S. Y., H. S. Cho, J. G. Pelton, D. Yan, R. K. Henderson, D. S. King, L. Huang, S. Kustu, E. A. Berry, and D. E. Wemmer.** 2001. Crystal structure of an activated response regulator bound to its target. Nat. Struct. Biol. **8:**52–56.
38. **Lewis, R. J., J. A. Brannigan, K. Muchova, I. Barak, and A. J. Wilkinson.** 1999. Phosphorylated aspartate in the structure of a response regulator protein. J. Mol. Biol. **294:**9–15.
39. **Lukat, G. S., B. H. Lee, J. M. Mottonen, A. M. Stock, and J. B. Stock.** 1991. Roles of the highly conserved aspartate and lysine residues in the response regulator of bacterial chemotaxis. J. Biol. Chem. **266:**8348–8354.
40. **Lupp, C., and E. G. Ruby.** 2004. *Vibrio fischeri* LuxS and AinS: comparative study of two signal synthases. J. Bacteriol. **186:**3873–3881.
41. **Lupp, C., and E. G. Ruby.** 2005. *Vibrio fischeri* utilizes two quorum-sensing systems for the regulation of early and late colonization factors. J. Bacteriol. **187:**3620–3629.
42. **Lupp, C., M. Urbanowski, E. P. Greenberg, and E. G. Ruby.** 2003. The *Vibrio fischeri* quorum-sensing systems *ain* and *lux* sequentially induce luminescence gene expression and are important for persistence in the squid host. Mol. Microbiol. **50:**319–331.
43. **Makino, K., H. Shinagawa, M. Amemura, and A. Nakata.** 1986. Nucleotide sequence of the phoB gene, the positive regulatory gene for the phosphate regulon of Escherichia coli K-12. J. Mol. Biol. **190:**37–44.
44. **Marchler-Bauer, A., and S. H. Bryant.** 2004. CD-Search: protein domain annotations on the fly. Nucleic Acids Res. **32:**W327–W331.
45. **Martinez-Hackert, E., and A. M. Stock.** 1997. The DNA-binding domain of OmpR: crystal structures of a winged helix transcription factor. Structure **5:**109–124.
46. **Martinez-Hackert, E., and A. M. Stock.** 1997. Structural relationships in the OmpR family of winged-helix transcription factors. J. Mol. Biol. **269:**301–312.
47. **Matsumura, P., J. J. Rydel, R. Linzmeier, and D. Vacante.** 1984. Overexpression and sequence of the *Escherichia coli cheY* gene and biochemical activities of the CheY protein. J. Bacteriol. **160:**36–41.
48. **McCann, J., E. V. Stabb, D. S. Millikan, and E. G. Ruby.** 2003. Population dynamics of *Vibrio fischeri* during infection of *Euprymna scolopes*. Appl. Environ. Microbiol. **69:**5928–5934.
49. **Millikan, D. S., and E. G. Ruby.** 2002. Alterations in *Vibrio fischeri* motility correlate with a delay in symbiosis initiation and are associated with additional symbiotic colonization defects. Appl. Environ. Microbiol. **68:**2519–2528.
50. **Millikan, D. S., and E. G. Ruby.** 2003. FlrA, a σ^{54}-dependent transcriptional activator in *Vibrio fischeri*, is required for motility and symbiotic light-organ colonization. J. Bacteriol. **185:**3547–3557.
51. **Miranda-Rios, J., R. Sanchez-Pescador, M. Urdea, and A. A. Covarrubias.** 1987. The complete nucleotide sequence of the *glnALG* operon of *Escherichia coli* K12. Nucleic Acids Res. **15:**2757–2770.
52. **Miyamato, C. M., Y. H. Lin, and E. A. Meighen.** 2000. Control of bioluminescence in *Vibrio fischeri* by the LuxO signal response regulator. Mol. Microbiol. **36:**594–607.
53. **Mizuno, T.** 1997. Compilation of all genes encoding two-component phosphotransfer signal transducers in the genome of *Escherichia coli*. DNA Res. **4:**161–168.
54. **Morett, E., and L. Segovia.** 1993. The σ^{54} bacterial enhancer-binding protein family: mechanism of action and phylogenetic relationship of their functional domains. J. Bacteriol. **175:**6067–6074.
55. **North, A. K., K. E. Klose, K. M. Stedman, and S. Kustu.** 1993. Prokaryotic enhancer-binding proteins reflect eukaryote-like modularity: the puzzle of nitrogen regulatory protein C. J. Bacteriol. **175:**4267–4273.
56. **Nyholm, S. V., and M. J. McFall-Ngai.** 2004. The winnowing: establishing the squid-*Vibrio* symbiosis. Nat. Rev. Microbiol. **2:**632–642.
57. **Nyholm, S. V., E. V. Stabb, E. G. Ruby, and M. J. McFall-Ngai.** 2000. Establishment of an animal-bacterial association: recruiting symbiotic vibrios from the environment. Proc. Natl. Acad. Sci. USA **97:**10231–10235.
58. **O'Shea, T. M., A. H. Klein, K. Geszvain, A. J. Wolfe, and K. L. Visick.** 2006. Diguanylate cyclases control magnesium-dependent motility of *Vibrio fischeri*. J. Bacteriol. **188:**8196–8205.
59. **Popham, D. L., D. Szeto, J. Keener, and S. Kustu.** 1989. Function of a bacterial activator protein that binds to transcriptional enhancers. Science **243:**629–635.
60. **Prouty, M. G., N. E. Correa, and K. E. Klose.** 2001. The novel σ^{54}- and σ^{28}-dependent flagellar gene transcription hierarchy of *Vibrio cholerae*. Mol. Microbiol. **39:**1595–1609.
61. **Rabin, R. S., and V. Stewart.** 1993. Dual response regulators (NarL and NarP) interact with dual sensors (NarX and NarQ) to control nitrate- and nitrite-regulated gene expression in *Escherichia coli* K-12. J. Bacteriol. **175:**3259–3268.
62. **Rosario, M. M., K. L. Fredrick, G. W. Ordal, and J. D. Helmann.** 1994. Chemotaxis in *Bacillus subtilis* requires either of two functionally redundant CheW homologs. J. Bacteriol. **176:**2736–2739.
63. **Ruby, E. G.** 1996. Lessons from a cooperative, bacterial-animal association: the *Vibrio fischeri-Euprymna scolopes* light organ symbiosis. Annu. Rev. Microbiol. **50:**591–624.
64. **Ruby, E. G., and K. H. Nealson.** 1977. Pyruvate production and excretion by the luminous marine bacteria. Appl. Environ. Microbiol. **34:**164–169.
65. **Ruby, E. G., M. Urbanowski, J. Campbell, A. Dunn, M. Faini, R. Gunsalus, P. Lostroh, C. Lupp, J. McCann, D. Millikan, A. Schaefer, E. Stabb, A. Stevens, K. Visick, C. Whistler, and E. P. Greenberg.** 2005. Complete genome sequence of *Vibrio fischeri*: a symbiotic bacterium with pathogenic congeners. Proc. Natl. Acad. Sci. USA **102:**3004–3009.
66. **Sambrook, J., E. F. Fritsch, and T. Maniatis.** 1989. Molecular cloning: a laboratory manual, 2nd ed. Cold Spring Harbor Laboratory, Cold Spring Harbor, NY.
67. **Schaffer, A. A., L. Aravind, T. L. Madden, S. Shavirin, J. L. Spouge, Y. I. Wolf, E. V. Koonin, and S. F. Altschul.** 2001. Improving the accuracy of PSI-BLAST protein database searches with composition-based statistics and other refinements. Nucleic Acids Res. **29:**2994–3005.
68. **Shingler, V.** 1996. Signal sensing by sigma 54-dependent regulators: derepression as a control mechanism. Mol. Microbiol. **19:**409–416.
69. **Simon, G., V. Mejean, C. Jourlin, M. Chippaux, and M. C. Pascal.** 1994. The *torR* gene of *Escherichia coli* encodes a response regulator protein involved in the expression of the trimethylamine *N*-oxide reductase genes. J. Bacteriol. **176:**5601–5606.
70. **Smith, J. G., J. A. Latiolais, G. P. Guanga, S. Citineni, R. E. Silversmith, and R. B. Bourret.** 2003. Investigation of the role of electrostatic charge in activation of the *Escherichia coli* response regulator CheY. J. Bacteriol. **185:**6385–6391.
71. **Stabb, E. V., M. S. Butler, and D. M. Adin.** 2004. Correlation between osmolarity and luminescence of symbiotic *Vibrio fischeri* strain ES114. J. Bacteriol. **186:**2906–2908.
72. **Stabb, E. V., K. A. Reich, and E. G. Ruby.** 2001. *Vibrio fischeri* genes *hvnA* and *hvnB* encode secreted NAD^+-glycohydrolases. J. Bacteriol. **183:**309–317.
73. **Stabb, E. V., and E. G. Ruby.** 2002. RP4-based plasmids for conjugation between *Escherichia coli* and members of the Vibrionaceae. Methods Enzymol. **358:**413–426.

74. **Stock, A. M., V. L. Robinson, and P. N. Goudreau.** 2000. Two-component signal transduction. Annu. Rev. Biochem. **69:**183–215.
75. **Tatusova, T. A., and T. L. Madden.** 1999. BLAST 2 Sequences, a new tool for comparing protein and nucleotide sequences. FEMS Microbiol. Lett. **174:** 247–250.
76. **Thompson, J. D., D. G. Higgins, and T. J. Gibson.** 1994. CLUSTAL W: improving the sensitivity of progressive multiple sequence alignment through sequence weighting, position-specific gap penalties and weight matrix choice. Nucleic Acids Res. **22:**4673–4680.
77. **Throup, J. P., K. K. Koretke, A. P. Bryant, K. A. Ingraham, A. F. Chalker, Y. Ge, A. Marra, N. G. Wallis, J. R. Brown, D. J. Holmes, M. Rosenberg, and M. K. Burnham.** 2000. A genomic analysis of two-component signal transduction in *Streptococcus pneumoniae*. Mol. Microbiol. **35:**566–576.
78. **Visick, K. L., J. Foster, J. Doino, M. McFall-Ngai, and E. G. Ruby.** 2000. *Vibrio fischeri lux* genes play an important role in colonization and development of the host light organ. J. Bacteriol. **182:**4578–4586.
79. **Visick, K. L., and L. M. Skoufos.** 2001. A two-component sensor required for normal symbiotic colonization of *Euprymna scolopes* by *Vibrio fischeri*. J. Bacteriol. **183:**835–842.
80. **Weiss, D. S., J. Batut, K. E. Klose, J. Keener, and S. Kustu.** 1991. The phosphorylated form of the enhancer-binding protein NTRC has an ATPase activity that is essential for activation of transcription. Cell **67:**155–167.
81. **West, A. H., and A. M. Stock.** 2001. Histidine kinases and response regulator proteins in two-component signaling systems. Trends Biochem. Sci. **26:**369–376.
82. **Weston, L. A., and R. J. Kadner.** 1988. Role of *uhp* genes in expression of the *Escherichia coli* sugar-phosphate transport system. J. Bacteriol. **170:**3375–3383.
83. **Whistler, C. A., T. A. Koropatnick, A. Pollack, M. J. McFall-Ngai, and E. G. Ruby.** 2007. The GacA global regulator of *Vibrio fischeri* is required for normal host tissue responses that limit subsequent bacterial colonization. Cell. Microbiol. **9:**766–778.
84. **Whistler, C. A., and E. G. Ruby.** 2003. GacA regulates symbiotic colonization traits of *Vibrio fischeri* and facilitates a beneficial association with an animal host. J. Bacteriol. **185:**7202–7212.
85. **Wolfe, A. J., and H. C. Berg.** 1989. Migration of bacteria in semisolid agar. Proc. Natl. Acad. Sci. USA **86:**6973–6977.
86. **Wurtzel, E. T., M. Y. Chou, and M. Inouye.** 1982. Osmoregulation of gene expression. I. DNA sequence of the *ompR* gene of the *ompB* operon of *Escherichia coli* and characterization of its gene product. J. Biol. Chem. **257:**13685–13691.
87. **Yamamoto, K., K. Hirao, T. Oshima, H. Aiba, R. Utsumi, and A. Ishihama.** 2005. Functional characterization in vitro of all two-component signal transduction systems from Escherichia coli. J. Biol. Chem. **280:**1448–1456.
88. **Yildiz, F. H., N. A. Dolganov, and G. K. Schoolnik.** 2001. VpsR, a member of the response regulators of the two-component regulatory systems, is required for expression of *vps* biosynthesis genes and EPS^{ETr}-associated phenotypes in *Vibrio cholerae* O1 El Tor. J. Bacteriol. **183:**1716–1726.
89. **Yip, E. S., K. Geszvain, C. R. Deloney-Marino, and K. L. Visick.** 2006. The symbiosis regulator RscS controls the *syp* gene locus, biofilm formation and symbiotic aggregation by *Vibrio fischeri*. Mol. Microbiol. **62:**1586–1600.
90. **Yip, E. S., B. T. Grublesky, E. A. Hussa, and K. L. Visick.** 2005. A novel, conserved cluster of genes promotes symbiotic colonization and σ^{54}-dependent biofilm formation by *Vibrio fischeri*. Mol. Microbiol. **57:**1485–1498.

JOURNAL OF BACTERIOLOGY, Dec. 2006, p. 8196–8205 Vol. 188, No. 23
0021-9193/06/$08.00+0 doi:10.1128/JB.00728-06

Diguanylate Cyclases Control Magnesium-Dependent Motility of *Vibrio fischeri*[▽]

Therese M. O'Shea, Adam H. Klein, Kati Geszvain, Alan J. Wolfe, and Karen L. Visick*

Department of Microbiology and Immunology, Loyola University Chicago, 2160 S. First Ave., Bldg. 105, Maywood, Illinois 60153

Received 21 May 2006/Accepted 5 September 2006

Flagellar biogenesis and hence motility of *Vibrio fischeri* depends upon the presence of magnesium. In the absence of magnesium, cells contain few or no flagella and are poorly motile or nonmotile. To dissect the mechanism by which this regulation occurs, we screened transposon insertion mutants for those that could migrate through soft agar medium lacking added magnesium. We identified mutants with insertions in two distinct genes, VF0989 and VFA0959, which we termed *mifA* and *mifB*, respectively, for *m*agnesium-dependent *i*nduction of *f*lagellation. Each gene encodes a predicted membrane-associated protein with diguanylate cyclase activity. Consistent with that activity, introduction into *V. fischeri* of medium-copy plasmids carrying these genes inhibited motility. Furthermore, multicopy expression of *mifA* induced other phenotypes known to be correlated with diguanylate cyclase activity, including cellulose biosynthesis and biofilm formation. To directly test their function, we introduced the wild-type genes on high-copy plasmids into *Escherichia coli*. We assayed for the production of cyclic di-GMP using two-dimensional thin-layer chromatography and found that strains carrying these plasmids produced a small but reproducible spot that migrated with an R_f value consistent with cyclic di-GMP that was not produced by strains carrying the vector control. Disruptions of *mifA* or *mifB* increased flagellin levels, while multicopy expression decreased them. Semiquantitative reverse transcription-PCR experiments revealed no significant difference in the amount of flagellin transcripts produced in either the presence or absence of Mg^{2+} by either vector control or *mifA*-overexpressing cells, indicating that the impact of magnesium and cyclic-di-GMP primarily acts following transcription. Finally, we present a model for the roles of magnesium and cyclic di-GMP in the control of motility of *V. fischeri*.

The limiting step in understanding signal transduction most often is the identification of the environmental signal that induces a physiological change. This has been true for two-component signaling (13, 58) and may also be true for the pathways that control the production of cyclic di-GMP (c-di-GMP) (45). This newly appreciated second messenger is synthesized from two GTP molecules by diguanylate cyclases (DGCs). These enzymes, found in numerous and diverse bacterial genomes, are readily identifiable through their signature GGDEF domains (19, 39, 40, 50, 53, 56). Furthermore, many bacterial species possess multiple proteins with domains that contain this GGDEF domain (for a recent review, see reference 45). Degradation of c-di-GMP is accomplished by phosphodiesterases containing either EAL or HD-GYP domains (8, 15, 49, 52, 57). Together, these activities maintain the steady-state concentration of c-di-GMP (46).

c-di-GMP first was discovered as a component of the cellulose biosynthesis enzyme complex from *Gluconacetobacter xylinus*, where it plays a vital role in promoting cellulose biosynthesis (46). c-di-GMP is now known to control exopolysaccharide production, rugose colony morphology, biofilm formation, and motility in a number of organisms (23, 27, 44, 53). In general, c-di-GMP production appears to promote a sessile, nonmotile lifestyle (45).

Numerous studies have shown that multicopy expression of DGCs inhibits motility (e.g., see references 3, 7, 34, and 53). However, the mechanism(s) by which this inhibition occurs has not been determined. In contrast, there exist a more limited number of studies in which mutations in DGC genes have been demonstrated to impact motility (1, 12, 23, 25, 43). Perhaps the best-characterized motility-associated DGC is the *Caulobacter crescentus* protein PleD, a two-component response regulator that contains a C-terminal GGDEF domain. During development, *C. crescentus* must eject its polar flagellum and grow a stalk in its stead. Flagellar ejection depends on cleavage of FliF, the protein that forms the MS ring at the base of the flagellum (1, 2, 23, 39). The ejection of the flagellum depends upon the production of c-di-GMP by PleD (1, 2, 23, 39).

Vibrio fischeri, naturally found free-living in seawater or in symbiotic association with the Hawaiian squid *Euprymna scolopes* (37), controls its flagellar biogenesis in response to magnesium (Mg^{2+}) in the environment: when Mg^{2+} is abundant, as it is in seawater, *V. fischeri* cells possess flagella; when this cation is limiting, they do not (38). In contrast to PleD, loss of flagella in *V. fischeri* does not occur through ejection (38). To understand how Mg^{2+} controls flagellation, we sought mutants that could migrate through soft agar medium lacking added Mg^{2+}. We report here the identification and characterization of two DGC genes, *mifA* and *mifB*, that inhibit migration in the absence of magnesium. We propose that these two DGCs constitute the keystone of an Mg^{2+}-sensitive signaling pathway that regulates flagellar biogenesis in *V. fischeri*.

MATERIALS AND METHODS

Strains and media. The strains used in this study are shown in Table 1. *V. fischeri* strain ESR1 (21) was used as the wild-type control for motility experi-

* Corresponding author. Mailing address: Department of Microbiology and Immunology, Loyola University Chicago, 2160 S. First Ave., Bldg. 105, Maywood, IL 60153. Phone: (708) 216-0869. Fax: (708) 216-9574. E-mail: kvisick@lumc.edu.

▽ Published ahead of print on 15 September 2006.

TABLE 1. Strains and plasmids used in this study

Strain or plasmid	Genotype	Source or reference
Strains		
V. fischeri		
ES114	Wild type	11
ESR1	Rif^r	21
KV1421	Tn*7*::*erm*	This study
KV1897	Rif^r *mifA*::Tn*10lacZ* + delivery vector	This study
KV1902	Rif^r *mifA*::Tn*10lacZ*	This study
KV1903	Rif^r *mifB*::Tn*10lacZ* + delivery vector	This study
KV2530	*mifC*::pTMO123	This study
KV2532	*mifB*::pTMO125	This study
KV2672	*mifA*::pKV217	This study
KV2825	Δ*mifB*	This study
KV2826	Δ*mifB mifA*::pKV217	This study
E. coli		
AJW678	*thi-1 thr-1*(Am) *leuB6 metF159*(Am) *rpsL136* Δ*lacX74*	29
DH5α	*endA1 hsdR17* (r_K^- m_K^+) *supE44 thi-1 recA1 relA* Δ(*lacIZYA-argF*)*U169 phoA* [ϕ80d*lac* Δ(*lacZ*)*M15*]	62
CC118 λ *pir*	Δ(*ara-leu*) *araD* Δ*lac74 galE galK phoA20 thi-1 rpsE rpsB argE*(am) *recA* λ *pir*	24
TAM1 λ *pir*	*mcrA* Δ(*mrr-hsdRMS-mcrBC*) F80 *lacZ*Δ*M15* Δ*lacX74 recA1 araD139* Δ(*ara-leu*)*7697 galU galK rpsL endA1 nupG* λ *pir*	Active Motif, Carlsbad, CA
Plasmids		
pAHMS16	pUC18-*hmsT*	28
pCR2.1 TOPO	Cloning vector, Kan^r Ap^r	Invitrogen
pKV69	Low-copy vector, Cm^r Tet^r	60
pTMO105	*mifA* in pKV69 (pKV69 BamHI/SphI + 2.2-kb BamHI/SphI [*mifA*$^+$] fragment from pTMO92; Tet^r Cm^r)	This study
pTMO126	*mifA* in pCR2.1 TOPO (pCR2.1 TOPO + 2,163-bp PCR fragment of *mifA* amplified with primers Up989Fwd and Down989Rev; Kan^r Ap^r)	This study
pTMO142	*mifCB* in pCR2.1 TOPO (pCR2.1 TOPO + *mifCB* amplified with primers Upfus959F and Down959Rev; Kan^r Ap^r)	This study
pTMO149	*mifCB* in pKV69 (pKV69 SmaI + BamHI/XbaI-filled fragment of *mifCB* from pTMO142; Tet^r Cm^r)	This study
pTMO155	*mifB* in pKV69 (pTMO149 with SalI deleted, which removes upstream sequences between the multiple cloning site and the 3′ end of *mifC*)	This study
pUC19	Cloning vector, Ap^r	63

ments with transposon insertion mutants. The wild-type *V. fischeri* strain ES114 (11) was used as the genetic background for construction of non-Tn-based *mif* mutants. Strain KV1421, a derivative of ES114 that contains a chromosomal erythromycin-resistant cassette (Tn*7*::*erm*) (32), was used as the wild-type control for motility experiments with erythromycin-resistant strains. *E. coli* strains Top10F′ (Invitrogen, Carlsbad, CA), CC118 λ *pir* (24), or TAM1 λ *pir* (Active Motif, Carlsbad, CA) were used for cloning. Triparental matings to introduce plasmid DNA into *V. fischeri* utilized *Escherichia coli* strain CC118λ*pir* carrying the conjugation helper plasmid, pEVS104 (55).

V. fischeri strains were grown in the following media. For routine culturing, LBS medium (54) was used. For experiments, cells were grown in Tris-buffered saline (TBS), which contains 342 mM NaCl and 1% Bacto-tryptone (Becton Dickinson and Company, Sparks, MD) (17) or TBS-Mg^{2+} (TBS with 35 mM $MgSO_4$) (38). In some experiments, $MgSO_4$ was added to final concentrations between 35 and 200 mM, as indicated in the text. HEPES minimal medium (HMM) (47) containing 100 mM HEPES, pH 7.5, 0.3% Casamino Acids, and 0.2% glucose, was used for biofilm experiments. *E. coli* strains were grown in LB (16), brain heart infusion medium (Becton, Dickinson and Company, Sparks, MD), or SOC medium (51). For c-di-GMP assays in *E. coli*, MOPS (morpholinepropanesulfonic acid) medium was prepared as described by Neidhardt et al. (36), with the following exceptions: 0.4% glucose, 0.2 mM K_2HPO_4, and 1/50 the micronutrients were used. Where appropriate, antibiotics were added to the following final concentrations: rifampin at 100 μg/ml; tetracycline at 5 μg/ml; chloramphenicol at 5 μg/ml for *V. fischeri* and 25 μg/ml for *E. coli*; and erythromycin at 5 μg/ml for *V. fischeri* and 150 μg/ml for *E. coli*. Agar was added to a final concentration of 1.5% for solid media and either 0.225% or 0.25% for motility plates.

Cloning, sequencing, and mutant construction. Plasmids constructed or used in this study are shown in Table 1 (and see data at http://www.meddean.luc.edu/lumen/DeptWebs/microbio/pub/pub.htm). Standard molecular biology techniques were used for all plasmid constructions. Restriction and modifying enzymes were purchased from New England Biolabs (Beverly, Mass.) or Promega (Madison, Wis.). DNA oligonucleotides used for amplifying *mif* genes (see supplemental material at http://www.meddean.luc.edu/lumen/DeptWebs/microbio/pub/pub.htm) were obtained from MWG Biotech (High Point, NC). The site of insertion of the transposon (Tn) in each mutant strain (KV1897, KV1902, and KV1903) was determined by cloning the Tn and flanking DNA to generate plasmids pTMO73, pTMO78, and pTMO85 (see data at http://www.meddean.luc.edu/lumen/DeptWebs/microbio/pub/pub.htm), respectively; plasmid pTMO85 was further subcloned to generate pTMO93. We sequenced DNA adjacent to the Tn in plasmids pTMO73, pTMO78, and pTMO93 with Tn- or plasmid-specific primers, using the services of Davis Sequencing, Inc. (Davis, CA).

We constructed vector-integration (Campbell insertion) (14) mutants by cloning an internal fragment of the appropriate genes into a suicide vector, pESY20, that cannot replicate in *V. fischeri*. The appropriate plasmid DNA was introduced into ES114 by triparental conjugation, followed by selection on erythromycin-supplemented LBS. The correct mutants were verified by Southern analysis. To construct the *mifB* deletion derivative, plasmid pKV231 (see data at http://www.meddean.luc.edu/lumen/DeptWebs/microbio/pub/pub.htm) was introduced into ES114. Cells containing the plasmid were selected on LBS containing chloramphenicol. The resulting colonies were passaged with or without chloramphenicol, and screened for increased motility on TBS soft agar plates. The presence of the *mifB* deletion was determined by PCR with primers complementary to regions flanking the insertion. The correctness of the resulting strain was verified by

Southern analysis with a probe for the *mifCB* region. To construct the double mutant, the *mifA* Campbell construct, pKV217, was introduced into the *mifB* deletion strain by conjugation, followed by selection on LBS containing erythromycin. KV1421 was constructed by introducing plasmid pEVS107 (Tn*7*::*erm*) (32) into ES114 by conjugation in a mating that also included *E. coli* strains carrying the Tn*7* transposase plasmid pUX-BF13 (6) and the conjugal plasmid pEVS104 (55).

Motility assays. To assay motility of *V. fischeri*, individual mutants and control strains were grown to mid-exponential phase (optical density [OD] of ~0.3), and 10-μl aliquots were spotted onto TBS or TBS-Mg^{2+} motility plates (containing as necessary the appropriate antibiotics). The diameter of migrating rings was measured over the course of 4 to 5 h of incubation at 28°C (17, 61). A similar strategy was used to assay motility of *E. coli*, except that the motility plates were based upon TB, which contains 86 mM NaCl and 1% Bacto-tryptone, and incubated for up to 12 h at 33°C.

Diguanylate cyclase activity assays. *E. coli* cells were grown at 37°C in phosphate-limited MOPS medium supplemented with 45 μCi/ml of $^{32}P_i$ (obtained as carrier-free orthophosphate in dilute HCl, pH 2 to 3, from Amersham). One-hundred-microliter samples were collected in 1.5-ml Eppendorf Safe-Lock tubes (Fisher Scientific) to which 10 μl of cold (4°C) 11 N formic acid (88% formic acid; Fisher Scientific) had been aliquoted and incubated in an ice bath for 30 min. The unincorporated orthophosphate was precipitated with 16.5 μl Na-tungstate–tetraethylammonium chloride–procaine precipitate solution as described previously (10) and centrifuged at 14,000 × *g* for 15 min at 4°C. A 10-μl aliquot of the supernatant was immediately neutralized with 10 μl of 2-picoline, as described previously (9). The neutralized sample was processed by two-dimensional thin-layer chromatography (2D-TLC) on polyethyleneimine cellulose F plates (EMD Chemicals), as described previously (59). To avoid inconsistencies associated with difference of exposure, all plates from any given experiment were exposed simultaneously to the same PhosphorImager screen.

c-di-GMP-dependent phenotype analyses. To assay the phenotypic consequences of c-di-GMP overproduction, we grew *V. fischeri* cells on chloramphenicol-containing LBS plates on which was spread 125 μl of a 0.2% stock of calcofluor (Fluorescent Brightener 28; Sigma Chemical, St. Louis, MO) dissolved in 1 M Tris, pH 9. We visualized fluorescence of the resulting colonies with UV light. We also examined cellulose production as described previously (22) using plates containing Congo red and Coomassie blue at final concentrations of 40 μg/ml and 15 μg/ml, respectively. To examine biofilm formation, cells were grown in HMM for 24 h with shaking. After staining with a 1% solution of crystal violet, the test tubes were rinsed three times with water and then photographed.

Western analysis. Western blot analysis was performed as previously described (38) with rabbit anti-*Vibrio parahaemolyticus* flagellin antibody (33).

RT-PCR. To analyze flagellin mRNAs from *V. fischeri* cells grown to early exponential phase (OD = 0.3 at 600 nm) in TBS or TBS-Mg^{2+}, RNA was first extracted using the RNeasy Mini kit from QIAGEN (Valencia, CA). DNA contamination was removed by treatment with 5 U of RQ1 RNase-free DNase (Promega, Madison, WI) in 1× RQ1 DNase buffer for 2 h at 37°C, followed by phenol-chloroform extraction and ethanol precipitation. To make cDNA, 0.7 μg RNA was incubated with 11.5 μM random hexamer primers from IDT (Skokie, IL) at 75°C for 3 min and then cooled to 4°C, to allow primers to anneal to the RNA. Next, 1× Stratascript buffer, 0.5 μM deoxynucleoside triphosphates (dNTPs), and 50 U of Stratascript reverse transcriptase (Stratagene, La Jolla, CA) were added and cDNA was generated by incubation at 42°C for 1 h, followed by 5 min at 95°C. DNase contamination was determined by performing a mock cDNA reaction lacking reverse transcriptase and dNTPs. Then, gene-specific primers (see data at http://www.meddean.luc.edu/lumen/DeptWebs/microbio/pub/pub.htm) were used in a PCR (30 cycles of 94°C for 20 s, 54°C for 30 s, and 72°C for 1 min, followed by a final 5-min 72°C extension.) For *flaA*, *flaB*, *flaD*, and *flaF*, 2.5 μl cDNA was used as a template; for *flaC*, *flaE*, and S16 reactions, 2.5 μl 5× dilute cDNA was used. PCR mixtures contained 0.4 μM primers, 0.25 μM dNTPS, 1.5 mM $MgCl_2$, 1× *Taq* buffer, and 1 U *Taq* (Promega, Madison, WI). Reactions were run on 1.5% agarose–Tris-borate-EDTA gels and photographed using a charge-coupled device camera and AlphaEaseFC software (AlphaInnotech Corp., San Leandro, CA).

RESULTS

Negative regulation controls motility of *V. fischeri*. Mg^{2+} controls migration of *V. fischeri* by promoting flagellar biogenesis (38). To account for this Mg^{2+}-dependent migration, we hypothesized that Mg^{2+} could enhance the activity of a positive regulator or prevent the function of a negative regulator. The latter hypothesis predicts that it should be possible to identify mutants defective for a negative regulator of flagellar biogenesis. Such a mutant would exhibit increased migration in the absence of Mg^{2+}. To test this possibility, we screened transposon mutant libraries for strains that exhibited enhanced migration on TBS (a tryptone-based medium lacking added $MgSO_4$) soft agar. In a screen of approximately 4,500 mutants, we identified 11 strains with increased migration on TBS. Careful measurements of migration rates of three of these revealed that they migrated substantially faster on TBS than ESR1, their parent (Fig. 1A and B and Table 1). In the absence of added Mg^{2+}, displacement of the outer edge of the swarm produced by each of the mutants began within an hour of inoculation (data not shown). Furthermore, this outer edge

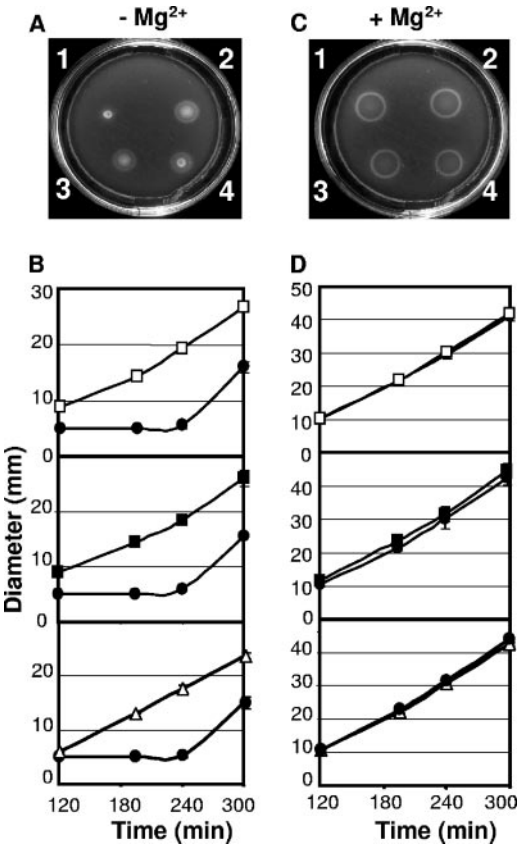

FIG. 1. Motility of transposon mutants in the absence and presence of Mg^{2+}. Exponential-phase cells of parent strain ESR1 (1; closed circles) and Tn insertion mutants KV1897 (2; open squares), KV1902 (3; closed squares), and KV1903 (4; open triangles), grown in TBS, were inoculated onto TBS or TBS-Mg^{2+} (containing 35 mM $MgSO_4$) soft agar plates (labeled $-Mg^{2+}$ and $+Mg^{2+}$, respectively) and incubated at 28°C. (A and C) Photographs of the migration of indicated strains after about 4 h of migration. (B and D) Migration was determined by measuring at hourly intervals the diameter of the outer migrating rings. At the last time point for the $-Mg^{2+}$ condition, only a small percentage of ESR1 cells contributed to the ring formed; the majority remained in the spot at the center of the plate. The error bars represent the standard deviations of a representative experiment performed in triplicate. The same data for ESR1 are plotted on multiple panels for comparison. Note the difference in the *y*-axis scales of the graphs.

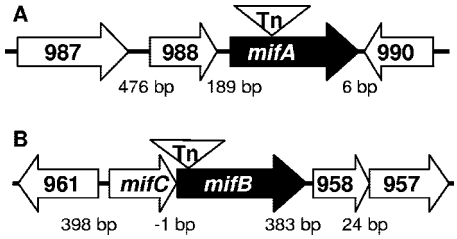

FIG. 2. Schematic representation of the *mifA*, *mifCB*, and flanking genes. (A) The *mifA* (VF0989) gene and genes flanking it on *V. fischeri* chromosome 1 are depicted as arrows. (B) The *mifC* (VFA0960) and *mifB* (VFA0959) genes and the genes flanking them on *V. fischeri* chromosome 2 are depicted as arrows. The numbers below indicate the spacing between the genes.

quickly developed into a tight, migrating ring of cells that responded to thymidine (17) (Fig. 1A and data not shown). In contrast, wild-type displacement was delayed by at least 4 h and the characteristic ring of thymidine-responsive cells never fully formed. In the presence of Mg^{2+}, both the migration and the thymidine-responsive rings of the three mutants were indistinguishable from those of their parent (Fig. 1C and D). These data are not consistent with the behavior of hypermotile mutants, but rather with a specific increase in migration caused by the disruption of a negative regulator. Since none of the mutants migrated to the same extent in the absence of Mg^{2+} as they did with Mg^{2+} addition (Fig. 1), we conclude that more than one gene product contributes to the inhibition of motility observed in the absence of Mg^{2+}.

Two putative diguanylate cyclase genes control motility. To understand the pathway of Mg^{2+}-dependent migration control, we cloned and sequenced DNA flanking the sites of the three transposon insertions. Two of the strains (KV1897 and KV1902) contained insertions in VF0989 (Fig. 2A). The transposons mapped to the same location within VF0989, although one of the insertions also included sequences from the delivery vector. The third strain contained an insertion in VFA0959 (KV1903; Fig. 2B). In a subsequent Tn*5* mutagenesis and motility screen to identify additional genes involved in Mg^{2+}-dependent migration control, we isolated 17 more *mifA* mutants, at least 11 of which were independently derived. These data further support the identification of *mifA* as an important and specific regulator of Mg^{2+}-dependent migration.

Both VF0989 and VFA0959 encode proteins with C-terminal GGDEF domains (GGEEF in the case of VF0989), indicating that they may encode DGCs. The amino termini of the predicted proteins each contain two putative membrane-spanning domains and a potential periplasmic loop. Finally, VFA0959 contains a predicted PAS sequence. Immediately upstream of VFA0959 is an open reading frame (VFA0960) that overlaps by 1 bp; thus, VFA0959 and VFA0960 likely constitute an operon (Fig. 2B). VFA0960 encodes a predicted periplasmic protein. Due to the roles of these genes in *M*g^{2+}-dependent *i*nduction of *f*lagellar biogenesis (along with supporting documentation described below), we designate VF0989 as *mifA*, VFA0959 as *mifB*, and VFA0960 as *mifC*.

Control of motility involves MifA and MifB. To begin to elucidate the roles of *mifA*, *mifB*, and *mifC* in Mg^{2+}-dependent migration and to rule out any potential complications from the

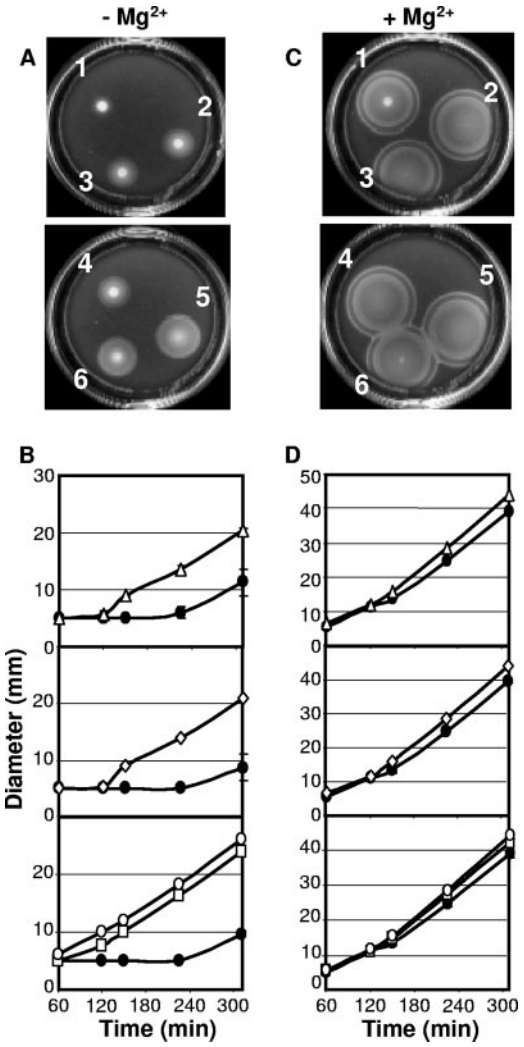

FIG. 3. Effects on motility of mutations in *mif* genes. Migration of *mif* mutants was assayed as described in the legend to Fig. 1. Photographs of the migration of indicated strains were taken after about 5 h of migration. Strains include the Erm^r control KV1421 (1; closed circles), KV2532 (*mifB*) (2 and 4; open triangles), KV2530 (*mifC*) (3; open diamonds), KV2826 (*mifA mifB*) (5; open circles), and KV2672 (*mifA*) (6; open squares). The error bars represent the standard deviations of a representative experiment performed in triplicate. In the absence of Mg^{2+}, only a small percentage of KV1421 cells contributed to the ring formed at the last time point; the majority remained in the spot at the center of the plate. The same data for KV1421 are plotted on multiple graphs for comparison.

study of transposon insertion mutants (derived from the rifampin-resistant strain ESR1), we used a vector-integration approach (18) to disrupt each of these genes in the wild-type strain ES114. Because we had only obtained the *mifB* mutant once, we particularly sought to verify its role in Mg^{2+}-dependent migration. In the course of these studies, we determined that the *erm* gene (in the vector portion of the insertion) in *V. fischeri* caused a slight motility defect; therefore, where appropriate for subsequent experiments, we used as our control KV1421, a derivative of ES114 that contains the *erm* gene inserted at the Tn*7* site. KV1421 and ES114 exhibited two behaviors that distinguished them from ESR1; both were ob-

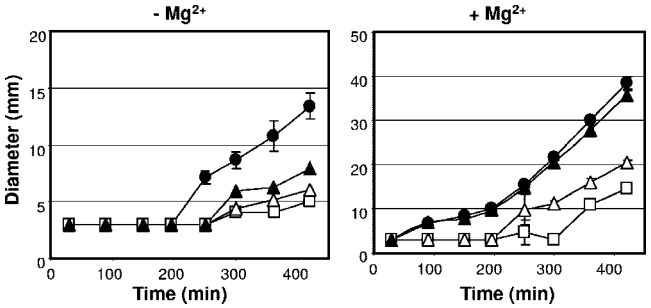

FIG. 4. Effects on motility of multicopy *mifA*, *mifCB*, and *mifB*. Migration of wild-type strain ES114 carrying the vector control (pKV69; closed circles) or plasmid pTMO105 (p*mifA*; open squares), pTMO149 (p*mifCB*; open triangles), or pTMO155 (p*mifB*; filled triangles) was assayed as described in the legend to Fig. 1, except that chloramphenicol was added at a final concentration of 2.5 μg/ml.

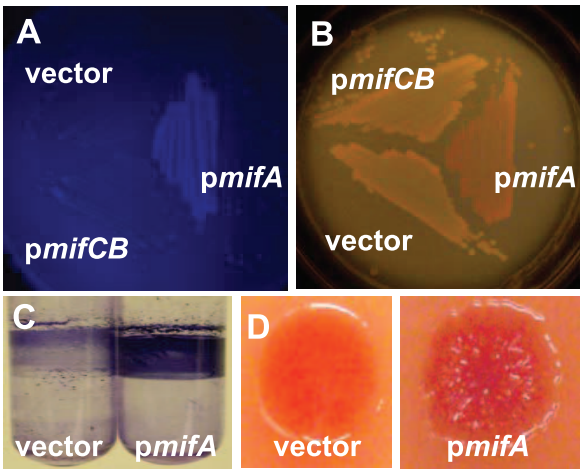

FIG. 5. Phenotype analysis of *V. fischeri* overexpressing *mifA* or *mifCB*. Cells of wild-type ES114 carrying vector (pKV69), multicopy *mifA* (p*mifA*; pTMO105), or multicopy *mifCB* (p*mifCB*; pTMO149) were examined for phenotypes consistent with increased c-di-GMP production. (A) Strains were grown on LBS plates with calcofluor and then exposed to UV light. (B) Strains were grown on LBS plates containing Congo red and Coomassie blue. (C) Strains were grown in HMM with shaking for 24 h and then stained with crystal violet as described in Materials and Methods. (D) Colony morphology of the vector control and multicopy *mifA* strains after prolonged growth on the LBS plates shown in panel B.

servable in the presence of Mg^{2+}. First, a substantial proportion of KV1421 (and ES114) cells remained at the site of inoculation (compare Fig. 3C to Fig. 1C; data not shown). Second, the characteristic inner band of cells that migrate in response to serine (17) appeared more rapidly with KV1421 and ES114 (Fig. 3C and data not shown) than it did with ESR1 (data not shown). As predicted from our original results (Fig. 1), however, disruption of either *mifA* or *mifB* allowed the cells to migrate in the absence of Mg^{2+} but did not substantially impact migration in its presence (Fig. 3B and D and data not shown). These data confirmed specific roles for *mifA* and *mifB* in the inhibition of migration in the absence of Mg^{2+}.

Due to the putative operon structure comprising *mifC* and *mifB*, we also asked whether *mifC* contributed to Mg^{2+}-dependent induction of motility. Indeed, a strain in which *mifC* was insertionally inactivated through vector integration displayed motility characteristics typical of the *mifB* mutant (Fig. 3). These data suggest that *mifC* is important, at least for providing a promoter for *mifB* transcription and potentially as a component in its own right. A more precise characterization of the role of *mifC* will depend upon the construction of unmarked nonpolar mutations. Finally, we constructed a double mutant containing an insertion in *mifA* and an unmarked deletion in *mifB*. Relative to the parent strains, the double mutant exhibited a slight but consistent increase in migration in the absence of Mg^{2+} (Fig. 3A and B and data not shown). Because the loss of both MifA and MifB does not bring migration to the same level as does the addition of Mg^{2+}, we conclude that another Mif component(s) likely exists.

Multicopy expression of *mifA* or *mifB* inhibits motility and promotes biofilm formation. To further understand the functions of MifA, MifB, and MifC, we cloned wild-type copies of *mifA* and the putative *mifCB* operon and introduced them on a medium copy plasmid (about 10 copies per cell; E. Stabb, personal communication) into wild-type or transposon mutant strains. This multicopy expression reduced the migration of the resulting cells, relative to the vector control, regardless of the strain background (e.g., wild-type and *mifA* or *mifB* mutant strains; Fig. 4 and data not shown). Microscopic examination showed that multicopy expression of *mifA* and *mifCB* also reduced the percentage of motile cells relative to the vector control (data not shown). This result is similar to that observed for other bacteria in which DGCs are overexpressed (for examples, see references 3, 7, 34, and 53). On motility plates, the inhibition of migration caused by multicopy *mifA* expression was not substantially overcome by Mg^{2+} addition, as the vast majority of the cells remained at the site of the initial inoculation (Fig. 4) (data not shown). This was true even when the concentration of Mg^{2+} was increased above the optimal 35 mM level, to upwards of 200 mM (data not shown). To clarify the role of MifB, we removed most of the upstream *mifC* sequences from the *mifCB* plasmid construct and asked whether it retained the ability to inhibit motility. We found that multicopy expression of *mifB* alone similarly decreased migration of the wild-type strain in the absence of Mg^{2+}. Intriguingly, however, addition of Mg^{2+} restored full motility to strains carrying multicopy *mifB*. These data suggest a role for MifC in modulating the activity of MifB.

Because the observed motility phenotype of wild-type cells carrying either multicopy *mifA* or *mifCB* resembled that of other overexpressed DGCs, we asked whether these strains produced other phenotypes known to be correlated with DGC activity, including cellulose biosynthesis, biofilm formation, and wrinkled colony morphology. First, we tested cellulose biosynthesis by examining the ability of *V. fischeri* cells to fluoresce under UV light on plates containing the cellulose-binding dye, calcofluor. We found that multicopy expression of *mifA* induced bright fluorescence, but *mifCB* and the vector control did not (Fig. 5A). These data indicate that MifA induced an alteration in the sugar composition of the cell surface. We further examined this phenotype using Congo red plates, another indicator of cellulose biosynthesis, and similarly found that multicopy *mifA* increased the dye binding properties of the cell (Fig. 5B). Second, we tested biofilm formation

by cells carrying *mifA*, *mifCB*, or the vector control by growing cells in a minimal medium, followed by staining adherent material with crystal violet. Consistent with the increased cellulose biosynthesis, multicopy expression of *mifA*, but not *mifCB*, substantially enhanced biofilm formation (Fig. 5C and data not shown). Finally, we investigated colony morphology of cells containing multicopy *mifA*, *mifCB*, or the vector control. After prolonged growth at room temperature, cells containing multicopy *mifA* formed wrinkled colonies, whereas cells carrying multicopy *mifCB* or the vector control produced smooth, round colonies characteristic of the wild-type strain (Fig. 5D and data not shown). Together, these data indicate that whereas multicopy expression of *mifCB* impacts only motility, multicopy *mifA* both inhibits motility and alters other cell surface characteristics.

MifA and MifB exhibit diguanylate cyclase activity. To further elucidate the roles of MifA and MifB, we assayed their activity in the heterologous microbe, *E. coli*. First, we introduced high-copy plasmids containing either *mifA* or *mifCB* and evaluated their effect on migration of *E. coli* on soft agar. Both *mifA* and *mifCB* (Fig. 6) decreased migration of *E. coli*, although not to the same extent as similar plasmids did to *V. fischeri* (Fig. 4). Then, we assayed potential DGC activity in these strains by separating small phosphorylated compounds by 2D-TLC. The *mifA* and *mifCB* constructs induced the production of a spot that migrated with an R_f value similar to that of the positive control, *E. coli* carrying the DGC HmsT from *Yersinia pestis* (Fig. 6B and C and data not shown). This spot was absent from the vector controls (Fig. 6D and data not shown). Quantification of these spots revealed that MifA produced more c-di-GMP than MifCB (Fig. 6E). Our data are consistent with the notion that MifA and MifCB harbor DGC activity (see Discussion).

***mifA* and *mifCB* impact flagellin levels.** Previously, we reported that *V. fischeri* cells grown in the absence of Mg^{2+} had little flagellin protein and either were aflagellate or contained, at most, a single flagellum (38). Since the *mif* mutants were capable of migrating in the absence of Mg^{2+}, we hypothesized that disruption of *mif* genes promotes migration by permitting the synthesis and assembly of functional flagella, which are composed primarily of flagellins. To determine whether *mif* pathway components contributed to the decreased flagellin levels in wild-type cells grown without Mg^{2+}, we probed whole-cell extracts from cells grown with or without Mg^{2+} using an anti-*V. parahaemolyticus* flagellin antibody (33). This antibody has been previously shown to recognize at least five of the six distinct flagellin proteins (FlaA to -E) produced by *V. fischeri* (35, 38). Consistent with the observed motility phenotypes, when grown in the absence of Mg^{2+}, strains with mutations in *mifA*, *mifB*, or both exhibited an increase in flagellin levels relative to the wild-type strain; when grown with Mg^{2+}, they produced equivalent levels of flagellins (Fig. 7A). In contrast, multicopy expression of either *mifA* or *mifCB* substantially reduced the levels of flagellins produced by cells, in both the absence and presence of Mg^{2+} (Fig. 7B and C). These data are consistent with a model that has MifA and MifB influencing motility by controlling flagellin levels.

***mifA* and *mifCB* appear to act posttranscriptionally.** In all bacteria studied extensively, the flagellin genes reside at the bottom of the flagellar transcriptional hierarchy, potentially due to the need to tightly control these highly expressed genes (31, 42). However, many of the characterized pathways for c-di-GMP control appear to act posttranscriptionally (27, 41, 45). We therefore analyzed whether environmental Mg^{2+} or *mif* pathway components impacted steady-state levels of flagellin transcripts, using semiquantitative RT-PCR (Fig. 8). First, we found that the Mg^{2+} content of the medium did not substantially alter the levels of flagellin transcripts. Then, we determined that they were largely unaltered by the presence of multicopy *mifA*, despite the fact that this plasmid abolishes motility (Fig. 4) and dramatically reduces flagellin protein lev-

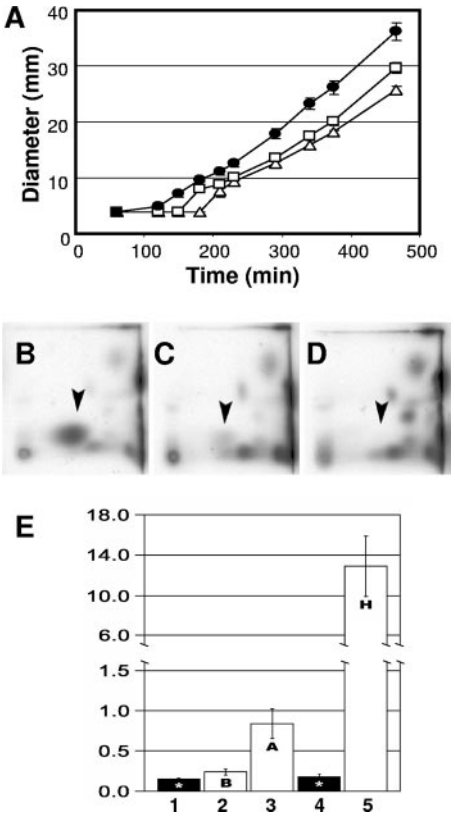

FIG. 6. Production of c-di-GMP by MifA and MifB. (A) Multicopy expression of *mifA* and *mifCB* inhibits migration of *E. coli*. Aliquots (5 μl) of *E. coli* strain AJW678 carrying pTMO126 (p*mifA*; open squares), pTMO142 (p*mifCB*; open triangles), or the vector control (pCR2.1 TOPO; closed circles), grown overnight in TB, were spotted onto the surface of TB motility plates and incubated at 34°C. The experiment was performed in triplicate at least twice. Error bars indicate standard deviation. (B to D) Multicopy expression of *mifA* in *E. coli* results in the accumulation of c-di-GMP. Cells of *E. coli* strain AJW678 carrying (B) pAhms16 (p*hmsT*), (C) pTMO126 (p*mifA*), or (D) pUC19 (vector) were grown at 37°C in low-phosphate MOPS medium supplemented with 0.4% glucose, harvested during mid-exponential growth, and subjected to formic acid extraction. Small phosphorylated molecules were separated by 2D-TLC as described in Materials and Methods. The arrowheads indicate the signal corresponding to c-di-GMP or its position. The experiment was performed at least twice, each time with multiple samples. (E) Histogram summarizing c-di-GMP production as a percentage of phosphorylated compounds in extracts of *E. coli* cells from the data of panels B to D and data not shown. 1, vector (pCR2.1 TOPO); 2, p*mifCB* (pTMO142); 3, p*mifA* (pTMO126); 4, vector (pUC19); and 5, p*hmsT* (pAhms16). The error bars represent standard deviation.

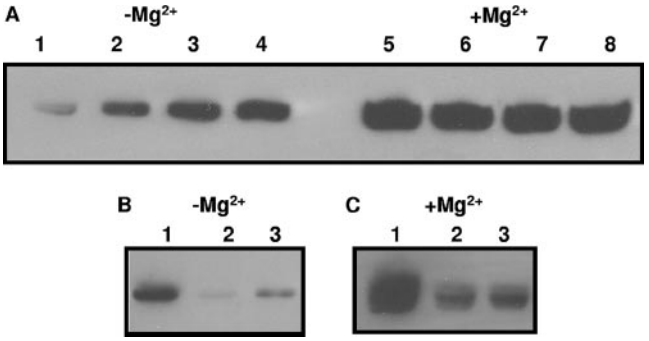

FIG. 7. Immunoblot analysis of *mif* mutant and overexpression strains. Flagellin proteins extracted from cells grown to mid-exponential phase in TBS or TBS-Mg^{2+} were separated by sodium dodecyl sulfate-polyacrylamide gel electrophoresis, transferred to a membrane, and detected by a *V. parahaemolyticus* antiflagellin antibody. The strains used in panel A were ES114 (lanes 1 and 5), KV2532 (*mifB*; lanes 2 and 6), KV2672 (*mifA*; lanes 3 and 7), and KV2826 (*mifA mifB*; lanes 4 and 8). Panels B and C were derived from ES114 with (lanes 1) vector pKV69, (lanes 2) pTMO105 (p*mifA*), or (lanes 3) pTMO149 (p*mifCB*). Strains were grown in TBS with or without Mg^{2+}, as indicated.

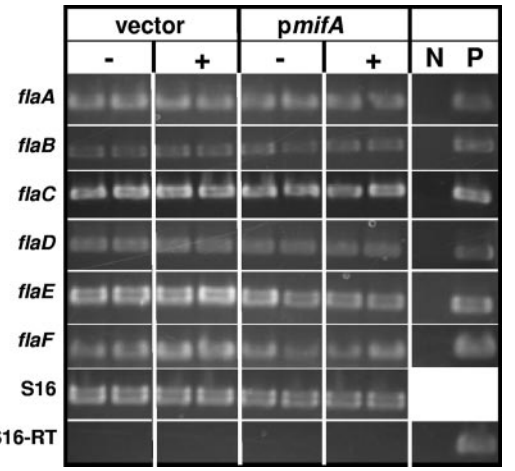

FIG. 8. Regulation of flagellin gene transcription by Mg^{2+} and multicopy expression of *mifA*. The gene amplified in each RT-PCR is labeled to the left of the panel. S16 is a ribosomal protein gene whose levels would be predicted to be unchanged by Mg^{2+} or MifA and was therefore used as a control for the efficiency of cDNA production. S16-RT represents reactions performed using the mock cDNA generated in the absence of reverse transcriptase and control for the presence of DNA contamination in the RNA. N, negative control (dH_2O as PCR template); P, positive control (genomic DNA as PCR template). − and +, presence and absence, respectively, of 35 mM $MgSO_4$ in the growth media.

els (Fig. 7B and C). Taken together, these data argue against a model for *mif* pathway control of flagellar biogenesis that relies primarily on a transcriptional mechanism.

DISCUSSION

We previously reported that flagellation and motility of *V. fischeri* depended upon Mg^{2+} in the medium. Here, we describe two novel flagellar regulators, MifA and MifB, that contribute to the poor motility of *V. fischeri* in the absence of Mg^{2+}. When either *mifA* or *mifB* was disrupted, the cells exhibited a substantial increase in migration on TBS soft agar plates. Because wild-type cells under these conditions are largely aflagellate, the increase in migration of *mif* mutants most likely stems from an increase in the number of assembled flagella. In support of this conclusion, these mutations caused an increase in the levels of flagellin proteins in cells grown without Mg^{2+}.

Both MifA and MifB are predicted to contain conserved GGDEF domain sequences, indicating that they likely function as DGCs. For MifA, our experiments demonstrate such a role, as follows: (i) *E. coli* strains carrying *mifA* on a multicopy plasmid synthesized a molecule that migrated on 2D-TLC plates with an R_f value similar to the positive control (Fig. 6); (ii) multicopy *mifA* expression inhibited motility of *V. fischeri*, and to a lesser extent, *E. coli* (Fig. 4 and 6A); and (iii) multicopy *mifA* expression promoted some of the same phenotypes induced by known DGCs, including increased cellulose biosynthesis and biofilm formation (Fig. 5). For MifB, our experiments are less conclusive: the impact of multicopy *mifCB* was primarily at the level of inhibiting motility; neither biofilm formation nor cellulose biosynthesis was noticeably impacted, and c-di-GMP production was difficult to discern. Like MifA, however, MifB contains a GGDEF domain and neither protein contains an EAL domain that would promote c-di-GMP degradation. Similar to that observed for *mifA* mutants, *mifB* mutants exhibited an increase in Mg^{2+}-independent migration. Finally, like multicopy *mifA*, multicopy *mifCB* reduced flagellin levels of wild-type cells. Together, these data suggest that MifB functions like MifA, albeit with lower activity. This weaker effect could be due to differences in expression or activity of the protein expressed from the *mifCB* plasmid tested. Indeed, *mifC* and *mifB* are likely to be translationally coupled, and our overexpression data suggest that MifC influences the activity of MifB.

V. fischeri is predicted to contain about 30 genes with GGDEF domains (48). This abundance suggests a network of pathways that integrates multiple signals into a single second messenger (20). Alternatively, single pathways or subsets of pathways might work in relative isolation due to their localization or the existence of microenvironments (25, 39, 53). Our screens for Tn insertion mutants with increased motility in the absence of Mg^{2+} consistently yielded insertions in the *mifA* gene. These data suggest that MifA plays a specific role in flagellar biogenesis and not a more general role as a contributor to the intracellular pool of c-di-GMP. To date, we have identified only one insertion mutant disrupted for *mifB*; however, the phenotypes of the original and two newly constructed *mifB* mutants exhibit motility phenotypes similar to that of the *mifA* mutants, suggesting that MifB also is a specific component of the Mif pathway. MifA and MifB each contain a predicted periplasmic loop, which potentially could permit membrane localization. If these proteins were directed to the flagellated cell pole, the localized production of c-di-GMP could be an efficient means of specifically interfering with flagellar biogenesis and not other cellular processes. Such localization might, in fact, be critical: the relatively insensitive TLC assay failed to detect c-di-GMP production by *V. fischeri* cells carrying multicopy *mifA* or *mifCB* (A. Klein and A. Wolfe, unpublished data),

despite the fact that these plasmids profoundly impacted motility. Where these proteins are localized and whether localization is critical to Mg^{2+}-dependent motility will be the subject of further research.

The mechanisms used by c-di-GMP to influence behavior remain obscure, although the recent identification of a putative c-di-GMP binding domain, PilZ, has substantially advanced our understanding of this small molecule (4). Similar to cAMP, which requires only the transcription factor CRP (also known as CAP) (5, 30), c-di-GMP is predicted to work by direct interaction with its targets (19). Such is the case with the biosynthesis of cellulose, an extracellular polysaccharide (EPS), in *G. xylinus* and *Salmonella enterica* serovar Typhimurium (44). In these organisms, multiple DGCs and phosphodiesterases regulate the intracellular concentration of c-di-GMP, which binds directly to a cellulose synthesis complex that includes BcsA, a glycosyltransferase that possesses a predicted PilZ domain (4).

Like cellulose synthesis, several c-di-GMP-associated behaviors (e.g., ejection of the *C. crescentus* flagellum, the hemin storage [Hms] phenotype of *Yersinia pestis*, and twitching motility in *Pseudomonas aeruginosa*) appear to be regulated posttranslationally (1, 23, 25, 28, 41). Our work to date similarly suggests a mechanism of posttranscriptional control by Mg^{2+} and c-di-GMP: (i) Mg^{2+} does not substantially impact levels of any of the six flagellin transcripts (Fig. 8), but does impact flagellin levels (38) (Fig. 7A); (ii) in the absence of Mg^{2+}, cells disrupted for either *mifA* or *mifB* exhibit increased motility (Fig. 1 and 3) and flagellin levels (Fig. 7A) but no changes in the levels of flagellin transcripts (Fig. 8); and (iii) in the absence of Mg^{2+}, multicopy *mifA* nearly abolishes motility (Fig. 4) and substantially decreases flagellin levels (Fig. 7B), but does not significantly alter flagellin transcripts (Fig. 8). Our work has not yet fully elucidated the mechanism by which loss of motility occurs in the absence of Mg^{2+}; however, because the levels of flagellin proteins are impacted, Mg^{2+} and/or c-di-GMP may affect translation or protein stability. Intriguingly, multicopy expression in *C. crescentus* of constitutively active versions of the *P. aeruginosa* DGC WspR inhibited motility but apparently not flagellation (3). The difference between this behavior and the one we describe in the present report indicates that the level at which large amounts of c-di-GMP impact motility may not be universal.

On the basis of the data presented here, we have constructed a model for known and predicted components of the *mif* pathway (Fig. 9). We propose that, in the absence of Mg^{2+}, MifA and MifB use GTP to produce c-di-GMP, which inhibits flagellation, potentially through inhibiting translation, enhancing degradation of flagellar proteins, or inhibiting assembly. In the presence of Mg^{2+}, flagellation may occur if MifA and MifB become inactivated and thus fail to produce c-di-GMP or, alternatively, if c-di-GMP degradation is increased. A periplasmic binding protein (e.g., MifC) may modulate the activities of these proteins.

It remains a formal possibility that Mg^{2+} and Mif form parallel pathways that each impact flagellation, such that the cation does not influence the activity of the Mif proteins. For example, Mg^{2+} may enhance flagellin synthesis through another mechanism, while Mif could potentially control degradation regardless of Mg^{2+} levels. In this scenario, the influence

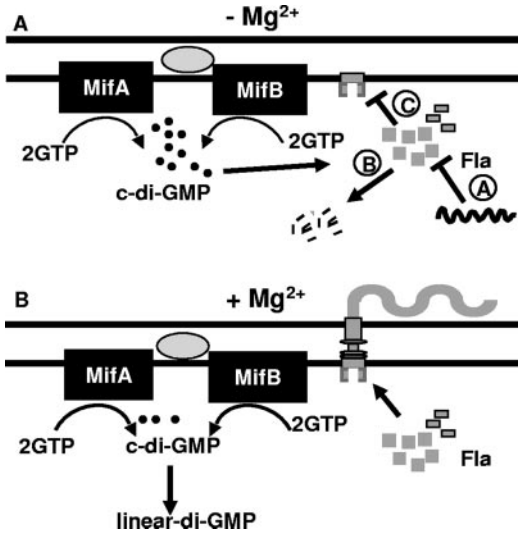

FIG. 9. Model for Mg^{2+}-dependent induction of flagellation. In the absence of Mg^{2+}, MifA and MifB use GTP to produce c-di-GMP, which inhibits flagellation, potentially through (A) inhibiting translation, (B) enhancing degradation of flagellar proteins, or (C) inhibiting assembly. In the presence of Mg^{2+}, flagellation may occur if MifA and MifB become inactivated and thus fail to produce c-di-GMP, or, alternatively, if c-di-GMP degradation is increased. A periplasmic binding protein (e.g., MifC [gray oval]), may modulate the activities of these proteins.

of the loss of Mif would be most discernible when little flagellin is being synthesized. Such a possible alternative could be supported by some of the data that we collected. First, mutation of both *mifA* and *mifB* together failed to restore the same level of motility that occurs in the presence of Mg^{2+}. Second, multicopy expression of *mifA* inhibited migration of *V. fischeri*, even in the presence of 200 mM Mg^{2+}. Alternatively, there may be missing components, such as an Mg^{2+}-responsive component. Indeed, the activity of MifB and its responsiveness to Mg^{2+} vary, depending on the presence of MifC. In addition to a Mg^{2+}-responsive component, we predict the involvement of a phosphodiesterase, as such proteins have been shown to play important roles in controlling c-di-GMP levels (8, 15, 57) and flagellar biogenesis (26); the activity of this protein could be impacted by Mg^{2+} levels. Finally, we also predict the existence of a c-di-GMP-binding protein, such as a PilZ domain protein (4), that interferes with translation or protein stability or prevents flagellar assembly. Intriguingly, *V. fischeri* contains genes that encode four PilZ domain proteins, one of which, VF1838, is situated between the flagellar export genes *flhA* and *flhB*. This gene is a prime candidate for playing a role in flagellar assembly. Our screens have yielded 10 additional mutants for which we have not yet determined the location of the Tn (T. O'Shea, A. Wolfe, and K. Visick, unpublished data); the identification of the disrupted genes may allow us to refine our model for the role of Mg^{2+} and Mif in promoting motility.

In summary, this work establishes a novel pathway that impacts Mg^{2+}-sensitive motility through an apparent posttranscriptional mechanism. Several studies have shown that overexpression of c-di-GMP inhibits motility in other organisms.

However, this study is among the first to identify an environmental signal and discrete regulators specifically involved in flagellar control.

ACKNOWLEDGMENTS

This work was supported by the Estate of William G. Potts in support of medical research at the Stritch School of Medicine at Loyola University Chicago and by NIH grant GM59690 awarded to K.L.V. and NIH grant GM066130 awarded to A.J.W.

We thank Cindy DeLoney-Marino for constructing KV1421, Linda McCarter for antiflagellin antibody, and R. D. Perry for pAHMS16.

REFERENCES

1. **Aldridge, P., and U. Jenal.** 1999. Cell cycle-dependent degradation of a flagellar motor component requires a novel-type response regulator. Mol. Microbiol. **32:**379–391.
2. **Aldridge, P., J. E. Karlinsey, and K. T. Hughes.** 2003. The type III secretion chaperone FlgN regulates flagellar assembly via a negative feedback loop containing its chaperone substrates FlgK and FlgL. Mol. Microbiol. **49:**1333–1345.
3. **Aldridge, P., R. Paul, P. Goymer, P. Rainey, and U. Jenal.** 2003. Role of the GGDEF regulator PleD in polar development of *Caulobacter crescentus*. Mol. Microbiol. **47:**1695–1708.
4. **Amikam, D., and M. Y. Galperin.** 2006. PilZ domain is part of the bacterial c-di-GMP binding protein. Bioinformatics **22:**3–6.
5. **Baker, D. A., and J. M. Kelly.** 2004. Structure, function and evolution of microbial adenylyl and guanylyl cyclases. Mol. Microbiol. **52:**1229–1242.
6. **Bao, Y., D. P. Lies, H. Fu, and G. P. Roberts.** 1991. An improved Tn7-based system for the single-copy insertion of cloned genes into chromosomes of Gram-negative bacteria. Gene **109:**167–168.
7. **Beyhan, S., A. D. Tischler, A. Camilli, and F. H. Yildiz.** 2006. Transcriptome and phenotypic responses of *Vibrio cholerae* to increased cyclic di-GMP level. J. Bacteriol. **188:**3600–3613.
8. **Bobrov, A. G., O. Kirillina, and R. D. Perry.** 2005. The phosphodiesterase activity of the HmsP EAL domain is required for negative regulation of biofilm formation in *Yersinia pestis*. FEMS Microbiol. Lett. **247:**123–130.
9. **Bochner, B. R., and B. N. Ames.** 1982. Complete analysis of cellular nucleotides by two-dimensional thin layer chromatography. J. Biol. Chem. **257:**9759–9769.
10. **Bochner, B. R., D. M. Maron, and B. N. Ames.** 1981. Detection of phosphate esters on chromatograms: an improved reagent. Anal. Biochem. **117:**81–83.
11. **Boettcher, K. J., and E. G. Ruby.** 1990. Depressed light emission by symbiotic *Vibrio fischeri* of the sepiolid squid *Euprymna scolopes*. J. Bacteriol. **172:**3701–3706.
12. **Boles, B. R., and L. L. McCarter.** 2002. *Vibrio parahaemolyticus scrABC*, a novel operon affecting swarming and capsular polysaccharide regulation. J. Bacteriol. **184:**5946–5954.
13. **Calva, E., and R. Oropeza.** 2006. Two-component signal transduction systems, environmental signals, and virulence. Microb. Ecol. **51:**166–176.
14. **Campbell, A.** 1962. Episomes. Adv. Genet. **11:**101–145.
15. **Christen, M., B. Christen, M. Folcher, A. Schauerte, and U. Jenal.** 2005. Identification and characterization of a cyclic di-GMP-specific phosphodiesterase and its allosteric control by GTP. J. Biol. Chem. **280:**30829–30837.
16. **Davis, R. W., D. Botstein, and J. R. Roth.** 1980. Advanced bacterial genetics. Cold Spring Harbor Laboratory, Cold Spring Harbor, N.Y.
17. **DeLoney-Marino, C. R., A. J. Wolfe, and K. L. Visick.** 2003. Chemoattraction of *Vibrio fischeri* to serine, nucleosides and *N*-acetylneuraminic acid, a component of squid light-organ mucus. Appl. Environ. Microbiol. **69:**7527–7530.
18. **Dunn, A. K., M. O. Martin, and E. Stabb.** 2005. Characterization of pES213, a small mobilizable plasmid from *Vibrio fischeri*. Plasmid **54:**114–134.
19. **Galperin, M. Y.** 2004. Bacterial signal transduction network in a genomic perspective. Environ. Microbiol. **6:**552–567.
20. **Garcia, B., C. Latasa, C. Solano, F. Garcia-del Portillo, C. Gamazo, and I. Lasa.** 2004. Role of the GGDEF protein family in *Salmonella* cellulose biosynthesis and biofilm formation. Mol. Microbiol. **54:**264–277.
21. **Graf, J., P. V. Dunlap, and E. G. Ruby.** 1994. Effect of transposon-induced motility mutations on colonization of the host light organ by *Vibrio fischeri*. J. Bacteriol. **176:**6986–6991.
22. **Hammar, M., Z. Bian, and S. Normark.** 1996. Nucleator-dependent intercellular assembly of adhesive curli organelles in *Escherichia coli*. Proc. Natl. Acad. Sci. USA **93:**6562–6566.
23. **Hecht, G. B., and A. Newton.** 1995. Identification of a novel response regulator required for the swarmer-to-stalked-cell transition in *Caulobacter crescentus*. J. Bacteriol. **177:**6223–6229.
24. **Herrero, M., V. de Lorenzo, and K. N. Timmis.** 1990. Transposon vectors containing non-antibiotic resistance selection markers for cloning and stable chromosomal insertion of foreign genes in gram-negative bacteria. J. Bacteriol. **172:**6557–6567.
25. **Huang, B., C. B. Whitchurch, and J. S. Mattick.** 2003. FimX, a multidomain protein connecting environmental signals to twitching motility in *Pseudomonas aeruginosa*. J. Bacteriol. **185:**7068–7076.
26. **Huitema, E., S. Pritchard, D. Matteson, S. K. Radhakrishnan, and P. H. Viollier.** 2006. Bacterial birth scar proteins mark future flagellum assembly site. Cell **124:**1025–1037.
27. **Jenal, U.** 2004. Cyclic di-guanosine-monophosphate comes of age: a novel secondary messenger involved in modulating cell surface structures in bacteria? Curr. Opin. Microbiol. **7:**185–191.
28. **Kirillina, O., J. D. Fetherston, A. G. Bobrov, J. Abney, and R. D. Perry.** 2004. HmsP, a putative phosphodiesterase, and HmsT, a putative diguanylate cyclase, control Hms-dependent biofilm formation in *Yersinia pestis*. Mol. Microbiol. **54:**75–88.
29. **Kumari, S., C. M. Beatty, D. F. Browning, S. J. W. Busby, E. J. Simel, G. Hovel-Miner, and A. J. Wolfe.** 2000. Regulation of acetyl coenzyme A synthetase in *Escherichia coli*. J. Bacteriol. **182:**4173–4179.
30. **Lory, S., M. Wolfgang, V. Lee, and R. Smith.** 2004. The multi-talented bacterial adenylate cyclases. Int. J. Med. Microbiol. **293:**479–482.
31. **Macnab, R. M.** 1996. Flagella and motility, p. 123–145. *In* F. C. Neidhardt, R. Curtiss III, J. L. Ingraham, E. C. C. Lin, K. B. Low, B. Magasanik, W. S. Reznikoff, M. Riley, M. Schaechter, and H. E. Umbarger (ed.), *Escherichia coli* and *Salmonella*: cellular and molecular biology, 2nd ed., vol. 1. ASM Press, Washington, D.C.
32. **McCann, J., E. V. Stabb, D. S. Millikan, and E. G. Ruby.** 2003. Population dynamics of *Vibrio fischeri* during infection of *Euprymna scolopes*. Appl. Environ. Microbiol. **69:**5928–5934.
33. **McCarter, L. L.** 1995. Genetic and molecular characterization of the polar flagellum of *Vibrio parahaemolyticus*. J. Bacteriol. **177:**1595–1609.
34. **Mendez-Ortiz, M. M., M. Hyodo, Y. Hayakawa, and J. Membrillo-Hernandez.** 2006. Genome wide transcriptional profile of *Escherichia coli* in response to high levels of the second messenger c-di-GMP. J. Biol. Chem. **281:**8090–8099.
35. **Millikan, D. S., and E. G. Ruby.** 2004. *Vibrio fischeri* flagellin A is essential for normal motility and for symbiotic competence during initial squid light organ colonization. J. Bacteriol. **186:**4315–4325.
36. **Neidhardt, F. C., P. L. Bloch, and D. F. Smith.** 1974. Culture medium for enterobacteria. J. Bacteriol. **119:**736–747.
37. **Nyholm, S. V., and M. J. McFall-Ngai.** 2004. The winnowing: establishing the squid-*Vibrio* symbiosis. Nat. Rev. Microbiol. **2:**632–642.
38. **O'Shea, T. M., C. R. DeLoney-Marino, S. Shibata, S.-I. Aizawa, A. J. Wolfe, and K. L. Visick.** 2005. Magnesium promotes flagellation of *Vibrio fischeri*. J. Bacteriol. **187:**2058–2065.
39. **Paul, R., S. Weiser, N. C. Amiot, C. Chan, T. Schirmer, B. Giese, and U. Jenal.** 2004. Cell cycle-dependent dynamic localization of a bacterial response regulator with a novel di-guanylate cyclase output domain. Genes Dev. **18:**715–727.
40. **Pei, J., and N. V. Grishin.** 2001. GGDEF domain is homologous to adenylyl cyclase. Proteins **42:**210–216.
41. **Perry, R. D., A. G. Bobrov, O. Kirillina, H. A. Jones, L. Pedersen, J. Abney, and J. D. Fetherston.** 2004. Temperature regulation of the hemin storage (Hms^+) phenotype of *Yersinia pestis* is posttranscriptional. J. Bacteriol. **186:**1638–1647.
42. **Prüβ, B. M., D.-J. Kim, S. Forst, R. T. Fleming, K. L. Visick, and A. J. Wolfe.** 2005. Genomics of flagella, p. 1–12. *In* B. M. Prüβ (ed.), Global regulatory networks in enteric bacteria. Research Signpost, Kerala, India.
43. **Rashid, M. H., C. Rajanna, A. Ali, and D. K. Karaolis.** 2003. Identification of genes involved in the switch between the smooth and rugose phenotypes of *Vibrio cholerae*. FEMS Microbiol. Lett. **227:**113–119.
44. **Romling, U.** 2005. Characterization of the rdar morphotype, a multicellular behaviour in Enterobacteriaceae. Cell Mol. Life Sci. **62:**1234–1246.
45. **Romling, U., M. Gomelsky, and M. Y. Galperin.** 2005. C-di-GMP: the dawning of a novel bacterial signaling system. Mol. Microbiol. **57:**629–639.
46. **Ross, P., R. Mayer, and M. Benziman.** 1991. Cellulose biosynthesis and function in bacteria. Microbiol. Rev. **55:**35–58.
47. **Ruby, E. G., and K. H. Nealson.** 1977. Pyruvate production and excretion by the luminous marine bacteria. Appl. Environ. Microbiol. **34:**164–169.
48. **Ruby, E. G., M. Urbanowski, J. Campbell, A. Dunn, M. Faini, R. Gunsalus, P. Lostroh, C. Lupp, J. McCann, D. Millikan, A. Schaefer, E. Stabb, A. Stevens, K. Visick, C. Whistler, and E. P. Greenberg.** 2005. Complete genome sequence of *Vibrio fischeri*: a symbiotic bacterium with pathogenic congeners. Proc. Natl. Acad. Sci. USA **102:**3004–3009.
49. **Ryan, R. P., Y. Fouhy, J. F. Lucey, L. C. Crossman, S. Spiro, Y. W. He, L. H. Zhang, S. Heeb, M. Camara, P. Williams, and J. M. Dow.** 2006. Cell-cell signaling in *Xanthomonas campestris* involves an HD-GYP domain protein that functions in cyclic di-GMP turnover. Proc. Natl. Acad. Sci. USA **103:**6712–6717.

49a. **Ryjenkov, D. A., R. Simm, U. Romling, and M. Gomelsky.** 2006. The PilZ domain is a receptor for the second messenger c-di-GMP: the PilZ domain protein YcgR controls motility in enterobacteria. J. Biol. Chem. **281:**30310–30314.

50. **Ryjenkov, D. A., M. Tarutina, O. V. Moskvin, and M. Gomelsky.** 2005. Cyclic

diguanylate is a ubiquitous signaling molecule in bacteria: insights into biochemistry of the GGDEF protein domain. J. Bacteriol. **187:**1792–1798.
51. **Sambrook, J., E. F. Fritsch, and T. Maniatis.** 1989. Molecular cloning: a laboratory manual, 2nd ed. Cold Spring Harbor Laboratory, Cold Spring Harbor, N.Y.
52. **Schmidt, A. J., D. A. Ryjenkov, and M. Gomelsky.** 2005. The ubiquitous protein domain EAL is a cyclic diguanylate-specific phosphodiesterase: enzymatically active and inactive EAL domains. J. Bacteriol. **187:**4774–4781.
53. **Simm, R., M. Morr, A. Kader, M. Nimtz, and U. Romling.** 2004. GGDEF and EAL domains inversely regulate cyclic di-GMP levels and transition from sessility to motility. Mol. Microbiol. **53:**1123–1134.
54. **Stabb, E. V., K. A. Reich, and E. G. Ruby.** 2001. *Vibrio fischeri* genes *hvnA* and *hvnB* encode secreted NAD^+-glycohydrolases. J. Bacteriol. **183:**309–317.
55. **Stabb, E. V., and E. G. Ruby.** 2002. RP4-based plasmids for conjugation between *Escherichia coli* and members of the *Vibrionaceae*. Methods Enzymol. **358:**413–426.
56. **Tal, R., H. C. Wong, R. Calhoon, D. Gelfand, A. L. Fear, G. Volman, R. Mayer, P. Ross, D. Amikam, H. Weinhouse, A. Cohen, S. Sapir, P. Ohana, and M. Benziman.** 1998. Three *cdg* operons control cellular turnover of cyclic di-GMP in *Acetobacter xylinum*: genetic organization and occurrence of conserved domains in isoenzymes. J. Bacteriol. **180:**4416–4425.
57. **Tamayo, R., A. D. Tischler, and A. Camilli.** 2005. The EAL domain protein VieA is a cyclic diguanylate phosphodiesterase. J. Biol. Chem. **280:**33324–33330.
58. **Tapparel, C., A. Monod, and W. L. Kelley.** 2006. The DNA-binding domain of the *Escherichia coli* CpxR two-component response regulator is constitutively active and cannot be fully attenuated by fused adjacent heterologous regulatory domains. Microbiology **152:**431–441.
59. **Tischler, A. D., and A. Camilli.** 2004. Cyclic diguanylate (c-di-GMP) regulates *Vibrio cholerae* biofilm formation. Mol. Microbiol. **53:**857–869.
60. **Visick, K. L., and L. M. Skoufos.** 2001. Two-component sensor required for normal symbiotic colonization of *Euprymna scolopes* by *Vibrio fischeri*. J. Bacteriol. **183:**835–842.
61. **Wolfe, A. J., and H. C. Berg.** 1989. Migration of bacteria in semisolid agar. Proc. Natl. Acad. Sci. USA **86:**6973–6977.
62. **Woodcock, D. M., P. J. Crowther, J. Doherty, S. Jefferson, E. DeCruz, M. Noyer-Weidner, S. S. Smither, M. Z. Michael, and M. W. Graham.** 1989. Quantitative evaluation of *Escherichia coli* host strains for tolerance to cystosine methylation in plasmid and phage recombinants. Nucleic Acids Res. **17:**3469–3478.
63. **Yanisch-Perron, C., J. Vieira, and J. Messing.** 1985. Improved M13 phage cloning vectors and host strains: nucleotide sequences of the M13mp18 and pUC19 cloning vectors. Gene **33:**103–119.

O'Shea, T. M., A. H. Klein, K. Geszvain, A. J. Wolfe, and K. L. Visick. 2006. Diguanylate cyclases control magnesium-dependent motility of *Vibrio fischeri*. J. Bacteriol.

Supplemental Table 1. Additional plasmids used in this study.

Plasmid	**Description**	**Source or reference**
pBS	Cloning vector, Ap^R	Stratagene, LaJolla CA
pESY20	pEVS122 with EcoRI site disrupted; Erm^R	This study
pEVS104	*tra*$^+$, Kan^R	(4)
pEVS107	mini-Tn*7*; mob, Erm^R Kan^R	(3)
pEVS122	low copy *oriR6K* suicide vector, Erm^R	(2)
pEVS79	High copy cloning vector, Cm^R	(4)
pKV217	pESY20 EcoRI + *mifA* (EcoRI) fragment from pTMO88	This study
pKV220	pCR2.1 TOPO + *mifB* and flanking DNA, PCR amplified with primers Upfus959F and VFA0957Rev; Kan^R Ap^R	This study
pKV228	pEVS79 XbaI + 4.9 kb SpeI/XbaI fragment from pKV220; Cm^R	This study
pKV231	pKV228 deleted for NdeI (Δ*mifB*); Cm^R	This study
pTMO73	Self-ligation of chromosomal DNA from Tn*10lacZ* mutant KV1897 following SphI digestion; Cm^R	This study
pTMO78	Self-ligation of chromosomal DNA from Tn*10lacZ* mutant KV1902 following SphI digestion; Cm^R	This study
pTMO85	Self-ligation of chromosomal DNA from Tn*10lacZ* mutant KV1903 following NheI digestion; Cm^R	This study

pTMO88	pCR2.1 TOPO + 312 bp fragment of *mifA* amplified with primers 989F and 989R; Kan^R Ap^R	This study
pTMO92	pCR2.1 TOPO + 2163 bp PCR fragment of *mifA* amplified with primers Up989Fwd and Down989Rev; Kan^R Ap^R	This study
pTMO93	pBS SacI + SacI fragment of pTMO85; Ap^R	This study
pTMO107	pCR2.1 TOPO + 306 bp (*mifB*) PCR fragment generated with primers VFA0959Fwd and VFA0959Rev; Kan^R Ap^R	This study
pTMO116	pCR2.1 + 321 bp (*mifC*) PCR fragment generated with primers 960F and 960R; Kan^R Ap^R	This study
pTMO123	pESY20 EcoRI + *mifC* (EcoRI) fragment from pTMO116	This study
pTMO125	pESY20 EcoRI + *mifB* (EcoRI) fragment from pTMO107	This study
pUX-BF13	Tn*7* transposase; Ap^R	(1)

References

1. **Bao, Y., D. P. Lies, H. Fu, and G. P. Roberts.** 1991. An improved Tn*7*-based system for the single-copy insertion of cloned genes into chromosomes of Gram-negative bacteria. Gene **109:**167-168.
2. **Dunn, A. K., M. O. Martin, and E. Stabb.** 2005. Characterization of pES213, a small mobilizable plasmid from *Vibrio fischeri*. Plasmid **54:**114-134.
3. **McCann, J., E. V. Stabb, D. S. Millikan, and E. G. Ruby.** 2003. Population dynamics of *Vibrio fischeri* during infection of *Euprymna scolopes*. Appl Environ Microbiol. **69:**5928-5934.
4. **Stabb, E. V., and E. G. Ruby.** 2002. RP4-based plasmids for conjugation between *Escherichia coli* and members of the Vibrionaceae. Methods Enzymol **358:**413-26.

Supplemental Table 2. Primers used in this study.

Name	Sequence
VFA0957Rev	TAACGACAAGTACGCTAAAACCAG
VFA0959Fwd	GCAAGAGATAGTGGTGGAGTTCG
VFA0959Rev	TGGCTCTGAGTAAAACAGTGTCTTAG
VFA0960Fwd	CCTTCTGATTTTCTTGGGTTGC
VFA0960Rev	GATCAAGCGGTATCTCTGGATG
989F	ACTTGAATCTCTATGGGCACTAACTG
989R	CAAATACCCTTTTCGCTCATCAG
Down 959Rev	CTAAGATAAAGTGCCATCACGTTG
Down 989Rev	GCCTGTACCAAGTGAACGCC
Upfus959F	TGACAAATTGGCATCGGTAATG
Up989Fwd	AGTTCGGATACATAATTGGCGTC
flaA rev 1	GATTGACCGTTGATGTATGTTGC
flaA fwd 2	AATCCTAATCAAGTTACCGTCAGTTC
flaB fwd	CGTTCAACTTACTTTAGGTAGTATGCG
flaB rev	GCACCACCAATGGCTAACTCAG
flaC fwd	CCTCTTTCGGTGGTTCTCGTC
flaC rev	GCTCAATATCATCACCAGACTTAGC
flaD fwd	GAAGTGGTTGCTTTGAATGACG
flaD rev	TCTGTATTTTCAGCACCCACTTTC
flaE fwd	CTTTCGGTGGCACACGTCTAC
flaE rev	CGATAGCTTGCTCTTCACCATTC
flaF fwd	ACTGATGCTGATCGTGCTGC
flaF rev	CCAGTTAATGTCACGACCTTCTTC
S16-F	ATGGTTACCATTCGTTTGGC
S16-R	CGCTTTTTTAGCGTCTTTAAC

Roles of Bacterial Regulators in the Symbiosis between *Vibrio fischeri* and *Euprymna scolopes*

Kati Geszvain, Karen L. Visick

1 Introduction

In a symbiosis, two or more evolutionarily distinct organisms communicate with one another in order to co-exist and co-adapt in their shared environment. The mutualistic symbiosis between the bioluminescent marine bacterium *Vibrio fischeri* and the Hawaiian squid *Euprymna scolopes* provides a model system that allows scientists to examine the mechanisms by which this communication occurs (McFall-Ngai and Ruby 1991). The squid, although *V. fischeri*-free (aposymbiotic) at hatching, rapidly acquires this bacterium and promotes its growth in a special symbiotic organ called the light organ (LO). In exchange for nutrients and a niche safe from competing bacteria, *V. fischeri* provides the bioluminescence used by *E. scolopes* to camouflage itself from predators.

In this chapter, we will give an overview of the early events in establishing the symbiosis and describe associated developmental changes triggered in each organism by the interaction. We will then discuss bacterial regulators and, where known, the traits they control that are necessary for a productive interaction between *V. fischeri* and *E. scolopes*. Finally, we will conclude by highlighting important directions for future investigation.

2 Early Events in the *Euprymna scolopes – Vibrio fischeri* Symbiosis

2.1 *Vibrio fischeri* strains are specifically recruited from the seawater

V. fischeri comprises less than 0.1% of the total bacterial population in the seawater inhabited by the squid (Lee and Ruby 1992), yet this organism alone

K. Geszvain, K. Visick (e-mail: kvisick@lumc.edu)
Dept. Microbiology and Immunology, Loyola University Chicago, 2160 S. First Ave. Bldg. 105, Maywood, IL 60153, USA

Progress in Molecular and Subcellular Biology
Jörg Overmann (Ed.)
Molecular Basis of Symbiosis

is found in the light organ association (Boettcher and Ruby 1990). Furthermore, inoculation in the laboratory with bacteria closely related to *V. fischeri*, including *V. harveyi* and *V. parahaemolyticus*, fails to result in colonization (McFall-Ngai and Ruby 1991; Nyholm et al. 2000). In addition to this species-specific selection, strain-specific enrichment also occurs. Both visibly luminescent and non-visibly luminescent strains of *V. fischeri* co-exist in the seawater, but only the latter strains colonize the squid LO in nature (Lee and Ruby 1994b). This strict limitation on the species and strains of bacteria capable of colonizing the LO suggests that a specific exchange of signals must occur between the squid and the bacteria early during colonization.

Within hours of hatching, *E. scolopes* recruits *V. fischeri* from the surrounding seawater. The presence of bacteria or the bacterial cell wall component peptidoglycan in the seawater causes the squid to secrete mucus (Nyholm et al. 2002), allowing *V. fischeri* cells to aggregate near pores leading into the LO (Fig. 1). Other bacteria such as *V. parahaemolyticus* also exhibit the ability to aggregate in squid mucus, suggesting that *E. scolopes* does not distinguish between *V. fischeri* and other Gram negative bacteria at this stage (Nyholm et al. 2000). However, when both *V. parahaemolyticus* and *V. fischeri* are present, the latter organism becomes the dominant species in the aggregate (Nyholm and McFall-Ngai 2003), indicating that *V. fischeri* may participate in establishing specificity at this stage.

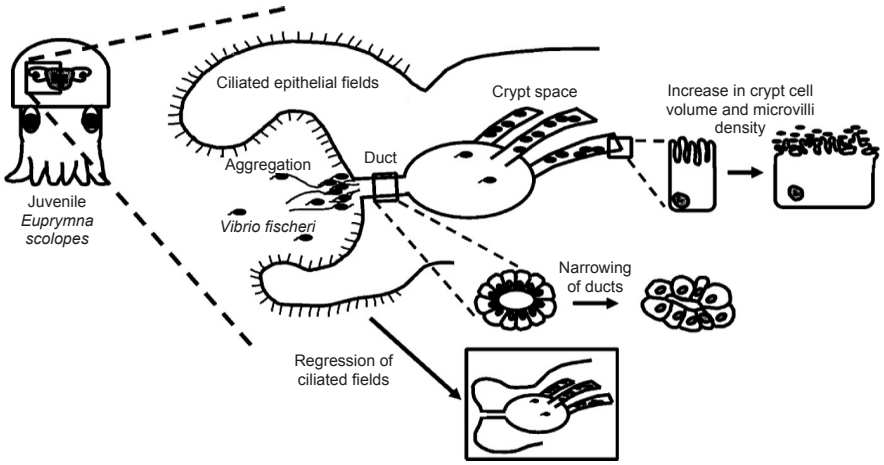

Fig. 1. Cartoon depicting the structure of and developmental changes in the juvenile squid LO during colonization. The position of the LO in a juvenile squid is shown on the *left*, while an enlarged cross section is shown on the *right*. The juvenile LO contains three pores on each side (six total), only one of which is depicted at the opening of the duct. *Arrows* indicate developmental events that occur within the first 4 days after exposure to *V. fischeri*. *Dashed lines* indicate an enlargement of the boxed area. *V. fischeri* cells are shown as *black ovals* aggregated in the mucus (depicted as *wavy lines*) outside the pore and in the crypt spaces (without flagella). This depiction of the light organ is based on Visick and McFall-Ngai (2000) and references described therein.

2.2 *Vibrio fischeri* cells navigate physical and chemical barriers to colonize *Euprymna scolopes*

From the aggregates, the *V. fischeri* cells migrate through LO pores, reaching ducts that ultimately lead into crypts, the sites of colonization (Fig. 1). In the ducts, the bacteria must move through mucus against an outward current generated by ciliated cells lining the passageway (McFall-Ngai and Ruby 1998). As a further barrier to colonization, the ducts contain high levels of nitric oxide, an anti-microbial agent that may function as a layer of defense against invasion by non-specific bacteria (Davidson et al. 2004). In the crypts, *V. fischeri* cells may encounter macrophage-like cells, a potential immune surveillance system (Nyholm and McFall-Ngai 1998). In addition, the bacteria may be exposed to toxic oxygen radicals such as hypohalous acid, produced by a halide peroxidase enzyme secreted by epithelial cells within the crypts (Weis et al. 1996; Small and McFall-Ngai 1999). Despite this plethora of potential host defenses, *V. fischeri* cells can enter the LO and grow to high cell density, approximately 10^{11} cells/cm^3 (Visick and McFall-Ngai 2000). Thus, *V. fischeri* must possess mechanisms by which it can evade host defenses and thrive in the LO environment.

Growth to high cell density does not represent the endpoint of the symbiosis. Rather, the symbiosis is dynamic. Each morning the squid expels between 90 and 95% of the bacterial population from its LO (Lee and Ruby 1994a). During the day, the *V. fischeri* cells retained in the squid divide to repopulate the LO. Therefore, persistent colonization actually consists of cycles of expulsion and re-growth, requiring the symbiotic bacteria to adapt to changing environments within the LO.

2.3 Both Organisms Undergo Developmental Changes in Response to the Symbiosis

The interaction between *E. scolopes* and *V. fischeri* induces a number of developmental and morphological changes in each organism (Fig. 1). Ciliated epithelial cells, present on a field that projects outward from the LO, likely function to facilitate recruitment of *V. fischeri* by drawing the bacteria-laden seawater into the mucus matrix near the LO pores. Once the symbiont has successfully migrated into the LO, apoptosis and subsequently regression of these ciliated fields results in their loss over the course of four days (Montgomery and McFall-Ngai 1994; Foster and McFall-Ngai 1998). The consequence, presumably, is a reduction in any further recruitment of additional symbiotic bacteria.

A bacterial signal that triggers some of the developmental changes in the epithelial fields is the bacterial cell wall component lipopolysaccharide (LPS). Purified LPS is sufficient to induce apoptosis in the fields (Foster et al. 2000). Most likely, the highly conserved lipid A portion of LPS is responsible, as LPS purified from many species of Gram negative bacteria can induce apoptosis. Possibly, an LPS detection pathway similar to the Toll-like receptor pathway found in many organisms (Gerard 1998) recognizes bacterial LPS and triggers apoptosis.

The LPS signal, however, is not sufficient to trigger regression of the epithelial fields; this suggests that more than one signal is required for this developmental change (Foster et al. 2000). *V. fischeri* strains that do not enter the LO fail to induce regression, suggesting signaling occurs between the bacteria and squid cells in the LO (Doino and McFall-Ngai 1995). Although regression requires a bacterial signal, the program continues regardless of the presence of bacteria: removing *V. fischeri* with antibiotic treatment after 12 h does not stop or reverse regression (Doino and McFall-Ngai 1995).

Another developmental event in the squid may also function to reduce LO accessibility. Within 12 h after symbiotic colonization, a two- to three-fold increase in actin levels occurs within the apical surface of epithelial cells lining the LO ducts (Kimbell and McFall-Ngai 2004). This increase in actin is correlated with a narrowing of the ducts, which decrease in size two-fold (Fig. 1). The narrowing of the ducts, along with the loss of the ciliated fields on the LO surface, likely limits entry into the LO. However, the LO remains at least somewhat open to the environment, as marked bacteria introduced into the seawater can subsequently be isolated from the adult LO (Lee and Ruby 1994b). Because *V. fischeri* remains the only bacterial resident, mechanisms must remain in place to prevent other species from infecting the LO.

Changes also occur in crypt epithelial cells immediately adjacent to the colonizing *V. fischeri* bacteria. Within 72 h of symbiotic colonization, these cells increase in volume as they develop from columnar to cuboidal cells (Fig. 1) (Montgomery and McFall-Ngai 1994). Concurrently, the microvilli on their surfaces increase in density and complexity (Lamarcq and McFall-Ngai 1998). These alterations likely increase the surface area available for interactions with the symbiotic bacteria. These structural changes require the persistent presence of bacteria (Doino 1998; Lamarcq and McFall-Ngai 1998), suggesting that a continual signal exchange occurs between the squid and bacteria throughout the symbiosis.

V. fischeri cells also undergo developmental changes upon colonization of the LO. Planktonic *V. fischeri* are flagellated and motile, traits that are essential for the bacteria to enter the LO (Graf et al. 1994; Millikan and Ruby 2003). Within 24 h of colonization, however, most of the bacteria lose their flagella and become non-motile. The cells re-grow flagella and regain motility shortly after expulsion from the LO (Ruby and Asato 1993). The bacteria also decrease in size in the LO and, after attaining high cell density, induce light

production (Ruby and Asato 1993) to a level 100-fold higher than in culture (Boettcher and Ruby 1990; Stabb et al. 2004). This luminescence is essential for persistent infection (Visick et al. 2000). Thus, in addition to signaling *E. scolopes* to induce developmental changes during the onset of symbiosis, *V. fischeri* also recognizes signals within the LO environment and adapts accordingly.

3 Regulatory Systems Employed by *Vibrio fischeri* to Promote the Symbiosis

3.1 Two-Component Signal Transduction Systems

Many bacteria, including *V. fischeri*, recognize and respond to their environments using two-component regulatory systems (Fig. 2A, reviewed in Stock et al. 2000). These systems are composed of a sensor histidine kinase

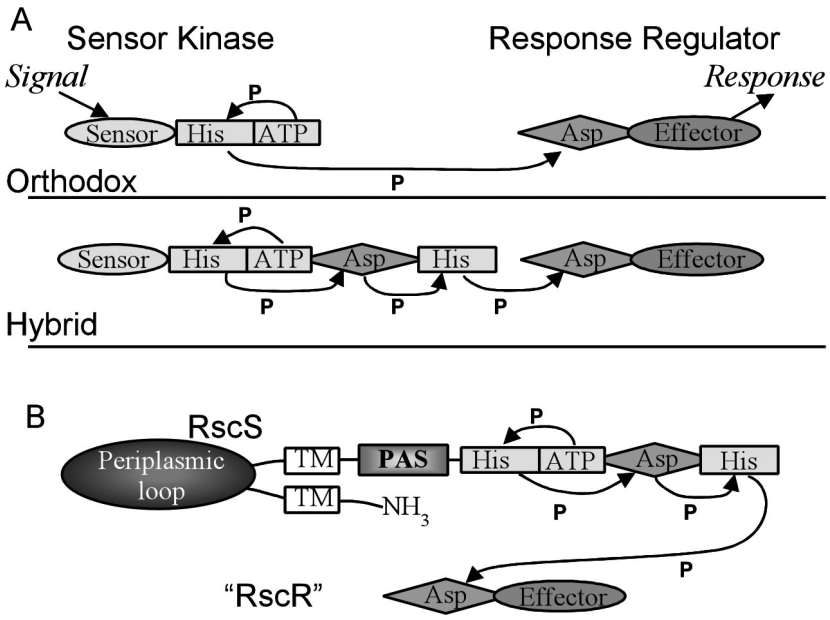

Fig. 2. Two-component regulatory systems. A. The phospho-relay in orthodox (*top*) and hybrid (*bottom*) two-component systems. Upon detection of signal, phosphate generated from a bound ATP is passed from conserved His to Asp residues until finally being transferred to an Asp in the response regulator, resulting in a response, either altered transcription or protein function. B. RscS is a hybrid sensor kinase. The sensor domain of RscS is composed of two transmembrane helices (*TM*), a large periplasmic loop and a PAS domain

protein that recognizes and transmits an environmental signal (through autophosphorylation on a His residue) to a second protein, the response regulator, which (when phosphorylated on a conserved Asp residue) carries out a response. Most frequently, the response consists of a change in gene expression; alternatively, changes in protein activity can result.

Given the changes in environmental conditions that *V. fischeri* cells experience as they travel from seawater into the LO, it is not surprising that colonization by *V. fischeri* requires two-component regulators. At least two such regulators are required for efficient initiation of symbiotic colonization: the sensor kinase RscS (Visick and Skoufos 2001) and the response regulator, GacA (Whistler and Ruby 2003). A transcriptional regulator, FlrA, which exhibits limited similarity to response regulators and is required for initiation (Millikan and Ruby 2003) will also be discussed here.

rscS. Mutations in *rscS* severely reduce the ability of *V. fischeri* to initiate symbiotic colonization: most animals remain uncolonized following exposure to *rscS* mutants, although other animals become colonized after a delay of several hours (Visick and Skoufos 2001). These results suggest that mutants are blocked at an early stage of colonization, but that they can occasionally by-pass this block and ultimately achieve what appears to be normal colonization. In culture, *rscS* mutants do not exhibit defects in growth, motility, or the timing and level of bioluminescence induction, traits known to be important for colonization (Visick and Skoufos 2001). Thus, to date no clues to *rscS* function have been garnered by phenotypes observed in culture.

The sequence of *rscS* suggests that it encodes a hybrid sensor kinase similar to ArcB and BvgS (Fig. 2B) (Visick and Skoufos 2001). These proteins contain, in addition to the conserved His residue that serves as the site of autophosphorylation, two additional domains with conserved residues (Asp and His) predicted to be sequentially phosphorylated and that may serve as sites of additional regulation (Fig. 2B). Upon receipt of a colonization signal, RscS is predicted to autophosphorylate and transfer the phosphate to an as-yet-unidentified response regulator, termed RscR, which may regulate genes or activities essential for symbiosis.

What serves as the colonization signal, and how is it detected by RscS? Clearly, many possibilities exist, and include in addition to bacterially produced molecules and seawater signals, components of the LO mucus, cell surface signals and nutrients. Determining the portion of RscS responsible for detecting the colonization signal will advance our understanding of symbiotic signal exchange. In many cases, the amino terminal periplasmic portion of sensor kinase proteins receives the environmental signal (Stock et al. 2000). For example, *Salmonella* PhoQ detects Mg^{2+} in the environment through its periplasmic domain; binding of Mg^{2+} to this domain results in a conformational

change and inactivation of the response regulator PhoP (Vescovi et al. 1997). RscS is predicted to possess a periplasmic domain of ~200 residues (Visick and Skoufos 2001); the large size of this region suggests it may play a role in RscS function, possibly signal detection.

In addition to a potential periplasmic signaling domain, RscS contains a second input domain, known as PAS. In other proteins, PAS detects signals such as small ligands, or changes in light levels, oxygen concentration or redox potential (Taylor and Zhulin 1999). Whether the PAS domain contributes to signal detection by RscS during colonization remains unknown. However, the transition from seawater to the nutrient-rich LO could plausibly affect the energy status of the *V. fischeri* cells thereby altering their redox potential or oxygen concentration, which could be sensed by the PAS domain. Thus, investigations of the PAS and periplasmic domains of RscS will be fruitful for exploring bacteria-host interactions. Perhaps each domain detects a distinct condition, allowing RscS to integrate multiple signals from the squid environment to regulate the initiation of colonization.

What is the identity of the cognate response regulator, RscR, and what genes or proteins are controlled by the RscS/R regulatory system? In many cases, the genes for sensor kinases and their cognate response regulators are linked on the chromosome, and in some cases, genes controlled by the regulators are also nearby. This is not the case for *rscS* and the gene encoding its response regulator. The advent of the *V. fischeri* genome sequencing project (http://ergo. integratedgenomics.com/Genomes/VFI), has made it possible to use bioinformatics to look for RscR. Using the sequences of known regulators, we have searched and identified about 40 response regulators (Hussa and Visick, unpubl. data). At least 14 appear unlinked to sensor kinase genes, and thus represent the best candidates for RscR. Current work is aimed at mutagenizing these candidates and asking whether any mutants exhibit *rscS*-like colonization defects. If *rscR* encodes a DNA binding protein, then newly available DNA microarrays will be used to explore the regulon controlled by RscS/R. Identification of the targets of RscS/R regulation may also suggest a role for this regulon in symbiosis initiation. Once a target(s) of these regulators is identified, experiments aimed at identifying the colonization signal can be formulated.

gacA. In a number of pathogenic bacteria, the two-component system GacS/A regulates expression of virulence and host association traits, such as production of exoenzymes in *Pseudomonas* spp. (Heeb and Haas 2001) and motility in *Salmonella* (Goodier and Ahmer 2001). *V. fischeri* GacA also plays a role in host association. Mutants defective for *gacA* exhibit severe defects in initiating colonization: only about 10% of animals become colonized and those animals that become colonized exhibit a nearly 100-fold reduction in the level of colonization (i.e., the number of bacteria residing in the LO) (Whistler and Ruby 2003). The role of GacA is likely to be quite complex. In culture, it is associated with a number of phenotypes known to be important for

symbiosis, including motility, nutrient acquisition, siderophore activity and luminescence (Whistler and Ruby 2003). The global control of disparate traits, all of which contribute to host-association, highlights the importance of such regulators in the evolution of symbiotic associations. As with RscS/R, neither the signal nor the gene/protein targets for GacA/S are known. Identification of targets of GacA regulation, possibly through DNA microarray experiments, will help elucidate the role of this regulator in symbiosis and potentially reveal previously unknown traits important for host-microbe interaction.

flrA. FlrA, a transcription regulator with limited sequence similarity to response regulators, functions as a master regulator of flagellar biosynthesis (Millikan and Ruby 2003). Given the absolute requirement for motility in symbiotic initiation, the requirement for FlrA seems straightforward as mutations lead to a lack of flagella. However, complemented *flrA* mutants showed restored motility but not normal colonization: initiation was delayed and the level of colonization at 48 h post-inoculation was reduced by 10-fold.

One explanation for the above result is that the timing and level of flagellar biosynthesis are critical for optimal initiation and colonization and these characteristics were not properly restored in the complemented strains. In support of this hypothesis, hyper-motile (hyper-flagellated) *V. fischeri* mutants also exhibit severe delays in initiating colonization and defects in the level of colonization 24 h post-inoculation (Millikan and Ruby 2002). Alternatively, an equally plausible explanation is that FlrA controls genes other than those involved in flagellar biosynthesis (Millikan and Ruby 2003) that are also required for colonization.

Several non-flagellar genes appear to be regulated by FlrA (Millikan and Ruby 2003). One gene that appears to be repressed by FlrA, *hvnC*, encodes a protein related to HvnA and HvnB, two secreted NAD^+ glycohydrolases found in *V. fischeri*. However, neither *hvnA* nor *hvnB* appears necessary for colonization (Stabb et al. 2001); therefore, the relevance of FlrA-mediated regulation of *hvnC* is unclear. A second putative FlrA-repressed gene is homologous to *V. cholerae kefB*. In *E.coli*, KefB is a potassium efflux protein that is important for protecting cells from toxic metabolites during growth on a poor carbon source (Ferguson et al. 2000). Possibly, the *V. fischeri* KefB homolog provides protection from a LO-specific toxin.

Are FlrA-repressed genes relevant to symbiotic colonization? FlrA-controlled flagella, which are required for initiation, become dispensable to colonized bacteria. Thus, a switch in flagella gene transcription may be coordinated with induction or repression of non-flagellar genes through FlrA. The regulation of FlrA itself may be at the level of transcription, analogous to cAMP-CRP mediated control of the master flagellar regulators *flhDC* in *E. coli* (Soutourina et al. 1999). In addition, the limited similarity of FlrA to response regulators suggests its activity could be regulated via phosphorylation by a sensor kinase. Future work will likely focus on

determining whether FlrA itself is transcriptionally controlled, whether over-expression of FlrA during colonization affects the level or timing of transcription of putative FlrA-controlled genes and whether such genes themselves promote (or interfere with) colonization.

3.2 Quorum-Sensing Regulatory Systems

First described in *V. fischeri*, quorum sensing is used by many bacteria to detect the presence of other bacteria in their surroundings (reviewed in Taga and Bassler 2003). This method of monitoring the environment involves the production of a small molecule known as an autoinducer (AI) by an autoinducer synthase. Secreted into the environment, AIs can be recognized in recipient cells either by a specific two-component sensor kinase, or more frequently in Gram-negative bacteria, by a DNA-binding protein in the LuxR family. In either case, the AI signal results in transcriptional control of target genes.

V. fischeri uses both the LuxR DNA binding protein and specific sensor kinases to detect at least three AI signals (Fig. 3). Both pathways contribute to the control of bioluminescence, a trait required for symbiosis. A mutant

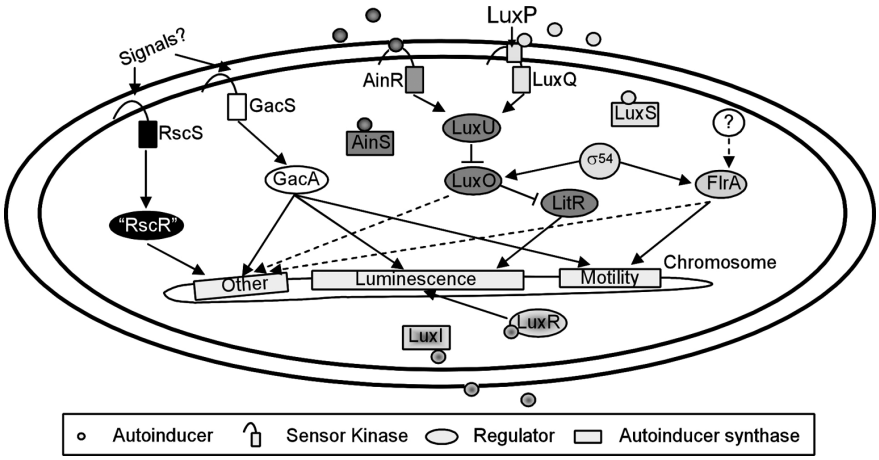

Fig. 3. Regulatory circuits required for symbiosis. *Dotted lines* represent hypothesized regulatory events. Activities required for symbiosis –"luminescence," "motility," and "other" – are represented as genes on the *V. fischeri* chromosome. Regulation of these activities may be through activation of transcription, as is the case for FlrA, through activation of transcription of a repressor, as is predicted to be the case for LuxO, or through modulating the activity of the protein product. The *V. fischeri* proteins AinS, AinR, and LitR are homologous to *V. harveyi* proteins LuxM, LuxN and LuxR, respectively

defective for *luxA*, one of two genes that encode bacterial luciferase, exhibits a three- to four-fold reduction in colonization level within 48 h post-inoculation (Visick et al. 2000). Encoded upstream of *luxA* are LuxR and LuxI, an AI synthase that produces the AI detected by LuxR. Mutations in either *luxR* or *luxI* result in a colonization defect similar to that of the *luxA* mutant, suggesting that these regulators are required for symbiosis due to their role in transcriptional control of the *lux* operon.

A second AI synthase, AinS, produces a distinct AI that also is required for symbiosis. The pathway through which the AinS-synthesized AI is detected and transmitted is predicted based on studies in the related bacterium, *V. harveyi* (reviewed in Taga and Bassler 2003). In *V. harveyi*, AIs signal through two hybrid sensor kinases, LuxN and LuxQ, using a phosphotransferase protein, LuxU, to ultimately affect the activity of a response regulator, LuxO. In the absence of AIs, LuxO negatively regulates *lux* genes by indirectly controlling transcription of a transcriptional activator (LitR in *V. fischeri* [Fidopiastis et al. 2002]). In *V. fischeri*, the AinS-produced AI likely is recognized by AinR, a sensor kinase with significant homology to *V. harveyi* LuxN (Gilson et al. 1995; Lupp et al. 2003) (Fig. 3).

A mutant defective for *ainS* exhibits a colonization level indistinguishable from that of *luxA*, *luxI* and *luxR* mutants (Lupp et al. 2003). However, whereas the *luxA*, *luxI*, and *luxR* mutants produce no symbiotic bioluminescence (at least 1000-fold decreased [Visick et al. 2000]), the *ainS* mutant produces approximately 10–20% of the wild-type bioluminescence. Thus, it seems probable that the role of *ainS* in colonization may be independent of its role in bioluminescence regulation. These phenotypes are difficult to separate, however: mutations in *luxO*, the response regulator through which the AI signals are transmitted, restore to wild-type levels both the slightly decreased symbiotic bioluminescence and the colonization defect of the *ainS* mutant (Lupp et al. 2003). Thus, an important direction will be to determine whether this pathway controls genes, other than *lux*, necessary for colonization.

V. fischeri encodes a third AI synthase, LuxS (Lupp and Ruby 2004). In *V. harveyi*, LuxS produces an AI that is detected by sensor kinase LuxQ through its interaction with the periplasmic protein LuxP (Taga and Bassler 2003). Because *V. fischeri* contains homologs for all of these genes (Lupp and Ruby 2004), it seems likely that this AI system functions similarly in the symbiotic organism (Fig. 3). A strain of *V. fischeri* in which *luxS* is mutated colonizes the LO as well as the wild-type strain; however the *luxS* mutation appreciably decreases the colonization efficiency of an *ainS* mutant, but not its per cell luminescence (Lupp and Ruby 2004). These data provide further support for a role of the AinS system in symbiosis distinct from that of luminescence. Further investigation of the three quorum sensing pathways likely will provide insight both into genes necessary for symbiotic colonization and, because the signals are known, signal transduction during symbiotic colonization.

4
Future Directions

The initiation of the symbiosis between *E. scolopes* and *V. fischeri* involves several regulatory systems, many of which affect traits known to be involved in colonization (Fig. 3). Many important questions remain. First, what is the relation of these regulatory circuits to one another? Both FlrA and the luminescence regulator LuxO modulate transcription by σ^{54}-containing RNA polymerase (Lilley and Bassler 2000; Millikan and Ruby 2003). Not surprisingly, a σ^{54} mutant is defective for colonization, motility and luminescence (Wolfe et al. 2004). Links between luminescence and motility also are found with the GacA mutant (Whistler and Ruby 2003) as well as with one class of hyper-motile mutants (Millikan and Ruby 2002), supporting coordinate regulation of motility and luminescence. Therefore, global regulation of the colonization response by *V. fischeri* may involve regulation of σ^{54} activity. Epistasis experiments could help to determine how these systems integrate to regulate colonization.

Second, what other traits, aside from luminescence and motility, are required for initiation of symbiosis? RscS is required for initiation, yet has no effect on motility or luminescence. GacA and FlrA both appear to regulate other functions as well. The major outer membrane protein OmpU is required for initiation of colonization (Aeckersberg et al. 2001) as is a recently identified gene cluster (Yip et al. 2005). These genes are possible targets of the systems described here. Identification of additional targets will be greatly aided by the *V. fischeri* genome sequence and available microarrays.

Finally, what signals are detected by the bacteria to regulate symbiosis? Aside from AIs produced by the quorum sensing systems, the signals received by the bacteria remain unknown. Predictions of the signals can be made based on our current knowledge of the environmental conditions in the LO. Furthermore, the recent sequencing of an *E. scolopes* expressed sequence tag library (http://trace.ensembl.org/) will facilitate identification of squid genes important for colonization and thus provide clues as to the conditions/signals the bacteria encounter in the LO. The answers to these questions will advance our understanding of the communication between and adaptation by *V. fischeri* and its host *E. scolopes*.

Acknowledgements. The authors would like to thank Drs. Joerg Graf, Margaret McFall-Ngai, Deborah Millikan, Eric Stabb and Cheryl Whistler and members of the Visick lab for their helpful comments in the preparation of this manuscript. We also thank Emily Yip for her drawing of juvenile light organ development shown in Fig. 1.

References

Aeckersberg F, Lupp C, Feliciano B, Ruby EG (2001). *Vibrio fischeri* outer membrane protein OmpU plays a role in normal symbiotic colonization. J Bacteriol 183:6590–6597

Boettcher KJ, Ruby EG (1990). Depressed light emission by symbiotic *Vibrio fischeri* of the sepiolid squid *Euprymna scolopes*. J Bacteriol 172:3701–3706

Davidson SK, Koropatnick TA, Kossmehl R, Sycuro L, McFall-Ngai MJ (2004) NO means 'yes' in the squid-vibrio symbiosis: nitric oxide (NO) during the initial stages of a beneficial association. Cell Microbiol 6(12):1139–1151

Doino JA (1998) The role of light organ symbionts in signaling early morphological and biochemical events in the sepiolid squid *Euprymna scolopes*, University of Southern California, Los Angeles

Doino JA, McFall-Ngai MJ (1995) A transient exposure to symbiosis-competent bacteria induces light organ morphogenesis in the host squid. Biol Bull 189:347–355

Ferguson GP, Battista JR, Lee AT, Booth IR (2000) Protection of the DNA during the exposure of *Escherichia coli* cells to a toxic metabolite: the role of the KefB and KefC potassium channels. Mol Microbiol 35:113–122

Fidopiastis PM, Miyamoto CM, Jobling MG, Meighen EA, Ruby EG (2002) LitR, a new transcriptional activator in *Vibrio fischeri*, regulates luminescence and symbiotic light organ colonization. Mol Microbiol 45:131–143

Foster JS, McFall-Ngai MJ (1998) Induction of apoptosis by cooperative bacteria in the morphogenesis of host epithelial tissues. Dev Genes Evol 208:295–303

Foster JS, Apicella MA, McFall-Ngai MJ (2000) *Vibrio fischeri* lipopolysaccharide induces developmental apoptosis, but not complete morphogenesis, of the *Euprymna scolopes* symbiotic light organ. Dev Biol 226:242–254

Gerard C (1998) Bacterial infection. For whom the bell tolls. Nature 395:217, 219

Gilson L, Kuo A, Dunlap PV (1995) AinS and a new family of autoinducer synthesis proteins. J Bacteriol 177:6946–6951

Goodier RI, Ahmer BM (2001) SirA orthologs affect both motility and virulence. J Bacteriol 183:2249–2258

Graf J, Dunlap PV, Ruby EG (1994) Effect of transposon-induced motility mutations on colonization of the host light organ by *Vibrio fischeri*. J Bacteriol 176:6986–6991

Heeb S, Haas D (2001) Regulatory roles of the GacS/GacA two-component system in plant-associated and other gram-negative bacteria. Mol Plant Microbe Interact 14:1351–1363

Kimbell JR, McFall-Ngai MJ (2004) Symbiont-induced changes in host actin during the onset of a beneficial animal-bacterial association. Appl Environ Microbiol 70:1434–1441

Lamarcq LH, McFall-Ngai MJ (1998) Induction of a gradual, reversible morphogenesis of its host's epithelial brush border by *Vibrio fischeri*. Infect Immun 66:777–785

Lee K, Ruby E (1992) Detection of the light organ symbiont, *Vibrio fischeri*, in Hawaiian seawater by using *lux* gene probes. Appl Environ Microbiol 58:942–947

Lee K, Ruby E (1994a) Effect of the squid host on the abundance and distribution of symbiotic *Vibrio fischeri* in nature. Appl Environ Microbiol 60:1565–1571

Lee KH, Ruby EG (1994b) Competition between *Vibrio fischeri* strains during initiation and maintenance of a light organ symbiosis. J Bacteriol 176:1985–1991

Lilley BN, Bassler BL (2000) Regulation of quorum sensing in *Vibrio harveyi* by LuxO and σ^{54}. Mol Microbiol 36:940–954

Lupp C, Ruby EG (2004) Vibrio fischeri LuxS and AinS: comparative study of two signal synthases. J Bacteriol 186:3873–3881

Lupp C, Urbanowski M, Greenberg EP, Ruby EG (2003) The *Vibrio fischeri* quorum-sensing systems *ain* and *lux* sequentially induce luminescence gene expression and are important for persistence in the squid host. Mol Microbiol 50:319–331

McFall-Ngai MJ, Ruby EG (1991) Symbiont recognition and subsequent morphogenesis as early events in an animal-bacterial mutualism. Science 254:1491–1494

McFall-Ngai M, Ruby EG (1998) Sepiolids and Vibrios: when first they meet. Reciprocal interactions between host and symbiont lead to the creation of a complex light-emitting organ. BioScience 48:257–265

Millikan DS, Ruby EG (2002) Alterations in *Vibrio fischeri* motility correlate with a delay in symbiosis initiation and are associated with additional symbiotic colonization defects. Appl Environ Microbiol 68:2519–2528

Millikan DS, Ruby EG (2003) FlrA, a σ^{54}-dependent transcriptional activator in *Vibrio fischeri*, is required for motility and symbiotic light-organ colonization. J Bacteriol *185*, 3547–3557

Montgomery MK, McFall-Ngai M (1994) Bacterial symbionts induce host organ morphogenesis during early postembryonic development of the squid *Euprymna scolopes*. Development 120:1719–1729

Nyholm SV, McFall-Ngai MJ (1998) Sampling the light-organ microenvironment of *Euprymna scolopes*: description of a population of host cells in association with the bacterial symbiont *Vibrio fischeri*. Biol Bull 195:89–97

Nyholm SV, McFall-Ngai MJ (2003) Dominance of *Vibrio fischeri* in secreted mucus outside the light organ of *Euprymna scolopes*: the first site of symbiont specificity. Appl Environ Microbiol 69:3932–3937

Nyholm SV, Stabb EV, Ruby EG, McFall-Ngai MJ (2000) Establishment of an animal-bacterial association: recruiting symbiotic *vibrios* from the environment. Proc Natl Acad Sci USA 97:10231–10235

Nyholm SV, Deplancke B, Gaskins HR, Apicella MA, McFall-Ngai MJ (2002) Roles of *Vibrio fischeri* and nonsymbiotic bacteria in the dynamics of mucus secretion during symbiont colonization of the *Euprymna scolopes* light organ. Appl Environ Microbiol 68:5113–5122

Ruby EG, Asato LM (1993) Growth and flagellation of *Vibrio fischeri* during initiation of the sepiolid squid light organ symbiosis. Arch Microbiol 159:160–167

Small AL, McFall-Ngai MJ (1999) Halide peroxidase in tissues that interact with bacteria in the host squid *Euprymna scolopes*. J Cell Biochem 72:445–457

Soutourina O, Kolb A, Krin E, Laurent-Winter C, Rimsky S, Danchin A, Bertin P (1999) Multiple control of flagellum biosynthesis in *Escherichia coli*: role of H-NS protein and the cyclic AMP-catabolite activator protein complex in transcription of the *flhDC* master operon. J Bacteriol 181:7500–7508

Stabb EV, Reich KA, Ruby EG (2001) *Vibrio fischeri* genes *hvnA* and *hvnB* encode secreted NAD(+)-glycohydrolases. J Bacteriol 183:309–317

Stabb EV, Butler MS, Adin DM (2004) Correlation between osmolarity and luminescence of symbiotic *Vibrio fischeri* strain ES114. J Bacteriol 186:2906–2908

Stock AM, Robinson VL, Goudreau PN (2000) Two-component signal transduction. Annu Rev Biochem 69:183–215

Taga ME, Bassler BL (2003) Chemical communication among bacteria. Proc Natl Acad Sci USA 100 [Suppl 2]:14549–14554

Taylor BL, Zhulin IB (1999) PAS domains: internal sensors of oxygen, redox potential, and light. Microbiol Mol Biol Rev 63:479–506

Vescovi EG, Ayala YM, di Cera E, Groisman EA (1997) Characterization of the bacterial sensor protein PhoQ. Evidence for distinct binding sites for Mg^{2+} and Ca^{2+}. J Biol Chem 272:1440–1443

Visick KL, McFall-Ngai MJ (2000) An exclusive contract: specificity in the *Vibrio fischeri-Euprymna scolopes* partnership. J Bacteriol 182:1779–1787

Visick KL, Skoufos LM (2001) Two-component sensor required for normal symbiotic colonization of *Euprymna scolopes* by *Vibrio fischeri*. J Bacteriol 183:835–842

Visick KL, Foster J, Doino J, McFall-Ngai M, Ruby EG (2000) *Vibrio fischeri lux* genes play an important role in colonization and development of the host light organ. J Bacteriol 182:4578–4586

Weis VM, Small AL, McFall-Ngai MJ (1996) A peroxidase related to the mammalian antimicrobial protein myeloperoxidase in the *Euprymna-Vibrio* mutualism. Proc Natl Acad Sci USA 93:13683–13688

Whistler CA, Ruby EG (2003) GacA regulates symbiotic colonization traits of *Vibrio fischeri* and facilitates a beneficial association with an animal host. J Bacteriol 185:7202–7212

Wolfe AJ, Millikan DS, Campbell JM, Visick KL (2004) *Vibrio fischeri* σ^{54} controls motility, biofilm formation, luminescence, and colonization. Appl Environ Microbiol 70:2520–2524

Yip ES, Grublesky BT, Hussa EA, Visick KL (2005) A novel, conserved cluster of genes promotes symbiotic colonization and sigma^{54}-dependent biofilm formation by *Vibrio fischeri*. Mol Microbiol. 57:1485–1498

Molecular Microbiology (2006) **62**(6), 1586–1600
doi:10.1111/j.1365-2958.2006.05475.x
First published online 6 November 2006

The symbiosis regulator RscS controls the *syp* gene locus, biofilm formation and symbiotic aggregation by *Vibrio fischeri*

Emily S. Yip,[1] Kati Geszvain,[1]
Cindy R. DeLoney-Marino[2] and Karen L. Visick[1]*
[1]*Department of Microbiology and Immunology, Loyola University Chicago, Maywood, IL, USA.*
[2]*Department of Biology, University of Southern Indiana, Evansville, IN, USA.*

Summary

Successful colonization of a eukaryotic host by a microbe involves complex microbe–microbe and microbe–host interactions. Previously, we identified in *Vibrio fischeri* a putative sensor kinase, RscS, required for initiating symbiotic colonization of its squid host *Euprymna scolopes*. Here, we analysed the role of *rscS* by isolating an allele, *rscS1*, with increased activity. Multicopy *rscS1* activated transcription of genes within the recently identified symbiosis polysaccharide (*syp*) cluster. Wild-type cells carrying *rscS1* induced aggregation phenotypes in culture, including the formation of pellicles and wrinkled colonies, in a *syp*-dependent manner. Colonies formed by *rscS1*-expressing cells produced a matrix not found in control colonies and largely lost in an *rscS1*-expressing *sypN* mutant. Finally, multicopy *rscS1* provided a colonization advantage over control cells and substantially enhanced the ability of wild-type cells to aggregate on the surface of the symbiotic organ of *E. scolopes*; this latter phenotype similarly depended upon an intact *syp* locus. These results suggest that transcription induced by RscS-mediated signal transduction plays a key role in colonization at the aggregation stage by modifying the cell surface and increasing the ability of the cells to adhere to one another and/or to squid-secreted mucus.

Introduction

Communication between bacteria and their plant or animal hosts is an essential component of both beneficial symbioses and pathogenic associations. Perhaps equally important are interactions within the community of bacterial cells as they colonize their host. For example, during *Vibrio cholerae* infection of the mouse intestine, interactions mediated by the TCP pilus allow the bacteria to aggregate into microcolonies, possibly affording protection from antimicrobial agents within the intestine (Kirn *et al*., 2000). Notably, biofilm formation by *V. cholerae* increases its resistance to the toxicity of the bile acids found in the intestine (Hung *et al*., 2006). Similarly, biofilm formation by *Pseudomonas aeruginosa* in the cystic fibrosis lung is thought to contribute to chronic infection by increasing resistance of the bacterial community to antibiotics (Whiteley *et al*., 2001). In addition to pathogenic functions, biofilm formation is implicated in the maintenance of the complex microbial community found within the mammalian gut (Sonnenburg *et al*., 2004); therefore, bacterial cell–cell interactions also appear to be a component of beneficial symbioses.

An elegant model system for studying bacteria–host and inter-bacterial interactions during colonization of a host is the symbiosis between the Hawaiian bobtail squid *Euprymna scolopes* and the marine bioluminescent bacterium *Vibrio fischeri* (reviewed in Nyholm and McFall-Ngai, 2004). The specialized symbiotic organ (the light organ) of *E. scolopes* is exclusively colonized by its bacterial symbiont, *V. fischeri*. Newly hatched squid lack symbionts but rapidly become colonized upon exposure to *V. fischeri* in the seawater. In the squid, symbiotic initiation is facilitated by ciliated cells located on the surface of the light organ that direct the flow of bacteria-containing seawater towards pores that lead into the organ. The squid also promotes colonization by secreting mucus on the surface of the light organ (Nyholm *et al*., 2000). Early in the association, *V. fischeri* cells form a tight, dense aggregate in this mucus (Nyholm *et al*., 2000). The cells then migrate from the aggregate into the pores and through ducts that lead to crypt spaces where finally they multiply to high cell density and luminesce (Nyholm and McFall-Ngai, 2004).

The specificity of the *Vibrio*–squid symbiosis is first manifested at the aggregation stage. Several species of Gram-negative bacteria, including the closely related *Vibrio parahaemolyticus*, can aggregate on the light organ surface (Nyholm *et al*., 2000). However, when both

Accepted 9 October, 2006. *For correspondence. E-mail kvisick@lumc.edu; Tel. (+1) 708 216 0869; Fax (+1) 708 216 9574.

V. fischeri and *V. parahaemolyticus* are present, the symbiotic *V. fischeri* cells dominate in the aggregate (Nyholm and McFall-Ngai, 2003). These data suggest that *V. fischeri* actively promotes aggregation; however, the bacterial factors that contribute to this activity are unknown (Nyholm and McFall-Ngai, 2003).

Studies investigating the genetic requirements for the symbiosis have revealed a number of mutants defective for initiating colonization, some of which have been characterized with respect to aggregation (Nyholm *et al*., 2000). A mutant defective for the flagellar master regulator, FlrA, forms smaller aggregates than those produced by wild-type *V. fischeri* (Millikan and Ruby, 2003). Hypermotile mutants, which are delayed in initiating colonization, also form smaller aggregates, typically after a lag period (Millikan and Ruby, 2002). While appropriate levels of motility appear to be required for optimal aggregation, it is unclear what other bacterial factors promote aggregation in the squid-secreted mucus. Furthermore, characteristics associated with bacterial aggregation in other bacteria – such as biofilm formation, wrinkled colony morphology and clumping of cells (Romling *et al*., 1998; Del Re *et al*., 2000) – have not been reported to date for *V. fischeri* cells grown in culture. This lack of culture phenotypes has hampered genetic investigation of the basis for aggregation within the squid mucus.

In bacteria, two-component regulatory systems detect environmental signals and respond by autophosphorylation of a sensor kinase and subsequent transfer of the phosphate to a response regulator. Signalling through these systems, in many cases, regulates transcription of a target gene(s) (reviewed in Stock *et al*., 2000). Previously, we reported that a mutant defective for the putative sensor kinase RscS exhibited a severe defect in colonization (Visick and Skoufos, 2001). However, known symbiosis traits, including motility and bioluminescence, were unaltered under laboratory conditions. Subsequently, we reported the identification of the symbiosis polysaccharide (*syp*) gene locus (Yip *et al*., 2005) involved in symbiotic initiation. Mutation of *syp* genes causes over a 1000-fold decrease in symbiotic colonization. The 18 genes (*sypA-R*) in this cluster encode proteins with predicted roles as glycosyltransferases and other polysaccharide metabolism and export functions. In addition, four genes encode putative regulatory proteins such as response regulators. Consistent with a possible role of *syp* in glycosylation of a surface molecule(s), we found that multicopy expression of a *syp*-encoded putative response regulator, SypG, caused a substantial increase in biofilm formation by cells grown in both static and shaking liquid cultures.

Here, we demonstrate that one role of RscS is regulation of the *syp* gene cluster. Multicopy expression of an allele of *rscS* with increased activity induced *syp* transcription and dramatic *syp*-dependent cell–cell aggregation phenotypes, including the formation of wrinkled colonies on solid media and pellicles in static liquid culture. We then show the relevance of these phenotypes to symbiosis by identifying a role for *rscS* in promoting aggregation of *V. fischeri* cells in squid-secreted mucus on the light organ surface. Our results reveal central roles for RscS and *syp* in cell–cell aggregation by this bacterium, both in culture and during symbiotic initiation, and provide a basis for understanding one of the earliest known stages of symbiotic colonization of squid by *V. fischeri*.

Results

RscS controls the syp *gene cluster*

Our preliminary data showed that the putative sensor kinase, RscS, could autophosphorylate, suggesting it did indeed function as a sensor kinase (E.S. Yip and K.L. Visick, unpublished). However, this gene was not linked to a response regulator, and our attempts to identify *rscS*-controlled genes through global screens with a wild-type copy of *rscS* on the multicopy plasmid pLMS33 (Visick and Skoufos, 2001) were unsuccessful. We therefore hypothesized that RscS might exhibit only a low basal level of activity under laboratory culture conditions and that isolation of an *rscS* allele with increased activity could make it possible to detect *rscS*-dependent phenotypes and gene regulation. We further speculated that one potential target of RscS could be the *syp* cluster, which we recently identified as essential for symbiotic colonization (Yip *et al*., 2005). Like disruption of *rscS*, *syp* mutations caused severe initiation defects but no discernible alterations in traits required for symbiosis. Furthermore, the *syp* genes were not detectably transcribed under laboratory conditions unless a *syp*-encoded regulator, SypG, was expressed from a multicopy plasmid (Yip *et al*., 2005). Therefore, we asked whether we could identify an allele of *rscS* capable of inducing *syp* transcription.

To isolate mutations in *rscS*, we passaged pLMS33 through an *E. coli* mutator strain and we introduced the resulting library of randomly mutagenized plasmids into reporter strains. To monitor the induction of *syp* transcription, we employed strains containing a promoterless *lacZ* gene carried on Tn*10* inserted in either *sypD* or *sypN* (KV1635 and KV1601 respectively; Table 1) which are located within two different putative operons of the *syp* cluster (Yip *et al*., 2005). We then screened for blue colonies, and found them at a frequency of about 1 in 1000. We confirmed that the plasmid was responsible for the elevated *syp* transcription for six such plasmids, and following subcloning experiments (see *Experimental procedures*), we identified two alleles, *rscS1* and *rscS2*, for

Table 1. Strains and plasmids.

Strains	Genotype or characteristics	Reference
E. coli		
CC118λ*pir*	Δ(*are-leu*) *araD* Δ*lacX74 galE galK phoA20 thi-1 rpsE rpoB argE* (Am) *recA1* λ*pir*	Herrero *et al*. (1990)
CC130	F-, *ara*D139, Δ(*ara-leu*)7697 Δ*lac*-74 *gal*U *gal*K *rps*L Δ (*pho*A-*pro*C) *pho*R *tsx*::Tn*5 mut*D5	Manoil and Beckwith (1985)
DH5α	*endA1 hsdR17* (r_K^- m_K^+) *glnV44 thi-1 recA1 gyrA* (Nal^r) *relA* Δ(*lacIZYA-argF*) *U169 deoR* [ϕ80d*lac*Δ(*lacZ*)M15]	Woodcock *et al*. (1989)
TOP10F′	F′ [*lacI*^{q} Tn10 (Tet^R)] *mcr*A Δ(*mrr-hsd*RMS-*mcr*BC) ϕ80*lac*Z ΔM15 Δ*lacX*74 *rec*A1 *ara*D139 Δ(*ara-leu*)7697 *gal*U *gal*K *rps*L (Str^R) *en*dA1 *nup*G	Invitrogen
V. fischeri		
ES114	Wild type	Boettcher and Ruby (1990)
ESR1	Rif^R	Graf *et al*. (1994)
KV905	pKV69/ESR1	Visick and Skoufos (2001)
KV1066	pKV111/ES114	This study
KV1223	pKV111/Rif^R*rscS*::*erm*	This study
KV1228	pKV111/Rif^R	This study
KV1339	pKV111/ES114 *rscS*::*erm*	This study
KV1421	ES114 att Tn*7*::*erm*	O'Shea *et al*., 2006)
KV1601	Rif^R*sypN*::Tn*10lacZ*	Yip *et al*. (2005)
KV1635	Rif^R*sypD*::Tn*10lacZ*	Yip *et al*. (2005)
KV1838	ES114 *sypN*::pTMB54	Yip *et al*. (2005)
KV1844	pKV69/ES114	Visick and Skoufos (2001)
KV1845	pLMS33/ES114	This study
KV1956	pKG11/ES114	This study
KV1958	pKV69/KV1601	Yip *et al*. (2005)
KV1959	pLMS33/KV1601	This study
KV1960	pKG11/KV1601	This study
KV1962	pKV69/KV1635	Yip *et al*. (2005)
KV1963	pLMS33/KV1635	This study
KV1964	pKG11/KV1635	This study
KV1980	pKG11/ESR1	This study
KV1992	pKG11/KV1838	This study
KV2273	pKG13/KV1601	This study
KV2274	pKG13/KV1635	This study
KV2435	pKV69/KV1421	This study
KV2437	pKG11/KV1421	This study
KV2608	pVSV208/ES114	This study
KV2613	pKG11/KV2608	This study
KV2617	pKV69/KV2608	This study
KV2682	pESY37/ES114	This study
KV2683	pESY37/KV1838	This study
KV2685	pKV69/KV2682	This study
KV2686	pKV69/KV2683	This study
KV2688	pKG11/KV2682	This study
KV2689	pKG11/KV2683	This study
KV2888	pESY48/KV1838	This study
KV2976	pKV69/KV2888	This study
KV2977	pKG11/KV2888	This study

Plasmids	Characteristics or construction	Reference
pCR2.1-TOPO	Commercial cloning vector; Amp^R, Kan^R	Invitrogen
pESY36	pCR2.1-TOPO + 4.6 kb fragment of *sypMNO*; Amp^R, Kan^R	This study
pESY37	pVSV105 (KpnI) + 1.3 bp BamHI/XmnI fragment from pKV111 containing *gfp*; Cm^R	This study
pESY47	pEVS107 (KpnI) + 4.6 kb KpnI fragment from pESY36 encoding *sypMNO*; Kan^R, Em^R	This study
pESY48	pESY47 (EcoRV) + 1.2 kb fragment encoding Cm^R; Kan^R, Cm^R	This study
pEVS107	Mini-Tn*7* delivery plasmid; mob; Kan^R, Em^R	McCann *et al*. (2003)
pKG11	pKV69 (SalI) + 3 kb SalI fragment from mutagenized pLMS33 containing *rscS1* allele; Cm^R, Tet^R	This study
pKG13	pKV69 (SalI) + 3 kb SalI fragment from mutagenized pLMS33 containing *rscS2* allele; Cm^R, Tet^R	This study
pKV69	Mobilizable vector; Cm^R, Tet^R	Visick and Skoufos (2001)
pKV111	Mobilizable vector containing *gfp*; Cm^R	Stabb and Ruby (2002)
pLMS33	pKV69 containing wild-type *rscS*; Cm^R, Tet^R	Visick and Skoufos (2001)
pVSV105	Mobilizable vector; Cm^R	Dunn *et al*. (2006)
pVSV208	Mobilizable vector containing *rfp*; Cm^R	Dunn *et al*. (2006)

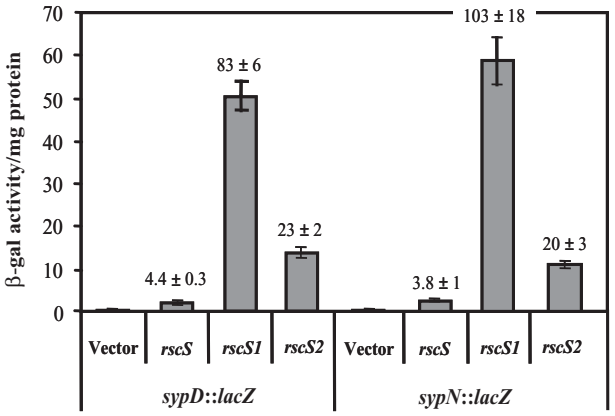

Fig. 1. Transcription of *syp* genes by *rscS*. After 24 h growth at 22°C in HMM, β-galactosidase activity levels were determined for *syp*::*lacZ* reporter strains carrying vector (pKV69), *rscS* (pLMS33), *rscS1* (pKG11) or *rscS2* (pKG13) (see *Experimental procedures*). Error bars represent the standard deviation of three replicate cultures. Numbers above the bars indicate the fold induction relative to the β-galactosidase activity produced by the vector control strain.

which the mutation mapped within the subcloned *rscS* portion of the plasmid (carried by pKG11 and pKG13 respectively). The effect of these two alleles on *syp* transcription was quantified by β-galactosidase assays. The presence of multicopy *rscS1* or *rscS2* increased the amount of β-galactosidase activity generated from the *sypN*::*lacZ* fusion strain by 103 ± 18-fold and 20 ± 3-fold, respectively, relative to the vector control (Fig. 1). Similar levels of induction were seen for the *sypD*::*lacZ* fusion strain (Fig. 1).

Sequence analysis of *rscS1* and *rscS2* revealed mutations within or near the putative *rscS* ribosome binding site, while *rscS1* contained a second, silent mutation at codon Leu25 (see *Experimental procedures*). Because the *rscS1* allele exerted the greatest effect on *syp* transcription, we used the plasmid (pKG11) carrying this allele in all of our subsequent investigations. Semi-quantitative RT-PCR revealed no difference in the amount of *rscS* transcripts produced by pKG11 relative to pLMS33 (data not shown); therefore, the mutations present in *rscS1* do not appear to affect transcription of the gene and thus we hypothesize that they affect translation. We verified that *syp* induction and the resulting *syp*-dependent phenotypes induced by multicopy *rscS1* in culture (described below) did indeed depend upon the *rscS* gene carried by pKG11 (data not shown). Furthermore, because the *rscS1* allele encodes wild-type protein, we anticipate that any observed effect on *syp* transcription is likely to represent a normal activity of RscS. Indeed, when we introduced multicopy wild-type *rscS* into the *syp* reporter strains, we observed a small but reproducible increase in β-galactosidase activity (approximately fourfold) relative to vector control (Fig. 1). Semi-quantitative RT-PCR experiments verified *rscS1*-induced expression of *sypD* and *sypN* in a wild-type background and demonstrated *rscS1*-dependent induction of at least two other genes within the cluster (*sypB* and *sypE*; K. Geszvain and K.L. Visick, unpubl. data). Therefore, *rscS1*-mediated induction of the *syp* cluster is neither an artefact of the particular mutations present within *rscS1* nor a consequence of the Tn*10lacZ* insertion present in the reporter strains.

From these data, we conclude that the sensor kinase RscS regulates expression of the *syp* cluster. Furthermore, these experiments have generated mutagenized alleles of *rscS* that can be employed to increase RscS expression, allowing us to investigate the role of the regulator in culture and during symbiosis.

RscS induces novel aggregation phenotypes in culture

Given the large increase in *syp* transcription induced by *rscS1* relative to wild-type *rscS*, we anticipated that phenotypic effects of RscS activity would be more readily observed in strains carrying *rscS1*. Indeed, we found that *rscS1* induced a novel phenotype following prolonged incubation on complex solid medium. Normally, *V. fischeri* colonies are round, smooth and wet-appearing, as are colonies carrying the vector (Fig. 2Ai). Colonies containing *rscS1*, however, appeared dry, flat and wrinkled (Fig. 2Aiii). These wrinkled colonies formed a film that could be peeled off the plate in a continuous sheet (data not shown). This phenotype depended upon *rscS1*-mediated induction of the *syp* cluster. When a representative *syp* gene, *sypN*, which encodes one of six putative *syp* glycosyltransferases (Yip *et al*., 2005), was disrupted, *rscS1* failed to induce wrinkling (Fig. 2Aiv). Wrinkling of the *sypN* mutant was restored upon complementation with the *sypMNO* operon (data not shown), further demonstrating the dependence on *syp* of this phenotype. Finally, wrinkling could be weakly induced by pLMS33 (Fig. 2Aii), indicating that this phenotype reflects the natural activity of RscS.

Wrinkled colony morphology is frequently associated with increased cell aggregation phenotypes (Branda *et al*., 2005); therefore, we screened cells for such phenotypes. First, we observed that after prolonged static growth in liquid Hepes minimal media (HMM), wild-type cells containing *rscS1* formed a pellicle at the air/liquid interface that exhibited high tensile strength. In fact, the pellicle was sufficiently strong to retain the culture when the tube was completely inverted (Fig. 2Biii). Disruption of *sypN* resulted in the loss of this thick pellicle while complementation with *sypMNO* restored it (data not shown), demonstrating that this phenotype similarly depended upon *syp*. Second, during growth with shaking in HMM, we observed that *rscS1* cultures formed stringy aggregates of cells (Fig. 2Ciii), which were difficult to disrupt

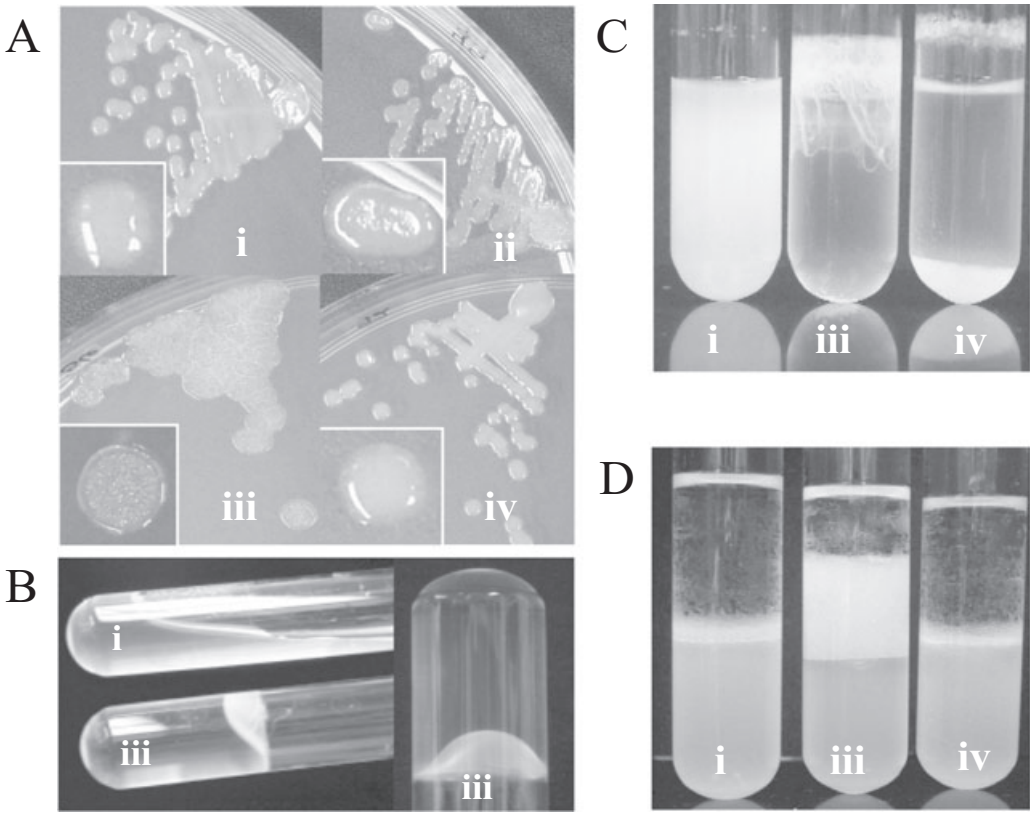

Fig. 2. Culture phenotypes of *V. fischeri* expressing *rscS*. (i) vector (pKV69) in ES114 (KV1844), (ii) *rscS* (pLMS33) in ES114 (KV1845), (iii) *rscS1* (pKG11) in ES114 (KV1956), (iv) *rscS1* (pKG11) in *sypN* (KV1992).
A. Growth phenotypes on solid media. Strains were streaked onto LBS with Tet and incubated at RT for 48 h. Inserts show a close-up view of a representative colony for each strain.
B. Pellicle formation in static cultures. Cultures were grown in HMM at RT for 7 days, then photographed after inverting the tubes 90 (left panel) and 180 degrees (right panel).
C. Growth phenotypes in shaking cultures. Cultures were grown in HMM with shaking at 22°C for 24 h. The experiment was performed in triplicate; representative results are shown.
D. Hydrophobicity of *V. fischeri* cultures. The organic solvent hexadecane was added to cultures that had been grown in HMM at 28°C for 24 h. After vortexing, cells were allowed to partition into the lower, aqueous phase or the upper, hydrophobic phase. The experiment was performed in triplicate; representative results are shown.

even with vigorous vortexing. This phenotype suggested that RscS greatly increases the 'stickiness' of the cell surface, allowing the cells to form aggregates even during agitation. In a *sypN* mutant, *rscS1* did not induce the strings of aggregated cells seen in the wild-type background; however, the cells settled on the bottom of the tube (Fig. 2Civ) rather than remaining suspended as in the vector control (Fig. 2Ci). Together, these data demonstrate that RscS induces *syp*-dependent cell–cell aggregation.

In some organisms, such as Lactobacilli and *Bifidobacterium longum*, autoaggregation and adhesion have been correlated with hydrophobic cell surfaces (Wadstrom *et al*., 1987; Del Re *et al*., 2000). Given the aggregation phenotypes induced by *rscS1*, we hypothesized that *rscS1* might increase hydrophobicity of *V. fischeri* cells. When cultures of wild-type *V. fischeri* carrying vector were vortexed with an equal volume of hexadecane (an organic solvent), the bulk of the cells remained in the aqueous phase (Fig. 2Di; bottom layer). However, for cells carrying *rscS1*, a substantial proportion of the cells partitioned to the organic, hexadecane layer (Fig. 2Diii; top, 'creamy' layer). The shift to the organic phase induced by *rscS1* was largely lost in the *sypN* mutant (Fig. 2Div). These data suggest that RscS-induced expression of the *syp* locus results in an altered, hydrophobic cell surface that might contribute to the above aggregation phenotypes.

RscS promotes the formation of thick biofilm on a glass surface

To further understand the nature of the RscS-mediated aggregation phenotypes, we asked whether multicopy *rscS1* enhanced the ability of *V. fischeri* to form biofilms. We used confocal microscopy to quantify the biomass of biofilms produced by GFP-labelled strains carrying either

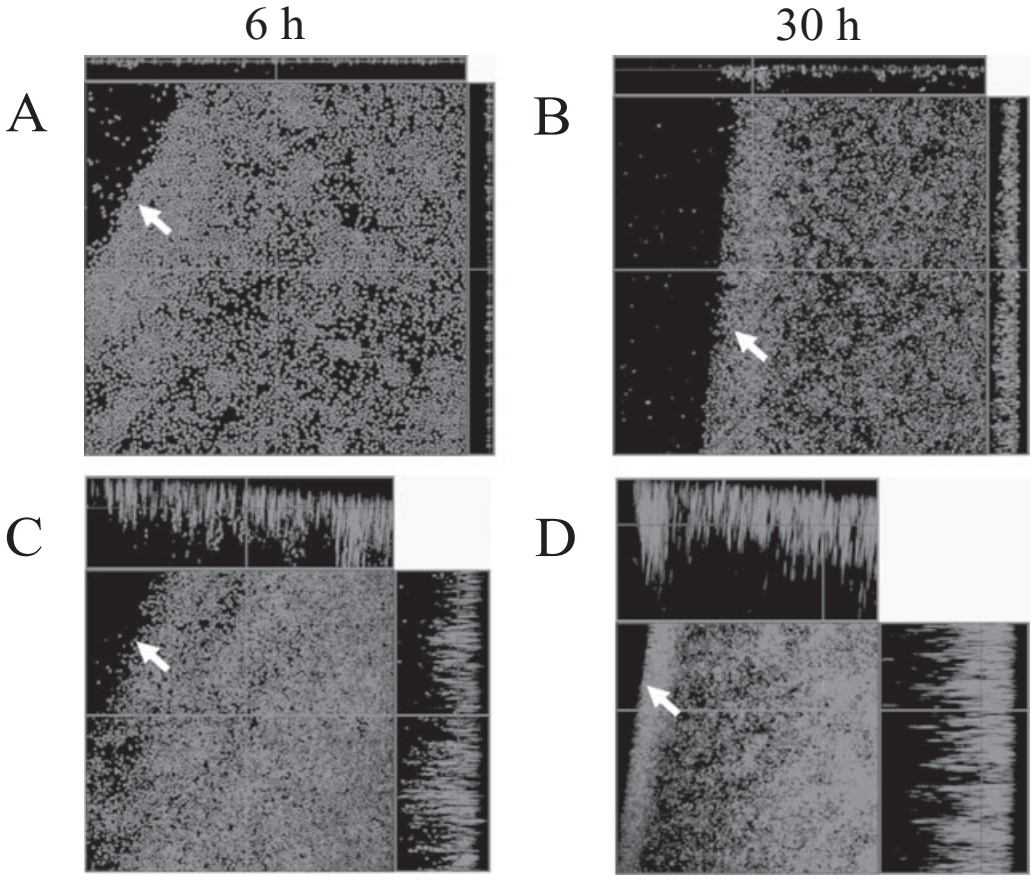

Fig. 3. Confocal microscopy of biofilm formation on a glass surface. Development of *V. fischeri* biofilms formed on glass coverslips was visualized by confocal microscopy. Representative views of the *xy* plane and *z* sections were shown for GFP-labelled (A and B) vector-containing (KV2685) and (C and D) *rscS1*-expressing wild-type *V. fischeri* cells (KV2688) at 6 h and 30 h post inoculation. Arrows indicate the air–liquid interface.

rscS1 or the vector control. These strains were grown statically in HMM medium in microtiter wells. To facilitate microscopy, glass coverslips were submerged vertically into medium immediately following inoculation, then removed either 6 or 30 h later. At 6 h, both vector control and *rscS1*-containing cells showed adherence to the glass surface. Even at this early time point, however, *z* sections showed that the thickness of the adherent cells was substantially greater for *rscS1*-containing cells (~18 μm) relative to the control (~2 μm) (Fig. 3A and C). At 30 h, the difference between the two cell types was even more dramatic (Fig. 3B and D). Whereas the biofilm of vector control cells was approximately 7 μm thick, that of the *rscS1*-containing cells was approximately 45 μm. Furthermore, at this time point, an even thicker region (about 56 μm) could be seen for the *rscS1* cells present at the air–liquid interface, where the pellicle eventually forms. These data suggest that multicopy *rscS1*, while not necessary for *V. fischeri* cells to adhere to a solid surface, substantially promotes the events that lead to the formation of a thick biofilm.

RscS induces a polysaccharide extracellular matrix

In nature, many bacteria reside in biofilms that are composed mainly of polysaccharides (Yildiz and Schoolnik, 1999; Enos-Berlage and McCarter, 2000; Zogaj *et al*., 2001; Solano *et al*., 2002; Friedman and Kolter, 2004a,b; Jackson *et al*., 2004; Matsukawa and Greenberg, 2004). To investigate the nature of *rscS1*-dependent biofilms, we first performed both scanning electron microscopy (SEM) and transmission electron microscopy (TEM) on colonies derived from *rscS1*-containing or vector control cells. SEM images revealed the existence of a smooth, sheet-like matrix produced by *rscS1*-expressing wild-type (Fig. 4B) but not vector control cells (Fig. 4A). Consistent with other culture phenotypes, the dense matrix induced by *rscS1* in the wild type was largely absent in the *sypN* mutant strain (Fig. 4C), indicating that matrix formation required an intact *syp* cluster.

We therefore further characterized the nature of the *rscS1*-dependent matrix by TEM using ruthenium red, which is commonly used to detect acidic polysaccharides

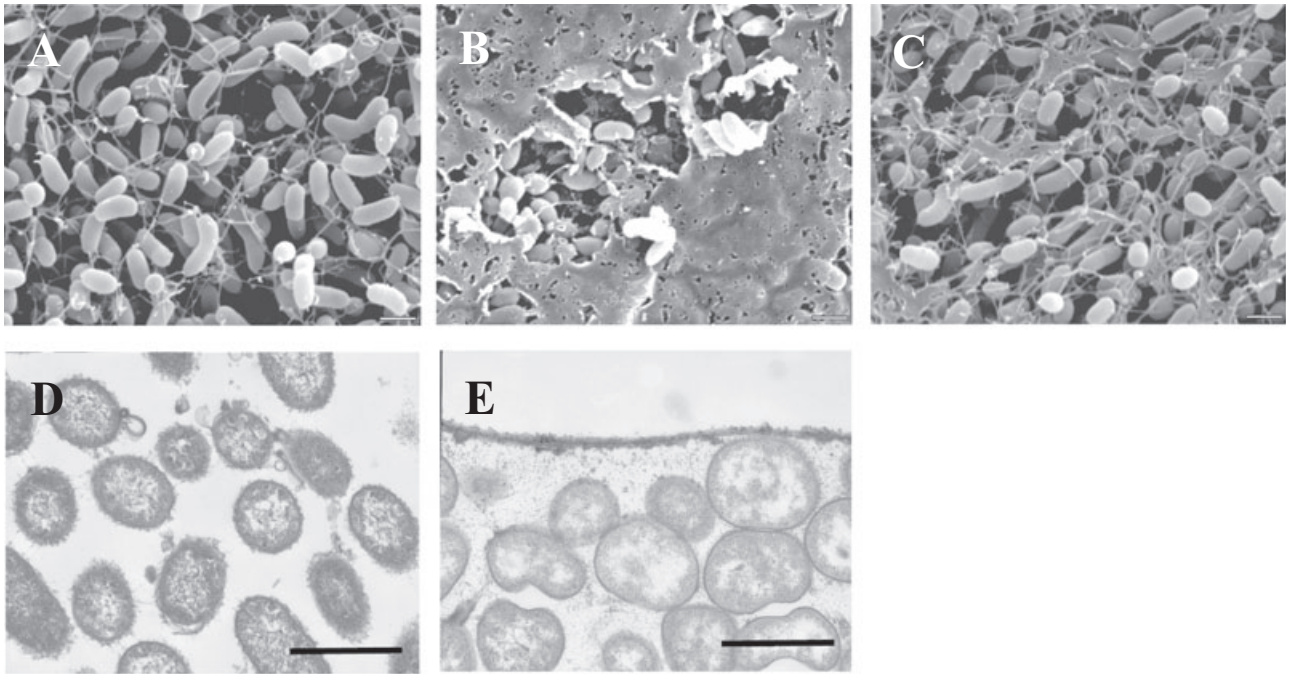

Fig. 4. SEM and TEM analysis of *V. fischeri* cells expressing *rscS1*. The production of an extracellular matrix was examined by SEM from (A) vector control wild-type cells (KV1844), (B) *rscS1*-expressing wild-type cells (KV1956) and (C) *rscS1*-expressing *sypN* mutant cells (KV1992) and by TEM analysis of (D) vector control and (E) *rscS1*-containing wild type cells stained with ruthenium red. Bars represent 1 μm.

(Luft, 1971). Colonies were fixed and stained with ruthenium red and thin sections examined by TEM. The *rscS1*-containing wild-type cells exhibited two types of ruthenium red-stained materials that were absent in vector control (Fig. 4D). First, an electron-dense layer was located at the colony surface which probably corresponds to the sheet-like matrix detected by SEM (Fig. 4E). Second, electron-dense material was also observed between cells, indicative of an extracellular matrix. Together, these data suggest that *rscS1* promotes the production of an extracellular matrix composed at least in part of acidic polysaccharides.

The observations by SEM and TEM of a matrix produced by *syp*-expressing cells supported our hypothesis that the *syp* cluster functions to modify the cell surface. To begin characterization of this matrix, we extracted surface-associated polysaccharide from smooth colonies and wrinkled colonies formed by vector-containing cells and *rscS1*-containing cells, respectively, using a capsule extraction protocol established for *V. parahaemolyticus* (Enos-Berlage and McCarter, 2000). Extractions from *rscS1*-containing wild-type cells yielded a high-molecular-weight polysaccharide (Fig. 5A). This polysaccharide was absent from vector control and largely missing from *rscS1*-expressing *sypN* mutant extracts. These data support the hypothesis that the alteration induced by *rscS1* involves increased surface polysaccharide.

Purification of the large polysaccharide has proven difficult to date due to its insolubility. Therefore, to further characterize its nature, we performed lectin binding assays with a panel of seven biotinylated lectins. A single lectin, Concanavalin A (ConA), reacted strongly with the *rscS1*-induced polysaccharide (Fig. 5B), while the other six lectins tested exhibited no binding (data not shown).

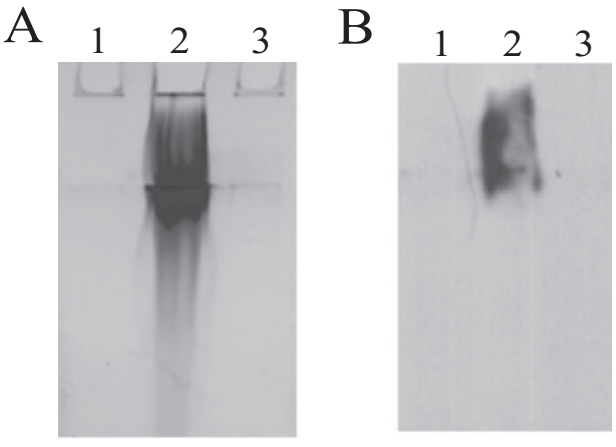

Fig. 5. Polysaccharide extraction of *V. fischeri* expressing *rscS1*. Polysaccharide extracts were resolved on SDS-PAGE gel and (A) stained with Stains-All or (B) transferred onto membrane and probed with the lectin ConA. Lane 1: vector control (KV905); 2: *rscS1*-expressing wild type (KV1980) and 3: *rscS1*-containing *sypN* mutant (KV1960).

ConA is specific for glucose and α-linked mannose residues, indicating that one (or more) of these sugars is present in the surface-associated polysaccharide produced by *rscS1*-containing wild-type *V. fischeri*.

RscS enhances colonization efficiency by promoting aggregation outside the light organ

V. fischeri cells lacking RscS exhibit a significant colonization defect (Visick and Skoufos, 2001). We therefore wanted to determine the relevance to symbiosis, if any, of phenotypes associated with multicopy expression of *rscS1*. Given the dramatic aggregation phenotypes induced in culture, we hypothesized that *rscS1* could either enhance or impede colonization through its role in cell–cell aggregation. Preliminary experiments, in which juvenile squid were incubated with cells containing either vector or *rscS1*, indicated that the *rscS1*-containing cells initiated the symbiosis earlier than vector-containing cells (data not shown). These data suggested that *rscS1* provided an advantage; however, the effect was difficult to quantify. As a more sensitive assay for colonization phenotypes, we performed competition assays. In these experiments, juvenile squid were inoculated with a mixture of two strains, one of which was marked with an erythromycin resistance (Em^R) gene on the chromosome. As a control, we competed vector-containing cells that were either erythromycin sensitive (Em^S) or resistant (Em^R) against each other at a ratio of about 1:1 and screened bacteria recovered from the light organ after colonization for antibiotic resistance. The majority of these animals (8 of 11) were colonized with a roughly equal number of each strain (Fig. 6, white circles), demonstrating that the Em^R cassette did not severely impact colonization fitness. Next, we inoculated squid with a mixture of vector-containing (Em^R) cells and *rscS1*-containing (Em^S) cells present at a ratio of about 2:1. All of the bacteria recovered from the light organ were Em^S and therefore were derived from the *rscS1*-containing cells (Fig. 6, black circles). Reciprocal experiments in which the Em^R marker was present in the *rscS1*-containing strain produced similar results: the *rscS1*-containing strain dominated in the light organ (data not shown). We conclude that multicopy expression of *rscS1* conferred a significant advantage to the cells during colonization.

To understand the mechanism by which RscS controls colonization proficiency, we asked at which stage of colonization RscS exerts its influence. Specifically, we asked whether the *rscS* gene was required for the ability of *V. fischeri* cells to aggregate in squid-secreted mucus, one of the earliest known stages of symbiotic colonization. We hypothesized that disruption of *rscS* would result in a loss of aggregates, while multicopy *rscS1* would enhance aggregate formation.

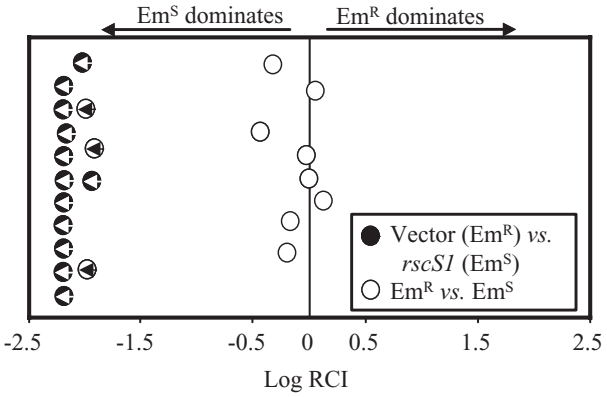

Fig. 6. Colonization by strains carrying multicopy *rscS1*. The log of the relative competitive index (log RCI) for each juvenile squid in the experiment is plotted on the *x*-axis. Log RCI is calculated as the log of the fraction of Em^R bacteria in the homogenate divided by the fraction of Em^R bacteria in the inoculum. Each circle represents a single animal. Circles with arrows represent animals in which no Em^R bacteria were present in the 100–200 colonies screened from the homogenate; therefore, the log RCI is below the limit of detection and the values plotted for these animals are approximate. In the competition between vector- and *rscS1*-containing cells, all of the colonies screened from the homogenate were the Em^S*rscS1*-containing strain (black circles). The position of the circles on the *y*-axis is merely for spacing.

To determine if *rscS* mutants exhibit a defect in aggregation, we inoculated newly hatched, aposymbiotic squid with either wild-type or *rscS* mutant strains constitutively expressing GFP. At times ranging from 2 to 6 h post inoculation, we dissected the animals and examined light organs for the presence of bacterial aggregates. Within 3–5 h of inoculation, animals exposed to GFP-labelled wild-type cells (KV1066 or KV1228) contained tightly packed aggregates of bacteria (~20 μm in diameter; Fig. 7A), either at or above a light organ pore, as observed previously (Nyholm *et al*., 2000). In contrast, animals inoculated with similar numbers of *rscS* mutant cells (KV1339 or KV1223) did not contain such aggregates (Fig. 7B); in fact, of 49 animals, 46 contained no visible GFP-labelled cells, while the remaining three animals showed only small clusters of about three to five cells. These data suggest that the defect of the *rscS* mutant in initiating symbiotic colonization stems from an inability of the cells to interact with one another and/or with mucus on the surface of the light organ.

Next, we evaluated the effect of *rscS1* on the ability of *V. fischeri* to aggregate in squid mucus. Whereas vector control cells formed aggregates of approximately 10–20 μm in diameter, similar to what we and others have seen for wild-type cells (Fig. 7C; Nyholm *et al*., 2000), *rscS1*-containing wild-type cells formed substantially larger aggregates (50–200 μm in diameter; Fig. 7D and E). These data strongly suggest that the aggregation phenotypes induced by *rscS1* in culture indeed reflect the role

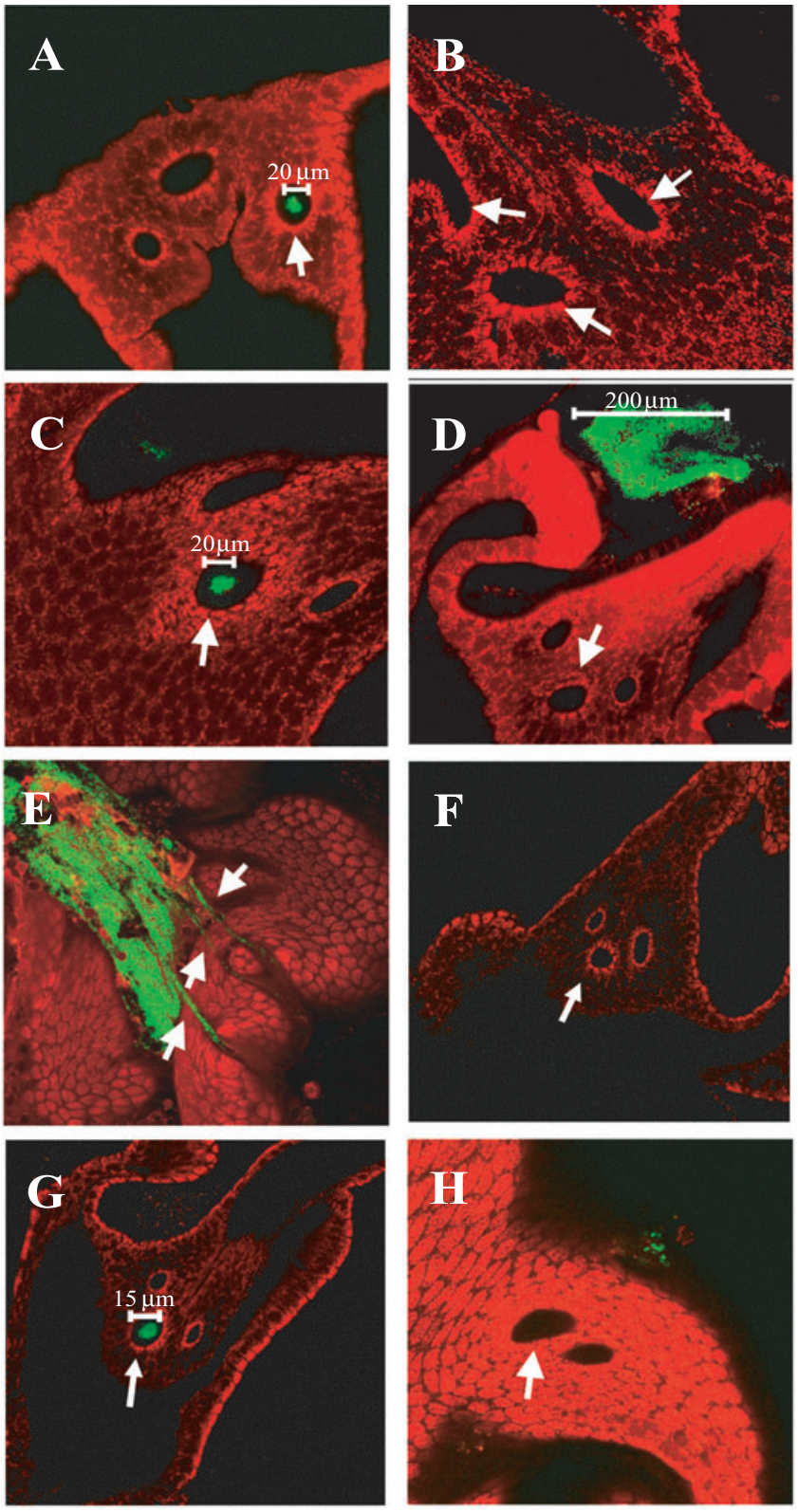

Fig. 7. Aggregate formation on the light organ by *V. fischeri*. Newly hatched juvenile squid were inoculated with GFP-labelled bacteria. After 2–6 h, animals were stained with Cell Tracker Orange (red colour) and the light organs examined by confocal microscopy. Representative images of aggregated *V. fischeri* cells at or near a light organ pore are shown. Animals were inoculated with (A) ES114 (KV1066), (B) *rscS* mutant cells (KV1339), (C) wild-type cells carrying the vector control (KV2685), (D and E) wild-type cells carrying *rscS1* (KV2688), (F and G) *rscS1*-expressing *sypN* mutant cells (KV2689), and (H) *sypN* mutant cells carrying vector (KV2686). Arrows indicate pores of the light organ.

of *rscS* in symbiosis. In further support of this hypothesis, we found that multicopy expression of *rscS1* in a *sypN* mutant largely eliminated the production of large aggregates: four of 28 animals contained no detectable *V. fischeri* (Fig. 7F), 12 contained only a few cells and the remaining 12 animals had aggregates that were substantially smaller than those produced by wild-type cells expressing *rscS1* (Fig. 7G; about wild type in size, 5–10 μm in diameter). These data demonstrate a role for *syp* in symbiotic aggregation. Furthermore, they are consistent with what we observed in culture: disruption of *sypN* reduces but does not eliminate aggregation induced by *rscS1*. Intriguingly, the *sypN* mutant carrying the vector control exhibited a more severe defect: of 18 animals examined, 15 contained no bacterial aggregates, while three contained only a few bacterial cells (Fig. 7H). These data further support a role for *sypN* in squid aggregation and suggest that *rscS1* might partially compensate for the loss of *sypN* function.

Discussion

The process by which *V. fischeri* establishes itself as the sole species within the symbiotic organ of the squid *E. scolopes* is poorly understood. Here, we demonstrate that a key step, aggregation on the surface of the squid light organ, is facilitated by the action of the bacterial regulator, RscS. Our experiments show that RscS promotes aggregation in culture and initiation of symbiotic colonization in the squid light organ by regulating expression of genes that alter the cell surface. Our data thus provide an important correlation between laboratory-based biofilm studies and natural interactions that occur during the course of colonization and as well as a basis for further genetic analysis of the regulatory pathway.

Through the isolation of an allele (*rscS1*) with increased activity, we demonstrated that RscS regulates expression of the recently discovered *syp* gene cluster (Yip *et al*., 2005). Consistent with the predicted role of the *syp* genes in the production of an extracellular polysaccharide, induction of *syp* transcription by multicopy *rscS1* resulted in phenotypes associated with cell–cell aggregation in culture: wrinkled colony morphology, biofilm and pellicle formation, clumping in liquid culture, and increased hydrophobicity. In further support of this role, cells expressing *rscS1* produce an extractable extracellular matrix visible by SEM and TEM and recognized by the lectin ConA. With this RscS-induced cell surface alteration, the ability of *V. fischeri* to colonize its host was greatly enhanced, as demonstrated by (i) competition experiments in which *rscS1*-containing cells dramatically out-competed vector control cells and (ii) microscopy studies that uncovered the role of *rscS* in promoting bacterial aggregation on the surface of the light organ.

To determine the role of the *syp* cluster in the production of *rscS1*-dependent phenotypes, we disrupted a representative *syp* gene, *sypN*, and found that most of the phenotypes depended on *sypN*. We chose *sypN* because it is a structural gene (encoding a putative glycosyltransferase), the loss of which should impact primarily the product of the *syp* cluster, rather than producing pleiotropic effects as would deletion of a regulatory gene such as *sypG*. Indeed, mutations in other *syp* genes similarly disrupt *rscS1*-dependent phenotypes. For example, disruption of most of the *syp* genes either eliminated or reduced the formation of wrinkled colonies and pellicles (E.S. Yip and K.L. Visick, unpubl. data). However, disruption of *sypN* (or other genes in the cluster) did not always render *rscS1*-containing cells indistinguishable from vector control cells. For example, shaking liquid cultures of *rscS1*-containing *sypN* mutants exhibited a cell settling phenotype unlike vector control cells (Fig. 2C). This phenotype may result either from the activities of the remaining intact *syp* genes or from RscS-dependent regulation of genes outside of the *syp* cluster.

It is not yet clear how RscS exerts its impact on *syp*. As a sensor kinase, it is predicted to function by signalling to a response regulator, and the *syp*-encoded response regulator SypG seems a prime candidate for this target regulator. Both regulators control *syp* transcription (Yip *et al*., 2005; Fig. 1) and *rscS1*-dependent *syp* induction requires SypG (K. Geszvain and K.L. Visick, unpubl. results). However, induction of the *syp* cluster through multicopy expression of *sypG* produces a different array of culture phenotypes from that which *rscS1* produces. First, multicopy *sypG* induces substantial adherence to the test tube when cells are grown with shaking (Yip *et al*., 2005), while *rscS1* does not (data not shown). Second, unlike *rscS1*, multicopy *sypG* fails to induce wrinkled colonies (E.A. Hussa and K.L. Visick, unpubl. data). Although cognate response regulators and sensor kinases can induce distinct phenotypes (for example, see Yap *et al*., 2005), it is also possible that these two regulators control the expression of distinct subsets of genes. The *syp* cluster includes two additional two-component regulators, a putative sensor kinase (SypF) and a putative response regulator (SypE) that is not predicted to bind DNA, suggesting that *syp* regulation may be complex.

Why is a sensor kinase necessary for one of the earliest steps of colonization? Presumably RscS recognizes an environmental signal and subsequently induces *syp* transcription such that surface modification can occur prior to aggregation. Potentially, a component of the seawater itself could serve as the signal for RscS. However, our preliminary experiments have provided no evidence for seawater-mediated induction of *syp* transcription (K. Geszvain and K.L. Visick, unpubl. data). Therefore, it is

likely that the environmental signal is found in proximity to the squid but external to the light organ.

The work presented here suggests that the *syp* cluster functions to modify the cell surface. Biotinylated lectin assays revealed that the surface polysaccharides produced by *syp* likely contain glucose or α-linked mannose residues. Intriguingly, the *rscS1*-induced matrix promotes the formation of a strong pellicle at the air–liquid interface similar to the cellulose-based pellicle produced by *Gluconacetobacter xylinum* (Ross *et al*., 1991). Cellulose biosynthetic genes are present in the *V. fischeri* genome (Ruby *et al*., 2005; K.L. Visick, unpubl. data); however, our preliminary data suggest that the *V. fischeri* matrix is not composed of cellulose, as the addition of cellulase did not dissolve it and *rscS1*-containing cells failed to bind either Congo Red or calcofluor (E.S. Yip and K.L. Visick, unpubl. data). It is worth noting that addition of a mannose analogue to the seawater interfered with the ability of *V. fischeri* to initiate the symbiosis (McFall-Ngai *et al*., 1998), supporting a role for a mannose-based interaction between the bacteria and their host, or perhaps among the bacteria, during colonization.

The increased surface hydrophobicity we detected in cells expressing *rscS1* may be relevant to the function of RscS and the *syp* cluster in symbiosis. In a number of systems, bacterial hydrophobicity has been correlated with adherence to plant and animal tissues (reviewed in Doyle, 2000). In the oral bacterium *Streptococcus gordonii*, fibrils composed of CshA render the cell surface hydrophobic and are required for colonization of the oral cavity in mice (McNab *et al*., 1999). In addition, the rugose phase variant of *V. cholerae* is more hydrophobic than the smooth variant due to the production of the VPS^{EITor} exopolysaccharide (Yildiz *et al*., 2004). For *V. fischeri*, it is possible that hydrophobic interactions among the bacterial cells, between the bacterium and its host, or both, could provide a substantial advantage, because the initial interactions occur in the context of an aqueous seawater environment. Indeed, it has been estimated that seawater flows in and out of the mantle cavity of the juvenile squid every 0.3 s (Visick and McFall-Ngai, 2000), creating a difficult environment for specific, receptor–ligand type interactions to occur between the two organisms.

After aggregation, *V. fischeri* cells must migrate through ducts into the light organ crypts in order to establish the symbiotic association. This migration was apparently not impaired in *rscS1* cells, despite the increased cell–cell aggregation on the light organ surface that could potentially impair subsequent cell movement. However, in our aggregation experiments we detected *rscS1*-containing bacteria beginning to move into the ducts in continuous streams of cells (Fig. 7E). This streaming of the bacteria into the ducts has also been observed with wild-type cells (Nyholm *et al*., 2000), indicating that colonization by *rscS1*-containing cells proceeds normally after aggregate formation. Indeed, the presence of *rscS1* does not impair the migration of *V. fischeri* through complex soft agar media (data not shown), supporting the conclusion that these cells can freely migrate away from the aggregate.

The ability of bacteria to form biofilm communities within their host organisms is thought to play a central role in both pathogenesis and symbiosis, by rendering the bacteria resistant to antimicrobial agents and enhancing adherence to host tissues, such as infection of lungs of cystic fibrosis patients by *P. aeruginosa* (Singh *et al*., 2000). Mutants which decrease the ability of pathogenic bacteria to form biofilms in culture show a concomitant decrease in virulence in animal models of infection (Paranjpye and Strom, 2005; Kulasakara *et al*., 2006). However, in many cases, these studies did not examine loss of biofilm within the host. Here, we report a mutualistic symbiosis where biofilm production in culture is directly linked to biofilm production in the host. Therefore, our work provides critical support for the importance of bacterial biofilm formation during the establishment of a natural bacteria–animal association.

Experimental procedures

Strains, plasmids and media

Strains used in this study are listed in Table 1. *V. fischeri* strains constructed in this work were generated by conjugation as previously described (Visick and Skoufos, 2001; DeLoney *et al*., 2002). A bacterial isolate from *E. scolopes*, ES114 (Boettcher and Ruby, 1990), and its rifampicin-resistant derivative, ESR1 (Graf *et al*., 1994), were the symbiosis-competent parent strains used in this study. The *E. coli* strains DH5α, TOP10 (Invitrogen, Carlsbad, CA) and CC118λ*pir* (Herrero *et al*., 1990) were used as hosts for cloning and conjugation. *V. fischeri* strains were grown in complex media [seawater tryptone, SWT (Yip *et al*., 2005) or LBS (Graf *et al*., 1994; Stabb *et al*., 2001)] or in HMM (Ruby and Nealson, 1977) containing 0.3% Casamino acids and 0.2% glucose (Yip *et al*., 2005). The following antibiotics were added, as needed, to the final concentrations indicated: chloramphenicol (Cm), 5 μg ml^{-1}; erythromycin (Em) 5 μg ml^{-1}; and tetracycline (Tet), 5 μg ml^{-1} in LBS, 30 μg ml^{-1} in SWT and HMM. Agar was added to a final concentration of 1.5% for solid media. Juvenile *E. scolopes* were maintained in artificial seawater (Instant Ocean; Aquarium Systems, Mentor, OH). In some experiments, natural seawater collected in *E. scolopes*-free waters off the coast of Oahu, Hawaii, was used. This seawater does not contain sufficient *V. fischeri* cells to colonize the squid. For motility assays, bacteria were grown at 28°C to mid-exponential phase and inoculated onto SWT, TBS or TB-SW soft agar plates (DeLoney-Marino *et al*., 2003).

Molecular techniques

Plasmids were constructed using standard molecular biology techniques, with restriction and modifying enzymes obtained

from New England Biolabs (Beverly, MA) or Promega (Madison, WI). Plasmids used or constructed in this study are shown in Table 1.

Random mutagenesis of rscS

A plasmid encoding wild-type *rscS*, pLMS33, was introduced into mutator strain CC130 (*mutD5*; Manoil and Beckwith, 1985; Schaaper, 1988) by transformation. Five independent transformations were performed to obtain a total of approximately 24 000 single colonies on selective media. Colonies were scraped off the plates into six separate pools; each pool of mutagenized plasmids was then conjugated into *syp* reporter strains KV1601 and KV1635 (Table 1). Transconjugants were selected for the presence of the plasmid and screened for induction of β-galactosidase expression on SWT Tet containing 80 μg ml^{-1} Xgal (Molecular Probes). After incubation at room temperature (RT) for 2 days, approximately 200 blue (i.e. *syp*-expressing) colonies were found among the ~200 000 colonies plated. Plasmids were isolated from the six colonies that exhibited the greatest amount of *syp* expression (based on the intensity of blue colour), the *rscS* gene from these plasmids was subcloned into unmutagenized vector (pKV69, Table 1) and the resulting constructs were examined again for their ability to induce *syp* transcription. Two subcloned *rscS* alleles (*rscS1* and *rscS2*, encoded on plasmids pKG11 and pKG13 respectively) retained the ability to induce *syp* expression.

Sequencing

The mutations in *rscS1* and *rscS2* were identified by automated sequencing (MWG Biotech, Highpoint, NC) of the *rscS* gene present on pKG11 and pKG13 respectively, using primers specific to *rscS*. The *rscS1* allele contains a C to T transition in the sixth position of the putative ribosome binding site (AGGAGC to AGGAGT) and a C to T transition at the wobble position within a Leu codon at amino acid 25 (CTC to CTT). The *rscS2* allele contains a T to C transition immediately 3′ of the ribosome binding site (AGGAGCT to AGGAGCC).

β-Galactosidase assay

Strains were grown in HMM with Tet at 22°C overnight, then subcultured into fresh medium and grown for 24 h. Aliquots (1 ml) were removed and β-galactosidase activity in triplicate was assayed as described (Miller, 1972). Protein concentration was measured as described (Lowry *et al*., 1951).

Hydrophobicity assay

Strains were grown in HMM with Tet at 28°C overnight, subcultured into fresh medium and grown for 24 h. Next, an equal volume of hexadecane (Acros Organics, NJ) was added to the culture tubes and vortexed until the suspension was homogeneous (at least 1 min). Then, the hydrophobic (hexadecane) and hydrophilic fractions were allowed to separate. Partitioning of the cells to the hydrophobic layer was visualized as an increase in turbidity of the top layer (Rosenberg *et al*., 1980; Araujo *et al*., 1994).

Confocal microscopy

Cells expressing fluorescent proteins (RFP or GFP) were grown statically in HMM in 12 well microtiter plates with glass coverslips submerged partially into the culture medium. Coverslips were incubated with bacteria at RT for up to 30 h and removed at specific time points for biofilm examination. A Zeiss LSM 510 confocal microscope (65× objective) was used to collect *xy* plane and *z* sections (*xz* and *yz* plane) images of the biofilms. Images were prepared using the Zeiss LSM Image Browser software.

Scanning electron microscopy

Colonies grown on cellulose membranes overlaid on LBS Tet plates were prepared as described (Yildiz *et al*., 2001) with the following modifications: cells were fixed in 2% glutaraldehyde in 0.45 M cacodylate buffer (pH 7.3), washed with 0.45 M cacodylate buffer, post-fixed with 1% osmium tetroxide for 1 h and washed again with cacodylate buffer. The samples were subjected to dehydration with ethanol, critical point drying and sputter-coating with gold-palladium. Finally, samples were examined with a scanning electron microscope (JEOL JSM-840A).

Transmission electron microscopy

Colonies were grown on LBS Tet plates at RT for 3 days and fixed as described (Luft, 1971; Patterson *et al*., 1975) with the following modifications: colonies were fixed overnight in a solution containing 1.2% glutaraldehyde, 0.45 M cacodylate buffer (pH 7.3) and 0.1% (wt/vol) ruthenium red. After fixation, cells were washed, post-fixed with 1% osmium tetroxide for 1 h, washed again and subjected to serial dehydration with ethanol. Samples were embedded in resin, thin-sectioned and stained with uranyl acetate and lead citrate. Finally, the samples were examined with a transmission electron microscope (Hitachi H-600) operating at an accelerating voltage of 75 kV.

Polysaccharide extraction

Polysaccharides were extracted as described by Enos-Berlage and McCarter (2000) with the following modifications: bacterial strains were grown in a lawn on LBS Tet until *rscS1*-containing WT cells became wrinkled. Cells scrapped off of the plates were resuspended in 5 ml of phosphate-buffered saline (20 mM sodium phosphate, 100 mM sodium chloride, pH 7.3). Cell suspensions were shaken at 28°C for 90 min, vortexed and shaken for another 90 min. Cultures were centrifuged at 10 000 *g* for 15 min to remove cells and cellular debris. Supernatants were transferred to fresh tubes and incubated for 3 h at 37°C with $MgCl_2$, RNase (Sigma, St Louis, MO) and RQ1 DNase (Promega, Madison, WI) at

final concentrations of 10 mM, 50 μg ml^{-1} and 50 μg ml^{-1} respectively. Proteinase K (Fisher, Fair Lawn, NJ) was subsequently added to a final concentration of 200 μg ml^{-1} and the samples were incubated at 37°C overnight. Polysaccharides were extracted using phenol/chloroform and precipitated with ethanol. Samples were boiled in loading buffer containing 10% β-mercaptoethanol prior to gel electrophoresis. However, only a portion of the samples were solubilized and thus loaded onto the gels for Stains-All (Kelley and Parker, 1981) staining and lectin binding assays.

Lectin binding assay

Polysaccharide extracts were evaluated using a panel of biotinylated lectins. Extracts were subjected to electrophoresis on a Tris glycine-polyacrylamide (14%) gel and then transferred onto a polyvinylidene fluoride membrane (Millipore, Bedford, MA). The membrane was blocked with Tris-buffered saline containing 0.2% Tween (TBST) and 2% (v/v) bovine serum albumin for 1 h. After blocking, the membrane was incubated in TBST for 45 min with 1 μg ml^{-1} (final concentration) of one of seven biotinylated lectins in the biotinylated lectin kit I, which contains ConA, DBA, PNA, RCA_{120}, SBA, UEA I and WGA (Vector Laboratory, Burlingame, CA). Then, the membrane was washed with TBST three times for 10 min each and subsequently incubated with horseradish peroxidase-conjugated streptavidin (Jackson ImmunoResearch, West Grove, PA) for 30 min. Reactive carbohydrates were detected by incubating the membrane with an equal volume of solution 1 (2.5 mM luminal, 0.4 mM p-coumaric acid and 100 mM Tris pH 8.5) and solution 2 (0.02% H_2O_2, 100 mM Tris pH 8.5).

Colonization assays

Both single-strain and competition assays were performed as described (Lee and Ruby, 1994; Ruby, 1996; Visick and Skoufos, 2001). For the competition assays, vector and *rscS1* were both introduced into *V. fischeri* strain KV1421, which is marked with an Em^R cassette inserted at the Tn*7* attachment site (DeLoney *et al*., 2002). Strains used in the colonization experiments were grown in SWT with Tet for about 4 h before inoculation; these conditions did not promote significant aggregation or growth defects in culture. These strains also exhibited no motility defect when tested for their ability to migrate through complex soft agar media (DeLoney-Marino *et al*., 2003). To test for a competitive defect, we inoculated 12 juveniles with a mixture of the Em^R vector strain (KV2435, 1750 cfu ml^{-1}) and the Em^S*rscS1* strain (KV1956, 750 cfu ml^{-1}) (a ratio of 2.3:1). In a control experiment, 11 juveniles were inoculated with a mixture of cells with vector in the Em^R strain background (KV2435, 2477 cfu ml^{-1}) and vector in the Em^S strain (KV1844, 3283 cfu ml^{-1}) (a ratio of 0.75:1). Approximately 20 h after inoculation, the individual squid were monitored for luminescence, rinsed with bacteria-free artificial seawater and frozen at −80°C. The following day, the squid were homogenized and plated on SWT. In these experiments, all animals luminesced and were colonized to at least 10^4 cfu per squid. Between 100 and 200 colonies from each squid homogenate were patched onto LBS with Em to determine the ratio of Em^S to Em^R bacteria within the light organ.

Squid aggregation assays

Log-phase cells (OD_{600} 0.3–0.6) were grown in 2 ml SWT medium at 28°C. Bacterial cells were then inoculated into unfiltered natural seawater or filtered artificial seawater at concentrations of between 10^6 and 10^8 cells per ml. Juvenile squid were then placed into inoculated seawater and the two organisms were allowed to associate at RT for between 2 and 6 h prior to dissection. At various times, the juvenile squid were removed to vials containing 2 ml filter-sterilized seawater and 5 μM of the counter-stain, Cell Tracker Orange (Molecular Probes, Eugene, OR). The animals were then anaesthetized in seawater or filtered artificial seawater containing 2% ethanol. Each squid was placed ventral side up on a depression well slide and dissected to remove the mantle and funnel and expose the light organ. Fluorescently labelled light organs (red) and GFP-labelled (green) bacteria were viewed using a Zeiss LSM 510 confocal microscope.

Acknowledgements

We thank Ned Ruby and Margaret McFall-Ngai for the use of *E. scolopes* juveniles and a confocal microscope and Eric Stabb for generous donation of plasmid vectors. We also thank Ned Ruby and Cheryl Whistler for helpful advice and Jon Visick, Joerg Graf and members of our lab for critical reading of our manuscript. This work was supported by NIH Grant GM59690 awarded to K.L.V., by the Estate of William G. Potts in support of medical research at the Stritch School of Medicine at Loyola University Chicago, by the National Science Foundation under a Research Fellowship in Microbial Biology awarded in 2001 and National Science Foundation Microbial Biology Research Starter Grant awarded in 2004 to C.R.D-M, and by the NIH under the Ruth L. Kirschstein National Research Service Award 1 F32 G073523 from the NIGMS awarded to K.G.

References

Araujo, R.S., Robleto, E.A., and Handelsman, J. (1994) A hydrophobic mutant of *Rhizobium etli* altered in nodulation competitiveness and growth in the rhizosphere. *Appl Environ Microbiol* **60:** 1430–1436.

Boettcher, K.J., and Ruby, E.G. (1990) Depressed light emission by symbiotic *Vibrio fischeri* of the sepiolid squid *Euprymna scolopes*. *J Bacteriol* **172:** 3701–3706.

Branda, S.S., Vik, S., Friedman, L., and Kolter, R. (2005) Biofilms: the matrix revisited. *Trends Microbiol* **13:** 20–26.

Del Re, B., Sgorbati, B., Miglioli, M., and Palenzona, D. (2000) Adhesion, autoaggregation and hydrophobicity of 13 strains of *Bifidobacterium longum*. *Lett Appl Microbiol* **31:** 438–442.

DeLoney, C.R., Bartley, T.M., and Visick, K.L. (2002) Role for phosphoglucomutase in *Vibrio fischeri-Euprymna scolopes* symbiosis. *J Bacteriol* **184:** 5121–5129.

DeLoney-Marino, C.R., Wolfe, A.J., and Visick, K.L. (2003) Chemoattraction of *Vibrio fischeri* to serine, nucleosides,

and N-acetylneuraminic acid, a component of squid light-organ mucus. *Appl Environ Microbiol* **69:** 7527–7530.

Doyle, R.J. (2000) Contribution of the hydrophobic effect to microbial infection. *Microbes Infect* **2:** 391–400.

Dunn, A.K., Millikan, D.S., Adin, D.M., Bose, J.L., and Stabb, E.V. (2006) New rfp- and pES213-derived tools for analyzing symbiotic *Vibrio fischeri* reveal patterns of infection and lux expression in situ. *Appl Environ Microbiol* **72:** 802–810.

Enos-Berlage, J.L., and McCarter, L.L. (2000) Relation of capsular polysaccharide production and colonial cell organization to colony morphology in *Vibrio parahaemolyticus*. *J Bacteriol* **182:** 5513–5520.

Friedman, L., and Kolter, R. (2004a) Two genetic loci produce distinct carbohydrate-rich structural components of the *Pseudomonas aeruginosa* biofilm matrix. *J Bacteriol* **186:** 4457–4465.

Friedman, L., and Kolter, R. (2004b) Genes involved in matrix formation in *Pseudomonas aeruginosa* PA14 biofilms. *Mol Microbiol* **51:** 675–690.

Graf, J., Dunlap, P.V., and Ruby, E.G. (1994) Effect of transposon-induced motility mutations on colonization of the host light organ by *Vibrio fischeri*. *J Bacteriol* **176:** 6986–6991.

Herrero, M., DeLorenzo, V., and Timmis, K.N. (1990) Transposon vectors containing non-antibiotic resistance selection markers for cloning and stable chromosomal insertion of foreign genes in gram-negative bacteria. *J Bacteriol* **172:** 6557–6567.

Hung, D.T., Zhu, J., Sturtevant, D., and Mekalanos, J.J. (2006) Bile acids stimulate biofilm formation in *Vibrio cholerae*. *Mol Microbiol* **59:** 193–201.

Jackson, K.D., Starkey, M., Kremer, S., Parsek, M.R., and Wozniak, D.J. (2004) Identification of *psl*, a locus encoding a potential exopolysaccharide that is essential for *Pseudomonas aeruginosa* PAO1 biofilm formation. *J Bacteriol* **186:** 4466–4475.

Kelley, J.T., and Parker, C.D. (1981) Identification and preliminary characterization of *Vibrio cholerae* outer membrane proteins. *J Bacteriol* **145:** 1018–1024.

Kirn, T.J., Lafferty, M.J., Sandoe, C.M., and Taylor, R.K. (2000) Delineation of pilin domains required for bacterial association into microcolonies and intestinal colonization by *Vibrio cholerae*. *Mol Microbiol* **35:** 896–910.

Kulasakara, H., Lee, V., Brencic, A., Liberati, N., Urbach, J., Miyata, S., *et al.* (2006) Analysis of *Pseudomonas aeruginosa* diguanylate cyclases and phosphodiesterases reveals a role for bis-(3′-5′)-cyclic-GMP in virulence. *Proc Natl Acad Sci USA* **103:** 2839–2844.

Lee, K.H., and Ruby, E.G. (1994) Competition between *Vibrio fischeri* strains during initiation and maintenance of a light organ symbiosis. *J Bacteriol* **176:** 1985–1991.

Lowry, O.H., Rosebrough, N.J., Farr, A.L., and Randall, R.J. (1951) Protein measurement with the folin phenol reagent. *J Biol Chem* **193:** 265–275.

Luft, J.H. (1971) Ruthenium red and violet. I. Chemistry, purification, methods of use for electron microscopy and mechanism of action. *Anat Rec* **171:** 347–368.

McCann, J., Stabb, E.V., Millikan, D.S., and Ruby, E.G. (2003) Population dynamics of *Vibrio fischeri* during infection of *Euprymna scolopes*. *Appl Environ Microbiol* **69:** 5928–5934.

McFall-Ngai, M., Brennan, C., and Lamarcq, L. (1998) *Mannose Adhesin–Glycan Interactions in the Euprymna Scolopes-Vibrio Fischeri Symbiosis*. New York: Plenum Press.

McNab, R., Forbes, H., Handley, P.S., Loach, D.M., Tannock, G.W., and Jenkinson, H.F. (1999) Cell wall-anchored CshA polypeptide (259 kilodaltons) in *Streptococcus gordonii* forms surface fibrils that confer hydrophobic and adhesive properties. *J Bacteriol* **181:** 3087–3095.

Manoil, C., and Beckwith, J. (1985) Tn phoA: a transposon probe for protein export signals. *Proc Natl Acad Sci USA* **82:** 8129–8133.

Matsukawa, M., and Greenberg, E.P. (2004) Putative exopolysaccharide synthesis genes influence *Pseudomonas aeruginosa* biofilm development. *J Bacteriol* **186:** 4449–4456.

Miller, J.H. (1972) *Experiments in Molecular Genetics*. Cold Spring Harbor, NY: Cold Spring Harbor Laboratory Press.

Millikan, D.S., and Ruby, E.G. (2002) Alterations in *Vibrio fischeri* motility correlate with a delay in symbiosis initiation and are associated with additional symbiotic colonization defects. *Appl Environ Microbiol* **68:** 2519–2528.

Millikan, D.S., and Ruby, E.G. (2003) FlrA, a sigma54-dependent transcriptional activator in *Vibrio fischeri*, is required for motility and symbiotic light-organ colonization. *J Bacteriol* **185:** 3547–3557.

Nyholm, S.V., and McFall-Ngai, M. (2003) Dominance of *Vibrio fischeri* in secreted mucus outside the light organ of *Euprymna scolopes*: the first site of symbiont specificity. *Appl Environ Microbiol* **69:** 3932–3937.

Nyholm, S.V., and McFall-Ngai, M. (2004) The winnowing establishing the squid *Vibrio* symbiosis. *Nat Rev Microbiol* **2:** 632–642.

Nyholm, S.V., Stabb, E.V., Ruby, E.G., and McFall-Ngai, M.J. (2000) Establishment of an animal–bacterial association: recruiting symbiotic *Vibrios* from the environment. *Proc Natl Acad Sci USA* **97:** 10231–10235.

O'Shea, T.M., Klein, A.H., Geszvain, K., Wolfe, A.J., and Visick, K.L. (2006) Diguanylate cyclases control magnesium-dependent motility of *Vibrio fischeri*. *J Bacteriol* **188:** 23.

Paranjpye, R.N., and Strom, M.S. (2005) A *Vibrio vulnificus* type IV pilin contributes to biofilm formation, adherence to epithelial cells, and virulence. *Infect Immun* **73:** 1411–1422.

Patterson, H., Irvin, R., Costerton, J.W., and Cheng, K.J. (1975) Ultrastructure and adhesion properties of *Ruminococcus albus*. *J Bacteriol* **122:** 278–287.

Romling, U., Sierralta, W.D., Eriksson, K., and Normark, S. (1998) Multicellular and aggregative behaviour of *Salmonella typhimurium* strains is controlled by mutations in the *agfD* promoter. *Mol Microbiol* **28:** 249–264.

Rosenberg, M., Gutnick, D., and Rosenberg, E. (1980) Adherence of bacteria to hydrocarbons: a simple method for measuring cell-surface hydrophobicity. *FEMS Microbiol Lett* **9:** 29–33.

Ross, P., Mayer, R., and Benziman, M. (1991) Cellulose biosynthesis and function in bacteria. *Microbiol Rev* **55:** 35–58.

Ruby, E.G. (1996) Lessons from a cooperative, bacterial–animal association: the *Vibrio fischeri-Euprymna scolopes* light organ symbiosis. *Annu Rev Microbiol* **50:** 591–624.

Ruby, E.G., and Nealson, K.H. (1977) Pyruvate production and excretion by the luminous marine bacteria. *Appl Environ Microbiol* **34:** 164–169.

Ruby, E.G., Urbanowski, M., Campbell, J., Dunn, A., Faini, M., Gunsalus, R., *et al.* (2005) Complete genome sequence of *Vibrio fischeri*: a symbiotic bacterium with pathogenic congeners. *Proc Natl Acad Sci USA* **102:** 3004–3009.

Schaaper, R.M. (1988) Mechanisms of mutagenesis in the *Escherichia coli* mutator mutD5: role of DNA mismatch repair. *Proc Natl Acad Sci USA* **85:** 8126–8130.

Singh, P.K., Schaefer, A.L., Parsek, M.R., Moninger, T.O., Welsh, M.J., and Greenberg, E.P. (2000) Quorum-sensing signals indicate that cystic fibrosis lungs are infected with bacterial biofilms. *Nature* **407:** 762–764.

Solano, C., Garcia, B., Valle, J., Berasain, C., Ghigo, J.M., Gamazo, C., and Lasa, I. (2002) Genetic analysis of *Salmonella enteritidis* biofilm formation: critical role of cellulose. *Mol Microbiol* **43:** 793–808.

Sonnenburg, J.L., Angenent, L.T., and Gordon, J.I. (2004) Getting a grip on things: how do communities of bacterial symbionts become established in our intestine? *Nat Immunol* **5:** 569–573.

Stabb, E.V., and Ruby, E.G. (2002) New RP4-based plasmids for conjugation between *Escherichia coli* and members of the *Vibrionaceae*. *Methods Enzymol* **358:** 413–426.

Stabb, E.V., Reich, K.A., and Ruby, E.G. (2001) *Vibrio fischeri* genes *hvnA* and *hvnB* encode secreted NAD(+)-glycohydrolases. *J Bacteriol* **183:** 309–317.

Stock, A.M., Robinson, V.L., and Goudreau, P.N. (2000) Two-component signal transduction. *Annu Rev Biochem* **69:** 183–215.

Visick, K.L., and McFall-Ngai, M.J. (2000) An exclusive contract: specificity in the *Vibrio fischeri-Euprymna scolopes* partnership. *J Bacteriol* **182:** 1779–1787.

Visick, K.L., and Skoufos, L.M. (2001) Two-component sensor required for normal symbiotic colonization of *Euprymna scolopes* by *Vibrio fischeri*. *J Bacteriol* **183:** 835–842.

Wadstrom, T., Andersson, K., Sydow, M., Axelsson, L., Lindgren, S., and Gullmar, B. (1987) Surface properties of *lactobacilli* isolated from the small intestine of pigs. *J Appl Bacteriol* **62:** 513–520.

Whiteley, M., Bangera, M.G., Bumgarner, R.E., Parsek, M.R., Teitzel, G.M., Lory, S., and Greenberg, E.P. (2001) Gene expression in *Pseudomonas aeruginosa* biofilms. *Nature* **413:** 860–864.

Woodcock, D.M., Crowther, P.J., Doherty, J., Jefferson, S., DeCruz, E., Noyer-Weidner, M., *et al.* (1989) Quantitative evaluation of *Escherichia coli* host strains for tolerance to cytosine methylation in plasmid and phage recombinants. *Nucleic Acids Res* **17:** 3469–3478.

Yap, M.N., Yang, C.H., Barak, J.D., Jahn, C.E., and Charkowski, A.O. (2005) The *Erwinia chrysanthemi* type III secretion system is required for multicellular behavior. *J Bacteriol* **187:** 639–648.

Yildiz, F.H., and Schoolnik, G.K. (1999) *Vibrio cholerae* O1 El Tor: identification of a gene cluster required for the rugose colony type, exopolysaccharide production, chlorine resistance, and biofilm formation. *Proc Natl Acad Sci USA* **96:** 4028–4033.

Yildiz, F.H., Dolganov, N.A., and Schoolnik, G.K. (2001) VpsR, a member of the response regulators of the two-component regulatory systems, is required for expression of *vps* biosynthesis genes and EPS (ETr)-associated phenotypes in *Vibrio cholerae* O1 El Tor. *J Bacteriol* **183:** 1716–1726.

Yildiz, F.H., Liu, X.S., Heydorn, A., and Schoolnik, G.K. (2004) Molecular analysis of rugosity in a *Vibrio cholerae* O1 El Tor phase variant. *Mol Microbiol* **53:** 497–515.

Yip, E.S., Grublesky, B.T., Hussa, E.A., and Visick, K.L. (2005) A novel, conserved cluster of genes promotes symbiotic colonization and sigma-dependent biofilm formation by *Vibrio fischeri*. *Mol Microbiol* **57:** 1485–1498.

Zogaj, X., Nimtz, M., Rohde, M., Bokranz, W., and Romling, U. (2001) The multicellular morphotypes of *Salmonella typhimurium* and *Escherichia coli* produce cellulose as the second component of the extracellular matrix. *Mol Microbiol* **39:** 1452–1463.

Molecular Microbiology (2005) **57**(5), 1485–1498 doi:10.1111/j.1365-2958.2005.04784.x

A novel, conserved cluster of genes promotes symbiotic colonization and σ^{54}-dependent biofilm formation by *Vibrio fischeri*

Emily S. Yip, Brian T. Grublesky, Elizabeth A. Hussa and Karen L. Visick*
Department of Microbiology and Immunology, Loyola University Chicago, 2160 S. First Ave. Bldg. 105, Maywood, IL 60153, USA.

Summary

Vibrio fischeri **is the exclusive symbiont residing in the light organ of the squid** ***Euprymna scolopes*****. To understand the genetic requirements for this association, we searched a library of** ***V. fischeri*** **transposon insertion mutants for those that failed to colonize** ***E. scolopes*****. We identified four mutants that exhibited severe defects in initiating colonization. Sequence analysis revealed that the strains contained insertions in four different members of a cluster of 21 genes oriented in the same direction. The predicted gene products are similar to proteins involved in capsule, exopolysaccharide or lipopolysaccharide biosynthesis, including six putative glycosyltransferases. We constructed mutations in five additional genes and found that they also were required for symbiosis. Therefore, we have termed this region** ***syp*****, for symbiosis polysaccharide. Homologous clusters also exist in** ***Vibrio parahaemolyticus*** **and** ***Vibrio vulnificus*****, and thus these genes may represent a common mechanism for promoting bacteria–host interactions. Using** ***lacZ*** **reporter fusions, we observed that transcription of the** ***syp*** **genes did not occur under standard laboratory conditions, but could be induced by multicopy expression of** ***sypG*****, which encodes a response regulator with a predicted σ^{54} interaction domain. This induction depended on σ^{54}, as a mutation in** ***rpoN*** **abolished** ***syp*** **transcription. Primer extension analysis supported the use of putative σ^{54} binding sites upstream of** ***sypA*****,** ***sypI*** **and** ***sypM*** **as promoters. Finally, we found that multicopy expression of** ***sypG*** **resulted in robust biofilm formation. This work thus reveals a novel group of genes that** ***V. fischeri*** **controls through a σ^{54}-dependent response regulator and uses to promote symbiotic colonization.**

Accepted 20 June, 2005. *For correspondence. E-mail kvisick@lumc.edu; Tel. (+1) 708 216 0869; Fax (+1) 708 216 9574.

Introduction

The symbiotic colonization of the Hawaiian bobtail squid *Euprymna scolopes* by the marine bioluminescent bacterium *Vibrio fischeri* serves as a model for studying bacteria–host interactions (Ruby, 1999; Nyholm and McFall-Ngai, 2004). Like well-studied pathogenic associations, the formation of this symbiosis requires the bacterium to express traits that allow it to enter and multiply within a host organ. Furthermore, colonization by *V. fischeri* promotes developmental changes within the host, including tissue remodelling (Foster and McFall-Ngai, 1998; Foster *et al*., 2000).

Factors involved in establishing the exclusive relationship between *V. fischeri* and its invertebrate host have been examined from the perspective of both organisms. The surface of the symbiotic organ, known as the light organ, includes ciliated epithelial appendages that project into the body cavity of the squid and help direct the flow of the seawater towards this organ (Montgomery and McFall-Ngai, 1993). *V. fischeri* cells in the seawater then aggregate in squid-secreted mucus on the surface of the light organ (Nyholm *et al*., 2000). In addition to *V. fischeri*, other Gram-negative bacteria, such as *Vibrio parahaemolyticus*, also exhibit the capability to aggregate on the light organ (Nyholm *et al*., 2000). However, if both *V. fischeri* and *V. parahaemolyticus* are introduced into the seawater, *V. fischeri* rapidly becomes the dominant species in the mixed bacterial aggregate (Nyholm and McFall-Ngai, 2003). These data suggest that *V. fischeri* cells contribute to the observed specificity of the interaction.

After 2–3 h of aggregation, during which bacteria–bacteria and bacteria–host signalling likely occurs (Nyholm *et al*., 2000; Lupp and Ruby, 2005), *V. fischeri* cells enter the light organ. First, they migrate into one of six openings known as pores (Nyholm *et al*., 2000). This migration requires bacterial motility: non-motile bacteria aggregate but fail to migrate into the light organ (Graf *et al*., 1994; Nyholm *et al*., 2000; Millikan and Ruby, 2003). Next, they passage through ducts that contain

nitric oxide, which may provide protection against colonization by non-symbionts (Davidson *et al*., 2004). Finally, they reach nutrient-filled crypts, where they multiply to high cell density and induce bioluminescence (Ruby and Asato, 1993; Graf and Ruby, 1998). Mutants defective for structural or regulatory genes required for light production (*luxA*, *luxR* and *luxI*) reach this stage of colonization, but subsequently fail to persist at wild-type levels within the light organ (Visick *et al*., 2000). Within the crypts, additional signalling occurs between the two organisms. Specifically, colonization by *V. fischeri* triggers apoptosis and subsequent regression of the surface ciliated appendages and a decrease in duct size (Foster and McFall-Ngai, 1998; Foster *et al*., 2000; Kimbell and McFall-Ngai, 2004). These changes presumably reduce the likelihood of colonization by other bacteria.

Besides motility and luminescence, other bacterial factors are required for various stages of symbiosis. Colonization requires the outer membrane protein OmpU for initiation, the metabolic enzyme Pgm for growth to high cell density, and the nitrogen and siderophore regulator GlnD for persistence (Graf and Ruby, 2000; Aeckersberg *et al*., 2001; DeLoney *et al*., 2002). In addition to these factors, a number of regulators have been identified as important for symbiotic colonization. These include quorum-sensing regulators (AinS, LuxS and LuxO), members of the class of two-component regulators (RscS, GacA and FlrA) and an alternative sigma factor (σ^{54}, encoded by *rpoN*). Other than RscS, for which targets have not been identified, these regulators control multiple factors known or predicted to play roles in symbiotic colonization (Visick and Skoufos, 2001; Lupp *et al*., 2003; Whistler and Ruby, 2003; Lupp and Ruby, 2004; 2005; Wolfe *et al*., 2004). Two of these regulators, FlrA and LuxO, are predicted to work with σ^{54} to control expression of flagella and bioluminescence respectively (Lupp *et al*., 2003; Millikan and Ruby, 2003). Indeed, *rpoN* mutants exhibit defects in motility and bioluminescence regulation, as well as in nitrogen metabolism and biofilm formation (Wolfe *et al*., 2004). Mutants defective for *rpoN* fail to initiate symbiotic colonization; however, whether this defect is due solely to the loss of motility exhibited by these strains or also to other σ^{54}-dependent phenotypes, such as biofilm formation, remains unclear.

Genes controlled by σ^{54}-containing RNA polymerase require transcription factors (such as FlrA and LuxO) to promote formation of an open, initiation-competent, complex by RNA polymerase (Reitzer and Schneider, 2001). Often, the transcription factor is a two-component response regulator activated by phosphorylation in response to an environmental signal received by a membrane-associated sensor kinase. The result is a tightly controlled, environment-specific regulation of gene expression.

In this article, we report the identification of a novel cluster of genes required for symbiotic initiation by *V. fischeri*. These genes are co-ordinately regulated by σ^{54} and a previously uncharacterized response regulator, SypG. Multicopy expression of *sypG* resulted in a dramatic, σ^{54}-dependent, enhancement of biofilm formation. This cluster, which includes putative genes for polysaccharide biosynthesis, is strongly conserved in the pathogens *V. parahaemolyticus* and *V. vulnificus* and thus may define a new paradigm for bacteria–host interactions in *Vibrio* species.

Results

Isolation of symbiosis-defective mutants

To identify novel bacterial genes required for establishing symbiosis, we screened a transposon (Tn)-mutagenized library of *V. fischeri* using newly hatched juveniles of *E. scolopes* as described previously (Visick and Skoufos, 2001; DeLoney *et al*., 2002). Briefly, we inoculated animals with individual mutant strains. We measured successful colonization by monitoring bacterial bioluminescence, produced when *V. fischeri* reaches high cell density in the symbiotic light organ. We then determined colonization levels by homogenizing the animals and counting the resulting number of colony-forming units (cfu). Mutants defective in symbiotic initiation were further confirmed using additional animals.

Using this assay, we identified four independent mutant strains, from among about 600 screened, that exhibited severe defects in initiating symbiotic colonization. None of the animals exposed to these strains achieved symbiotic luminescence above background levels within 17 h post inoculation (Fig. 1A). In contrast, 90% of the animals exposed to the parent strain, ESR1, began to emit light within 10 h, and all 10 animals inoculated with ESR1 produced detectable levels of light by 17 h (Fig. 1A). In culture, the mutant bacteria grew like their parent on a variety of media. They also exhibited normal kinetics of bioluminescence induction and similar overall levels of light relative to the parent strain (data not shown). These data suggested that the lack of symbiotic luminescence reflected either a delay in or an absence of colonization. In support of this prediction, we found that most animals exposed to the Tn mutants remained uncolonized while the few that were colonized contained less than 1% of the symbionts found in animals inoculated with ESR1 (Fig. 1B). Because the majority of the animals remained uncolonized, these data indicated that the defect in initiation was severe.

We next investigated whether these mutant strains were defective for known symbiotic factors. Non-motile strains of *V. fischeri* fail to colonize (Graf *et al*., 1994;

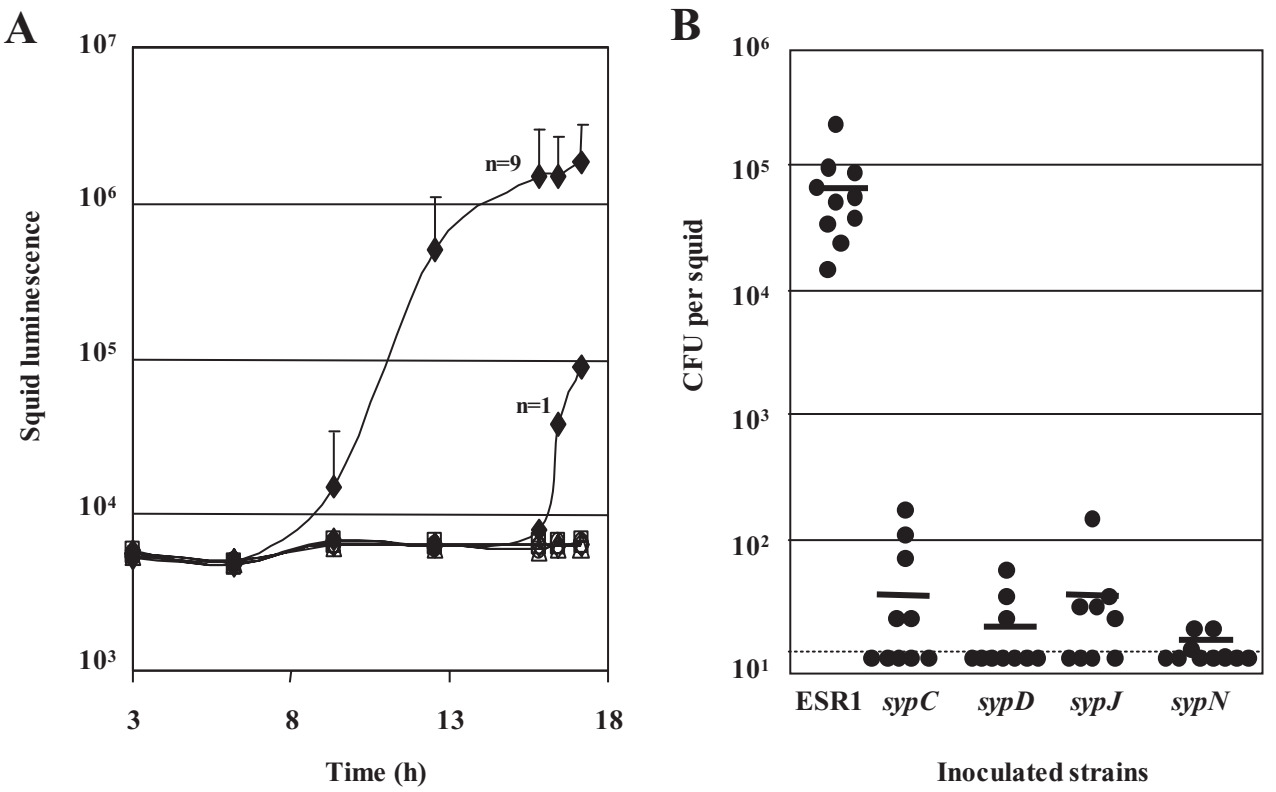

Fig. 1. Symbiotic colonization by transposon insertion mutants. Newly hatched juvenile squid were inoculated with either the parent strain, ESR1, or the transposon insertion mutants defective for *sypC*, *sypD*, *sypJ* or *sypN* (KV1637, KV1635, KV1636 and KV1601 respectively) with approximately 2300–3300 cfu ml^{-1} for 3 h.
A. Bioluminescence emission was monitored for 10 individual squid inoculated with ESR1 (solid diamonds) or the transposon insertion mutants *sypC* (open triangles), *sypD* (open squares), *sypJ* (open circles) or *sypN* (open diamonds). One ESR1-inoculated animal emitted bioluminescence after a significant delay, but achieved a high level of colony-forming units (cfu).
B. Within 1 h of the last time point shown in (A), the animals were homogenized and plated to determine the number of cfu in each squid. Each solid circle represents the number of cfu from an individual animal, while the bars represent the average of 10 (ESR1, *sypC*, *sypD* and *sypN*) or nine (*sypJ*) animals. The dotted line represents the limit of detection.

Millikan and Ruby, 2003; Wolfe *et al*., 2004), while hypermotile strains, if they colonize, do so with a significant delay (Millikan and Ruby, 2002). The four Tn mutants exhibited migration indistinguishable from that of their parent strain in a tryptone-based soft agar medium (data not shown). Symbiotic initiation also requires the outer membrane protein, OmpU (Aeckersberg *et al*., 2001); however, all four Tn mutants contained outer membrane protein profiles similar to that of the parent strain (data not shown). These data suggested that the Tns had inserted into genes not previously characterized as symbiosis determinants of *V. fischeri*.

Identification of a novel symbiotic gene cluster

We further characterized these novel colonization-defective mutants by examining the number and location of the Tn insertions by Southern analysis, cloning and sequencing. Each of the four mutant strains contained a single Tn insertion (data not shown; see *Experimental procedures*). Each insertion mapped to a distinct and previously uncharacterized gene within a cluster of 21 genes oriented in the same direction on chromosome 2 of *V. fischeri* (Fig. 2).

BLAST analyses (Altschul *et al*., 1990; 1997) and motif searches (Marchler-Bauer and Bryant, 2004) indicated that many of the genes in this cluster exhibited weak similarities to those involved in lipopolysaccharide (LPS), capsule or polysaccharide biosynthesis or export (Table 1). Six predicted proteins exhibited sequence similarities to glycosyltransferases, enzymes that transfer a sugar moiety from an activated donor (typically nucleotide sugar derivatives) to a specific acceptor (Kikuchi *et al*., 2003; Zhang *et al*., 2003). Target acceptors could be a growing carbohydrate chain of LPS, capsule or glycoproteins (Upreti *et al*., 2003). In addition, four genes were predicted to encode regulatory proteins such as two-component regulators. Based on these and other analyses (see below), we designated the genes in this locus as *syp*, for symbiosis polysaccharide.

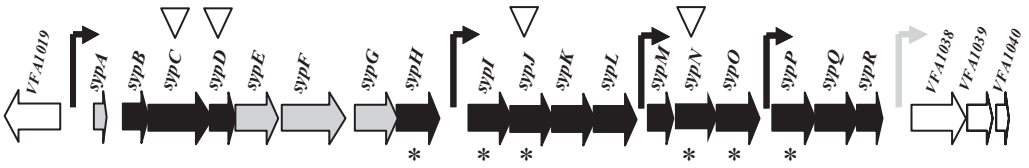

Fig. 2. Schematic representation of the *syp* cluster. Each gene in the *syp* cluster is represented by a block arrow. Grey arrows indicate genes with predicted regulatory function and solid arrows indicate genes with similarity to those involved in polysaccharide biosynthesis. Genes that encode putative glycosyltransferases are indicated by asterisks. Open arrows indicate genes flanking the *syp* cluster (*VFA1019* and *VFA1038–1040*). Bent black arrows indicate promoter sequences containing putative σ^{54} binding sites. The grey line arrow indicates a potential promoter region. Inverted triangles indicate transposon insertions.

To verify the importance of the *syp* cluster, we constructed derivatives of the wild-type strain, ES114, with mutations in this region. We cloned internal portions of specific genes into a suicide vector and introduced the constructs into *V. fischeri*. The resulting insertional mutants were confirmed by Southern analysis (see *Experimental procedures*). The ability of each mutant to initiate symbiotic colonization was compared with that of the wild-type strain. We used *sypN* as a control for this approach, as this gene was disrupted in one of the original Tn mutants and thus was not expected to colonize successfully. Indeed, like the original mutant, the insertional mutant of *sypN* colonized poorly (Fig. 3). Similarly, mutations in *sypL*, *sypO*, *sypP*, *sypQ* and *sypR* resulted in substantial defects (more than three orders of magnitude) in symbiotic colonization. In contrast, mutations in two downstream genes, *VFA1038* (Fig. 2; Table 1) and *VFA1043* (a putative ABC transporter), did not affect colonization of *V. fischeri* cells (Fig. 3). These data supported our hypothesis that this region functions in symbiotic colonization and suggested that the *syp* cluster does not extend to *VFA1038* or beyond.

Identification of Syp homologues in related Vibrio *species*

Significant similarities of the Syp proteins to others in the database were largely limited to predicted proteins found in two marine pathogens, *V. parahaemolyticus* (Makino *et al.*, 2003) and *V. vulnificus* (Chen *et al.*, 2003). Further analysis using the TIGR database (http://

Table 1. Putative functions of the *V. fischeri* Syp proteins and VFA1038–1040.

Syp	VFA[a]	RPS-BLAST[b]	E-value
A	1020	Sulphate transporter and anti-sigma factor antagonist	7e-11
B	1021	Outer membrane protein and related peptidoglycan-associated (lipo) proteins	2e-19
C	**1022**	**Wza, periplasmic protein involved in polysaccharide export**	4e-16
D	**1023**	**Mrp, ATPases involved in chromosome partitioning**	1e-11
E	1024	Response regulator receiver domain	3e-21
		Sigma factor PP2C-like phosphatases	4e-13
F	1025	Signal transduction histidine kinase	3e-41
		Response regulator receiver domain	1e-24
G	1026	Sigma-54 interaction domain	3e-84
		Response regulator receiver domain	1e-22
		HTH_8, bacterial regulatory protein, Fis family	1e-05
H	1027	Glycosyl transferases group 1	2e-22
I	1028	Glycosyl transferases group 1	5e-27
J	**1029**	**Glycosyl transferases group 1**	3e-09
K	1030	RfbX, membrane protein involved in the export of O-antigen and teichoic acid	5e-12
L	1031	RfaL, lipid A core-O-antigen ligase and related enzymes	1e-07
M	1032	WbbJ, acetyltransferase (isoleucine patch superfamily)	3e-19
N	**1033**	**RfaG, Glycosyltransferase**	1e-08
O	1034	GumC, uncharacterized protein involved in exopolysaccharide biosynthesis	3e-15
P	1035	RfaG, glycosyltransferase	4e-27
Q	1036	Glycosyltransferase, probably involved in cell wall biogenesis	2e-21
R	1037	WczJ, sugar transferase involved in lipopolysaccharide synthesis	1e-53
	1038	EAL domain	1e-61
		DUF1, domain of unknown function with GGDEF motif	3e-09
	1039	COG3310, uncharacterized protein conserved in bacteria	1e-67
	1040	Glutaredoxin	8e-06

a. The transposons inserted into *sypC*, *sypD*, *sypJ* and *sypN*, shown in bold.
b. Protein sequences were submitted to BLASTP. The most significant matches over the length of the protein are listed, along with the *e*-value to the motif. No conserved domains were noted for VFA1019. The alignments spanned over 70% of the protein sequence for all of the Syp proteins, except SypJ (51.7%).

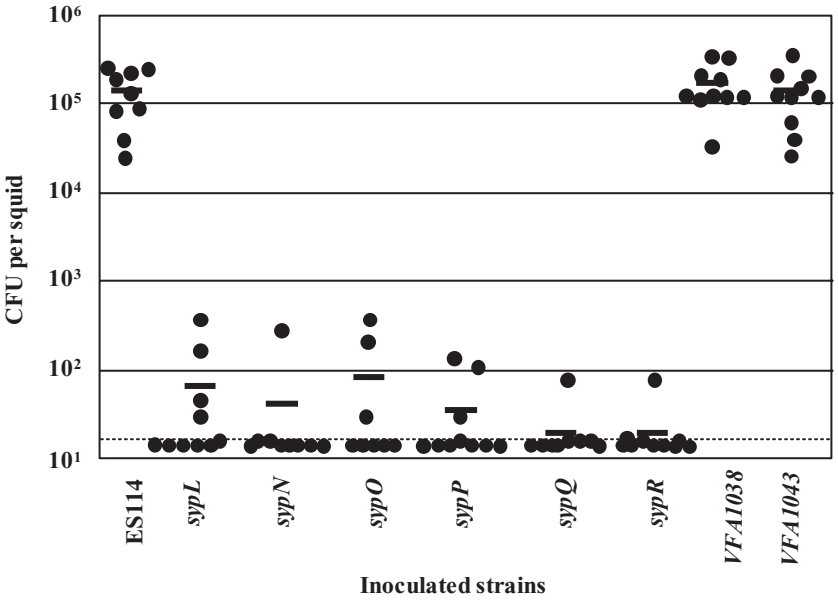

Fig. 3. Colonization by insertional mutants. Juvenile squid were inoculated for 3 h with approximately 2300–5000 cfu ml^{-1} of the wild-type strain, ES114, or insertional mutants defective for *syp* or downstream genes (*VFA1038* and *VFA1043*) (strains KV1816–18, KV1837–41). Animals were homogenized at ~18 h post inoculation for cfu determination. Each solid circle represents an individual animal and the bar represents the average of 10 (*sypL*, *sypP*, *sypQ*, *sypR*, *VFA1038* and *VFA1043*), nine (ES114 and *sypN*) or eight animals (*sypO*). The dotted line represents the limit of detection.

www.tigr.org/) revealed that homologues of almost all of the *syp* genes were present and similarly clustered in the above pathogens but not in *Vibrio cholerae* (Heidelberg *et al*., 2000) (Table S1). The *syp* cluster was located on the small chromosome of *V. fischeri*, but on the larger of two chromosomes in both *V. parahaemolyticus* and *V. vulnificus* (Chen *et al*., 2003; Makino *et al*., 2003; Ruby *et al*., 2005).

The three genes (*VFA1038–1040*) immediately downstream of the *syp* cluster, although apparently conserved in *V. parahaemolyticus*, *V. vulnificus* and *V. cholerae* (Table S1), were not found in proximity to the other 18 genes in these organisms. The lack of clustering of the *VFA1038–1040* homologues in *V. parahaemolyticus* and *V. vulnificus* suggests that these genes may not contribute to the function of this locus. This hypothesis is supported by our observation that a mutant defective for *VFA1038* is not deficient for colonization. Therefore, at this time, we designate only first 18 genes of the *V. fischeri* cluster as *syp*. Similarly, a homologue of *VFA1019*, the gene immediately upstream of and transcribed divergently to the cluster genes, exists in *V. parahaemolyticus* ($e = 1.2e^{-298}$) and potentially in *V. vulnificus* ($e = 1.9e^{-22}$); however, these genes were unlinked to the respective clusters. Our preliminary data suggested that this gene also is not required for colonization (B.T. Grublesky and K.L. Visick, unpublished data).

In *V. fischeri*, the G+C content of the *syp* cluster genes ranged from 34% to 42% and averaged 37.6%, a value similar to the overall G+C content of *V. fischeri* genome (38.85%). For *V. parahaemolyticus* and *V. vulnificus*, the values of the *syp* homologues also reflected that of the average G+C content. Thus, the *syp* cluster does not appear to represent an 'island'.

Transcriptional regulation of syp *genes by SypG and* σ^{54}

Nine of the open reading frames in the *syp* cluster appear to overlap their upstream neighbours, suggesting that these genes may be co-ordinately regulated. Close examination revealed larger gaps (~140 bp to 400 bp) between four sets of genes within the cluster as well as between *sypA* and the divergent gene *VFA1019* (Fig. 2). We examined these five intergenic regions and found four potential promoters that could be recognized by RNA polymerase containing the alternative sigma factor, σ^{54} (Fig. 4A). Unlike other sigma factors, σ^{54} recognizes sequences at positions –24 and –12 relative to the transcriptional start site. The consensus sequence of the σ^{54} binding site (mrNrYTGGCACG-N4-TTGCWNNw) is well conserved in a number of organisms (Barrios *et al*., 1999). The most important nucleotides in the consensus sequence (GG-N10-GC) (Barrios *et al*., 1999) are absolutely conserved at three of the four predicted promoters in the cluster (Fig. 4A).

Transcription by σ^{54}-containing RNA polymerase requires an interaction with an activator protein, often a response regulator whose ability to promote transcription is limited to specific environmental or cellular conditions. Sequence analysis of the *syp* cluster revealed a putative σ^{54}-dependent response regulator, SypG. This putative regulator was highly conserved in *V. parahaemolyticus*, *V. vulnificus* and *V. cholerae* (Table S1). Using Multiple Em for Motif Elicitation (MEME) analysis (see *Experimental procedures*), we identified a conserved 22 bp sequence in each of the four intergenic regions, upstream of the putative σ^{54} binding site (Fig. 4A). This sequence could potentially serve as a binding site for an activator. Both the putative σ^{54} binding sites and 22 bp sequences also

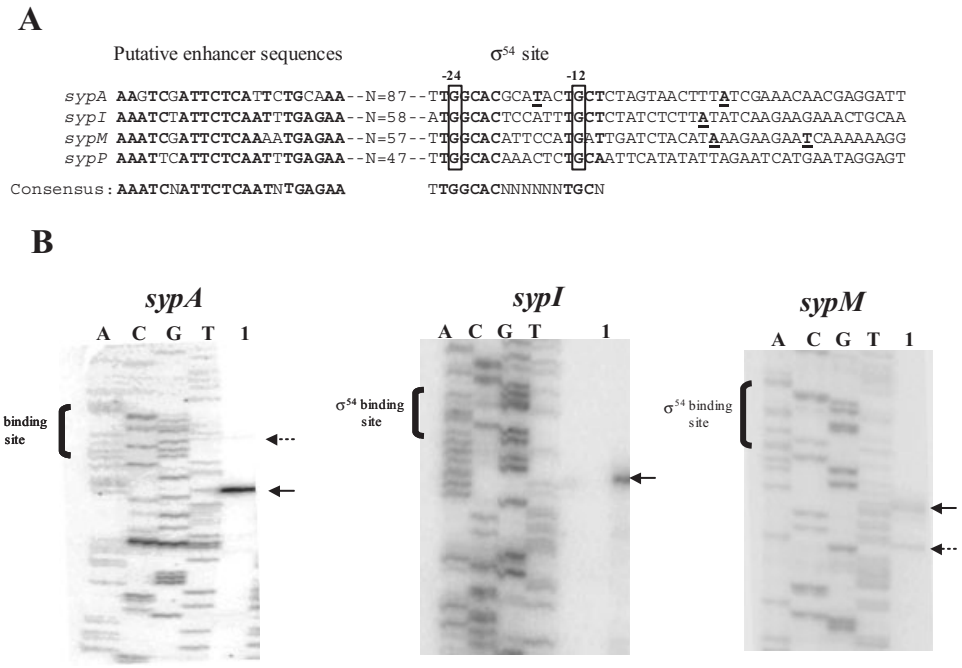

Fig. 4. Primer extension-based mapping of the transcriptional start sites of *sypA*, *sypI* and *sypM* genes.
A. Putative σ^{54} binding sites and potential enhancer binding sequences identified upstream of *sypA*, *sypI*, *sypM* and *sypP* are indicated. Conserved bases (three of four identical) are shown in bold. The –24 and –12 nucleotides of the predicted σ^{54} binding sites are boxed. The transcriptional start sites of each gene, based on primer extension experiments (B), are shown in bold and underlined.
B. Primer extension products obtained for transcripts initiating upstream of *sypA*, *sypI* and *sypM* are shown in lane 1 of the indicated panel. Bold line arrows indicate primer extension products predicted to be derived from the upstream σ^{54}-based promoter, while dashed line arrows indicate products from as yet undetermined sources. Lanes labelled A, C, G and T represent bands obtained from DNA sequencing reactions using the same primers.

are conserved in *V. parahaemolyticus* and *V. vulnificus* (data not shown).

To investigate the transcriptional control of the *syp* cluster, we used as reporter strains two of the Tn mutants, *sypD* and *sypN*, each of which contained a promoterless *lacZ* gene oriented correctly for *syp*-dependent transcription. Surprisingly, we observed no β-galactosidase activity from these strains under a variety of media and growth conditions (data not shown). We therefore hypothesized that SypG, in concert with σ^{54}, might control transcription of the *syp* genes in *V. fischeri*. Although response regulators typically depend on activation (by phosphorylation) from cognate sensor kinases, this requirement often can be overridden by multicopy expression of the response regulator. Thus, to investigate our hypothesis, we cloned a wild-type copy of *sypG* under the control of the *lac* promoter on a multicopy plasmid. We then introduced the resulting construct, pEAH40, into the Tn*10lacZ* reporter strains and observed the formation of blue colonies on X-gal-containing media, suggesting that SypG could induce *syp* transcription. We quantified this induction by measuring β-galactosidase activity, and found that multicopy expression of *sypG* increased the activity 37- to 70-fold over that of the vector control (Fig. 5). To determine whether the ability of SypG to induce *syp* transcription required the activity of σ^{54}, as predicted, we constructed double mutants (containing a mutation in *rpoN* and the *lacZ* reporter in either *sypD* or *sypN*). Indeed, a mutation in *rpoN* abolished the SypG-dependent activation of *syp* transcription (Fig. 5). These data suggest that SypG activates *syp* cluster expression in a σ^{54}-dependent manner.

Finally, to provide further support for the use of the identified σ^{54} binding sites, we determined the transcriptional start sites for *sypA*, *sypI* and *sypM* using primer extension experiments. Briefly, mRNA, isolated from wild-type cells containing multicopy *sypG*, was hybridized to a radiolabelled primer complementary to the gene of interest and subjected to reverse transcription. The resulting cDNA product was compared with a sequencing ladder (Fig. 4B). This analysis revealed two *sypA*-specific transcripts, with the primary band located 14 bp downstream from the putative σ^{54} binding site. Similarly, a *sypI* transcript initiated 12 bp downstream of the putative σ^{54} binding site. Finally, one of the *sypM* transcripts initiated at 13 bp downstream of the binding site. As these transcripts initiated within the range of start sites (8–16 bp) typical for σ^{54}-dependent transcription (Barrios *et al.*, 1999), these

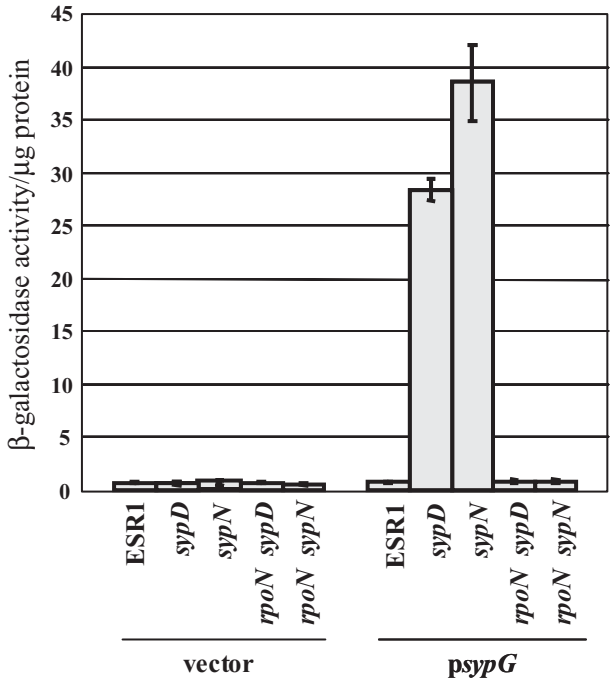

Fig. 5. Transcription of the *syp* genes. All strains were cultured in MM with shaking for 24 h before assaying activity. β-Galactosidase activity was measured in parent or *rpoN* mutant strains that contained a promoterless *lacZ* fusion to *sypD* or *sypN*. These strains also carried either the vector control or the *sypG*-expressing multicopy plasmid, pEAH40. As a control, β-galactosidase activity in parent strain, ESR1, which lacks a *lacZ* fusion, also was measured.

data further support a role for σ^{54} in promoting transcription of the *syp* genes.

Formation of biofilms under syp*-inducing conditions*

In nature, bacteria often exist in biofilms in which bacterial cells are embedded within a matrix of extracellular polysaccharides. Due to the putative functions of the *syp* genes in polysaccharide biosynthesis, we hypothesized that the *syp* cluster may function to alter the surface properties of *V. fischeri* to enhance biofilm formation. We therefore asked whether *syp* cluster members contributed to biofilm formation by *V. fischeri*. Not surprisingly, given the lack of *syp* transcription in culture, we noticed little difference in biofilm formation between the *syp* mutant strains and their parent when grown in static culture (data not shown). However, the addition of the *sypG* multicopy plasmid caused a significant, 3.5-fold, increase ($P = 0.0041$) in the ability of the parent strain, ESR1, to produce a biofilm in static culture (Fig. 6A and C). The *sypG*-expressing plasmid caused a similar increase in biofilm formation in all of the *syp* mutants except *sypC*, suggesting that *sypC* plays role in enhancing biofilm formation. Finally, consistent with our β-galactosidase results, a mutation in *rpoN* eliminated the *sypG*-dependent induction of biofilm formation, further supporting the roles of these two regulators in controlling the *syp* cluster.

During the course of our β-galactosidase experiments, we observed that cells containing multicopy *sypG*, when grown with shaking, produced a substantial ring of cells around the test tube. This large biofilm ring seemed inconsistent with the relatively modest increase in biofilm production we observed using the static culture assay. We therefore examined biofilms formed by these strains during growth with shaking. We found that these conditions dramatically increased the magnitude of the *sypG*- and *rpoN*-dependent biofilm formation (Fig. 6B and D). The parent strain containing multicopy *sypG* exhibited a >30-fold increase relative to the vector control and a > 12-fold increase relative to that achieved under static conditions. This increase in stainable material stemmed from an increase in adherent cells: we observed a 7.8-fold increase of adherent cells when they contained the *sypG* plasmid, relative to the vector control. Among *syp* mutant strains, biofilms of the *sypC*, and to a lesser extent, *sypJ*, mutants were substantially reduced relative to their parent strain. In contrast, mutants defective for *sypD* or *sypN* exhibited biofilm formation similar to that of the parent strain. Finally, the formation of biofilms under these conditions depended on a functional copy of *rpoN*. These data further demonstrate the dependence of *syp* biofilm formation on SypC, SypG and σ^{54}, and provide an *in vitro* function for the *syp* cluster members.

Discussion

Identification of a novel cluster that is required for symbiotic colonization

In this study, we identified four Tn mutants of *V. fischeri* that exhibited severe defects in initiating symbiotic colonization of *E. scolopes*. The Tns in the four strains mapped to four genes within a cluster of genes, termed *syp*, that encodes proteins with putative functions in LPS or capsule biosynthesis. Our investigations of these mutants in culture revealed no defects in traits known to be important for symbiotic colonization, including motility and luminescence. Insertional mutations in five other genes within this locus similarly caused severe initiation defects, supporting the hypothesis that this locus represents a novel gene cluster that functions in symbiotic initiation.

Transcriptional control of the syp *genes*

Two of the *syp* mutants contained insertions in which a promoterless *lacZ* reporter was oriented correctly for *syp*-dependent transcription. Surprisingly, we observed no β-galactosidase activity under any of a variety of media and growth conditions. Through a bioinformatics approach, we

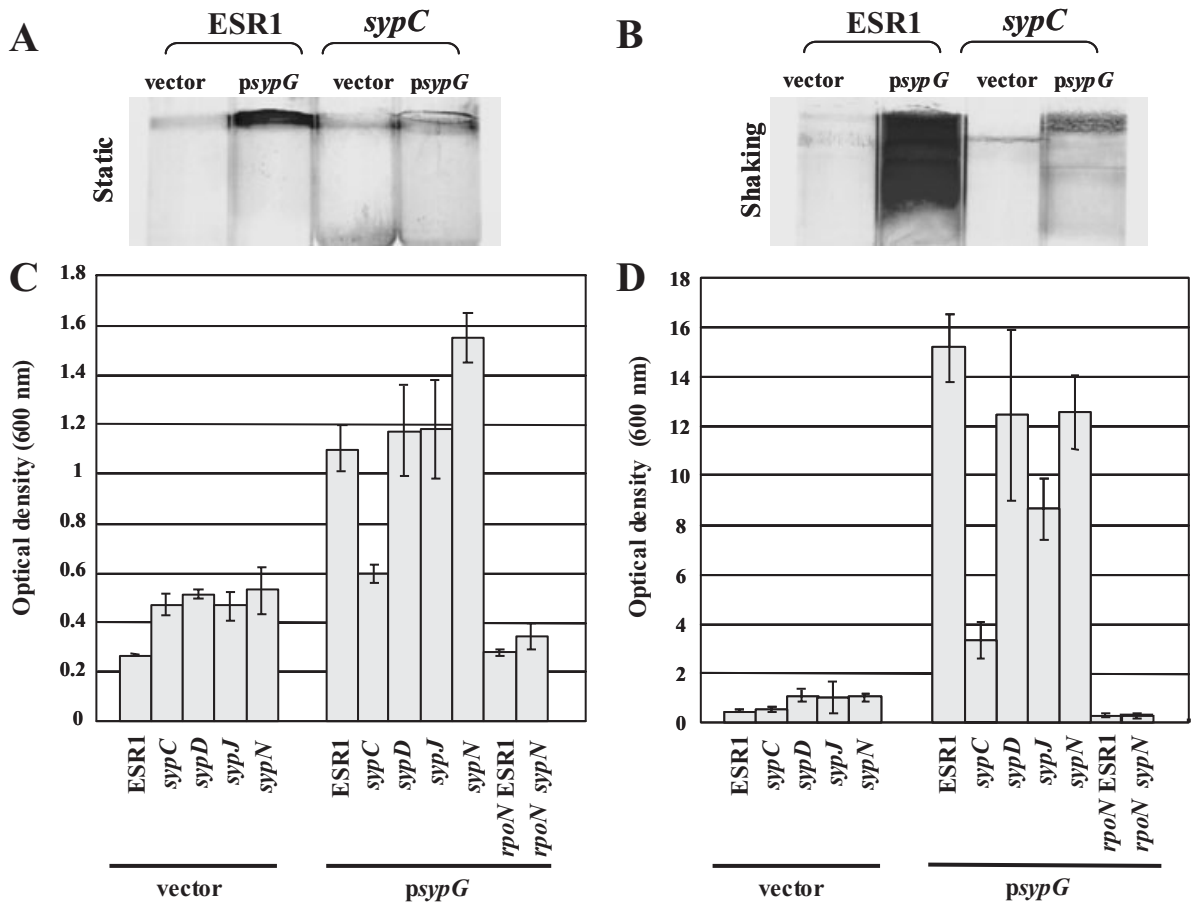

Fig. 6. Biofilm formation by *syp* mutants and their parent. Biofilm formation by parent strain ESR1, the transposon mutants and *rpoN* mutants was determined by growing strains in MM either statically for 30 h (A and C) or with shaking for 24 h (B and D). Biofilms on the surface of the test tubes were visualized by crystal violet staining (A and B), and quantified by measuring the absorbance at 600 nm of ethanol-solubilized crystal violet (C and D). Note that scale of *y*-axis in (D) is different from that of (C).

identified both SypG, a putative σ^{54}-dependent transcriptional activator encoded by the *syp* cluster, and potential binding sites for RNA polymerase carrying σ^{54}. Multicopy expression of *sypG* induced transcription of the two *lacZ* reporters (in *sypD* and *sypN*) by 37- to 70-fold. This induction depended on σ^{54}, as mutations in *rpoN* abolished β-galactosidase activity by these strains. Similarly, multicopy expression of *sypG* in a wild-type strain resulted in *sypA*, *sypI* and *sypM* transcripts that initiated between 12 and 14 based downstream of putative σ^{54} consensus sequences, a common range of initiation sites for such promoters (Barrios *et al.*, 1999). In addition, in preliminary experiments, we have fused the putative *sypP* promoter region to the *lacZ* reporter, introduced it in single copy in the chromosome, and similarly observed a *sypG*-dependent induction of transcription (E.A. Hussa and K.L. Visick, unpubl. data). Together, these data support the existence of multiple operons within *syp* that depend on both SypG and σ^{54}.

Control by σ^{54}-containing RNA polymerase is an effective method for keeping transcription turned off: because the σ^{54}-bound RNA polymerase fails to promote transcription without the aid of a regulatory protein, transcription of target genes is largely off until the appropriate, activated transcription factor binds and interacts with the polymerase. For *syp*, this presumably occurs through the binding of the two-component response regulator, SypG, to its target, perhaps the conserved 22 bp sequence we identified in four intergenic regions. We postulate that a colonization signal transduced by a sensor kinase activates SypG and turns on *syp* transcription to permit symbiotic initiation. A sensitive assay for gene expression in the host, such as recombination-based *in vivo* expression technology (RIVET) (Camilli and Mekalanos, 1995; Angelichio and Camilli, 2002), will be needed to determine whether the *syp* genes are induced early in symbiotic colonization. Consistent with the predicted importance of *sypG* in colonization, our preliminary results suggest that a *sypG* mutant initiates colonization poorly (E.A. Hussa, T. O'Shea and K.L. Visick, unpubl. data).

If SypG functions as a response regulator that is activated during symbiotic colonization, then what is the identity of its cognate sensor kinase? Sensor kinases typically detect a particular environmental signal and respond by autophosphorylating and subsequently serving as a phospho-donor to a response regulator. Just upstream of *sypG* are two additional putative two-component regulator genes: *sypE*, which likely encodes a response regulator, and *sypF*, which encodes a putative sensor kinase. The SypF sensor could potentially function with SypG, or, alternatively, with both SypE and SypG in a complex phosphorelay such as that which controls capsule biosynthesis in *Escherichia coli* (the *rcs* system) (Takeda *et al*., 2001). Another possibility is the sensor kinase, RscS, that we have previously identified as essential for symbiotic initiation (Visick and Skoufos, 2001). The *rscS* gene is not located within the *syp* cluster, and to date, we have not identified its cognate response regulator nor any members of its regulon. Clear identification of the cognate sensor kinase for SypG may require simulation of the host conditions that induce *syp* transcription, or the construction of constitutively active sensor kinase genes.

Role for SypG in promoting biofilm formation

We found that multicopy expression of *sypG* substantially enhanced biofilm formation by *V. fischeri*. Biofilms, dynamic mixtures of cells encased within an extracellular matrix, are being intensively studied in part due to their importance in medicine (Parsek and Singh, 2003; Parsek and Fuqua, 2004). Work in other organisms has shown that the biofilm structures formed by a single organism may vary substantially depending on the exact environmental condition, perhaps due to the environment-specific expression of factors that contribute to the extracellular matrix. For example, experiments in *Pseudomonas aeruginosa* indicate that decreased oxygen availability is a factor in robust biofilm formation (Yoon *et al*., 2002). Our studies in *V. fischeri* revealed that multicopy *sypG* expression enhanced biofilm formation to a greater extent when the cells were grown with shaking, relative to static growth. We thus hypothesize that aeration plays a role in biofilm formation under these conditions. Alternatively, it is possible that another difference between the two conditions, such as fluid distribution, which plays a role in *Bordetella* biofilms (Mishra *et al*., 2005), or the relative amounts of cell growth, accounts for the differences observed. Future work will address these possibilities.

Multicopy *sypG* expression also substantially increased biofilm formation by mutants defective for *sypD*, *sypJ* and *sypN*, but not *sypC*. Multiple explanations are possible. For example, SypG could control a locus, in addition to *syp*, that promotes biofilm formation. Alternatively, SypG-mediated overexpression of *sypC*, which encodes a protein with similarity to those involved in capsule export (KpsD, OtnA and Wza) (Bik *et al*., 1996; Arrecubieta *et al*., 2001; Nesper *et al*., 2003), could result in inappropriate export of a biofilm-promoting factor. It is also possible that the *syp* genes encode redundant functions with respect to biofilm formation, and thus multiple mutations are necessary to counteract the effect of multicopy *sypG*. Regardless of the explanation, these data make it clear that, in contrast to what has been assumed from this and previous studies of biofilm formation by wild-type strains (Wolfe *et al*., 2004), *V. fischeri* is not a poor biofilm former; rather, like pathogenic bacteria, this symbiont can produce substantial biofilms, under the appropriate conditions.

Function of the syp *gene cluster*

Our biofilm results suggest that, under conditions in which the *syp* genes are expressed, *V. fischeri* cells are producing an extracellular matrix that enables them to adhere to a glass surface and, perhaps, to a host tissue. The tentative functional assignments for Syp proteins in capsule, exopolysaccharide or LPS synthesis, macromolecules that contribute to biofilm formation by other bacteria, are consistent with that hypothesis. Our studies to date have yielded no differences in the overall carbohydrate levels produced by multicopy *sypG* or vector containing cells (E.S. Yip and K.L. Visick, unpubl. data). This result is similar to recent studies of *P. aeruginosa psl* (polysaccharide synthesis locus) – a locus that, like *syp*, contains multiple putative glycosyltransferase genes (Frideman and Kolter, 2004; Jackson *et al*., 2004; Matsukawa and Greenberg, 2004): a comparison of matrix carbohydrate levels in a *psl* mutant relative to the wild-type strain revealed similar overall yields (Matsukawa and Greenberg, 2004). Mutations in the *psl* locus result in an altered carbohydrate composition; this could potentially be true for *syp* as well. Recently, we have identified another phenotype consistent with potential exopolysaccharide production: prolonged static growth of *V. fischeri* with multicopy *sypG* results in the formation of a pellicle at the air/liquid interface, a phenotype that we do not observe in cultures of wild-type or vector-control cells (E.S. Yip and K.L. Visick, unpublished). We anticipate that investigation of this pellicle will provide insights into the nature of the product of the *syp* cluster.

Homologues of syp *genes in related* Vibrio *species*

Our analysis of the *syp* gene cluster of *V. fischeri* revealed similar clusters, with the same gene order, in the related human pathogens, *V. parahaemolyticus* and *V. vulnificus*. Neither of these two species is competent to colonize *E. scolopes*, although at least one strain of *V. parahaemolyticus* can adhere to the surface of the squid light organ

(Nyholm *et al*., 2000). We speculate that the *syp* cluster may be used by all of these *Vibrio* species in the early stages of colonization with their hosts, either marine invertebrates, or, potentially, human hosts. If so, then comparative studies of the three loci will aid our understanding of such bacteria–host interactions. Although there is high overall conservation, a number of individual genes exhibit significant sequence divergence; these differences could potentially account for the observed differences in host range. Further study of the role and regulation of the *syp* cluster may enhance our knowledge not only of the communication between *V. fischeri* and its symbiotic host but also of the signals and responses leading to initiation of pathogenic associations.

Experimental procedures

Bacterial strains and media

Vibrio fischeri strains used in this study are listed in Table 2. Strain ES114 (Boettcher and Ruby, 1990) was used as the wild-type strain, and ESR1, a rifampin-resistant (Rif^R) derivative of ES114 (Graf *et al*., 1994), was used as the parent

Table 2. Strains and plasmids used or constructed in this study.

	Genotype or characteristics	Reference
Strains		
E. coli		
DH5α	*endA1 hsdR17* (r_K^- m_K^+) *glnV44 thi-1 recA1 gyrA* (Nal^r) *relA* Δ(*lacIZYA-argF*)*U169 deoR* [φ80 *dlac*Δ(*lacZ*)M15]	Woodcock *et al*. (1989)
CC118λ*pir*	Δ(*ara-leu*) *araD* Δ*lacX74 galE galK phoA20 thi-1 rpsE rpoB argE* (Am) *recA1* λ*pir*	Herrero *et al*. (1990)
V. fischeri		
ES114	Wild type	Boettcher and Ruby (1990)
ESR1	Rif^R derivative of ES114	Graf *et al*. (1994)
KV1601	ESR1 *sypN*::Tn*10lacZ*	This study
KV1635	ESR1 *sypD*::Tn*10lacZ*	This study
KV1636	ESR1 *sypJ*::Tn*10lacZ*	This study
KV1637	ESR1 *sypC*::Tn*10lacZ*	This study
KV1816	ES114 *sypP*::pESY9	This study
KV1817	ES114 *VFA1038*::pESY10	This study
KV1818	ES114 *VFA1043*::pESY11	This study
KV1837	ES114 *sypL*::pTMB53	This study
KV1838	ES114 *sypN*::pTMB54	This study
KV1839	ES114 *sypO*::pTMB55	This study
KV1840	ES114 *sypQ*::pTMB56	This study
KV1841	ES114 *sypR*::pTMB57	This study
KV2080	ESR1 *rpoN*::pESY17	This study
KV2082	KV1601 *rpoN*::pESY17	This study
KV2083	KV1635 *rpoN*::pESY17	This study
Plasmids	Characteristics or construction	
pCR2.1-TOPO	commercial cloning vector; Amp^R, Kan^R	Invitrogen
pEAH40	pKV69 (BamHI/SphI) + 3.3 kb *sypG*$^+$ fragment; Tet^R	This study
pESY9	pKV194 (EcoRI) + 389 bp internal fragment of *sypP*; Cm^R	This study
pESY10	pKV194 (EcoRI) + 307 bp internal fragment of *VFA1038*; Cm^R	This study
pESY11	pKV194 (EcoRI) + 254 bp internal fragment of *VFA1043*; Cm^R	This study
pESY16	pKV194 (SmaI) + 252 bp XbaI/HindIII fragment from pLD1 (Wolfe *et al*., 2004) containing internal fragment of *rpoN*; Cm^R	This study
pESY17	pESY16 (MluI) + 1.2 kb fragment encoding Em^R from pKV168	This study
pEVS104	Conjugal helper plasmid (*tra trb*); Kan^R	Stabb and Ruby (2002)
pEVS122	R6Kγ *oriV*, *oriT*RP4, Em^R, *lacZα*, *cosN, loxP, incD*	Dunn *et al*. (2005)
pKV69	Mobilizable vector; Tet^R, Cm^R	Visick and Skoufos (2001)
pKV124	Mini-Tn*10lacZ* delivery plasmid	Visick and Skoufos (2001)
pKV168	Vector containing a 1.2 kb fragment encoding Em^R	Visick and Ruby (1998)
pKV189	pCR2.1-TOPO + 1.8 kb fragment of *VFA1019-sypA* intergenic DNA	This study
pKV190	pCR2.1-TOPO + 294 bp fragment of *sypH-sypI* intergenic DNA	This study
pKV191	pCR2.1-TOPO + 398 bp fragment of *sypL-sypM* intergenic DNA	This study
pKV194	1.4 kb BamHI/SacI fragment from pKV124 + 1.6 kb SspI/XmnI fragment from pEVS122; Cm^R, *oriR6K, oriT, lacZ*	This study
pTMB53	pEVS122 (EcoRI) + 386 bp internal fragment of *sypL*; Em^R	This study
pTMB54	pEVS122 (EcoRI) + 406 bp internal fragment of *sypN*; Em^R	This study
pTMB55	pEVS122 (EcoRI) + 375 bp internal fragment of *sypO*; Em^R	This study
pTMB56	pEVS122 (EcoRI) + 364 bp internal fragment of *sypQ*; Em^R	This study
pTMB57	pEVS122 (EcoRI) + 341 bp internal fragment of *sypR*; Em^R	This study

Amp^R, ampicillin resistance; Cm^R, chloramphenicol resistance; Em^R, erythromycin resistance; Kan^R, kanamycin resistance; Tet^R, tetracycline resistance.

strain in Tn mutagenesis and mutant analyses. *E. coli* strains DH5α and CC118*λpir* (Herrero *et al*., 1990) were used as hosts for cloning and conjugation. *V. fischeri* strains were grown on SWT medium (0.5% tryptone, 0.3% yeast extract, 210 mM NaCl, 35 mM $MgSO_4$, 7 mM $CaCl_2$ and 7 mM KCl) for all colonization experiments and Hepes-minimal medium (MM) (Ruby and Nealson, 1977) supplemented with 0.2% glucose and 0.3% Casamino acids for β-galactosidase and biofilm experiments. For motility assays, *V. fischeri* cells were spotted on tryptone-based soft agar medium containing 0.25% Bacto-Agar (Difco, Detroit, MI). Antibiotics were added to media, where appropriate, to the following final concentrations: ampicillin (Amp), 100 μg ml^{-1} for *E. coli*; chloramphenicol (Cm), 25 μg ml^{-1} for *E. coli* and 2.5 μg ml^{-1} for *V. fischeri*; erythromycin (Em), 150 μg ml^{-1} for *E. coli* and 5 μg ml^{-1} for *V. fischeri*; tetracycline (Tet), 15 μg ml^{-1} for *E. coli* and 30 μg ml^{-1} for *V. fischeri*.

Plasmid and mutant constructions

Transposon mutagenesis was performed using the mini-Tn*10lacZ* delivery plasmid pKV124 (Visick and Skoufos, 2001). Cloning of the Tn and flanking DNA was carried out as described previously (Visick and Skoufos, 2001), using the origin of replication and Cm-resistance gene contained within the Tn. All plasmids were constructed using standard molecular biology techniques, with restriction and modifying enzymes from New England Biolabs (Beverly, MA) or Promega (Madison, WI). To construct *syp* and *rpoN* mutants of *V. fischeri*, we first amplified, by polymerase chain reaction (PCR), an internal fragment of specific genes using DNA oligonucleotides (Table S2) from MWG Biotech (High Point, NC). The PCR fragments were then cloned into cloning vector pCR2.1-TOPO (Invitrogen, Carlsbad, CA) and subcloned into one of two 'suicide' plasmids [pEVS122 (Dunn *et al*., 2005) or pKV194], which do not replicate but integrate into genomic DNA via homologous recombination between the inserted *V. fischeri* sequence and the chromosome. Triparental matings were performed and potential insertional mutants were selected on the appropriate antibiotic-containing plates.

Colonization assays

To screen for Tn mutants defective in colonizing the light organ, *V. fischeri* mutant strains were inoculated into artificial seawater (Instant Ocean; Aquarium Systems, Mentor, OH) containing individual newly hatched juvenile squid. After 3 h incubation, juvenile squid were washed and transferred to symbiont-free seawater. Colonization of the light organ was monitored by measuring luminescence over the course of 18 h in a scintillation counter as described previously (Ruby, 1996). To quantify the number of bacteria present in the light organ, juvenile squid were homogenized, serially diluted and plated on SWT agar. The limit of detection is 14 bacterial cells per squid.

Luminescence assays

ESR1 and the Tn mutants were diluted 1:100 from overnight cultures and grown in SWT/IO medium [0.5% tryptone, 0.3% yeast extract, 0.3% glycerol and 43 g l^{-1} Instant Ocean (Aquarium Systems) (Stabb *et al*., 2004)]. Samples were taken for luminescence and optical density measurements over the course of 4 h. A TD-20/20 luminometer (Turner Designs, Sunnyvale, CA) was used to determine the level of bioluminescence.

Protein analysis

To examine the outer membrane protein (OMP) profiles of the mutant strains, cellular protein extracts were obtained as described previously (Aeckersberg *et al*., 2001). Upon extraction, OMP-enriched fractions were separated by electrophoresis on a 8% SDS-polyacrylamide gel and visualized by staining with either Coomassie brilliant blue (Sigma, St Louis, MO) or SYPRO Red protein gel stain (Molecular Probes, Eugene, OR).

Southern blot analysis

We analysed both the original Tn mutants and our constructed insertional mutants by Southern blot experiments. Chromosomal DNA was extracted, digested and separated by a 0.6% agarose gel, transferred onto a nylon membrane (Hybond XL; Amersham-Pharmacia Biotech, Piscataway, NJ) and cross-linked using UV light. Detection of DNA fragments was performed by using the Boehringer Mannheim DIG DNA labelling kit (Roche Molecular Biochemicals, Indianapolis, IN) as previously described (Visick and Skoufos, 2001) using either Tn or vector probes. We found that all Tn mutant strains carried a single Tn insertion. The insertion in *sypC* also contained the delivery vector integrated into the chromosome at the site of the insertion. Similarly, for the ES114-derived *syp* insertional mutants, the resulting banding pattern showed that each contained a single insertion of suicide plasmid vector at the appropriate location in the chromosome.

Bioinformatics

In this work, we examined potential Syp function and searched for *syp* homologues using the sequence-based similarity searching methods, BLAST and RPS-BLAST (Altschul *et al*., 1990; 1997). To search for homologues in *V. parahaemolyticus*, *V. vulnificus* and *V. cholerae*, we submitted Syp protein sequences to the TIGR website (http://www.tigr.org/) which uses WU BLAST analysis (W. Gish, 1996–2003; available at: http://blast.wustl.edu). To search for σ^{54}-dependent promoter sequences and a potential enhancer consensus sequence, we used the PROMSCAN program (http://www.promscan.uklinux.net/home.html) and MEME (http://meme.sdsc.edu/meme/website/meme.html) respectively.

Primer extension

Twenty-five millilitres of cultures of strain ES114 containing either pEAH40 or pKV69 were grown in MM for 24 h at 28°C. The cells were lysed in GITCN lysis buffer (Totten and Lory, 1990), and mRNA was isolated by ultracentrifugation through

a cesium chloride gradient. Oligonucleotide primers (VFA1020PER, VFA1028PER and VFA1032PER; see Table S2) complementary to *sypA*, *sypI* and *sypM* sequences were radiolabelled via T4 polynucleotide kinase (USB) and [γ^{32}-P]-ATP (Amersham-Pharmacia Biotech, Piscataway, NJ). The labelled primers were hybridized to 32 μg of mRNA and incubated with Moloney murine leukaemia virus (MMLV) reverse transcriptase (Stratagene, LaJolla, CA) and nucleotides per the manufacturer's instructions. Primer extension products were visualized upon separation on a 6% polyacrylamide gel. To determine the start of transcription, the extension product was compared with a sequencing ladder generated from pKV189 (*sypA*), pKV190 (*sypI*) or pKV191 (*sypM*) using Sequenase Version 2.0 DNA Sequencing Kit (USB) with the same primer used for the primer extension.

β-Galactosidase measurements

To measure the expression of *syp* genes, Tn reporter strains which carried either pKV69 or pEAH40 were grown in MM with shaking for 24 h; β-galactosidase activity was measured as described (Miller, 1972). Total protein concentrations were determined by the method of Lowry *et al*. (1951). All experiments were performed in triplicate.

Biofilm assays

To quantify biofilm formation, we used methods modified from Djordjevic *et al*. (2002). Briefly, all *V. fischeri* strains were grown in triplicate in MM. Overnight cultures were diluted to an optical density at 600 nm (OD_{600}) ~0.1 and then incubated in test tubes with and without shaking for 24 and 30 h respectively. We quantified biofilm by adding 1 ml of 1% crystal violet to each culture. After 30 min of staining, all liquid was removed from the tubes and each was rinsed 10 times with dH_2O. Tubes were then dried by aspiration and 4 ml of 100% ethanol was added to each for destaining. Samples were destained for 1 h with vortexing every 15 min. Each crystal violet-containing sample was diluted, if necessary, and quantified by measuring its absorbance at OD_{600}. In parallel, samples were grown over the same time-course, vortexed and the optical density was determined to assess growth of the strains. Under these experimental conditions, strains containing multicopy *sypG* exhibited a decreased growth yield (and increased biofilm formation) relative to vector controls. Statistical analysis was performed using the Student's *t*-test.

To quantify viable cells within biofilms we inoculated cells as described above to generate biofilms in triplicate. After incubation, we removed the liquid from the culture without staining and rinsed tubes with 70% artificial seawater (Instant Ocean; Aquarium Systems, Mentor, OH) 10 times each. We then added 3 ml of 70% artificial seawater to each tube and 1 mm glass beads. After 15 min of incubation with vortexing every 5 min, we plated dilutions of biofilm material and calculated viable cell recovery.

Acknowledgements

We would like to thank Eric Stabb for generous donation of plasmid vectors in advance of publication and Therese O'Shea for the construction of *syp* mutant plasmids. We also thank Kati Geszvain, Therese O'Shea, Jon Visick and Alan Wolfe for their insightful experimental suggestions and critical review of the article. This work was supported by NIH Grant GM59690 awarded to K.L.V.

References

Aeckersberg, F., Lupp, C., Feliciano, B., and Ruby, E.G. (2001) *Vibrio fischeri* outer membrane protein OmpU plays a role in normal symbiotic colonization. *J Bacteriol* **183:** 6590–6597.

Altschul, S.F., Gish, W., Miller, W., Myers, E.W., and Lipman, D.J. (1990) Basic local alignment search tool. *J Mol Biol* **215:** 403–410.

Altschul, S.F., Madden, T.L., Schaffer, A.A., Zhang, J., Zhang, Z., Miller, W., and Lipman, D.J. (1997) Gapped BLAST and PSI-BLAST: a new generation of protein database search programs. *Nucleic Acids Res* **25:** 3389–3402.

Angelichio, M.J., and Camilli, A. (2002) *In vivo* expression technology. *Infect Immun* **70:** 6518–6523.

Arrecubieta, C., Hammarton, T.C., Barrett, B., Chareonsudjai, S., Hodson, N., Rainey, D., and Roberts, I.S. (2001) The transport of group 2 capsular polysaccharides across the periplasmic space in *Escherichia coli*. Roles for the KpsE and KpsD proteins. *J Biol Chem* **276:** 4245–4250.

Barrios, H., Valderrama, B., and Morett, E. (1999) Compilation and analysis of sigma(54)-dependent promoter sequences. *Nucleic Acids Res* **27:** 4305–4313.

Bik, E.M., Bunschoten, A.E., Willems, R.J., Chang, A.C., and Mooi, F.R. (1996) Genetic organization and functional analysis of the *otn* DNA essential for cell-wall polysaccharide synthesis in *Vibrio cholerae* O139. *Mol Microbiol* **20:** 799–811.

Boettcher, K.J., and Ruby, E.G. (1990) Depressed light emission by symbiotic *Vibrio fischeri* of the sepiolid squid *Euprymna scolopes*. *J Bacteriol* **172:** 3701–3706.

Camilli, A., and Mekalanos, J.J. (1995) Use of recombinase gene fusions to identify *Vibrio cholerae* genes induced during infection. *Mol Microbiol* **18:** 671–683.

Chen, C.Y., Wu, K.M., Chang, Y.C., Chang, C.H., Tsai, H.C., Liao, T.L., *et al.* (2003) Comparative genome analysis of *Vibrio vulnificus*, a marine pathogen. *Genome Res* **13:** 2577–2587.

Davidson, S.K., Koropatnick, T.A., Kossmehl, R., Sycuro, L., and McFall-Ngai, M.J. (2004) NO means 'yes' in the squid–vibrio symbiosis: nitric oxide (NO) during the initial stages of a beneficial association. *Cell Microbiol* **6:** 1139–1151.

DeLoney, C.R., Bartley, T.M., and Visick, K.L. (2002) Role for phosphoglucomutase in *Vibrio fischeri–Euprymna scolopes* symbiosis. *J Bacteriol* **184:** 5121–5129.

Djordjevic, D., Wiedmann, M., and McLandsborough, L.A. (2002) Microtiter plate assay for assessment of *Listeria monocytogenes* biofilm formation. *Appl Environ Microbiol* **68:** 2950–2958.

Dunn, A.K., Martin, M.O., and Stabb, E.V. (2005) Characterization of pES213, a small mobilization plasmid from *Vibrio fischeri*. *Plasmid* (in press).

Foster, J.S., and McFall-Ngai, M.J. (1998) Induction of apo-

ptosis by cooperative bacteria in the morphogenesis of host epithelial tissues. *Dev Genes Evol* **208:** 295–303.

Foster, J.S., Apicella, M.A., and McFall-Ngai, M.J. (2000) *Vibrio fischeri* lipopolysaccharide induces developmental apoptosis, but not complete morphogenesis, of the *Euprymna scolopes* symbiotic light organ. *Dev Biol* **226:** 242–254.

Frideman, L., and Kolter, R. (2004) Genes involved in matrix formation in *Pseudomonas aeruginosa* PA14 biofilms. *Mol Microbiol* **51:** 675–690.

Graf, J., and Ruby, E.G. (1998) Host-derived amino acids support the proliferation of symbiotic bacteria. *Proc Natl Acad Sci USA* **95:** 1818–1822.

Graf, J., and Ruby, E.G. (2000) Novel effects of a transposon insertion in the *Vibrio fischeri glnD* gene: defects in iron uptake and symbiotic persistence in addition to nitrogen utilization. *Mol Microbiol* **37:** 168–179.

Graf, J., Dunlap, P.V., and Ruby, E.G. (1994) Effect of transposon-induced motility mutations on colonization of the host light organ by *Vibrio fischeri*. *J Bacteriol* **176:** 6986–6991.

Heidelberg, J.F., Eisen, J.A., Nelson, W.C., Clayton, R.A., Gwinn, M.L., Dodson, R.J., *et al.* (2000) DNA sequence of both chromosomes of the cholera pathogen *Vibrio cholerae*. *Nature* **406:** 477–483.

Herrero, M., DeLorenzo, V., and Timmis, K.N. (1990) Transposon vectors containing non-antibiotic resistance selection markers for cloning and stable chromosomal insertion of foreign genes in gram-negative bacteria. *J Bacteriol* **172:** 6557–6567.

Jackson, K.D., Starkey, M., Kremer, S., Parsek, M.R., and Wozniak, D.J. (2004) Identification of *psl*, a locus encoding a potential exopolysaccharide that is essential for *Pseudomonas aeruginosa* PAO1 biofilm formation. *J Bacteriol* **186:** 4466–4475.

Kikuchi, N., Kwon, Y.D., Gotoh, M., and Narimatsu, H. (2003) Comparison of glycosyltransferase families using the profile Hidden Markov Model. *Biochem Biophys Res Comm* **310:** 574–579.

Kimbell, J.R., and McFall-Ngai, M.J. (2004) Symbiont-induced changes in host actin during the onset of a beneficial animal–bacterial association. *Appl Environ Microbiol* **70:** 1434–1441.

Lowry, O.H., Rosebrough, N.J., Farr, A.L., and Randall, R.J. (1951) Protein measurement with the Folin phenol reagent. *J Biol Chem* **193:** 265–275.

Lupp, C., and Ruby, E.G. (2004) *Vibrio fischeri* LuxS and AinS: comparative study of two signal synthases. *J Bacteriol* **186:** 3873–3881.

Lupp, C., and Ruby, E.G. (2005) *Vibrio fischeri* utilizes two quorum-sensing systems for the regulation of early and late colonization factors. *J Bacteriol* **187:** 3620–3629.

Lupp, C., Urbanowski, M., Greenberg, E.P., and Ruby, E.G. (2003) The *Vibrio fischeri* quorum-sensing systems *ain* and *lux* sequentially induce luminescence gene expression and are important for persistence in the squid host. *Mol Microbiol* **50:** 319–331.

Makino, K., Oshima, K., Kurokawa, K., Yokoyama, K., Uda, T., Tagomori, K., *et al.* (2003) Genome sequence of *Vibrio parahaemolyticus*: a pathogenic mechanism distinct from that of *V. cholerae*. *Lancet* **361:** 743–749.

Marchler-Bauer, A., and Bryant, S.H. (2004) CD-Search: protein domain annotations on the fly. *Nucleic Acids Res* **32:** W327–W331.

Matsukawa, M., and Greenberg, E.P. (2004) Putative exopolysaccharide synthesis genes influence *Pseudomonas aeruginosa* biofilm. *J Bacteriol* **186:** 4449–4456.

Miller, J.H. (1972) *Experiments in Molecular Genetics.* Cold Spring Harbor, NY: Cold Spring Harbor Laboratory Press.

Millikan, D.S., and Ruby, E.G. (2002) Alterations in *Vibrio fischeri* motility correlate with a delay in symbiosis initiation and are associated with additional symbiotic colonization defects. *Appl Environ Microbiol* **68:** 2519–2528.

Millikan, D.S., and Ruby, E.G. (2003) FlrA, a sigma54-dependent transcriptional activator in *Vibrio fischeri*, is required for motility and symbiotic light-organ colonization. *J Bacteriol* **185:** 3547–3557.

Mishra, M., Parise, G., Jackson, K.D., Wozniak, D.J., and Deora, R. (2005) The BvgAS signal transduction system regulates biofilm development in *Bordetella*. *J Bacteriol* **187:** 1474–1484.

Montgomery, M.K., and McFall-Ngai, M. (1993) Embryonic development of the light organ of the sepiolid squid *Euprymna scolopes*. *Berry Biol Bull* **184:** 296–308.

Nesper, J., Hill, C., Paiment, A., Harauz, G., Beis, K., Naismith, J., and Whitfield, C. (2003) Translocation of group 1 capsular polysaccharide in *Escherichia coli* serotype K30. *J Biol Chem* **278:** 49763–49772.

Nyholm, S.V., and McFall-Ngai, M.J. (2003) Dominance of *Vibrio fischeri* in secreted mucus outside the light organ of *Euprymna scolopes*: the first site of symbiont specificity. *Appl Environ Microbiol* **69:** 3932–3937.

Nyholm, S.V., and McFall-Ngai, M. (2004) The winnowing: establishing the squid–*Vibrio* symbiosis. *Nat Rev Microbiol* **2:** 632–642.

Nyholm, S.V., Stabb, E.V., Ruby, E.G., and McFall-Ngai, M.J. (2000) Establishment of an animal–bacterial association: recruiting symbiotic *Vibrios* from the environment. *Proc Natl Acad Sci USA* **97:** 10231–10235.

Parsek, M.R., and Singh, P.K. (2003) Bacterial biofilms: an emerging link to disease pathogenesis. *Annu Rev Microbiol* **57:** 677–701.

Parsek, M.R., and Fuqua, C. (2004) Biofilms 2003: emerging themes and challenges in studies of surface-associated microbial life. *J Bacteriol* **186:** 4427–4440.

Reitzer, L., and Schneider, B.L. (2001) Metabolic context and possible physiological themes of sigma(54)-dependent genes in *Escherichia coli*. *Microbiol Mol Biol Rev* **65:** 422–444.

Ruby, E.G. (1996) Lessons from a cooperative, bacterial–animal association: the *Vibrio fischeri–Euprymna scolopes* light organ symbiosis. *Annu Rev Microbiol* **50:** 591–624.

Ruby, E.G. (1999) The *Euprymna scolopes–Vibrio fischeri* symbiosis: a biomedical model for the study of bacterial colonization of animal tissue. *J Mol Microbiol Biotechnol* **1:** 13–21.

Ruby, E.G., and Asato, L.M. (1993) Growth and flagellation of *Vibrio fischeri* during initiation of the sepiolid squid light organ symbiosis. *Arch Microbiol* **159:** 160–167.

Ruby, E.G., and Nealson, K.H. (1977) Pyruvate production and excretion by the luminous marine bacteria. *Appl Environ Microbiol* **34:** 164–169.

Ruby, E.G., Urbanowski, M., Campbell, J., Dunn, A., Faini, M., Gunsalus, R., *et al.* (2005) Complete genome sequence of *Vibrio fischeri*: a symbiotic bacterium with pathogenic congeners. *Proc Natl Acad Sci USA* **102:** 3004–3009.

Stabb, E.V., and Ruby, E.G. (2002) New RP4-based plasmids for conjugation between *Escherichia coli* and members of the Vibrionaceae. *Methods Enzymol* **358:** 413–426.

Stabb, E.V., Butler, M.S., and Adin, D.M. (2004) Correlation between osmolarity and luminescence of symbiotic *Vibrio fischeri* strain ES114. *J Bacteriol* **186:** 2906–2908.

Takeda, S., Fujisawa, Y., Matsubara, M., Aiba, H., and Mizuno, T. (2001) A novel feature of the multistep phosphorelay in *Escherichia coli*: a revised model of the RcsC $\rightarrow$ YojN $\rightarrow$ RcsB signalling pathway implicated in capsular synthesis and swarming behaviour. *Mol Microbiol* **40:** 440–450.

Totten, P.A., and Lory, S. (1990) Characterization of the type a flagellin gene from *Pseudomonas aeruginosa* PAK. *J Bacteriol* **172:** 7188–7199.

Upreti, R.K., Kumar, M., and Shankar, V. (2003) Bacterial glycoproteins: functions, biosynthesis and applications. *Proteomics* **3:** 363–379.

Visick, K.L., and Ruby, E.G. (1998) The periplasmic, group III catalase of *Vibrio fischeri* is required for normal symbiotic competence and is induced both by oxidative stress and by approach to stationary phase. *J Bacteriol* **180:** 2087–2092.

Visick, K.L., and Skoufos, L.M. (2001) Two-component sensor required for normal symbiotic colonization of *Euprymna scolopes* by *Vibrio fischeri*. *J Bacteriol* **183:** 835–842.

Visick, K.L., Foster, J., Doino, J., McFall-Ngai, M., and Ruby, E.G. (2000) *Vibrio fischeri lux* genes play an important role in colonization and development of the host light organ. *J Bacteriol* **182:** 4578–4586.

Whistler, C.A., and Ruby, E.G. (2003) GacA regulates symbiotic colonization traits of *Vibrio fischeri* and facilitates a beneficial association with an animal host. *J Bacteriol* **185:** 7202–7212.

Wolfe, A.J., Millikan, D.S., Campbell, J.M., and Visick, K.L. (2004) *Vibrio fischeri* σ^{54} controls motility, biofilm formation, luminescence, and colonization. *Appl Environ Microbiol* **70:** 2520–2524.

Woodcock, D.M., Crowther, P.J., Doherty, J., Jefferson, S., DeCruz, E., Noyer-Weidner, M., *et al.* (1989) Quantitative evaluation of *Escherichia coli* host strains for tolerance to cytosine methylation in plasmid and phage recombinants. *Nucleic Acids Res* **17:** 3469–3478.

Yoon, S.S., Hennigan, G.M., Hilliard, G.M., Ochsner, U.A., Parvatiyar, K., Kamani, M.C., *et al.* (2002) *Pseudomonas aeruginosa* anaerobic respiration in biofilms: relationships to cystic fibrosis pathogenesis. *Dev Cell* **3:** 593–603.

Zhang, Z., Kochhar, S., and Grigorov, M. (2003) Exploring the sequence-structure protein landscape in the glycosyltransferase family. *Protein Sci* **12:** 2291–2302.

Supplementary material

The following supplementary material is available for this article online:

Table S1. Conservation of the *syp* cluster and flanking genes among sequenced *Vibrio* strains.

Table S2. Oligonucleotides used in this study.

V. fischeri ES114 chromosome 2

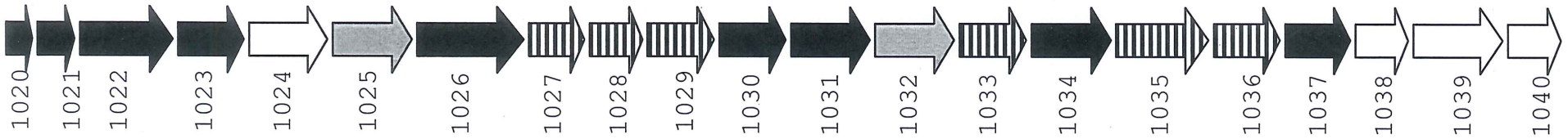

V. vulnificus CMCP6 chromosome 1

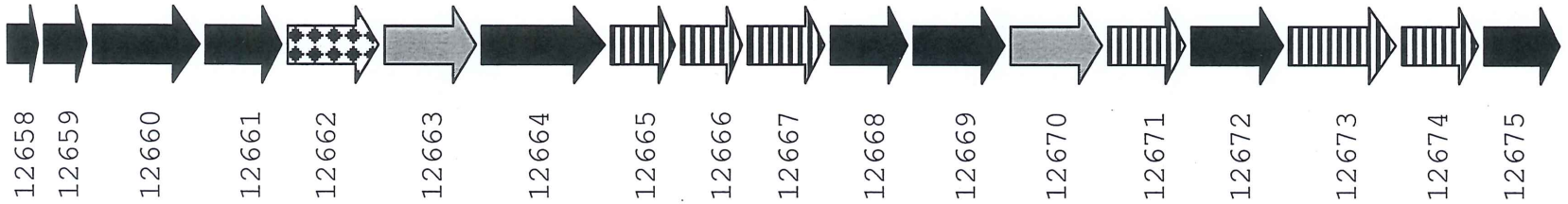

V. parahaemolyticus RIMD 2210633 chromosome 1

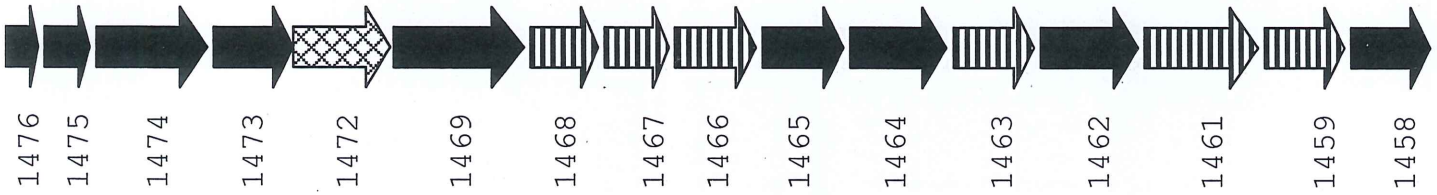

Table S1. Conservation of the *syp* cluster and flanking genes among sequenced *Vibrio* strains.*

syp	*V. fischeri*	*V. parahaemolyticus*	e-value	*V. vulnificus*	e-value	*V. cholerae*	e-value
	VFA1019	VPA1172	1.2e-198	VV13143	1.9e-22	VC2612	0.28
A	VFA1020	**VP1476**	2.3e-30	**VV12658**	2.1e-27	VCA1087	3.6e-06
B	VFA1021	**VP1475**	2.9e-71	**VV12659**	8.7e-70	VC1835	5.7e-11
C	VFA1022	**VP1474**	8.5e-246	**VV12660**	2.0e-262	**VC0936**	1.1e-06
D	VFA1023	**VP1473**	2.3e-39	**VV12661**	4.5e-34	**VC0937**	0.088
E	VFA1024	VPA0148	2.4e-12	VV12140	3.7e-12	VC1719	8.1e-14
F	VFA1025	VPA1130	2.3e-93	**VV12663**	5.0e-154	VC2453	3.4e-64
G	VFA1026	**VP1469**	6.3e-179	**VV12664**	5.4e-180	VC1021	1.7e-126
H	VFA1027	**VP1468**	5.8e-73	**VV12665**	1.1e-64	**VC0925**	8.7e-09
I	VFA1028	**VP1467**	2.5e-79	**VV12666**	1.3e-66	VC0259	2.5e-18
J	VFA1029	**VP1466**	6.3e-60	**VV12667**	5.4e-70	VC0511	0.098
K	VFA1030	**VP1465**	3.1e-67	**VV12668**	3.1e-65	**VC0921**	1.2e-07
L	VFA1031	**VP1464**	1.1e-126	**VV12669**	6.2e-124	VC1244	6.2e-124
M	VFA1032	VP1758	1.2e-15	**VV12670**	1.2e-51	VCA0473	2.0e-13
N	VFA1033	**VP1463**	1.6e-102	**VV12671**	1.4e-91	VC0862	0.7
O	VFA1034	**VP1462**	1.2e-120	**VV12672**	1.4e-117	VC0057	0.0068
P	VFA1035	**VP1461**	2.7e-91	**VV12673**	2.1e-84	**VC0925**	6.1e-13
Q	VFA1036	**VP1459**	1.5e-99	**VV12674**	2.1e-100	VC1052	0.56
R	VFA1037	**VP1458**	8.5e-72	**VV12675**	7.6e-71	**VC0934**	1.9e-26
	VFA1038	VPA0869	1.4e-149	VV20264	1.0e-155	VCA0785	2.7e-143
	VFA1039	VP1314	2.3e-78	VV12779	4.9e-76	VC1619	1.8e-75
	VFA1040	VP1317	7.6e-32	*VV12776*	7.5e-32	VC1616	3.1e-32

*We used *V. fischeri* protein sequences to search the TIGR Web site (http://www.tigr.org/) for homologs in *V. parahaemolyticus* (VP) , *V. vulnificus* (VV) , and *V. cholerae* (VC). Gene numbers shown in bold represent genes that are closely linked to one another in that organism (not in bold-face for *V. fischeri*). Note that *V. cholerae* gene *VC0925* is listed twice. This gene exhibits weak sequence similarity to both *sypH* and *sypP*. For each organism, the letter A in the gene name represents genes found on chromosome 2, while its absence reflects genes found on chromosome 1.

Table S2. Oligonucleotides used in this study.

Primer	Gene	Sequence
VFA1019 intR	*VFA1019*	TTTTTCGTACGTGATGGGAAATGACGTTGTG
VFA1020PER	*sypA*	CCGATGGCGTCCATATCAC
VFA1028PER	*sypI*	GGTATTTCTGATGGTTGATGC
5147 (SacI)	*sypJ*	AAAAAGAGCTCGTCTGCTTATCAAATTTAATTTG
ORF1031F	*sypL*	AAACACGACAATGGGTTACAGC
ORF1031R	*sypL*	TGAAATACTCAATGGCTAAAGGATG
VFA1031-RTF	*sypL*	GTTAATGGGAACCATAGTATCG
VFA1032PER	*sypM*	GGCGAGGAGTTGGCAACTC
ORF1033F	*sypN*	TTACGCCAACCTCGCTTCTC
ORF1033R	*sypN*	GTAACTCTTTACTGGCGGCTAGG
ORF1034F	*sypO*	TGCCTTTTATTGGACTGACTGTTG
ORF1034R	*sypO*	TGTTCAGTAAAATGACGGCTCAC
3642F	*sypP*	GTCCAACACCTTTCACCTG
3642R	*sypP*	GACAGAGAAAGAGCAAATCG
VFA1035PER	*sypP*	CTCCAACATATCTAATACCATAC
ORF1036F	*sypQ*	GCTGGTTTGCTTCTCGTCAC
ORF1036R	*sypQ*	CAGAGCAATGACATCACTTGACTG
ORF1037F	*sypR*	GCGATTAAGTTAGATTCAAAAGGC
ORF1037R	*sypR*	CGGTAATACTCCATAAGTTCTTTCAC
3645F	*VFA1038*	GCCATCGACATTCCTGAAC
3645R	*VFA1038*	GCGGATAACACCCAATGG
3650F	*VFA1043*	GACCTTGCTTGCAGGATTGG
3650R	*VFA1043*	CTCGTCCAGACAGCCCAAC

JOURNAL OF BACTERIOLOGY, June 2005, p. 3603–3606 Vol. 187, No. 11
0021-9193/05/$08.00+0 doi:10.1128/JB.187.11.3603–3606.2005

GUEST COMMENTARY

Layers of Signaling in a Bacterium-Host Association

Karen L. Visick*

Department of Microbiology and Immunology, 2160 S. First Ave., Bldg. 105, Maywood, Illinois 60153

Quorum sensing, the monitoring of population density by bacteria, is used to coordinately control gene expression and therefore particular behaviors under conditions of high cell density. Such group behaviors provide advantages to organisms under certain conditions, such as during pathogenic colonization when virulence traits are induced by a group of bacteria. In the accompanying paper, Lupp and Ruby describe the requirement for a quorum-sensing system at relatively low cell density during colonization by *Vibrio fischeri* of its symbiotic host, *Euprymna scolopes* (18).

Quorum-sensing systems in *Vibrio fischeri* and *Vibrio harveyi*. Quorum sensing is a field built from laboratory-based investigations of luminous marine bacteria, namely, *Vibrio fischeri* and *Vibrio harveyi* (25). It was in *V. fischeri* that the quorum-sensing regulators LuxR (a transcriptional activator) and LuxI (a signal synthase) first were discovered (reviewed in reference 6). The LuxI-produced signaling molecule, an acyl homoserine lactone (acyl-HSL), diffuses out of and then (under conditions of high cell density) back into the cell, where it activates LuxR and thus the *lux* (luminescence) genes, which are under LuxR control (11, 14). Homologs of these proteins have been found in most gram-negative quorum-sensing bacteria studied to date.

Studies of quorum sensing in *V. harveyi* subsequently revealed a much more complex system for *lux* control (Fig. 1) (reviewed in reference 28). This organism uses three sensor kinase proteins to detect its three quorum-sensing molecules (one of which is an acyl-HSL) (1, 2, 13). At low cell density, the sensor proteins autophosphorylate. The phosphate is sequentially transferred to LuxU, a phosphotransferase protein, and LuxO, a transcriptional activator. Phosphorylated LuxO activates the transcription of five small RNA (sRNA) genes (16). The resulting sRNAs work in conjunction with the Hfq protein to destabilize the transcript encoding $LuxR_{VH}$, a transcriptional regulator that is not homologous to *V. fischeri* LuxR (16). The consequence is that $LuxR_{VH}$ is not synthesized, and thus the *lux* genes are not transcribed. Increasing population densities sequentially signal the three sensor proteins to switch from kinases to phosphatases. The consequence is dephosphorylation of LuxO, loss of sRNA synthesis, increased translation of LuxR, and thus transcription of *lux* and production of light.

For some time, it has been known that *V. fischeri* encodes a second acyl-HSL synthase, termed AinS (8). AinS is homologous to LuxM of *V. harveyi* yet produces a distinct acyl-HSL (8, 15). More recently, homologs of the other *V. harveyi* quorum-sensing components have been identified (Fig. 1) (7, 17, 19, 24). Although only a few of these components have been examined at a molecular level, the results to date suggest that this second *V. fischeri* system functions like that of *V. harveyi*. The *ain* system is integrated with the *lux* system at LitR, a $LuxR_{VH}$ homolog that is controlled by LuxO and itself controls transcription of *luxR* (Fig. 1) (7, 24), thereby controlling *lux* expression.

Roles for AinS and LuxO in symbiotic initiation. Lupp and Ruby report the novel finding that the acyl-HSL synthase AinS is required for initiation of symbiotic colonization of the squid *E. scolopes* by *V. fischeri* (18). Loss of *ainS* delayed both colonization and the luminescence emission that results from the symbiotic association (Fig. 2A). No such delay of colonization was observed for *lux* mutants, suggesting that AinS may control factors other than *lux* that are required for symbiotic initiation. Surprisingly, a mutation in *luxO*, which might be expected to counteract the consequences of an *ainS* mutation, also prevented normal symbiotic initiation. Together, these data suggested that an optimal level of AinS/LuxO-controlled (non-*lux*) target gene transcription is necessary for symbiotic initiation.

To identify potential AinS-controlled genes, Lupp and Ruby used microarray analysis (the first such published for the recently sequenced *V. fischeri* [27]). Their screen yielded 30 positively and negatively controlled genes, including, notably, negatively controlled motility genes (18). The effect of the AinS signal on motility was supported experimentally by the finding that the *ainS* mutant migrated through soft agar faster than the wild-type strain. Is the increase in motility sufficient to account for the colonization defect? Perhaps. Previous work has demonstrated that motility is essential for symbiotic colonization: nonmotile bacteria fail to colonize, while hypermotile mutants exhibit a severe delay (9, 22). Interestingly, a *luxO* mutant also displayed a defect in motility, in this case a decreased rate of migration through soft agar. These data support the idea that mutations in *ainS* and *luxO* can differentially unbalance regulation of a downstream target. Besides motility genes, however, there were a number of other, equally interesting, targets identified that could be the cause of the initiation defect observed and which will presumably be the focus of future investigations.

Sequential activation of two quorum-sensing systems. In laboratory culture, induction of *lux* depends primarily upon *ainS*. Whereas *luxI* mutants exhibit near-wild-type levels of light emission, no luminescence can be detected from *ainS* mutants (19, 29). During symbiotic colonization, the opposite is true: *luxI* mutants fail to produce any detectable light, while

* Mailing address: Department of Microbiology and Immunology, 2160 S. First Ave., Bldg. 105, Maywood, IL 60153. Phone: (708) 216-0869. Fax: (708) 216-0896. E-mail: kvisick@lumc.edu.

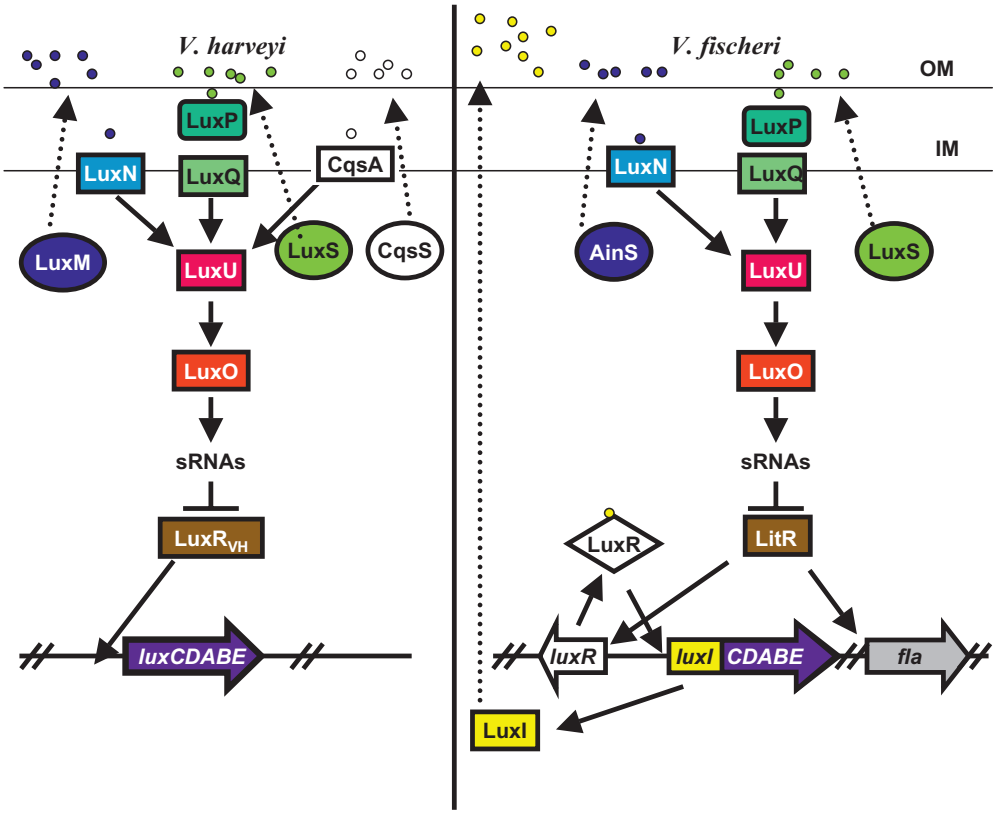

FIG. 1. A comparison of the *V. harveyi* and *V. fischeri* quorum-sensing systems. Parts of the pathway in *V. fischeri* are modeled after those described for *V. harveyi* and are described further in the text. The colors reflect proteins that are homologous between the two species. The acyl-HSL synthases are depicted as ovals. Although the *V. fischeri* AinS and LuxS proteins are homologous to LuxM and LuxS of *V. harveyi*, the acyl-HSL signaling molecules (represented by small circles) produced by the different bacteria are distinct. It is not known whether sRNAs are involved in bioluminescence control in *V. fischeri*. OM, outer membrane; IM, inner membrane.

ainS mutants exhibit only a small decrease in light. These data led Lupp and Ruby to suggest a model in which the AinS signal promotes luminescence at low cell densities, which occur in culture and the early stages of symbiotic colonization; their results that *ainS*, but not *luxI*, is required for initiation support this low cell density role for AinS. At higher cell densities, which occur in the symbiotic light organ, LuxI produces the signal necessary for high-level light production.

Colonization by *V. fischeri* occurs in a series of stages that occur immediately after hatching of the juvenile squid (Fig. 2) (reviewed in reference 26). First, *V. fischeri* cells in the seawater aggregate in mucus on the surface of the symbiotic (light) organ (Fig. 2A). Next, after a short period of time, during which signaling likely occurs between the bacteria themselves (as suggested by the results of Lupp and Ruby) as well as between the bacteria and their host, motile bacteria migrate into the light organ. After entry into nutrient-rich crypts, the bacteria begin to multiply to high cell density, induce the *lux* genes, and lose their flagella (Fig. 2B). The last stage, termed persistence, occurs once the animals are fully colonized (Fig. 2C). This stage requires the adaptation of the microbe to a changing environment: certain host developmental events are triggered by the bacteria, including an increase in size of the epithelial cells lining the bacterium-containing crypts. Furthermore, 90% of *V. fischeri* cells are expelled each morning, while the remaining 10% regrow to high cell density.

At the persistence stage of colonization, mutants defective for one of the quorum regulators, *luxR* and *luxI*, or the LuxR/I target gene, *luxA* (encoding one subunit of the luciferase enzyme), fail to achieve the same levels of colonization (regrowth) as the wild-type strain (29) (Fig. 2C). Furthermore, normal host development requires *luxA*, as *luxA* mutants fail to induce the typical epithelial cell swelling (29). It is not yet understood how the function (or lack thereof) of this quorum-sensing-controlled gene is communicated to the host.

Lupp et al. (19) previously reported that the acyl-HSL synthase AinS is similarly required for symbiotic persistence (Fig. 2C). Whereas mutations in *luxI* abolish symbiotic bioluminescence, mutations in *ainS* only slightly decrease light levels. Thus, although the colonization defect of the *luxI* mutant can be attributed to control of *lux* transcription, it is not clear that the same is true for the defect of the *ainS* mutant. Indeed, in culture, this mutant is unable to achieve the same growth yield as the wild-type strain, suggesting that an AinS-controlled factor other than *lux* may be involved in symbiotic persistence. The array experiments performed by Lupp and Ruby thus may also yield a (non-*lux*) factor required for symbiotic persistence as well. Taken together, these studies support sequential roles

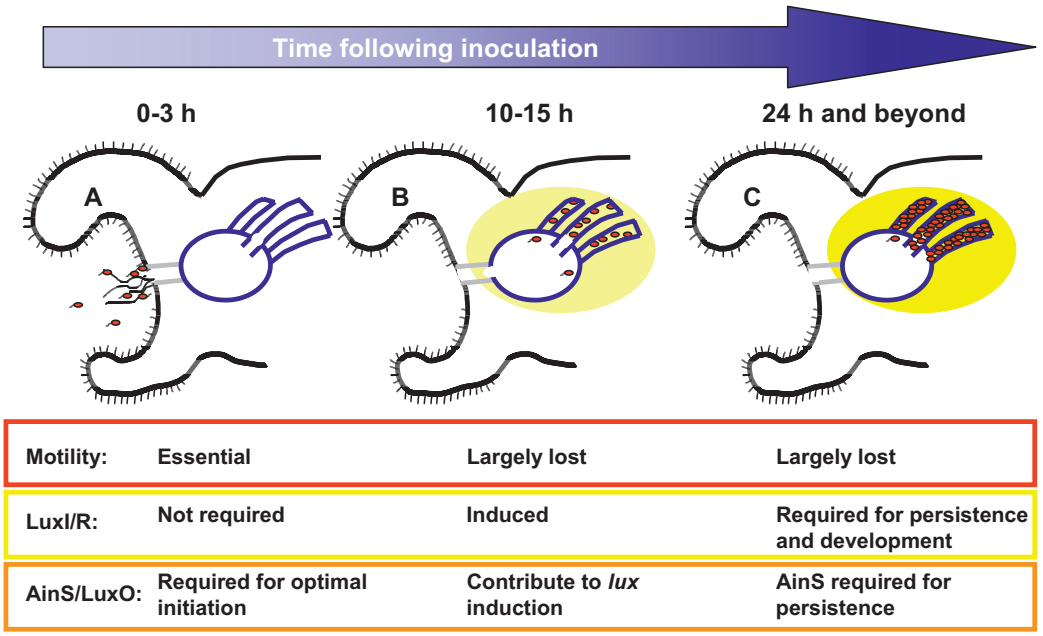

FIG. 2. Time course of bacterial colonization in the *V. fischeri-E. scolopes* symbiosis. Panels A to C depict a one side of the bilaterally symmetric light organ from juvenile *E. scolopes*, containing one of three crypts (outlined in blue). Each panel represents a different stage of symbiotic colonization. *V. fischeri* bacteria are shown as red ovals, with or without flagella. The yellow ovals surrounding the crypt spaces represent bioluminescence emission from the bacteria. The states of motility and of LuxI/R and AinS/LuxO activity are indicated below each stage. The cartoon reflects data reviewed in reference 26.

in symbiotic colonization for the AinS-produced signal (early control of a *lux*-independent target and later control of *lux* and/or a *lux*-independent target) and the LuxI-produced signal (later control of *lux*) (Fig. 2). Thus, it has been shown, for the first time, that sequential signaling by two acyl-HSLs occurs, and is important, during colonization of host tissue.

Quorum sensing in *Vibrio* spp. Although LuxI/LuxR homologs have been found in most gram-negative quorum-sensing organisms studied to date, homologs of the *V. harveyi* quorum-sensing components have been found only in other *Vibrio* species, including *V. cholerae* (10, 21, 30), *V. vulnificus* (3), *V. parahaemolyticus* (12, 20), *V. anguillarum* (4, 5, 23), and *V. fischeri* (17, 19). Of the four sequenced *Vibrio* species (*V. cholerae*, *V. parahaemolyticus*, *V. vulnificus*, and *V. fischeri*), only *V. fischeri* appears to encode both LuxR/LuxI- and LuxO-based systems of quorum sensing. Why are the vibrios distinct from other gram-negative bacteria in the mechanism by which quorum sensing occurs, and why does *V. fischeri* contain both systems? These questions await further study, including genomic sequencing of additional *Vibrio* strains (including other luminescent isolates), but insights into these questions may be gained from research into the roles of the two systems in *V. fischeri*.

In summary, this work represents an important leap forward in terms of elucidating factors necessary for the *V. fischeri*-squid symbiosis. Significantly, the dissection by Lupp and Ruby of the relative roles of two distinct quorum-sensing systems at specific stages of colonization, and in particular during an early, low-cell-density stage, provides important insights for the larger field of quorum sensing as well.

I am grateful to Emily Yip for her contribution to Fig. 2 and to Bonnie Bassler for her helpful comments.

Research on the *Vibrio fischeri-E. scolopes* symbiosis in the Visick lab is supported by NIH grant GM59690.

REFERENCES

1. **Bassler, B. L., M. Wright, R. E. Showalter, and M. R. Silverman.** 1993. Intercellular signalling in *Vibrio harveyi*: sequence and function of genes regulating expression of luminescence. Mol. Microbiol. **9:**773–786.
2. **Bassler, B. L., M. Wright, and M. R. Silverman.** 1994. Multiple signalling systems controlling expression of luminescence in *Vibrio harveyi*: sequence and function of genes encoding a second sensory pathway. Mol. Microbiol. **13:**273–286.
3. **Chen, C. Y., K. M. Wu, Y. C. Chang, C. H. Chang, H. C. Tsai, T. L. Liao, Y. M. Liu, H. J. Chen, A. B. Shen, J. C. Li, T. L. Su, C. P. Shao, C. T. Lee, L. I. Hor, and S. F. Tsai.** 2003. Comparative genome analysis of *Vibrio vulnificus*, a marine pathogen. Genome Res. **13:**2577–2587.
4. **Croxatto, A., V. J. Chalker, J. Lauritz, J. Jass, A. Hardman, P. Williams, M. Camara, and D. L. Milton.** 2002. VanT, a homologue of *Vibrio harveyi* LuxR, regulates serine, metalloprotease, pigment, and biofilm production in *Vibrio anguillarum*. J. Bacteriol. **184:**1617–1629.
5. **Croxatto, A., J. Pride, A. Hardman, P. Williams, M. Camara, and D. L. Milton.** 2004. A distinctive dual-channel quorum-sensing system operates in *Vibrio anguillarum*. Mol. Microbiol. **52:**1677–1689.
6. **Dunlap, P. V.** 1999. Quorum regulation of luminescence in *Vibrio fischeri*. J. Mol. Microbiol. Biotechnol. **1:**5–12.
7. **Fidopiastis, P. M., C. M. Miyamoto, M. G. Jobling, E. A. Meighen, and E. G. Ruby.** 2002. LitR, a new transcriptional activator in *Vibrio fischeri*, regulates luminescence and symbiotic light organ colonization. Mol. Microbiol. **45:** 131–143.
8. **Gilson, L., A. Kuo, and P. V. Dunlap.** 1995. AinS and a new family of autoinducer synthesis proteins. J. Bacteriol. **177:**6946–6951.
9. **Graf, J., P. V. Dunlap, and E. G. Ruby.** 1994. Effect of transposon-induced motility mutations on colonization of the host light organ by *Vibrio fischeri*. J. Bacteriol. **176:**6986–6991.
10. **Hammer, B. K., and B. L. Bassler.** 2003. Quorum sensing controls biofilm formation in *Vibrio cholerae*. Mol. Microbiol. **50:**101–104.
11. **Hanzelka, B. L., and E. P. Greenberg.** 1995. Evidence that the N-terminal region of the *Vibrio fischeri* LuxR protein constitutes an autoinducer-binding domain. J. Bacteriol. **177:**815–817.
12. **Henke, J. M., and B. L. Bassler.** 2004. Quorum sensing regulates type III

secretion in *Vibrio harveyi* and *Vibrio parahaemolyticus*. J. Bacteriol. **186:** 3794–3805.
13. **Henke, J. M., and B. L. Bassler.** 2004. Three parallel quorum-sensing systems regulate gene expression in *Vibrio harveyi*. J. Bacteriol. **186:**6902–6914.
14. **Kaplan, H. B., and E. P. Greenberg.** 1985. Diffusion of autoinducer is involved in regulation of the *Vibrio fischeri* luminescence system. J. Bacteriol. **163:**1210–1214.
15. **Kuo, A., N. V. Blough, and P. V. Dunlap.** 1994. Multiple *N*-acyl-L-homoserine lactone autoinducers of luminescence in the marine symbiotic bacterium *Vibrio fischeri*. J. Bacteriol. **176:**7558–7565.
16. **Lenz, D. H., K. C. Mok, B. N. Lilley, R. V. Kulkarni, N. S. Wingreen, and B. L. Bassler.** 2004. The small RNA chaperone Hfq and multiple small RNAs control quorum sensing in *Vibrio harveyi* and *Vibrio cholerae*. Cell **118:**69–82.
17. **Lupp, C., and E. G. Ruby.** 2004. *Vibrio fischeri* LuxS and AinS: comparative study of two signal synthases. J. Bacteriol. **186:**3873–3881.
18. **Lupp, C., and E. G. Ruby.** 2005. *Vibrio fischeri* uses two quorum-sensing systems for the regulation of early and late colonization factors. J. Bacteriol. **187:**3620–3629.
19. **Lupp, C., M. Urbanowski, E. P. Greenberg, and E. G. Ruby.** 2003. The *Vibrio fischeri* quorum-sensing systems *ain* and *lux* sequentially induce luminescence gene expression and are important for persistence in the squid host. Mol. Microbiol. **50:**319–331.
20. **Makino, K., K. Oshima, K. Kurokawa, K. Yokoyama, T. Uda, K. Tagomori, Y. Iijima, M. Najima, M. Nakano, A. Yamashita, Y. Kubota, S. Kimura, T. Yasunaga, T. Honda, H. Shinagawa, M. Hattori, and T. Iida.** 2003. Genome sequence of *Vibrio parahaemolyticus*: a pathogenic mechanism distinct from that of *V. cholerae*. Lancet **361:**743–749.
21. **Miller, M. B., K. Skorupski, D. H. Lenz, R. K. Taylor, and B. L. Bassler.** 2002. Parallel quorum sensing systems converge to regulate virulence in *Vibrio cholerae*. Cell **110:**303–314.
22. **Millikan, D. S., and E. G. Ruby.** 2002. Alterations in *Vibrio fischeri* motility correlate with a delay in symbiosis initiation and are associated with additional symbiotic colonization defects. Appl. Environ. Microbiol. **68:**2519–2528.
23. **Milton, D. L., A. Hardman, M. Camara, S. R. Chhabra, B. W. Bycroft, G. S. A. B. Stewart, and P. Williams.** 1997. Quorum sensing in *Vibrio anguillarum*: characterization of the *vanI*/*vanR* locus and identification of the autoinducer *N*-(3-oxodecanoyl)-L-homoserine lactone. J. Bacteriol. **179:**3004–3012.
24. **Miyamoto, C. M., P. V. Dunlap, E. G. Ruby, and E. A. Meighen.** 2003. LuxO controls *luxR* expression in *Vibrio harveyi*: evidence for a common regulatory mechanism in *Vibrio*. Mol. Microbiol. **48:**537–548.
25. **Nealson, K. H., and J. W. Hastings.** 1979. Bacterial bioluminescence: its control and ecological significance. Microbiol. Rev. **43:**496–518.
26. **Nyholm, S. V., and M. J. McFall-Ngai.** 2004. The winnowing: establishing the squid-*Vibrio* symbiosis. Nat. Rev. Microbiol. **2:**632–642.
27. **Ruby, E. G., M. Urbanowski, J. Campbell, A. Dunn, M. Faini, R. P. Gunsalus, P. Lostroh, C. Lupp, J. McCann, D. Millikan, A. Schaefer, E. Stabb, A. Stevens, K. Visick, C. Whistler, and E. P. Greenberg.** 2005. Complete genome sequence of *Vibrio fischeri*: a symbiotic bacterium with pathogenic congeners. Proc. Natl. Acad. Sci. USA **102:**3004–3009.
28. **Schauder, S., and B. L. Bassler.** 2001. The languages of bacteria. Genes Dev. **15:**1468–1480.
29. **Visick, K. L., J. Foster, J. Doino, M. McFall-Ngai, and E. G. Ruby.** 2000. *Vibrio fischeri lux* genes play an important role in colonization and development of the host light organ. J. Bacteriol. **182:**4578–4586.
30. **Zhu, J., M. B. Miller, R. E. Vance, M. Dziejman, B. L. Bassler, and J. J. Mekalanos.** 2002. Quorum-sensing regulators control virulence gene expression in Vibrio cholerae. Proc. Natl. Acad. Sci. USA **99:**3129–3134.

The views expressed in this Commentary do not necessarily reflect the views of the journal or of ASM.

JOURNAL OF BACTERIOLOGY, Mar. 2005, p. 2058–2065 Vol. 187, No. 6
0021-9193/05/$08.00+0 doi:10.1128/JB.187.6.2058–2065.2005

Magnesium Promotes Flagellation of *Vibrio fischeri*

Therese M. O'Shea,[1] Cindy R. DeLoney-Marino,[2] Satoshi Shibata,[3] Shin-Ichi Aizawa,[3] Alan J. Wolfe,[1] and Karen L. Visick[1]*

Department of Microbiology and Immunology, Loyola University Chicago, Maywood, Illinois[1]; Department of Biology, University of Southern Indiana, Evansville, Indiana[2]; and CREST, Japan Science and Technology Agency, Hirata, Takanezawa, Shioya-gun, Tochigi, Japan[3]

Received 30 November 2004/Accepted 1 December 2004

The bacterium *Vibrio fischeri* requires bacterial motility to initiate colonization of the Hawaiian squid *Euprymna scolopes*. Once colonized, however, the bacterial population becomes largely unflagellated. To understand environmental influences on *V. fischeri* motility, we investigated migration of this organism in tryptone-based soft agar media supplemented with different salts. We found that optimal migration required divalent cations and, in particular, Mg^{2+}. At concentrations naturally present in seawater, Mg^{2+} improved migration without altering the growth rate of the cells. Transmission electron microscopy and Western blot experiments suggested that Mg^{2+} addition enhanced flagellation, at least in part through an effect on the steady-state levels of flagellin protein.

The symbiosis between the marine bacterium *Vibrio fischeri* and the Hawaiian squid *Euprymna scolopes* provides a model for exploring the communication that occurs between a bacterium and its host in a natural setting (30, 39, 45, 55). Juveniles of *E. scolopes* hatch without *V. fischeri* cells present inside the symbiotic organ (the light organ), and rapidly acquire these bacteria from the surrounding seawater (31, 57). Colonization begins with aggregation of *V. fischeri* cells in mucus on the surface of the light organ (37, 38, 40), followed by movement of these bacteria through pores into ducts, apparently toxic passageways that limit nonspecific invaders (11, 40), and ultimately into crypts where the bacteria multiply (46).

Only motile cells of *V. fischeri* initiate symbiotic colonization of *E. scolopes*. Nonmotile mutants fail to colonize (16, 33, 59), presumably because they fail to migrate out of the bacterial aggregates formed on the surface of the light organ (40). Apparently, normal initiation also requires optimal motility, because several hypermotile mutants colonize with delayed kinetics (32).

Once *V. fischeri* cells initiate colonization, the majority of symbiotic bacteria within the *E. scolopes* light organ become nonflagellated (33, 46). However, within an hour of their release from the light organ into seawater, *V. fischeri* cells regrow their flagella (46). These observations suggest that environmental conditions inside the light organ inhibit flagellation, while those outside favor it (46).

Environmental influences on the motility of the enteric bacteria *Escherichia coli* and *Salmonella enterica* serovar Typhimurium have been well documented (for reviews, see references 3 and 29). These influences include nutrient availability, temperature, ionic composition, pH, and surface interactions (2, 21, 23, 27, 35, 48, 50). Most known environmental influences act at the level of transcription initiation or, to a lesser extent, message stability. These operate through at least one nucleoid protein (H-NS) and a host of transcription factors, including the cyclic AMP (cAMP) receptor protein, LrhA (CRP), and several two-component response regulators (1, 7, 14, 15, 21, 22, 26, 41, 49-51, 54). Control of message stability involves the small RNA-binding protein CsrA (56).

Environmental conditions also can affect flagellation post-transcriptionally. For example, flagellation of *Rhizobium* spp. depends on divalent cations to maintain cross-links between flagellin subunits. In the absence of those cations, the flagellin subunits dissociate, resulting in nonmotile cells (44).

During studies of *V. fischeri* chemotaxis (13), we noticed differences in migration through soft agar depending on the medium used. In this study, we determined that optimal migration of *V. fischeri* required divalent cations. In particular, we found that Mg^{2+} influenced motility by promoting flagellation of this organism.

MATERIALS AND METHODS

Strains and media. Strains used in this study are described in Table 1. Cells were grown in TBS (1% tryptone, 342 mM NaCl) (13) or TB-SW (1% tryptone, 210 mM NaCl, 35 mM $MgSO_4$, 7 mM $CaCl_2$, and 7 mM KCl) (13). TBS was supplemented with $MgSO_4$, $MgCl_2$, $CaCl_2$, KCl, $BaCl_2$, or $SrOH_2$ at a variety of concentrations. Agar was added to a final concentration of 0.25% for soft agar and 1.5% for solid agar.

Soft agar and motility assays. Bacteria were grown at 28°C to mid-exponential phase (A_{600} of ca. 0.3 to 0.7) in TBS or TB-SW. For soft agar motility studies, 10-ml aliquots of approximately equal numbers of bacterial cells were inoculated on the surface of soft agar motility plates and incubated at 28°C for 4 to 7 h. Soft agar motility plates were handled as described previously (58). Images were taken with a Kodak DX3600 Zoom digital camera (Eastman Kodak Company, Rochester, N.Y.).

Visualization of flagella by electron microscopy. Wild-type *V. fischeri* cells (ES114) were grown to exponential phase in either TBS or TBS containing 35 mM $MgSO_4$. Samples were negatively stained with 2% phosphotungstic acid (pH 7.0) and observed with a JEM-1200EXII electron microscope (JEOL, Tokyo, Japan). Micrographs were taken at an accelerating voltage of 80 kV.

Western blot analysis. ES114 cells were grown in the indicated medium, concentrated by microcentrifugation (2 min), resuspended in 10 mM Tris (pH 7.5), and then lysed by sonication. Equal amounts of proteins (10 μg), as determined by Lowry assay (28), were separated by sodium dodecyl sulfate-polyacrylamide gel electrophoresis (12.5% acrylamide) and transferred to a nylon membrane. After blocking with dry milk in TBS-T (10 mM Tris, 150 mM sodium chloride, and 0.05% Tween 20), the membrane was treated with rabbit anti-

* Corresponding author. Mailing address: Department of Microbiology and Immunology, Loyola University Chicago, 2160 S. First Ave., Bldg. 105, Maywood, IL 60153. Phone: (708) 216-0869. Fax: (708) 216-9574. E-mail: kvisick@lumc.edu.

TABLE 1. Strains used in this study

Species	Strain	Description	Source or reference
V. anguillarum	PKJ	Wild-type isolate	E. G. Ruby
V. fischeri	ES114	Isolate from *E. scolopes*	8
V. fischeri	ES235	Isolate from *E. scolopes*	9
V. fischeri	EM17	Isolate from *E. morsei*	8
V. fischeri	H905	Seawater isolate	24
V. fischeri	MJ1	Isolate from monocentrid fish	47
V. fischeri	MJ11	Isolate from monocentrid fish	25
V. harveyi	B392	Wild-type isolate	36, 43
V. orientalis	ATCC 33934	Seawater isolate	60
V. parahaemolyticus	KNH1	Isolate from Kaneohe Bay, Hawaii	40
V. splendidus	ATCC 33869	Wild-type isolate	43

Vibrio parahaemolyticus flagellin antibody (29a), followed by anti-rabbit immunoglobulin G secondary antibody conjugated to horseradish peroxidase (Jackson ImmunoResearch Laboratories, Inc., West Grove, Pa.). To visualize the flagellin proteins, the membrane was incubated with Western Lightning Western blot chemiluminescence reagents (Perkin-Elmer, Torrance, Calif.) and exposed to film.

Measurements of motile cells. Overnight cultures of *V. fischeri* strain ES114 were inoculated into two tubes of TBS broth (5 ml) or, as a control, TBS containing 35 mM $MgSO_4$ fresh medium. After incubation (3 h) at 28°C (A_{600} of ca. 0.3), 180 μl of 1 M $MgSO_4$ was added to one of the TBS cultures. At 10-min intervals, 75-μl samples were removed. Cell motility was observed with an Olympus BX41 microscope with dark-field background and video recorded through an Olympus charge-coupled device color camera for 5 s. The percentage of motile cells was calculated by comparing the position of cells after 5 s relative to their position after 1 s.

RESULTS

Effect of medium and pregrowth conditions on migration. During the course of experiments designed to investigate chemotaxis of *V. fischeri* cells in a tryptone-based soft agar medium (13), we observed enhanced migration in the presence of salts naturally present in seawater. For example, the cells migrated farther and formed rings that appeared denser when inoculated onto TB-SW (a tryptone-based medium that contains 210 mM NaCl, 35 mM $MgSO_4$, 7 mM $CaCl_2$, and 7 mM KCl) than when inoculated onto TBS (a tryptone-based medium with 342 mM NaCl) (compare Fig. 1A with B and 1C with D). Furthermore, the growth condition of the cells prior to inoculation onto soft agar (pregrowth) affected their subsequent migration. When inoculated onto TBS soft agar, cells pregrown in TBS broth migrated poorly relative to those pregrown in TB-SW broth (Fig. 1B and D). Although less dramatic, the same was true when cells were inoculated onto TB-SW soft agar (Fig. 1A and C).

To further investigate the influence of pregrowth conditions, we monitored the rate of migration. We harvested mid-exponential-phase cells grown in either medium, gently washed them with TBS to reduce salt carryover while minimizing flagellum breakage, and then inoculated soft agar medium. Cells pregrown in TB-SW, and inoculated onto the same medium, migrated rapidly (Fig. 2). After a 1-h lag, those pregrown in TBS, and inoculated onto TB-SW, migrated at about the same rate. Thus, the difference in ring diameter seen in Fig. 1A and C resulted from a lag, not a differential rate of migration. Similarly, pregrowth in TB-SW allowed cells to begin migrating immediately on TBS, albeit slowly (Fig. 2). This accounts for the difference in ring diameter seen in Fig. 1B and D. On the basis of these experiments, we hypothesized that the observed lags in and rates of migration resulted from the differential salt compositions of the pregrowth medium and the inoculated soft agar medium.

Effect of Mg^{2+} and Ca^{2+} on migration of *V. fischeri* in soft agar. To identify the salt component that caused the observed differences in lag and migration, we examined the behavior of *V. fischeri* on TBS medium supplemented with $MgSO_4$, $CaCl_2$, KCl, or additional NaCl. Addition of either $MgSO_4$ (35 mM) or $CaCl_2$ (7 mM) significantly enhanced migration (Fig. 1E and F and 3A), while KCl (7 mM) exerted, at most, a small effect (Fig. 1G and 3A). In contrast, addition of NaCl to TBS (to final concentrations between 220 and 380 mM) failed to alter migration (data not shown), suggesting that the observed effects did not result from a change in osmolarity. $MgSO_4$ also affected the appearance of the chemotactic rings. In particular, a gap occurred between the inner and outer rings of cells grown on TBS-Mg^{2+} (Fig. 1E) but not of cells grown on TB-SW (Fig. 1C). The reason for these differences remains unknown; however, like the rings formed by cells grown on TB-SW (13), the inner ring formed on TBS-Mg^{2+} responds to serine (arrow in Fig. 1H) and the outer ring responds to thymidine (data not shown). This observation argues that the salt composition does not substantially alter chemotaxis.

We then asked whether differences in growth could account for the observed differences in migration. The cells reached a higher optical density in TB-SW than in TBS. We attributed this growth difference to the presence of KCl, because its addition to TBS resulted in growth similar to that of TB-SW-grown cells (data not shown). Thus, the slight effect that KCl exerts on migration cannot be distinguished from growth, and we have not pursued its further investigation. In contrast, the addition of $MgSO_4$ or $CaCl_2$ exerted no effect upon growth (data not shown). Therefore, these salts must play specific roles in enhancing migration of *V. fischeri* cells.

Effect of divalent cations on migration of *V. fischeri*. To further explore the importance of salts in promoting migration of *V. fischeri*, we first determined the range of $MgSO_4$ concentrations that promote migration. Cells migrated farther with the addition of as little as 0.2 mM and as much as 200 mM $MgSO_4$; optimal migration occurred between 20 and 40 mM (Fig. 3B and data not shown). Because the addition of $MgCl_2$ (35 mM) enhanced migration to a similar extent as did $MgSO_4$

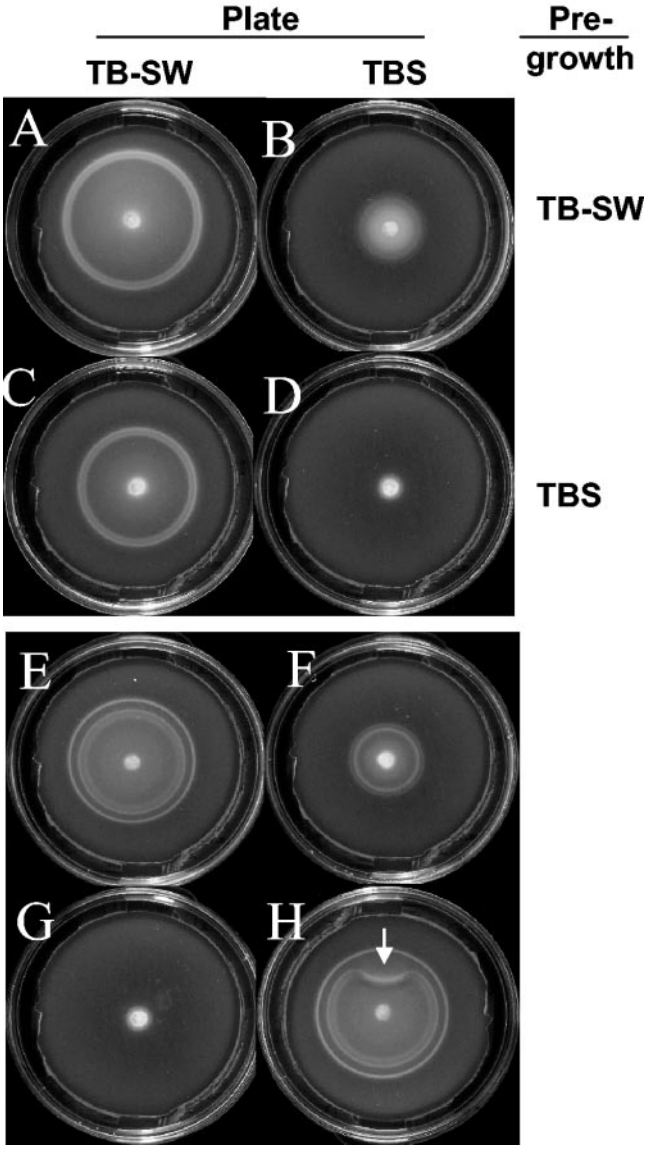

FIG. 1. Migration of *V. fischeri* on tryptone-based soft agar with various salt compositions. (A to D) Exponential-phase cells of *V. fischeri*, pregrown in TB-SW or TBS as indicted, were inoculated near the center of soft agar plates containing either TB-SW (A and C) or TBS (B and D). (E to H) Exponential-phase cells of *V. fischeri* grown in TBS were inoculated near the center of soft agar plates containing TBS containing 35 mM $MgSO_4$ (E and H), TBS containing 7 mM $CaCl_2$ (F), or TBS containing 7 mM KCl (G) and incubated at 28°C for 5 h. At 4 h, 5 μl of 2 M serine was spotted directly onto a TBS plate containing 35 mM $MgSO_4$ outside the migrating bands (arrow, H).

(35 mM) (data not shown), we concluded that the Mg^{2+} cation promotes migration of *V. fischeri*.

We next varied the $CaCl_2$ concentration. Addition of low concentrations of $CaCl_2$ (2 to 20 mM) to TBS enhanced migration (Fig. 3C). In contrast, higher concentrations of $CaCl_2$ (40 to 66 mM) inhibited migration of the cells (Fig. 3C and data not shown). However, this decreased migration likely stems from an effect on growth, as these amounts also decreased the growth rate and peak optical density in liquid culture (data not shown).

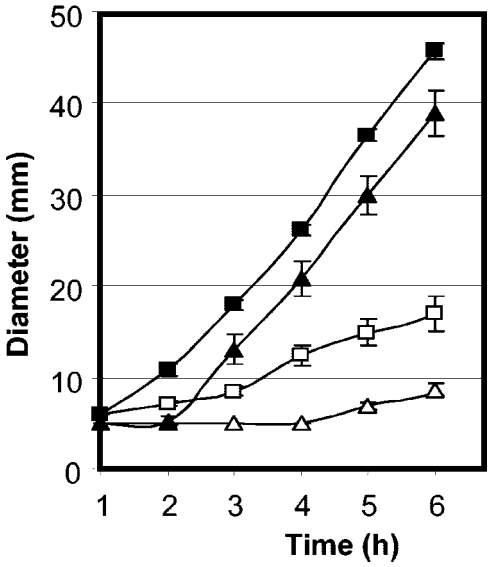

FIG. 2. Effect of pregrowth conditions on migration of *V. fischeri*. Cells of *V. fischeri* strain ES114 were pregrown to mid-exponential phase in TBS (triangles) or TB-SW (squares), inoculated onto TBS (open symbols) or TB-SW (solid symbols) soft agar plates, and incubated at 28°C. Migration of the cells was determined hourly by measuring the diameter of the outer migrating rings. Error bars represent the standard deviations of a representative experiment performed in triplicate.

Because both Mg^{2+} and Ca^{2+} could enhance migration, albeit not to the same extent, we asked whether migration of *V. fischeri* depended upon divalent cations, in general. We found that low concentrations of $BaCl_2$ (2 to 8 mM) enhanced migration to nearly the same degree as did 8 mM $MgSO_4$ (data not shown), while higher concentrations inhibited migration. Similarly, low concentrations of $SrOH_2$ (2 to 5 mM) also enhanced migration (data not shown). We could not test the effects of higher concentrations, as this salt was insoluble at higher concentrations. These results support a general divalent cation effect. They also suggest that optimal *V. fischeri* motility occurs under the conditions of high concentrations of Mg^{2+} that naturally exist in seawater (about 50 mM) (12).

Role of Mg^{2+} in migration of other bacterial species. Because Mg^{2+}-dependent migration has not been reported previously, we asked whether the ability to migrate farther in the presence of Mg^{2+} represents a common trait of marine *Vibrio* spp. We therefore examined migration of other marine isolates in TBS and TBS containing 35 mM Mg^{2+} (Fig. 4; Table 1; also data not shown). Mg^{2+} significantly enhanced migration of other *V. fischeri* isolates, including strains isolated from the fish *Monocentris japonica* (MJ1 and MJ11), the squids *E. scolopes* (ES235) and *Euprymna morsei* (EM17), and seawater (H905). Mg^{2+} also significantly enhanced migration of *Vibrio orientalis* (ATCC 33934) (data not shown). Migration of *Vibrio splendidus* (ATCC 33869), *V. parahaemolyticus* (KNH1), and *Vibrio anguillarum* (PKJ) was also enhanced; however, the effect of this salt on migration was relatively minor (Fig. 4 and data not shown). Finally, Mg^{2+} did not significantly influence migration of *Vibrio harveyi* B392 (Fig. 4). Furthermore, addition of low concentrations of $MgSO_4$ (2.5 to 10 mM) to TBS did not affect

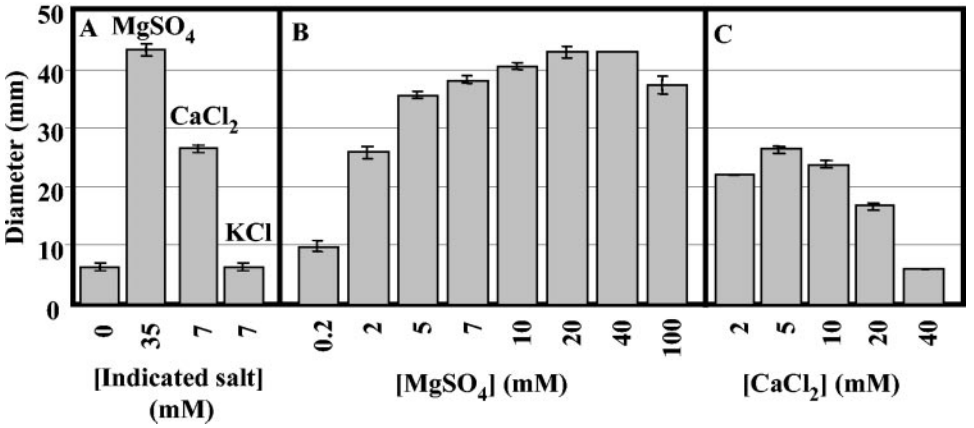

FIG. 3. Mean migration of *V. fischeri* on tryptone-based soft agar plates with various salt compositions. (A) Exponential-phase cells of *V. fischeri*, grown in TBS, were inoculated near the center of TBS soft agar plates or TBS plates containing 35 mM $MgSO_4$, 7 mM $CaCl_2$, or 7 mM KCl. (B) Exponential-phase cells of *V. fischeri*, grown in TBS, were inoculated near the center of TBS soft agar plates containing the specified concentration of $MgSO_4$. (C) Exponential-phase cells of *V. fischeri*, grown in TBS, were inoculated near the center of TBS soft agar plates containing the specified concentration of $CaCl_2$. All plates were incubated at 28°C for 5 h, after which time the diameters of the outer migrating bands were measured. Error bars represent the standard deviations of a representative experiment performed in triplicate.

the migration of *E. coli* (data not shown), while high concentrations (20 to 80 mM) decreased migration, as reported previously (27).

Effect of Mg^{2+} on flagellation of *V. fischeri*. We hypothesized that Mg^{2+} and other divalent cations could affect migration of *V. fischeri* by altering the kinetics or direction of flagellar rotation, altering the length of the filaments, increasing the number of flagella per cell, and/or increasing the proportion of flagellated bacteria. To distinguish among these possibilities, we first examined cells by phase-contrast microscopy. Those

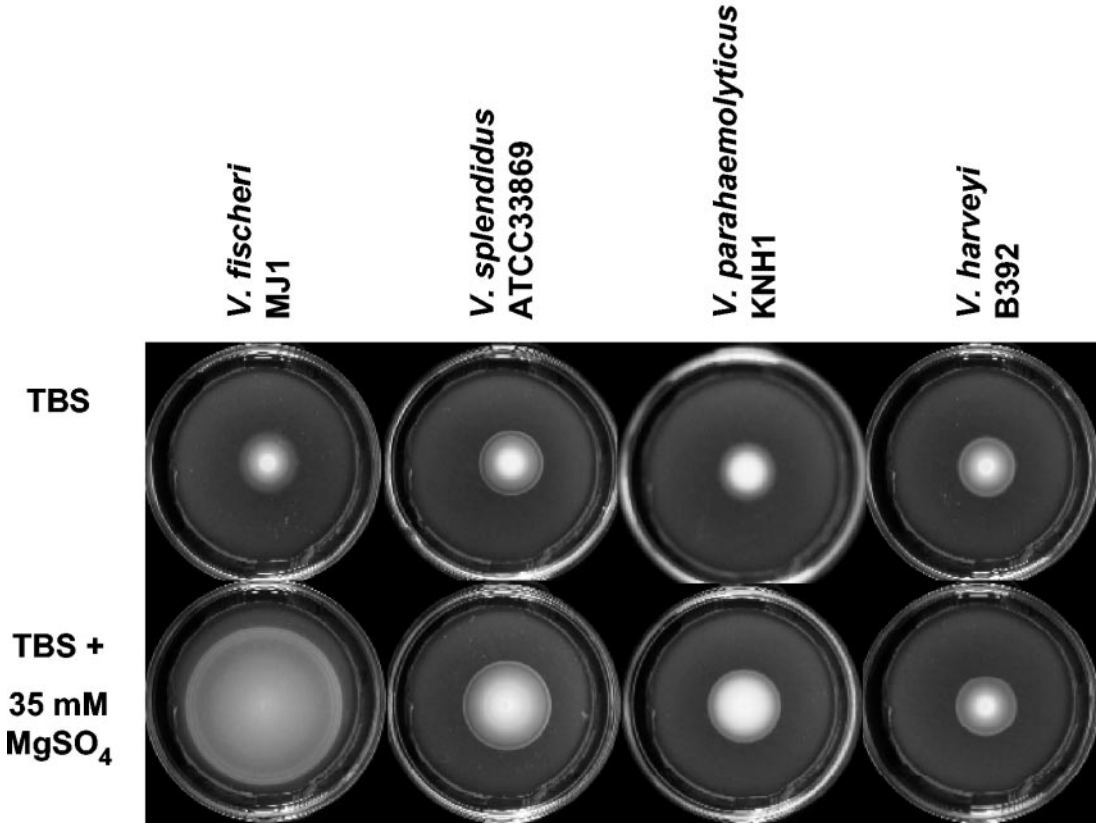

FIG. 4. Migration of various *Vibrio* strains on TBS soft agar supplemented with Mg^{2+}. Exponential-phase cells of *V. fischeri* MJ1, *V. splendidus* ATCC 33869, *V. parahaemolyticus* KNH1, and *V. harveyi* B392, grown in TBS, were inoculated near the center of TBS soft agar plates or TBS supplemented with 35 mM $MgSO_4$. Pictures were taken after 7 h of incubation at 28°C.

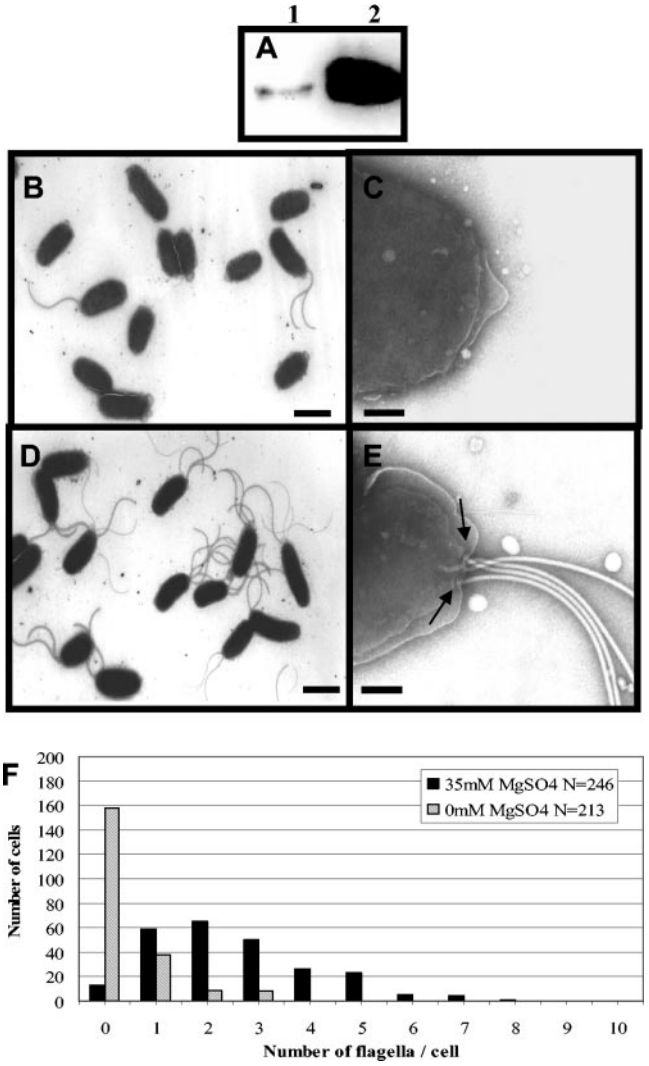

FIG. 5. Analysis of flagella from *V. fischeri* ES114 grown in the presence and absence of Mg^{2+}. (A) Ten micrograms of protein extracted from cells grown to mid-exponential phase in TBS (lane 1) or TBS supplemented with 35 mM $MgSO_4$ (lane 2) was separated by sodium dodecyl sulfate-polyacrylamide gel electrophoresis, transferred to a membrane, and probed with antiflagellin antibody. The observed bands were located between the 36.2- and 49.9-kDa size standards, similar to that observed previously (34). (B and C) TEM of ES114 cells grown in TBS. (D and E) TEM of ES114 grown in TBS containing 35 mM $MgSO_4$. Scale bars, 200 μm (B and D) and 200 nm (C and E). (F) Histogram indicating the number of ES114 cells containing the indicated number of flagella per cell. ES114 was grown in TBS (shaded bars) or TBS containing 35 mM $MgSO_4$ (black bars). Arrows point to basal body structures.

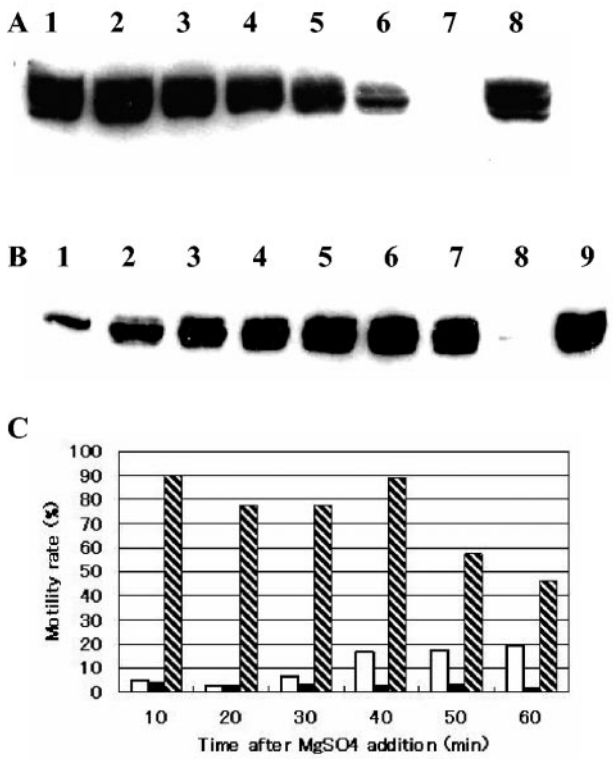

FIG. 6. Response of *V. fischeri* flagellation and motility to changes in $MgSO_4$. (A) ES114 cells were grown in TBS containing 35 mM $MgSO_4$ to mid-exponential phase, collected, and resuspended in TBS lacking $MgSO_4$. Samples were collected over time and analyzed by a Western blot procedure as described for Fig. 5. Lanes 1 to 6 contain samples collected at the indicated times (min): 1, $t = 0$; 2, $t = 15$; 3, $t = 30$; 4, $t = 45$; 5, $t = 60$; 6, $t = 120$. Lanes 7 and 8 contain samples prepared from ES114 cells treated similarly to those in lanes 1 to 6 but grown for the duration of the experiment (overnight and $t = 120$ min) in either TBS (lane 7) or TBS containing 35 mM $MgSO_4$ (lane 8). (B) ES114 cells were grown in TBS to mid-exponential phase and then subcultured in TBS containing 35 mM $MgSO_4$. Samples were collected over time and analyzed by a Western blot procedure as described for Fig. 5. Lanes 1 to 7 contain samples collected at the indicated times (min): 1, $t = 0$; 2, $t = 5$; 3, $t = 15$; 4, $t = 30$; 5, $t = 45$; 6, $t = 60$; 7, $t = 120$. Lanes 8 and 9 contain samples prepared from ES114 cells treated similarly to those in lanes 1 to 7 but grown for the duration of the experiment (overnight and $t = 120$ min) in either TBS (lane 8) or TBS containing 35 mM $MgSO_4$ (lane 9). (C) ES114 cells grown overnight in TBS (white and black bars) or TBS containing 35 mM $MgSO_4$ (striped bars) were subcultured into the same medium to an A_{600} of 0.3. Then, 35 mM $MgSO_4$ was added to one of the TBS cultures (white bars). Samples were examined for motility as described in Materials and Methods.

cells grown in TBS-Mg^{2+} were highly motile, while those grown in TBS exhibited poor to no motility (data not shown). We then determined by Western analysis that the Mg^{2+}-grown cells contained higher amounts of flagellin protein than did those grown without Mg^{2+} (Fig. 5A). We next sheared and collected surface-associated flagellin and found that Mg^{2+}-exposed bacteria possessed larger amounts (data not shown). Finally, we analyzed *V. fischeri* cells by using transmission electron microscopy (TEM). The majority of cells grown in TBS were nonflagellated (Fig. 5B and F). Furthermore, we observed no obvious basal-body-like structures at the poles of nonflagellated cells (Fig. 5C). In contrast, the majority of cells grown in TBS-Mg^{2+} expressed between one and three flagella (Fig. 5D to F and data not shown). Thus, Mg^{2+} enhances migration of *V. fischeri* by increasing both the number of flagella per cell and the proportion of cells that have flagella.

Effect of Mg^{2+} on the kinetics of flagellin biosynthesis and motility. To understand the migration kinetics shown in Fig. 2, we determined the rate of disappearance or appearance of flagellin protein following a Mg^{2+} shift-down (Fig. 6A) or

shift-up (Fig. 6B). We observed a steady decline in cell-associated flagellin following the shift-down. However, even after 2 h of growth in TBS, some cell-associated flagellin protein remained. This result explains why cells pregrown in media containing Mg^{2+} consistently exhibited more rapid migration over the first few hours of incubation than did those pregrown without added Mg^{2+} (Fig. 2).

Shift-up experiments (Fig. 6B) showed a progressive increase in *V. fischeri* flagellin, with a large increase by 40 min and a maximum level reached between 1 and 2 h. This amount of time is similar to that required for *E. coli* and *S. enterica* serovar Typhimurium to become fully flagellated and motile (about 40 min) (4, 19). To determine whether this timing was similar for *V. fischeri*, we examined motility of the cells during this time frame. Within 40 min of $MgSO_4$ addition to TBS, we observed about a threefold increase in occurrence of motile cells (Fig. 6C). However, the percentage of motile cells in cultures exposed for 60 min to Mg^{2+} remained substantially lower than that for cells grown under conditions that included Mg^{2+} for the duration of the experiment. This suggests that additional time is required for the population to achieve full flagellation and motility following Mg^{2+} exposure under these conditions.

DISCUSSION

In this study, we demonstrated that divalent cations enhance the migration of *V. fischeri* cells. Mg^{2+} exerted the largest effect across a wide range of concentrations, including that present in seawater. Although Mg^{2+} enhanced the migration of some other marine *Vibrio* isolates, it exerted the most substantial influence on *V. fischeri*. This effect occurred at the level of flagellation and represents a novel mechanism for the control of motility.

In attempting to understand the effect of Mg^{2+} on motility of *V. fischeri*, we found that monitoring migration over a time course rather than examining a single arbitrarily chosen time point provided insight into the problem. In particular, we observed a lag in migration when cells were pregrown without Mg^{2+} relative to those grown in its presence. However, the lack of Mg^{2+} during pregrowth did not cause any defects in the rate of migration on Mg^{2+}-containing soft agar—a phenotype not evident from examining a single time point. Migration is a complex behavior. It involves transport, metabolism, growth, and motility (6). Our results make it clear that it also depends upon the status of the cells in the inoculum.

How does Mg^{2+} influence flagellation of *V. fischeri*? In *E. coli*, *S. enterica* serovar Typhimurium, and other enteric bacteria, environmental factors influence flagellation predominantly by controlling transcription of the operon that encodes the master activator FlhDC (10). This may also be true for *V. fischeri*. Although relatively little is known about the regulatory genes that exert control over flagellar transcription in *V. fischeri*, it is apparent that its flagellar hierarchy is distinct from that of *E. coli* and likely similar to that of the closely related pathogen *Vibrio cholerae* (20, 33). Flagellation of both *Vibrio* species depends on σ^{54} (20, 59) and FlrA, a σ^{54}-dependent master regulator of flagellar gene transcription (20, 33, 42). In *V. cholerae*, and likely in *V. fischeri*, distinct subsets of flagellar genes also are controlled by the two-component regulatory system FlrBC and by the flagellum-specific sigma factor σ^{28} (20, 33). Although the flagellar hierarchy of *V. fischeri* is not fully understood, our preliminary experiments suggest that Mg^{2+} does not operate at the level of transcription (T. M. O'Shea and K. L. Visick, unpublished data). Rather, it appears to act at a posttranscriptional level.

Posttranscriptional control of flagellation has been documented (5, 18, 44, 53, 56). Notably, Mg^{2+} exerts an effect on the stability of flagella in *Sinorhizobium meliloti*. In this soil organism, divalent cations, present at relatively low concentrations (200 μM), provide cross-bridges between the flagellin subunits that form the flagellar filament (44). In contrast, 200 μM Mg^{2+} only slightly enhanced migration of *V. fischeri* cells, while substantial enhancement required about 1 to 2 mM (Fig. 3 and data not shown). Unlike those of *S. meliloti*, *V. fischeri* flagella are sheathed, encased within an extension of the outer membrane (32) (Fig. 5C). Furthermore, when grown without added Mg^{2+}, the resulting nonflagellated *V. fischeri* cells do not possess basal body structures (Fig. 5E). One would predict the presence of such structures, if the lack of Mg^{2+} simply caused the disassembly of the flagellar filament. Together, these observations suggest that Mg^{2+} affects a different level, such as (i) the translation of all or a subset of flagellar transcripts, (ii) the stability of the resultant flagellar subunits, and/or (iii) the assembly of the basal body.

Mg^{2+} is a signal that the pathogen *S. enterica* serovar Typhimurium senses and uses to determine its location within a host (17). Does Mg^{2+} also serve as an environmental signal for *V. fischeri*? This organism primarily exists in seawater, where Mg^{2+} is abundant, as well as in the intestinal tracts of fishes and in the light organ of *E. scolopes*. The Mg^{2+} levels inside these host environments are unknown. However, recent evidence suggests that *E. scolopes* can control at least one environmental condition (osmolarity) within its symbiotic light organ (52).

Motility is absolutely required for *V. fischeri* cells to enter the light organ of *E. scolopes* (16, 32-34, 59). Following colonization, a switch occurs, resulting in a significant population of nonflagellated cells within the internal crypts of the light organ (33, 46). Furthermore, within about 45 to 60 min after their release from the light organ into seawater, *V. fischeri* cells regrow their flagella (46). This is similar to the time interval necessary for cells pregrown in TBS to produce flagellin and, at least for some, to become motile following exposure to Mg^{2+}.

Whether, like *S. enterica* serovar Typhimurium (17), *V. fischeri* experiences a reduction in Mg^{2+} concentration in its natural environment remains an open question. Regardless, data presented in this paper support a novel mechanism for the control of flagellar biogenesis in *V. fischeri*. Determining the mechanism by which Mg^{2+} influences flagellar biogenesis in *V. fischeri* likely will provide insight into the control of flagellar assembly by bacteria and, potentially, an increased understanding of the environmental control of bacterium-host associations.

ACKNOWLEDGMENTS

We thank Ana Mrejeru, Joy Campbell, and Debbie Millikan for their contributions to experiments described herein and members of our labs for critical reading of the manuscript. We are grateful to Linda McCarter for her generous gift of antiflagellin antibody.

This work was supported by NIH grant GM59690 awarded to K.L.V., by NSF grant MCB-9982762 awarded to A.J.W., and by the National Science Foundation under a Research Fellowship in Microbial Biology awarded in 2001 to C.R.D.-M.

REFERENCES

1. **Adams, P., R. Fowler, N. Kinsella, G. Howell, M. Farris, P. Coote, and C. D. O'Connor.** 2001. Proteomic detection of PhoPQ- and acid-mediated repression of *Salmonella* motility. Proteomics **1:**597–607.
2. **Adler, J., and B. Templeton.** 1967. The effect of environmental conditions on the motility of *Escherichia coli*. J. Gen. Microbiol. **46:**175–184.
3. **Aizawa, S.-I.** 2004. Flagella, p. 470–479. *In* M. Schaechter (ed.), The desk encyclopedia of microbiology. Academic Press, San Diego, Calif.
4. **Aizawa, S.-I., and T. Kubori.** 1998. Bacterial flagellation and cell division. Genes Cells **3:**1–10.
5. **Aldridge, P., and U. Jenal.** 1999. Cell cycle-dependent degradation of a flagellar motor component requires a novel-type response regulator. Mol. Microbiol. **32:**379–391.
6. **Berg, H. C., and L. Turner.** 1979. Movement of microorganisms in viscous environments. Nature **278:**349–351.
7. **Bertin, P., E. Terao, E. H. Lee, P. Lejeune, C. Colson, A. Danchin, and E. Collatz.** 1994. The H-NS protein is involved in the biogenesis of flagella in *Escherichia coli*. J. Bacteriol. **176:**5537–5540.
8. **Boettcher, K. J., and E. G. Ruby.** 1990. Depressed light emission by symbiotic *Vibrio fischeri* of the sepiolid squid *Euprymna scolopes*. J. Bacteriol. **172:** 3701–3706.
9. **Boettcher, K. J., and E. G. Ruby.** 1994. Occurrence of plasmid DNA in the sepiolid squid symbiont *Vibrio fischeri*. Curr. Microbiol. **29:**279–286.
10. **Chilcott, G. S., and K. T. Hughes.** 2000. Coupling of flagellar gene expression to flagellar assembly in *Salmonella enterica* serovar Typhimurium and *Escherichia coli*. Microbiol. Mol. Biol. Rev. **64:**694–708.
11. **Davidson, S. K., T. A. Koropatnick, R. Kossmehl, L. Sycuro, and M. J. McFall-Ngai.** 2004. NO means 'yes' in the squid-vibrio symbiosis: nitric oxide (NO) during the initial stages of a beneficial association. Cell. Microbiol. **6:**1139–1151.
12. **de Graaf, F.** 1973. Marine aquarium guide. The Pet Library Ltd., Harrison, N.J.
13. **DeLoney-Marino, C. R., A. J. Wolfe, and K. L. Visick.** 2003. Chemoattraction of *Vibrio fischeri* to serine, nucleosides, and *N*-acetylneuraminic acid, a component of squid light organ mucus. Appl. Environ. Microbiol. **69:**7527–7530.
14. **Francez-Charlot, A., B. Laugel, A. Van Gemert, N. Dubarry, F. Wiorowski, M. P. Castanie-Cornet, C. Gutierrez, and K. Cam.** 2003. RcsCDB His-Asp phosphorelay system negatively regulates the *flhDC* operon in *Escherichia coli*. Mol. Microbiol. **49:**823–832.
15. **Goodier, R. I., and B. M. Ahmer.** 2001. SirA orthologs affect both motility and virulence. J. Bacteriol. **183:**2249–2258.
16. **Graf, J., P. V. Dunlap, and E. G. Ruby.** 1994. Effect of transposon-induced motility mutations on colonization of the host light organ by *Vibrio fischeri*. J. Bacteriol. **176:**6986–6991.
17. **Groisman, E. A.** 2001. The pleiotropic two-component regulatory system PhoP-PhoQ. J. Bacteriol. **183:**1835–1842.
18. **Karlinsey, J. E., J. Lonner, K. L. Brown, and K. T. Hughes.** 2000. Translation/secretion coupling by type III secretion systems. Cell **102:**487–497.
19. **Karlinsey, J. E., S. Tanaka, V. Bettenworth, S. Yamaguchi, W. Boos, S.-I. Aizawa, and K. T. Hughes.** 2000. Completion of the hook-basal body complex of the *Salmonella typhimurium* flagellum is coupled to FlgM secretion and *fliC* transcription. Mol. Microbiol. **37:**1220–1231.
20. **Klose, K. E., and J. J. Mekalanos.** 1998. Distinct roles of an alternative sigma factor during both free-swimming and colonizing phases of the *Vibrio cholerae* pathogenic cycle. Mol. Microbiol. **28:**501–520.
21. **Komeda, Y., H. Suzuki, J.-I. Ishidsu, and T. Iino.** 1975. The role of cAMP in flagellation of *Salmonella typhimurium*. Mol. Gen. Genet. **142:**289–298.
22. **Kutsukake, K.** 1997. Autogenous and global control of the flagellar master operon, *flhD*, in *Salmonella typhiumurium*. Mol. Gen. Genet. **254:**440–448.
23. **Landini, P., and A. J. Zehnder.** 2002. The global regulatory *hns* gene negatively affects adhesion to solid surfaces by anaerobically grown *Escherichia coli* by modulating expression of flagellar genes and lipopolysaccharide production. J. Bacteriol. **184:**1522–1529.
24. **Lee, K.-H., and E. G. Ruby.** 1992. Detection of the light organ symbiont, *Vibrio fischeri*, in Hawaiian seawater by using *lux* gene probes. Appl. Environ. Microbiol. **58:**942–947.
25. **Lee, K.-H., and E. G. Ruby.** 1998. The *Vibrio fischeri-Euprymna scolopes* light organ association: current ecological paradigms. Appl. Environ. Microbiol. **64:**805–812.
26. **Lehnen, D., C. Blumer, T. Polen, B. Wackwitz, V. F. Wendisch, and G. Unden.** 2002. LrhA as a new transcriptional key regulator of flagella, motility and chemotaxis genes in *Escherichia coli*. Mol. Microbiol. **45:**521–532.
27. **Li, C., C. J. Louise, W. Shi, and J. Adler.** 1993. Adverse conditions which cause lack of flagella in *Escherichia coli*. J. Bacteriol. **175:**2229–2235.
28. **Lowry, O. H., N. J. Rosebrough, A. L. Farr, and R. J. Randall.** 1951. Protein measurement with the Folin phenol reagent. J. Biol. Chem. **193:**265–275.
29. **Macnab, R. M.** 1996. Flagella and motility, p. 123–145. *In* F. C. Neidhardt, R. Curtiss III, J. L. Ingraham, E. C. C. Lin, K. B. Low, B. Magasanik, W. S. Reznikoff, M. Riley, M. Schaechter, and H. E. Umbarger (ed.), *Escherichia coli* and *Salmonella*: cellular and molecular biology. ASM Press, Washington, D.C.

29a. **McCarter, L. L.** 1995. Genetic and molecular characterization of the polar flagellum of Vibrio parahaemolyticus. J. Bacteriol. **177:**1595–1609.

30. **McFall-Ngai, M. J.** 1999. Consequences of evolving with bacterial symbionts: insights from the squid-vibrio associations. Annu. Rev. Ecol. Syst. **30:**235–256.
31. **McFall-Ngai, M. J., and E. G. Ruby.** 1991. Symbiont recognition and subsequent morphogenesis as early events in an animal-bacterial mutualism. Science **254:**1491–1494.
32. **Millikan, D. S., and E. G. Ruby.** 2002. Alterations in *Vibrio fischeri* motility correlate with a delay in symbiosis initiation and are associated with additional symbiotic colonization defects. Appl. Environ. Microbiol. **68:**2519–2528.
33. **Millikan, D. S., and E. G. Ruby.** 2003. FlrA, a σ^{54}-dependent transcriptional activator in *Vibrio fischeri*, is required for motility and symbiotic light-organ colonization. J. Bacteriol. **185:**3547–3557.
34. **Millikan, D. S., and E. G. Ruby.** 2004. *Vibrio fischeri* flagellin A is essential for normal motility and for symbiotic competence during initial squid light organ colonization. J. Bacteriol. **186:**4315–4325.
35. **Morrison, R. B., and J. McCapra.** 1961. Flagellar changes in *Escherichia coli* induced by temperature of the environment. Nature **192:**774–776.
36. **Nealson, K. H.** 1977. Autoinduction of bacterial luciferase. Occurrence, mechanism and significance. Arch. Microbiol. **112:**73–79.
37. **Nyholm, S. V., B. Deplancke, H. R. Gaskins, M. A. Apicella, and M. J. McFall-Ngai.** 2002. Roles of *Vibrio fischeri* and nonsymbiotic bacteria in the dynamics of mucus secretion during symbiont colonization of the *Euprymna scolopes* light organ. Appl. Environ. Microbiol. **68:**5113–5122.
38. **Nyholm, S. V., and M. J. McFall-Ngai.** 2003. Dominance of *Vibrio fischeri* in secreted mucus outside the light organ of *Euprymna scolopes*: the first site of symbiont specificity. Appl. Environ. Microbiol. **69:**3932–3937.
39. **Nyholm, S. V., and M. J. McFall-Ngai.** 2004. The winnowing: establishing the squid-*Vibrio* symbiosis. Nat. Rev. Microbiol. **2:**632–642.
40. **Nyholm, S. V., E. V. Stabb, E. G. Ruby, and M. J. McFall-Ngai.** 2000. Establishment of an animal-bacterial association: recruiting symbiotic vibrios from the environment. Proc. Natl. Acad. Sci. USA **97:**10231–10235.
41. **Oshima, T., H. Aiba, Y. Masuda, S. Kanaya, M. Sugiura, B. L. Wanner, H. Mori, and T. Mizuno.** 2002. Transcriptome analysis of all two-component regulatory system mutants of *Escherichia coli* K-12. Mol. Microbiol. **46:**281–291.
42. **Prouty, M. G., N. E. Correa, and K. E. Klose.** 2001. The novel σ^{54}- and σ^{28}-dependent flagellar gene transcription hierarchy of *Vibrio cholerae*. Mol. Microbiol. **39:**1595–1609.
43. **Reichelt, J. L., and P. Baumann.** 1973. Taxonomy of the marine, luminous bacteria. Arch. Mikrobiol. **94:**283–330.
44. **Robinson, J. B., O. H. Tuovinen, and W. D. Bauer.** 1992. Role of divalent cations in the subunit associations of complex flagella from *Rhizobium meliloti*. J. Bacteriol. **174:**3896–3902.
45. **Ruby, E. G.** 1996. Lessons from a cooperative, bacterial-animal association: the *Vibrio fischeri-Euprymna scolopes* light organ symbiosis. Annu. Rev. Microbiol. **50:**591–624.
46. **Ruby, E. G., and L. M. Asato.** 1993. Growth and flagellation of *Vibrio fischeri* during initiation of the sepiolid squid light organ symbiosis. Arch. Microbiol. **159:**160–167.
47. **Ruby, E. G., and K. H. Nealson.** 1976. Symbiotic association of *Photobacterium fischeri* with the marine luminous fish *Monocentris japonica*: a model of symbiosis based on bacterial studies. Biol. Bull. **151:**574–586.
48. **Shi, W., C. Li, C. J. Louise, and J. Adler.** 1993. Mechanism of adverse conditions causing lack of flagella in *Escherichia coli*. J. Bacteriol. **175:**2236–2240.
49. **Shin, S., and C. Park.** 1995. Modulation of flagellar expression in *Escherichia coli* by acetyl phosphate and the osmoregulator OmpR. J. Bacteriol. **177:** 4696–4702.
50. **Silverman, M., and M. Simon.** 1974. Characterization of *Escherichia coli* flagellar mutants that are insensitive to catabolite repression. J. Bacteriol. **120:**1196–1203.
51. **Sperandio, V., A. G. Torres, and J. B. Kaper.** 2002. Quorum sensing *Escherichia coli* regulators B and C (QseBC): a novel two-component regulatory system involved in the regulation of flagella and motility by quorum sensing in *E. coli*. Mol. Microbiol. **43:**809–821.
52. **Stabb, E. V., M. S. Butler, and D. M. Adin.** 2004. Correlation between osmolarity and luminescence of symbiotic *Vibrio fischeri* strain ES114. J. Bacteriol. **186:**2906–2908.
53. **Tang, Y., J. R. Guest, P. J. Artymiuk, R. C. Read, and J. Green.** 2004. Post-transcriptional regulation of bacterial motility by aconitase proteins. Mol. Microbiol. **51:**1817–1826.
54. **Teplitski, M., R. I. Goodier, and B. M. Ahmer.** 2003. Pathways leading from BarA/SirA to motility and virulence gene expression in *Salmonella*. J. Bacteriol. **185:**7257–7265.

55. **Visick, K. L., and M. J. McFall-Ngai.** 2000. An exclusive contract: specificity in the *Vibrio fischeri-Euprymna scolopes* partnership. J. Bacteriol. **182:**1779–1787.
56. **Wei, B. L., A. M. Brun-Zinkernagel, J. W. Simecka, B. M. Pruss, P. Babitzke, and T. Romeo.** 2001. Positive regulation of motility and *flhDC* expression by the RNA-binding protein CsrA of *Escherichia coli*. Mol. Microbiol. **40:**245–256.
57. **Wei, S. L., and R. E. Young.** 1989. Development of symbiotic bacterial bioluminescence in a nearshore cephalopod, *Euprymna scolopes*. Mar. Biol. **103:**541–546.
58. **Wolfe, A. J., and H. C. Berg.** 1989. Migration of bacteria in semisolid agar. Proc. Natl. Acad. Sci. USA **86:**6973–6977.
59. **Wolfe, A. J., D. S. Millikan, J. M. Campbell, and K. L. Visick.** 2004. *Vibrio fischeri* σ^{54} controls motility, biofilm formation, luminescence, and colonization. Appl. Environ. Microbiol. **70:**2520–2524.
60. **Yang, Y., L. Yeh, Y. Cao, L. Baumann, P. Baumann, J. S. Tang, and B. Beaman.** 1983. Characterization of marine luminous bacteria isolated off the coast of China and description of *Vibrio orientalis* sp. nov. Curr. Microbiol. **8:**95–100.

APPLIED AND ENVIRONMENTAL MICROBIOLOGY, Apr. 2004, p. 2520–2524 Vol. 70, No. 4
0099-2240/04/$08.00+0 DOI: 10.1128/AEM.70.4.2520–2524.2004

Vibrio fischeri σ^{54} Controls Motility, Biofilm Formation, Luminescence, and Colonization

Alan J. Wolfe,[1] Deborah S. Millikan,[2] Joy M. Campbell,[1] and Karen L. Visick[1]*

Department of Microbiology and Immunology, Loyola University Chicago, Maywood, Illinois 60153,[1] and Pacific Biomedical Research Center, University of Hawaii, Honolulu, Hawaii 96813[2]

Received 19 September 2003/Accepted 29 December 2003

In this study, we demonstrated that the putative *Vibrio fischeri rpoN* gene, which encodes σ^{54}, controls flagellar biogenesis, biofilm development, and bioluminescence. We also show that *rpoN* plays a requisite role initiating the symbiotic association of *V. fischeri* with juveniles of the squid *Euprymna scolopes*.

The sigma factor σ^{54}, encoded by *rpoN*, is distributed widely among bacteria. The ability of σ^{54} to regulate nitrogen metabolism is well established (reviewed in reference 16). In *Escherichia coli*, about half of all σ^{54}-dependent operons function in the assimilation and metabolism of nitrogen (28). In other organisms, σ^{54} regulates diverse functions in addition to controlling nitrogen metabolism. In *Vibrio parahaemolyticus*, it controls the biogenesis of the polar flagella required for swimming and the lateral flagella necessary for swarming (31). In *Vibrio harveyi*, it regulates motility and bioluminescence (14). In *Pseudomonas aeruginosa*, it activates transcription of both the flagellin and pilin genes, negatively affects quorum-sensing genes, and promotes virulence (8–10, 32). In *Vibrio cholerae*, it regulates flagellin gene transcription and influences mouse colonization. Its role in colonization, however, appears distinct from the requirement for motility and nitrogen assimilation (13).

The symbiosis between the bioluminescent marine bacterium *Vibrio fischeri* and the Hawaiian squid *Euprymna scolopes* has become established as a model system for investigating mutualistic associations (reviewed in references 18 and 35). Colonization of newly hatched juvenile *E. scolopes* occurs rapidly and requires motility: nonmotile bacteria fail to colonize (5), while hypermotile mutants exhibit delays in colonization (21). A recent report characterized the symbiotic phenotype of a mutant defective for FlrA, the putative σ^{54}-dependent transcriptional activator likely to be at the top of the flagellar hierarchy in *V. fischeri* (22). The *flrA* mutant was defective for both motility and colonization. This mutant was fully complemented for motility but only partially complemented for colonization. Thus, the *flrA* colonization defect may result from more than a lack of flagella (22).

In this study, we identified a nonmotile mutant of *V. fischeri* defective for the putative *rpoN* gene, which encodes the sigma factor σ^{54}. Given the scope of its regulatory control in other bacteria and the importance of the putative σ^{54}-dependent transcriptional activator FlrA in establishing the *V. fischeri-E. scolopes* symbiotic relationship, we examined the role of *rpoN* in culture and during colonization. We asked whether *rpoN* regulates traits known to be or potentially associated with symbiotic colonization, including flagellar biogenesis (5, 21, 22), nitrogen metabolism, iron uptake (6), and bioluminescence (34).

Role for the *rpoN* gene in motility. In a search for flagellar mutants of *V. fischeri*, we identified a transposon insertion mutant, KV618 (Table 1), that failed to migrate in tryptone-based soft agar plates. We complemented the defect in this strain by introducing a plasmid library of BglII-digested chromosomal DNA and screening for motility in soft agar plates (38). From a motile clone, we isolated plasmid pES2-2 (Table 1), which carried a 2.5-kb chromosomal insert resembling the *rpoN* locus from a number of other organisms, including *E. coli*, *V. harveyi*, and *V. cholerae* (11, 13, 14). It contained putative genes for an ABC-type transporter (*yhbG*, open reading frame 1 [ORF1]), σ^{54} (*rpoN*), a σ^{54} regulatory gene (*yhbH*, ORF 95), and a nitrogen regulatory phosphotransferase component (*ptsN*) (Table 2). We cloned the DNA flanking the transposon insertion and determined that the transposon had inserted into codon 10 of the putative *rpoN* gene.

To characterize the *rpoN* gene further, we first constructed a null mutation in the symbiosis-competent wild-type *V. fischeri* strain ES114. We introduced plasmid pLMS71 (Table 1) into ES114 by conjugation and isolated a nonmotile recombinant, designated KV1513 (Table 1). We confirmed the identity of the mutant with Southern analysis. The mutation introduces a KpnI site; therefore, we probed KpnI-digested chromosomal DNA with pES2-2 and found, as expected, that the mutant contained two smaller bands in place of the single larger band of the wild-type strain.

Examination by transmission electron microscopy revealed that KV1513 lacked flagella (data not shown). Introduction of pES2-2 restored motility to KV1513 (data not shown), although migration of the complemented strain on soft agar plates was delayed relative to that of the plasmid-bearing wild-type counterpart. These data suggest that complementation with *rpoN* on a low-copy-number plasmid is not optimal for the motility of *V. fischeri*. Prolonged incubation of the *rpoN* null mutant KV1513 on soft agar plates failed to yield motile revertants (data not shown), an observation similar to that made with null mutants of *V. cholerae rpoN* (13) and *V. fischeri flrA*

* Corresponding author. Mailing address: Department of Microbiology and Immunology, Loyola University Chicago, 2160 S. First Ave., Bldg. 105, Rm. 3860A, Maywood, IL 60153. Phone: (708) 216-0869. Fax: (708) 216-9574. E-mail: kvisick@lumc.edu.

TABLE 1. List of strains and plasmids used in this study

Strain or plasmid	Relevant characteristic(s)	Reference
Strains		
DM127	*flrA*::*kan*	22
ES114	Wild-type isolate from *E. scolopes*	2
ESR1	Rif^r	5
KV150	Δ*luxA*::*erm* Rif^r	36
KV618	*rpoN*::Tn*luxAB* Δ*luxA*::*erm* Rif^r	This study
KV1513	*rpoN*::*erm-oriR6K-oriT*	This study
KV661	*fla*::Tn*luxAB* Δ*luxA*::*erm* Rif^r	This study
Plasmids		
pDM88	pEVS79 (30) HindIII + 3.2-kb (*flaA*) HindIII-digested ES114 chromosomal DNA	This study
pDM104-6	pVO8 BamHI/SalI + 3.2-kb BamHI/SalI (*flaA*) fragment from pDM88 into which a Tn::*lacZ* (promoterless) transposon was inserted about 400 bp downstream from the predicted *flaA* start codon	This study
pES2-2	pVO8 BamHI + 2.5-kb (*rpoN*$^+$) BglII-digested ES114 chromosomal DNA	This study
pLD1	KV618 chromosome, digested with NheI and self-ligated; contains Tn*10luxAB* insertion in *rpoN* and flanking DNA	This study
pLD6	pKV69 + EcoRI-PstI (*rpoN*$^+$) from pES2-2	This study
pLMS71	pLD1 SacI + *oriT*, *erm*^{r}, oriR6K cassette from pLMS65	This study
pLMS65	pBS containing *oriT*, *erm*^{r}, oriR6K on a SacI fragment	This study

(22). These results suggest that *V. fischeri* motility absolutely requires σ^{54}, which likely operates in conjunction with FlrA.

In *V. cholerae*, σ^{54} controls flagellar gene transcription on at least two levels (13, 27). In conjunction with the transcriptional activator FlrA, σ^{54} induces transcription of the class II genes *flrB* and *flrC*, which encode a two-component signaling pathway. With FlrC, σ^{54} then activates class III gene transcription, including the major flagellin subunit, *flaA*. Since *V. fischeri* motility also requires *flrA* and *flaA* homologs (22; D.S. Millikan and E.G. Ruby, unpublished data), we determined whether *rpoN* controls transcription of the *V. fischeri flaA* gene. Into the *rpoN* mutant KV1513 and its wild-type parent we introduced the plasmid pDM104-6 (Table 1), which carries a *lacZ* reporter gene fused downstream of the *flaA* promoter. We grew the resultant transconjugants in SWT medium (2) and measured β-galactosidase activity when the cells reached the mid-exponential phase of growth (A_{600} = 1.1 to 1.3). Transcription of the reporter gene was reduced by 10-fold in the *rpoN* mutant, a result similar to that achieved by the *flrA* mutant (Table 3). These data confirm that σ^{54} plays a role in motility by activating transcription of at least one flagellar gene.

Role for the *rpoN* gene in biofilm formation. In some organisms, biofilm formation is enhanced by the presence of flagella (25, 26, 33, 37). Therefore, we asked whether the ability of *V. fischeri* to form biofilms in culture was enhanced by the presence of the *rpoN* gene. To assay biofilm formation, we pregrew cells in SWT at 28°C with shaking and then transferred the cultures to glass test tubes. The cells were incubated without shaking for 10 h at 28°C and then exposed to a solution of 1% crystal violet to visualize cells that had formed a biofilm on the test tube (25). After further incubation for 15 min, the tubes were rinsed with distilled H_2O. Biofilms formed at the air-liquid interface were stained purple. Under these conditions (Fig. 1A) and others (data not shown), the *rpoN* mutant formed a biofilm that differed from that of the wild type: it was consistently broader and stained less intensely. Since levels of growth of the *rpoN* mutant and its wild-type parent were similar (Fig. 1B), these data support a role for *rpoN* in biofilm formation. To control for the role of flagella in biofilm formation, we examined the biofilm-forming ability of another mutant, KV661 (Table 1), that cannot form flagella because of a disruption in the key biosynthetic *flgB* operon. Since this mutant produced biofilms similar to those of its wild-type parent (data not shown), the role of *rpoN* in biofilm formation must be independent of its role in flagellar gene expression.

Nitrogen metabolism and iron sequestration by the *rpoN* mutant. In a number of organisms, a functional copy of the *rpoN* gene is required for the assimilation of nitrogen from nonammonia sources, e.g., glutamine and serine (19, 28). Thus, we examined growth of the *V. fischeri rpoN* mutant in the presence of a variety of nitrogen sources. The *rpoN* mutant was not defective for growth in rich media, such as SWT, at a variety of temperatures (data not shown), nor was it defective for growth in a glucose minimal medium (MM-G) (29) con-

TABLE 2. Sequence analysis of the *rpoN* locus

Sequence[a]	Protein length	Size (no. of amino acids) of homolog	Organism	% Identity	Predicted function	Reference
ORF1 (partial cds)	134	241	*V. parahaemolyticus*	87	ABC transporter	17
rpoN	489	489	*Vibrio alginolyticus*	75	σ^{54}	12
ORF95	95	95	*V. alginolyticus*	74	σ^{54} modulation	12
ptsN	147	148	*V. cholerae*	73	Nitrogen regulatory IIA component	7

[a] cds, coding sequence.

TABLE 3. Transcription of *flaA* in wild-type and mutant strains

Strain[a]	Genotype	Reporter activity[b]
ES114	Wild type	140 ± 1.3
KV1513	*rpoN*	16 ± 1.2
DM127	*flrA*	12 ± 1.5

[a] Strains carried plasmid pDM104-6, which contained the *flaA*::*lacZ* construct, and were grown to an optical density between 1.1 and 1.3 in SWT.
[b] Reporter activity is reported in Miller units (20). Values are averages ± standard deviations.

taining ammonium chloride and Casamino Acids (Fig. 2A), ammonium chloride (Fig. 2B), or glutamine (data not shown). In contrast to its parent, the *rpoN* mutant grew poorly in MM-G containing serine as the sole nitrogen source (Fig. 2C). Thus, the *V. fischeri rpoN* gene controls assimilation of nitrogen from serine.

In *V. fischeri*, siderophore production and thus iron uptake depend upon GlnD (6), a protein that modulates the *E. coli* and *Salmonella enterica* response to nitrogen availability (reviewed in reference 16). The pathway by which *V. fischeri* GlnD regulates siderophores remains unknown. However, in *E. coli*, GlnD (the uridylyltransferase/uridylyl-removing enzyme) modulates PII, a protein whose activity ultimately affects activation of the σ^{54}-dependent transcriptional activator NtrC. We anticipated, therefore, that a defect in σ^{54} might affect iron uptake in a manner similar to that of the *V. fischeri glnD* mutant. Instead, the *rpoN* mutant retained a significant ability to sequester iron from the environment, in contrast to the isogenic *glnD* mutant (data not shown). Although the *rpoN* mutant grew more slowly than did its wild-type parent on chrome azurol S siderophore assay plates, its growth was not significantly different from that of wild-type cells in the presence of the iron chelator ethylenediamine-di(*o*-hydroxyphenyl-acetic acid) (data not shown). Thus, GlnD likely controls siderophore production by a pathway that does not involve *rpoN*.

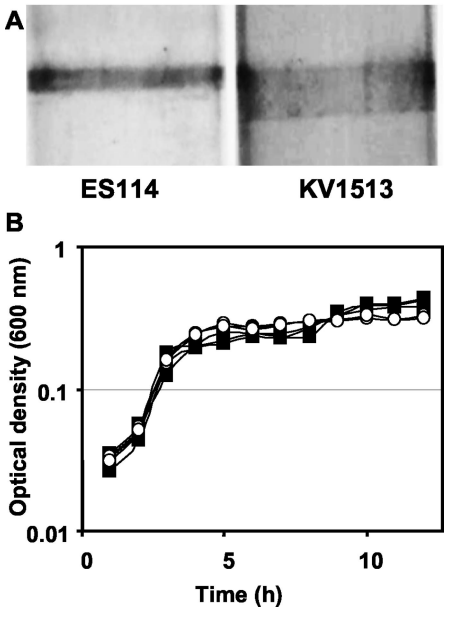

FIG. 1. Biofilm and static growth of the *rpoN* mutant and its parent. (A) Wild-type *V. fischeri* and *rpoN* mutant KV1513 were grown for 10 h in static culture in glass test tubes and then stained with 1% crystal violet. Representative biofilm bands are shown. (B) Growth of the wild type (filled squares) and *rpoN* mutant (open circles) strains in static culture is shown in triplicate.

Bioluminescence emission by the *rpoN* mutant. Luminescence regulation in *V. fischeri* requires the prototypical quorum-sensing system, which consists of the transcriptional activator LuxR (a member of the TetR family) and the autoinducer synthase LuxI (4). Regulation of *V. fischeri* luminescence also involves homologs of the *V. harveyi luxO* and *luxR* (distinct from the *V. fischeri luxR*) genes (3, 15, 23). Inactivation of the *V. fischeri luxR* homolog, *litR*, delayed and reduced light emission in culture (3), while inactivation of the *luxO* homolog in *V. fischeri* strains MJ1 and ES114 resulted in increased luminescence (15, 23). The latter phenotype is identical to that of a *V. harveyi luxO* mutant (1).

Because the *V. harveyi* LuxO protein functions as a σ^{54}-dependent transcriptional activator (14), we asked whether regulation of bioluminescence in *V. fischeri* involves the *rpoN* gene. We monitored the light emission of the *rpoN* mutant and its wild-type parent during growth of the cells in SWT medium. Under a variety of aeration, medium, and temperature conditions, the *rpoN* mutant consistently achieved higher bioluminescence levels, such as the three- to fourfold difference at the peak of luminescence shown in Fig. 3. This result is similar to that seen with a *V. fischeri luxO* mutant (15). This observation supports a role for *rpoN* in repressing luminescence in *V. fischeri*, likely in conjunction with the *luxO* homolog. The target for these regulators remains to be determined.

Colonization by the *rpoN* mutant. Because colonization of *E. scolopes* requires flagella and σ^{54} controls flagellar biogenesis, we determined whether colonization requires σ^{54} by exposing juvenile squid to the *rpoN* mutant KV1513 or to its wild-type parent. Consistent with previous reports of nonmotile strains (5, 22), the *rpoN* mutant did not initiate symbiotic colonization, as measured by symbiotic bioluminescence and viable counts of squid-associated bacteria in a representative experiment (seven squid). In contrast to wild-type-exposed squid, which contained on average 3.46×10^5 CFU/squid, animals inoculated with KV1513 either were uncolonized (four of seven animals) or exhibited colonization levels of <100 CFU/squid (three of seven animals). The apparent low level of colonization in the latter squid group likely reflects bacteria aggregated on the surface of the light organ rather than bacteria present inside the light organ, as previously reported (22, 24).

Complementation with a functional copy of *rpoN* (pLD6) restored the ability to initiate symbiotic colonization (84 to 90% of animals inoculated with the *rpoN* mutant versus 90 to 96% of animals inoculated with the wild-type parent). This rate of initiation was greater than that reported (49%) for the complemented *flrA* mutant (22) and likely reflects differences in the ways the assays were performed. The colonization levels achieved by squid inoculated with the complemented *rpoN* mutant varied, but some animals achieved wild-type levels of colonization. Thus, while these data clearly demonstrate a role for *rpoN* in symbiotic initiation, a role for this regulator in subsequent stages cannot be assessed with the tools currently available; further investigation of its role in symbiotic colonization will require construction of strains with a tightly regulated promoter upstream of the *rpoN* gene.

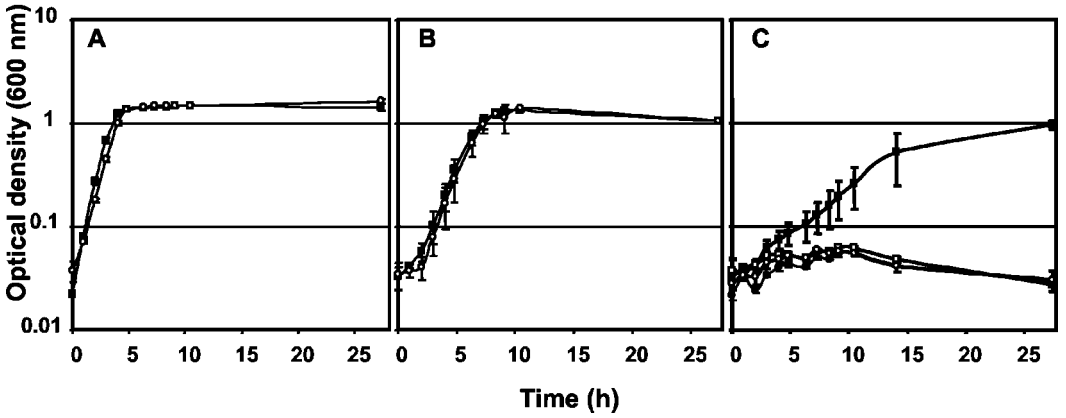

FIG. 2. Growth of the *rpoN* mutant in minimal media containing various nitrogen sources. Wild-type strain ES114 (filled squares) and the *rpoN* mutant KV1513 (open circles) were pregrown in MM-G containing NH_4Cl and Casamino Acids, washed with MM-G without a nitrogen source, and then inoculated into MM-G containing NH_4Cl and Casamino Acids (A), NH_4Cl (B), and Ser (C). ES114 (open squares) and KV1513 (filled circles) were also inoculated into MM-G lacking a nitrogen source as a control (C). Growth was measured using a spectrophotometer at 600 nm. The experiment was performed in triplicate, and the error bars represent the standard deviations. In panel C, growth of KV1513 in the presence of serine is indistinguishable from its growth in media lacking a nitrogen source. In some experiments, growth of KV1513 in MM-G with serine was delayed but reached an optical density measurement similar to that of the wild-type strain at the 24-h time point.

Summary. This work shows that σ^{54} of *V. fischeri* plays multiple roles. It controls flagellar biogenesis and, thus, motility. It contributes to biofilm development, nitrogen assimilation, and the regulation of bioluminescence. Finally, σ^{54} plays an essential role in the establishment of symbiotic colonization, most likely due to its requirement for motility. Whether other σ^{54}-dependent traits contribute to symbiotic initiation or to later stages of colonization remains to be determined. This work provides a foundation for a deeper understanding of the contributions to symbiotic colonization of σ^{54}-dependent determinants such as motility, bioluminescence, and biofilm development.

Nucleotide sequence accession number. The 2.5-kb chromosomal insert from plasmid pES2-2 has been assigned GenBank accession number AY082659.

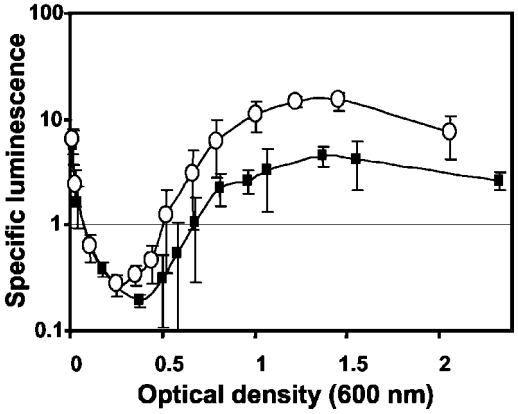

FIG. 3. Bioluminescence of the *rpoN* mutant and its parent in culture. The *rpoN* mutant KV1513 (open circles) and its parent ES114 (filled squares) were grown at 24°C in 125-ml flasks containing 25 ml of SWT (2). Luminescence was measured over time using a Turner 20/20 Biosystems luminometer at the factory settings. Specific luminescence was determined by dividing the relative luminescence per milliliter by the optical density at each time point. The experiment was repeated multiple times under a variety of temperature and aeration conditions. The *rpoN* mutant consistently emitted higher levels of luminescence. Data shown are from a representative experiment in which the average of values for three cultures of each strain are plotted. Error bars represent standard deviations.

We thank Cindy R. DeLoney for examining the *rpoN* mutant by transmission electron microscopy, Erika Simel for her assistance in cloning and sequencing the *rpoN* gene, Therese M. Bartley for expert technical assistance, and members of our labs for critical reading of the manuscript.

This work was supported by NIH grant GM59690 awarded to K.L.V.

REFERENCES

1. **Bassler, B. L., M. Wright, and M. R. Silverman.** 1994. Sequence and function of LuxO, a negative regulator of luminescence in *Vibrio harveyi*. Mol. Microbiol. **12:**403–412.
2. **Boettcher, K. J., and E. G. Ruby.** 1990. Depressed light emission by symbiotic *Vibrio fischeri* of the sepiolid squid *Euprymna scolopes*. J. Bacteriol. **172:** 3701–3706.
3. **Fidopiastis, P. M., C. M. Miyamoto, M. G. Jobling, E. A. Meighen, and E. G. Ruby.** 2002. LitR, a new transcriptional activator in *Vibrio fischeri*, regulates luminescence and symbiotic light organ colonization. Mol. Microbiol. **45:** 131–143.
4. **Fuqua, C., S. C. Winans, and E. P. Greenberg.** 1996. Census and consensus in bacterial ecosystems: the LuxR-LuxI family of quorum-sensing transcriptional regulators. Annu. Rev. Microbiol. **50:**727–751.
5. **Graf, J., P. V. Dunlap, and E. G. Ruby.** 1994. Effect of transposon-induced motility mutations on colonization of the host light organ by *Vibrio fischeri*. J. Bacteriol. **176:**6986–6991.
6. **Graf, J., and E. G. Ruby.** 2000. Novel effects of a transposon insertion in the *Vibrio fischeri glnD* gene: defects in iron uptake and symbiotic persistence in addition to nitrogen utilization. Mol. Microbiol. **37:**168–179.
7. **Heidelberg, J. F., J. A. Eisen, W. C. Nelson, R. A. Clayton, M. L. Gwinn, R. J. Dodson, D. H. Haft, E. K. Hickey, J. D. Peterson, L. A. Umayam, S. R. Gill, K. E. Nelson, T. D. Read, H. Tettelin, D. Richardson, M. D. Ermolaeva, J. Vamathevan, S. Bass, H. Qin, I. Dragoi, P. Sellers, L. McDonald, T. Utterback, R. D. Fleishmann, W. C. Nierman, O. White, S. L. Salzberg, H. O. Smith, R. R. Colwell, J. J. Mekalanos, J. C. Venter, and C. M. Fraser.** 2000. DNA sequence of both chromosomes of the cholera pathogen *Vibrio cholerae*. Nature **406:**477–483.
8. **Hendrickson, E. L., J. Plotnikova, S. Mahajan-Miklos, L. G. Rahme, and F. M. Ausubel.** 2001. Differential roles of the *Pseudomonas aeruginosa* PA14 *rpoN* gene in pathogenicity in plants, nematodes, insects, and mice. J. Bacteriol. **183:**7126–7134.
9. **Heurlier, K., V. Dénervaud, G. Pessi, C. Reimmann, and D. Haas.** 2003. Negative control of quorum sensing by RpoN (σ^{54}) in *Pseudomonas aeruginosa* PAO1. J. Bacteriol. **185:**2227–2235.

10. **Ishimoto, K. S., and S. Lory.** 1989. Formation of pilin in *Pseudomonas aeruginosa* requires the alternative σ factor (RpoN) subunit of RNA polymerase. Proc. Natl. Acad. Sci. USA **86:**1954–1957.
11. **Jones, D. H., F. C. Franklin, and C. M. Thomas.** 1994. Molecular analysis of the operon which encodes the RNA polymerase sigma factor σ^{54} of *Escherichia coli*. Microbiology **140:**1035–1043.
12. **Kawagishi, I., M. Nakada, N. Nishioka, and M. Homma.** 1997. Cloning of a *Vibrio alginolyticus rpoN* gene that is required for polar flagellar formation. J. Bacteriol. **179:**6851–6854.
13. **Klose, K. E., and J. J. Mekalanos.** 1998. Distinct roles of an alternative sigma factor during both free-swimming and colonizing phases of the *Vibrio cholerae* pathogenic cycle. Mol. Microbiol. **28:**501–520.
14. **Lilley, B. N., and B. L. Bassler.** 2000. Regulation of quorum sensing in *Vibrio harveyi* by LuxO and Sigma-54. Mol. Microbiol. **36:**940–954.
15. **Lupp, C., M. Urbanowski, E. P. Greenberg, and E. G. Ruby.** 2003. The *Vibrio fischeri* quorum-sensing systems *ain* and *lux* sequentially induce luminescence gene expression and are important for persistence in the squid host. Mol. Microbiol. **50:**319–331.
16. **Magasanik, B.** 1996. Regulation of nitrogen utilization, p. 1344–1356. *In* F. C. Neidhardt et al. (ed.), *Escherichia coli* and *Salmonella*: cellular and molecular biology, 2nd ed., vol. 1. ASM Press, Washington, D.C.
17. **Makino, K., K. Oshima, K. Kurokawa, K. Yokoyama, T. Uda, K. Tagomori, Y. Iijima, M. Najima, M. Nakano, A. Yamashita, Y. Kubota, S. Kimura, T. Yasunaga, T. Honda, H. Shinagawa, M. Hattori, and T. Iida.** 2003. Genome sequence of *Vibrio parahaemolyticus*: a pathogenic mechanism distinct from that of *V. cholerae.* Lancet **361:**743–749.
18. **McFall-Ngai, M. J.** 1999. Consequences of evolving with bacterial symbionts: insights from the squid-vibrio associations. Annu. Rev. Ecol. Syst. **30:**235–256.
19. **Merrick, M. J.** 1993. In a class of its own—the RNA polymerase sigma factor σ 54 (σ N). Mol. Microbiol. **10:**903–909.
20. **Miller, J. H.** 1972. Experiments in molecular genetics. Cold Spring Harbor Laboratory, Cold Spring Harbor, N.Y.
21. **Millikan, D. S., and E. G. Ruby.** 2002. Alterations in *Vibrio fischeri* motility correlate with a delay in symbiosis initiation and are associated with additional symbiotic colonization defects. Appl. Environ. Microbiol. **68:**2519–2528.
22. **Millikan, D. S., and E. G. Ruby.** 2003. FlrA, a σ^{54}-dependent transcriptional activator in *Vibrio fischeri*, is required for motility and symbiotic light-organ colonization. J. Bacteriol. **185:**3547–3557.
23. **Miyamato, C. M., Y. H. Lin, and E. A. Meighen.** 2000. Control of bioluminescence in *Vibrio fischeri* by the LuxO signal response regulator. Mol. Microbiol. **36:**594–607.
24. **Nyholm, S. V., E. V. Stabb, E. G. Ruby, and M. J. McFall-Ngai.** 2000. Establishment of an animal-bacterial association: recruiting symbiotic vibrios from the environment. Proc. Natl. Acad. Sci. USA **97:**10231–10235.
25. **O'Toole, G. A., and R. Kolter.** 1998. Flagellar and twitching motility are necessary for *Pseudomonas aeruginosa* biofilm development. Mol. Microbiol. **30:**295–304.
26. **Pratt, L. A., and R. Kolter.** 1998. Genetic analysis of *Escherichia coli* biofilm formation: roles of flagella, motility, chemotaxis and type I pili. Mol. Microbiol. **30:**285–293.
27. **Prouty, M. G., N. E. Correa, and K. E. Klose.** 2001. The novel σ54- and σ28-dependent flagellar gene transcription hierarchy of *Vibrio cholerae*. Mol. Microbiol. **39:**1595–1609.
28. **Reitzer, L., and B. L. Schneider.** 2001. Metabolic context and possible physiological themes of ó^{54}-dependent genes in *Escherichia coli*. Microbiol. Mol. Biol. Rev. **65:**422–444.
29. **Ruby, E. G., and K. H. Nealson.** 1977. Pyruvate production and excretion by the luminous marine bacteria. Appl. Environ. Microbiol. **34:**164–169.
30. **Stabb, E. V., and E. G. Ruby.** 2002. RP4-based plasmids for conjugation between *Escherichia coli* and members of the Vibrionaceae. Methods Enzymol. **358:**413–426.
31. **Stewart, B. J., and L. L. McCarter.** 2003. Lateral flagellar gene system of *Vibrio parahaemolyticus*. J. Bacteriol. **185:**4508–4518.
32. **Totten, P. A., J. C. Lara, and S. Lory.** 1990. The *rpoN* gene product of *Pseudomonas aeruginosa* is required for expression of diverse genes, including the flagellin gene. J. Bacteriol. **172:**389–396.
33. **Vatanyoopaisarn, S., A. Nazli, C. E. R. Dodd, C. E. D. Rees, and W. M. Waites.** 2000. Effect of flagella on initial attachment of *Listeria monocytogenes* to stainless steel. Appl. Environ. Microbiol. **66:**860–863.
34. **Visick, K. L., J. Foster, J. Doino, M. McFall-Ngai, and E. G. Ruby.** 2000. *Vibrio fischeri lux* genes play an important role in colonization and development of the host light organ. J. Bacteriol. **182:**4578–4586.
35. **Visick, K. L., and M. J. McFall-Ngai.** 2000. An exclusive contract: specificity in the *Vibrio fischeri-Euprymna scolopes* partnership. J. Bacteriol. **182:**1779–1787.
36. **Visick, K. L., and E. G. Ruby.** 1996. Construction and symbiotic competence of a *luxA*-deletion mutant of *Vibrio fischeri*. Gene **175:**89–94.
37. **Watnick, P. I., C. M. Lauriano, K. E. Klose, L. Croal, and R. Kolter.** 2001. The absence of a flagellum leads to altered colony morphology, biofilm development and virulence in *Vibrio cholerae* O139. Mol. Microbiol. **39:**223–235.
38. **Wolfe, A. J., and H. C. Berg.** 1989. Migration of bacteria in semisolid agar. Proc. Natl. Acad. Sci. USA **86:**6973–6977.

APPLIED AND ENVIRONMENTAL MICROBIOLOGY, Dec. 2003, p. 7527–7530 Vol. 69, No. 12
0099-2240/03/$08.00+0 DOI: 10.1128/AEM.69.12.7527–7530.2003

Chemoattraction of *Vibrio fischeri* to Serine, Nucleosides, and *N*-Acetylneuraminic Acid, a Component of Squid Light-Organ Mucus

Cindy R. DeLoney-Marino,† Alan J. Wolfe, and Karen L. Visick*

Department of Microbiology and Immunology, Loyola University Chicago, Maywood, Illinois 60153

Received 23 June 2003/Accepted 19 August 2003

Newly hatched juveniles of the Hawaiian squid *Euprymna scolopes* rapidly become colonized by the bioluminescent marine bacterium *Vibrio fischeri*. Motility is required to establish the symbiotic colonization, but the role of chemotaxis is unknown. In this study we analyzed chemotaxis of *V. fischeri* to a number of potential attractants. The bacterium migrated toward serine and most sugars tested. *V. fischeri* also exhibited the unusual ability to migrate to nucleosides and nucleotides as well as to N-acetylneuraminic acid, a component of squid mucus.

Upon hatching, the light organ of the juvenile Hawaiian squid, *Euprymna scolopes*, is specifically colonized by the luminous marine bacterium *Vibrio fischeri* (reviewed in references 7 and 13). *V. fischeri* cells present in the seawater aggregate in mucus secreted from the light organ and then appear to stream into the openings of the light organ (10), suggesting directed movement by the bacterium. The light-organ mucus, secreted upon bacterial exposure (10) and subsequently within the light organ in response to symbiotic colonization (9), contains two sugars, *N*-acetylgalactosamine (NAGal) and *N*-acetylneuraminic acid (NANA) (10). These sugars, as well as amino acids and peptides within the light organ (6), may serve as nutrient sources and/or chemoattractants to enhance entry by *V. fischeri*, which must be motile to colonize successfully (5). To begin investigating the potential role of chemotaxis in symbiotic initiation, we characterized the response of the bacterium to various nutrients.

Motile cells inoculated onto a soft agar medium containing two attractants form an outermost ring in response to a spatial gradient that results from the consumption and subsequent diffusion of the preferred attractant (14). Similarly, an inner ring forms to the second attractant (11 and B. M. Pruss and A. J. Wolfe, unpublished data). When inoculated onto TB-SW soft agar plates (1% tryptone, 0.88% NaCl, 0.62% $MgSO_4$, 0.072% $CaCl_2$, 0.038% KCl, 0.25% agar), cells of *V. fischeri* strain ES114 (2) formed two concentric rings (Fig. 1A). Cells of *Escherichia coli* also form two rings on tryptone-based soft agar, with the outer and inner rings sensing serine and aspartate, respectively (1). We therefore tested whether *V. fischeri* also migrated to serine and aspartate. While the bacterium did not respond to aspartate (data not shown), the addition of increasing concentrations of serine to the soft agar slowed the migration of the inner ring of *V. fischeri*, indicating that the cells present in that ring consume, sense, and migrate to serine (Fig. 1B and C). We used an excess of serine to disrupt the gradient and found that serine perturbed migration of the inner ring (arrows in Fig. 1 depict the location of the spot of serine). Closer inspection of the rings revealed that a doublet we occasionally observed (e.g., Fig. 1B) consisted of faster-migrating cells on the surface of the plate and slower-migrating cells deeper in the agar, both of which responded to serine. Because the doublet responded as a unit to the addition of serine, we believe it should be considered a single, serine-responsive ring. Serine can be metabolized anaerobically by organisms such as *E. coli* (1); thus, the separation may result from a lag in migration due to the less-oxygenated environment deep in the plate. This would explain the apparent discrepancy between this report of two migrating rings and a recent report that mentions three (8).

We sought further evidence that the cells in the inner ring sensed serine, taking advantage of the fact that rings of bacteria migrating toward the same attractant will fuse when they meet (1). Using TBS soft agar plates (1% tryptone, 2% NaCl, and 0.25% agar), we coinoculated *V. fischeri* cells with *E. coli* cells. The inner ring of *V. fischeri* fused with the outer (serine-sensing) ring formed either by wild-type *E. coli* (Fig. 1D) or a *tar* mutant that cannot sense aspartate (Fig. 1E); the fused ring was perturbed when an excess of serine was spotted just beyond the ring. In contrast, neither ring of *V. fischeri* fused with the single aspartate-sensing ring of an *E. coli tsr* mutant (Fig. 1F). These results confirmed that *V. fischeri* cells in the inner ring migrate toward serine and that those in the outer ring do not sense aspartate.

To identify the substrate sensed by the outer ring of *V. fischeri*, we spotted each of the other 18 amino acids onto Tris-buffered TB-SW soft agar plates just beyond the migrating rings. Although alanine, arginine, asparagine, histidine, and threonine slightly perturbed the inner ring, no amino acid perturbed the outer ring (data not shown), suggesting that the cells in the outer ring do not recognize an amino acid. We therefore investigated the ability of *V. fischeri* to migrate toward other components of tryptone and found that the outer

* Corresponding author. Mailing address: Department of Microbiology and Immunology, Loyola University Chicago, 2160 S. First Ave., Bldg. 105, Maywood, IL 60153. Phone: (708) 216-0869. Fax: (708) 216-9574. E-mail: kvisick@lumc.edu.

† Present address: University of Southern Indiana, Department of Biology, Evansville, IN 47712.

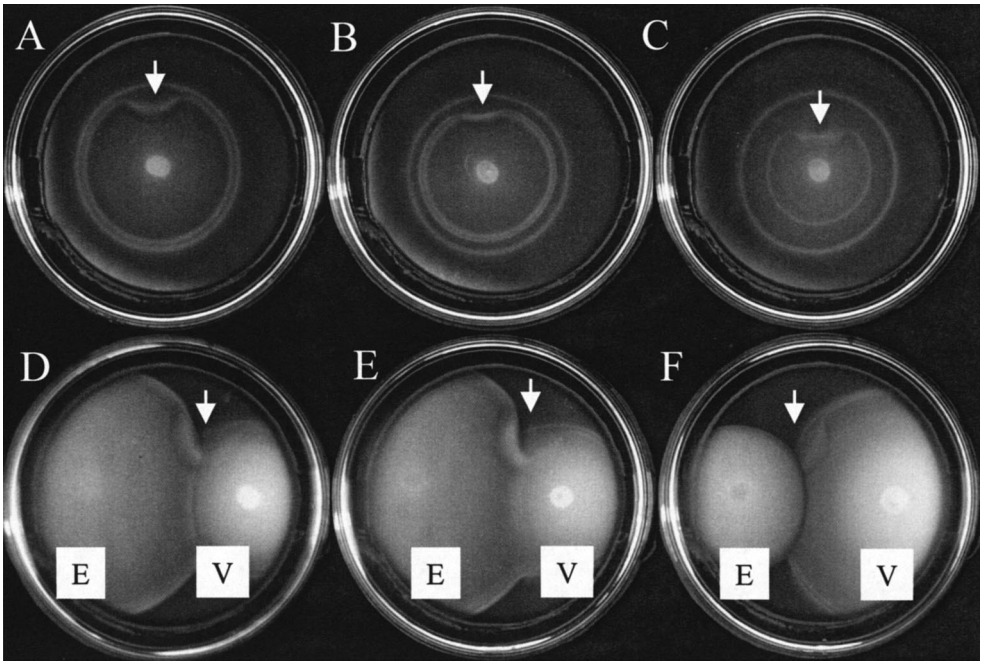

FIG. 1. (A-C) Migration of *V. fischeri* to serine. *V. fischeri* cells were inoculated onto TB-SW plates in the absence (A) or presence of increasing concentrations of serine (0.75 mM [B] or 2 mM [C]). Plates were incubated at 28°C for 5 h. Arrows indicate where an excess of serine was spotted directly onto the plate just beyond the migrating rings. (D-F) Cells of *V. fischeri* (V) and *E. coli* (E) were coinoculated on TBS soft agar plates. (D) *E. coli* strain RP437, wild-type for chemotaxis. (E) *E. coli* strain RP5854, *tar*. (F) *E. coli* strain RP5714, *tsr*. *E. coli* cells were inoculated at 28°C for 7 to 12 h prior to inoculation with *V. fischeri*, followed by incubation for an additional 5 h. Arrows indicate where an excess of serine was spotted directly onto the plate just beyond the migrating rings.

ring of cells responded to the nucleoside thymidine (Fig. 2A). Increasing concentrations of thymidine added to Tris-buffered TB-SW plates caused cells in the outer ring to migrate more slowly, and an excess of thymidine perturbed that migration (data not shown). This suggests that in TB-SW this organism preferentially consumes and senses thymidine over serine. Indeed, *V. fischeri* cells grew with thymidine as a sole carbon source (data not shown). Supplementation with other ribonucleosides (adenosine, guanosine, uridine, and cytodine) similarly slowed the migration of the outer ring of *V. fischeri* cells, and spotting with an excess of these ribonucleosides just beyond the rings formed on TB-SW perturbed only the outer ring (Fig. 2B and C and data not shown), indicating that these cells could respond to any ribonucleoside. We also spotted with deoxynucleotide triphosphates (dATP, dCTP, dGTP, dTTP), which similarly perturbed only the outer ring (data not shown). Because deoxynucleoside triphosphates differ from ribonucleosides in two ways, the sugar moiety (deoxyribose versus ribose) and the phosphorylation state (triphosphate versus unphosphorylated), these data suggest that neither the sugar

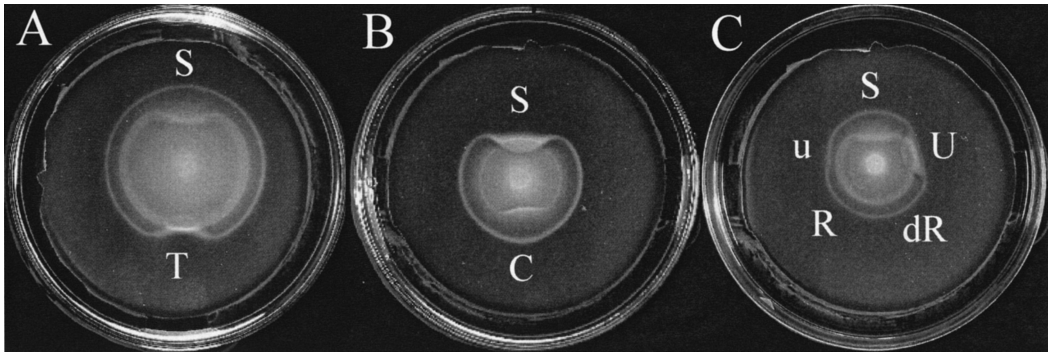

FIG. 2. Migration of *V. fischeri* to nucleosides and their components. *V. fischeri* cells were inoculated onto Tris-buffered TB-SW soft agar plates for 5 h at 28°C. (A) Aliquots (10 μl) of 0.121 M thymidine (T) and 2 M serine (S) were spotted just beyond the migrating rings of *V. fischeri*. (B) Serine (2 M) (S) and cytidine (0.171 M) (C) were spotted just beyond the migrating rings formed on Tris-buffered TB-SW plates containing 1 mM cytidine. Note that the ring perturbed by serine is now located on the outside of the ring perturbed by cytidine. (C) Aliquots (10 μl) of equimolar concentrations (0.066 M) of uridine (U), uracil (u), ribose (R), and deoxyribose (dR) were spotted onto plates just beyond the migrating rings. Serine (2 mM) was added to all plates to provide a better separation of the inner and outer rings for visualization of the response to nucleoside or nucleoside component addition. An excess of serine (S) was spotted at the top of each plate as a comparison.

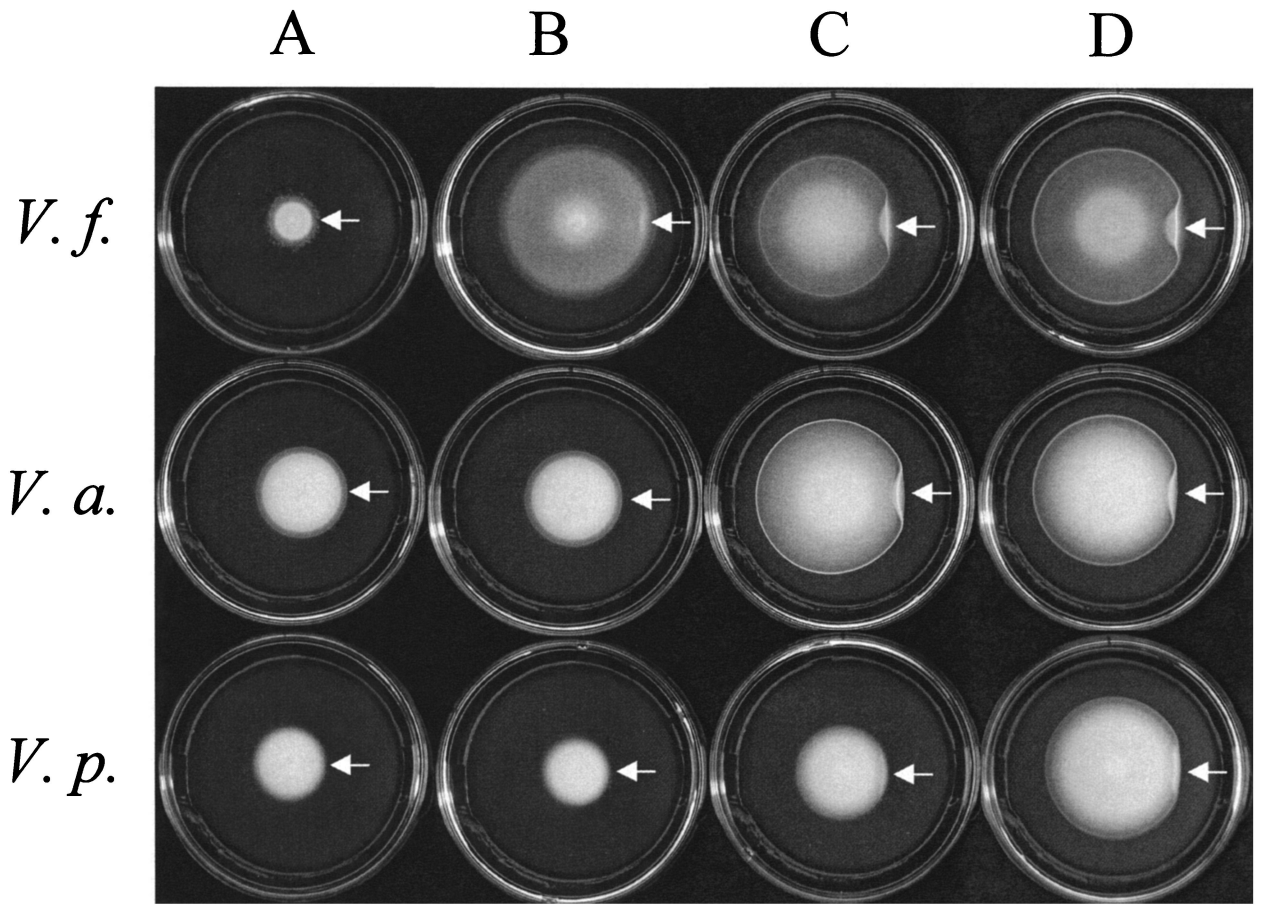

FIG. 3. Migration of various *Vibrio* strains to NANA and other sugars. Cells of *V. fischeri* (*V.f.*), *V. anguillarum* strain PKJ (*V.a.*), and *V. parahaemolyticus* strain KNH1 (*V.p.*) were inoculated near the center of MM-M soft agar plates (column A) or MM-M soft agar plates containing either 1 mM NANA (column B), 1 mM glucose (column C), or 1 mM NAG (column D). Plates were incubated at 28°C for approximately 24 h. Arrows indicate where an excess of the respective carbon source was spotted onto the plate just beyond the migrating rings.

component nor the phosphorylation state constitutes a critical component of recognition.

We then tested whether *V. fischeri* cells in the outer ring responded to the whole nucleoside molecule or to its components (base or sugar) by spotting equimolar concentrations (0.066 M) of these substrates just beyond the outer ring. *V. fischeri* cells preferentially responded to the entire molecule (Fig. 2C and data not shown). Neither ribose nor deoxyribose perturbed the outer ring (Fig. 2C). Uracil and thymine occasionally caused only slight perturbations, while cytosine, guanine, or adenine did not (Fig. 2C and data not shown). When uracil and thymine were tested at higher concentrations, a slight perturbation was consistently observed (data not shown). Adenine, cytosine, and guanine were not tested at higher concentrations due to their insolubility. Thus, *V. fischeri* can consume, sense, and migrate to nucleosides and nucleotides. To our knowledge this is the first report of bacterial migration toward the building blocks of DNA and RNA. Whether this ability enhances colonization of *E. scolopes* by *V. fischeri* is unknown; however, it is not unreasonable to expect a higher concentration of nucleic acids in the vicinity of the squid, particularly because surface cells of the light organ undergo apoptosis during early stages of symbiotic colonization (4).

In addition to serine and nucleosides and nucleotides, *V. fischeri* may perform chemotaxis to sugars. Surface molecules of host cells frequently contain sugar moieties, and the mucus secreted by *E. scolopes* contains the sugars NANA and NAGal. We therefore tested the ability of *V. fischeri* to migrate in response to a variety of sugars and other substrates. Potential chemoattractants were either added to or spotted on one of two media: TB-SW and HEPES minimal medium (12) containing 25 mM mannitol (MM-M). Mannitol serves as a carbon source but not as an attractant for *V. fischeri* (Fig. 3, first row, column A). As shown in Table 1, *V. fischeri* migrated toward a variety of substrates (13 of 18 tested), including glucose, cellobiose, and to a lesser extent, ribose. Ribose caused a faint additional inner ring to form but did not slow migration of the outer ring, implying that the receptors for thymidine and ribose are distinct. The same was true for cyclic AMP (3).

When we tested the two sugars present in squid mucus, we found that whereas NANA served as a chemoattractant for *V. fischeri*, NAGal did not (Fig. 3, first row, column B, and Table 1). To test whether this attraction is a common trait among other vibrio species, we examined the ability of the marine isolates *V. anguillarum* and *V. parahaemolyticus* to migrate to the sugar. Unlike that of *V. fischeri*, migration of *V. anguillarum*

TABLE 1. Response of *V. fischeri* to various substrates added to TB-SW or MM-M

Substrate	Medium	
	TB-SW[a]	MM-M[b]
Cyclic AMP	+	+
Cellobiose	++	ND
Choline	−	−
Deoxyribose	−	ND
Fructose	++	+
Galactose	+	ND
Glucose	++	++
Glucosamine	−	−
Glycerol	+	−
Maltose	+	ND
Mannitol	−	−
Mannose	+	++
NAGal	−	−
NAG	++	++
NANA	+	++
Raffinose	+	ND
Ribose	+	ND
Sucrose	++	ND

[a] For TB-SW, a positive response was noted if an additional concentric ring formed that was subsequently perturbed by spotting the appropriate substrate. ++, dense ring; +, faint ring; − no ring.

[b] For MM-M, a positive response was noted if addition of a substrate, added at concentrations of 1 μM to 10 mM, allowed the cells to form a ring that migrated beyond the zone of growth formed in the presence of MM-M alone. ++, radius of >10 mm; +, radius of <10 mm; −, no difference. ND, migration to this substrate was not tested under these conditions.

and *V. parahaemolyticus* was not improved by the addition of NANA to MM-M, nor was migration perturbed by spotting with NANA (Fig. 3, columns A and B). In contrast, all three organisms formed rings in response to either 1 mM glucose or 1 mM *N*-acetylglucosamine (NAG), which were perturbed by an excess of either glucose or NAG, respectively (Fig. 3, columns C and D). This potentially unique chemotaxis to NANA, combined with the ability of *V. fischeri* to use NANA as a carbon source (data not shown), raises the intriguing possibility that migration toward this sugar could contribute to initiating symbiotic colonization.

Given the absolute requirement for motility in symbiotic colonization (5), the data reported here provide an important first step in assessing the contribution of chemotaxis to colonization. *V. fischeri* apparently encodes an unusually large number of chemoreceptors; over 40 genes contain putative chemotaxis signaling motifs (C. R. DeLoney-Marino, unpublished observations). We are presently working to identify receptors specific for the identified attractants by constructing and characterizing chemotaxis mutants. These mutants will permit more direct testing of a potential role for chemotaxis in establishing the *Vibrio*-squid symbiosis.

We thank Joy Campbell and Therese Bartley for expert technical assistance, E. G. Ruby for experimental suggestions, J. S. Parkinson and E. G. Ruby for strains, and members of our labs for critical reading of the manuscript. Genome information was provided by the *Vibrio fischeri* Genome Project, at http://ergo.integratedgenomics.com/Genomes/VFI, supported by the W. M. Keck Foundation.

This work was supported by NIH grant GM59690 awarded to K.L.V. and by the National Science Foundation under a Research Fellowship in Microbial Biology awarded in 2001 to C.R.D.

REFERENCES

1. **Adler, J.** 1966. Chemotaxis in bacteria. Science **153:**708–716.
2. **Boettcher, K. J., and E. G. Ruby.** 1990. Depressed light emission by symbiotic *Vibrio fischeri* of the sepiolid squid *Euprymna scolopes.* J. Bacteriol. **172:** 3701–3706.
3. **Dunlap, P. V., U. Mueller, T. A. Lisa, and K. S. Lundberg.** 1992. Growth of the marine luminous bacterium Vibrio fischeri on 3′:5′-cyclic AMP: correlation with a periplasmic 3′:5′-cyclic AMP phosphodiesterase. J. Gen. Microbiol. **138:**115–123.
4. **Foster, J. S., and M. J. McFall-Ngai.** 1998. Induction of apoptosis by cooperative bacteria in the morphogenesis of host epithelial tissues. Dev. Genes Evol. **208:**295–303.
5. **Graf, J., P. V. Dunlap, and E. G. Ruby.** 1994. Effect of transposon-induced motility mutations on colonization of the host light organ by *Vibrio fischeri.* J. Bacteriol. **176:**6986–6991.
6. **Graf, J., and E. G. Ruby.** 1998. Host-derived amino acids support the proliferation of symbiotic bacteria. Proc. Natl. Acad. Sci. USA **95:**1818–1822.
7. **McFall-Ngai, M. J.** 1999. Consequences of evolving with bacterial symbionts: insights from the squid-vibrio associations. Annu. Rev. Ecol. Syst. **30:**235–256.
8. **Millikan, D. S., and E. G. Ruby.** 2002. Alterations in *Vibrio fischeri* motility correlate with a delay in symbiosis initiation and are associated with additional symbiotic colonization defects. Appl. Environ. Microbiol. **68:**2519–2528.
9. **Nyholm, S. V., B. Deplancke, H. R. Gaskins, M. A. Apicella, and M. J. McFall-Ngai.** 2002. Roles of *Vibrio fischeri* and nonsymbiotic bacteria in the dynamics of mucus secretion during symbiont colonization of the *Euprymna scolopes* light organ. Appl. Environ. Microbiol. **68:**5113–5122.
10. **Nyholm, S. V., E. V. Stabb, E. G. Ruby, and M. J. McFall-Ngai.** 2000. Establishment of an animal-bacterial association: recruiting symbiotic vibrios from the environment. Proc. Natl. Acad. Sci. USA **97:**10231–10235.
11. **Pruss, B. M., J. M. Nelms, C. Park, and A. J. Wolfe.** 1994. Mutations in NADH:ubiquinone oxidoreductase of *Escherichia coli* affect growth on mixed amino acids. J. Bacteriol. **176:**2143–2150.
12. **Ruby, E. G., and K. H. Nealson.** 1977. Pyruvate production and excretion by the luminous marine bacteria. Appl. Environ. Microbiol. **34:**164–169.
13. **Visick, K. L., and M. J. McFall-Ngai.** 2000. An exclusive contract: specificity in the *Vibrio fischeri-Euprymna scolopes* partnership. J. Bacteriol. **182:**1779–1787.
14. **Wolfe, A. J., and H. C. Berg.** 1989. Migration of bacteria in semisolid agar. Proc. Natl. Acad. Sci. USA **86:**6973–6977.

JOURNAL OF BACTERIOLOGY, Sept. 2002, p. 5121–5129 Vol. 184, No. 18
0021-9193/02/$04.00+0 DOI: 10.1128/JB.184.18.5121–5129.2002

Role for Phosphoglucomutase in *Vibrio fischeri-Euprymna scolopes* Symbiosis

Cindy R. DeLoney, Therese M. Bartley, and Karen L. Visick*

Department of Microbiology and Immunology, Loyola University Chicago, Maywood, Illinois 60153

Received 3 June 2002/Accepted 19 June 2002

***Vibrio fischeri*, a luminescent marine bacterium, specifically colonizes the light organ of its symbiotic partner, the Hawaiian squid *Euprymna scolopes*. In a screen for *V. fischeri* colonization mutants, we identified a strain that exhibited on average a 10-fold decrease in colonization levels relative to that achieved by wild-type *V. fischeri*. Further characterization revealed that this defect did not result from reduced luminescence or motility, two processes required for normal colonization. We determined that the transposon in this mutant disrupted a gene with high sequence identity to the *pgm* (phosphoglucomutase) gene of *Escherichia coli*, which encodes an enzyme that functions in both galactose metabolism and the synthesis of UDP-glucose. The *V. fischeri* mutant grew poorly with galactose as a sole carbon source and was defective for phosphoglucomutase activity, suggesting functional identity between *E. coli* Pgm and the product of the *V. fischeri* gene, which was therefore designated *pgm*. In addition, lipopolysaccharide profiles of the mutant were distinct from that of the parent strain and the mutant exhibited increased sensitivity to various cationic agents and detergents. Chromosomal complementation with the wild-type *pgm* allele restored the colonization ability to the mutant and also complemented the other noted defects. Unlike the *pgm* mutant, a galactose-utilization mutant (*galK*) of *V. fischeri* colonized juvenile squid to wild-type levels, indicating that the symbiotic defect of the *pgm* mutant is not due to an inability to catabolize galactose. Thus, *pgm* represents a new gene required for promoting colonization of *E. scolopes* by *V. fischeri*.**

One of the most intimate interactions between organisms occurs during the establishment of a long-term symbiotic relationship between a microorganism and its host, as exemplified by the *Vibrio*-squid symbiosis. Upon hatching, juveniles of *Euprymna scolopes*, a nocturnal Hawaiian squid, quickly become colonized by the luminescent marine bacterium *Vibrio fischeri*, establishing a symbiosis that persists throughout the lifetime of the squid (see reference 40 for a review). The bacterial symbionts colonize a specialized structure in the squid host, the light organ, located within the mantle cavity of the animal. When a sufficient cell density is reached, the bacteria luminesce, providing the counterillumination ability believed to be an antipredation mechanism for the squid host (see reference 49 for a review). Various studies characterizing the *Vibrio*-squid symbiosis have identified several genetic determinants involved in establishing this association (2, 14, 48, 50, 52); however, much remains to be learned about how these symbiotic partners interact.

Despite the presence of other bacteria in the seawater, the light organ of the juvenile *E. scolopes* is colonized primarily by *V. fischeri* (6); even other *Vibrio* species are generally unable to colonize under lab conditions (29, 36). *V. fischeri* cells colonize the newly hatched aposymbiotic (symbiont-free) juveniles of *E. scolopes* within a few hours, reaching between 10^5 and 10^6 CFU per squid within 24 h (41). The bacteria are drawn to the vicinity of the light organ by currents created by specialized ciliated appendages of the organ as seawater is vented through the mantle cavity of the juvenile squid (see reference 49 for a review). The bacterial cells embed and aggregate in a mucus-like material sloughed off the appendages and secreted from pores located at the base of the light organ (36). As they enter the pores, they encounter mucus-filled ducts (27) and an outwardly directed current created by dense cilia lining the duct walls (see reference 49 for a review); not surprisingly, nonmotile *V. fischeri* are symbiosis defective (14, 36). The ducts ultimately lead to the site of colonization, the internal crypts, where the microbes likely encounter a relatively hostile environment due to the presence of macrophage-like cells (35) and halide peroxidase, an enzyme implicated in oxidative stress (53). A *V. fischeri* mutant that cannot produce catalase does not successfully compete with a catalase-positive strain for colonization (50).

Once inside the crypts of the light organ, the bacteria multiply to a high cell density, where the microbes are exposed to amino acids and peptides which likely serve as a nutrient source (15). Inside the crypts the microbes may attach by using fimbriae to sugar residues (such as mannose [28]) on the surfaces of host epithelial cells: certain *V. fischeri* mutants defective in the ability to hemagglutinate animal red blood cells (a characteristic correlated with the presence of fimbriae in some bacteria) showed a decreased ability to colonize juvenile squid (B. Feliciano and E. Ruby, Abstr. 99th Gen. Meet. Am. Soc. Microbiol. 1999, abstr. N-75, 1999). The presence of surface sugars may also serve as a nutrient source for the symbionts, a strategy employed in other host-microbe interactions. For example, *Bacteroides thetaiotaomicron*, a common mammalian gut commensal, induces fucosylation on the surface of ileal enterocytes in mice. The bacteria then use the fucose residues as an energy source (22).

Within hours of the onset of colonization, the squid under-

* Corresponding author. Mailing address: Department of Microbiology and Immunology, Loyola University Chicago, 2160 S. First Ave., Bldg. 105, Maywood, IL 60153. Phone: (708) 216-0869. Fax: (708) 216-9574. E-mail: kvisick@lumc.edu.

goes bacterium-induced morphological changes, including increased microvillar density (25) and swelling of the epithelial lining of the crypts (30). The specialized ciliated appendages of the light organ also undergo bacterium-induced morphological changes, including lipopolysaccharide (LPS)-mediated apoptosis (12) and complete regression within 4 days of colonization (30). Thus, bacteria colonizing the light organ face continuously changing conditions, including stresses within the light organ and the dramatic morphological changes in the host, which may contribute to the specific colonization by *V. fischeri*. Interestingly, *V. fischeri* luminescence mutants, although able to establish the initial colonization, cannot induce swelling in the crypt epithelial cells and are also unable to maintain persistent symbiosis (48).

More recently identified colonization factors include RscS, a sensor kinase hypothesized to regulate symbiosis-specific genes (52), and OmpU, an outer membrane protein (2). Because colonization appears to require active participation on the part of both the bacterium and the squid host (36), it is likely that this exclusive association depends upon numerous additional host and bacterial genes. Other important bacterial factors may include those involved in chemotaxis, attachment, and protection against host stresses; however, the necessary genetic determinants for such processes have yet to be described.

In an effort to identify additional factors necessary for establishing the *Vibrio*-squid symbiosis, we screened a transposon mutant library and identified a colonization mutant that exhibited on average a 10-fold decrease in colonization ability relative to wild-type *V. fischeri*. We report here the characteristics of this symbiosis mutant of *V. fischeri*.

MATERIALS AND METHODS

Strains and media. The strains used in the present study are listed in Table 1. ESR1, the parent strain used here, was derived from *V. fischeri* ES114. *V. fischeri* cells were grown in SWT medium (6), LBS medium (9), or HEPES minimal medium (MM) (42) containing either glucose or galactose at a final concentration of 0.2%. *Escherichia coli* strains were grown in Luria-Bertani medium (8). Conditioned medium (CM), made from LM medium (31) as described previously (52), was utilized to determine whether the colonization mutant KV733 was defective for bioluminescence in culture. Where appropriate, antibiotics were added to the following final concentrations: chloramphenicol (CHL), 1 to 5 μg ml^{-1} for *V. fischeri* and 30 μg ml^{-1} for *E. coli*; erythromycin (ERY), 1 to 5 μg ml^{-1} for *V. fischeri* and 150 μg ml^{-1} for *E. coli*; rifampin, 100 μg ml^{-1}; kanamycin, 100 μg ml^{-1} for *V. fischeri* and 50 μg ml^{-1} for *E. coli*. Agar was added to a final concentration of 1.5% for solid media or 0.25% for motility plates.

Molecular techniques. All plasmid constructions were carried out by standard molecular biology techniques, with restriction and modifying enzymes obtained from New England Biolabs (Beverly, Mass.) or Promega (Madison, Wis.). Plasmids used or constructed in the present study are shown in Table 1. Cloning of DNA flanking the Tn*10* transposon insertion in *V. fischeri* strain KV733 was accomplished by using the *oriR6K* (the *pir*-dependent origin of replication from plasmid R6K [24]) and CHL resistance elements contained within the transposon.

Genetic techniques. Transposon mutagenesis by using the Tn*10* delivery plasmid pKV124 was described previously (52). Conjugations were performed as described previously (52) by using the appropriate *V. fischeri* recipient strain and two *E. coli* strains: DH5α carrying the plasmid to be transferred and DH5α carrying a conjugal plasmid (either pRK2013 or pEVS104).

The *pgm* and *galK* mutants were constructed with strains and plasmids as follows. The *pgm*::*erm* mutant was derived from pPS24 introduced into ESR1; a recombinant, KV1069, that was ERY resistant and CHL sensitive and grew poorly on MM containing galactose (MM-galactose) was subsequently identified. Similarly, the Δ*pgm* mutant was derived by introducing pPS33 into KV1069 by conjugation. An isolate, KV1177, was sensitive to both ERY and CHL and defective for growth on MM-galactose. The *galK* mutant was obtained by introducing pTMB9 into ESR1. KV1358, a CHL-sensitive strain unable to grow on MM-galactose, was identified.

The *pgm*::Tn*10* mutation was complemented with a wild-type copy of the *seqA-pgm* region inserted in single copy at the Tn*7* insertion site (*att*Tn*7*) in the *V. fischeri* chromosome (4; E. Stabb, unpublished data). Briefly, *E. coli* cells carrying the Tn*7*::*pgm*$^+$-containing plasmid pCD3 served as a donor in a tetraparental mating, which also included *E. coli* cells carrying pUX-BF13 and the *V. fischeri* recipient (ESR1 or KV733). Because an ERY resistance cassette was included within the Tn*7* ends along with *pgm*, ERY-resistant colonies were selected and screened for the loss of kanamycin resistance encoded by the Tn*7* vector. Strains with presumptive Tn*7*::*pgm* insertions were confirmed by Southern blot analysis.

Southern blotting. Chromosomal DNA isolated from *V. fischeri* strain KV733 was digested with *Eco*RV, which cuts once within the mini-Tn*10* transposon, or *Bsr*GI, which cuts outside the transposon. Chromosomal DNA isolated from *V. fischeri* strains KV733 (*pgm*::Tn*10*), KV1069 (*pgm*::*erm*), and KV1177 (Δ*pgm*) was digested with *Hin*dIII. DNA fragments were separated by using a 0.6% agarose gel, transferred onto a nylon membrane (Hybond XL; Amersham-Pharmacia Biotech, Piscataway, N.J.), and UV-cross-linked. Detection was carried out by using the Boehringer Mannheim DIG DNA labeling kit (Roche Molecular Biochemicals, Indianapolis, Ind.). Either random priming or a PCR-based technique was used to generate digoxigenin-labeled DNA complementary to the transposon or to the *pgm* gene. Hybridization and detection were carried out as described previously (52).

Colonization assays. To determine whether mutant *V. fischeri* strains were able to form a symbiotic association with *E. scolopes*, juvenile squids were placed in artificial seawater (Instant Ocean; Aquarium Systems, Mentor, Ohio) containing an inoculum of 1,000 to 5,000 cells of the desired *V. fischeri* strain per ml of fluid and then analyzed for the presence of bacteria in the light organ as previously described (40). The limit of detection is 14 *V. fischeri* cells per squid.

Luminescence assays. KV733 and ESR1 were diluted 1:100 from an overnight culture and grown in CM in the presence or absence of synthetic *V. fischeri* autoinducer (600 ng of 3-oxo-hexanoyl-L-homoserine lactone [Sigma, St. Louis, Mo.] per ml). At various times after inoculation, 1-ml samples were taken for luminescence and optical density (OD) measurements. A TD-20/20 luminometer (Turner Designs, Sunnyvale, Calif.) was used to determine the level of bioluminescence of KV733 and its parent.

Phosphoglucomutase assay. Phosphoglucomutase activity was determined by the method of Adhya and Schwartz (1).

Polymixin B, sodium dodecyl sulfate (SDS), and deoxycholate sensitivity determinations. Polymyxin B MIC determinations were made by using a protocol modified from that of Steinberg and Lehrer (46). Briefly, polymyxin B (Sigma) was diluted to a concentration of 1,280 μg ml^{-1} in 0.01% acetic acid and kept frozen at −20°C. Twofold serial dilutions of the stock antibiotic ranging from 0.04 to 80 μg ml^{-1} were prepared in the first row of a 96-well plate in 0.01% acetic acid–0.1% bovine serum albumin. Tenfold dilutions of these concentrations (0.004 to 8 μg ml^{-1}) were then made in SWT medium in the remaining wells. Log-phase cultures of each strain were inoculated into each dilution in triplicate to a starting concentration of 4×10^5 CFU ml^{-1}, incubated for 24 h, and visually examined for turbidity. The lowest concentration of polymyxin B inhibiting growth was designated the MIC.

We assayed for growth of the cells in the presence of SDS by first preparing SDS to a final concentration of 10% in SWT medium. This medium was inoculated to a starting concentration of 4×10^5 CFU ml^{-1} with log-phase cultures in triplicate which were grown at 28°C with shaking. Then, 1-ml samples were taken for OD measurements over time.

Sensitivity to deoxycholate was determined by diluting overnight cultures 1:1,000 in SWT containing 1% deoxycholate and incubating the cells with shaking at 28°C for 6 h. Growth of the cultures was monitored hourly by diluting and plating onto SWT and then counting the resulting CFU.

LPS gel analysis. LPS fractions were prepared by using a protocol modified from the method of B. L. Reuhs and J. S. Kim (as described in reference 39) with the following modifications: 1.5-ml samples were harvested from cultures grown to an OD at 600 nm of 0.5 to 0.7 in SWT medium, pelleted, decanted, and frozen at −80°C prior to a phenol-water extraction. The resulting LPS fractions were desalted by using MicroSpin G-25 columns (Amersham), and the volume was reduced by lyophilization in a Labconco freeze dryer 4.5 (Labconco, Kansas City, Mo.). The isolated LPS fractions were then resuspended in 20 μl of sample buffer, separated by deoxycholic acid-polyacrylamide gel electrophoresis (PAGE) on 14% acrylamide and silver stained with the Owl silver stain staining kit for electrophoresis (Owl Separation Systems, Portsmouth, N.H.) according to the manufacturer's instructions.

TABLE 1. Bacterial strains and plasmids used in this study

Strain or plasmid	Genotype or characteristics[a]	Reference or source
Strains		
E. coli		
DH5α	*endA1 hsdR17* (r_K^- m_K^+) *glnV44 thi-1 recA1 gyrA* (Nal^r) *relA* Δ(*lacIZYA-argF*)*U169 deoR* [ϕ80d*lac*Δ(*lacZ*)M15]	54
CC118λ*pir*	Δ(*ara-leu*) *araD* Δ*lacX74 galE galK phoA20 thi-1 rpsE rpoB argE*(Am) *recA1* λ*pir*	20
S17-1λ*pir*	*thi pro hsdR hsdM*$^+$ *recA* λ*pir*	43
CGSC4982	*galK*	CGSC[b]
V. fischeri		
ES114	WT	6
ESR1	Rf^r	14
KV733	Rf^r *pgm*::Tn*10*	This study
KV828	Rf^r, carries pPS18 integrated into the chromosome	This study
KV1069	Rf^r *pgm*::*erm*	This study
KV1170	Rf^r *att*Tn*7*::*seqA-pgm*$^+$	This study
KV1171	Rf^r *pgm*::Tn*10 att*Tn*7*::*seqA-pgm*$^+$	This study
KV1177	Rf^r Δ*pgm*	This study
KV1306	Rf^r, carries pKV161 integrated into the chromosome	This study
KV1358	Rf^r, Δ*galK*	This study
Plasmids		
pBS	Blue-white screen cloning vector; Ap^r	Stratagene
pCD3	pEVS107 (*Spe*I) + 3-kb *Nhe*I fragment from pPS21, contains *seqA* and *pgm* inside the Tn*7* transposon	This study
pCNW1	pVO8 *Bam*HI + 5-kb *galK*$^+$ *Bgl*II fragment	This study
pEVS79	pBC + *mob*; Cm^r	44
pEVS104	Conjugal helper plasmid (*tra trb*); Kn^r	44
pEVS107	Tn*7* delivery plasmid; Kn^r Em^r	Eric Stabb
pKV25	pUC19::*erm*	50
pKV36	pUC19::*cat*	This study
pKV124	pBSL181 containing promoterless *lacZ* and *oriR6K* within Tn*10* ends	52
pKV161	pEVS79 *Hin*dIII + 2.8-kb *galK*$^+$ *Hin*dIII fragment from pCNW1	This study
pPS8	11-kb *Nhe*I fragment cloned from KV733, contains *pgm*::Tn*10* and flanking DNA	This study
pPS12	pBS (*Sac*I) + 6-kb *Sac*I fragment from pPS8, contains DNA flanking the Tn*10* insertion	This study
pPS15	pBS (*Xba*I) + 2.6-kb *Nhe*I fragment from pPS12, contains DNA upstream of *pgm*	This study
pPS18	pPS15 *Bgl*II + 1.1-kb *Bam*HI fragment encoding Cm^r from pKV36 (results in *fur*::*cat* mutation)	This study
pPS19	14-kb *Nsi*I fragment cloned from KV828, contains *seqA*$^+$ and a portion of *pgm*	This study
pPS20	pEVS79 (*Bam*HI) + 2.2-kb *Bam*HI/*Bgl*II fragment from pPS19, contains a portion of the *pgm* locus	This study
pPS21	20-kb *Xba*I fragment cloned from KV828, contains *seqA*$^+$ and *pgm*$^+$	This study
pPS24	pPS20 *Sph*I/filled + 1.2-kb *Sma*I/*Eco*RV fragment encoding Em^r from pKV25 (results in a *pgm*::*erm* mutation)	This study
pPS27	pEVS79 (*Xba*I) + 3-kb *Nhe* fragment from pPS21	This study
pPS33	pPS20 with two *Msc*I sites internal to *pgm* deleted (results in a 606-bp deletion)	This study
pRK2013	Conjugal helper plasmid (*tra trb*); Kn^r	10
pTMB7	9.6-kb *Cla*I fragment cloned from KV1306, contains *galK*$^+$ and flanking DNA	This study
pTMB9	pTMB7 deleted between two *Ase*I sites (results in 250-bp deletion at the 5′ end of *galK*)	This study
pUX-BF13	Encodes Tn*7* transposase (*tnsABCDE*); Ap^r	4
pVO8	Blue-white screen cloning vector; Cm^r Em^r	51

[a] Nal^r, nalidixic acid resistance; WT, wild type; Rf^r, rifampin resistance; Ap^r, ampicillin resistance; Kn^r, kanamycin resistance; Cm^r, CHL resistance; Em^r, ERY resistance.
[b] CGSC, *E. coli* Genetic Stock Center, Yale University, New Haven, Conn.

Sequencing. Automated sequencing was carried out with forward and reverse primers complementary to vector and insert sequences. Similarity searches were performed by using the National Center for Biotechnology Information BLAST program (3, 19). Oligonucleotides were obtained from the Loyola Macromolecular Analysis Facility, Integrated DNA Technologies (Coralville, Iowa), or MWG Biotech (High Point, N.C.).

Nucleotide sequence accession number. The following GenBank accession number was assigned to the *seqA-pgm-ybgI* sequence: AF474148.

RESULTS

Isolation of a symbiosis-defective *V. fischeri* mutant. Individual transposon insertion mutants of *V. fischeri* ESR1 were screened for their ability to form a symbiotic association with juveniles of the squid *E. scolopes* as described previously (52). Briefly, individual mutants were inoculated into seawater containing newly hatched juvenile *E. scolopes*. Colonization was monitored noninvasively by using bioluminescence as an indirect indicator of symbiont density in the light organ of *E. scolopes*. One mutant, KV733, could not achieve the high levels of luminescence sustained by ESR1 in the symbiosis with *E. scolopes* (Fig. 1A).

To confirm that the decreased level of symbiotic bioluminescence corresponded to decreased colonization, levels of colonization by KV733 and its parent were measured directly (Fig. 2). Juveniles inoculated with KV733 exhibited on average

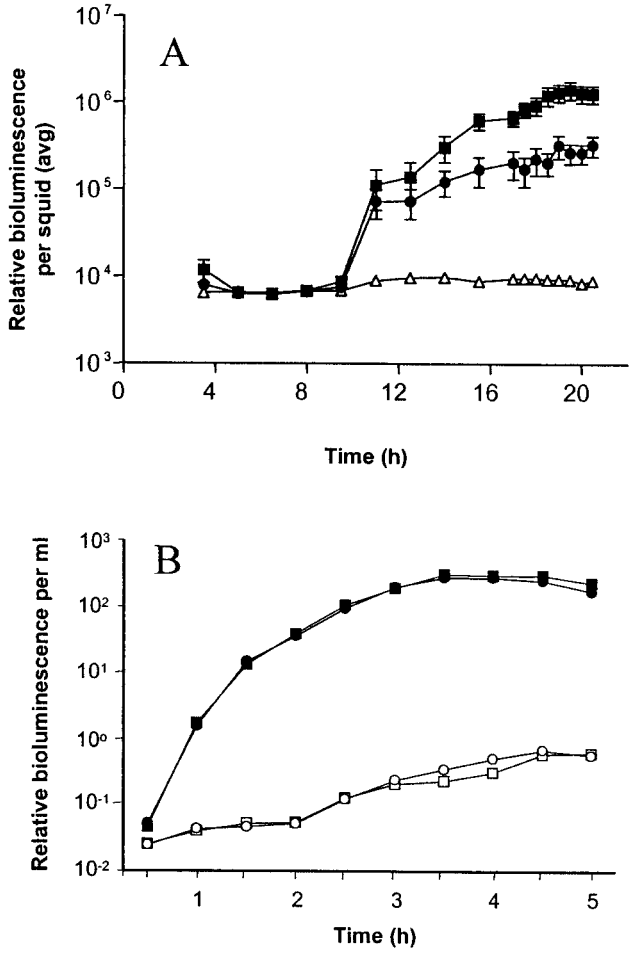

FIG. 1. Luminescence of colonization mutant KV733 and its parent. (A) Newly hatched juvenile *E. scolopes* squid were incubated in artificial seawater containing no *V. fischeri* (△), the parent strain ESR1 (■), or the colonization mutant KV733 (●). Bioluminescence emission was measured over time and represents an average of 11 animals for ESR1 and KV733. Error bars show the standard errors of the mean (SEM). (B) ESR1 (squares) and KV733 (circles) were grown in CM in the absence (open symbols) or presence (solid symbols) of autoinducer (3-oxo-hexanoy-L-homoserine lactone). The data shown are from a representative experiment of several replicates.

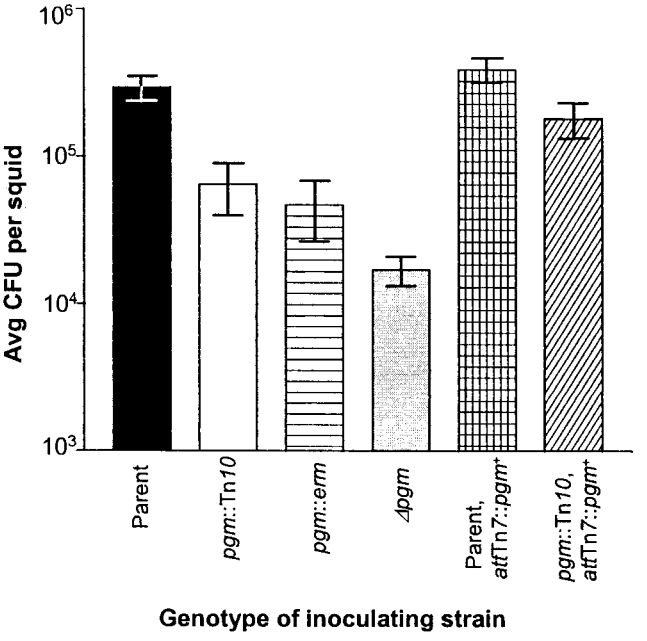

FIG. 2. Symbiotic colonization by *pgm* mutant and control strains. Newly hatched juvenile *E. scolopes* were inoculated with the following strains: ESR1 (■), KV733 (□), KV1069 (▤), KV1177 (▨), KV1170 (▩), or KV1171 (▨). The juveniles were exposed to ca. 1,000 cells of the parental and complemented strains or 2,000 cells of the mutant strains per ml of seawater for 3 h. The level of colonization achieved by these strains was determined by homogenization and plating 20 h after the organisms were placed together. The data shown are from a representative experiment, and the bars indicate an average of 11 squids. Error bars indicate the SEM.

a 10-fold reduction in colonization levels relative to those inoculated with ESR1. This putative symbiosis-defective mutant was further characterized in culture by examining motility on soft agar plates (data not shown), growth on minimal medium (data not shown), natural bioluminescence, and response to autoinducer (Fig. 1B). In these assays, KV733 behaved like its parent, suggesting that the symbiotic defect in KV733 was not due to deficiency in motility, amino acid biosynthesis, or luminescence, all factors previously identified as important in the symbiosis. It therefore seemed likely that KV733 was defective for an as-yet-unknown symbiotic locus.

Identification of the locus disrupted in KV733. To identify the genetic defect in KV733, we determined the number and location of the transposon insertion(s) in this strain by Southern analysis. A single, large (>12-kb) *Bsr*GI fragment that carried the transposon was identified by probing with DNA complementary to the transposon delivery plasmid, providing evidence that the strain carried a single transposon insertion (data not shown). Further analysis of KV733 chromosomal DNA revealed that the entire transposon delivery plasmid had incorporated into the chromosome at this site (data not shown).

We cloned the transposon and flanking chromosomal DNA. Sequence analysis revealed that the transposon had inserted after codon 189 of a 548-codon open reading frame (ORF). This putative protein exhibited high sequence similarity (69% identity, 83% similarity) to Pgm (phosphoglucomutase) of *E. coli* (26) and *V. cholerae* (80% identity, 89% similarity [17]). Directly upstream of the putative *pgm* gene in *V. fischeri* was an ORF that encoded a putative protein with high sequence similarity to SeqA, encoded by a gene upstream of *pgm* in both *E. coli* (51% identity, 71% similarity [5]) and *V. cholerae* (65% identity, 79% similarity [17]). Directly downstream of *pgm* in *V. fischeri* was an ORF encoding a predicted protein similar to proteins of unknown function in *V. cholerae* (74% identity, 81% similarity [17]) and *Haemophilus influenzae* (YbgI, 62% identity, 78% similarity [11]). Directly downstream of this gene and in the opposite orientation is an ORF encoding a product with high sequence similarity, based on partial sequence data, to GltA encoded by the *gltA* gene of *E. coli* (5).

In *E. coli*, phosphoglucomutase interconverts glucose-1-phosphate and glucose-6-phosphate and thus plays roles in both galactose metabolism and polysaccharide biosynthesis

(13). The protein is part of a family of phosphoserine enzymes which contain a highly conserved serine residue within a conserved 5-amino-acid sequence critical for enzyme activity (38, 55). The deduced amino acid sequence of this region in *V. fischeri*, *V. cholerae*, and *E. coli* is Thr-Pro-Ser-His-Asn at amino acids 144 to 148, differing in a single Ala-Pro change from the rabbit muscle phosphoglucomutase consensus sequence Thr-Ala-Ser-His-Asn (38). On the basis of the presence of this conserved active site region in the putative *V. fischeri pgm* gene, as well as on the overall high sequence similarity to the *pgm* genes of both *V. cholerae* and *E. coli*, we conclude that the locus disrupted in KV733 is the *V. fischeri pgm* gene. The phenotypic and biochemical data described below further support this conclusion.

Role for *pgm* in the symbiosis. Because the transposon insertion in KV733 also contains the delivery plasmid (encoding transposase), it is conceivable that, during symbiotic colonization, additional insertions that might inhibit the ability of KV733 to colonize could be generated. To determine whether the transposon insertion in KV733 was retained in the *pgm* gene during colonization, chromosomal DNA extracted from KV733 harvested after symbiotic colonization was subjected to Southern analysis. In each of 10 independent clones from individual animals, the transposon was present only in the *pgm* gene (data not shown).

Additionally, it was formally possible that KV733 carried a secondary mutation; therefore, in order to confirm that the *pgm* gene itself plays a role in the symbiosis, we constructed additional *pgm* mutants (Table 1). A *pgm*::*erm* insertion mutant (KV1069) and a Δ*pgm* (in-frame deletion) mutant (KV1177 with a region that includes the conserved 5-amino-acid active-site sequence deleted) also exhibited defects in the ability to colonize juvenile squid similar to that of the original transposon insertion mutant, as shown in Fig. 2 (the mean colonization levels of the three *pgm* mutants were not statistically different [$P = 0.2$] as determined by one-way analysis of variance analysis). Additionally, when a pgm^+ gene was inserted in single copy into the chromosome of KV733 (KV1171), the complemented strain achieved a colonization level similar to that of the wild-type parent (Fig. 2). These data indicate that the *pgm* gene plays a critical role in symbiotic colonization.

Phosphoglucomutase assay. To determine whether our sequence analysis correctly predicted the function of the putative Pgm protein, we measured phosphoglucomutase activity of our wild-type and mutant strains. Whereas wild-type extracts displayed Pgm activity, the *pgm* mutants tested were deficient (Fig. 3). Complementation restored Pgm activity to the *pgm* mutant and, not surprisingly, the strain with two wild-type copies of *pgm* exhibited approximately twice as much Pgm activity.

Growth of the *pgm* mutant in culture. An *E. coli pgm* mutant exhibits a decreased ability to grow on minimal medium containing galactose as the sole carbon source (26). We hypothesized that if Pgm has the same function in *V. fischeri*, then the *pgm* mutants would be similarly defective. This was the case for all three *pgm* mutants (KV733, KV1069, and KV1177), whereas the complemented strain (KV1171) exhibited a restored ability to grow on MM-galactose as the sole carbon source (data not shown).

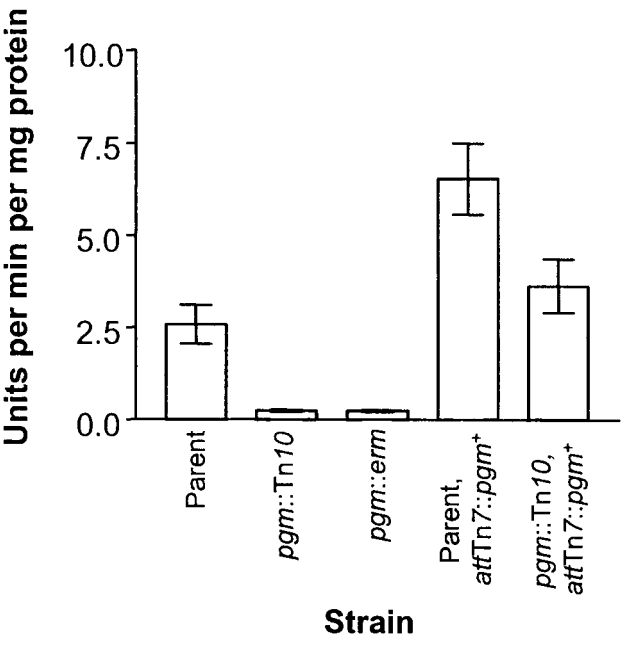

FIG. 3. Phosphoglucomutase assay. Phosphoglucomutase activity of strains ESR1 (parent), KV733 (*pgm*::Tn*10*), KV1069 (*pgm*::*erm*), KV1170 (ESR1 with chromosomal pgm^+ complementation), and KV1171 (*pgm*::Tn*10* with chromosomal pgm^+ complementation). The data shown are averages from four independent experiments. Error bars show the SEM.

We also examined the ability of the *pgm* mutant KV733 to grow in different complex nutrient media. When grown in SWT (a seawater-based medium), the *pgm* mutant KV733 grew identically to its parent, ESR1, suggesting that KV733 does not possess a general growth defect (Fig. 4A). In contrast, when grown in LBS medium, a medium containing NaCl as the only added salt, KV733 displayed a growth defect when inoculated to a starting cell density of $<10^6$ CFU ml^{-1}. As shown in Fig. 4B, when the *pgm* mutant KV733 was inoculated to a starting density of 10^5 CFU ml^{-1}, its growth leveled off at an OD of ca. 0.1.

Given the differences in the ability of the mutant to grow in the two complex media under conditions of a low inoculum, we examined the possibility that the salts present in SWT medium may be rescuing the growth defect of the *pgm* mutant in LBS medium. SWT medium contains NaCl, KCl, $MgSO_4$, and $CaCl_2$, whereas LBS medium contains NaCl as the only added salt. The growth experiments were repeated with LBS medium supplemented with the individual SWT salts (Fig. 4C). The addition of either $MgSO_4$ or $CaCl_2$, both salts containing divalent cations, to LBS medium allowed the *pgm* mutant to grow to wild-type levels when it was inoculated to a starting density of 10^5 CFU ml^{-1}, whereas the addition of the monovalent salt KCl did not affect the mutant's growth. The growth of ESR1 was not affected by the addition of any of the three salts (data not shown). The consequences of this ion requirement in nature are unclear because seawater and most likely the internal crypts of the light organ contain plentiful amounts of Mg^{2+} and Ca^{2+}.

Susceptibility of the *pgm* mutant to polymyxin B, deoxy-

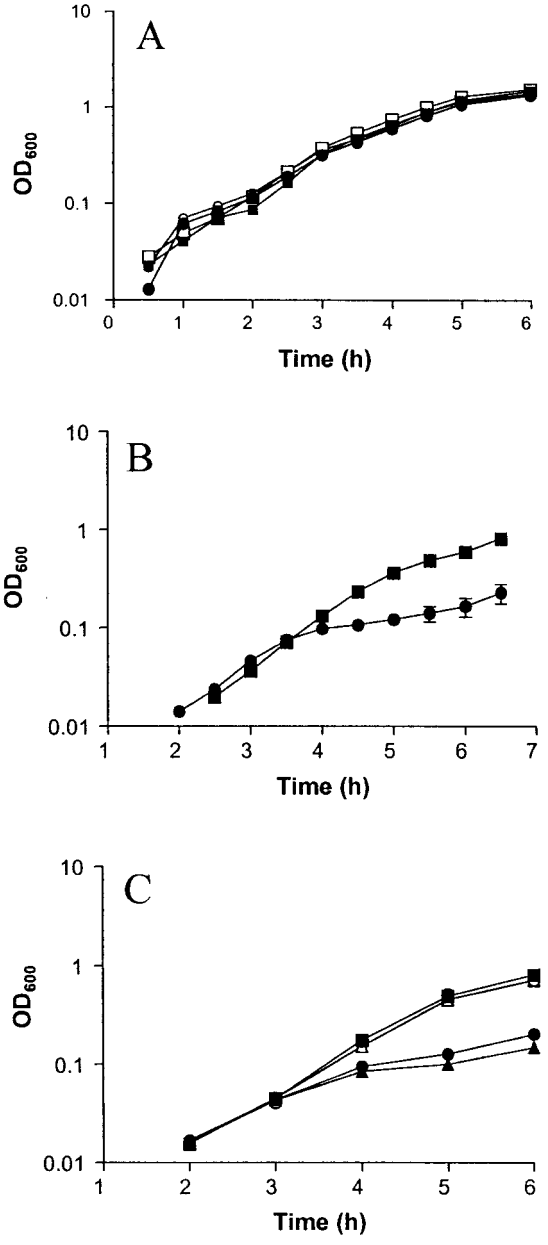

FIG. 4. Growth of ESR1 and KV733 in liquid media. (A) ESR1 (squares) and KV733 (circles) were inoculated to a starting concentration of 10^6 CFU ml^{-1} in either SWT (solid symbols) or LBS (open symbols) medium and grown for 6.0 h. (B) ESR1 (■) and KV733 (●) were inoculated to a starting concentration of 10^5 CFU ml^{-1} and grown in LBS medium for 6.5 h. Error bars indicate the SEM. (C) ESR1 (■) was inoculated to a starting concentration of 10^5 CFU ml^{-1} and grown in LBS medium for 6 h. In parallel, KV733 was inoculated to a starting concentration of 10^5 CFU ml^{-1} and grown in LBS medium (●), LBS medium supplemented with $MgSO_4$ (○), LBS medium supplemented with $CaCl_2$ (△), or LBS medium supplemented with KCl (▲) for 6 h. The data from ESR1 grown in LBS medium supplemented with individual salts were omitted for clarity.

cholate, and SDS. An *E. coli pgm* mutant exhibits increased susceptibility to environmental stresses (26). To investigate whether the *V. fischeri pgm* mutants also exhibited this phenotype, we determined the MIC of the cationic antibiotic polymyxin B for each *pgm* mutant and for ESR1 grown in SWT medium. All three *pgm* mutants had an MIC of 2 μg ml^{-1}, a threefold increase in susceptibility relative to the MIC for ESR1 of 6 μg ml^{-1}. Complementation with *pgm*$^+$ restored the MIC to 5 to 6 μg ml^{-1}.

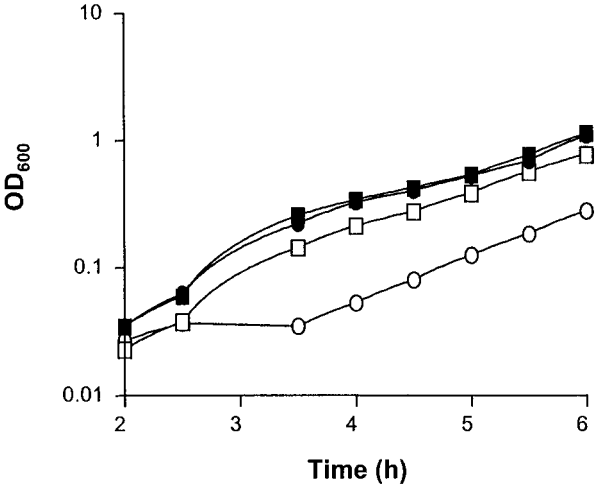

FIG. 5. Growth of ESR1 and KV733 in the presence of SDS. ESR1 (squares) and KV733 (circles) were inoculated in triplicate to a starting density of 4×10^5 CFU ml^{-1} in either SWT medium (solid symbols) or SWT medium with 10% SDS (open symbols) and grown for 6.0 h. Error bars show the SEM. The data shown are from a representative experiment.

We also examined the ability of the *pgm* mutant to grow in SWT in the presence of either 10% SDS or 1% deoxycholate. The presence of SDS interfered with the growth of KV733 to a greater extent than it did the parent strain (Fig. 5). The growth of KV733 (but not the parent strain) was similarly affected in the presence of 1% deoxycholate (data not shown). Taken together, these data indicate that the *pgm* mutant is more susceptible to environmental stresses.

LPS structure of the *pgm* mutant. *E. coli* (1) and *Agrobacterium tumefaciens* (47) *pgm* mutants exhibit defects in LPS production due to an inability to produce sufficient amounts of UDP-glucose. To determine whether the *V. fischeri pgm* mutant had a similar defect in LPS biosynthesis, we analyzed LPS from the *pgm* mutant and wild-type strains by separating the LPS molecules with deoxycholic acid-PAGE and then visualizing them by silver staining (Fig. 6). The LPS extracted from the *pgm* mutant KV733 had a banding pattern distinct from that of ESR1, containing additional species that migrated faster than that of the smallest LPS band of ESR1 (Fig. 6). An altered banding pattern was also observed with LPS extracted from the other two *pgm* mutant strains (data not shown). Complementation restored the LPS banding pattern to that of the parent strain (Fig. 6 and data not shown), suggesting that the altered LPS profile of the mutant is due to the loss of *pgm*.

Colonization assay of the *V. fischeri galK* mutant. To test whether the inability of the *pgm* mutants to utilize galactose accounts for the colonizaton defect of these strains, we constructed a mutant defective for galactokinase (encoded by the *galK* gene) and examined the strain's ability to form a symbiotic association with *E. scolopes*. The *galK* mutant, KV1358, colonized to wild-type levels (Fig. 7). These data indicate that an

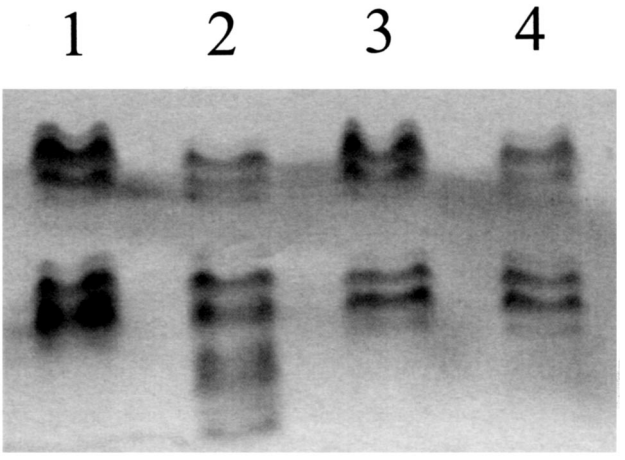

FIG. 6. LPS profiles of the *pgm* mutant and wild-type strains. LPS fractions were prepared as described in Materials and Methods, separated by deoxycholic acid-PAGE, and visualized by silver staining. Lane 1, ESR1 (parent); lane 2, KV733 (*pgm*::Tn*10*); lane 3, KV1170 (ESR1 with chromosomal pgm^+ complementation); and lane 4, KV1171 (*pgm*:: Tn*10* with chromosomal pgm^+ complementation). The gel is from a representative experiment.

inability to catabolize galactose does not account for the symbiotic defect in KV733.

DISCUSSION

In the present study we identified a mutant of *V. fischeri* that failed to colonize *E. scolopes* to wild-type levels. This mutant, KV733, carried a transposon insertion in an ORF with high identity to the *pgm* (phosphoglucomutase) gene of *E. coli*. Our data suggest that the locus interrupted in KV733 encodes a functional homolog of the *E. coli* Pgm protein and that this locus, which we have designated *pgm*, plays a role in symbiotic colonization.

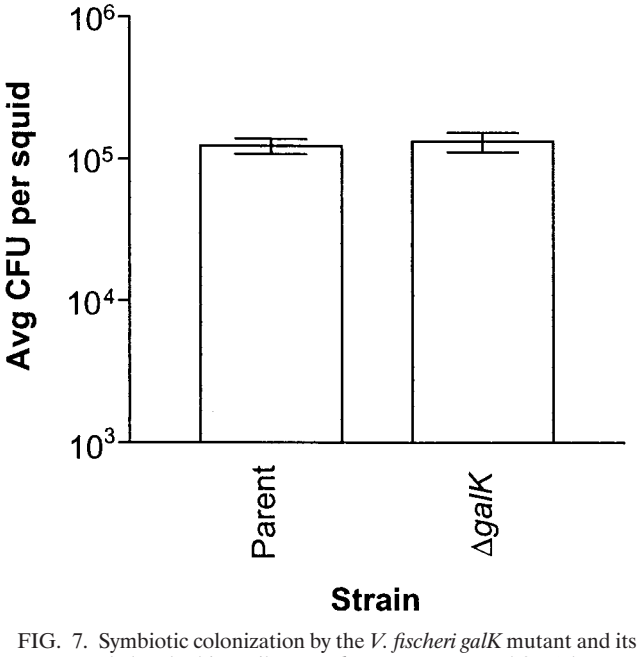

FIG. 7. Symbiotic colonization by the *V. fischeri galK* mutant and its parent. Newly hatched juvenile *E. scolopes* were exposed for 3 h at ca. 3,000 cells per ml of either ESR1 or KV1358. The level of colonization was determined by homogenization and plating 20 h after the organisms were placed together. The data shown are from a representative experiment. The bars indicate the average colonization level of 12 squids. Error bars show the SEM.

In *E. coli*, Pgm plays roles both in catabolizing galactose and in promoting the production of UDP-glucose, an activated form of glucose that serves as a building block for a number of polysaccharides, including LPS. Strains with a deficiency in UDP-glucose production exhibit a number of phenotypes, including an altered LPS profile (21, 32) and increased susceptibility to hydrophobic agents, bile salts, and cationic antimicrobial peptides (32). Similarly, the *V. fischeri pgm* mutant displayed a decrease in phosphoglucomutase activity, grew poorly on MM-galactose, exhibited an altered LPS profile, and displayed an increased susceptibility to polymyxin B, deoxycholate, and SDS. Taken together, our data indicate that KV733 exhibits phenotypes consistent with a defect in a gene with the same function as that of the *E. coli pgm* gene.

Interestingly, in the seawater-based SWT medium, wild-type *V. fischeri* grew to high cell densities despite the presence of 10% SDS. This is in contrast to a recent report indicating that wild-type *V. fischeri* cells grown in LBS medium were susceptible to 0.009% SDS (2). It is possible that the three additional salts found in SWT medium ($MgSO_4$, $CaCl_2$, and KCl) protect the cells against lysis by the detergent. In support of this hypothesis, the addition of Mg^{2+} to growth medium has been shown to stabilize the outer membrane of a *Salmonella enterica* serovar Typhimurium LPS mutant (45). Similarly, we saw that divalent cations were required for optimal growth of the *pgm* mutant in LBS medium.

In addition, our data suggested that the *pgm* gene itself is required for symbiotic colonization: the original transposon insertion mutant and two other *pgm* mutants that we constructed exhibited similar defects in colonization, and complementation restored the ability of KV733 to colonize. The colonization defect conferred by the mutation in *pgm* is similar to that caused by some amino acid auxotrophies (15). It is more severe than either a mutation in the *luxA* gene, which causes a fourfold decrease only after the first day of colonization (48), or a mutation in catalase, which results in a competitive defect (50). We have observed that the *pgm* mutant is at least 10-fold reduced in colonization as early as 12 h postinoculation, a time at which the wild-type strain has not yet achieved its population maximum (C. R. DeLoney and K. L. Visick, unpublished observations). These data suggest that the *pgm* mutant is not simply growing normally until it reaches a population maximum that is 10-fold reduced from that which can be achieved by the wild-type strain. Rather, it appears that this mutant is deficient at even earlier stages of colonization. This result is consistent with our hypothesis that the *pgm* mutant fails to resist host-imposed stresses (see below).

What role does *pgm* play in symbiotic colonization? Given the pleiotrophic effects of *pgm* mutants, several explanations could be proposed to explain the symbiotic defect. One possibility was that the symbiotic defect resulted from the inability of the *pgm* mutant to use galactose as a carbon source. We speculated that galactose moieties on the surfaces of cells in the light organ might serve as a carbon source for the bacteria.

A similar mechanism seems to be employed during colonization of the mouse gut by *B. thetaiotaomicron*, which induces the presentation of the sugar fucose on host cells and then uses it as an energy source (22). However, our construction of a second galactose utilization mutant, one not defective for LPS biosynthesis (data not shown) that colonized normally suggested that this hypothesis was incorrect.

A second possible explanation is that alterations in LPS, correlated with susceptibility to stresses, prevent the mutant from colonizing to wild-type levels because it cannot withstand environmental stresses in the squid. Although relatively little is known about the environment of the light organ, the presence of defensive host cells (primitive macrophages [35]) and proteins (halide peroxidase [53]), as well as the exclusivity of the symbiosis, suggests that the bacteria likely encounter host-derived stresses during colonization.

Comprising the vast majority of the outer leaflet of the outer membrane of gram-negative bacteria, LPS plays a crucial role in maintaining membrane integrity (see reference 34 for a review). Divalent cations such as magnesium form cross-bridges between neighboring LPS molecules by binding to phosphate residues on inner core heptose components (which are often derived from UDP-glucose [see reference 37 for a review]). These interactions give strength and rigidity to the otherwise fluid outer membrane. *H. influenzae pgm* mutants, presumably defective for UDP-glucose synthesis, contain LPS species with a reduced number of sugar residues in the inner core (21). If the *pgm* mutation caused a parallel defect on the inner core of *V. fischeri* LPS, which would not be surprising given the conserved nature of LPS structure among gram-negative bacteria (16), then the strength of the outer membrane likely would be reduced. Our sensitivity assays suggest that this is indeed the case. However, it is not clear whether the moderate increase in susceptibility to agents such as polymyxin B that the *pgm* defect confers in culture can account for the 10-fold decrease in colonization ability.

A third explanation for the symbiotic defect in KV733 could be the loss or reduction of outer membrane proteins necessary for colonization. Some LPS mutants ("deep rough") that are devoid of part of the core oligosaccharide (for reviews, see references 33 and 37) show significant decreases in the amounts of the major outer membrane proteins. The *V. fischeri* outer membrane protein OmpU plays a role in symbiotic colonization (2) and may be affected by the LPS defect. Our preliminary data suggest that this is not the case; we have detected no distinct differences in the banding patterns of proteins extracted from wild-type and *pgm* mutant cells (K. Visick, unpublished observations).

In *E. coli*, UDP-glucose plays a number of roles other than LPS synthesis, including (i) protecting against thermal and osmotic stresses through the production of trehalose (7); (ii) serving as a building block for periplasmic β-D-glucans, which are implicated both in osmotic adaptation and in cell signaling (23); and (iii) regulating (negatively) σ^S, the stationary-phase sigma factor (18). Defects in any of these cellular processes could potentially result in the observed symbiotic phenotype in *V. fischeri*, and future research will have to address these possibilities.

The role of Pgm in colonization is not limited to the *Vibrio*-squid symbiosis. *V. cholerae* (32) and *H. influenzae* (21) *pgm* mutants similarly display defects in pathogenic colonization. The requirement of a metabolic enzyme in establishment of the symbiosis between *V. fischeri* and *E. scolopes* demonstrates the complexity of the association, as well as how little is known about the necessary genetic determinants. We anticipate that our characterization of the role of Pgm in this symbiotic association will provide opportunities for the comparison of symbiotic and pathogenic colonization. As we continue to search for insights on how these mutualistic partners interact, studies such as these will add to our knowledge of how symbiotic relationships—both beneficial and detrimental—are established between bacteria and animals.

ACKNOWLEDGMENTS

We thank Paul Smith for his assistance in the characterization of the *pgm* gene and many plasmid constructions, Erika Enk for the construction of KV1069, Cionne Wolfe for isolating the *V. fischeri galK* gene, and Eric Stabb for plasmids and advice in advance of publication. We also thank David Keating, Ned Ruby, Eric Stabb, Jon Visick, and Alan Wolfe for their insightful comments and critical review of the manuscript.

This work was supported by NIH grant GM59690 awarded to K.L.V. and by the National Science Foundation Research Fellowship in Microbial Biology awarded in 2001 to C.R.D.

REFERENCES

1. **Adhya, S., and M. Schwartz.** 1971. Phosphoglucomutase mutants of *Escherichia coli* K-12. J. Bacteriol. **108:**621–626.
2. **Aeckersberg, F., C. Lupp, B. Feliciano, and E. G. Ruby.** 2001. *Vibrio fischeri* outer membrane protein OmpU plays a role in normal symbiotic colonization. J. Bacteriol. **183:**6590–6597.
3. **Altschul, S. F., T. L. Madden, A. A. Schäffer, J. Zhang, Z. Zhang, W. Miller, and D. J. Lipman.** 1997. Gapped BLAST and PSI-BLAST: a new generation of protein database search programs. Nucleic Acids Res. **25:**3389–3402.
4. **Bao, Y., D. P. Lies, F. Haian, and G. P. Roberts.** 1991. An improved Tn7-based system for the single-copy insertion of cloned genes into chromosomes of gram-negative bacteria. Gene **109:**167–168.
5. **Blattner, F. R., G. Plunkett III, C. A. Bloch, N. T. Perna, V. Burland, M. Riley, J. Collado-Vides, J. D. Glasner, C. K. Rode, G. F. Mayhew, J. Gregor, N. W. Davis, H. A. Kirkpatrick, M. A. Goeden, D. J. Rose, B. Mau, and Y. Shao.** 1997. The complete genome sequence of *Escherichia coli* K-12. Science **277:**1453–1474.
6. **Boettcher, K. J., and E. G. Ruby.** 1990. Depressed light emission by symbiotic *Vibrio fischeri* of the sepiolid squid *Euprymna scolopes*. J. Bacteriol. **172:** 3701–3706.
7. **Csonka, L. N., and W. Epstein.** 1996. Osmoregulation, p. 1210–1223. *In* F. C. Neidhardt, R. Curtiss III, J. L. Ingraham, E. C. C. Lin, K. B. Low, B. Magasanik, W. S. Reznikoff, M. Riley, M. Schaechter, and H. E. Umbarger (ed.), *Escherichia coli* and *Salmonella*: cellular and molecular biology, 2nd ed. ASM Press, Washington, D.C.
8. **Davis, R. W., D. Botstein, and J. R. Roth.** 1980. Advanced bacterial genetics. Cold Spring Harbor Laboratory, Cold Spring Harbor, N.Y.
9. **Dunlap, P. V.** 1989. Regulation of luminescence by cyclic AMP in *cya*-like and *crp*-like mutants of *Vibrio fischeri*. J. Bacteriol. **171:**1199–1202.
10. **Figurski, D. H., and D. R. Helinski.** 1979. Replication of an origin-containing derivative of plasmid RK2 dependent on a plasmid function provided in trans. Proc. Natl. Acad. Sci. USA **76:**1648–1652.
11. **Fleischmann, R. D., M. D. Adams, O. White, R. A. Clayton, E. F. Kirkness, A. R. Kerlavage, C. J. Bult, J. F. Tomb, B. A. Dougherty, J. M. Merrick, K. McKenney, G. Sutton, W. Fitzhugh, C. A. Fields, J. D. Gocayne, J. D. Scott, R. Shirley, L. I. Liu, A. Glodek, J. M. Kelley, J. F. Weidman, C. A. Phillips, T. Spriggs, E. Hedblom, M. D. Cotton, T. R. Utterback, M. C. Hanna, D. T. Nguyen, D. M. Saudek, R. C. Brandon, L. D. Fine, J. L. Fritchman, J. L. Fuhrmann, N. S. M. Geoghagen, C. L. Gnehm, L. A. McDonald, K. V. Small, C. M. Fraser, H. O. Smith, and J. C. Venter.** 1995. Whole-genome random sequencing and assembly of *Haemophilus influenzae* Rd. Science **269:**496–512.
12. **Foster, J. S., M. A. Apicella, and M. J. McFall-Ngai.** 2000. *Vibrio fischeri* lipopolysaccharide induces developmental apoptosis, but not complete morphogenesis, of the *Euprymna scolopes* symbiotic light organ. Dev. Biol. **226:** 242–254.
13. **Fraenkel, D. G.** 1996. Glycolysis, p. 189–198. *In* F. C. Neidhardt, R. Curtiss III, J. L. Ingraham, E. C. C. Lin, K. B. Low, B. Magasanik, W. S. Reznikoff, M. Riley, M. Schaechter, and H. E. Umbarger (ed.), *Escherichia coli* and

Salmonella: cellular and molecular biology, 2nd ed. ASM Press, Washington, D.C.
14. **Graf, J., P. V. Dunlap, and E. G. Ruby.** 1994. Effect of transposon-induced motility mutations on colonization of the host light organ by *Vibrio fischeri*. J. Bacteriol. **176:**6986–6991.
15. **Graf, J., and E. G. Ruby.** 1998. Host-derived amino acids support the proliferation of symbiotic bacteria. Proc. Natl. Acad. Sci. USA **95:**1818–1822.
16. **Gronow, S., and H. Brade.** 2001. Lipopolysaccharide biosynthesis: which steps do bacteria need to survive? J. Endotoxin Res. **7:**3–23.
17. **Heidelberg, J. F., J. A. Eisen, W. C. Nelson, R. A. Clayton, M. L. Gwinn, R. J. Dodson, D. H. Haft, E. K. Hickey, J. D. Peterson, L. A. Umayam, S. R. Gill, K. E. Nelson, T. D. Read, H. Tettelin, D. Richardson, M. D. Ermolaeva, J. Vamathevan, S. Bass, H. Qin, I. Dragoi, P. Sellers, L. McDonald, T. Utterback, R. D. Fleischmann, W. C. Nierman, O. White, S. L. Salzberg, H. O. Smith, R. R. Colwell, J. J. Mekalanos, J. C. Venter, and C. M. Fraser.** 2000. DNA sequence of both chromosomes of the cholera pathogen *Vibrio cholerae*. Nature **406:**477–483.
18. **Hengge-Aronis, R.** 1996. Regulation of gene expression during entry into stationary phase, p. 1497–1512. *In* F. C. Neidhardt, R. Curtiss III, J. L. Ingraham, E. C. C. Lin, K. B. Low, B. Magasanik, W. S. Reznikoff, M. Riley, M. Schaechter, and H. E. Umbarger (ed.), *Escherichia coli* and *Salmonella*: cellular and molecular biology, 2nd ed. ASM Press, Washington, D.C.
19. **Henikoff, S., and J. G. Henikoff.** 1992. Amino acid substitution matrices from protein blocks. Proc. Natl. Acad. Sci. USA **89:**10915–10919.
20. **Herrero, M., V. DeLorenzo, and K. N. Timmis.** 1990. Transposon vectors containing non-antibiotic resistance selection markers for cloning and stable chromosomal insertion of foreign genes in gram-negative bacteria. J. Bacteriol. **172:**6557–6567.
21. **Hood, D. W., M. E. Deadman, T. Allen, H. Masoud, A. Martin, J. R. Brisson, R. Fleischmann, J. C. Venter, J. C. Richards, and E. R. Moxon.** 1996. Use of the complete genome sequence information of *Haemophilus influenzae* strain Rd to investigate lipopolysaccharide biosynthesis. Mol. Microbiol. **22:**951–965.
22. **Hooper, L. V., J. Xu, P. G. Falk, T. Midtvedt, and J. I. Gordon.** 1999. A molecular sensor that allows a gut commensal to control its nutrient foundation in a competitive ecosystem. Proc. Natl. Acad. Sci. USA **96:**9833–9838.
23. **Kennedy, E. P.** 1996. Membrane-derived oligosaccharides (periplasmic β-D-glucans) of *Escherichia coli*, p. 1064–1071. *In* F. C. Neidhardt, R. Curtiss III, J. L. Ingraham, E. C. C. Lin, K. B. Low, B. Magasanik, W. S. Reznikoff, M. Riley, M. Schaechter, and H. E. Umbarger (ed.), *Escherichia coli* and *Salmonella*: cellular and molecular biology, 2nd ed. ASM Press, Washington, D.C.
24. **Kolter, R., M. Inuzuka, and D. R. Helinski.** 1978. Trans-complementation-dependent replication of a low molecular weight origin fragment from plasmid R6K. Cell **15:**1199–1208.
25. **Lamarcq, L. H., and M. J. McFall-Ngai.** 1998. Induction of a gradual, reversible morphogenesis of its hosts epithelial brush border by *Vibrio fischeri*. Infect. Immun. **66:**777–785.
26. **Lu, M., and N. Kleckner.** 1994. Molecular cloning and characterization of the *pgm* gene encoding phosphoglucomutase of *Escherichia coli*. J. Bacteriol. **176:**5847–5851.
27. **McFall-Ngai, M. J.** 1999. Consequences of evolving with bacterial symbionts: insights from the squid-vibrio associations. Annu. Rev. Ecol. Syst. **30:**235–256.
28. **McFall-Ngai, M., C. Brennan, V. Weis, and L. Lamarcq.** 1998. Mannose adhesin-glycan interactions in the *Euprymna scolopes-Vibrio fischeri* symbiosis, p. 273–276. *In* Y. L. Gal and H. O. Halvorson (ed.), New developments in marine biothechnology. Plenum Press, New York, N.Y.
29. **McFall-Ngai, M. J., and E. G. Ruby.** 1991. Symbiont recognition and subsequent morphogenesis as early events in an animal-bacterial mutualism. Science **254:**1491–1494.
30. **Montgomery, M. K., and M. McFall-Ngai.** 1994. Bacterial symbionts induce host organ morphogenesis during early postembryonic development of the squid *Euprymna scolopes*. Development **120:**1719–1729.
31. **Nealson, K. H.** 1978. Isolation, identification, and manipulation of luminous bacteria. Methods Enzymol. **57:**153–166.
32. **Nesper, J., C. M. Lauriano, K. E. Klose, D. Kapfhammer, A. Kraiss, and J. Reidl.** 2001. Characterization of *Vibrio cholerae* O1 El Tor *galU* and *galE* mutants: influence on lipopolysaccharide structure, colonization, and biofilm formation. Infect. Immun. **69:**435–445.
33. **Nikaido, H.** 1996. Outer membrane, p. 29–47. *In* F. C. Neidhardt, R. Curtiss III, J. L. Ingraham, E. C. C. Lin, K. B. Low, B. Magasanik, W. S. Reznikoff, M. Riley, M. Schaechter, and H. E. Umbarger (ed.), *Escherichia coli* and *Salmonella*: cellular and molecular biology, 2nd ed. ASM Press, Washington, D.C.
34. **Nikaido, H., and M. Vaara.** 1985. Molecular basis of bacterial outer membrane permeability. Microbiol. Rev. **49:**1–32.
35. **Nyholm, S. V., and M. J. McFall-Ngai.** 1998. Sampling the light-organ microenvironment of *Euprymna scolopes*: description of a population of host cells in association with the bacterial symbiont *Vibrio fischeri*. Biol. Bull. **195:**89–97.
36. **Nyholm, S. V., E. V. Stabb, E. G. Ruby, and M. J. McFall-Ngai.** 2000. Establishment of an animal-bacterial association: recruiting symbiotic vibrios from the environment. Proc. Natl. Acad. Sci. USA **97:**10231–10235.
37. **Raetz, C. R. H.** 1996. Bacterial lipopolysaccharides: a remarkable family of bioactive macroamphiphiles, p. 1035–1063. *In* F. C. Neidhardt, R. Curtiss III, J. L. Ingraham, E. C. C. Lin, K. B. Low, B. Magasanik, W. S. Reznikoff, M. Riley, M. Schaechter, and H. E. Umbarger (ed.), *Escherichia coli* and *Salmonella*: cellular and molecular biology, 2nd ed. ASM Press, Washington, D.C.
38. **Ray, W. J., Jr., M. A. Hermodson, J. M. Puvathingal, and W. C. Mahoney.** 1983. The complete amino acid sequence of rabbit muscle phosphoglucomutase. J. Biol. Chem. **258:**9166–9174.
39. **Reus, B. L., D. P. Geller, J. S. Kim, J. E. Fox, V. S. Kumar Kolli, and S. G. Pueppke.** 1998. *Sinorhizobium fredii* and *Sinorhizobium meliloti* produce structurally conserved lipopolysaccharides and strain-specific K antigens. Appl. Environ. Microbiol. **64:**4930–4938.
40. **Ruby, E. G.** 1996. Lessons from a cooperative, bacterial-animal association: the *Vibrio fischeri-Euprymna scolopes* light organ symbiosis. Annu. Rev. Microbiol. **50:**591–624.
41. **Ruby, E. G., and L. M. Asato.** 1993. Growth and flagellation of *Vibrio fischeri* during initiation of the sepiolid squid light organ symbiosis. Arch. Microbiol. **159:**160–167.
42. **Ruby, E. G., and K. H. Nealson.** 1977. Pyruvate production and excretion by the luminous marine bacteria. Appl. Environ. Microbiol. **34:**164–169.
43. **Simon, R., U. Priefer, and A. Puhler.** 1983. A broad host range mobilization system for in vivo genetic engineering: transposon mutagenesis in gram-negative bacteria. Bio/Technology **1:**784–791.
44. **Stabb, E. V., and E. G. Ruby.** New RP4-based plasmids for conjugation between *Escherichia coli* and members of the *Vibrionaceae*. Methods Enzymol., in press.
45. **Stan-Lotter, H., M. Gupta, and K. E. Sanderson.** 1979. The influence of cations on the permeability of the outer membrane of *Salmonella typhimurium* and other gram-negative bacteria. Can. J. Microbiol. **25:**475–485.
46. **Steinberg, D. A., and R. L. Lehrer.** 1997. Designer assays for antimicrobial peptides: disputing the "one size fits all" theory. Methods Mol. Biol. **78:**169–186.
47. **Uttaro, A. D., G. A. Cangelosi, R. A. Geremia, E. W. Nester, and R. A. Ugalde.** 1990. Biochemical characterization of avirulent *exoC* mutants of *Agrobacterium tumefaciens*. J. Bacteriol. **172:**1640–1646.
48. **Visick, K. L., J. Foster, J. Doino, M. McFall-Ngai, and E. G. Ruby.** 2000. *Vibrio fischeri lux* genes play an important role in colonization and development of the host light organ. J. Bacteriol. **182:**4578–4586.
49. **Visick, K. L., and M. J. McFall-Ngai.** 2000. An exclusive contract: specificity in the *Vibrio fischeri-Euprymna scolopes* partnership. J. Bacteriol. **182:**1779–1787.
50. **Visick, K. L., and E. G. Ruby.** 1998. The periplasmic, group III catalase of *Vibrio fischeri* is required for normal symbiotic competence and is induced both by oxidative stress and by approach to stationary phase. J. Bacteriol. **180:**2087–2092.
51. **Visick, K. L., and E. G. Ruby.** 1997. New genetic tools for use in the marine bioluminescent bacterium *Vibrio fischeri*, p. 119–122. *In* J. W. Hastings, L. J. Kricka, and P. E. Stanley (ed.), Bioluminescence and chemiluminescence, John Wiley & Sons, Ltd., Chichester, England.
52. **Visick, K. L., and L. M. Skoufos.** 2001. Two-component sensor required for normal symbiotic colonization of *Euprymna scolopes* by *Vibrio fischeri*. J. Bacteriol. **183:**835–842.
53. **Weis, V. M., A. L. Small, and M. J. McFall-Ngai.** 1996. A peroxidase related to the mammalian antimicrobial protein myleperoxidase in the *Euprymna-Vibrio* mutualism. Proc. Natl. Acad. Sci. USA **93:**13683–13688.
54. **Woodcock, D. M., P. J. Crowther, J. Doherty, S. Jefferson, E. DeCruz, M. Noyer-Weidner, S. S. Smith, M. Z. Michael, and M. W. Graham.** 1989. Quantitative evaluation of *Escherichia coli* host strains for tolerance to cytosine methylation in plasmid and phage recominants. Nucleic Acids Res. **17:**3469–3478.
55. **Zielinski, N. A., A. M. Chakrabarty, and A. Berry.** 1991. Characterization and regulation of the *Pseudomonas aeruginosa algC* gene encoding phosphomannomutase. J. Biol. Chem. **266:**9754–9763.

JOURNAL OF BACTERIOLOGY, Feb. 2001, p. 835–842 Vol. 183, No. 3
0021-9193/01/$04.00+0 DOI: 10.1128/JB.183.3.835–842.2001

Two-Component Sensor Required for Normal Symbiotic Colonization of *Euprymna scolopes* by *Vibrio fischeri*

KAREN L. VISICK* AND LINE M. SKOUFOS

Department of Microbiology and Immunology, Loyola University Chicago, Maywood, Illinois 60153

Received 15 August 2000/Accepted 14 November 2000

The light organ of the squid *Euprymna scolopes* is specifically colonized to a high density by the marine bacterium *Vibrio fischeri*. To date, only a few factors contributing to the specificity of this symbiosis have been identified. Using a genetic screen for random transposon mutants defective in initiating the symbiotic association or in colonizing the light organ to high density, we identified a mutant of *V. fischeri* that exhibited an apparent defect in symbiosis initiation. This mutant was not defective in motility, luminescence, or growth in minimal medium, suggesting that it lacks an essential, previously unidentified symbiotic function. By sequence analysis, we showed that the locus inactivated in this mutant encodes a predicted 927-amino-acid protein with a high degree of similarity to the sensor component of hybrid two-component regulatory systems. We have therefore designated this locus *rscS*, for regulator of symbiotic colonization—sensor. Sequence analysis revealed two hydrophobic regions which may result in the formation of a periplasmic loop involved in signal recognition; PhoA fusion data supported this proposed membrane topology. We have investigated the start site of *rscS* transcription by primer extension and identified a putative promoter region. We hypothesize that RscS recognizes a signal associated with the light organ environment and responds by stimulating a putative response regulator that controls protein function or gene expression to coordinate early colonization events. Further studies on RscS, its cognate response regulator, and the signaling conditions will provide important insight into the interaction between *V. fischeri* and *E. scolopes*.

The bioluminescent marine bacterium *Vibrio fischeri* forms an intimate symbiotic association with the Hawaiian squid *Euprymna scolopes*. Juvenile *E. scolopes* squid hatch from eggs uncolonized by *V. fischeri* cells but become rapidly and exclusively colonized by this bacterium despite potential competition from the many other bacterial species present in seawater (46, 48). Initiation of this mutualism typically requires only a short exposure (1 to 3 h) to *V. fischeri*, after which normal colonization will result even if the squid are removed to *Vibrio*-free seawater (40). Within 24 h, the *V. fischeri* cells reach a population of between 10^5 and 10^6 CFU in the symbiotic light organ, equivalent to approximately 10^8 CFU/cm^3 (40).

Because of the exclusive nature of the relationship between *V. fischeri* and *E. scolopes*, it is likely that both bacterial and host genes function in actively establishing this specific, long-term association. Through the study of bacterial mutants, three major stages of symbiotic colonization have been identified. These stages include (i) initiation of the association (initiation), (ii) colonization to the high cell density typically achieved by the wild type (accommodation), and (iii) persistence at a high cell density (persistence) (reviewed in reference 39).

Mutants defective for each of the stages have been identified. Initiation mutants include those defective for motility, because neither nonflagellated nor flagellated but nonmotile mutants can colonize the host (21). It is thought that a thick mucus layer present in the ducts leading to the light organ crypts, where colonization occurs, may prevent entry of nonmotile bacteria (47). Accommodation mutants include bacteria defective in one of several amino acid-biosynthetic genes. The ability of these strains to colonize, albeit at lower levels, suggests that the light organ environment is nutrient rich and that the required amino acids are being supplied by the squid host. The discovery of peptides present at high concentration in the fluid of the light organ supports this hypothesis (22).

Persistence mutants include two distinct subclasses. One subclass mutant lacks the ability to produce and take up siderophores. This mutant exhibited a decreasing level of colonization over the course of 3 days (23), suggesting that sequestration of iron from the light organ environment is an important factor in maintaining the symbiotic association. The second subclass includes bioluminescence mutants, defective in either structural or regulatory genes. The bioluminescence mutants colonize to a level comparable to the wild-type strain during the first day and thereafter show a decreased level of colonization (45, 47). At present, the exact relationship between defects in light production and reduced colonization remains unclear, but it has been speculated that utilization of oxygen by the bioluminescence machinery may reduce host-imposed oxidative stress (45).

Although these symbiosis-impaired mutants have provided valuable clues to the environmental conditions in the light organ, no comprehensive screen for bacterial genetic determinants of symbiotic competence has been described. We anticipate the existence of bacterial genes that are essential to initiate the symbiosis, including surface markers or receptors, as well as additional genes required for accommodation. It is also likely that regulatory factors controlling one or more regulons involved in the symbiosis will be found, particularly in view of the developmental events taking place in both partners as their association progresses (33, 39).

* Corresponding author. Mailing address: Department of Microbiology and Immunology, Loyola University Chicago, 2160 S. First Ave., Bldg. 105, Maywood, IL 60153. Phone: (708) 216-0869. Fax: (708) 216-9574. E-mail: kvisick@luc.edu.

In the present study, we have screened the ability of mutants generated by a random transposon insertion mutagenesis to colonize juvenile *E. scolopes*. We present here the characterization of one mutant with a severe symbiosis defect. This mutant colonizes poorly and thus may be defective in the ability to overcome a barrier(s) associated with early colonization events. We also present sequence data that predict that the defective gene interrupted by the transposon insertion in this mutant strain may encode a regulatory protein. We hypothesize that this putative regulator may play a key role in the expression of genes essential for, or even induced by, this bacterium-animal association.

MATERIALS AND METHODS

Strains and media. *V. fischeri* strain ES114 (9) and its rifampin-resistant derivative ESR1 (21) were the parent strains used in this study. *Escherichia coli* strains DH5α and CC118λ*pir* (27) were used as host strains for cloning, and S17-1λ*pir* (43) was used as the donor strain in conjugations.

V. fischeri cells were grown in SWT (9), LBS (15), or HEPES-minimal medium (41) containing ribose as a carbon source. *E. coli* strains were grown in Luria-Bertani (LB) medium (12). Conditioned medium (CM) was used to determine whether the colonization mutant KV712 was defective for bioluminescence in culture and was made as follows. *V. harveyi* B392 (38) was grown in LM (35) to an optical density of approximately 0.8 at 600 nm. The cells were removed by centrifugation followed by passage of the supernatant through a 0.2-μm-pore-sized filter. Where appropriate, antibiotics were added to the following final concentrations: ampicillin, 100 μg/ml; chloramphenicol (CHL), 1 to 5 μg/ml for *V. fischeri* and 30 μg/ml for *E. coli*; erythromycin, 1 to 5 μg/ml for *V. fischeri* and 150 μg/ml for *E. coli*; rifampin, 100 μg/ml; and tetracycline (TET), 5 μg/ml for *V. fischeri* and 15 μg/ml for *E. coli*. Agar was added to a final concentration of 1.5% for solid medium or 0.25% for motility plates.

Genetic techniques. Transposon mutagenesis was carried out using the Tn*10-lacZ* delivery plasmid pKV124 (see below). Conjugations were performed as follows. The donor strain (S17-1λ*pir* carrying the plasmid to be delivered) and the recipient *V. fischeri* strain (typically either ES114 or ESR1) were grown to mid-log phase at 37°C in LB and at 28°C in LBS, respectively. The strains were mixed, concentrated by centrifugation, and allowed to mate on solid medium. After an incubation of 6 to 14 h at 28°C, cells were diluted in LBS and transferred to selective medium. In some cases, triparental conjugations were performed using the appropriate *V. fischeri* recipient strain and two *E. coli* strains, DH5α carrying the plasmid to be transferred and DH5α carrying pRK2013 (13, 17), to supply conjugation functions.

Molecular techniques. All plasmid constructions were carried out by standard molecular biology techniques, using restriction and modifying enzymes obtained from New England Biolabs (Beverly, Mass.) or Promega (Madison, Wis.). The mini-Tn*10-lacZ* transposon in pKV124 was derived from pBSL181 (1) by the insertion of both a promoterless *lacZ* gene and *ori*R6K, the *pir*-dependent origin of replication from plasmid R6K (31). This plasmid is therefore a "suicide" plasmid in hosts lacking the *pir* gene, including *V. fischeri*. Cloning of DNA flanking the transposon insertion in *V. fischeri* strain KV712 was accomplished using the *ori*R6K and CHL resistance elements contained within the transposon. Chromosomal DNA was isolated and digested with a restriction enzyme that does not cleave within the insertion sequences. Fragments were then self-ligated using T4 DNA ligase and transformed into the permissive host CC118λ*pir* or S17-1λ*pir*. Clones carrying the transposon and flanking DNA were selected on CHL-containing LB plates. Two plasmids, pKV132 (containing about 3.8 kb of flanking DNA) and pKV133 (containing about 8.0 kb of flanking DNA), were obtained by digestion with *Nhe*I and *Bsr*GI, respectively. DNA fragments from clones pKV132 and pKV133 were subcloned into pBluescript (Stratagene, La Jolla, Calif.), pBC (Stratagene), or pEVS79 (E. V. Stabb and E. G. Ruby, submitted for publication). One of these subclones, pLMS22, contained a 2-kb *Hin*dIII-*Pst*I fragment; this plasmid was recombined into *V. fischeri* strain ESR1. Chromosomal DNA isolated from the resulting recombinant was used to clone the wild-type copy of the *rscS* gene and flanking DNA, resulting in pLMS25. Plasmid pLMS26 was derived from pLMS25 by the insertion of a 6-kb (*rscS*$^+$) fragment into pKV69, a TET^r CHL^r mobilizable vector.

Sequencing was carried out using forward and reverse primers complementary to vector and insert sequences. Manual sequencing for primer extension was carried out using the Sequenase sequencing kit (Amersham-Pharmacia Biotech, Piscataway, N.J.). Similarity searches were performed using the NCBI Blast program (2). Oligonucleotides were obtained from either the Loyola Macromolecular Analysis Facility or Integrated DNA Technologies (Coralville, Iowa).

Southern blotting. Chromosomal DNA isolated from *V. fischeri* strain KV712 was digested with *Eco*RV, which cuts once within the mini-Tn*10-lacZ* transposon, or *Bsr*GI, which cuts outside the transposon. DNA fragments were separated using a 0.6% agarose gel, transferred onto a nylon membrane (Hybond XL; Amersham-Pharmacia Biotech), and UV cross-linked. Detection was carried out using the Boehringer Mannheim digoxigenin DNA labeling kit (Roche Molecular Biochemicals, Indianapolis, Ind.) as follows. Random priming was used to generate biotinylated DNA fragments complementary to the transposon sequences, and these fragments were hybridized to the chromosomal DNA in a buffer containing 50% formamide, 0.1% *N*-lauroylsarcosine, 0.02% sodium dodecyl sulfate, 750 mM NaCl, and 75 mM sodium citrate. Blocking reagent was added to 2% for the prehybridization step. Washing, blocking, treatment with primary and secondary antibodies, and colorimetric detection were carried out under conditions of high stringency according to the manufacturer's instructions.

Primer extension. A 25-ml culture of *V. fischeri* strain ES114 was grown in LBS to an optical density of 1 at 600 nm. The cells were lysed in GITCN lysis buffer (44), and mRNA was isolated by centrifugation through a cesium chloride gradient as previously described (44). An oligonucleotide primer, 10R3 (5′-GATT GTGATAAGGCTATAACG-3′), complementary to the 5′ end of the *rscS* locus was radiolabeled by treatment with T4 polynucleotide kinase (Amersham-Pharmacia Biotech) in the presence of [γ-^{32}P]ATP (Amersham-Pharmacia Biotech). The radiolabeled primer was hybridized to the mRNA and incubated with Moloney murine leukemia virus (MMLV) reverse transcriptase (Stratagene) and nucleotides per the manufacturer's instructions. Extension products were visualized by autoradiography after separation on an 8% polyacrylamide gel and compared to a sequencing ladder generated using the same oligonucleotide primer to sequence from plasmid pLMS35, containing the *rscS* locus and flanking DNA.

Colonization assays. To determine whether mutant *V. fischeri* strains were able to form a symbiotic association with *E. scolopes*, juvenile squid were placed in artificial seawater (Instant Ocean; Aquarium Systems, Mentor, Ohio) containing an inoculum of 1,000 to 5,000 cells of the desired *V. fischeri* strain per ml of fluid as previously described (39). Luminescence was monitored over the course of 16 to 24 h using a Packard Tri-carb 2100TR scintillation counter (Packard Instruments, Meriden, Conn.) modified to detect bioluminescence. At specific intervals, juvenile *E. scolopes* were sacrificed by homogenization to directly quantify the number of bacteria present in the light organ. Homogenates were serially diluted, and aliquots were spread on SWT agar for viable-cell counts. The limit of detection is 14 *V. fischeri* cells per squid.

Luminescence assays. KV712 and ESR1 were diluted 1:100 and grown in CM prepared as described above, in the presence or absence of a synthetic *V. fischeri* autoinducer (600 ng of 3-oxo-hexanoyl-L-homoserine lactone [Sigma, St. Louis, Mo.] per ml). At various times after inoculation, 1-ml samples were taken for luminescence and optical density measurements. A TD-20/20 luminometer (Turner Designs, Sunnyvale, Calif.) was used to determine the level of bioluminescence of KV712 and its parent.

Construction and analysis of *phoA* fusions. A mini-Tn*10* derivative carrying the *phoA* and *lacZ* genes fused in frame was obtained from M. Alexeyev. This transposon, carried by pMA651, was introduced by conjugation into DH5α carrying pBlueScript with a 3-kb *rscS*$^+$ insert. After conjugation and selection for recipient strains carrying the transposon (carried out as described above for *V. fischeri*), the selected cells were pooled and subjected to a plasmid extraction procedure. The pooled plasmids were sequentially introduced into DH5α and CC118λ*pir* which were then grown on LB medium containing CHL and ampicillin to select for the presence of plasmids containing a transposon insertion. CC118λ*pir* recipient cells were plated on LB containing CHL and 5-bromo-4-chloro-3-indolylphosphate, an indicator of alkaline phosphatase activity. Colonies that turned blue on this medium (indicating an active fusion to PhoA) were identified; the plasmids from these colonies were analyzed by restriction digestion to ascertain the location of the transposon fusion. Fusions that mapped to the *rscS* gene were further localized by sequence analysis.

Nucleotide sequence accession number. The GenBank accession number assigned to the *rscS* sequence is AF319618.

RESULTS

Identification of a novel symbiotic locus. We have developed a genetic screen to identify bacterial genes important for the symbiotic interaction between *V. fischeri* and *E. scolopes*. Upon entering the light organ of a newly hatched juvenile squid,

wild-type *V. fischeri* rapidly reaches a high cell density (40). A cell density-dependent (quorum-sensing) mechanism regulates *V. fischeri* bioluminescence; therefore, the amount of light produced by the bacteria in the light organ serves as an indirect measure of colonization. We constructed transposon insertion mutants of *V. fischeri* strain ESR1 (see Materials and Methods) and inoculated newly hatched *E. scolopes* juveniles with individual mutant strains. Automated monitoring of luminescence over a 16- to 24-h period was used to determine the ability of these mutants to enter and proliferate within the light organ. This screen should identify mutants of the initiation class, which would be unable to colonize the light organ. The screen should also identify mutants of the accommodation class, which would be unable to reach normal cell densities after initial colonization.

From a collection of approximately 2,000 transposon insertion mutants, we identified a strain, KV712, that failed to exhibit the wild-type pattern (Fig. 1A, top) of bioluminescence in the symbiotic association: during the first 16 h post inoculation, 7 of 10 juvenile squid exposed to this mutant failed to emit light, while 3 exhibited delayed onset of bioluminescence (Fig. 1A, bottom). However, KV712 showed no detectable defect relative to the parent strain ESR1 in producing bioluminescence in culture or in inducing luminescence in response to the addition of an autoinducer (3-oxo-hexanoyl L-homoserine lactone) (Fig. 1B). Thus, the symbiotic luminescence defect apparently did not result from a mutation in the *lux* operon, which encodes the structural genes for bioluminescence.

In addition to *lux* mutants, nonmotile mutants and some amino acid auxotrophs fail to establish normal levels of colonization (21, 23). When tested for motility in a soft agar plate, strain KV712 exhibited motility identical to that of the parent strain (data not shown). Growth in a minimal medium was also comparable to that of ESR1 (data not shown). These data suggested that KV712 carries a mutation in a previously unidentified locus that affects the symbiotic interaction.

To confirm a potential colonization defect of KV712, we determined the number of CFU present in the light organ of the juvenile squid at 19 h postinoculation (Fig. 2). Of the 10 juveniles inoculated with KV712, 4 exhibited no detectable colonization (the limit of detection in this experiment was approximately 14 CFU), while an additional 3 were colonized at a level approximately 100-fold reduced from that of juveniles exposed to the wild-type strain. The three remaining juveniles, which had exhibited a delay in onset of bioluminescence (Fig. 1A), contained *V. fischeri* cells at a level comparable to that of the wild-type-colonized squid.

These data suggest that although KV712 is capable of bioluminescence, in squid assays it fails to emit the typical wild-type pattern of bioluminescence due to a symbiotic defect. We hypothesize that this mutant lacks the ability to properly initiate the symbiotic association. Occasionally, however, some mutant cells succeed in bypassing the "block" to initiation, after which colonization (i.e., multiplication) within the squid proceeds normally. In support of this idea, we observed that squid in which mutant cells apparently overcame the block more quickly (as judged by luminescence [Fig. 1A]) exhibited higher colonization levels at the assay time than those that experienced a greater delay. Furthermore, in preliminary experiments we have observed that the relative frequency of high-level colonization by KV712 was reduced with smaller inoculum and a shorter duration of inoculation (Skoufos and Visick, unpublished data). Thus, we believe that the observed variation in the data represents random events during the interaction of a homogeneous population of mutants with an animal host.

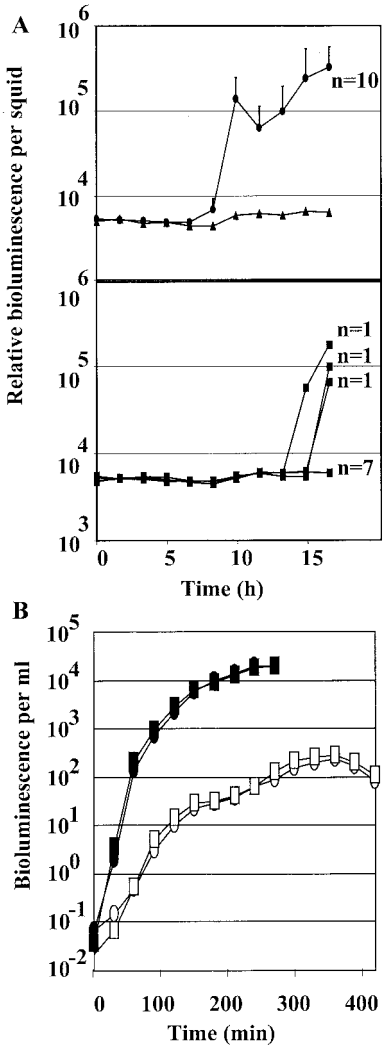

FIG. 1. Luminescence levels of colonization mutant KV712 and its parent. (A) Newly hatched juvenile *E. scolopes* squid were incubated in artificial seawater containing no *V. fischeri* (solid triangles, top panel) or either the parent strain ESR1 (solid circles, top panel) or the colonization mutant KV712 (solid squares, bottom panel). Bioluminescence was measured over time. The light levels of 10 animals inoculated with ESR1 (indicated by $n = 10$) and of 7 animals inoculated with KV712 (indicated by $n = 7$), were averaged, while three squid colonized by KV712 are represented singly (indicated by $n = 1$). Error bars are shown, representing the standard deviation of luminescence readings for ESR1-colonized animals; the level of light observed for seven of the KV712-inoculated squid was not above the limit of detection for the machine, and thus error bars are not displayed. (B) ESR1 (circles) and KV712 (squares) were grown in CM in the absence (open symbols) or presence (solid symbols) of an autoinducer of bioluminescence (3-oxo-hexanoyl-L-homoserine lactone). The level of luminescence was measured using a Turner 20/20 luminometer. The two strains grew at essentially the same rate.

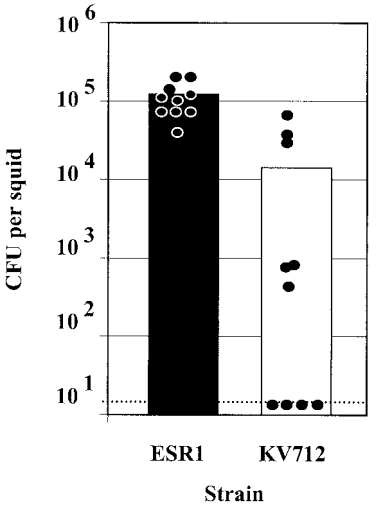

FIG. 2. Symbiotic colonization by *V. fischeri* strain KV712 and its parent, ESR1. Newly hatched juvenile *E. scolopes* were exposed for 15 h to either KV712 or ESR1. The level of colonization achieved by these strains was determined by homogenization and plating 19 h after the organisms were placed together. Each circle represents the number of *V. fischeri* cells in an individual squid, and the bar indicates the average colonization level of the 10 squid in each inoculation condition (2,300 cells per ml). The level of colonization of four squid inoculated with KV712 was below the limit of detection, as indicated by the dashed line.

Molecular characterization of KV712. Our data suggested that KV712 carries a mutation in a novel symbiosis locus. Because the mutation in this strain was generated by transposon mutagenesis, the number and location of transposon insertions could be easily determined by Southern blot analysis. DNA probes complementary to the transposon and its delivery plasmid were hybridized to chromosomal DNA isolated from KV712 and digested either with *Bsr*GI (which does not cut within the inserted sequences) or *Eco*RV (which recognizes a single site within the transposon). Consistent with a single transposon insertion event in KV712, we observed a single band for *Bsr*GI-digested DNA and two bands for *Eco*RV-digested DNA (approximately 5 and 7kb) (data not shown). When the same probe was hybridized to *Eco*RV-digested chromosomal DNA extracted from ESR1, no bands were observed (data not shown).

To further investigate the locus that was disrupted in KV712, we cloned the transposon and flanking chromosomal DNA. The presence of an origin of replication (*ori*R6K) and a CHL resistance marker within the transposon permitted rapid cloning by recircularization of chromosomal DNA fragments and transformation into a permissive *E. coli* host strain. Subcloning and sequencing revealed that the transposon had inserted into a large open reading frame (ORF), encoding a predicted 105-kDa protein of 927 amino acids.

Sequencing of flanking DNA demonstrated that the genes adjacent to this ORF possess a high degree of similarity to *E. coli* genes involved in glycerol metabolism and regulation. Located 581 nucleotides upstream of the putative translational start of the large ORF, there is an apparent homolog of the *glpR* gene (10), while 68 nucleotides downstream there is a *glpK* analog (37). Both genes are transcribed divergently relative to the large ORF (Fig. 3A), precluding the possibility that the ORF is part of an operon and suggesting that the transposon insertion in strain KV712 affects expression only of that single, large ORF. KV712 and its parent, ESR1, both fail to grow on glycerol as a carbon source, but a mutation of this ORF in ES114 (N. D. Montgomery and K. L. Visick, unpublished data) did not alter that strain's ability to grown on glycerol (data not shown).

Comparison of the ORF sequence to known sequences revealed significant amino acid sequence identity with the sensory component of hybrid two-component regulatory systems (Fig. 3B). Close matches included LuxQ (39% identity, 62% similarity) (7), ArcB (28% identity, 48% similarity) (30), and BvgS (26% identity, 45% similarity) (4), as well as a number of hypothetical *V. cholerae* sensor kinases (26). Each of these proteins (LuxQ, ArcB, and BvgS) plays a role in sensing an environmental signal and transducing the signal through a phosphorelay cascade (3, 29, 36) to a response regulator protein (LuxO [8], ArcA [14], and BvgA [4], respectively). Each response regulator protein then up- or downregulates transcription of a set of genes.

The domains involved in nucleotide binding and in the phosphorelay cascade are highly conserved among these proteins. The strongest similarity between the ORF disrupted in KV712 and these sensor kinases occurs in these domains (Fig. 3B). From these sequence alignments, we believe that this ORF likely encodes a hybrid two-component sensor kinase. Thus, we tentatively assign this locus the name *rscS*, for regulator of symbiotic colonization—sensor.

Complementation of the symbiotic defect. To determine whether the disruption of *rscS* caused the symbiotic defect of KV712, we cloned the wild-type copy of the locus. We performed complementation assays using a subclone, pLMS26, that contained *rscS*$^+$ and approximately 3 kb of upstream DNA to ensure the presence of regulatory sequences. We infected juvenile *E. scolopes* with cells either wild-type (ESR1) or defective for *rscS* (KV712), carrying either the vector (pKV69) or the *rscS*$^+$ complementing plasmid pLMS26. Plasmid pLMS26 but not pKV69 apparently restored symbiotic competence to KV712, as monitored indirectly by bioluminescence measurements over a 17-h period (data not shown). The presence of either plasmid did not affect symbiotic luminescence levels of the parent strain (data not shown).

After 17 h, we directly determined the level of colonization achieved by each strain. As predicted from the luminescence patterns, pLMS26 complemented the disrupted *rscS* gene in KV712: the complemented strain reached colonization levels comparable to those of the parent strain carrying either vector or pLMS26 (Fig. 4). We also observed wild-type levels of colonization when we inoculated juvenile squid with KV712 complemented with a construct containing only the 3-kb *rscS*$^+$ locus (data not shown). In contrast, KV712 carrying the vector alone remained defective in properly initiating the symbiotic interaction. These results are consistent with the conclusion that the transposon insertion in *rscS* caused the symbiotic defect displayed by KV712.

Analysis of the *rscS* promoter region. To confirm transcription of the *rscS* gene and to identify a putative promoter region, we mapped the transcriptional start of *rscS* using primer extension. A radiolabeled primer complementary to the 5′

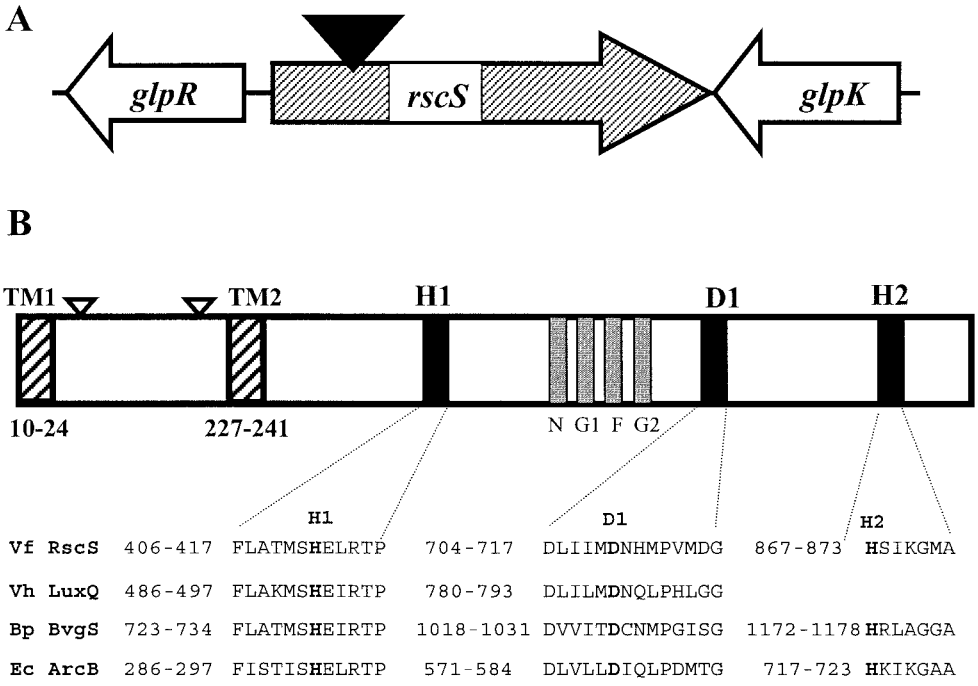

FIG. 3. Schematic diagram of the *rscS* locus and flanking genes. (A) The region of the chromosome flanking the transposon insertion in KV712 is indicated. The transposon (solid triangle) inserted in a large ORF, *rscS*, which is flanked by genes with high sequence similiarity to the *E. coli glpR* and *glpK* genes. The direction of transcription is indicated. (B) Noteworthy regions of the 927-amino-acid RscS protein are diagrammed. RscS exhibits sequence similarity to the *V. harveyi* (Vh) LuxQ, *Bordetella pertussis* (Bp) BvgS, and *E. coli* (Ec) ArcB proteins, particularly, as indicated below the black bars, in the regions flanking the histidine and aspartic acid residues (H1, D1, and H2) thought to be involved in the phosphorelay cascade. RscS also exhibits sequence similarity to the nucleotide-binding sites depicted by the gray boxes and labeled N, G1, F, and G2. Two putative transmembrane (TM) regions are indicated by striped bars and are designated TM1 and TM2. The locations of active *phoA* transposon insertions are indicated by open triangles.

region of the putative *rscS* ORF (spanning nucleotides 19 to 39 downstream from the putative translational start) was hybridized to mRNA isolated from the wild-type *V. fischeri* strain ES114. This served as the template for reverse transcription by MMLV reverse transcriptase. The resulting product was compared to a sequencing ladder generated from the same primer. We observed a major band (Fig. 5A), which places the transcriptional start site (+1) at the A residue located 34 nucleotides upstream of the predicted ATG translational start codon (Fig. 5B), and a minor band, which maps to an A residue 46 bases further upstream. The significance of the minor transcriptional start is unclear.

We have identified possible regulatory elements upstream of the putative translational start, based on the location of the major transcriptional start site and consensus sequences found in *E. coli*. These assignments are tentative because there has been little research identifying such elements in *V. fischeri*. A possible Shine-Dalgarno sequence, AGGAGC (shown in boldface and underlined), is located 8 bases upstream of the proposed translational start and matches five of six bases of the consensus *E. coli* sequence AGGAGG (42). A putative −10 promoter sequence (dotted underline), TAAAAT, is centered at base −11 with respect to the transcriptional start. This sequence is similar to that identified by primer extension mapping of the *V. fischeri lux* operon (16) and is identical at five of six bases to the canonical *E. coli* −10 sequence, TATAAT (25). Fifteen nucleotides upstream of this sequence (dotted underline) is a potential −35 sequence, TTGTAA, that matches the *E. coli* −35 consensus (TTGACA) (25) at four of six bases. In addition to predicting a possible promoter, these primer extension results provide evidence that the *rscS* locus is transcriptionally active in cells grown in laboratory culture.

PhoA fusions predict a periplasmic loop. LuxQ and BvgS hypothetically recognize their respective environmental signals by means of an amino-terminal periplasmic loop (4, 7). These periplasmic loops exhibit no sequence similarity to each other despite the strong conservation of other domains in the proteins, suggesting that this region gives each protein its unique function. Similarly, the amino terminus of the putative RscS shows no significant similarity to any other known protein.

Initial support for the hypothesis that RscS may possess a periplasmic loop resulted from a hydrophobicity analysis (dense alignment surface method) (11). Two highly hydrophobic regions were found in the N-terminal third of the protein (amino acids 10 to 24 and 227 to 241). A second program (SOUSI) (28) predicted two transmembrane (TM) regions, from 6 to 28 and 222 to 244, as well as a third TM from 312 to 334.

To investigate whether these hydrophobic regions result in a periplasmic loop, we mutagenized an *E. coli* strain (Materials and Methods) carrying a plasmid-borne copy of *rscS* with a mini-Tn*phoA* transposon. Insertion of this transposon in frame into the *rscS* gene would result in synthesis of an RscS-PhoA fusion protein, but the PhoA portion would be active only if

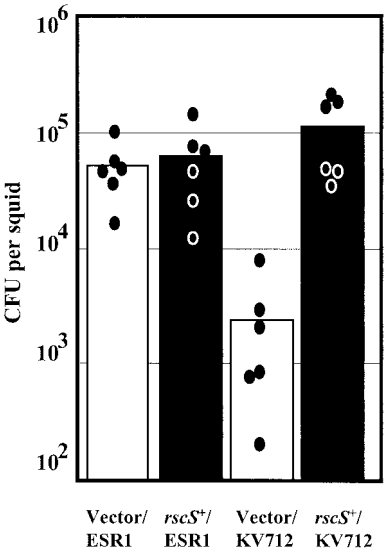

FIG. 4. Complementation of the colonization defect in KV712. Newly hatched juvenile *E. scolopes* were inoculated with one of four strains: KV712 or its parent ESR1, each carrying either vector pKV69 or *rscS*$^+$ plasmid pLMS26. The squid were exposed to approximately 1,000 cells of *V. fischeri* per ml of seawater for 3 h. The level of colonization achieved by these strains 17 h after the organisms were placed together was determined by homogenization and plating as described in Materials and Methods. Each circle represents the number of *V. fischeri* cells in an individual squid, and the bar indicates the average colonization level of the six squid in each inoculation condition.

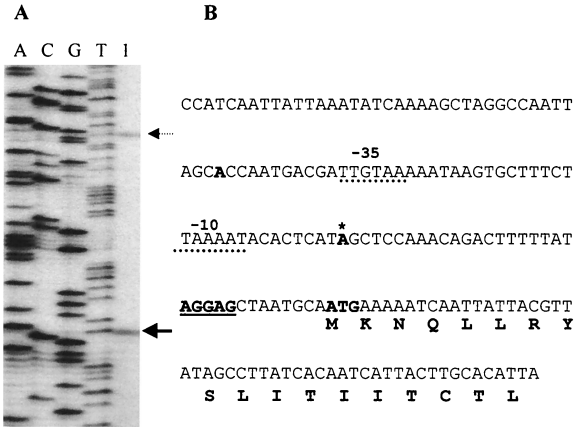

FIG. 5. Promoter mapping by primer extension. (A) The primer extension products obtained using a primer complementary to the *rscS* coding sequence (see Materials and Methods) appear in lane 1 and are indicated by arrows. Contained within the adjacent lanes, labeled A, C, G, and T, are the bands obtained by DNA sequencing using the same primer. (B) The DNA sequence at the beginning of the *rscS* ORF and upstream is shown. The putative ATG translational start is indicated by the bold ATG. Centered 11 bp upstream of the possible translational start is a potential Shine-Dalgarno site, boldface and underlined. The possible transcriptional starts identified by primer extension are Mboldface; the more significant product is also indicated by an asterisk. A possible promoter region is indicated by a dashed underline and labeled above with −10 and −35.

localized to the periplasm (32). An alkaline phosphatase indicator medium was used to identify fusions with alkaline phosphatase activity; four independent insertions which had this activity were identified. Two of the four active insertions were located after amino acid 40 of RscS, and the other two were both inserted after amino acid 200. Both of these sites are within the region flanked by the two putative membrane-spanning segments, providing strong evidence that this region lies in the periplasm. These data also demonstrate that *rscS* is not only transcribed but also translated in vivo.

DISCUSSION

This paper reports the first major result of a genetic screen for *V. fischeri* mutants defective in symbiotic initiation and accommodation: a novel symbiotic locus, *rscS*, that appears to play an important role in symbiotic initiation. A single transposon insertion in *rscS* severely impaired the ability of *V. fischeri* to initiate a symbiotic association with juvenile *E. scolopes* (Fig. 2), a defect that could be complemented by a wild-type copy of the *rscS* gene. We identified putative promoter and ribosome-binding sequences on the basis of the transcriptional start site and *E. coli* consensus sequences. Given a paucity of data for regulatory elements in *V. fischeri* genes, however, positive confirmation of these sequences will require mutational and other analyses.

Molecular characterization of *rscS* revealed a predicted 927-amino-acid protein, RscS, that exhibited strong sequence similarity (Fig. 3B) to hybrid two-component sensor kinases. Each of these kinases participates in a series of four phosphorelay reactions that occur in response to particular environmental conditions (such as a specific level of osmolarity or the presence of a particular ion [3, 36]). Initially, autophosphorylation occurs on a histidine residue (H1). This phosphate sequentially transfers to an aspartic acid (D1), another histidine (H2), and finally to another aspartic acid residue (D2).

Although as many as four distinct proteins may be utilized in this phosphorelay, there are typically two key proteins: a sensor that recognizes the environmental cue and begins the phosphorelay, and a response regulator that contains the conserved final aspartic acid residue and effects changes in gene expression or protein function (3, 29, 36). The module arrangement of the RscS protein most resembles that of BvgS and ArcB, both of which contain three of the four conserved phosphorylation domains (H1, D1, and H2). RscS therefore appears to be a sensor component belonging to the subclass of hybrid two-component regulators. The amino acid sequence in the periplasmic loop domain, however, diverges from other known sequences, suggesting that it may respond to a distinct environmental condition.

The predicted RscS protein most resembles LuxQ of *V. harveyi* (39% identity). LuxQ functions as one of two "redundant" quorum-sensing proteins that sense cell density and regulate luminescence through the recognition of an autoinducer signaling molecule (6, 7). Individually, LuxQ and a second sensor, LuxN, funnel their signals through a common histidine phosphotransferase protein, LuxU, which then modulates phosphorylation of LuxO, a DNA-binding protein that represses transcription of the *V. harveyi lux* operon (8, 18, 19). In recent years, proteins with sequence similarity to these and other *V. harveyi* quorum-sensing components have been identified in *V. fischeri*. The *V. fischeri* AinR protein (20) shows

some sequence similarity with a portion of the *V. harveyi* LuxN sensor kinase. Furthermore, proteins with high sequence identity to the *V. harveyi* LuxO (65%) and LuxU proteins have recently been identified in *V. fischeri* (34). The *V. fischeri* LuxO plays a role similar to that of the *V. harveyi* protein in repressing luminescence (34).

The identification of a *V. fischeri* protein, RscS, with sequence similarity to LuxQ makes it tempting to speculate that RscS plays a role in recognizing an autoinducer and participating in *lux* gene regulation. Unlike LuxQ, which carries only two of the modules predicted to be involved in a phosphorelay cascade (H1 and D1), RscS contains three of the four modules (H1, D1, and H2). Thus, a LuxU intermediate would likely be unnecessary. The two proteins, RscS and LuxQ, show no apparent sequence similarity in the proposed periplasmic loops, suggesting that they recognize different signals. This prediction is supported by a lack of cross-stimulation of *V. harveyi* bioluminescence by *V. fischeri* culture supernatants (5, 24). Furthermore, our data to date indicate no apparent defect in luminescence gene regulation (Fig. 1B). It is formally possible that, similar to the *V. harveyi* system, RscS and a second sensor kinase, such as AinR, may function redundantly to control *lux* expression. Thus, we would be unable to detect a defect by removing only one of these two proteins. Further work needs to be performed to test this hypothesis by constructing *ainR* and possibly *luxO* mutations singly and in combination with an *rscS* mutation in our squid-symbiont strain of *V. fischeri*. These mutants can then be tested for both luminescence in culture and colonization in the symbiosis.

Regardless of a hypothetical additional role for RscS in controlling luminescence, normal symbiotic colonization by *V. fischeri* requires this protein. Given the sequence similarity of RscS to two-component sensors and the colonization defect observed in the *rscS* mutant strain, we believe that RscS may be a key regulatory factor in the *Vibrio-Euprymna* symbiosis. We propose that RscS responds to some factor unique to the light organ environment and subsequently communicates to a hypothetical "RscR" the information that the cell now occupies a special niche. The phosphorelay hypothetically initiated by RscS could then alter gene expression and/or protein activity, switching the bacteria into symbiotic mode and perhaps activating the developmental programs that permit *V. fischeri* to permanently colonize its host.

We expect that further characterization of the role of RscS will contribute to a better understanding of the mechanism(s) by which *V. fischeri* senses the symbiotic environment and of the nature of the response that permits these bacteria to colonize their host. We anticipate the discovery of a cognate response regulator that acts in conjunction with RscS to control a symbiotic gene function(s) and the identification of these downstream targets. In so doing, we may learn the environmental cues that permit *V. fischeri* to sense that it has entered the light organ and modulate specific functions required for the interaction between the bacteria and their animal host.

ACKNOWLEDGMENTS

We thank C. Beatty for her assistance with the primer extension experiments, P. Smith for his assistance with the bioluminescence assays, and the following individuals for experimental ideas and comments on the manuscript: A. Driks, F. Catalano, J. Graf, N. Montgomery, E. Ruby, J. Visick, and A. Wolfe.

This work was supported by an internal award to K.L.V. from the Potts Foundation and by NIH grant 1 RO1 GM59690-01A1 to K.L.V.

REFERENCES

1. **Alexeyev, M. F., and I. N. Shokolenko.** 1995. Mini-Tn*10* transposon derivatives for insertion mutagenesis and gene delivery into the chromosome of Gram-negative bacteria. Gene **160:**59–62.
2. **Altschul, S. F., T. L. Madden, A. A. Schäffer, J. Zhang, Z. Zhang, W. Miller, and D. J. Lipman.** 1997. Gapped BLAST and PSI-BLAST: a new generation of protein database search programs. Nucleic Acids Res. **25:**3389–3402.
3. **Appleby, J. L., J. S. Parkinson, and R. B. Bourret.** 1996. Signal transduction via the multi-step phosphorelay: not necessarily a road less traveled. Cell **86:**845–848.
4. **Arico, B., V. Scarlato, D. M. Monack, S. Falkow, and R. Rappuoli.** 1991. Structural and genetic analysis of the *bvg* locus in *Bordetella* species. Mol. Microbiol. **5:**2481–2491.
5. **Bassler, B. L., E. P. Greenberg, and A. M. Stevens.** 1997. Cross-species induction of luminescence in the quorum-sensing bacterium *Vibrio harveyi*. J. Bacteriol. **179:**4043–4045.
6. **Bassler, B. L., M. Wright, R. E. Showalter, and M. R. Silverman.** 1993. Intercellular signalling in *Vibrio harveyi*: sequence and function of genes regulating expression of luminescence. Mol. Microbiol. **9:**773–786.
7. **Bassler, B. L., M. Wright, and M. R. Silverman.** 1994. Multiple signalling systems controlling expression of luminescence in *Vibrio harveyi*: sequence and function of genes encoding a second sensory pathway. Mol. Microbiol. **13:**273–286.
8. **Bassler, B. L., M. Wright, and M. R. Silverman.** 1994. Sequence and function of LuxO, a negative regulator of luminescence in *Vibrio harveyi*. Mol. Microbiol. **12:**403–412.
9. **Boettcher, K. J., and E. G. Ruby.** 1990. Depressed light emission by symbiotic *Vibrio fischeri* of the sepiolid squid *Euprymna scolopes*. J. Bacteriol. **172:** 3701–3706.
10. **Choi, Y. L., S. Kawase, T. Nishida, H. Sakai, T. Komano, M. Kawamukai, R. Utsumi, Y. Kohara, and K. Akiyama.** 1988. Nucleotide sequence of the *glpR* gene encoding the repressor for the glycerol-3-phosphate regulon of *Escherichia coli* K12. Nucleic Acids Res. **16:**7732.
11. **Cserzo, M., E. Wallin, I. Simon, G. von Heijne, and A. Elofsson.** 1997. Prediction of transmembrane alpha-helices in procaryotic membrane proteins: the dense alignment surface method. Protein Eng. **10:**673–676.
12. **Davis, R. W., D. Botstein, and J. R. Roth.** 1980. Advanced bacterial genetics. Cold Spring Harbor Laboratory, Cold Spring Harbor, N.Y.
13. **Ditta, G., S. Stanfield, D. Corbin, and D. R. Helinski.** 1980. Broad host range DNA cloning system for Gram-negative bacteria: construction of a gene bank of *Rhizobium meliloti*. Proc. Natl. Acad. Sci. USA **77:**7347–7351.
14. **Drury, L. S., and R. S. Buxton.** 1985. DNA sequence analysis of the *dye* gene of *Escherichia coli* reveals amino acid homology between the Dye and OmpR proteins. J. Biol. Chem. **260:**4236–4242.
15. **Dunlap, P. V.** 1989. Regulation of luminescence by cyclic AMP in *cya*-like and *crp*-like mutants of *Vibrio fischeri*. J. Bacteriol. **171:**1199–1202.
16. **Egland, K. A., and E. G. Greenberg.** 1999. Quorum sensing in *Vibrio fischeri*: elements of the *luxI* promoter. Mol. Microbiol. **31:**1197–1204.
17. **Figurski, D. H., and D. R. Helinski.** 1979. Replication of an origin-containing derivative of plasmid RK2 dependent on a plasmid function provided in trans. Proc. Natl. Acad. Sci. USA **76:**1648–1652.
18. **Freeman, J. A., and B. L. Bassler.** 1999. Sequence and function of LuxU, a two-component phosphorelay protein that regulates quorum sensing in *Vibrio harveyi*. J. Bacteriol. **181:**899–906.
19. **Freeman, J. A., B. N. Lilley, and B. L. Bassler.** 2000. A genetic analysis of the functions of LuxN: a two-component hybrid sensor kinase that regulates quorum sensing in *Vibrio harveyi*. Mol. Microbiol. **35:**139–149.
20. **Gilson, L., A. Kuo, and P. V. Dunlap.** 1995. AinS and a new family of autoinducer synthesis proteins. J. Bacteriol. **177:**6946–6951.
21. **Graf, J., P. V. Dunlap, and E. G. Ruby.** 1994. Effect of transposon-induced motility mutations on colonization of the host light organ by *Vibrio fischeri*. J. Bacteriol. **176:**6986–6991.
22. **Graf, J., and E. G. Ruby.** 1998. Host-derived amino acids support the proliferation of symbiotic bacteria. Proc. Natl. Acad. Sci. USA **95:**1818–1822.
23. **Graf, J., and E. G. Ruby.** 2000. Novel effects of a transposon insertion in the *Vibrio fischeri glnD* gene: defects in iron uptake and symbiotic persistence in addition to nitrogen utilization. Mol. Microbiol. **37:**168–179.
24. **Greenberg, E. P., J. W. Hastings, and S. Ulitzur.** 1979. Induction of luciferase synthesis in *Beneckea harveyi* by other marine bacteria. Arch. Microbiol. **120:**87–91.
25. **Hawley, D. K., and W. R. McClure.** 1983. Compilation and analysis of *Escherichia coli* promoter DNA sequences. Nucleic Acids Res. **11:**2237–2255.
26. **Heidelberg, J. F., J. A. Eisen, W. C. Nelson, R. A. Clayton, M. L. Gwinn, R. J. Dodson, D. H. Haft, E. K. Hickey, J. D. Peterson, L. A. Umayam, S. R. Gill, K. E. Nelson, T. D. Read, H. Tettelin, D. Richardson, M. D. Ermolaeva, J. Vamathevan, S. Bass, H. Qin, I. Dragoi, P. Sellers, L. McDonald, T. Utterback, R. D. Fleishmann, W. C. Nierman, O. White, S. L. Salzberg, H. O. Smith, R. R. Colwell, J. J. Mekalanos, J. C. Venter, and C. M. Fraser.** 2000.

DNA sequence of both chromosomes of the cholera pathogen *Vibrio cholerae*. Nature **406:**477–483.
27. **Herrero, M., V. de Lorenzo, and K. N. Timmis.** 1990. Transposon vectors containing non-antibiotic resistance selection markers for cloning and stable chromosomal insertion of foreign genes in gram-negative bacteria. J. Bacteriol. **172:**6557–6567.
28. **Hirokawa, T., S. Boon-Chieng, and S. Mitaku.** 1998. SOSUI: classification and secondary structure prediction system for membrane proteins. Bioinformatics **14:**378–379.
29. **Hoch, J. A., and T. J. Silhavy (ed.).** 1995. Two-component signal transduction. ASM Press, Washington, D.C.
30. **Iuchi, S., Z. Matsuda, T. Fujiwara, and E. C. C. Lin.** 1990. The *arcB* gene of *Escherichia coli* encodes a sensor-regulator protein for anaerobic repression of the *arc* modulon. Mol. Microbiol. **4:**715–727.
31. **Kolter, R., M. Inuzuka, and D. R. Helinski.** 1978. Trans-complementation-dependent replication of a low molecular weight origin fragment from plasmid R6K. Cell **15:**1199–1208.
32. **Manoil, C., and J. Beckwith.** 1986. A genetic approach to analyzing membrane protein topology. Science **233:**1403–1408.
33. **McFall-Ngai, M. J.** 1999. Consequences of evolving with bacterial symbionts: insights from the squid-vibrio associations. Annu. Rev. Ecol. Syst. **30:**235–256.
34. **Miyamato, C. M., Y. H. Lin, and E. A. Meighen.** 2000. Control of bioluminescence in *Vibrio fischeri* by the LuxO signal response regulator. Mol. Microbiol. **36:**594–607.
35. **Nealson, K. H.** 1978. Isolation, identification, and manipulation of luminous bacteria. Methods Enzymol. **57:**153–166.
36. **Parkinson, J. S.** 1993. Signal transduction schemes of bacteria. Cell **73:**857–871.
37. **Pettigrew, D. W., D. P. Ma, C. A. Conrad, and J. R. Johnson.** 1988. *Escherichia coli* glycerol kinase: cloning and sequencing of the *glpK* gene and the primary structure of the enzyme. J. Biol. Chem. **263:**135–139.
38. **Reichelt, J. L., and P. Baumann.** 1973. Taxonomy of the marine, luminous bacteria. Arch. Mikrobiol. **94:**283–330.
39. **Ruby, E. G.** 1996. Lessons from a cooperative, bacterial-animal association: the *Vibrio fischeri-Euprymna scolopes* light organ symbiosis. Annu. Rev. Microbiol. **50:**591–624.
40. **Ruby, E. G., and L. M. Asato.** 1993. Growth and flagellation of *Vibrio fischeri* during initiation of the sepiolid squid light organ symbiosis. Arch. Microbiol. **159:**160–167.
41. **Ruby, E. G., and K. H. Nealson.** 1977. Pyruvate production and excretion by the luminous marine bacteria. Appl. Environ. Microbiol. **34:**164–169.
42. **Shine, J., and L. Dalgarno.** 1974. The 3′-terminal sequence of *Escherichia coli* 16S ribosomal RNA: complementarity to nonsense triplets and ribosome binding sites. Proc. Natl. Acad. Sci. USA **71:**1342–1346.
43. **Simon, R., U. Priefer, and A. Puhler.** 1983. A broad host range mobilization system for *in vivo* genetic engineering: transposon mutagenesis in gram negative bacteria. Bio/Technology **1:**784–791.
44. **Totten, P. A., and S. Lory.** 1990. Characterization of the type a flagellin gene from *Pseudomonas aeruginosa* PAK. J. Bacteriol. **172:**7188–7199.
45. **Visick, K. L., J. Foster, J. Doino, M. McFall-Ngai, and E. G. Ruby.** 2000. *Vibrio fischeri lux* genes play an important role in colonization and development of the host light organ. J. Bacteriol. **182:**4578–4586.
46. **Visick, K. L., and M. J. McFall-Ngai.** 2000. An exclusive contract: specificity in the *Vibrio fischeri-Euprymna scolopes* partnership. J. Bacteriol. **182:**1779–1787.
47. **Visick, K. L., and E. G. Ruby.** 1996. Construction and symbiotic competence of a *luxA*-deletion mutant of *Vibrio fischeri*. Gene **175:**89–94.
48. **Wei, S. L., and R. E. Young.** 1989. Development of symbiotic bacterial bioluminescence in a nearshore cephalopod, *Euprymna scolopes*. Mar. Biol. **103:**541–546.